

http://waikato.researchgateway.ac.nz/

Research Commons at the University of Waikato

Copyright Statement:

The digital copy of this thesis is protected by the Copyright Act 1994 (New Zealand).

The thesis may be consulted by you, provided you comply with the provisions of the Act and the following conditions of use:

- Any use you make of these documents or images must be for research or private study purposes only, and you may not make them available to any other person.
- Authors control the copyright of their thesis. You will recognise the author's right to be identified as the author of the thesis, and due acknowledgement will be made to the author where appropriate.
- You will obtain the author's permission before publishing any material from the thesis.

A TEPHRA-DATED RECORD OF PALAEOENVIRONMENTAL CHANGE SINCE ~ 5,500 YEARS AGO FROM LAKE ROTORUA, NORTH ISLAND, NEW ZEALAND

A thesis submitted in partial fulfillment
of the requirements for the degree of

MASTER OF SCIENCE

In Earth and Ocean Sciences and Chemistry
at The University of Waikato
by

RACHEL CARA PICKETT



THE UNIVERSITY OF
WAIKATO
Te Whare Wānanga o Waikato

UNIVERSITY OF WAIKATO

2008

Abstract

A palaeolimnological study was carried out on a high-resolution, 7.62 m long core (RU188-07) from Lake Rotorua. The core consists predominantly of olive diatomaceous ooze, laminated in places, and contains five tephra including Tarawera (1886 A.D.), Kaharoa (c. 1314 A.D.), Taupo (c. 233 A.D.) and Whakatane (c. 5500 cal. years B.P.). The core terminated in the Whakatane Tephra giving the sediment a maximum age of 5530 ± 60 cal. years B.P. An age model was developed using the five tephra layers. Radiocarbon dates obtained returned ages, too old because of contamination by old CO_2 or CH_4, or both. Investigations carried out on the core, included spectrophotometry, sedimentological, and geochemical analyses, which provided a number of proxy from which inferences were made about lake history, catchment development, and palaeoclimate. Sediment geochemistry indicates that the Rotorua catchment has undergone several changes since the Whakatane eruption, alternating between periods of variable and stable environmental conditions. Following the Whakatane and Waimihia eruptions and up until around 3000 cal. years B.P. the catchment surrounding Lake Rotorua was rather unstable. Fluctuations in many of the proxies during this period are likely to be associated with a fluctuating climate, and coincidently this phase corresponds to around the time ENSO was becoming established in New Zealand. One of the most notable features of the inferred catchment and lake histories is the two phases of stability following the Taupo eruption and again from c. 580 to c. 300 cal. years B.P. The latest, most significant change in the catchment history of Lake Rotorua was the settlement of Polynesians in the area. Pollen profiles are commonly used to infer the initial presence of human settlement and suggest settlement was present around the time of the Kaharoa eruption (c. 630 cal years B.P.; c. 1314 A.D.), however, the sediment chemistry and erosion profiles for the north-east section of Lake Rotorua's catchment indicate that although there may have been some early clearing in that area for tracks or buildings, large-scale clearing and subsequent settlement probably did not occur until around c. 300 cal. years B.P, later than what has been previously suggested from pollen profiles. This later timing coincides closely with dates suggested for the occupation of the lake shore around Hamurana. Also contained within the sediments

are three layers of reworked glass shards. These reworked layers are inferred to be caused by the reworking of coarse grained tephra in shallow water, which are then deposited in the deeper lake basin, and these reworked layers are thought to be due to large storms (c. 1300, 520, and 220 cal years B.P). Because of Lake Rotorua's position away from the BOP coast, these storm events probably represent only the largest events over that period of time, with each of these layers coinciding with similar events from lacustrine records on the east coast of the North Island. Further grain size analysis and the development of a disturbance index (the amount of reworked glass grains) may help indicate the number of small storm events that having progressed this far inland.

Acknowledgements

Firstly a big thank you to my supervisors, Associate Professor Chris Hendy and Professor David Lowe. Chris, thank you for your assistance and advice throughout the course of this thesis, especially the hours spent retrieving cores from Lake Rotorua and your constant enthusiasm throughout the project. David, thank you for encouragement and knowledgeable advice, both greatly appreciated, and especially the hours spent reading and editing.

I am especially grateful to the Comer Foundation of Science and Education for providing funding for the project and a scholarship – The Gary Comer Abrupt Climate Change Fellowship. I'd also like to acknowledge the University of Waikato for supporting me with a Masters Research Scholarship and the Fernhill Charitable Trust for its financial assistance.

Thank you to Alison Graettinger, Janine Krippner, Kurt Joy and Mum for all your hard work in retrieving cores, finding tools and generally getting covered in mud – I hope it made the hot pools at the end of the day all the more worth it. I would also like to thank Rob French from Environment Bay of Plenty for driving and manoeuvring the boat into all sorts of places, towing the barge into the middle of Lake Rotorua, setting anchors and generally helping with the coring. I also acknowledge Hartly Contractors, of Kawerau, for the use of their boat – *Surveyor*.

A big thank you to the many staff members whom have offered precious time, advice and help during the course of this project. Special thanks go to:

- Associate Professor Rodger Briggs for his assistance with the ferromagnesian mineralogy and for booking the electron microprobe;
- Annie Barker for her assistance with lab work and allowing me take over benches in her lab for sampling;
- Steve Cameron for running the digested samples on the ICP-MS;
- Helen Turner for her assistance in capturing images on the SEM;

- Dr Vivienne Cassie-Cooper and Wendy Paul for the help with diatom identification;
- Intern students Elodie and Pauline for spending hours helping me weigh samples out for digesting and carbon and nitrogen analyses;
- Will Esler, of Rotorua, for advice and encouragement in the field; and
- Dirk Immenga, Brad Scarfe and Alexandre Schimel from the Coastal Marine Group for carrying out the geophysical survey and providing the fantastic bathymetric image used when finding coring sites.

All the other staff in the Earth and Ocean Sciences and Chemistry departments at the University of Waikato who helped me in some way are thanked.

Cheers to my fellow Masters students in particular – Alison Graettinger, Kate Jackson and Orla Hanson. You girls are great and made my years at Waikato full of fun, adventure and laughter.

Last but certainly not least, I would like to thank my family, especially my parents (Vern and Chris), who have always been interested in what I was doing and have provided love, support and encouragement to get me this far. Thanks Mum for coming coring on Lake Rotorua, and providing the best coffee and lunches of any fieldtrip. Thanks Dad for your hours spent reading and helping edit my thesis. My brother Davie, thanks for all the hours spent stitching photographs. Damian, I am eternally grateful for all your love and continuing support through all the highs and lows.

Table of Contents

TITLE PAGE i

ABSTRACT iii

ACKNOWLEDGEMENTS v

TABLE OF CONTENTS vii

LIST OF FIGURES AND TABLES xiii

CHAPTER ONE – INTRODUCTION

1.0 Introduction 3

1.1 Objectives 5

1.2 Nomenclature 5

1.3 Location of study area – Lake Rotorua 6

1.4 Structure of thesis 7

CHAPTER TWO – LITERATURE REVIEW

2.0 Introduction 11

2.1 Lakes 11

2.1.1 Formation 12

2.1.2 Tectonic and climatic settings 12

2.2 The Rotorua Basin 14

2.2.1 Geology 16

2.2.2 Rotorua Volcanic Centre 19

2.2.2.1 Introduction 19

2.2.2.2 Rotorua caldera 19

2.2.2.3 Eruptive history of Rotorua 22

2.2.2.3.1 Caldera-forming eruption 22

2.2.2.3.2 Post-caldera formation 22

2.2.2.3.3 Modern hydrothermal activity 22

2.2.3 Lake-level changes 24

2.2.4 Previous sediment studies on Lake Rotorua 25

2.3 Late Quaternary climate records 29

2.3.1 New Zealand records 30

2.3.2 New Zealand mid-late Holocene climate 30

2.3.3 Palaeolimnological studies in NZ 31

2.4 How elements behave in lake sediments 33

2.4.1 Phosphorus (P) 34

2.4.2 Iron (Fe) 35

2.4.3 Manganese (Mn) 36

2.4.4 Arsenic (As) 36

2.4.5 Trace metals 37

2.5 Additional regional volcanic geology 37

2.5.1 Taupo Volcanic Zone (TVZ) 37

2.5.1.1 Okataina Volcanic Centre (OVC) 40

2.5.1.1.1 Basaltic eruptions 42

2.5.1.1.2 Modern hydrothermal activity 42

2.5.1.2 Taupo Volcanic Centre (TVC) 42

2.5.1.3 Tongariro Volcanic Centre (TgVC) 45

2.5.2 Mt Egmont (Taranaki) 46

2.6 Tephrostratigraphy 48

2.6.1 New Zealand tephrostratigraphy 48

2.6.2 Correlation techniques 50

2.6.2.1 Ferromagnesian mineral assemblages 50

2.6.2.2 Glass chemistry 52

2.6.3 Tephrostratigraphy: post-c. 60 ka deposits 54

CHAPTER THREE – METHODOLOGY

3.1 Coring 57

3.2 Core location 57

3.3 Onboard methodology 60

3.3.1 Coring 61

3.3.1 Core processing 63

3.4 Core description 63

3.5	Sampling			64
	3.5.1	*Tephra*		64
	3.5.2	*Radiocarbon samples*		64
	3.5.3	*Sediment samples*		64
3.6	Laboratory methods			65
	3.6.1	*Sample preparation*		65
	3.6.2	*Non-destructive techniques*		65
		3.6.2.1	*X-ray images*	65
		3.6.2.2	*Colour reflection*	66
		3.6.2.3	*Magnetic susceptibility*	67
	3.6.3	*Tephra samples*		67
		3.6.3.1	*Magnetic separation*	67
		3.6.3.2	*Grain mounts*	68
		3.6.3.3	*Resin mounts for EMPA and LA-ICP-MS*	69
	3.6.4	*Sediment samples*		70
		3.6.4.1	*Elemental analysis*	70
			3.6.4.1.1 Sediment digestion using Aqua Regia	70
			3.6.4.1.2 Digestion analysis	70
		3.6.4.2	*Grain size analysis*	71
		3.6.4.3	*Carbon and nitrogen analysis*	71
		3.6.4.4	*Scanning electron microscopy*	72
		3.6.4.5	*Biogenic silica*	73
		3.6.4.6	*Radiocarbon dating*	73

CHAPTER FOUR – CORE STRATIGRAPHY AND CHRONOLOGY

4.0	Introduction	77
4.1	Coring site	77
4.2	Sediment stratigraphy	78

4.3	Chronology			82
	4.3.1	*Radiocarbon dating*		82
	4.3.2	*Magnetic susceptibility*		83
	4.3.3	*Stratigraphy, chronology, mineralogy, and correlation of tephra preserved in Lake Rotorua sediments*		84
		4.3.3.1	*Tephrostratigraphy*	84
		4.3.3.2	*Glass chemistry of tephra from Lake Rotorua*	86
4.4	Rates of sedimentation			95
	4.4.1	*Mean sedimentation rate*		95
	4.4.2	*Variations in sedimentation rates*		96
	4.4.3	*Radiocarbon dating*		98
4.5	Summary			98

CHAPTER FIVE – PHYSICAL CHARACTERISTICS: SEDIMENT STRUCTURE AND COMPOSITION

5.0	Introduction			103
5.1	Photography			104
5.2	X-radiography			104
5.3	Colour reflection			107
	5.3.1	*Colour*		107
	5.3.2	*Spectrophotometry reflectance*		109
5.4	Scanning electron microscopy			112
	5.4.1	*Diatom record*		114
		5.4.1.1	*30-32 cm*	114
		5.4.1.2	*350-359 cm*	137
		5.4.1.3	*390-400 cm*	137
5.5	Grain-size analysis			138
5.6	Summary			144

CHAPTER SIX – GEOCHEMICAL CHARACTERISTICS

6.0 Introduction 149

6.1 Chemical composition 149

6.1.2 Sediment elemental geochemistry 151

6.1.2.1 Phosphorus (P) 151

6.1.2.2 Iron (Fe) 153

6.1.2.3 Manganese (Mn) 154

6.1.2.4 Arsenic (As) 155

6.1.2.5 Sulfur (S) 156

6.1.2.6 Trace elements 157

6.1.2.7 Effect of tephra deposition 169

6.2 Organic matter elemental geochemistry 169

6.2.1 Biogenic silica 170

6.2.2 Total organic carbon and total nitrogen 170

6.3 Summary 174

CHAPTER SEVEN –PALAEOENVIRONMENTAL INTERPRETATIONS

7.0 Introduction 179

7.1 Chronological model 179

7.2 Geochemical changes 180

7.3 Human disturbance in the catchment 184

7.4 Identification and descriptions of facies 189

7.4.1 Facies 1, 2, 3, 4, and 7 (disturbed) 189

7.4.1.1 Facies 1 189

7.4.1.2 Facies 2 189

7.4.1.3 Facies 3 190

7.4.1.4 Facies 6 190

7.4.1.4 Facies 7 191

7.4.2 Facies 4 and 5 (stable or 'quiet') 191

7.4.2.1 Facies 4 191

7.4.2.2 Facies 5 192

7.5	Lake history		197
	7.5.1	*Pre-human occupation*	197
	7.5.2	*Post-human occupation*	198
7.6	Palaeoclimatic reconstruction		200
	7.6.1	*Multi-record of the eastern North Island*	201
	7.6.2	*Waitomo speleothem record*	201
	7.6.3	*Dendrochronology*	
		– Libocedrus bidwillii *(NZ cedar)*	202
	7.6.4	*Lake Maratoto*	203
	7.6.5	*Lake Rotorua*	203
7.7	Summary		205

CHAPTER EIGHT – CONCLUSIONS

8.1	Conclusions	211
8.2	Areas of future study	213

REFERENCES 217

APPENDICES

Appendix A:	Core log data	247
Appendix B:	Radiocarbon dates	257
Appendix C:	Magnetic susceptibility	259
Appendix D:	Spectrophotometry data	261
Appendix E:	Grain-size data	271
Appendix F:	Glass data	281
Appendix G:	Sediment geochemistry data	295
Appendix H:	Carbon and nitrogen analysis	305
Appendix I:	Photography and x-radiography	CD

List of Figures and Tables

CHAPTER TWO – LITERATURE REVIEW

Figure 2.1: The Rotorua Basin. 15

Figure 2.2: Maps showing location of the Rotorua geothermal system. 17

Figure 2.3: Rotorua Caldera. 20

Figure 2.4: Satellite image of Rotorua Caldera. 21

Figure 2.5: Map of Rotorua Geothermal Field. 23

Figure 2.6: Probable shorelines of Lake Rotorua. 24

Figure 2.7: Changing levels of Lake Rotorua. 25

Figure 2.8: General map showing plate tectonic setting, the main volcanic centres that have erupted soil-forming tephras, and the general dispersal of tephra on North Island. 38

Figure 2.9: Map of the Taupo Volcanic Zone and the Central Volcanic Zone. 39

Figure 2.10: Map of Okataina Volcanic Centre (OVC). 40

Figure 2.11: Map of Taupo Volcanic Centre (TVC). 43

Figure 2.12: Andesite massifs and cones of the Tongariro Volcanic Centre (TgVC). 45

Figure 2.13: Location of Taranaki volcanoes. 47

Table 2.1: Stratigraphy of Tongariro Subgroup and Tukino Subgroup. 46

Table 2.2: Dominant ferromagnesian mineral assemblages – Quaternary volcanics. 51

Table 2.3: Major element composition of glass from NZ tephra marker beds. 53

CHAPTER THREE – METHODOLOGY

Figure 3.1: *Surveyor* and barge at Sulfur Point, Lake Rotorua. 57

Figure 3.2: Bathymetric map of Lake Rotorua (constructed by Brad Scarfe). 58

Figure 3.3: Low frequency echo sounder example of reflectors, inferred to be tephra layers. 59
Figure 3.4: Coring set up. 61
Figure 3.5: Coring method. 62
Figure 3.6: Core labelling procedure. 63
Figure 3.7: Steps for constructing a mount for EMPA and LA-ICP-MS. 69

Table 3.1: List of Lake Rotorua coring locations. 60

CHAPTER FOUR – CORE STRATIGRAPHY AND CHRONOLOGY
Figure 4.1: Satellite image of Lake Rotorua. 77
Figure 4.2: Photos showing examples of massive diatomaceous ooze (a) and laminated diatomaceous ooze (b & c). 78
Figure 4.3: Summary of RU188-07. 79
Figure 4.4: Plot of magnetic susceptibility. 84
Figure 4.5: Plot showing glass chemistry. 88
Figure 4.6: Plot of glass data from unit 2. 89
Figure 4.7: Plot of glass data from unit 3. 90
Figure 4.8: Plot of glass data from unit 4. 90
Figure 4.9: Plot of glass data for unit 5. 91
Figure 4.10: Plot of glass chemistry for unit 6. 92
Figure 4.11: Plots of glass data from unit 7. 93
Figure 4.12: Plot of unit 8 glass populations. 94
Figure 4.13: Plot of glass data from unit 9. 95
Figure 4.14: Sedimentation rate based on dated tephra ages (cal. yr B.P.). 97
Figure 4.15: Plot showing rhyolitic glass data. 99

Table 4.1: Summary of radiocarbon samples and calibration. 82
Table 4.2: Glass composition of tephra beds in core RU188-07. 87

CHAPTER FIVE – PHYSICAL CHARACTERISTICS: SEDIMENT STRUCTURE AND COMPOSITION

Figure 5.1: Photos and x-ray images. 105

Figure 5.2: Combination plots of L*, a* and b*. 107

Figure 5.3: Whole core multi-plot of L*, a* and b*. 108

Figure 5.4: Whole core plot of b* variable. 109

Figure 5.5: A) Reflective data from 560nm and B) Reflective data from 660nm. 110

Figure 5.6: Down core changes of first derivative values. 111

Figure 5.7: Representative SEM images from RU188. 113

Figure 5.8: Examples of benthic taxa. 114

Figure 5.9: Diatoms from sample at 30 cm depth. 115

Figure 5.10: Diatoms from sample at 32 cm depth. 117

Figure 5.11: Diatoms from sample at 350 cm depth. 119

Figure 5.12: Diatoms from sample at 351 cm depth. 121

Figure 5.13: Diatoms from sample at 358 cm depth. 123

Figure 5.14: Diatoms from sample at 359 cm depth. 125

Figure 5.15: Diatoms from sample at 390 cm depth. 127

Figure 5.16: Diatoms from sample at 391 cm depth. 129

Figure 5.17: Diatoms from sample at 392 cm depth. 131

Figure 5.18: Diatoms from sample at 396 cm depth. 133

Figure 5.19: Diatoms from sample at 400 cm depth. 135

Figure 5.20: Grain size analysis of representative samples. 139

Figure 5.21: Mean grain size of representative samples from RU188. 140

Figure 5.22: Representative samples showing percentage of grains > 32 microns. 141

Figure 5.23: Representative samples showing percentage of grains > 63 microns. 143

CHAPTER SIX – GEOCHEMICAL CHARACTERISTICS

Figure 6.1: Phosphorus concentration for RU188. 152
Figure 6.2: Phosphorus flux in the sediments. 153
Figure 6.3: Iron concentration for RU188. 154
Figure 6.4: Manganese concentration for RU188. 155
Figure 6.5: Arsenic concentration for RU188. 156
Figure 6.6: Sulfur concentration for RU188. 157
Figure 6.7: Heavy metal elements. 163
Figure 6.8: Alkali earth elements and earth elements. 165
Figure 6.9: Other trace elements. 167
Figure 6.10: An example of element comparisons made from sediment samples pre- and post tephra layers. 169
Figure 6.11: Biogenic Silica. 170
Figure 6.12: Representative elemental and carbon isotopic compositions of organic matter. 171
Figure 6.13: Organic carbon content of the sediment in Lake Rotorua. 172
Figure 6.14: Organic nitrogen content of the sediment in Lake Rotorua. 172
Figure 6.15: Plot showing percentage carbon, nitrogen, and the ratio of carbon:nitrogen. 173
Figure 6.16: Plot of redox related elements. 176

CHAPTER SEVEN –PALAEOENVIRONMENTAL INTERPRETATIONS

Figure 7.1: Plot of elements related to the dissolution of volcanic derived rocks and tephra. 181
Figure 7.2: Plot of elements related silicate mineral inputs. 181
Figure 7.3: Plot of elements related to geothermal inputs. 183
Figure 7.4: Plot of heavy metal element trends. 183
Figure 7.5: *Pteridium* (bracken) spore profiles, North Island, New Zealand. 186
Figure 7.6: Composite diagram illustrating changes in pollen, sedimentation and production from Lake Rotorua over the last 5,500 years. 188
Figure 7.7: Multi proxy core summary. 193

Figure 7.8: Illustration of lake history and development. 195

Figure 7.9: A sketch of tephra layers at Holden's Bay, Rotorua. 199

Figure 7.10: Comparison of lake data with North Island climate records. 207

Table 7.1: A list of the five coldest and warmest 25-year intervals as indicated by the temperature reconstruction of *Libocedrus bidwillii* (Palmer and Xiong, 2004). 203

Chapter One

Introduction



Chapter One: Introduction

1.0 INTRODUCTION

New Zealand has been recognised by many in the geo-scientific community as being a valuable archive of Quaternary climate records (e.g. Newnham et al., 1999). Moreover, New Zealand's Quaternary climate records are of global importance for four main reasons (Alloway et al., 2007b).

1. Well-dated terrestrial records of Late Quaternary change can be used to calibrate and corroborate evidence from equivalent records from deep-sea cores in the adjacent oceans. Because of New Zealand's small size and oceanic climate, the two sets of climate records should show a high degree of correspondence in timing, duration and structure.

2. New Zealand's remote southwest Pacific position means that it should directly reflect hemispheric-wide changes in the ocean – atmospheric system.

3. New Zealand's small size and high mountains meant that an ice cap was present during the Last Glaciation, ensuring that a range of biotic environments persisted and was able to respond rapidly to climatic change.

4. The late arrival of humans in New Zealand (since c. 1280 A.D.) means that most records are not affected by anthropologic activities until the last 700 years or so.

Although much is known about New Zealand's oceanographic setting, principal currents and water masses, extent of glaciers and distribution of vegetation zones during the last glacial through to modern times (Alloway et al., 2007b), and despite the growing body of literature regarding the past climate conditions in New Zealand, there is still a great deal to be examined. At present there are numerous records e.g. Auckland maars, various marine cores (in particular MD97-2121 and MD97-2122), speleothems from both the North and South islands (Williams, 1996; Williams et al., 2004; Lorrey et al., 2008; Whittaker, in prep),

wetland records such as Kopouatai Bog (Newnham et al., 1995), Kaipo Bog (Newnham and Lowe, 2000), Okarito Wetland (Vandergoes and Fitzsimons, 2003; Vandergoes et al., 2005), and numerous lake studies including from Lake Maratoto (Green and Lowe, 1985), Lake Rotoiti (Pickrill et al., 1991), Lake Poukawa (Shulmeister et al., 2001; McGlone, 2002; Shane et al., 2002), Lake Tutira (Eden and Froggatt, 1996; Wilmshurst et al., 1997; Eden and Page, 1998), Lake Waikaremoana (Newnham et al., 1998a), and Lake Forsyth (Woodward and Shulmeister, 2001). These records have provided insight into palaeoclimate reconstructions for the late Quaternary.

A common problem with previous studies is that they either lack high chronological precision or high climatic sensitivity. Lake Rotorua has a long history and is within close proximity to many active volcanics, and is likely to be a place from which a long sediment core could be retrieved. The lake's general history is known to have undergone many complex changes in level, some of which are largely unrelated to climate change, e.g. faulting and volcanic events. The lake is also situated at an altitude (~ 280 m.a.s.l.) where it would be on the verge of changes tending towards montane climate, so if there was a cooling shift in climate it should be reflected rapidly in the lake sediments.

The study of lakes and the reconstruction of past environmental conditions and processes affecting them is known as palaeolimnology. These reconstructions are established primarily through the analysis of sediment cores. One of the most important factors when carrying out this type of analysis is the ability to constrain the timeframe which it covers. In much of North Island such chronologies have involved the identification of tephra beds but radiocarbon dating, ^{210}Pb, and magnetic susceptibility have also been used. The stratigraphy and dating of these sediments from within a lake aids in the understanding of a lake's history and how such a history relates to records from other locations. Tephra layers are important stratigraphic markers in the interpretation of sediment deposits in lakes in volcanic areas. They potentially provide a chronological framework for tying together lake and catchment histories, and for linking these (using tephrochronology) with records derived from other regions. They are often widespread and many have well documented ages. New Zealand is fortunate to have tephra records from the many volcanic centres located in the North Island and these provide numerous

marker beds in sediments found both on- and off-shore. Some of these 'marker bed' tephras now have very well constrained dates and distinctive geochemical signatures and thus allow horizons of known age to be identified.

The principle aim of this study is to establish a partial palaeolimnologic history for Lake Rotorua and to provide a palaeoclimate reconstruction for the middle to late Holocene using a tephrostratigraphic record to constrain the timeframe. A number of sediment cores were taken from the lake and one of these has been sampled in detail. It has been dated using tephrochronology to c. 5,500 calendar (cal.) years ago, and the core thus spans the middle to late Holocene period.

1.1 Objectives

This study was under taken with the following objectives in mind.

- To identify from the sediment core a well constrained tephrostratigraphy, together with ^{14}C dating, to provide a chronology and correlation tie points for palaeoenvironment reconstructions in the mid-late Holocene.

- Examine a range of proxies from lake sediments to assist in palaeoenvironmental and paleoclimatic reconstructions for the mid-late Holocene in the Rotorua area.

- Examine the sediment geochemistry of lake sediments in the core to establish the trophic status of the lake during the mid-late Holocene, and investigate the role of tephra fall in lake trophic status and other properties.

- Identify when humans first arrived in the surrounding area and to ascertain the effect these Polynesian settlers may have had on the lake and its catchment.

1.2 Nomenclature

The nomenclature of Lowe and Hunt (2001) and Alloway et al. (2007a) has been adopted for this work. 'Tephra' is defined as an all-embracing term for the explosively erupted, loose fragmental (pyroclastic) products of a volcanic eruption, and includes all grain sizes. Tephra may include fall deposits

(commonly called tephra-fall or tephra fallout) and unconsolidated deposits derived from pyroclastic flows or surges (also known as pyroclastic density currents). 'Tephrostratigraphy' refers to the study of sequences of tephra layers and related deposits and their relative ages. It involves defining, describing, and characterising or 'finger-printing' tephra or tephra sequences using their physical, mineralogical, and geochemical properties, and fundamentally underpins tephrochronology.

'Tephrochronology' in one sense has been used as a broad term to cover all aspects of tephra related study. However, within this work it refers to the use of tephra deposits as an isochron (an 'instant' in time or a time parallel marker bed) to link sequences in different settings via precise tie-points, and to establish and transfer relative or numerical ages from site to site (Lowe and Hunt, 2001).

Tephra ages come primarily from Lowe et al. (2008), unless otherwise stated. This paper is the most recently published work presenting new glass compositional data for many of the key markers beds and revised age models using recently obtained radiocarbon dates, Bayesian based wiggle-matching, and IntCal04 calibration curves via both OxCal and Bpeat.

1.3 Location of study area – Lake Rotorua

The Rotorua region in the Bay of Plenty lies in the central part of the Taupo Volcanic Zone. Like most of the lakes in the Rotorua area, Lake Rotorua formed as a result of late Quaternary volcanic processes which produced some voluminous rhyolitic and ignimbrite eruptions. Some of these eruptions left large collapse features (calderas), such as the Rotorua Caldera, and explosion craters which then filled with water to form some of the lakes around Rotorua. Other lakes were formed when pre-existing drainage was blocked by lavas or pyroclastic deposits (Lowe and Green, 1992; Nairn, 2002). The volcanic eruptions from this region have additionally provided many of the tephra layers, forming time markers, needed for constraining the chronology and for synchronzing palaeoclimate records. The present-day Lake Rotorua is situated at 280 m.a.s.l. and occupies part of the Rotorua caldera within the Rotorua Volcanic Centre (RVC). The RVC consists of a 215 km^2 basin comprising the caldera and multiple rhyolitic domes. The Rotorua caldera is approximately 20 x 21 km and

forms a near circular depression, within which lies the lake. Several rhyolite domes are located in and around the lake. Mokoia Island is a small dome located in the centre of the lake, Kawaha and Hinemoa Points are situated on the southern shoreline on either side of Rotorua City, and Pukeroa (Hospital Hill) is found right in the centre of the city near Kuirau Park and Ohinemutu geothermal systems. Mount Ngongotaha is the largest of the rhyolite dome complexes in the landscape surrounding the lake, rising to 757 m elevation.

1.4 Structure of thesis

Chapter 2 comprises of a literature review that describes the landscape features and deposits within the Rotorua Basin, a detailed geological history of the Rotorua region including the formation of the caldera and its eruptive history, and earlier work on lake-level changes and sediment studies previously undertaken on Lake Rotorua. It also provides a summary of the nearby volcanic centres which have erupted tephras in the period of time since Lake Rotorua's formation, and a description of lakes and why they are important and what information they can provide relating to climate, and tephrostratigraphy in New Zealand.

The coring method used and the locations of coring sites in Lake Rotorua are detailed in Chapter 3. Non-destructive techniques including magnetic susceptibility, colour reflectance and x-radiography are explained. Laboratory techniques for core analysis are described; these include the separation, treatment, and mounting procedures for tephra-derived minerals and glass, and separation of sediment samples including preparation for digestion, analysis of samples and calculations for ICPMS element concentrations. Methods are also included for grain-size analysis, carbon and nitrogen analysis, scanning electron microscopy (SEM), biogenic silica and radiocarbon dating.

Chapters 4 to 6 present and discuss the results from this study. Chapter 4 examines the stratigraphy and chronological record, sediment stratigraphy and rates of sedimentation. Chapter 5 provides results from investigations on the physical characteristics of the sediments, including those deriving from both destructive and non-destructive techniques. Photographs, x-rays and colour-reflection data provide detailed records of the nature of the sediment whereas SEM images and grain size analysis provide the actual characteristics of the

sediment – including clastic sediment accumulation, mean grain size and the make up of diatom species. Chapter 6 describes the elemental geochemistry of sediments and the organic matter locked within them. This chapter looks in particular at the behaviour of elements within the sediments, and the composition of the organic matter. In particular, the carbon and nitrogen analyses indicate the type of organic material present and lead to possible inferences regarding lake trophic states and catchment history. These parameters combined allow for possible reconstructions of the regional climate.

The implications of the proxies used are discussed in Chapter 7. The changes in the sediment geochemistry, and interpretation of the human impacts on the lake catchment, are used to reconstruct both the lake and the palaeoclimatic histories with reference to other New Zealand (NZ) palaeoclimate records for the last c. 5,500 years.

The final chapter (Ch. 8) presents a summary of the findings, in relation to the initial aims, associated with the palaeolimnological history of Lake Rotorua.

Chapter Two

Literature Review



Chapter Two – Literature Review

2.0 INTRODUCTION

The Rotorua Basin or caldera and associated deposits are located in the central Taupo Volcanic Zone. The Basin has been the focus of intense geological, geophysical and geochemical investigations over the past fifteen or so years. During the 1980s and 1990s this research was driven by increasing conflict between exploitation of subsurface geothermal fluid and consequential negative effects on New Zealand's last remaining geyser field at Whakarewarewa. More recently this focus has moved to re-identifying calderas and caldera development, structural controls, volcanism and magmatic bodies, gas flux, and ignimbrite source and properties. The dramatic deterioration of the water quality in Lake Rotorua in the last few years especially has led to new research on limnological aspects (e.g. Burger et al., 2007; Pearson, 2007).

In this review I look firstly at the formation of lakes in general and the influences climate can have on them. I then specifically examine the Rotorua Basin – its general landscape features, geology and a brief history of formation – and note the influences this geological history has had on Lake Rotorua. I then provide a summary of the tephrostratigraphy as it relates to this region. Finally, I will touch briefly on historical lake level changes, and previous sediment studies, on Lake Rotorua.

2.1 Lakes

Lakes are inland bodies of water which are not connected directly to the open ocean. Lacustrine environments occur on about 1% of today's land surface (Nichols, 1999; Boggs, 2001).

2.1.1 Formation

The basins or depressions in which lakes form can be created by a variety of mechanisms, including:

- Tectonic movements such as faulting and rifting
- Glacial processes such as ice scouring, ice damming, and moraine damming
- Landslides or other mass movements
- Volcanic activity such as damming by lavas or pyroclastic material, explosion's or caldera collapse
- Deflation by wind scour or damming by wind-blown sand
- Fluvial activity such as the formation of oxbow lakes and levee lakes

(Lowe and Green, 1992; Boggs, 2001; Cohen, 2003).

2.1.2 Tectonic and climatic settings

Lakes also occur in a variety of tectonic and climatic settings. Tectonic processes are responsible for the evolution of a vast number of lakes, including the largest, deepest, and oldest lakes on the planet (Cohen, 2003).

Lakes with sediments suitable for climate change reconstruction are varied in origin, geographical distribution, age, and chemistry. Although some regions have very few lakes, by and large lakes are widely distributed around the world and potentially provide a global network of sites that can be used to assess regional variations in climate change across continents (Battarbee, 2000).

Climate factors affect lake sedimentation in numerous ways, responding physically (e.g. landscape erosion), chemically (e.g. chemical and isotopic composition) and biologically (e.g. lacustrine biota and catchment plant cover). Sediments usually accumulate quite rapidly, often > 1 mm per year, and sediment cores can normally be sub-sampled finely to provide data with potentially a decadal or sub-decadal resolution. Climate reconstruction relies on relationships between the sediment record and the water column that can be calibrated with climate (Battarbee, 2000).

The global distribution of lakes strongly reflects global climate patterns, and regional patterns of lake size indicate regional variability of global climate. Water levels in lakes are maintained by the balance between evaporation and precipitation. Climate can determine whether a lake is filled to overflowing (open) or acts as an internal drainage basin (closed). The kind of chemical sedimentation occurring in lakes also strongly reflects climatic conditions. Sediment input into lakes is influenced by the vegetation cover in the drainage area of the lakes and is greatest in regions with low vegetation cover. Climate and physiography of lake settings also determine the local weather conditions over lakes. Severe, localised storms with high winds can cause considerable shore erosion, coupled with sediment transport and deposition, over short periods of time (Boggs, 2001).

Biogenic deposition in lakes is sensitive to climatic and tectonic influences and is strongly dependent upon lake hydrology and morphology. Climate controls the rate and nature of biogenic productivity, influences chemical weathering, erosion, and runoff rates in the catchment area, and thus determines nutrient supply. Tectonic controls determine the rate of subsidence and thus influence sedimentation rates (Platt and Wright, 1991).

One type of sedimentation process that appears to be particularly characteristic of cold-climate (high latitude or high altitude) lakes is the formation of varves, which are very thin, alternating light- and dark-coloured sediment layers. Varves are generated in so-called glacial lakes because of seasonal freezing and melting. These seasonal changes are generally caused by periodic fluctuations in sediment inputs into the lake by inflows. During summer months when lakes are open, thick, light-coloured, coarse-grained laminae accumulate. Sediment input is limited during winter, when the lakes are frozen over, resulting in deposition of thinner, finer-grained laminae that are coloured dark by the presence of fine organic matter that settles slowly from suspension (Goodwin, 1984; Boggs, 2001). Varves may also form in non-glacial lakes, owing to seasonal variations in carbonate production (e.g. meromictic lakes). Greater carbonate production in warm water during summer months tends to mask fine organic matter, which accumulates very slowly throughout the year, producing a thick, light-coloured lamina of carbonate sediment. A very thin, clayey, organic layer forms during the

winter months when cold water inhibits carbonate production (Lowe et al., 1997; Boggs, 2001).

Battarbee (2000) looked at many palaeolimnological sediment methodologies and found that most records are used primarily to reconstruct changes in effective moisture (precipitation-evaporation, P-E) and temperature, although there have also been attempts to relate sediment records to wind regimes (e.g. Bradbury et al., 1993, as cited in Battarbee, 2000), moisture sources and atmospheric circulation patterns (e.g. McKenzie and Hollander, 1993, as cited in Battarbee, 2000) and atmospheric pressure of CO_2 (e.g Street-Perrott et al., 1997, as cited in Battarbee, 2000). It is often difficult to separate some of these influences, especially the individual effects of temperature, moisture and wind regimes. Some proxies can be used to reconstruct climatic variables directly, but most approaches are indirect requiring an understanding of the relationship between the sediment record and water-column processes and between water-column processes and climate (Green, 1994; Battarbee, 2000).

2.2 The Rotorua Basin

The Rotorua Basin covers an area of 215 km^2 which includes an area in the Waipa and Kapenga localities south of the Hemo Gorge (Fig. 2.1) (Kennedy et al., 1978). Lake Rotorua covers ~ 78 km^2 but has a catchment area of ~ 520 km^2. The lake is fed by 10 major streams, seven of which are cold spring fed and three that are influenced by geothermal inflow. The lake currently has only one drainage passage through the Ohau Channel located to the north-east of the lake; this channel drains into Lake Rotoiti before entering the Kaituna River and draining out to sea, via (at its mouth) an artificial channel bordering the Maketu Estuary.

Lake Rotorua is surrounded by a series of terraces and fans formed by previous lake levels and old stream deposits. The widest of these deposits occupy the east, south-east and south-west lake shores. The northern side of the lake is steep faced and any previous terraces have been eroded away. The area south-west of the lake and south-east of Mt Ngongotaha is occupied by Rotorua City (Kennedy et al., 1978; Kennedy and Pullar, 1981). These terraces are estimated to have formed

between c. 60,000 and 27,100 cal. years ago, with the Kawakawa tephra (c. 27,100 cal. yrs B.P.) resting directly on the surface of the lacustrine deposits (Kennedy and Pullar, 1981). The fans comprise conglomerates of silt, sand, stones and boulders that have been transported by streams (Kennedy et al., 1978). These fans located on the western side of the lake around Mt Ngongotaha are thought to have been deposited around 20-25 cal. ka (ka = 1000 years) years ago. Modern fans occur mainly on the south-eastern side of the basin along the foot of the hills.

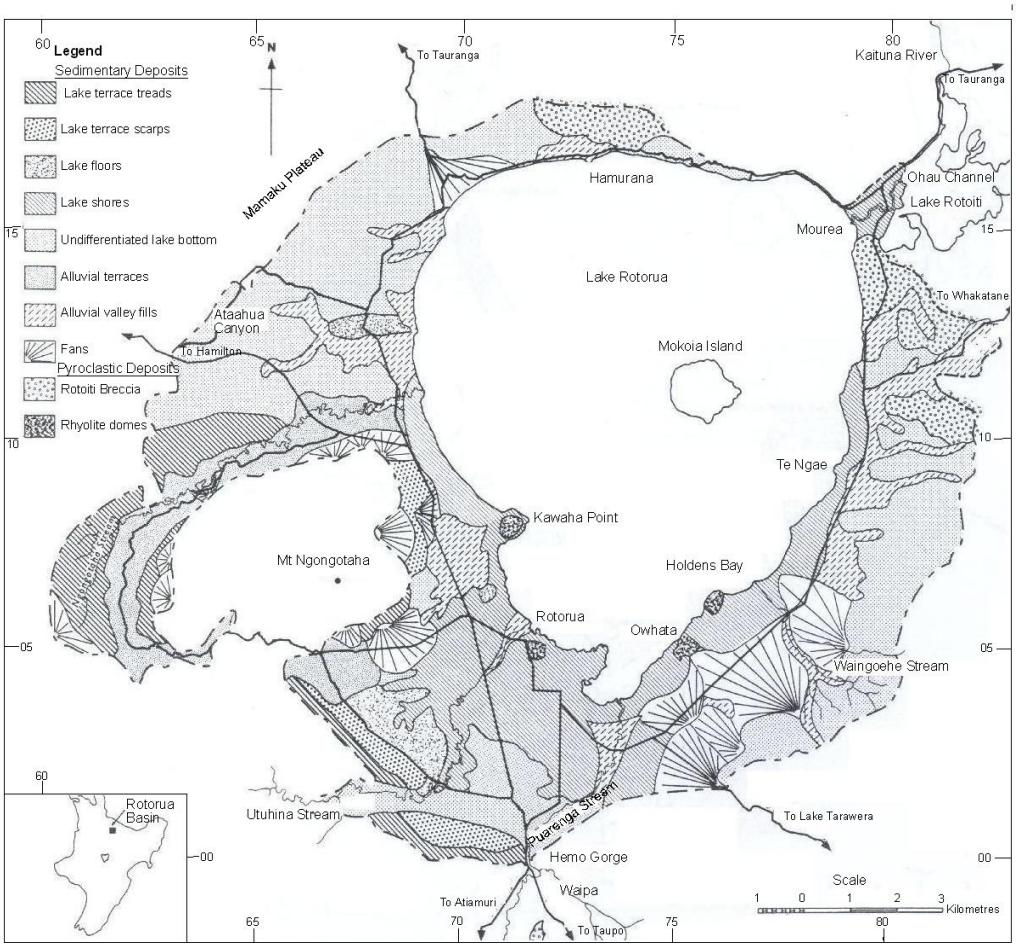

Figure 2.1: The Rotorua Basin showing the distribution of sedimentary and pyroclastic deposits and associated landforms (Kennedy et al., 1978).

Other landscape features and deposits identified by Kennedy et al. (1978) include loess or aeolian deposits, lake shore deposits, diatomite deposits and peat deposits (Fig. 2.1). Loess deposits comprise windblown silt and fine sands deposited generally during periods of colder climate when less vegetation covered the landscape (Kennedy et al., 1978). These cold climatic conditions last occurred between c. 29,000 and 18,000 cal. yrs ago during the last glacial coldest period (LGCP; Alloway et al., 2007b; Newnham et al., 2007a, 2007b).

Deposition of lake shore sediments in the Rotorua Basin has alternated with volcanism since the formation of the lake. Many of these volcanic products have originated in the neighbouring Okataina Volcanic Centre (OVC) or from within the basin itself (Houghton and Scott, 2002).

Remnant lake shore deposits have been found up to 120 m above the present lake level (Esler, 2006). These ancient deposits show that the lake has undergone many changes and has been much larger following its formation ~ 220,000 – 230,000 yrs ago. These features comprise diatomite deposits, containing the remains of siliceous diatom frustula that accumulated on the lake floor to produce a white or greenish-brown, compact, fine textured clay-like deposit when the lake level subsequently dropped. Peat deposits have occurred in the low-lying poorly drained areas close to the shores of the lake.

The Rotorua region is still very geothermally active. Hot springs and geysers provide direct geothermal input along the southern shore and through some of the streams. These geothermal waters are characterised by their extreme temperatures, pH, high sulphide and heavy metal concentrations. In New Zealand geothermal waters typically contain about 2000 ppm Na, 250 ppm K, 3000 ppm Cl, and 600 ppm $Si(OH)_4$ (C. Hendy, pers. comm. 2008).

2.2.1 Geology

Ferdinand von Hochstetter (following Dr Ernest Dieffenbach) was one of the first to describe the volcanics of the North Island, noting prior to his exploration that "the country over which I should there proceed, is inhabited almost exclusively by Maoris, and has hitherto been almost unknown and totally unsurveyed, both topographically and geologically". He found and described a number of volcanic cones (active and extinct), as well as a long line of boiling springs, fumaroles, and sulfataras found in a series stretching across the country in a north-north east direction from the active crater of Ngauruhoe in the Tongariro system to the active crater of White Island. The boiling springs of Whakarewarewa on the edge of Lake Rotorua were described in detail, and Hochstetter correctly suggested that the depression in which the lake resides originated through collapse of the ground.

Lake Rotorua is located in the central part of the Taupo Volcanic Zone (TVZ), which is an extensional NE–SW trending depression on the North Island of New Zealand (Fig. 2.2). The TVZ is a volcano-tectonic complex, 300 km long and up to 60 km wide, reflecting northwest-directed subduction of the Pacific plate beneath the North Island of New Zealand. The zone is defined by an envelope encapsulating all vent locations known or inferred to have been active during the past 2 million years and associated with a northeast structural trend.

The central TVZ is a broad structural depression, with a regional negative gravity anomaly containing local anomalies of 20-40 mgal, reflecting caldera centres and tectonic basins. At least 34 eruptions (inferred from their volume and/or facies associations to be associated with caldera collapse) have occurred from a complex sequence of relatively short-lived, nested, and/or overlapping volcanic centres in the central TVZ (Houghton et al., 1995).

Work by Sutton et al. (1995), based on the Taupo Volcanic Centre, implies that magmatic cycles in the TVZ may only last thousands to tens of thousands of years and can overlap both time and space.

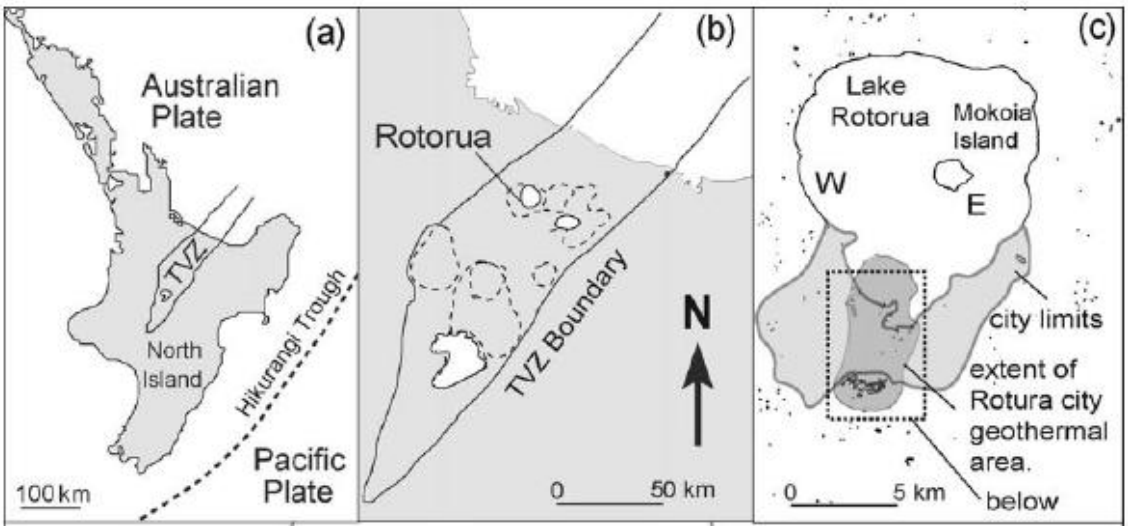

Figure 2.2: Maps showing location of the Rotorua geothermal system on the North Island of New Zealand. (a) Taupo Volcanic Zone (TVZ); the convergent boundary lies east of the TVZ; (b) Rotorua caldera boundary within the context of other volcanic calderas in New Zealand; (c) light grey shading indicates the extent of the city, and the dark grey the extent of Rotorua city geothermal system (Werner and Cardellini, 2006).

The Rotorua Basin, and the area surrounding it are composed exclusively of Quaternary rocks, either of volcanic origin or derived from volcanic rocks (Kennedy et al., 1978; Ballance, 1981). The geology of the Rotorua region and formational processes of the Rotorua Basin have been discussed in detail by Park (1910), Marshall (1905; 1912a; 1912b), Cotton (1922), Grange (1937) and Fleming (1959).

Marshall (1905) and Park (1910) discussed the formation of Rotorua Basin as a result of a volcanic explosion. In contrast Marshall's (1912a; 1912b) later work, and that of Cotton (1922), favoured the formation of the depression through subsidence. Hochstetter's theory of collapse was also supported by Grange (1937) and Fleming (1959), both of whom expanded the theory to suggest that the depression was formed by structural collapse probably after a volcanic eruption. It was not until 1964 when new work published by Healy and Thompson referred to the depression in which Lake Rotorua lies as a caldera.

Interest in the geology of the Rotorua region increased considerably again in the early 1980s with renewed interest in geothermal energy. The city of Rotorua lies at the southern end of the lake and is partially built over the Rotorua geothermal system (Fig. 2.2). Historically, geothermal waters from this system have been extracted from shallow depths (30–200 m) for private use (Wood, 1992). Since the 1920s, over 950 wells (the average well is about 120 m deep) have been drilled in the Rotorua geothermal field, with just over 100 still in use. These wells have been used primarily to supply hot water for domestic and commercial heating and for bathing (Glover and Mroczek, 1998; Houghton and Scott, 2002). However, during the 1970s-1980s continuous exploitation resulted in a noticeable decrease in the activity of the Whakarewarewa geyser field, the last remaining geyser field in New Zealand, and in the surface and near-surface geothermal activity found in the suburb of Ohinemutu and Kurau Park, all of which had a negative impact on tourism in the region. This decrease in geyser activity lead to research into the effects the increasing exploitation of the subsurface fluid was having on the geyser field. In 1986-1987 a government-lead programme initiated by geologist Tom Lloyd and physicist Ron Keam prompted the closure of many of the bores (Houghton and Scott, 2002), resulting in renewed geothermal activity at many of the geysers and hot springs. During this time there was a focussed

effort to establish baseline knowledge about the overall size, structure, and hydrology of the Rotorua geothermal field (Werner and Cardellini, 2006).

2.2.2 Rotorua Volcanic Centre

2.2.2.1 Introduction

The Rotorua Volcanic Centre (RVC) is located in the northern central TVZ 15–20 km NW of the junction between Okataina and Kapenga rift axes (Fig. 2.2). This volcanic centre's major eruption occurred between 220-230 ka, generating the Mamaku Ignimbrite (Shane et al., 1994; Houghton et al., 1995; Wilson et al., 1995a; Black et al., 1996; Milner et al., 2002, 2003). Following subsidence around the eruption centre, small eruptions around the caldera rim gave rise to a number of dome complexes (Houghton, 1982; Wood, 1992) and these, together with the ignimbrite, are the host rocks to the Rotorua geothermal system (Horwell et al., 2005).

The Rotorua region is situated close to the convergent margin where the Pacific plate subducts beneath the Australian plate (Fig. 2.8) to the east of the North Island, and is underlain by metamorphosed sedimentary units. Crustal thinning and basalt emplacement are thought to drive the continuous generation of magma in the upper crust of the TVZ; work by Houghton et al. (1995) indicated that Rotorua erupted during a period of intense volcanic activity in the TVZ. Milner et al. (2003) suggested rhyolitic volcanism at Rotorua was likely triggered by emplacement of high-temperature andesitic magma that is potentially derived from a basaltic magma such as those considered to have triggered eruptions in the Tarawera Volcanic Complex to the east of the Rotorua system (Leonard et al., 2002).

2.2.2.2 Rotorua caldera

The caldera formed after the eruption of the 220–230 ka Mamaku Ignimbrite. Although earlier events have been proposed (e.g. Wood, 1992), any evidence for these events in the region is buried beneath the Mamaku Ignimbrite and younger volcanic rocks (Houghton and Scott, 2002), and recent workers (Milner et al., 2002, 2003) have presented strong evidence indicating that Rotorua is a single-event caldera. Milner et al. (2002) studied the geochemistry of the Mamaku magma system and found three separate units. They found that the pre-caldera

rhyolite domes (e.g. Fryer Dome, Hamurana Dome, Endean Dome) scattered around the rim of the caldera are geochemically distinct from one another and from the Mamaku magma system. By contrast, most of the post-caldera dome-forming volcanism is geochemically similar to the Mamaku magma system.

The Rotorua Caldera is characterised by a N–S elongate negative residual gravity anomaly to the west and southwest of Lake Rotorua (Spinks et al., 2005). Surrounding gravity contours are not concentric to the caldera margin, defining an asymmetric rise towards NE and NW. A low Vp anomaly is consistent with the negative gravity anomaly and a collapse structure filled with volcaniclastic material (Sherburn, et al., 2003).

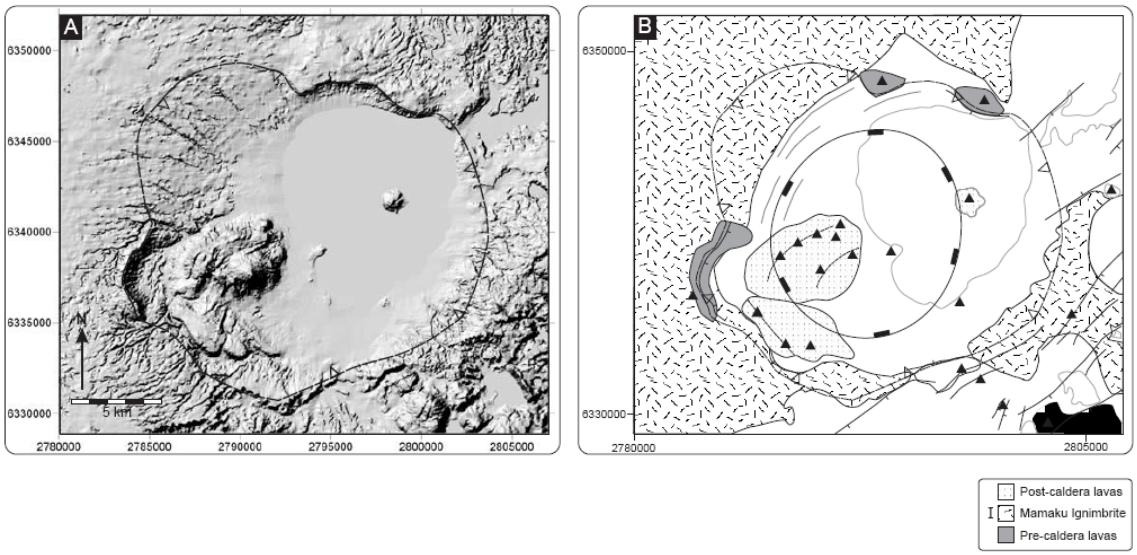

Figure 2.3: Rotorua Caldera. (A) Shaded relief image of Rotorua caldera. (B) Structure map of Rotorua Caldera generated from analysis of DEM data. Also shown are pre- and post-caldera lavas and the ignimbrite related to caldera formation (Spinks et al., 2005).

Digital elevation models (DEMs) and field data (Fig. 2.3 B) show that Rotorua Caldera is located several kilometres west of the present area of active tectonism within TVZ, with most of the active faults restricted to the junction between the Kapenga and Okataina segments (Spinks et al., 2005). Rotorua Caldera (Fig. 2.4), is expressed on DEM imagery as a sub-circular, fault controlled collapse structure, approximately 20 x 21 km (Milner et al., 2002; Werner and Cardellini, 2006), whereas the limit of deformation caused by collapse of the caldera is 21 x 22 km (Milner et al., 2002). The caldera floor is dominated by the ~ 9 km-wide lake and post-caldera dome complexes.

The topographic margin is semi-continuous around the caldera and is best expressed by scarps formed in pre-caldera rhyolite domes or Mamaku Ignimbrite (Figs. 2.3 A and 2.4); elsewhere the margin is marked by the limit of the inwards dipping Mamaku Ignimbrite, referred to as the limit of deformation by Milner et al. (2002). The southeast margin of the caldera roughly parallels NE-trending regional faults in the adjacent Okataina segment. Other lineaments in the caldera are arcuate and relate to caldera bounding scarps and associated deformation, rather than to regional structures (Spinks et al., 2005).

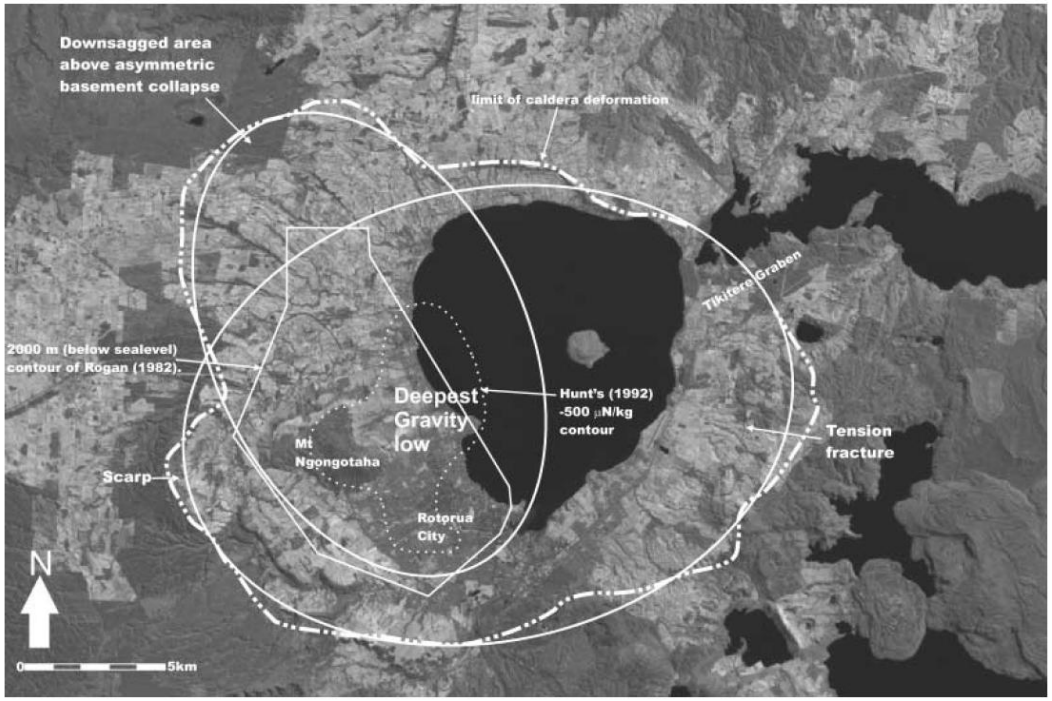

Figure 2.4: Satellite image of Rotorua Caldera showing major features outlined by Milner et al. (2002). The embayment in the northwest is thought to have been strongly influenced by NW–SE striking faults. The influence of NE–SW striking faults (associated with the main axis of rifting) can clearly be seen forming an elliptical collapse structure with a long axis oriented NE–SW

Milner et al. (2002) classified Rotorua caldera as a downsag collapse type, according to Lipman's (2000) four end-member collapse styles. This type of collapse occurs where ring faults either do not form or do not penetrate the ground surface, and instead some or all of the rocks overlying the magma chamber deform by bending without fracture (Milner et al., 2002). There are no distinct caldera walls and the ground surface dips gently towards the caldera collapse centre (Lipman, 2000).

2.2.2.3 Eruptive history of Rotorua

The eruptive history of the Rotorua Volcanic Centre can be divided into three main periods:

1) Large ignimbrite eruption that lead to the formation of the Rotorua Basin and caldera
2) Several effusive rhyolite eruptions producing the domes which surround the present day lake
3) Modern hydrothermal activity

2.2.2.3.1 Caldera-forming eruption (220-230 ka)

The Mamaku Ignimbrite eruption is considered to have a minimum volume of 145 km^3 dry-rock equivalent (DRE) including the intra-caldera ignimbrite (Milner et al., 2003). As a result of eruptive processes during the event, ground collapse occurred, forming a ring-faulted depression that is the Rotorua caldera.

2.2.2.3.2 Post-caldera formation

Soon after the Mamaku caldera eruption a lake began to form in the ring-faulted depression. The resulting lake sediments are known as the Huka Group – reworked fine ash, pumiceous sands, and diatomaceous silts.

Several rhyolite domes in and around the caldera post-date the Mamaku eruption, and these include Pukeroa Hill, Ngongotaha Complex, Pukehangi Complex, Hinemoa Point, Kawaha Point and Mokoia Island, but appear to pre-date the Rotoiti and Earthquake Flat pyroclastic eruptions that occurred ~ 60 cal. ka (Wood, 1992; Houghton and Scott, 2002). The caldera basin continued infilling with sediment and tephra was erupted from neighbouring volcanic centres, primarily the Okataina Volcanic Centre (Fig. 2.9). Thus, very little volcanic activity has occurred in the Rotorua caldera in the last ~ 60,000 years.

2.2.2.3.3 Modern hydrothermal activity

Altered rocks and sinter deposits in the region suggest that a hydrothermal system was active between c. 27,100 and c. 60,000 within Rotorua caldera, and migrated to its present location following a lowering of lake levels in the more recent geological past (Wood, 1992). Today, the only indication of continuing

underplating of basaltic magma in the Rotorua region is the sustained heat and volatile flux.

Resistivity data show that three hydrothermal areas exist within the Rotorua caldera. The main geothermal region is the Rotorua Geothermal Field (Fig 2.5) underlying much of Rotorua city. It extends at least 2 km northward under Lake Rotorua, with the majority of the activity concentrated in the Whakarewarewa area. This geothermal field is classified as acid-sulphate with some neutral chloride waters, and features include hot and boiling springs, geysers, bubbling mud pools, fumeroles, steaming ground and sinter deposits. The named features associated with this field are Whakarewarewa, Puarenga Stream, Kuirau Park, Ohinemutu, Arikikapakapa, Pohutu Geyser, Mokoia Island, Waipa, Ngapuna and Government Gardens.

The Tikitere Geothermal Field (8 km^2), located to the east of Lake Rotorua, appears as a thermal manifestation, and while linked by a resistivity band to the anomaly in Rotorua city, is unlikely to have shallow communication with the geothermal fluids in the area of the city of Rotorua. The West Lake Rotorua resistivity low does not have an associated thermal anomaly and is considered a fossil system (Werner and Cardellini, 2006).

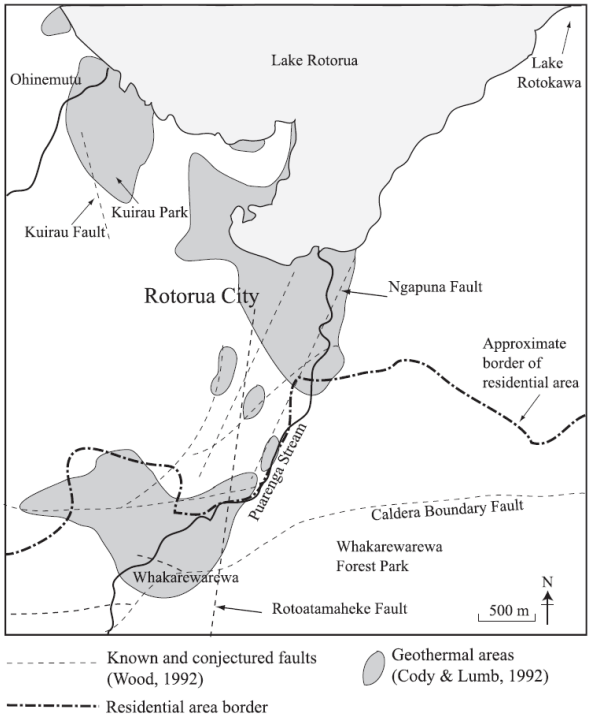

Figure 2.5: Map of Rotorua Geothermal Field showing geothermal areas and conjectured faults (Horwell et al., 2005).

2.2.3 Lake-level changes

The lake currently lies at about 280 metres above sea level. However, lake level over time has fluctuated markedly. The variations in lake level have been the result of volcanic disturbances in adjacent centres or climatic effects or (non-volcanic) geomorphic events. Deposits from volcanic eruptions, particularly from the Okataina Volcanic Centre (OVC), have periodically blocked the lake's outlet, and hence the lake has risen accordingly (Houghton and Scott, 2002). Kennedy et al. (1978) originally mapped the probable shorelines of Lake Rotorua, post eruption of the Rotoiti Breccia c. 60,000 years ago (Fig. 2.6). This eruption from the Haroharo volcano within the northern OVC formed a vast fan of non-welded ignimbrite that dammed the lake. A prominent terrace on the side of the hills from the Hemo Gorge to Mt Ngongotaha marks the old lake floor and indicates a rise of approximately 80 m above the present level (Houghton and Scott, 2002).

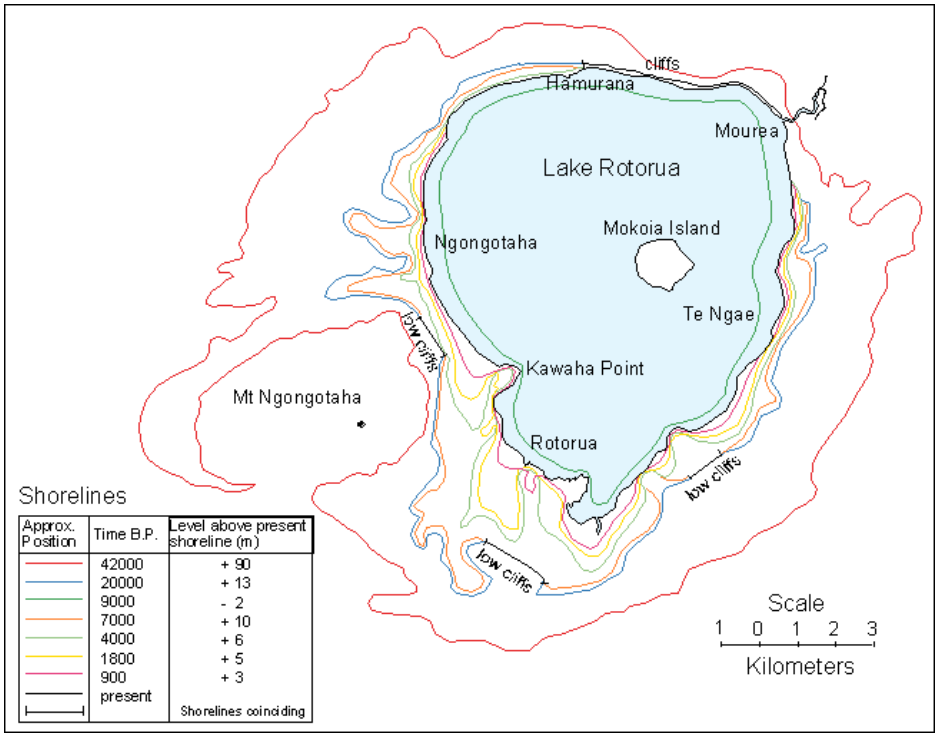

Figure 2.6: Probable shorelines of Lake Rotorua between about 60,000 cal. yrs ago and the present (after Kennedy et al., 1978).

Recent work by Dravitzki (1999) and Esler (2006) suggested that these fluctuations may be far more complicated than first thought. Esler (2006) has suggested at least seven periods of very high lake level, up to 120 m above present level, and its complete drainage at least twice (Fig. 2.7). Esler (2006) also discussed the formation a huge lake which may have extended as far as Atiamuri

or beyond. All of these drastic water level changes can be correlated in some way to major geological events.

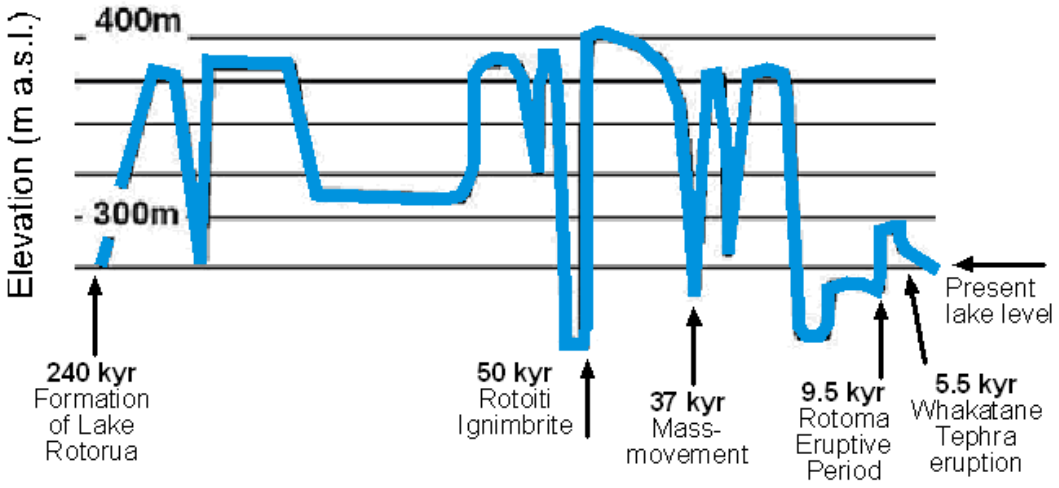

Figure 2.7: Changing levels of Lake Rotorua since ca. 230,000 years ago. Present level is ca. 280 m.a.s.l. (Pearson, 2007, adapted from Esler, 2006).

Additional interpretations of lake level history and the timeline of events have been proposed, the most recent including Marx (2004) and Hodgson and Nairn (2005). Marx (2004) supported a 'caldera breakout flood', whereas Hodgson and Nairn (2005) suggested that the drainage flowed to the east into the OVC.

2.2.4 Previous sediment studies on Lake Rotorua

Sediment studies are important to establish previous lake conditions via a number of proxies, and can lead to inferences about trophic status, lake levels and climate, as well as more general lake history. The deep (>10 m) sediments are comprised predominantly of organisms that live in the water column. When these die, they fall and accumulate on the bottom of the lake, carrying with them a proportion of their cell contents that become incorporated in the deposition of sediment. Sediments also reflect the chemical composition of the waters at the time of deposition, and how nutrients are retained and recycled.

Previous sediment studies carried out on Lake Rotorua have been related mainly to determining chemical composition of the accumulated material, and assessing nutrient budgets and sedimentation rates. Buried tephra layers in the sediment allow the stratigraphy of the sediment to be dated and accumulation rates calculated. During the late 1970s multiple studies were carried out on Lake

Rotorua's sediments. Fish (1979) conducted the first comprehensive study of Lake Rotorua's sediments. He collected 28 short sediment cores to study several tephra – in particular the amount and distribution of ejecta from the Tarawera eruption of 1886, and hence was able to calculate a sedimentation rate. The tephra deposits identified included Rotomahana Mud and Tarawera Ash (1886 A.D.), manifests as a thick grey mud deposit with smaller, gritty, black basaltic scoria along the base, and Kaharoa Tephra (c. 1314 A.D.), a white pumice layer found deeper in some of the cores between 1 and 1.5 m below the surface. The intervening deposit was described as mottled black-and-olive, fine lake sediment containing large numbers of diatom frustules – dominated by the species *Aulacoseira granulata*.

Fish (1979) found that in water depth less than 10 m, water movement is too vigorous to permit the permanent settling of the fairly light lake detritus. Hoare (1978) came to a similar conclusion when he studied sediment flows from the catchment into Lake Rotorua. Kennedy et al. (1978) suggested that because Mount Tarawera lies to the south-east of Lake Rotorua then the thickness of Rotomahana Mud and Tarawera ash would be expected to diminish in a northwest direction. This prediction was confirmed by Fish (1979). There were not enough data to make a reliable estimate of sediment accumulation between the Kaharoa and Tarawera eruptions. However, Fish (1979) suggested that the sediment deposition rate before the Tarawera eruption was less than at the present time and therefore the present state of Lake Rotorua is correspondingly more eutrophic.

White et al. (1978) examined the role of the sediment as a source and sink for plant nutrients in Lake Rotorua, and its role in the flux of salts assimilated and excreted in the biological cycles. They took depth profile samples from 30 sites across the lake. Each water sample was routinely analysed for various phosphorus and nitrogen components, as well as biomass and pigments. They estimated the nutrient exchanges between the lake sediments and the overlying water column using a mass balance approach, and came to the conclusion that, depending upon the extent of summer deoxygenation in the lake water, the sediments could potentially supply up to half the total income of phosphorus to the lake.

Matthews (1979) investigated the probable source of the sediment in various parts of the lake bed in an attempt to distinguish between different sediment types and the relationship between the sediments. Matthews (1979) studied a transect of cores from Ngongotaha to Mokoia Island. To determine how far sediment entering the lake off the land is distributed and to determine the sediment composition, Matthews (1979) used a variety of techniques including the scanning electron microscopy, x-ray diffraction, and radiometric dating.

Burnet and Davis (1980) examined the total production for Lake Rotorua. They found that production did not vary greatly from year to year, but that there is considerable seasonal fluctuation in the timing, intensity, and duration of the peaks. Burnet and Davis (1980) classified Lake Rotorua as a mixed lake, where maxima occur in summer or early autumn during which a thermocline occurs. The timing, duration, and extent of anoxic conditions are controlled predominantly by wind and insolation, and in turn these variables influence the possible releases of nutrients from the lake bed. Such release in turn influences the occurrence and intensity of the summer production maxima. Hence, Burnet and Davis (1980) concluded that the carbon production data can be used to predict oxygen fluctuations in the epilimnion, and to estimate probable depletion rates in the hypolimnion. They noted that the physical characteristics and climatological systems influencing the lake needed to be taken into consideration, however.

Fish and Andrew (1980) collected ten sediment cores from various locations during different seasons to determine whether the vertical distribution of nitrogen and phosphorus was affected by summer stratification (wind generally keeps the waters of Lake Rotorua well circulated and highly oxygenated, but there are times when the lake becomes thermally stratified for periods of days e.g. Burger et al., 2007) or if it was due to culturally enriched lake inflows. Fish and Andrew (1980) found large fluxes of nitrogen and phosphorus in many of the sediment cores. Nutrient concentrations were found to be higher at the sediment-water interface and then fell to a more constant value around 20 cm sediment depth. They concluded that the concentrations of nitrogen and phosphorus did not vary significantly with season and that bacteria and fungi at the interface probably assisted in the rapid decomposition of the plankton and other particulate matter that fell through the water column making the surface sediments more enriched.

More recent studies by Burger (2006; 2007) and Pearson (2007) have investigated sedimentation rates and nutrient budgets, but have yet to create a history of trophic states and development. Burger (2006) investigated variations in sedimentation rates of total particulate matter, total phosphorus, total nitrogen and chlorophyll-a using cylindrical sediment traps at three different depths in Lake Rotorua. He found that the sedimentation rate of particulate inorganic material increased with depth indicating that sediment resuspension is an important process in the lake. Burger (2007) also concluded from the proposed nutrient budget that nutrient sources derived from benthic fluxes within the lake were more important than external nutrient sources.

Pearson (2007) examined the sediments of Lake Rotorua from 163 cores. These cores were used to determine the distribution of elements in the sediments, the nature of the sedimentary processes involved in the lake, and finally a nutrient budget for the entire lake. Pearson (2007) reached conclusions similar to those of Fish (1979). Both scientists found two distinct types of sediments. In the lake margins, up to ~ 10 m water depth, the sediment is dominated by coarse clastic erosion products and coarse rhyolitic tephra fallout components. In this area wave action prevents the finer material from settling out and currents then focus these sediments towards deeper areas of the lake. Sediments in the remaining lake area, in water depths > 10 m, are dominated by diatomaceous ooze and contain a record of volcanic eruptions, in the form of tephra layers preserved within the fine sediments.

Decay of cyanobacteria and many other phytoplankton results in little material from this source accumulating in bottom sediments. However, diatom frustules remain largely intact and resistant to decay, and therefore dominate the bulk of the sediment. The diatom frustules are dominated by *Aulacoseira granulata* (formerly *Melosira granulata*). Detailed chemical analysis of the sediment revealed the bulk material consists primarily of silica derived from diatom frustules, with composition of other elements in the sediments related to the lake composition at the time of diatom deposition. Pearson (2007) expanded on the work of Fish and Andrews (1980), creating phosphorus maps covering the top 20 cm of the entire lake. These maps indicate concentrations in the centre of the lake

reach as high as 2500 µg/g but decline rapidly to 800 µg/g by 20 cm sediment depth. Pearson (2007) also looked at Fe, Mn, As and Pb. Fe and Mn were controlled by redox conditions whereas arsenic concentrations seem to be dependent on water depth. Both arsenic and lead were highly correlated with iron and manganese in the sediment and mimic the respective concentration profiles.

2.3 Late Quaternary climate records

Many records from around the world have focused recently on climate change during the transition from the last glaciation to the Holocene. INTIMATE (INTergration of Ice-core, MArine, and TErrestrial records) groups have been formed from different regions around the world to try and facilitate the precise correlation of major climatic events over the transition (e.g. Alloway et al., 2007b).

In the Northern Hemisphere, Holocene climate change events recorded in different paleoclimate archives have been demonstrated to be correlated in time, based on the comparison of glacier fluctuation records, ice core records, and marine sediments. However, many of these records do not correspond to changes in the Southern Hemisphere. For this reason global records are generally grouped into three regions: Northern Hemisphere (mid- to high-latitudes), low latitudes, and Southern Hemisphere (mid- to high-latitudes; Mayewski et al., 2004). Mayewski et al. (2004) examined ~ 50 globally distributed paleoclimate records from the Holocene and revealed there have been as many as six periods of significant rapid climate change. These periods were as follows: 9000–8000, 6000–5000, 4200–3800, 3500–2500, 1200–1000 (Medieval Warm Period), and 600–150 (Little Ice Age) calendar years before present (cal. yrs B.P.). Examination of these records demonstrates that, although generally weaker in amplitude than the dramatic shifts of the last glacial – post glacial transition, Holocene climate variations have been larger and more frequent than commonly recognized. Most of the climate change events in these records are characterized by polar cooling, tropical aridity, and major atmospheric circulation changes. One of the primary difficulties with trying to reconstruct Holocene temperature fluctuations, however, is that they were less than 1°C and few proxy records can yield temperatures with sufficient precision (Broecker, 2001).

2.3.1 New Zealand records

There are no measured climatic records for New Zealand prior to c. 1853 A.D. and therefore proxy information is required to provide evidence for earlier climate variation (Green, 1994). Some records of climatic variation are recorded by dendrochronology, speleothems, glacial moraines, palynolgy, fluvial terraces, loess, marine cores, and palaeolimnology. It is now widely recognised that the acquisition of high-resolution palaeoclimate records from southern mid-latitude sites is essential for establishing a coherent picture of inter-hemispheric climate change and for better understanding of the role of Antarctic climate dynamics in the global climate system (e.g. Newnham and Lowe, 2000). New Zealand is considered to be a sensitive monitor of climate change because it is one of a few sizeable landmasses in the Southern Hemisphere within the westerly circulation zone, a critical transition zone between subtropical and Antarctic influences (Alloway et al., 2007b). Many New Zealand records focus on the last glaciation, but more are beginning to investigate Holocene climate changes (e.g. Eden and Page, 1998; McGlone, 2002; Williams et al., 2004; Gomez et al., 2007; Lorrey et al., 2007). NZ-INTIMATE have identified what they consider the key records that collectively span the major climate transitions since 30,000 years ago, including the Holocene, and have developed a representative climate event stratigraphy using a variety of proxies (Alloway et al., 2007b; Lowe et al., 2008).

New Zealand's marked local and regional environmental variability has been recognised by numerous authors and is primarily attributed to complex terrain of mountain barriers and lowlands surrounded by extensive areas of ocean which produce rapid changes of climate over relatively short distances (e.g. Sturman et al., 1999; Lorrey et al., 2007). The current prevailing climatic regime is dominated by the El Nino-Southern Oscillation (ENSO). This regime is thought to have become established c. 4000 calibrated (cal.) years ago (c. 4 cal. ka), and that climate changed little during the late Holocene (McGlone et al., 1993; Gomez et al., 2004, 2007).

2.3.2 New Zealand mid-late Holocene climate

The Holocene climate has been relatively stable compared with previous glacial and interglacial regimes. Among the fluctuations are eleven periods of glacial advance in the Southern Alps (5.0-0.1 cal. ka) which demonstrate a cool or wetter

climate (NZ glaciers also respond to precipitation changes). Regional variability means that these cold temperatures (± wet) were not uniform across the country and speleothem records only indicate cooling ~ 3 cal. ka (Williams et al., 2004). Interspersed amongst the cooling events are periods of warmer climate, the most recent being the Medieval Warm Period (MWP). This period is defined loosely as the interval 0.8-1.1 cal. ka (or c. 900-1200 A.D.) and was first recognised in records from the North Atlantic (IPCC, 2007). Broecker (2001) suggested this natural warming event is the most recent in a series of similar warmings spaced at roughly 1500 year intervals. There are few records in New Zealand that contain evidence for this event. Williams et al. (2004) observed this event in speleothem records from Waitomo Caves, North Island, around 0.75 cal. ka. However, the same event in speleothems from the South Island was delayed until the period 0.7-0.57 cal. ka (Williams et al., 2005). The Little Ice Age (LIA) represents a period of cooler-than-present temperatures occurring approximately around 1200-1850 A.D. (IPCC, 2007). As with many other climate anomalies this period was first recognised in North Atlantic, but is thought to have a global extent (Broecker, 2001). The last climatic anomaly of this period is the subsequent post-1860 warming. This event has been recorded everywhere that there are ice covered mountains except Antarctica and hence is considered global (Broecker, 2001).

2.3.3 Palaeolimnological studies in NZ

Palaeolimnological studies in New Zealand have progressed a long way in the last 20 years, with research from lakes in both main islands (e.g. see Green and Lowe, 1992b, for a short review up to 1992). These studies have given us a greater understanding of the geological and climatological processes which have formed our landscape, as well as documenting some of the effects of both Maori and European settlement (Green and Lowe, 1992c). Some of these studies include work on Lake Pupuke (Horrocks et al., 2005; Augustinus, et al., 2006, 2008), Lake Rotoroa (Speirs, 1995), Lake Maratoto (Green, 1979; Green and Lowe, 1985), Lake Taharoa (Green, 1994), lakes on Matakana Is (Munro, 1994), Lake Rotoiti (Pickrill et al., 1991; Pickrill, 1993), Lake Rotorua (Fish, 1979; McGlone, 1983a; Rawlence, 1984; Burger et al., 2007, Pearson, 2007), Lake Rotoma (Nelson, 1983; Pickrill et al., 1991), Lake Waikaremoana (Newnham et al., 1998a), Lake Tutira (Eden et al., 1993; Eden and Froggatt, 1996; Eden and Page, 1998; Gomez et al., 2007), Lake Poukawa (Harper et al., 1986; Shulmeister et al.,

2001; Carter 2002; Harper and Collen, 2002; McGlone, 2002; Shane et al., 2002), and Lake Forsyth (Soons, 1998; Woodward and Shulmeister, 2005). Multi-lake studies have also been carried out to povide proxy data for environmental change. Examples of these include studies on chironomids (Woodward and Shulmeister, 2006), diatoms (Reid, 2005), and pollen (McGlone, 1989; Newnham et al., 1989; Newnham and Lowe, 2000; McGlone and Wilmshurst, 1999).

The North Island has many lake records ranging from the maars in Auckland to the small peat lakes of the Waikato and Hawke's Bay. One of these small peat lakes, Lake Poukawa, has been subject to extensive coring. Harper et al. (1986) studied the Holocene algal communities and found that Polynesian and European deforestation caused significant changes in the algal community as did the frequent depositions of tephra in the lake. More recent studies (Shulmeister et al., 2001; Carter, 2002; Harper and Collen, 2002; McGlone, 2002; Shane et al., 2002) have provided a reasonably sound chronology for pollen, diatom and phytoliths environmental interpretations. Lake Tutira, also in the Hawke's Bay, provides a detailed record of the last c. 6500 cal. yrs. This lake has had an extensive coring program looking in particular at sedimentation rates, assisted by a very detailed chronology. These studies have enabled storm erosion fluxes and a storm precipitation index to be developed, the only record like this in the country. Lakes of the central volcanic region have also had a significant amount of work carried out on them. These studies include sedimentation patterns (Lake Rotoiti and Rotoma; Pickrill et al., 1991), sediment nutrient levels (Lake Rotorua; Fish, 1979; Burger et al., 2007, Pearson, 2007), diatoms and pigments (Lake Rotorua; Rawlence, 1984), and pollen analysis (McGlone, 1983a, 1983b). Lake Pupuke, one of the Auckland maars, has been studied by Horrocks et al. (2005) and Augustinus et al. (2006, 2008). These studies examined sedimentation rates, geochemical signatures, pollen records and changes in biotic proxies as means for interpreting environmental change and provided one of the most complete records for the Holocene in the Auckland region.

2.4 How elements behave in lake sediments

In natural waters dissolved metals can form a wide variety of complexes. The sediment acts as source or sink, depending on the metal redox characteristics and on the geochemical conditions of the lake. Diffusion through redox boundaries, mixing processes, adsorption and resedimentation may lead to focusing effects with higher concentrations in deeper parts of the basin (Davison, 1993; Schaller et al., 1997).

Processes of oxidation and reduction, known as redox reactions, are common in the natural environment and particularly in aqueous environments. Usually only one oxidation state is stable, and this is the most commonly encountered oxidation state and is generally only stable in the presence of oxygen. However, this state changes when oxygen becomes depleted and then reduced forms may dominate. Oxygen is consumed by respiration and the decomposition of organic material in the lake sediment, and this leads to the formation of anoxic (reducing) environments which can sometimes extend into the main body of water.

Elements may be transformed from relatively immobile particulate forms to soluble components, free to move along hydraulic pathways. Many of these transformations are mediated by micro- organisms whose metabolisms depend upon the transfer of electrons to and from inorganic substrates. The study of redox processes in lakes reveals a picture of numerous, interdependent, chemical reactions. These various transformations are complex and the redox chemistry of the lake is closely reflected by the many and varied biological interactions and processes within it (Davison, 1993).

The preservation of geochemical signals in the sediment depends on primarily on the diagenetic processes occurring there. Formation of iron sulfides and precipitation of phosphates and carbonates are the main pathways to record changes in metal concentrations in lake sediments (Schaller et al., 1999).

Whole lake budgets for major ions (Na, K, Ca, Mg, SO_4, Cl, HCO_3) have been the topic of large number of studies and considerable speculation (Timperley and Vigor-Brown, 1985). Opinions vary about the relative contributions of many elements, but geochemists do agree that the sources of metals in most aquatic

systems are the products of the weathering of rocks and soils in the catchment, and occasionally the release of hydrothermal fluids. These processes result in metals being transferred in dissolved and/or particulate form (Boudreau, 1999).

2.4.1 Phosphorus (P)

Phosphorus is an essential nutrient in all aquatic environments and is sometimes a limiting agent for primary production. Therefore, the retention of phosphorus in aquatic sediments is a major factor regulating the trophic state of the overlying waters in a wide variety of environments (Carman et al., 2000; Katsev et al., 2006). However, though it is well established that the burial of organic phosphorus in the sediment composes a quantitatively important sink in most aquatic environments, its speciation is not well known (Carman et al., 2000).

The magnitude and timing of phosphorus release from aquatic sediments are affected by a multitude of factors, none of which is universally dominant (Katsev et al., 2006). The transfer of phosphate to and from sediments is largely determined by the redox cycling of iron. Phosphate is also, however, taken up by phytoplankton and bacteria, and so may eventually accumulate in the sediments within organic matter. There has been some debate recently as to whether phosphate is remobilized from anoxic sediments as a result of reduction of iron or due to rapid release from bacteria. Most probably both inorganic and organic mechanisms operate in most systems, their relative dominance depending on the microbial populations and the importance of the reductive remobilization of iron (Davison, 1993).

The most commonly used model to describe releases of phosphorus from sediment is linked to redox conditions at the sediment–water interface. Consequently, phosphorus releases are effectively controlled by the dissolved oxygen concentration in bottom water. When the sediment surface is oxic, strong adsorption of dissolved phosphate to solid iron oxyhydroxides limits phosphorus efflux by preventing phosphate diffusion into the water column from deeper, reduced, sediment. With onset of anoxia in the water overlying the sediment, iron oxyhydroxides reductively dissolve and phosphate is released into the water column. The apparent success of the classical model has resulted in widespread

attribution of phosphorus mobilization incidents to sediment redox conditions for a variety of situations and time scales (Katsev et al., 2006).

2.4.2 Iron (Fe)

The behaviour of iron and manganese in lakes and their sediments is well documented (Mackereth, 1966; Davison, 1993; Bryant et al., 1997; Schaller et al., 1997; Boudreau, 1999; Dean, 1999), and is related to redox conditions in the lake. Most iron enters lakes via rivers and streams in particulate form, which is eroded from the lattice of clay minerals in the surrounding catchment (Davison, 1993). In volcanic areas Fe (and Mn) may be added via tephra fallout, and also via dust and aerosol inputs.

Iron has two oxidation states of importance to aquatic chemistry, Fe(II) and Fe(III), and is released from sediments depending on the redox conditions present. Ferrous iron, Fe^{2+}, is stable in anoxic water and exists almost exclusively as a simple hydrated aqueous ion. It is very soluble with respect to most inorganic ions, but siderite ($FeCO_3$), amorphous iron sulphide (FeS) and vivianite ($Fe_3(PO_4)_2 \cdot 8\ H_20$) can be formed (Davison, 1993).

In well oxygenated waters, Fe^{3+} is the stable oxidation state. This acidic cation is completely hydrolysed at neutral pH, with its solubility being controlled by amorphous iron hydroxide. At pH 7, $Fe(OH)_3^0$ is the dominant species. In lakes, ferric iron has been found to be present as amorphous particles, which are negatively charged due to adsorption of organic substances (Davison, 1993). According to Davison (1993) sediment is often highly reducing due to the large amount of organic material settling out of the water column. Fe-reducing or Fe-oxidising bacteria can also affect the form of iron in the water (D.J. Lowe, pers. comm. 2008).

Mackereth (1966) suggested that iron and manganese are reasonable indicators of trophic status because their ratios should vary with the redox potential of the lake hypolimnion. Manganese should be depleted relative to iron in sediments where redox potentials are relatively low, whereas in highly anaerobic sediments both iron and manganese would be lost. Presumably, eutrophic lakes have highly anaerobic sediments and where stratified anoxic hypolimnia. Complications arise

because variations in the redox potential of catchment soils influence the rates of iron and manganese input into a lake (Brugam, 1984).

2.4.3 Manganese (Mn)

Manganese has three oxidation states of importance to aquatic chemistry, Mn(II), Mn(III) and Mn(IV). Manganous ions, Mn(II), are stable in anoxic waters where they are present as simple hydrated aquo ions. The basic chemistry of both Mn(III) and Mn(IV) oxidation states is poorly understood (Davison, 1993). The distribution of this element in aquatic systems is largely governed by pH-Eh equilibria (Bryant et al., 1997). Redox transformations dominate the chemistry of both iron and manganese in oxic and anoxic waters and in sediments (Davison, 1993; Bryant et al, 1997). While it is substantially true that ferrous and manganous ions predominate in anoxic waters, and that higher oxidation states mainly occur in well oxygenated systems, there are many exceptions to this rule (Davison, 1993).

Manganese (II) is present in many rock-forming minerals where it replaces iron (II) in the crystal lattice. Thus, olivine, pyroxene, hornblende, biotite, chlorite, serpentinite and magnetite may all contain appreciable amounts of manganese (II). Manganese primarily enters waterways through the weathering of rocks and soils containing these minerals. Suspended sediment or solutes travel in groundwater or down the rivers and streams into lakes where it accumulates in the sediments.

2.4.4 Arsenic (As)

Arsenic occurs naturally in some lake waters as a result of rock and soil weathering or geothermal activity. The mobility of arsenic is determined primarily by processes at mineral surfaces, particularly precipitation, dissolution, adsorption and desorption controlled by geochemical parameters such as pH, Eh, ionic composition, and mineral type (Bauer and Blodau, 2006).

Arsenate ($H_xAsO_4^{-3+x}$) is the dominant species of arsenic in oxidized natural waters. Under mildly reducing conditions arsenate is reduced to arsenite ($H_xAsO_3^{-3+x}$). In the presence of S(-II) the solubility of arsenite is controlled by amorphous FeS phases and, depending on the S(-II) concentration, arsenic sulfide. Reduced As(III) is quite stable in oxic environments, due to the relatively slow

oxidation kinetics (Schaller et al., 1999). Geothermal waters found in the TVC often contain significant arsenic concentrations (Smith, 1986).

2.4.5 Trace metals

The fate of trace metals in lakes is governed by numerous physical and biogeochemical processes. The relative importance of these processes depends on the geochemical conditions of the lake and on the chemical characteristics of each metal. The redox conditions in the deep water and in the sediment influence the fate of trace metals to a great extent. Adsorption, solubility and complexation characteristics of metals change with their oxidation state. Temporal and spatial redox gradients induce internal cycling of metals (Davison, 1993; Schaller et al., 1999). The combination of the many processes acting on these various elements makes them difficult to understand in many cases.

2.5 Additional regional volcanic geology

Current plate tectonic models for New Zealand show that the North Island lies on the leading edge of the Australasian Plate that is being obliquely underthrust by the subducting oceanic Pacific Plate. Volcanic activity resulting from the interaction of these lithospheric plates has been a feature of the geological development of much of the central North Island in the Quaternary (Fig. 2.8). The sites of volcanism in the North Island have varied largely over this timeframe and many of these centres have erupted great quantities of lava and pyroclastic material. Notably these include the TVZ volcanoes, and Mt Egmont and Mayor Island (Lowe, 1990; Froggatt and Lowe, 1990; Soengkono, 1995; Wilson et al., 1995a, 1995b).

2.5.1 Taupo Volcanic Zone

A number of authors have described the structural and volcanic features of the Taupo Volcanic Zone (TVZ) (Fig. 2.9) (e.g. Henderson, 1924; Marwick, Fyfe and Grange, 1937; Modriniak and Studt, 1959; Healy 1964; Suggate et al., 1978; Wilson et al., 1995a), and all have emphasised the pronounced subsidence that has occurred within it. Williams (1941) classed it as a volcanic-tectonic depression. The TVZ was originally named the "Taupo Zone" by Hochstetter (1864), who first recognised the structural unity and some of the large faults it contains. The term described the Quaternary eruptive centres extending from Ruapehu to White

Island, including boiling springs, geysers and sulfataras. The term was reintroduced by Steiner (1958) in the form the "Taupo volcanic zone".

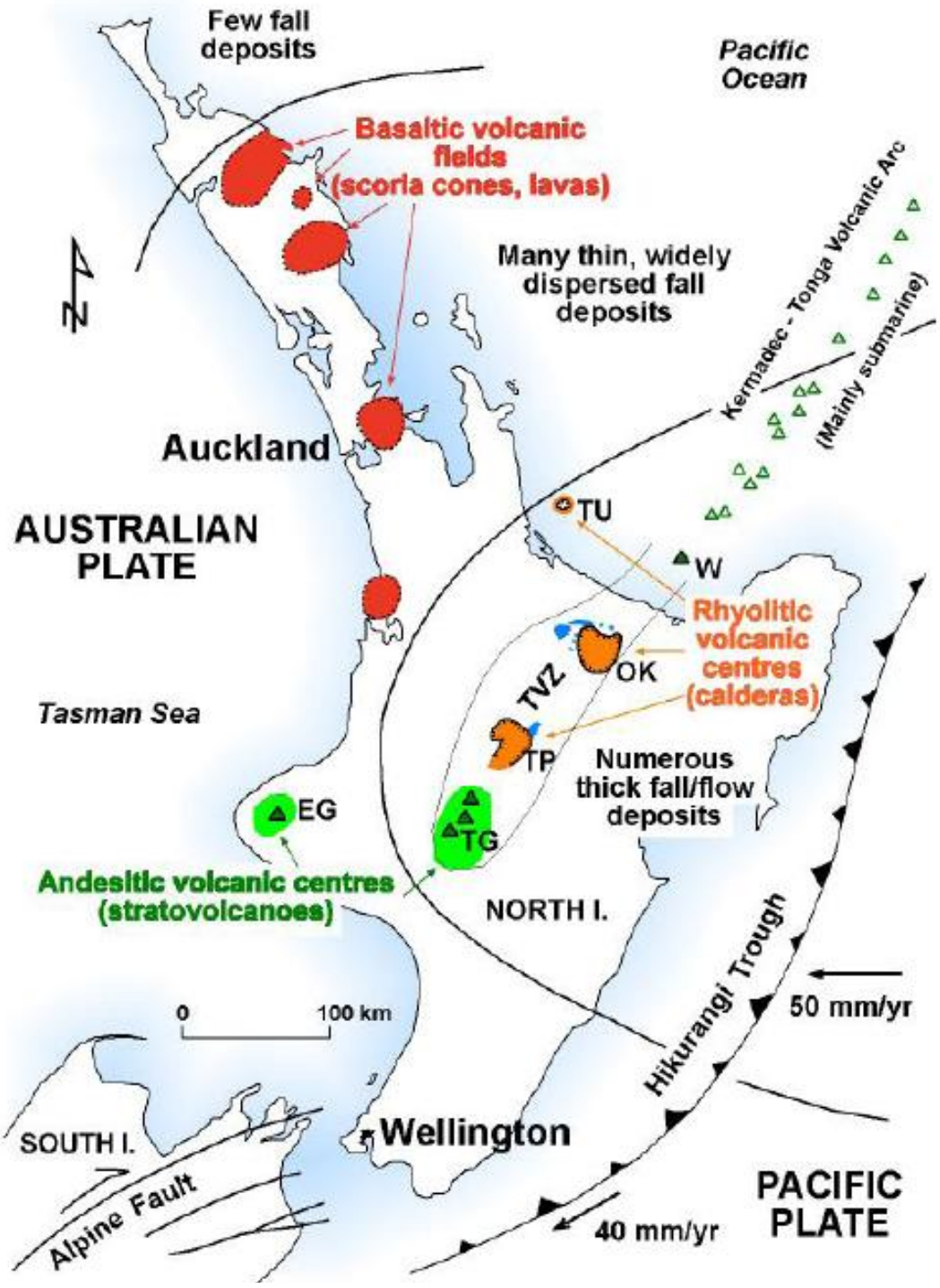

Figure 2.8: General map showing plate tectonic setting, the main volcanic centres that have erupted soil-forming tephras, and the general dispersal of tephra on North Island (Lowe and Palmer, 2005). EG, Egmont or Taranaki volcano; TG, Tongariro Volcanic Centre (includes Ngauruhoe, Tongariro, and Ruapehu volcanoes); TP, Taupo Volcanic Centre; OK, Okataina Volcanic Centre (includes Mt Tarawera and Haroharo volcanic complexes); TU, Tuhua Volcanic Centre (Mayor Is.); W, Whakaari (White Is.); TVZ, Taupo Volcanic Zone.

Healy (1964) redefined this term describing the relationship between the structure and volcanism in the zone, pointing out that the zone consists of all normal faults generally associated with subsidence, which is one of the results of volcanism. The Taupo Volcanic Zone has since been redefined multiple times as knowledge and technology has advanced. Maroa, Okataina, Rotorua and Taupo volcanic centres were identified by surface expression (Healy, 1964). Kapenga, Mangakino, and Tihoi from gravity and magnetic interpretations (Soengkono, 1995), and Reporoa from drill hole data. Houghton et al. (1995) redefined the zone as an envelope around all vent locations known or inferred to have been active during the past 2.0 million years.

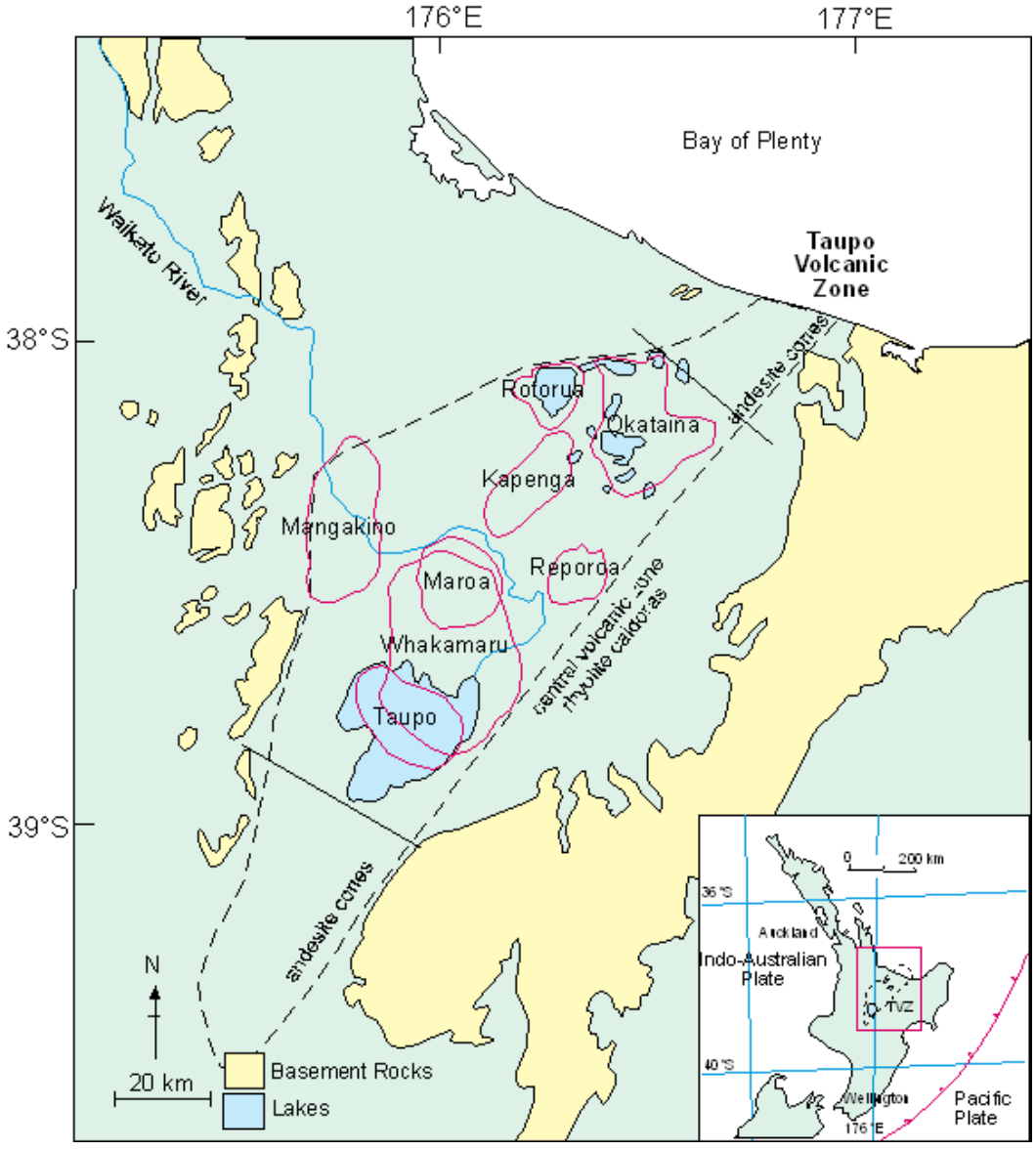

Figure 2.9: Map of the Taupo Volcanic Zone and the Central Volcanic Zone highlighting the volcanic centres (Marx, 2004, adapted from Bibbly et al., 2002 and Wilson et al., 1995a).

2.5.1.1 Okataina Volcanic Centre

The Okataina Volcanic Centre (OVC) is the most north-easterly of the rhyolitic centres located in the TVZ, and is also the most recently active (Jurado-Chichay and Walker, 2000). Okataina Volcanic Centre consists of the Haroharo linear vent zone, within which lie a number of overlapping vents, fissures, post-caldera rhyolites lavas and pyroclastic deposits, and several small lakes, and the Tarawera linear vent zone (Fig. 2.10). Temporal trends indicate that the OVC eruption episodes have tapped progressively more evolved (~71–77 wt. % SiO_2), cooler (940–730°C), and possibly shallower (~400–150 MPa) magmas.

Okataina, along with Taupo, remains highly active (average 0.08 m^3s^{-1} over the past c. 60 ka) and is among the most productive rhyolite volcanoes documented. Post-caldera activity at Okataina contrasts with Taupo in that there have been fewer but generally larger eruptions, often with substantial volumes of lava that have largely filled the younger caldera structure (Wilson et al., 1995a). The most recent activity was at Mt Tarawera in 1886 A.D. (the largest known TVZ basalt eruption) and the Kaharoa eruption 636 ± 12 cal. yrs B.P. (the youngest TVZ rhyolite eruption).

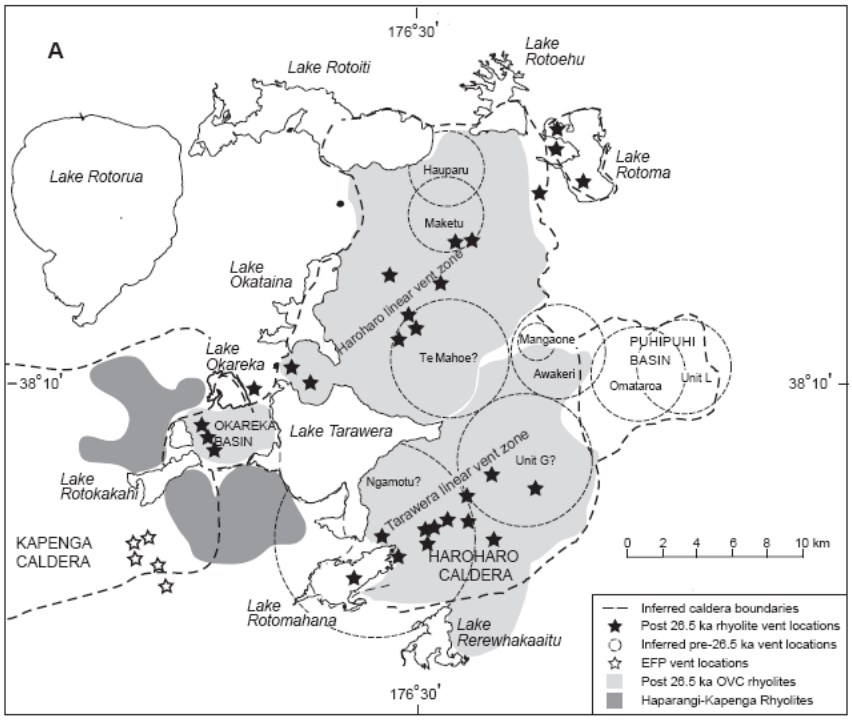

Figure 2.10: Map of Okataina Volcanic Centre (OVC) showing the outline of the Okataina (Haroharo) and Kapenga calderas, vent locations, and lavas (map constructed by Nairn, 2002; sourced from Smith et al., 2005).

The OVC eruptive history can be divided into two main periods:

1) A sequence of large caldera-forming eruptive episodes, concluding with the Rotoiti Tephra eruption. Explosive activity appears to have commenced at OVC around 340 ka. The OVC was previously thought to have erupted at least four major ignimbrites and possibly two smaller eruptions (Nairn 1981; 1989), others (Houghton et al., 1995; Wilson et al., 1995a) attributed only two ignimbrite eruptions (Matahina Ignimbrite 0.28 ± 0.01 Ma [Bailey and Carr, 1994; Houghton et al., 1995] and c. 60 cal. ka Rotoiti eruption [Nairn, 1981; Davis, 1985; Wilson et al., 1992]) to caldera collapse. Current literature propose at least three, large caldera-forming eruption episodes, together erupting > 240 km^3 of magma, and producing widespread ignimbrites (Bowyer, 2001; Nairn, 2002; Smith et al., 2005).

2) A phase of post-caldera formation activity (Mangaone Subgroup and Rotorua Subgroup) that intensified over the last c. 50,000 years. Post caldera activity has involved the eruption of rhyolite lava domes and flows interbedded with pyroclastic flow and fall deposits that have largely infilled the initial collapse structure (Bowyer, 2001). Numerous studies of eruptive activity since the Rotoiti event (e.g. Jurado-Chichay and Walker, 2000; Bowyer, 2001; Smith, 2001; Leonard et al., 2002) indicate that these eruptions involved multiple small magma batches. The following describes the two subgroups – Mangaone Subgroup and Rotorua Subgroup – erupted from the OVC over the last 40,000 years.

The most recent rhyolite eruption in New Zealand occurred in the OVC from the Tarawera Volcanic Complex, around 0.7 ka and is known as the Kaharoa episode (Nairn et al., 2004). During this episode, multiple batches of rhyolite magma were sequentially erupted along an 8 km chain of vents, following basaltic intrusion into a single silicic magma chamber. Further investigations by Smith et al. (2004; 2006) and Shane et al. (2005; 2007) have shown that rhyolite eruptions at Okataina vary significantly in magmatic and eruption dynamics. Some of these episodes were driven by the intrusion and mingling of different rhyolite magma bodies that had experienced separate crystallisation and cooling histories prior to eruption (Shane et al., 2007).

2.5.1.1.1 Basaltic eruptions

The only solely basalt episodes are the small scale 1886 A.D. Tarawera and c. 3.8 cal. ka Rotokawau eruptions. Basaltic phreatomagmatic eruptions occurred around 3.8 cal. ka, on the north-west margin of the OVC. This incident is known as the Rotokawau Eruptive Episode and formed four maars associated with the lakes of Rotokawau, Rotoatua, and Rotongata (Beanland and Houghton, 1991). The most recent (June 1886 A.D.) basaltic plinian eruption from Mt Tarawera erupted ~ 1 km^3 of basalt magma from multiple vents on a 17 km-long northeast-trending dike system (Nairn and Cole, 1981), commencing at Ruawahia Dome and extended both south-west and north-east across the rhyolite domes and flows of the Tarawera Volcanic Complex (Keam, 1988). Phreatomagmatic and phreatic explosion followed at Lake Rotomahana and Waimangu (Nairn and Cole, 1981; Keam, 1988). Thin basaltic deposits have been recognised in early deposits in a number of Okataina-derived rhyolitic eruptive episodes (e.g. see Smith et al., 2005).

2.5.1.1.2 Modern hydrothermal activity

The OVC remains active to this day, with activity found across the complete centre. The Waimangu Thermal Valley, located on the southwest shore of Lake Rotomahana, is a well known tourist attraction with steaming cliffs of hydrothermally altered rocks, boiling springs, geysers and fumaroles. Lake Okataina, Tarawera, and Rotomahana all show low levels of hydrothermal activity varying from visible gas bubbles to hot water spots and beaches (Nairn, 1989). Some minor activity has been noted on Mt Tarawera with fumaroles and hot springs found within the fissure craters. This activity is much reduced compared to the hydrothermal activity prior to the 1886 Tarawera eruption when the Rotomahana Basin was intensely active with boiling springs, geysers, fumaroles, and the siliceous sinter Pink and White Terraces, was considered one of the "Wonders of the World" and travellers from around the world came to see them.

2.5.1.2 Taupo Volcanic Centre (TVC)

The Taupo Volcanic Centre (TVC) is located in the southern central TVZ (Fig. 2.9), and is considered to be the most productive and frequently active rhyolite complex in the world (Houghton et al., 1995; Sutton et al., 1995; Wilson et al., 1995a). The Taupo magmatic system has had a complex evolution. Work by

Houghton (1995) and Sutton et al. (1995) indicate's magmatic cycles may only last thousands to tens of thousands of years. Evidence shows the magma which fuels Taupo's eruptions does not tap a single, gradually evolving magma chamber, hence there must be multiple magma chambers beneath the TVC feeding the volcanic activity in the region. Taupo has erupted compositions ranging from basalt through andesite and dacite to high-silica rhyolite, with rhyolite making up > 95% of the erupted volume (Sutton et al., 1995). The modern Lake Taupo partly infills the caldera formed following the 27.1 cal. ka Oruanui (or Kawakawa) eruption; the northern half of the lake is interpreted as occupying a genuine caldera, while the southern part of the lake occupies a structure which in part at least is tectonically controlled and may also pre-date the Oruanui (Kawakawa) event (Sutton et al., 1995). The 27.1 cal. ka caldera-forming eruption is well documented (Wilson, 1993; Self, 1993; Wilson, 1991; Sutton et al., 1995; Wilson, 2001; Wilson et al., 2006). The post-Oruanui activity has been studied in detail and a sequence of 28 eruptions has been identified (Wilson, 1993). The most powerful of these, the Taupo eruption, occurred in the eastern part of the lake (Wilson and Walker, 1985; Smith and Houghton, 1995) at 1717 ± 13 cal. B.P. Vents for pre-caldera lavas are located to the north and south of the caldera complex, and lie along NE-trending features, whereas the vents for post-Oruanui eruptions mostly occur along the eastern edge of the caldera complex (Fig. 2.11; Wilson, 1993; Spinks et al., 2005; Smith et al., 2005).

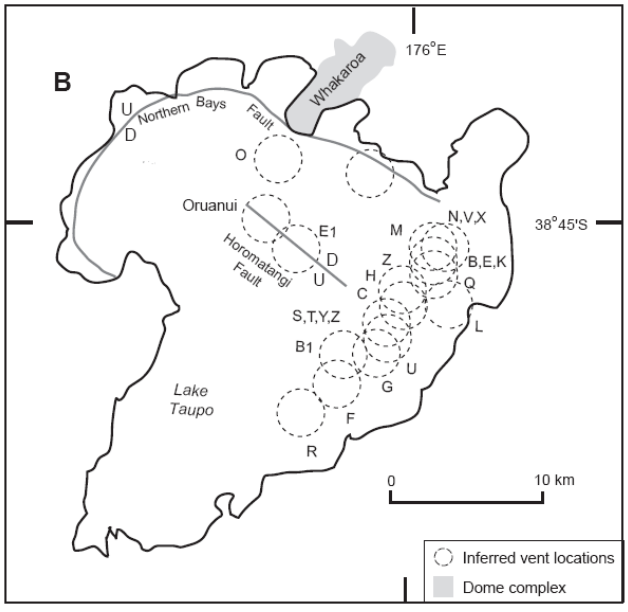

Figure 2.11: Map of Taupo Volcanic Centre (TVC) showing inferred vents from Wilson (2001). Vent locations for OSg eruptives are considered to be located in the northern part of modern Lake Taupo (Vucetich and Howorth, 1976) (Diagram sourced from Smith et al., 2005).

The eruptive history of the Taupo Volcanic Centre can be divided into four phases:

1) The early eruptive history, from 320 to ca. 50 ka is poorly constrained, largely due to burial by younger eruption products or engulfment by caldera collapse. This phase of activity is represented mostly by numerous lava domes and associated locally dispersed pyroclastics southwest, southeast and north of the modern lake. There are also two poorly welded ignimbrites, known from this time period. One is best exposed at Rangatira Point and the other at Kawakawa Bay, but due to poor exposure their extents and volumes are vague (Sutton et al., 1995; Wilson et al., 2006).

2) From ca. 50 to ca. 28 ka, dome building activity (Wilson et al., 1984) began to be accompanied by increasingly powerful explosive events – known as the Okaia Subgroup (~ 45–28 cal. ka; Vucetich and Howorth, 1976; Froggatt and Lowe, 1990; Sutton et al., 1995; Smith et al., 2005), culminating in the major phreatomagmatic Oruanui eruption at 22.6 ^{14}C ka (27.1 cal. ka; Lowe et al., 2008).

3) The 27.1 cal. ka Oruanui eruption is the largest known in the history of Taupo volcano (Self, 1983; Wilson, 1991) and marks a major turning point in the structural and magmatic evolution of TVC (Sutton et al., 1995). It was during this eruption that the structure of the modern volcano was established. This eruption generated an extremely widespread fall deposit and voluminous non-welded ignimbrite. It represents one of the youngest caldera-forming events in the central TVZ (Houghton et al., 1995; Wilson et al., 1995a).

4) Following the caldera-forming Oruanui eruption, twenty eight eruptions (labelled Ψ, Ω, A: Z.) known as the Taupo Subgroup, are recognised ranging in age from c. 20.5 ka to c. 1740 cal. years B.P. Twenty-seven of these events are represented by pyroclastic deposits, three of which (D, F and W) can be correlated with mappable lava extrusions preserved onshore. Juvenile obsidian observed in some deposits suggests that lava extrusions accompanied some of the episodes (Wilson, 1993; Sutton et al., 1995). The most voluminous and powerful post-Oruanui event was eruption Y (the Taupo eruption), and further caldera collapse in the northeast part of the Lake Taupo basin is inferred to have followed this

event. Precise vent locations for the Taupo subgroup are uncertain, as there are no proximal exposures to precisely constrain the isopachs (Wilson, 2001). Vents of the rhyolitic episodes appear to have been concentrated along the eastern edge of the modern Lake Taupo in a northeast–southwest trending zone. This corridor of vents parallels the regional tectonic regime of the TVZ (Wilson, 1993).

2.5.1.3 Tongariro Volcanic Centre

The Tongariro Volcanic Centre (TgVC) is a relatively young andesite-dacite complex located in the southern TVZ (Fig. 2.8). It consists of four major andesite massifs (Fig. 2.12): Kakaramea-Tihia, Pihanga, Tongariro (which includes multiple craters and the parasitic strato-cone Mt Ngauruhoe), and Ruapehu, and on the western side four smaller cones and flows, Maungakatote, Pukeonake, Hauhungatahi and Ohakune. Older lavas from Kakaramea, Pihanga and Tongariro were erupted from a series of vents aligned NW-SE and more recent lavas from vents aligned NNE-SSW two smaller eroded centres (Maungakatote, Hauhungatahi), and two satellite vents (Pukeonake scoria cone, Ohakune Craters; Cole, 1978; Cole et al., 1986).

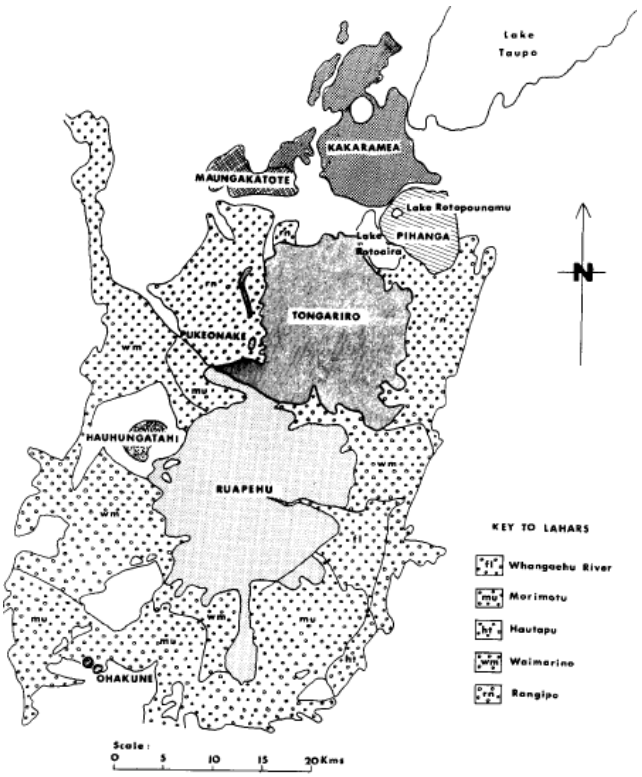

Figure 2.12: Andesite massifs and cones of the Tongariro Volcanic Centre (Cole, 1978)

The time at which volcanism commenced in the TgVC is not precisely known. Hobden et al. (1996) suggested that growth would have been visible by the time interval 250-275 ka. The most recent activity has occurred from Mt Ngauruhoe, Mt Tongariro, and Mt Ruapehu. Tongariro-derived units are particularly distinctive and are more widely dispersed than the Mt Ruapehu eruptives for this time period, the main difference being that most eruptives from Mt Ruapehu are products of small phreatomagmatic eruptions through Crater Lake located at the summit (Donoghue et al., 1996). The eruptive history of TgVC over the Holocene is recorded in nine andesitic tephra formations. Donoghue et al. (1995) grouped these tephras into two subgroups (Table 2.1): the Tongariro Subgroup (redefined) and the newly defined Tukino Subgroup.

Table 2.1: Stratigraphy of Tongariro Subgroup and Tukino Subgroup (Donoghue et al., 1995).

Subgroup	Formation	Age
TONGARIRO SUBGROUP	Tufa Trig Formation	c. 1,850 years B.P
	Ngauruhoe Formation	
	Mangatawai Tephra	
	Papakai Formation	
	Mangamate Formation	
	Pahoka Tephra	c. 10,000 years B.P
TUKINO SUBGROUP	Okupata Tephra	
	Rotoaira Lapilli	
	Bullot Formation	c. 22,500 years B.P

Cole (1978) contains a detailed outline of each of the components that make up the TgVC. Further details about the growth of the volcanic complex and the tephrochronology of the TgVC can be found respectively in the Hobden et al. (1996), and Donoghue et al. (1996), Donoghue et al. (1995), and Donoghue et al. (2007).

2.5.2 Mt Egmont (Taranaki)

The Taranaki Basin, located in the west coast of the North Island, is a large sedimentary basin through which the Taranaki volcanoes have erupted to form the Taranaki Peninsula (Fig. 2.13a) (Locke and Cassidy, 1997). Within this basin there are two groups of andesite volcanoes: one is a group of older buried Miocene volcanoes occurring offshore, the second is a more recently formed group located onshore (Hatherton et al., 1979; Knox, 1982). Volcanic activity on the Taranaki Peninsula began around the start of the Quaternary and has migrated

southeast at approximately right angles to the trend of the Taupo Volcanic Zone. This migration has left a succession of three relict volcanoes marking previous centres of activity: Paritutu (1.74 Ma), Kaitake (0.58 Ma) and Pouakai (0.23 Ma) (Fig. 2.13b). Mt Egmont (Taranaki) is the youngest and only still active volcano within the Taranaki Basin. It forms an almost perfect andesitic stratovolcano broken only by a small parasitic late Holocene cone called Fanthams Peak.

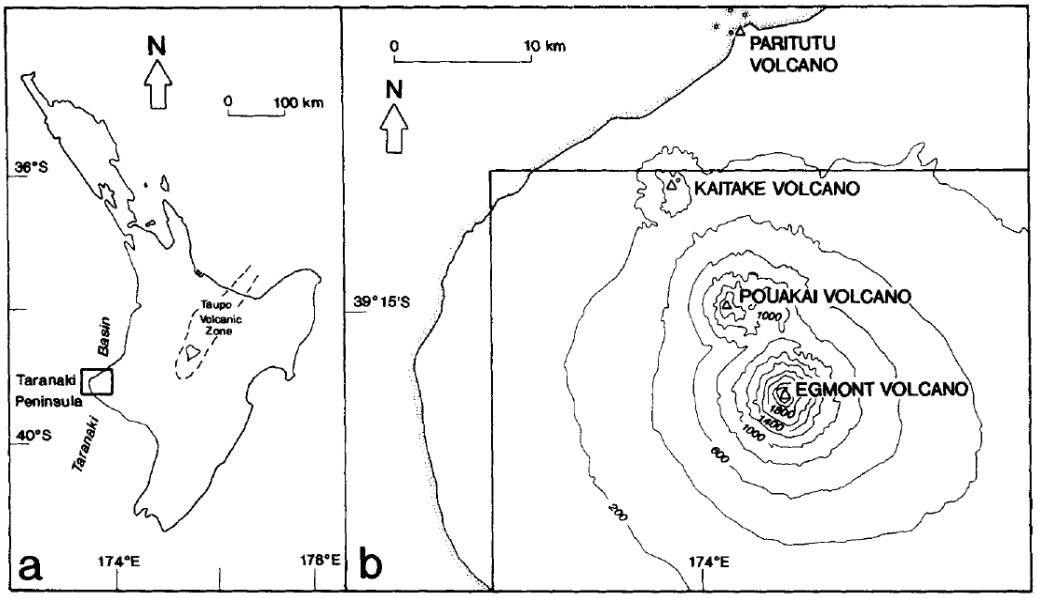

Figure 2.13: (a) North Island New Zealand showing location of Taranaki region [rectangle delimits area shown in (b)] and the Taupo Volcanic Zone. (b) Location of Taranaki volcanoes showing topographic surface (in metres a.s.1.) and peaks (Δ) (Locke and Cassidy, 1997).

The history of volcanic activity of Egmont Volcano is characterised by alternating phases of edifice construction and destruction (Palmer and Neall, 1991). The eruptive history of Mt Egmont is recorded in the units that make up the volcano and the surrounding ring plain. Deposits around the base of the Volcano record intermittent volcanic activity has occurred at this site for the at least the last 130,000 years (Neall and Alloway, 1991). Alloway et al. (1995) have describe the post-28 ka units. These units are complex consisting of multiple formations containing at least 76 tephras. These formations indicate that Egmont has been very active over the last 28 ka with an average eruption interval of once every c. 330 years. The latest definitive eruption of the volcano was in c. 1755 A.D., just before European settlement began (Alloway et al., 1995).

2.6 Tephrostratigraphy

The word "tephra" is derived from the Greek tephra (τεφρα), meaning ashes, and is a collective term for all the unconsolidated, primary pyroclastic products of a volcanic eruption (Froggatt and Lowe, 1990). It is inclusive of all grain sizes, including very fine ash (< 0.06 mm), medium ash (0.06-0.5 mm), coarse ash (0.5-2 mm), lapillus/i (2-64 mm), and block/s and bomb/s (> 64 mm) (Lowe and Hunt, 2001; Turney and Lowe, 2001).

Tephrochronology is the use of volcanic ash (tephra) beds as a stratigraphic tool to correlate and date volcanic and other geologic, geomorphological, palaeoenvironmental, and archaeological events. Large magnitude silicic eruptions can disperse tephra up to thousands of kilometres from the vent, producing a near instantaneous marker horizon (Shane, 2000). This 'instantaneous' atmospheric deposition of tephra following an eruption can often lead to tephra layers which are identifiable in a wide range of depositional environments including lakes, peats, loess, marine sediments, and glacier ice or ice sheets (Turney and Lowe, 2001). In addition to their geochronological and correlative value, tephra beds are a major source of data on the eruption frequency, magnitude, and geochemistry of large rhyolitic volcanoes (Shane, 2000; Shane et al., 2006). The dispersal of pyroclastic material around a volcanic region is strongly controlled by prevailing winds, topography and bathymetry. As a result, fall deposits may be distributed in different directions to pyroclastic flow and remobilised deposits.

2.6.1 New Zealand tephrostratigraphy

Quaternary silicic tephras have been studied in New Zealand for over 100 years, providing a detailed fundamental understanding of their stratigraphy, distribution, and processes of eruption (Froggatt and Lowe, 1990; Lowe, 1990; Shane, 2000). The first steps towards the development of modern tephrostratigraphy and tephrochronology began in the late 19th Century and early 20th Century when the first geologists arrived in New Zealand, with many noting the widespread pyroclastic material. During the mid to late 1920s and the 1930s more detailed studies were initiated including the completion of the first comprehensive "ash shower" maps and geological maps for the Rotorua-Taupo region. During the course of this work, many soil-forming tephra were named, described and mapped

(Grange. 1931; Grange and Taylor, 1932; Grange et al., 1939; Taylor, 1930, 1933, 1953). These maps were some of the first attempts in the world to utilise tephra horizons for correlation and geochronological control and are documented by authors such as Berry, (1928), Oliver, (1931), and Grange, (1931) (Lowe, 1990; Turney and Lowe, 2001). From the 1950s onwards more maps emerged and added supporting evidence to the volcanic history of the region. Much of post-1950s knowledge of tephrostratigraphy is due to the dedicated field work of two people, C. G. Vucetich and W. A. Pullar, and is embodied in three benchmark papers – Vucetich & Pullar 1964, 1969, 1973 (Froggatt and Lowe, 1990; Shane, 2000; Lowe et al., 2008b).

Continued mineralogical and chemical studies on many of these tephra has lead to the development of tephra "fingerprinting", which has further progressed with the development of new analytical techniques, allowing major element chemistry to characterise and distinguish many of New Zealand's late Quaternary tephra (Lowe, 1990, Shane, 2000). This technique of geochemical fingerprinting has become more important as the role of distal tephra has become significant, because these tephras tend to be thinner and mineral depleted (Shane, 2000; Shane et al., 2008). Careful analyses of the glass component, which represents the magma melt fraction quenched at the time of eruption, are used to match the tephra with source and possible correlatives.

As noted earlier, the central TVZ is considered to be one of the most frequently active and largest rhyolitic centres on Earth (Wilson et al., 1995a), and has been the focus of numerous large (> 100 km^3) caldera-forming ignimbrite and plinian eruptions. New Zealand Quaternary sequences and those of the surrounding oceans over 1000 km distant are well endowed with silicic tephra beds erupted from the TVZ (Fig. 2.9). The value of these beds as regional stratigraphic markers is well known (e.g., Froggatt and Lowe, 1990; Shane, 2000; Shane et al., 2006). Prior to the Quaternary, large-scale rhyolite volcanism was centred in the Coromandel Volcanic Zone starting at around 12 Ma (Fig. 2.8; Adams et al., 1994; Shane, 2000).

2.6.2 Correlation techniques

The key to both tephrostratigraphy and tephrochronology is the identification and correlation of tephra horizons. In the proximal setting < 50 km from vent, tephra beds can often be identified by their lithology, stratigraphic position and ferromagnesian mineralogy. Farther from source (> 50-100 km) most of these features become less diagnostic as units become thinner and mineral depleted, and in these cases geochemical fingerprinting, as discussed earlier, must be employed.

2.6.2.1 Ferromagnesian mineral assemblages

The first step in the identification of tephra using laboratory techniques is to identify the dominant ferromagnesian mineral assemblages. The relative abundances of various ferromagnesian minerals (e.g., pyroxenes, amphiboles, biotite) within silicic tephra beds have been used as an aid in the identification of many post-60 ka events in New Zealand. However, it is the presence not absence of characteristic minerals that is of most value (Froggatt and Lowe, 1990; Lowe and Newnham, 1999; Shane, 2000). As well as helping to identify the source volcano, the occurrence of particular minerals can aid in eliminating candidate eruptive events. The observed mineral assemblages fall into six main groups (Table 2.2). This grouping was first recognised in part by Ewart (1963, 1968, 1971) and developed by Kohn (1973) and then Froggatt and Lowe, (1990) and later Smith et al. (2005). The assemblages are listed below with mineral species in usual order of abundance, followed by minerals that may or may not be present in small amounts (±) (Froggatt and Lowe, 1990; Lowe et al., 2008). The cummingtonite-bearing tephra (with cummingtonite in more than minor amounts) are generally only found in eruptives from the Haroharo complex within Okataina Volcanic Centre (Ewart, 1968). During the last c. 60 ka only three widely dispersed tephra beds contain the mineral cummingtonite: Rotoehu (ca. 60 ka); Rotoma (9,505 ± 25 cal. yrs B.P) and Whakatane (5,530 ± 60 cal. yrs B.P). Biotite is normally abundant in only four post-22 ka tephra beds (all from Okataina): Okareka (c. 22 cal. ka), Rerewhakaaitu (c. 17.6 cal. ka), Rotorua (15.4 cal. ka) and Kaharoa (c. 636 cal. years B.P.). The occurrence of sodic phases such as aegirine, riebeckite, ferrohedenbergite and aenigmatite are indicative and restricted to pyroclastics from Tuhua Volcanic Centre, Mayor Island (Froggatt and Lowe, 1990; Shane, 2000).

Table 2.2: The dominant ferromagnesian mineral assemblages for the late Quaternary silicic tephra deposits, listed by volcanic centre and relative age (Froggatt and Lowe, 1990; Lowe, 1990; Lowe et al., 2008).

Tephra name[a]	Relative abundances of ferromagnesian minerals[b]	Eruption temperature[c] (°C)	Oxygen fugacity fO_2 (NNO)[d]
Taupo Volcanic Centre (rhyolitic)			
Taupo (Unit Y)	Opx ≫ Cpx	862 ± 17	−0.17 ± 0.11
Whakaipo (Unit V)	Opx	785 ± 10	−1.06 ± 0.12
Waimihia (Unit S)	Opx ≫ Hbe	816 ± 10	−0.72 ± 0.08
Unit K	Opx	822 ± 16	−0.59 ± 0.11
Opepe (Unit E)	Opx ≫ Cpx	812 ± 18	−0.54 ± 0.17
Poronui (Unit C)	Opx ≫ Cpx		
Karapiti (Unit B)	Opx ≫ Cpx + Hbe	788 ± 33	−0.75 ± 0.24
Kawakawa/Oruanui	Opx > Hbe	774 ± 12	−0.14 ± 0.10
Poihipi	Opx > Hbe > Bio	771 ± 6	0.07 ± 0.10
Okaia	Opx > Hbe	789 ± 17	0.21 ± 0.09
Okataina Volcanic Centre (rhyolitic)			
Kaharoa			
T1[e]	Bio ≫ Hbe ≫ Cgt ± Opx	731 ± 10	0.09 ± 0.14
T2	Bio ≫ Cgt > Hbe ± Opx		
Whakatane[f]			
T1	Hbe > Cgt > Opx	746 ± 13	0.33 ± 0.09
T2	Hbe > Cgt > Opx	737 ± 9	0.29 ± 0.11
T3	Opx > Hbe > Cgt	770 ± 5	0.52 ± 0.05
Mamaku[f]	Hbe > Opx ≫ ± Cgt	735 ± 19	0.18 ± 0.13
Rotoma[f]			
T1	Cgt > Hbe > Opx	752 ± 19	0.47 ± 0.12
T2	Hbe > Opx > Cgt	752 ± 19	0.47 ± 0.12
T3	Opx > Hbe > Cgt	752 ± 19	0.47 ± 0.12
Waiohau	Opx > Hbe	762 ± 23	0.36 ± 0.22
Rotorua			
T1	Opx > Hbe ≫ Cpx	871 ± 10	1.11 ± 0.13
T2	Bio > Hbe ≫ Opx	745 ± 30	0.17 ± 0.20
Rerewhakaaitu			
T1	Opx > Hbe	721	−0.31
T2	Hbe + Bio ≫ Opx	750 ± 18	0.43 ± 0.14
T3	Opx > Hbe		
Okareka			
T1	Opx + Hbe ≫ Cgt	759 ± 20	0.30 ± 0.20
T2	Hbe + Bio ≫ Opx	724 ± 14	0.05 ± 0.15
T3	Opx > Hbe	794 ± 12	0.82 ± 0.08
Te Rere			
T1	Opx + Hbe	801 ± 24	1.43 ± 0.16
T2	Opx + Hbe + Bio > Cpx	708 ± 3	−0.07 ± 0.01
T3	Opx + Hbe		
Tuhua Volcanic Centre (peralkaline rhyolitic)			
Tuhua	Aeg > Cpx > Opx ± Aen ± Rie ± Hbe ± Olv(fa) ± Tuh		
Tongariro Volcanic Centre (andesitic)			
Okupata	Opx > Cpx ≫ ± Olv(fo) ± Hbe	~900–1100	
Egmont Volcano (andesitic)			
Konini	Hbe > Cpx ≫ ± Opx	~950	

[a] See Table 1.

[b] Mineral data for rhyolitic tephras from Smith et al. (2005) and P.A.R. Shane and V.C. Smith (unpubl. data); for Tuhua after Lowe (1988a) and Manighetti et al. (2003); for Okupata and Konini after Lowe (1988a), Donoghue et al. (1999) and Lowe et al. (1999); ± indicates may or may not be present. All tephras additionally contain Fe–Ti oxides including spinel (titanomagnetite) and rhombohedral (ilmenite) phases (Smith et al., 2005). *Abbreviations*: Opx, orthopyroxene (mainly hypersthene); Cpx, clinopyroxene (mainly augite); Hbe, hornblende; Cgt, cummingtonite; Bio, biotite; Aeg, aegirine; Aen, aenigmatite; Rie, riebekite; Olv, olivine (fa, fayalite; fo, forsterite); Tuh, tuhualite.

[c] Pre-eruption temperature data for rhyolitic tephras are all from Smith et al. (2005) and were obtained via geothermometry using Fe–Ti oxide pairs (mean ± 1 standard deviation); broad estimates for Okupata and Konini generalised after Lowe (1988a, b).

[d] Oxygen fugacity data from Smith et al. (2005), reported in NNO units relative to the NiNiO buffer.

[e] T1–T3 represent separate magma types (early to late eruptive phases, respectively) identified by Smith et al. (2005) for some Okataina eruptive episodes (see also Table 5).

[f] See also Smith et al. (2006).

2.6.2.2 Glass chemistry

The chemical composition of ferromagnesian minerals is generally not characteristic of individual eruptions, and so the second step in identification is to determine the composition of the glass fragments. A major advance in tephra characterisation and hence correlation techniques has involved the use of the electron microprobe to analyse volcanic glass. This work began in New Zealand with Froggatt (1983) and has since been widely adopted (e.g. see Lowe et al., 2008). Grain-specific electron microprobe techniques are valuable for identifying both source volcano and individual eruptive events. From this technique glass and Fe–Ti oxide chemistry can be established, as well as eruption temperature and oxygen fugacity (estimated from oxide equilibrium pairs).

The composition of glass from many of New Zealand's post-60 ka tephra has been established and in many cases has allowed the volcanic source (Okataina, Taupo, Mayor Island, Tongariro, Egmont) to be identified (Table 2.3). Not all tephra beds have unique glass chemistry, and those erupted over short intervals (< 20 ka) from the same volcano are often similar with respect to major and trace elements. The composition of Fe–Ti oxides can also assist with the identification of source volcano (Taupo vs. Okataina), whilst simple binary (FeO vs. TiO_2) and ternary (Al–Mn–Mg) plots may aid in the identification of individual eruptive events. Such data allow some eruptions to be distinguished that are indistinguishable by glass chemistry.

Tephra beds are also valuable because they can be dated by a variety of methods, and therefore can provide direct age control for sequences that are not normally amenable to radiometric dating.

Table 2.3: Glass major element composition of tephra marker beds erupted in New Zealand since ca. 30,000 cal. yrs BP (Lowe et al., 2008).

	SiO_2	Al_2O_3	TiO_2	FeO	MnO	MgO	CaO	Na_2O	K_2O	Cl	H_2O	*n*
Taupo Volcanic Centre (rhyolitic)[b]												
Taupo (Unit Y)	75.04	13.45	0.30	1.99	0.07	0.22	1.47	4.49	2.85	0.19	4.63	19
	0.19	*0.12*	*0.04*	*0.08*	*0.03*	*0.10*	*0.05*	*0.12*	*0.07*	*0.01*	*1.85*	
Whakaipo (Unit V)	76.89	12.43	0.22	1.54	0.07	0.11	1.07	4.37	3.15	0.16	6.10	10
	0.14	*0.12*	*0.08*	*0.07*	*0.04*	*0.05*	*0.04*	*0.11*	*0.06*	*0.02*	*1.71*	
Waimihia (Unit S)	75.58	13.11	0.24	1.92	0.08	0.17	1.32	4.48	2.92	0.19	3.25	11
	0.18	*0.08*	*0.05*	*0.09*	*0.04*	*0.05*	*0.04*	*0.10*	*0.10*	*0.02*	*0.66*	
Unit K	75.83	12.81	0.26	1.64	0.03	0.14	1.30	4.86	2.98	0.16	5.63	9
	0.32	*0.11*	*0.08*	*0.16*	*0.03*	*0.05*	*0.07*	*0.13*	*0.08*	*0.03*	*1.05*	
Opepe (Unit E)	75.38	13.06	0.24	1.74	0.08	0.11	1.60	4.66	2.97	0.17	5.93	22
	0.50	*0.37*	*0.06*	*0.10*	*0.06*	*0.10*	*0.08*	*0.15*	*0.11*	*0.03*	*1.42*	
Poronui (Unit C)	76.26	12.91	0.19	1.57	0.03	0.16	1.45	4.14	3.15	0.15	2.92	10
	0.30	*0.16*	*0.04*	*0.12*	*0.02*	*0.04*	*0.16*	*0.15*	*0.15*	*0.03*	*0.94*	
Karapiti (Unit B)	76.16	12.75	0.20	1.57	0.06	0.11	1.42	4.42	3.14	0.16	6.26	18
	0.33	*0.12*	*0.06*	*0.12*	*0.05*	*0.08*	*0.10*	*0.15*	*0.08*	*0.03*	*1.88*	
Kawakawa/Oruanui	77.46	12.37	0.19	1.23	0.07	0.11	1.13	4.14	3.16	0.19	7.45	40
	0.41	*0.26*	*0.07*	*0.12*	*0.05*	*0.08*	*0.10*	*0.17*	*0.15*	*0.04*	*1.78*	
Poihipi	77.39	12.26	0.15	0.91	0.08	0.06	0.81	3.97	4.16	0.20	3.95	10
	0.34	*0.30*	*0.07*	*0.15*	*0.07*	*0.04*	*0.14*	*0.14*	*0.21*	*0.03*	*1.13*	
Okaia	77.50	12.42	0.18	1.29	0.04	0.10	1.20	3.90	3.28	0.19	5.99	19
	0.34	*0.21*	*0.06*	*0.10*	*0.04*	*0.06*	*0.09*	*0.14*	*0.10*	*0.02*	*2.36*	
Okataina Volcanic Centre (rhyolitic)[b]												
Kaharoa												
T1[c]	77.61	12.39	0.12	0.79	0.08	0.05	0.51	4.04	4.26	0.15	4.93	84
	0.19	*0.11*	*0.06*	*0.07*	*0.05*	*0.04*	*0.05*	*0.12*	*0.08*	*0.03*	*1.80*	
T2	77.75	12.32	0.13	0.82	0.07	0.05	0.58	4.01	4.13	0.15	1.83	30
	0.18	*0.07*	*0.05*	*0.07*	*0.05*	*0.04*	*0.05*	*0.13*	*0.05*	*0.03*	*0.50*	
Whakatane												
T1	77.84	12.24	0.16	0.85	0.07	0.09	0.77	4.22	3.67	0.16	2.94	98
	0.20	*0.11*	*0.07*	*0.09*	*0.05*	*0.06*	*0.05*	*0.13*	*0.08*	*0.04*	*1.48*	
T2	77.83	12.19	0.17	0.82	0.07	0.09	0.69	4.12	3.87	0.17	3.99	53
	0.23	*0.10*	*0.07*	*0.09*	*0.07*	*0.06*	*0.05*	*0.15*	*0.08*	*0.04*	*1.71*	
T3	77.83	12.19	0.19	0.88	0.07	0.12	0.85	4.17	3.52	0.15	2.43	19
	0.27	*0.07*	*0.07*	*0.15*	*0.04*	*0.06*	*0.05*	*0.12*	*0.09*	*0.04*	*0.73*	
Mamaku	78.15	12.15	0.16	0.89	0.06	0.01	0.76	4.03	3.69	0.13	na	34
	0.15	*0.08*	*0.02*	*0.06*	*0.02*	*0.01*	*0.07*	*0.09*	*0.16*	*0.01*	na	
Rotoma												
T1	77.84	12.23	0.16	0.86	0.09	0.11	0.80	4.28	3.57	0.15	2.77	39
	0.22	*0.09*	*0.07*	*0.10*	*0.06*	*0.07*	*0.07*	*0.16*	*0.19*	*0.03*	*1.31*	
T2	77.76	12.30	0.18	0.90	0.07	0.14	0.83	4.26	3.45	0.16	3.06	38
	0.21	*0.10*	*0.07*	*0.08*	*0.05*	*0.07*	*0.05*	*0.23*	*0.08*	*0.04*	*2.07*	
T3	77.73	12.24	0.18	0.94	0.06	0.13	0.93	4.29	3.36	0.15	2.99	32
	0.18	*0.10*	*0.06*	*0.10*	*0.04*	*0.07*	*0.05*	*0.18*	*0.08*	*0.04*	*1.53*	
Waiohau	78.11	12.15	0.19	0.98	0.08	0.04	0.91	4.02	3.39	0.14	3.68	97
	0.28	*0.13*	*0.06*	*0.15*	*0.06*	*0.04*	*0.07*	*0.17*	*0.11*	*0.03*	*2.08*	
Rotorua												
T1	76.50	12.77	0.29	1.29	0.07	0.23	1.35	4.33	3.02	0.15	5.74	55
	0.29	*0.23*	*0.08*	*0.13*	*0.06*	*0.08*	*0.08*	*0.12*	*0.09*	*0.03*	*1.65*	
T2	77.34	12.32	0.14	0.87	0.09	0.08	0.76	4.03	4.26	0.15	4.82	34
	0.20	*0.06*	*0.12*	*0.12*	*0.07*	*0.05*	*0.11*	*0.11*	*0.16*	*0.03*	*1.52*	
Rerewhakaaitu												
T1	77.73	12.16	0.18	0.96	0.07	0.11	0.92	4.27	3.44	0.17	5.80	69
	0.22	*0.11*	*0.07*	*0.09*	*0.05*	*0.07*	*0.06*	*0.12*	*0.09*	*0.04*	*1.47*	
T2	77.36	12.27	0.13	0.91	0.06	0.10	0.82	3.96	4.21	0.18	6.07	66
	0.32	*0.18*	*0.07*	*0.10*	*0.05*	*0.08*	*0.07*	*0.13*	*0.10*	*0.04*	*1.72*	
T3	77.37	12.38	0.20	1.05	0.05	0.15	0.99	4.62	3.14	0.15	8.00	10
	0.31	*0.15*	*0.08*	*0.10*	*0.04*	*0.06*	*0.08*	*0.12*	*0.06*	*0.07*	*0.49*	
Okareka												
T1	77.81	12.31	0.18	0.90	0.08	0.11	0.76	3.87	3.81	0.17	6.88	27
	0.23	*0.11*	*0.07*	*0.11*	*0.05*	*0.06*	*0.09*	*0.14*	*0.15*	*0.04*	*1.07*	
T2	77.67	12.28	0.15	0.86	0.09	0.10	0.77	3.76	4.16	0.15	4.12	13
	0.21	*0.08*	*0.07*	*0.08*	*0.04*	*0.05*	*0.05*	*0.09*	*0.05*	*0.02*	*1.75*	
T3	77.76	12.20	0.21	1.02	0.07	0.18	1.02	3.97	3.43	0.14	3.76	37
	0.19	*0.09*	*0.07*	*0.10*	*0.05*	*0.05*	*0.06*	*0.10*	*0.07*	*0.03*	*2.05*	
Te Rere												
T1	77.37	12.48	0.21	1.03	0.09	0.17	1.00	4.30	3.19	0.16	3.99	209
	0.35	*0.16*	*0.07*	*0.13*	*0.06*	*0.07*	*0.07*	*0.17*	*0.11*	*0.05*	*2.12*	
T2	77.60	12.12	0.15	0.86	0.08	0.07	0.64	3.84	4.47	0.18	5.43	33
	0.30	*0.21*	*0.06*	*0.10*	*0.05*	*0.04*	*0.12*	*0.35*	*0.24*	*0.05*	*1.36*	
T3	77.22	12.53	0.30	1.00	0.06	0.19	1.23	4.20	3.15	0.12	1.89	11
	0.18	*0.09*	*0.09*	*0.15*	*0.07*	*0.06*	*0.07*	*0.11*	*0.06*	*0.03*	*0.42*	
Tuhua Volcanic Centre (peralkaline)[d]												
Tuhua	73.40	9.57	0.26	5.89	0.15	0.05	0.25	5.94	4.28	0.25	4.14	58
	0.42	*0.29*	*0.05*	*0.17*	*0.06*	*0.04*	*0.04*	*0.30*	*0.08*	*0.04*	*1.30*	
Tongariro Volcanic Centre (andesitic)[e]												
Okupata												
Hydro Access Rd	67.52	16.14	0.79	3.86	0.20	0.78	4.10	3.57	2.86	0.24	1.40	10
	1.00	*1.08*	*0.19*	*0.66*	*0.06*	*0.14*	*0.59*	*0.27*	*0.21*	*0.04*	*1.30*	
Kaipo bog	68.71	15.61	0.79	3.41	0.15	0.90	3.37	3.93	2.97	0.16	3.19	11
	1.23	*0.84*	*0.11*	*0.25*	*0.09*	*0.10*	*0.69*	*0.16*	*0.16*	*0.04*	*2.21*	
Egmont Volcano (andesitic)[f]												
Konini												
Kaipo bog	65.24	17.40	0.72	3.25	0.21	1.03	2.79	4.97	4.23	0.19	2.16	8
	0.34	*0.50*	*0.09*	*0.51*	*0.04*	*0.25*	*0.46*	*0.34*	*0.21*	*0.04*	*0.75*	
Pukaki crater	64.31	17.02	0.73	4.03	0.20	1.32	2.86	4.58	4.72	0.21	0.70	10
	0.66	*0.26*	*0.06*	*0.23*	*0.08*	*0.10*	*0.22*	*0.38*	*0.29*	*0.04*	*0.60*	

[a]Analyses recalculated to 100% on a volatile-free basis and expressed as a mean and standard deviation (italics) in wt%. Total Fe as FeO, water by difference from original analytical total, *n* = number of shards analysed, na = not available. Analytical methods for rhyolitic and peralkaline tephras were described in Smith et al. (2005).

[b]Data for rhyolitic tephras all from Smith et al. (2005) except Okareka, Kawakawa/Oruanui, Okaia from P.A.R. Shane (unpubl. data). See also Smith et al. (2006) for data on Rotoma, Mamaku and Whakatane eruptives.

[c]T1–T3 represent separate magma types (early to late eruptive phases, respectively) identified by Smith et al. (2005).

[d]Data from P.A.R. Shane (unpubl.).

[e]Data from Donoghue et al. (1999) (Hydro Access Rd sample 10) and Lowe et al. (1999) (Kaipo bog, anal. 18).

[f]Data after Lowe et al. (1999) (Kaipo bog, anal. 19a) and Sandiford et al. (2001) (Pukaki crater, anal. AT191).

2.6.3 Tephrostratigraphy: post-60 ka deposits

The current New Zealand tephrostratigraphic record is neither complete nor uniform in space or time. Only the post-60 ka record is well established. However, there are chronologically well-constrained tephra beds dating back to more than 10 Ma. Some tephra beds cover most of the North Island of New Zealand, are also found in the South Island, and extend as much as 1400 km from vent into the Pacific Ocean. For the last 60 ka, most eruptions are well documented and source vents are known. The tephra beds provide a stratigraphy for much of the North Island.

Key palaeoenvironmental tephra markers beds include the Kaharoa (636 ± 12 cal. yrs B.P.), Taupo (1,717 ± 13 cal. yrs B.P.), Tuhua (7,005 ± 155 cal. yrs B.P.), Konini (11,720 ± 220 cal. yrs B.P.), Waiohau (13,635 ± 165 cal. yrs B.P.), Rerewhakaaitu (17,625 ± 425 cal. yrs B.P.), Kawakawa (27,097 cal. yrs B.P.) and Rotoehu (c. 60 ka) (Lowe et al., 2008). These and other tephras have been used widely as tephrochronological markers in a range of disciplines and environments (e.g. Lowe and Newnham, 1999; Alloway et al., 2007b).

The c. 27,100 cal. yrs B.P. Kawakawa eruption from Taupo centre provides a convenient marker to divide the post-60 ka tephra sequence, and also marks a major change in the chemistry and mineralogy of Taupo eruptive units. Tephra beds erupted from Taupo in the last c. 27,000 years can easily be distinguished from Okataina-derived units on the basis of electron microprobe analysis (EMPA) data (shown in Table 2.3) using simple binary plots of oxides, although individual eruptive events in this short time interval are difficult to distinguish. Taupo tephra beds (< 27 ka) are distinguished by their lower SiO and higher FeO contents compared with Okataina units. Ages on these and other tephra beds provide a framework for global climatic and sea-level change recorded in New Zealand, and allow direct correlation between the marine and terrestrial records (Shane, 2000).

Chapter Three

Methodology



3.1 Coring

Coring was carried out over the summer and autumn of 2007 using a boat, *Surveyor*, which had been specially modified for coring, and a small anchored twin-hulled coring barge built at the University of Waikato (Fig. 3.1).



Figure 3.1: *Surveyor* and barge at Sulfur Point, Lake Rotorua

3.2 Core location

A geophysical survey was undertaken on Lake Rotorua in late 2006-early 2007. This survey used two echo-sounding techniques that ran simultaneously: a multibeam echo-sounder and sub-bottom profiler with a low-frequency echo-sounder. The multibeam survey was undertaken on Lake Rotorua between August and November 2006 by Dirk Immenga, Brad Scarfe and Alex Schimel, from the University of Waikato's Coastal Marine Group within the Department of Earth and Ocean Sciences. They used a SIMRAD EM3000 Multibeam Echo-sounder at 300 kHz, aboard the University of Waikato vessel, *Tai Rangahu*. Tracks were run from the 10 m water depth contour. These data were then used in conjunction with shallow (< 10 m) echo-sounder tracks to create a detailed bathymetric map. A feature of the map is the revelation of large 'pockmark' features (Fig. 3.2). The lake floor has many pockmarks of 20-60 m diameter, 0.5-0.6 m deep that are circular, flat bottomed depressions. The pockmarks are usually located in areas where the sediments contain gas. The deeper pockmarks are only found in water depths greater than 15 m and show a 3-5 m decrease in the sediment surface elevation (Fig. 3.2).

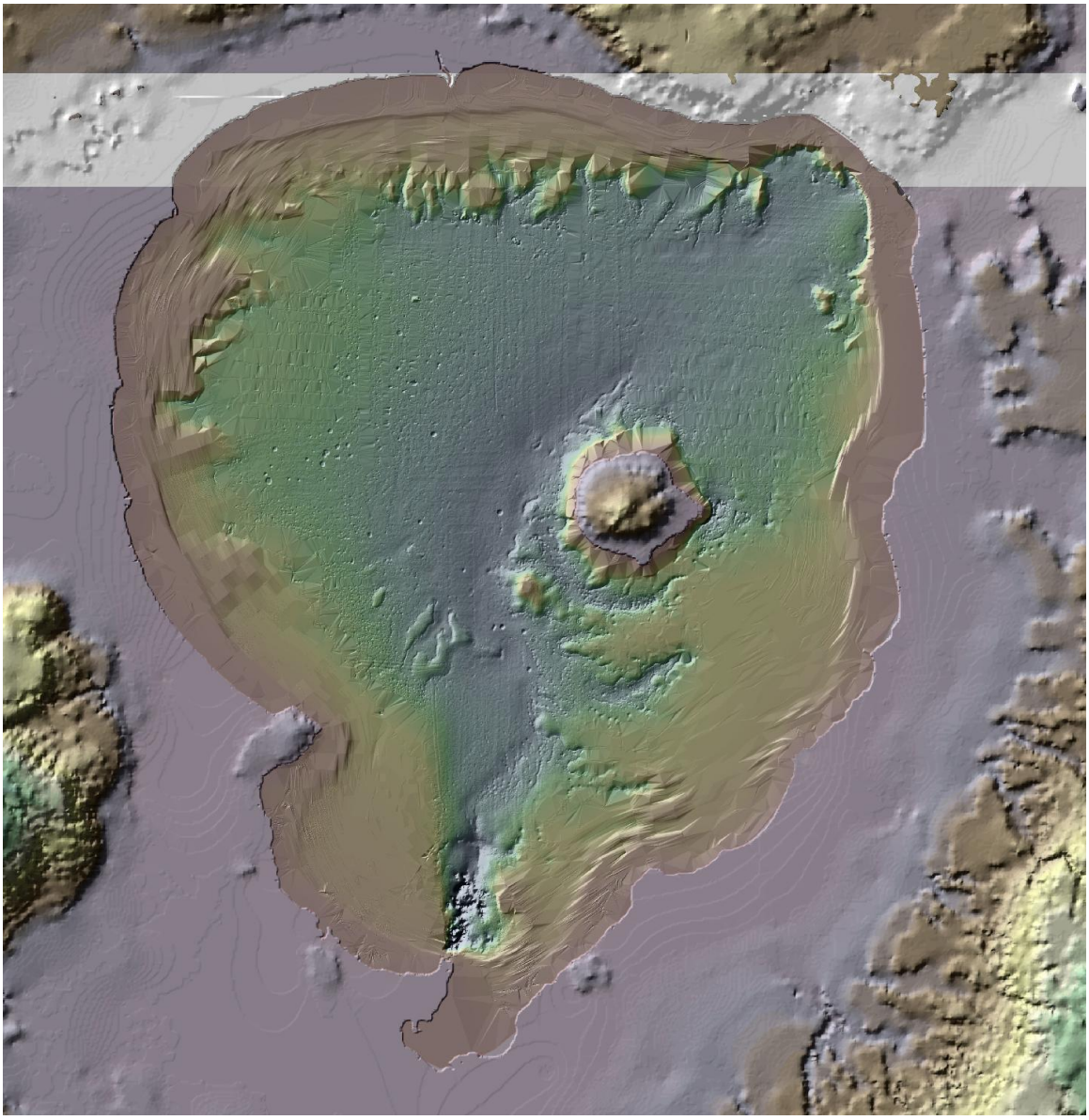

Figure 3.2: Bathymetric map of Lake Rotorua (constructed by Brad Scarfe)

Sub-bottom profiles of the pockmarks show that gas has been lost from the overlying sediment making the stratigraphy visible in the sediments associated with the pockmarks. Evidence of 'pockmarks' was first reported in the 1970s from side scan records off the Scotian Shelf. These pockmarks were first described as 'concave, crater-like depressions' (King and MacLean, 1970). Pockmark features have since been widely reported in a variety of continental margin settings, deltas, and areas of petroleum production or tectonic activity all over the world by numerous authors (e.g. Gay et al., 2006a, 2006b; Rodgers et al., 2006). Gas is not usually observed directly beneath a pockmark, allowing imaging of sub-bottom reflectors

beneath pockmarks that are obscured by gas nearby. This observation suggests that the escape of the gas and associated pore waters formed the pockmark (Rodgers et al., 2006). The examples found on the seafloor can be hundreds of metres wide and tens of metres deep, and thus the examples found in Lake Rotorua are relatively small by comparison.

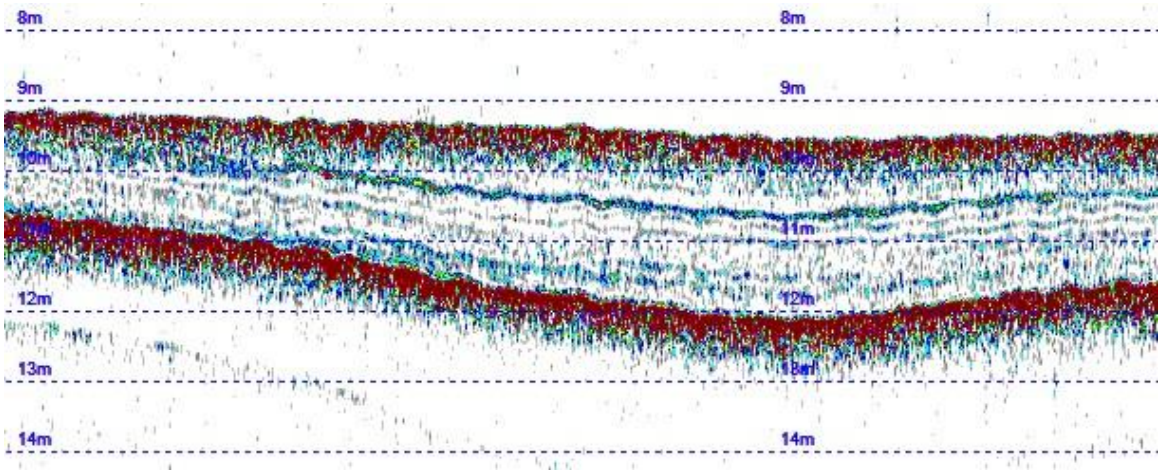

Figure 3.3: Low frequency echo sounder example of reflectors, inferred to be tephra layers

A low-frequency single beam echo-sounder (KNUDEN 320 MP) was used to give insight into the sediment layers. Sub-bottom profiling was carried out using the frequency 33 kHz. The echo-sounder was run in track lines from the shore to the 10 m water depth contour to complete the bathymetric map. The echo-sounder was also run in the centre of the lake but was unable to give a complete sediment record due to the interference by gas trapped in the sediment. However, the pockmarks found in these > 10 m water depths revealed detailed layers subsequently identified by coring as tephras (Fig 3.3).

Previous work carried out by Fish (1979) and Pearson (2007) revealed that sediment found in Rotorua in < 10 m water depths is subject to constant reworking from wind generated surface waves. A combination of bathymetric mapping and sub-bottom profiling was used to determine coring locations with cores taken only in areas in water depths greater than 10 m. The first cores were taken in a deep trench located west of Mokoia Island (Table 3.1) in one of the larger pockmarks found in the lake. This was thought to be an ideal place because sub-bottom profiling revealed the

likely presence of multiple tephra layers. However, coring of these pockmarks showed the sediment within them had been disturbed. This disruption was thought to be due to the release of methane gas trapped within them, so these cores proved to be of no use for this particular project.

Coring also proved difficult because of the weather – wind often prohibited coring or made the primary coring sites unworkable. Lake Rotorua's proximity to the Bay of Plenty coast results in weather being partly affected by the sea. Early in the afternoon each day the lake became influenced by a sea breeze which strengthened as the day progressed. Because of this wind, the coring barge was moved to the north-east of Mokoia Island providing a site that was sheltered for most of the day.

In total twelve cores (Table 3.1) were retrieved from Lake Rotorua before a suitable core was recovered. This core, RU188, has been used as the basis of this research. The core contains a number of rhyolitic tephra and one andesitic tephra, all derived from volcanoes in the TVZ.

Table 3.1: List of Lake Rotorua coring locations

Core	**Date collected**	**Latitude (south)**	**Longitude (easting)**
RU177-07	01/02/2007	38° 05' 00"	176° 17' 7.5"
RU178-07	01/02/2007	38° 05' 59.6"	176° 17' 6.7"
RU179-07	02/02/2007	38° 05' 59.7"	176° 15' 28.6"
RU180-07	02/02/2007	38° 06' 0.3"	176° 15' 33.5"
RU181-07 – RU183-07	Disturbed or short cores (26/02/2007 – 05/03/2007)		
RU184-07	08/03/2007	38° 07' 46.8"	176° 15' 51.2"
RU185-07	08/03/2007	38° 07' 46.8"	176° 15' 51.2"
RU186-07	08/03/2007	38° 04' 53.2"	176° 16' 08.5"
RU187-07	09/03/2007	Liquefied during retrieval	
RU188-07*	19/04/2007	38° 04' 32.9"	176° 17' 69.9"

* used in this project

3.3 Onboard methodology

As discussed above, geophysical and core data from previous research on Lake Rotorua were used to determine initial site selection. Onboard methodology follows

that of many other coring boats: in this case a modified Livingston piston coring method was used to retrieve the cores, followed by some processing onboard (separating and cutting). However, much of this processing (photography and description) was carried out on land whenever possible.

3.3.1 Coring

Lake sediments are collected using a variety of methods, mainly through piston coring. Typically a piston corer is rammed into the lake bed which allows the collection of sediment with relatively little deformation or compression (Green and Lowe, 1992b). All cores from Lake Rotorua were collected using a modified Livingston piston coring system. This system was modified to suit our requirements. The corer consists of a 3 m long, 50 mm diameter stainless steel tube core barrel fitted for wire-line piston coring, a stainless steel core catcher, a 3 m hammer rod, and a 20 kg lead hammer (Fig. 3.4).

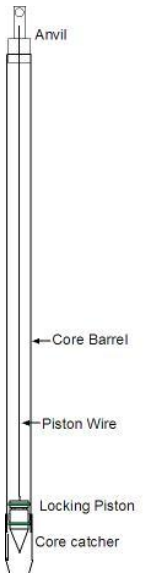

Figure 3.4: Coring set up consisting of and anvil which connects to the hammer rod, a 3 m long, 50 mm diameter, stainless steel core barrel fitted with a wire line connected to the locking piston, a locking piston, and a stainless steel core catcher.

Before deployment, a locking piston was fed through to the base of the core barrel and a core catcher attached to the base of a 3 m core barrel. The locking piston permitted control over core depth location allowing cores to be collected from the same spot but at different sediment depths.

A 3 m long hammer rod with a 20 kg hammer was attached to the top of the core barrel. The corer was then fed through 150 mm diameter PVC piping, adding additional aluminium tubing to the top of the hammer rod, down to the base of the water column (previously measured). The hammer was then manually lifted, driving the corer into the sediment. When the barrel had been driven approx. 3 m into the sediment the whole system was lifted up and dismantled piece by piece. This lifting triggers the core catcher which prevents the sediment from falling out the bottom of the core barrel (Fig. 3.5).

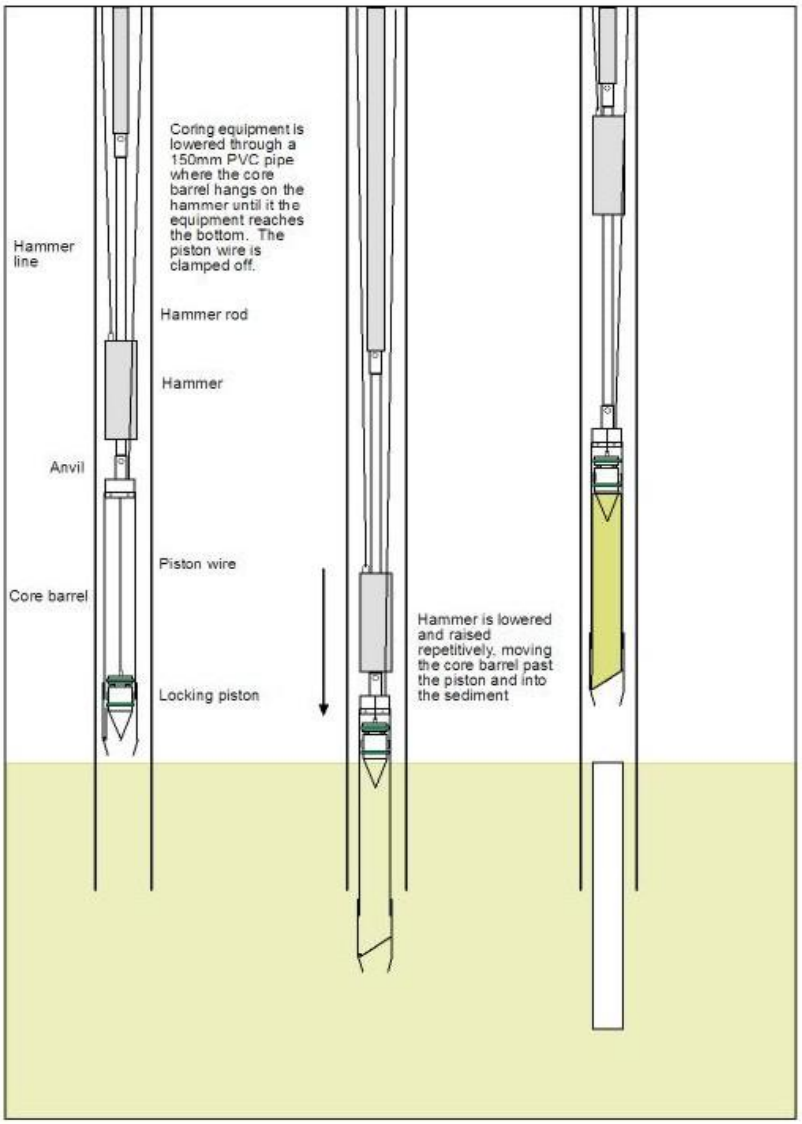

Figure 3.5: Coring method – Stage 1: the coring equipment is fed down through a PVC pipe; Stage 2: the hammer is manually lifted to push the core barrel into the sediment; Stage 3: the coring equipment is lifted up to the boat and the sediment is extruded.

3.3.2 Core processing

Following the removal of the core catcher, the sediment is extruded by winching a standard piston down through the core barrel. The sediment core is then feed into longitudinally sectioned PVC tubes to contain it.

Individual core sections were labelled according to convention (Fig. 3.6), with all core sections receiving a unique identifier including the year of core collection, the unique sequential number of the core, and the core section in Roman numerals with the uppermost section labelled as "I". The depth interval was also recorded on each core section.

The core was then split using a wire cutter and wrapped tightly in plastic wrap so it could then be photographed and described when back on land.

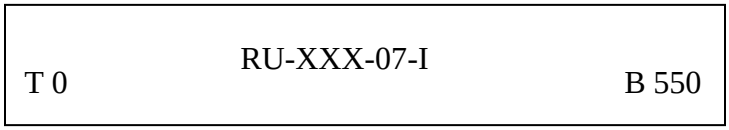

Figure 3.6: Core labelling procedure. Cores were then split into two halves and each covered in plastic wrap to prevent drying.

3.4 Core description

Following splitting, the most intact halves of the core sections were cleaned by scraping the exposed core surface back to a uniform flat surface to ensure any sedimentary or structural features became evident and distinguishable from any features originating from the core splitting process. Section lengths and top and bottom depths of the sections were checked and recorded on a standard sedimentary logging sheet (Appendix A). A visual core description was then made. Descriptions generally included lithology, sedimentary structure (if present), colour, evidence of bioturbation, texture (grain size), possible chemical changes (e.g. sulfide reduction), and any coring disturbance features.

3.5 Sampling

Few samples were collected during the description of the core. Most were collected once back at the laboratory. However, samples of seeds and leaves were removed and stored when found. Tephra and sediment samples were collected in the laboratory for elemental analysis, grain size analysis, total organic carbon and total nitrogen determinations, diatom identification, and biogenic silica analysis.

3.5.1 Tephra

Tephra horizons were recognised as white to pale grey, millimetre to centimetre thick layers within the lake sediment. They varied from laminar bedding to massive, pumice- or vitric-rich, coarse lapilli- to fine ash textured layers. The majority of the tephra layers exhibited primary depositional features with sharp bases. Some showed evidence of normal grading, possibly indicating different eruptive phases especially in those layers that were erupted from volcanoes proximal to the lake.

3.5.2 Radiocarbon samples

Seeds and leaves were removed from the cores and put into small, labelled plastic bags. Some of these were then sent to the University of Waikato Radiocarbon Dating Lab. Unfortunately these samples proved too small to be analysed even by AMS. Consequently, additional samples of bulk lake sediment were taken and used for dating instead.

3.5.3 Sediment samples

Sediment samples approximately 0.5 cm thick were cut from the core at 1 cm intervals. These samples included the thinner tephras but avoided the thick Kaharoa and Whakatane tephras, giving in total 689 samples. Each sample was placed on a small watch-glass and left to dry overnight in a 50°C oven. Once dry, the samples were lightly crushed and placed in labelled glass vials.

3.6 Laboratory methods

3.6.1 Sample preparation

The working half of core RU188 was used for analysis. High-resolution measurements of magnetic susceptibility and spectrophotometry were performed every 2 cm, and an x-ray record provided evidence of sediment structures and density changes within the core without destroying it.

Tephra samples were wet sieved. A beaker containing the sample and distilled water was placed in a sonic bath for 10 minutes to separate the grains and diatomaceous ooze and allow for easy movement through the mesh. This mixture was then washed through meshes > 1 mm, 1 mm-250 µm, 250 µm-63 µm, and <63 µm, and each fraction dried on glass watch-glasses in a 50°C oven. These samples were then transferred into small labelled glass vials. The 250 µm-63 µm fractions were then separated into heavy minerals, plagioclase and glass. The glass was mounted into resin blocks for major and trace element analysis using the electron microprobe (EMPA) and laser ablation inductively coupled plasma mass spectrometry (LA-ICP-MS), and the heavy minerals mounted on thin sections for optical analysis using a petrological microscope.

As stated above sediment samples were taken at 1 cm intervals. These samples were then separated as needed for various analyses.

3.6.2 Non-destructive techniques

3.6.2.1 X-ray images

Radiography is a technique of making a picture by some form of penetrating radiation such as X-rays. It has been widely used in medicine, industry and in various natural sciences, but its application to geology has been largely limited to palaeontology. However, it is very useful in identifying the laminations found in sediment cores (Hamblin et al., 1962) and for tephras (e.g. Lowe et al., 1981).

Images were taken at Hamilton Radiology, with the best images obtained with a fine focus lens and the following parameters: exposure for 39.6 ns at 40 kv and 8 mAs with from a distance of 1 m. One of the problems encountered with x-

radiography is a common phenomenon causing a slight blurring near the top of the x-ray. We tried multiple ways to eliminate this from the images but to no avail, hence the laminations were unable to be counted accurately enough to assist the chronology.

3.6.2.2 Colour reflection

Colour reflectance was measured on split-core surfaces, using diffuse-reflected spectrophotometry, to provide quantitative descriptions of sediment colour. Light reflected from the material is collected in an integration sphere, normalized to the source light of the reflectance, and calibrated with the measurement of a pure white standard (100% reflection) and a black box (zero reflection) over the entire wavelength spectrum of visible light. Reflectance spectra are related to colour using established international conventions. The reflectance was measured at NIWA in Wellington using a Minolta Spectrophotometer CM-5089 about 6 months after the cores were first opened. The colours may have changed a small amount even though the cores were stored in a 4° refrigerator to minimize redox-associated colour changes. The data are given using the CIELAB system, which provides lightness (L^*) and chromaticity (a^* and b^*) parameters. This method has allowed various parameters to be determined more easily than traditional methods and thus prevents destroying the core.

The colour and variations in colour can be used to interpret variations that occur within one core or between cores. A quantitative description allows the data to be analyzed in a formal manner and correlated with other data sets (e.g. carbonate content).

The two most common uses of colour reflectance data are:

(1) Colour components, such as L*a*b*, provide detailed time series of relative changes in the composition of the bulk material and are frequently used to correlate sections from core to core or hole to hole and to analyze the cyclicity of lithologic changes;

(2) Spectral data, which can be used to estimate the abundance of certain minerals.

3.6.2.3 Magnetic susceptibility

Magnetic susceptibility is used to measure and identify the magnetic properties of sediments. In particular it is a measure of the ease with which particular sediments are magnetised when subjected to a magnetic field. There are two primary reasons for doing this. The first is that, under specific conditions, lake sediments can preserve and record variations in the direction and strength of the Earth's geomagnetic field. The second is that the type, concentration and grain-size of magnetic minerals found in lake sediments varies according to a variety of processes operating in response to climate, human activity and lake processes (Sandgren and Snowball, 2001).

Strongly magnetisable minerals include the ferromagnetic minerals such as magnetite, hematite, iron titanium oxides, and pyrrhotite, making this technique valuable when identifying tephra within lake sediments. This technique can also identify moderately magnetisable (paramagnetic) minerals including a broad array of substances all of which contain Fe^{2+}, Fe^{3+}, or Mn^{2+} ions, and may include clay minerals (chlorite, smectite and glauconite), iron and manganese carbonates (siderite, rhodochrosite), ferromagnesian silicates (olivine, amphiboles, pyroxenes, etc.), as well as a variety of ferric-oxyhydroxide mineraloids.

Magnetic susceptibility was measured using the Bartington MS2F Magnetic Susceptibility probe at the National Institute of Water and Atmospheric Research (NIWA) in Wellington.

3.6.3 Tephra samples

3.6.3.1 Magnetic separation

Magnetic separation takes advantage of differences in the magnetic properties of minerals. Minerals fall into one of three magnetic properties: ferromagnetic, paramagnetic and diamagnetic. Ferromagnetic minerals are themselves magnetic (i.e., magnetite and pyrrhotite) and can be easily separated from other minerals with a magnet because they will stick to the poles of a magnet. Paramagnetic and diamagnetic minerals are not magnetic, but they differ in how they interact with a magnetic field.

Paramagnetic minerals are weakly attracted into a magnetic field and diamagnetic minerals are weakly repelled by a magnetic field. Therefore, if a mixture of paramagnetic and diamagnetic minerals is passed through a magnetic field, they will be pulled into the field (paramagnetic) or repelled from the field (diamagnetic) and may be separated.

The device used to separate minerals based on their magnetic properties is a Frantz Isodynamic Magnetic Separator. It consists of a large electromagnet through which mineral mixtures can be passed on a metal trough which is divided near its exit end. Varying the strength of the magnetic field and slope of the separation trough is used to separate minerals (Svoboda, 2004). Two separators were available, one set vertically and the other tilted. The vertical separator allows for the extraction of strongly magnetic ('heavy') minerals, whereas the tilted one permits the separation of paramagnetic and diamagnetic minerals (otherwise referred to as 'non-magnetic').

Tephra samples, 250 µm-63 µm fractions, were separated into magnetic ('heavy') and non-magnetic ('light' – glass and feldspar). Using a vertical Frantz magnetic separator initially removed the strongly magnetic minerals with a magnet. The light (less magnetic) fraction was further separated glass and feldspar using a tilted Franz.

3.6.3.2 Grain mounts

Standard thin sections were made using the 250 µm-63 µm heavy mineral fraction, extracted as described above, mounted into epoxy resin grain mounts. Optical microscopy techniques then allowed for the identification of heavy minerals common in New Zealand tephras such as hypersthene, hornblende, augite (especially high-Ca augite which is commonly associated with Egmont eruptives), and cummingtonite.

3.6.3.3 Resin mounts for EMPA and LA-ICP-MS

For EMPA and LA-ICP-MS analysis the 250 µm-63 µm glass fractions were mounted in small resin disks (Fig. 3.7) which were then polished using an alumina or fine diamond polish.

These blocks were taken to the Electron Microprobe Facility at Victoria University Wellington, where they were subjected to major element analysis (discussed in chapter 5).

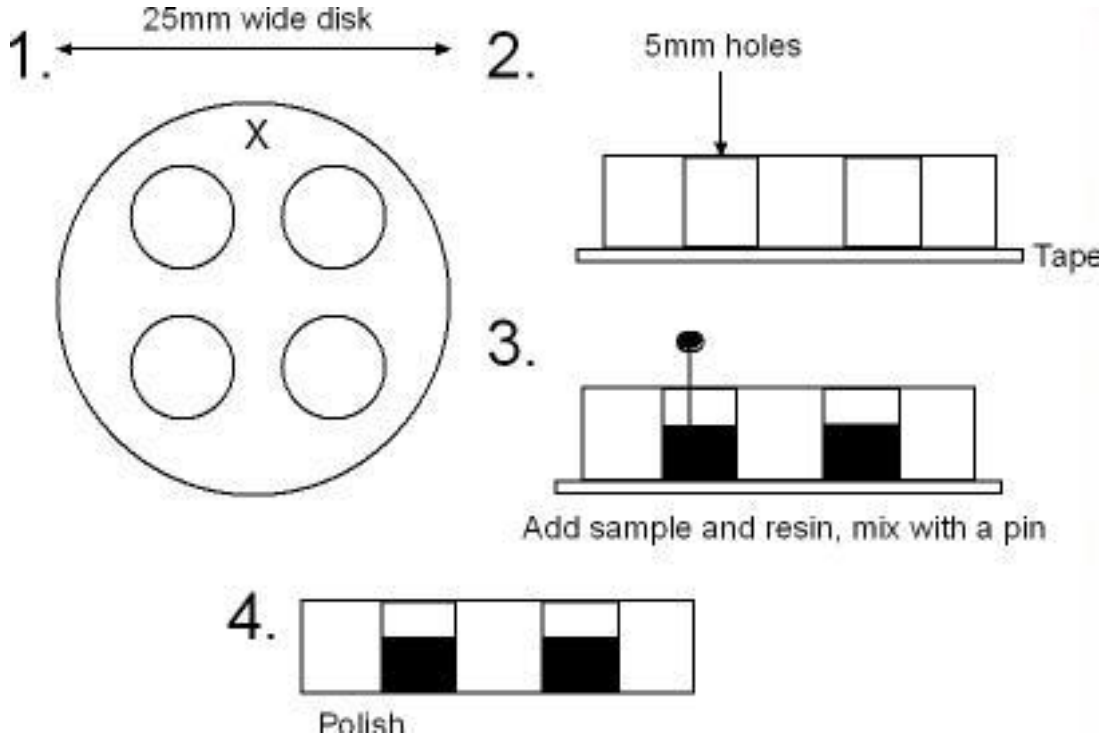

Figure 3.7: Steps for constructing a mount for EMPA and LA-ICP-MS. 1) Make a resin disk 25 mm wide, drill out 5 mm holes all the way through the block, and mark the top and the bottom so you can orientate your sample. 2) Tape the bottom, smooth side of the disk with double sided tape. 3) Pour some of your glass sample onto the tape and then fill the hole with resin, agitate with a pin to remove any air bubbles and ensure the glass is mounted correctly in the resin. 4) Remove the tape once the resin is set and polish carefully using either an alumina or diamond polish. NOTE: Do not use any polish with rare earths in it or you will ruin your sample for analysis of such elements.

3.6.4 Sediment samples

The sediment samples were separated for the various analyses – elemental analysis, total carbon and total nitrogen, grainsize analysis, diatom identification, biogenic silica, and ^{14}C dating. For some analyses, representative samples were taken from throughout the core. Because of the large number of samples some analyses were only carried out on representative samples, which provide windows at various depths. These representative "window" samples were taken at: 30-39, 60-70, 350-360, 390-400, 530-540, 556-566, 600-610 and 640-650 cm depth.

3.6.4.1 Elemental analysis

3.6.4.1.1 Sediment digestion using aqua regia

Sediment samples were digested using reverse *aqua regia* (3 HNO_3: 1 HCl). Approximately 0.1 g of dried sediment was weighted out and placed in a pre-weighed 50 ml centrifuge tube. The samples were placed in a digestion block where 0.6 ml of HNO_3 and 0.2 ml of HCl were added to each tube to form reverse *aqua regia*. The centrifuge tubes were left to stand in the digestion block to digest over night and remove the majority of the organic matter.

The next day the samples were heated in the digestion block at 50 °C for 1 hour. After digestion the samples were removed from the block and allowed to cool, then 30 ml of Type 1 water (ultra purified) was added (the amount of water depends on the amount of nitric acid added), capped, mixed and left to settle. Once the samples had settled they were placed in a centrifuge for 15 minutes at 4000 rpm. This centrifuging removes the residue from the liquid sample. A 10 ml sample of the centrifuged mixture was pipetted into a 15 ml tube for analysis by ICP-MS. The remaining acid solution was decanted into new 50 ml plastic centrifuge tubes and placed in storage. A blank reagent and quality assurance solution were run with each of the sample batches**.**

3.6.4.1.2 Digestion analysis

ICP-MS determines the concentration of a large number of elements. Phosphorus, iron, manganese, arsenic and sulfur are considered the most significant of these; the others have been classified into the following groups – heavy metals, alkalis, alkali

earth elements, and others of known and unknown source. The concentrations of each element were plotted against sample depths.

Concentrations of elements from ICP-MS analysis were calculated using the amount of material digested and dilution used for the analysis as follows: the concentration of an element in solution ($C_{x(soln)}$) (µg/L), divided by the weight of the dry sediment digested (M_s) (g) times the volume of solution made up to ($V_{(final)}$) (ml). This gives the final result in µg/g.

$$C_{x(soln)} = (R_{x(ICP)}/M_{(S)})*V_{(final)}$$

3.6.4.2 Grain size analysis

Grain size analysis was undertaken at 1 cm intervals, on eight 10 cm-long sections. The samples were treated with 10% H_2O_2 to remove organic matter, then when this solution stopped bubbling, 2M Na_2CO_3 was added to dissolve the diatoms. This solution was left until it stopped fizzing. Samples were mixed with a vortex mixer before being measured with a Malvern Mastersizer 2000 laser particle sizer. Grain size was measured from 0.05 µm up to 2000 µm, and each sample was analysed five times. These replicates were then averaged. Sample data are presented as mean size, sand/silt/clay proportions, and percentage > 32 µm and > 63 µm. The latter grain size ranges (> 32 µm and > 63 µm) are used as an indicator of clastic sediment influx into a lake (e.g. Augustinus et al., 2008).

3.6.4.3 Carbon and nitrogen analysis

Total organic carbon (TOC) and total nitrogen (TN) analyses were carried out at the Isotope Laboratory at the University of Waikato using a LECO TruSpec CN Carbon/Nitrogen Determinator. Approximately 0.1 g of each sample was weighed out into a tin foil cup and twisted to seal the contents in the foil. The sample was then placed in the CN analyzer and underwent the three phases in the analysis cycle: purge, combust and analyse. In the purge phase the encapsulated sample was placed in the loading head, sealed and purged of any atmospheric gases that may have entered during sample loading (LECO Corporation, 2006). The sample was then dropped into a hot furnace (950°C) and flushed with oxygen for a very rapid and

complete combustion. The products of the combustion phase were passed through a secondary furnace (850°C) for further oxidation and particulate removal. In the analysis phase, oxygen was mixed with the combustion gases and purged through a CO_2 infrared detector and a 3 cm^3 aliquot loop (LECO Corporation, 2006).

Once the gases had equilibrated, carbon was measured as carbon dioxide by the CO_2 detector. The gases in the aliquot loop were transferred to a helium carrier flow, swept through hot copper to remove oxygen and change NO_x to N_2, and then through 'Lecosord' and 'Anhydrone' to remove carbon dioxide and water, respectively (LECO Corporation, 2006). A thermal conductivity cell was used to determine nitrogen content. The final results were calculated and expressed as weight percentage of carbon and nitrogen in the dried sample.

3.6.4.4 Scanning electron microscopy (SEM)

Eleven samples were chosen to be examined using a SEM to identify the diatom compositions in different coloured laminations and to investigate causes for the changes in colour. The SEM at the University of Waikato is a Hitachi s-4100 Field Emission. The samples selected from the core were taken at 30, 32, 350, 351, 358, 359, 390, 391, 392, 396 and 400 cm depth. Samples were mounted on a small stub using double-sided carbon tape, with two samples per stub. A small amount of sample was placed on one section of the tape and then a small handheld pump was used to remove excess sediment from the tape. The first sample is then covered and this process repeated for the other sample. The stub was then placed in a Hitachi sputter (platinum) coater. This high vacuum chamber coats the sample in platinum providing a conductive surface preventing electron charging of the sample surface in the SEM.

The sample stub can then be screwed onto the mounting plate in the SEM and introduced, under vacuum, into the sample chamber. Hand controls on the microscope are used to navigate around the sample, zooming in to identify different diatoms in the sample. Images were taken via a computer by slowing the image capture rate of the SEM and pressing the capture button on the capture computer.

General images were taken at a lower magnification to get a representative sample before increasing magnification to focus on single diatoms in each of the samples.

3.6.4.5 Biogenic silica

Biogenic silica (BGS) estimation was measured at 1 cm intervals, on four 10 cm-long sections: 30-39, 350-360, 390-400, and 556-566 cm. These samples were digested using a modified method of Mortlock and Froelich (1989) (as reported in Augustinus et al., 2008), and then the silica concentration in each sample were measured by ICP-MS at the University of Waikato.

3.6.4.6 Radiocarbon dating

Accelerator mass spectrometry (AMS) ^{14}C age determinations were carried out on four sediment samples from depths of 541.5, 621.5, 670.5 and 694.5 cm, at the Waikato Radiocarbon Dating Laboratory, University of Waikato. The samples received standard acid–alkali–acid pretreatments, with radiocarbon age calibration undertaken using OxCal 3 using the INTCAL04 dataset (Reimer et al., 2004). Radiocarbon years (before AD 1950) are reported as ^{14}C yr BP. Calibrated ages were reported as cal. yr BP and expressed with 2 sigma errors (95%).

Chapter Four

Core Stratigraphy and Chronology



4.0 INTRODUCTION

In this chapter I examine the stratigraphy and characteristics of the sediment and tephra found within the core, provide a rate of sedimentation, and supply a detailed chronologic framework, through the use of sediment-derived radiocarbon ages and tephrochronology, from which further interpretations can be made.

4.1 Coring Site

In April 2007, a 7.62-m long core, RU188, was retrieved from the lake floor to the north-east of Mokoia Island (Fig. 4.1). It is this core which is the basis for the following research.



Figure 4.1: Satellite image of Lake Rotorua, showing location of coring site for RU188-07 (Google Earth)

4.2 Sediment stratigraphy

RU188 covers a period of ~ 5,500 years. However, the topmost water-rich sediment of the past ca. 100 years is missing (this is typically not recovered by piston coring), but has been documented previously from box cores in Pearson (2007).

The lake sediment is predominantly made up of fine, slightly sticky, diatomaceous ooze with subtle colour changes ranging from olive to dark olive grey. This sediment is interspersed with layers of coarser grained inorganic material – which have been identified as tephra.

Distinct laminations are evident discontinuously throughout the core (Fig. 4.2 & 4.3). Some of these laminae faded in colour over time, in particular the yellow and orange-gold ones. In order to determine the nature of these laminations they have been examined by SEM analysis: the darker laminae tend to be dominated by inorganic grains indicating they have probably been washed in from the surrounding catchment, and the lighter laminae by diatoms (see Ch. 5). These laminae possibly represent annual banding and fine inorganic material washed in from the surrounding catchment during events associated with storms or long periods of heavy precipitation or from human activities. Alternatively, the laminae may originate from small underwater slumps or slides.

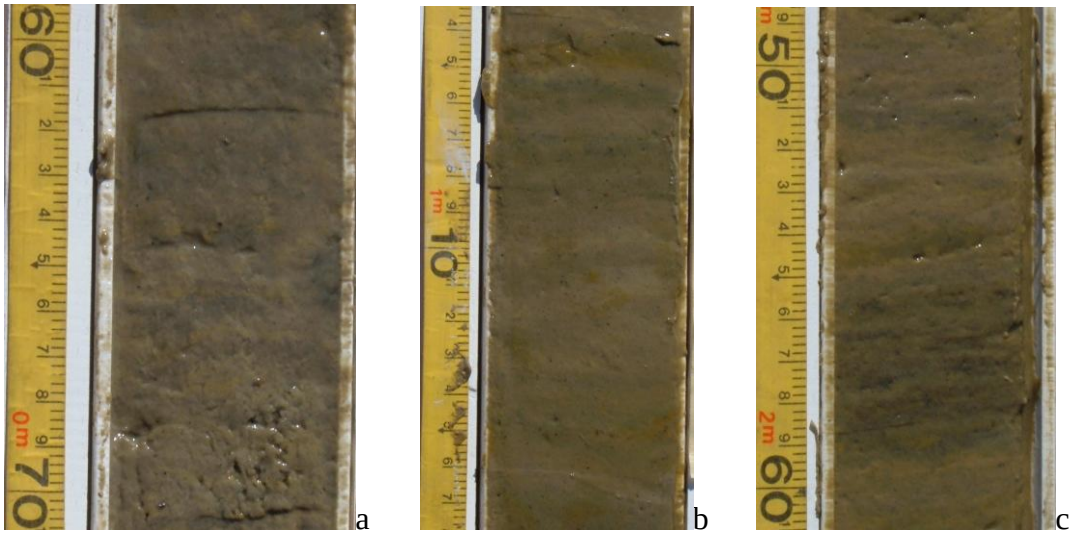

a b c

Figure 4.2: Photos showing examples of massive diatomaceous ooze (a) and laminated diatomaceous ooze (b & c).

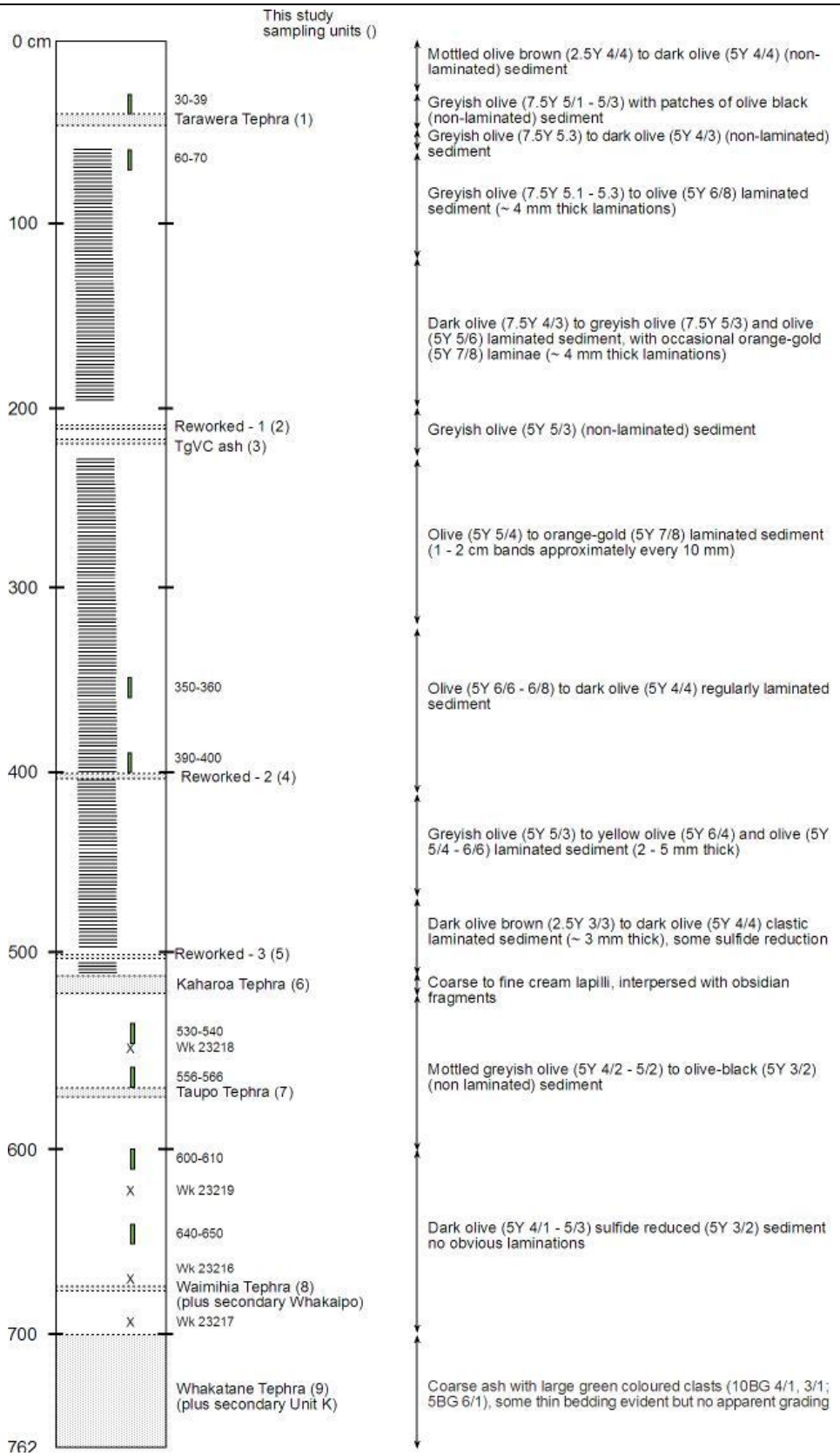

Figure 4.3: Summary of RU188-07, showing laminations, tephra depths, representative sampling positions (green blocks) and radiocarbon sampling positions (represented by X).

The uppermost 28 cm (Fig. 4.3) consists of a slightly mottled but massive olive diatomaceous ooze. This ooze is underlain by a thick layer (~ 15 cm) of grey (7.5Y 5/1; Munsell, 1967) Rotomahana Mud, extending from 28 cm and becoming denser to around 38 cm. This denser grey (N 6/0) mud is underlain by a small amount of black Tarawera Scoria. The first thin banding or laminations in the lake sediments are found at 65 cm depth. These bands ranged in colour from greyish olive (7.5Y 5/1 – 5/3) through to olive (5Y 6/8) and dark olive (7.5Y 4/3). There is also evidence of some sulfide reduction, in the form of dark mottled discolouration. Most bands are ~ 4 mm in thickness and are continuous to a depth of 210 cm.

The diatomaceous ooze between 210 cm and 225 cm is slightly different from the sediment above and below it in that it does not contain obvious banding, and is made up of light olive grey sediment, with a small amount of sulfide reduction evident near the top above the grey ash. There are two tephras contained within this greyish olive sediment. The upper tephra is a very thin band of reworked pale grey ash ("reworked 1") and the lower a thin reddish ash from the Tongariro Volcanic Centre ("TgVC ash"). The reddish ash is not evident as a definite bed as it is slightly diffused probably due to the nature of the sediment water interface when it fell. Its total thickness spans ~ 10 mm, but the actual bed as "pure" layer is only around 2-4 mm in places.

At around 230 cm depth the sediment is predominately olive (5Y 5/3) with thin (1-2 mm) intense orange-gold (5Y 7/8) laminations. These laminations occur at least every 10 mm, but some are very difficult to distinguish due to their light colour. The laminations continue down past 320 cm depth but the colour of the sediment is distinctly darker olive (5Y 6/6 – 6/8) to dark olive (5Y 4/4). A thin sloped band of slightly coarser, sand sized material is present around 340 cm. There is also a thin band of medium ash sized material around 400 cm. This lower layer has been identified as reworked tephra ("reworked 2").

Darker diatomaceous ooze ranging from grey to greyish olive and olive yellow begins at ~ 410 cm depth. A number of medium (2-5 mm) sized, yellow olive (5Y 6/4) and olive (5Y 5/4 – 6/6) laminations can be visually identified. However, there

is a large amount of sulfide reduction and the very mottled appearance makes it difficult to identify the true structure. The layers around 475 cm are darker indicating an increase of clastic inwashing after deposition of the Kahaora Tephra. At around 500 cm depth is a layer that is coarser than the normal sediment. This layer shows reverse grading from very fine sand to medium sand, and has been identified as reworked Kaharoa Tephra ("reworked 3"). The sediment between this layer and the actual Kaharoa Tephra is a very dark olive brown indicating a large amount of clastic material, also inferred to be inwash, within which small seed cases were found.

The Kaharoa Tephra, occurs at 504 cm and is largely made up of pumice, ranging from coarse to fine lapilli, and containing some smaller dark clasts of obsidian. The top boundary is slightly uneven with a flat base and a long tail on the left hand side due to disturbance during the coring process. This tephra is underlain by mottled olive and olive black diatomaceous ooze. At a depth of 556 cm is a dark layer of Taupo Tephra. This tephra consists of medium lapilli to coarse-ash-sized particles and is shaped like an upside down "U" which thins out on the outer edges to around 4 cm. This layer is up to 2 cm thick. The "U" shape is most likely due to deformation during the coring process.

The lower section of the core (pre-Taupo Tephra) is predominately made up of non-laminated dark diatomaceous ooze, indicating a large amount of sulfide reduction. There are some slight changes in texture from a mud to fine sand and the remains of seed cases have been recovered. They proved too small to be used for radiocarbon dating. The mottled appearance makes any fine structure difficult to distinguish. A 20 mm bed of lapilli is present around 674 cm, underlain by a section of dark olive (5Y 4/1 – 5/3) to greyish olive (5Y 3/2) diatomaceous ooze. This sediment gives way to a massive coarse ash with larger green coloured clasts at 700 cm, and continues to the base of this section. This ash is pale orange in colour and has been identified as the Whakatane Tephra.

4.4 Chronology

4.4.1 Radiocarbon dating

Four radiocarbon ages (Table 4.1) were obtained from samples of lake sediment submitted to the Radiocarbon Dating Laboratory at the University of Waikato (lab code Wk-) for dating using AMS ^{14}C. These samples were all obtained from sediment below the Kaharoa Tephra (1314 ± 12 A.D.) (Fig. 4.3). No samples were taken for dating above the Kaharoa Tephra because previous work has demonstrated that such lake sediments are invariably contaminated with "old" inwashed carbon (e.g. McGlone and Wilmshurst, 1999). Bulk carbon extracted from 541 cm provided an age of 3835 ± 30 ^{14}C yrs B.P., while the samples collected at 622, 670, and 694 cm depth provided ages in stratigraphic order ranging from 4763 ± 30 ^{14}C yrs B.P. to 5181 ± 30 ^{14}C yrs B.P. However, all these ages after calibration are too old to fit with the ages obtained from tephra identification. There are several potential reasons for this, all relating to contamination, e.g. hard water effect, remobilisation of old organics, ground water. In this case it is thought to be due to the introduction of old carbon into the system possibly through the release of methane gas from the lake sediments marked by pockmarks and possibly the geothermal vents.

Table 4.1: Summary of radiocarbon samples and calibration

	Depth (mm)	**Wk**	**δ C^{13} (‰)**	**% Modern**	**^{14}C ages (± 1σ)**	**Calibrated ages (cal. yrs B.P. (2 σ) ***
Sample 3, Core 8	5415-5420	23218	-24.6 ± 0.2	62.0 ± 0.1	3835 ± 30 BP	4290-4070 (87.8%) 4050-3990 (7.6%)
Sample 4, Core 9	6215-6220	23219	-18.7 ± 0.2	55.2 ± 0.1	4776 ± 34 BP	5590-5440 (54.7%) 5420-5320 (40.7%)
Sample 1, Core 10	6705-6710	23216	-31.8 ± 0.2	55.3 ± 0.1	4763 ± 30 BP	5490-5320 (70.6%) 5590-5500 (24.8%)
Sample 2, Core 10	6945-6950	23217	-27.7 ± 0.2	52.5 ± 0.1	5181 ± 30 BP	5940-5740 (95.4%)

* calibrated using OxCal 3 (Bronk Ramsey, 2001) and SHCal 04 (McCormack et al., 2004).

4.4.2 Magnetic susceptibility

The cores recovered from Lake Rotorua do not cover a period long enough to see changes in the Earth's magnetic field, but the application of identifying magnetic minerals, in particular the layers of tephra, proved to be very worthwhile and confirmed the suggestion that there are no obvious cryptotephras found within the core.

Lake Rotorua has a well defined catchment and receives sediment from numerous sources. The majority of minerals found in lake sediments are derived from erosion in the surrounding catchment and originate from bedrock and soils in the lake's drainage basin. They are transported as suspended load and/or bed load in the streams, or in some cases as overflow, which is eventually deposited in the lake. Magnetic minerals can also derive from atmospheric sources, from local and distant regions through aeolian processes (volcanic eruptions and dust transported by storms) or particles produced by anthropogenic activities such as the burning of fossil fuels (Sandgren and Snowball, 2001).

The magnetic susceptibility plot of core RU188-07 of Lake Rotorua shows little obvious input of magnetic minerals from the surrounding catchment. All the peaks appear to coincide with the tephra layers identified in the core, apart from one which corresponds to a slightly coarse layer likely to be clastic inwash. There are also a few small peaks believed to be reworked tephras, in particular Kaharoa Tephra, that have been deposited in the lake following significant erosion episodes in the catchment (Fig. 4.4).

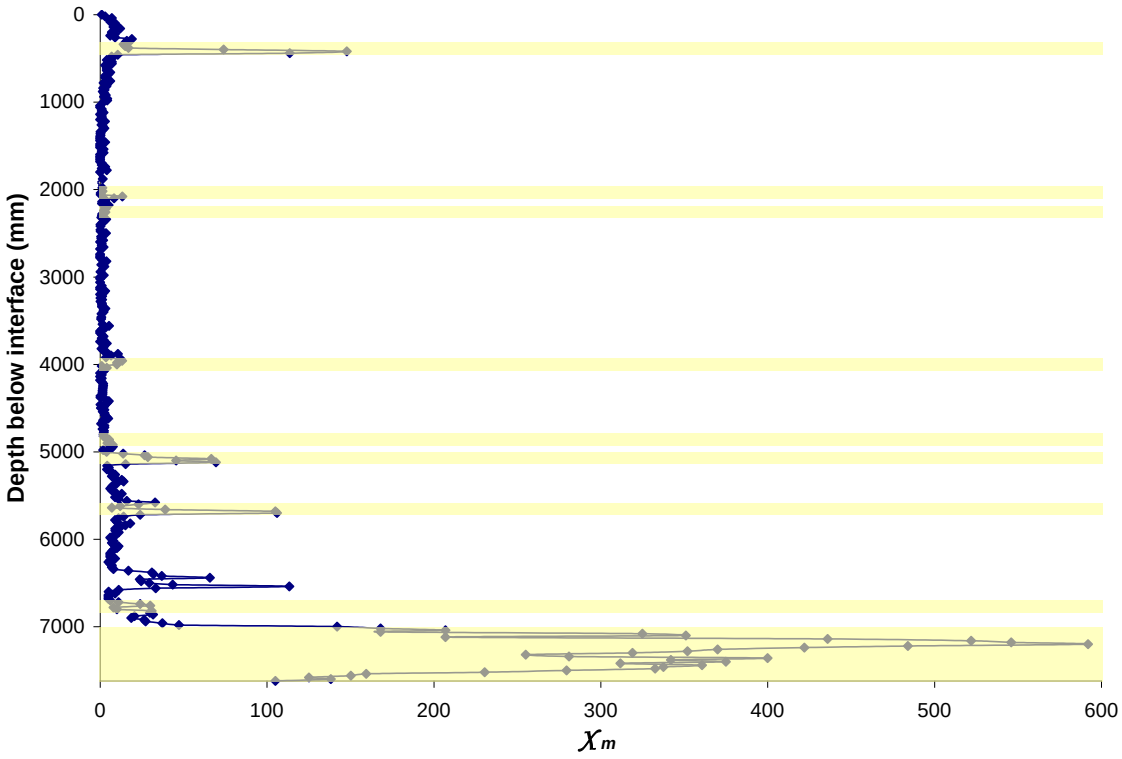

Figure 4.4: Plot of magnetic susceptibility. Peaks indicate large amounts of magnetic minerals present in the sediment and correlate to the tephras identified.

4.4.3 The stratigraphy, chronology, mineralogy, and correlation of tephras preserved in Lake Rotorua sediments

A total of nine tephra beds were located in RU188. These beds are informally numbered 1-9, 1 being the youngest, 9 being the oldest (Fig. 4.3). These tephra were identified on the basis of field appearance, stratigraphic position, ferromagnesian mineralogy, and major element glass chemistry.

4.4.3.1 Tephrostratigraphy

The nine tephra deposits ranged from a few millimetres in thickness to well over half a metre, and varied from fine normally graded ash to thick, non-graded lapilli sequences.

Rotomahana Mud (upper member of the Tarawera Tephra; Froggatt and Lowe 1990) forms a discontinuous grey medium ash layer up to 15 cm in thickness, and is underlain by a few millimetres of Tarawera Basalt (lower member of the Tarawera

Tephra; Froggatt and Lowe 1990). This eruption occurred on the 10th June 1886 A.D. from Tarawera Volcano in the Okataina Volcanic Centre (OVC).

Kaharoa Tephra (unit 6) is a 10 cm-thick layer comprising greyish-white, coarse pumiceous lapilli. This tephra is normally dominated by biotite, a diagonostic mineral for this tephra. Erupted from Tarawera Volcano, it has an age of 636 ± 12 cal. years B.P. (1314 ± 12 A.D.; Hogg et al., 2003).

Taupo Tephra (unit 7) is a creamy coloured, 2 cm-thick layer of coarse ash. It is derived from the Taupo Volcanic Centre. The Taupo Tephra corresponds to Unit Y of the volcanological units identified by Wilson (1993), and has an age of 1717 ± 13 cal. years B.P. (233 ± 13 A.D.; Sparks et al., 2008).

Informally-named, unit 8 is a 2 cm-thick bed of non-graded lapilli and fine ash. Identification was aided by major element analysis of glass. Glass from this layer closely matches analysis of Waimihia Tephra from other environments, including lakes Tutira and Poukawa (Hawke's Bay). This tephra was erupted from the TVC but the composition of glass differs from that of other Holocene eruptives from TVC by having lower CaO and FeO concentrations (Lowe, 1988; Stokes et al., 1992). Waimihia Tephra is also referred to as Unit S by Wilson (1993). Unit 8 also contained a second smaller population of glass that is possibly derived from the younger Whakaipo Tephra (Unit V of Wilson, 1993). Waimihia Tephra has an age of 3410 ± 40 cal. years B.P. (Lowe et al., 2008)

Petrological microscope analysis of ferromagnesian minerals was undertaken in only one of the nine beds – unit 9 comes from a massive bed of non-graded coarse ash and dark, hard lapilli sized material, occurring at 7 m to the base of the core. This unit's heavy minerals were found to contain an assemblage dominated by the pale green amphibole, cummingtonite. Only three beds, since c. 60 cal. ka, contain cummingtonite in high abundances and they are all characteristic of the nearby OVC eruptives, originating specifically from Haroharo volcano: Rotoehu (ca. 60 ka cal. yr B.P.); Rotoma (9505 ± 25 cal. yr B.P.) and Whakatane (5530 ± 60 cal. yr B.P.; Shane, 2000; Lowe et al., 2008). The glass chemistry of this bed (Table 4.2) supports

correlation with the Whakatane tephra. The Whakatane Tephra has been dated at 5530 ± 60 cal. yr B.P. by Lowe et al. (2008).

4.4.3.2 Glass chemistry of tephra from Lake Rotorua

A wide range of major, trace and rare earth elements can be determined rapidly and precisely by modern instrumental methods such as electron microprobe analysis (EMPA), X-ray fluorescence (XRF), instrumental neutron activation analysis (INAA), and laser ablation inductively coupled plasma mass spectrometry (LA-ICP-MS; Shane, 2000). One of the most widely used techniques for chemically characterising glass within tephra beds is individual shard analysis by EMPA. The efficiency of the technique for fingerprinting deposits in New Zealand was established by Froggatt (1983), and has since been widely used to characterise tephra beds in lake cores (e.g. Lowe, 1988); deep-sea cores (Wilmshurst et al., 1999; Shane et al., 2006); and various other tephra sequences (e.g. Shane, 2000; Smith et al., 2005; Lowe et al., 2008). Holocene tephra beds found in sedimentary basins in the North Island are typically calc–alkaline rhyolites with SiO_2 in the range 72–78 wt. % and K_2O in the range 2.6–4.5 wt. %, recalculated to 100% on a volatile-free basis (Shane, 2000).

For this study the major element compositions of glass shards from the nine beds were determined using this technique (Fig. 4.5; Table 4.2). The glass chemistry of the nine beds indicated eleven different units, with grains of Kaharoa Tephra found as background shards in sampling units 1, 2, 4, and 5. All these units, with the exception of the Tongariro derived andesite ash ("TgVC ash"), have well constrained ages ranging from the Whakatane tephra at 5530 ± 60 cal. yr BP to the most recent Tarawera eruption of 1886. In some cases, Na_2O values may be underestimated, presumably because of volatalisation during EMPA (the Na_2O values for several layers are less then would be expected).

Table 4.2: Glass composition of tephra beds in core RU188-07, presented as a mean (± standard deviation) of 10–20 shards determined by electron microprobe analysis (wt. %). Analyst: Rachel Pickett. Recalculated to 100% on a volatile free basis. Water by difference.

Informal units	Identifications	SiO_2	Al_2O_3	TiO_2	FeO*	MnO	MgO	CaO	Na_2O	K_2O	Cl	*n*
Unit 1	Tarawera	77.89 (0.62)	12.76 (0.3)	0.13 (0.03)	0.80 (0.27)	0.11 (0.07)	0.09 (0.04)	0.72 (0.21)	3.07 (0.45)	4.30 (0.79)	0.13 (0.07)	11
Unit 2	? Ka	78.32 (0.44)	12.51 (0.32)	0.18 (0.09)	0.96 (0.31)	0.07 (0.03)	0.13 (0.06)	0.93 (0.28)	3.62 (0.6)	3.13 (0.86)	0.14 (0.04)	11
Unit 3	TgVC Andesite	63.36 (0.74)	15.42 (0.2)	1.04 (0.06)	6.62 (0.42)	0.16 (0.05)	2.14 (0.13)	4.99 (0.37)	3.73 (0.12)	2.41 (0.11)	0.13 (0.03)	13
Unit 4	Group A ? Wk/Ka	78.41 (0.5)	12.60 (0.21)	0.15 (0.05)	0.98 (0.14)	0.09 (0.04)	0.12 (0.05)	0.75 (0.18)	3.12 (0.33)	3.58 (0.53)	0.19 (0.05)	17
Unit 4	Group B ? Tp	76.17 (0.31)	13.64 (0.39)	0.28 (0.06)	1.91 (0.04)	0.12 (0.04)	0.30 (0.03)	1.53 (0.09)	3.22 (0.1)	2.65 (0.08)	0.18 (0.04)	3
Unit 5	? Ka	78.10 (0.25)	12.63 (0.24)	0.12 (0.04)	0.84 (0.1)	0.12 (0.05)	0.09 (0.03)	0.61 (0.07)	3.42 (0.11)	3.90 (0.16)	0.16 (0.03)	20
Unit 6	Kaharoa	77.93 (0.29)	12.64 (0.16)	0.09 (0.04)	0.87 (0.08)	0.11 (0.05)	0.08 (0.02)	0.56 (0.05)	3.50 (0.08)	4.06 (0.15)	0.17 (0.03)	21
Unit 7	Taupo - Group A	76.14 (0.46)	13.51 (0.24)	0.27 (0.06)	1.95 (0.15)	0.14 (0.04)	0.29 (0.03)	1.52 (0.1)	3.25 (0.26)	2.73 (0.12)	0.18 (0.04)	13
Unit 7	Taupo - Group B ? Wk	78.25 (0.56)	12.46 (0.16)	0.14 (0.05)	1.07 (0.18)	0.10 (0.07)	0.13 (0.03)	0.87 (0.21)	3.30 (0.31)	3.49 (0.43)	0.19 (0.02)	7
Unit 8	Waimihia	75.55 (0.28)	13.87 (0.28)	0.27 (0.03)	2.05 (0.12)	0.12 (0.04)	0.30 (0.07)	1.55 (0.07)	3.26 (0.37)	2.87 (0.14)	0.17 (0.04)	11
Unit 8	Whakaipo	77.61 (1.02)	13.16 (0.71)	0.16 (0.09)	1.24 (0.36)	0.12 (0.09)	0.15 (0.04)	1.03 (0.24)	3.21 (0.34)	3.16 (0.29)	0.17 (0.02)	4
Unit 9	Whakatane	77.82 (0.3)	13.30 (0.28)	0.16 (0.04)	0.96 (0.1)	0.10 (0.04)	0.14 (0.02)	0.86 (0.15)	2.97 (0.24)	3.52 (0.18)	0.16 (0.05)	10
Unit 9	Unit K	76.80 (0.42)	13.49 (0.09)	0.20 (0.05)	1.65 (0.15)	0.14 (0.03)	0.19 (0.02)	1.27 (0.15)	2.99 (0.15)	3.11 (0.11)	0.17 (0.06)	5

* total Fe expressed as FeO

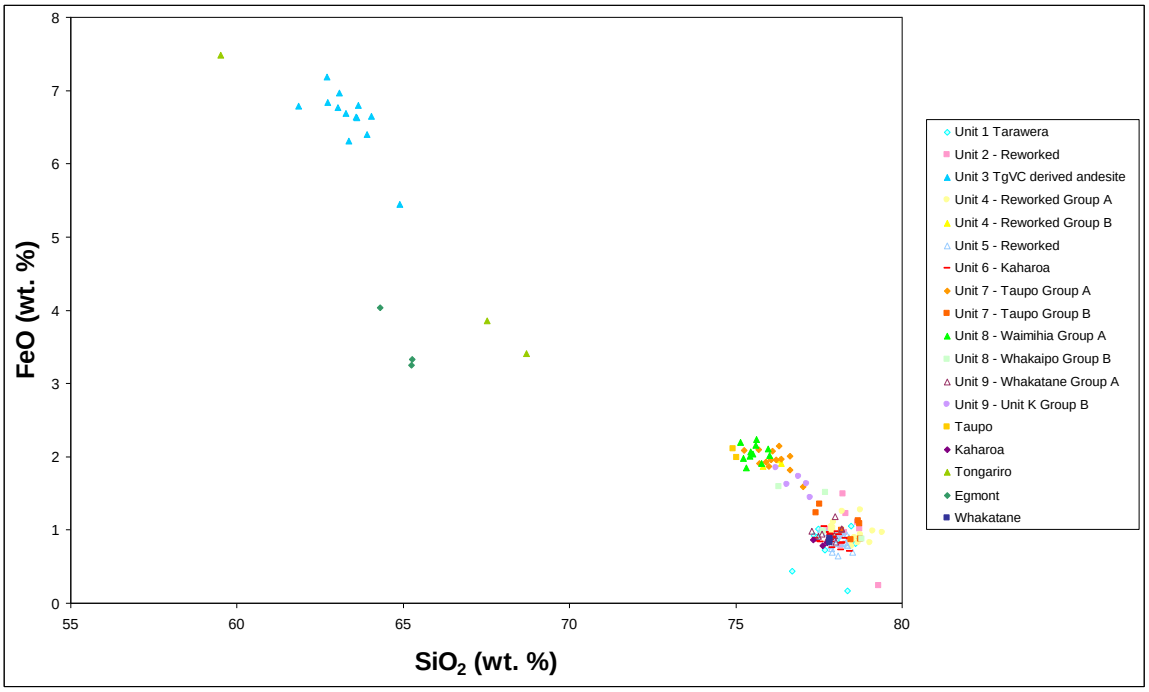

Figure 4.5: Plot showing glass chemistry for all samples taken from RU188, compared to data from Shane (2000) and Lowe et al. (2008).

Sampling unit 1 was identified positively from stratigraphic position and field characteristics as Tarawera Tephra. This unit can be split into two distinct phases, the first a coarse black scoria from the initial basaltic plinian eruption from multiple vents on Mt Tarawera during the 1886 eruption followed by the phreatomagmatic and phreatic explosion at Lake Rotomahana and in the Waimangu Valley (Nairn and Cole, 1981), distributing a fine grey ash of glass, lake sediments, and country rock across much of the Rotorua – Bay of Plenty region (see Keam, 1988; Lowe et al., 2002).

Sampling unit 2 was found have a varied composition, with possibly more than one population present. This unit is probably of Okataina source (Fig. 4.6) and is more than likely a reworked Kaharoa with some stray shards incorporated, and is of unknown age.

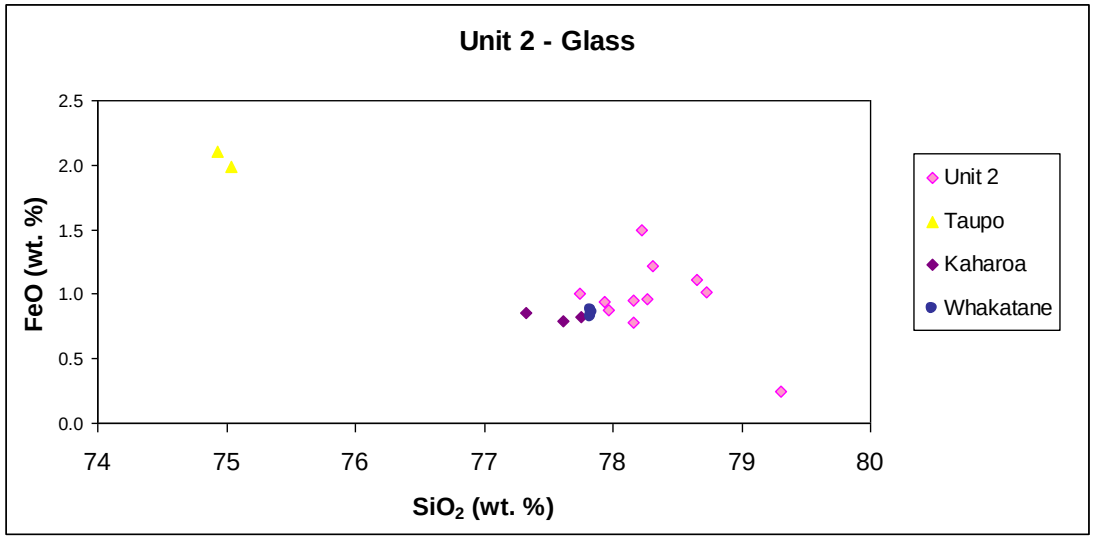

Figure 4.6: Plot of glass data from unit 2 – indicating an Okataina source. Data for Taupo, Kaharoa, and Whakatane are from Shane (2000) and Lowe et al. (2008).

Sampling unit 3 was unable to be correlated as a specific unit – only that it derives from the Tongariro Volcanic Centre. This unit has characteristically lower silica content (Fig 4.5) and high aluminium, magnesium, calcium (Fig. 4.7), iron, and titanium. Analyses of this unit were compared with glass data for both Egmont and Tongariro found in cores from Kaipo, Pukaki, and Okupata (Shane, 2000; Lowe et al., 2008); these data pointed to a Tongariro origin. The glass major element data are similar to analyses of Tufa Trig tephras, erupted from Mt Ruapehu and divided into 19 units in the post-Taupo Tephra period (Donoghue et al., 1995, 1997). It is possible that this tephra ("TgVC ash" in Fig 4.3) represents a member of the Tufa Trig Formation, presumably one of the later ones (e.g. Tf 14) based on its stratigraphic position high in the core.

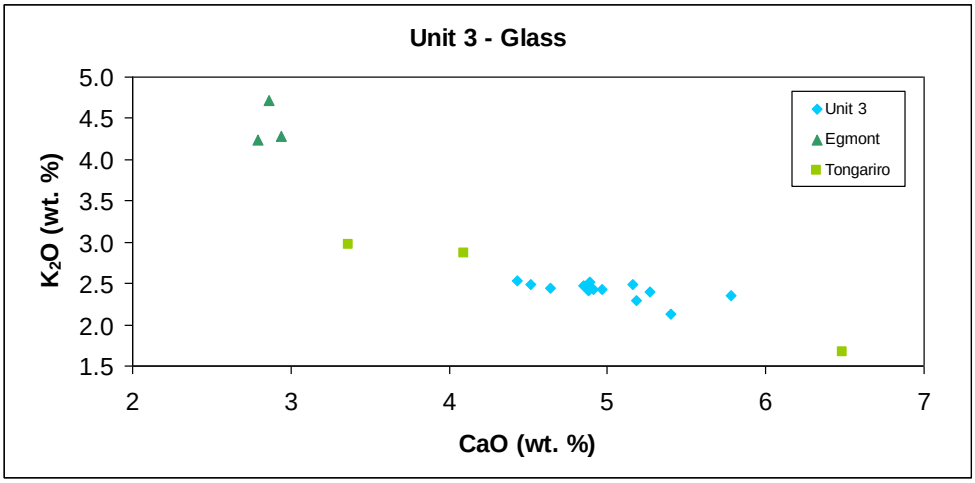

Figure 4.7: Plot of glass data from unit three showing slightly higher calcium and lower potassium than those samples from Mt Egmont. Egmont and Tongariro data are from Shane (2000) and Lowe et al. (2008).

The glass chemistry of sampling unit 4 (Fig. 4.8) indicates a bimodal composition (population Group B is similar to Taupo), but is dominated by probably Whakatane-derived shards. Unit 5 (Fig 4.9) on the other hand is made up of just one population very similar to the glass composition of the Kaharoa Tephra. Both these units are inferred to be deposits derived from reworking by a storm event causing widespread erosion in the catchment or reworking by waves in shallower waters. Both are of unknown age.

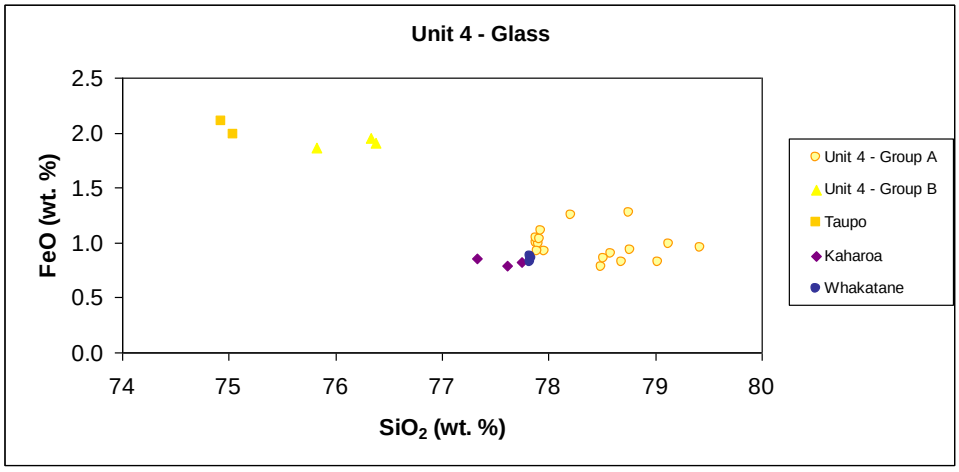

Figure 4.8: Plot of glass data from unit 4 indicating two separate sources one from Taupo and the other from Okataina. This unit has been inferred to be reworked grains of units found deeper in the lake record and are considered a reworked layer. Taupo, Kaharoa, and Whakatane data from Shane (2000) and Lowe et al. (2008).

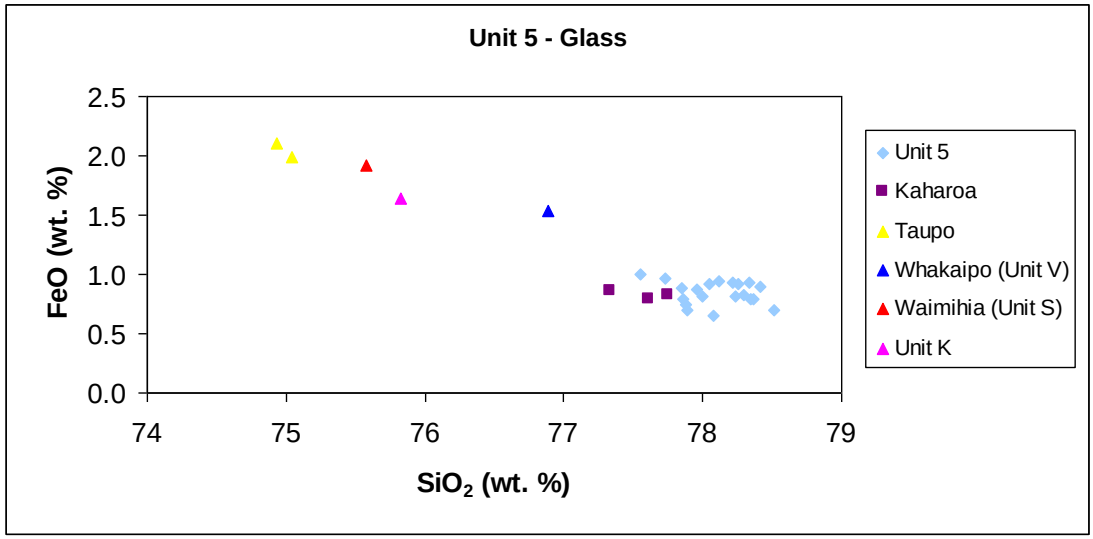

Figure 4.9: Plot of glass data for unit 5 indicates it to be a reworked layer of the initial Kaharoa Tephra. Data for deposits other than unit 5 are from Lowe et al. (2008).

Sampling unit 6 was positively identified by its stratigraphic position together with its field characteristics (coarse, very hard, dense pumice and visible biotite) as Kaharoa Tephra (636 ± 12 cal. years B.P.). Glass chemistry supports this identification, with silica, iron, calcium, magnesium and potassium closely matching other published data (Fig. 4.10). This unit represents fallout from the most recent rhyolite eruption in New Zealand. The eruption deposited a thick sequence over at least one quarter of North Island and offshore Bay of Plenty. It is an important marker bed in archaeological studies for two reasons (Lowe et al., 1998, 2000a). Firstly, as there is very limited cultural evidence beneath this layer of lapilli so it is inferred to have occurred just prior to the arrival and settlement of most Polynesians in the eastern North Island. Secondly, multiple pollen studies (e.g. Wilmshurst, 1997; Newnham et al., 1998b; Wilmshurst et al., 1999), indicate sustained deforestation very close to the time of its deposition reinforcing the theory of timing of human settlement in the region.

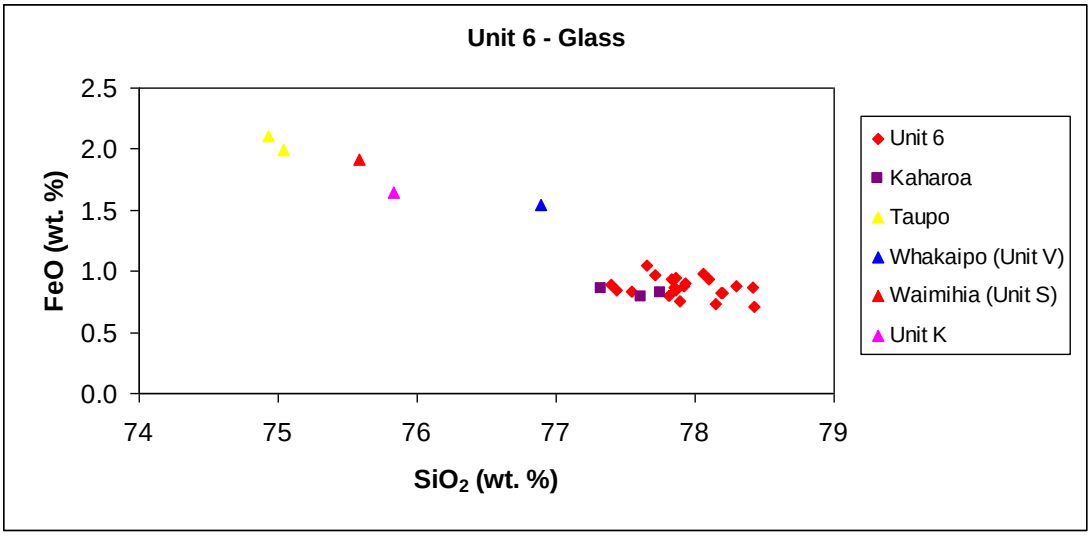

Figure 4.10: Plot of glass chemistry for Unit 6. Data for deposits other than unit 6 are from Lowe et al. (2008).

Glass chemistry from sampling unit 7 (Group A) indicates a Taupo source, consistent with Taupo Tephra (Unit Y; 1717 ± 13 cal. years B.P.). The eruption of the Taupo Tephra was the most powerful event in the Taupo Subgroup (since c. 27,100 yrs ago), and took place in vents in the northern part of Lake Taupo. This eruption is inferred to have caused further caldera collapse in the north-eastern section of the Lake Taupo Basin. There are two populations evident, with population A matching analyses of Taupo very closely (e.g. high FeO, high TiO_2, and low K_2O; Lowe et al., 2008; Fig. 4.11). Population B analyses in sampling unit 7 look to be very similar to those for Whakatane Tephra beneath it in the core and thus these shards may reflect reworking or contamination from that tephra.

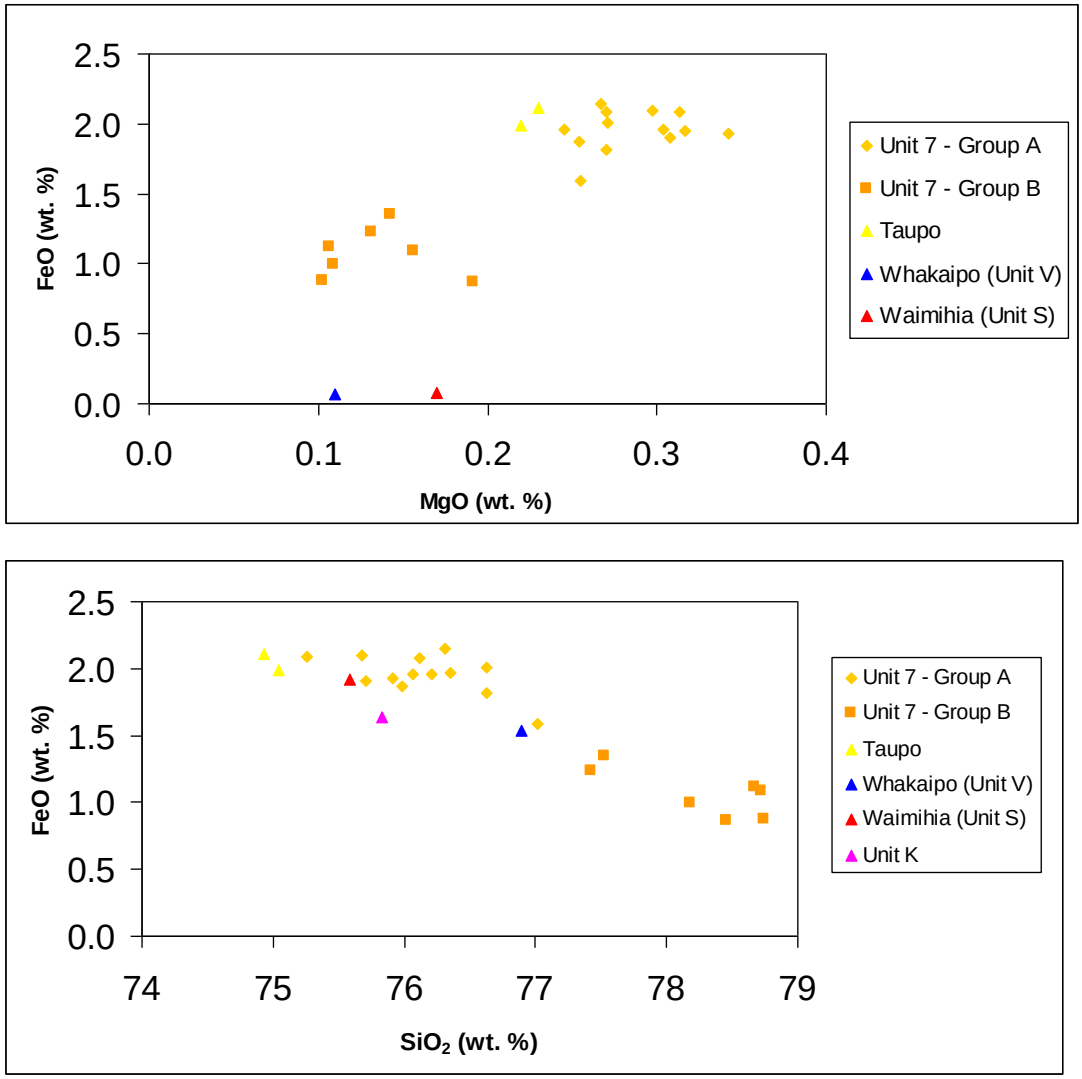

Figure 4.11: Plots of glass data from Unit 7 indicating two different but similar Taupo populations. Data for Taupo comes from Shane (2000) and Lowe et al. (2008); Whakaipo, Waimihia and Unit K data are from Lowe et al. (2008).

Two populations were evident from the glass shards extracted from sampling unit 8. Both are from the Taupo Volcanic Centre, and correspond to Unit V and Unit S (Wilson, 1993) or Whakaipo and Waimihia tephras, respectively. Waimihia (3410 ± 40 cal. years B.P.) dominates this assemblage, with a small number of younger Whakaipo (2760 ± 20 cal. years B.P.) grains (Fig. 4.12).

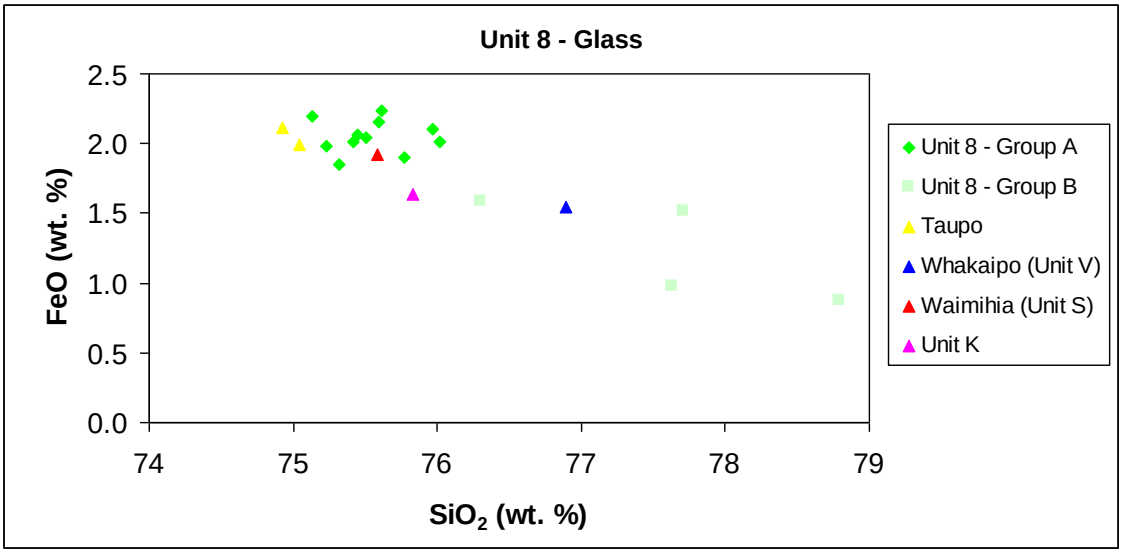

Figure 4.12: Plot of unit 8 glass populations, indicates the possible mixing of two tephras from the same source. Data for Taupo comes from Shane (2000) and Lowe et al. (2008); Whakaipo, Waimihia and Unit K are from Lowe et al. (2008).

Unit 9 was first identified by its ferromagnesian mineralogy, as it contained an assemblage dominated by the distinctive mineral cummingtonite. Additional work on glass characteristics (Fig. 4.13) confirmed the initial identification as Whakatane (5530 ± 60 cal. years B.P.), erupted from the Haroharo Volcano in the OVC. A small secondary population was identified, possibily of the TVC-derived Unit K (5120 ± 150 cal. years B.P.). Shane et al. (2008) proposed that the Whakatane eruption involved at least five vents spread along 11 km of the Haroharo Linear Vent Zone, with widespread pyroclastic falls and large volume lavas being erupted. Geochemical analysis of the pyroclastic sequences and lava flows revealed that three subtly different rhyolite magmas were involved (Smith et al., 2006), but glass compositions only show slight compositional differences between eruptives from the multiple vents, which could explain the spread of the glass data in Figure 4.13 (see also Lowe et al., 2008).

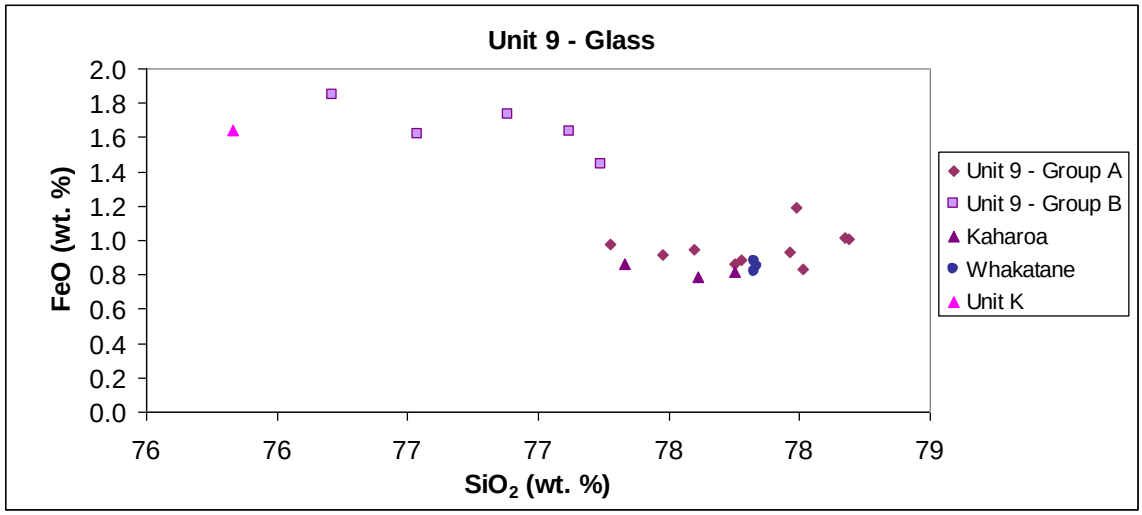

Figure 4.13: Plot of glass data from Unit nine indicates two groups possible indicating a secondary population of Unit K. Additional data comes from Lowe et al. (2008).

All glass data are available in appendix F.

4.4 Rates of Sedimentation

The tephra layers have used to calculate sediment accumulation rates. The rate at which the sediment accumulated in the lake changes significantly, from less than half a millimetre per annum on average prior to the Kaharoa eruption to around 3.5 mm per annum on average directly following the Kaharoa eruption in 1314 ± 12 A.D. (Fig. 4.14). The accumulation of sediment in most lakes changes when significant amounts of clastic material enter the lake. But in some lakes, Lake Rotorua especially, elements such as phosphate controls the production of diatoms and hence when the amount of available phosphate increases the amount of sediment accumulating also increases.

4.4.1 Mean sedimentation rate

The mean sedimentation rate varies from 0.12 mm yr^{-1} to 3.6 mm yr^{-1}, increasing in younger sediments as expected (Fig. 4.14). Sedimentation rates between known age points for tephra isochrons in the core are calculated as follows (on a tephra-thickness-free basis):

- Whakatane (5530 cal. yrs B.P.) → Waimihia (3410 cal. yrs B.P.)
  Depth 700 – 674 = 26 cm
  260 mm / 2120 yrs
  = 0.12 mm/yr

- Waimihia (3410 cal. yrs B.P.) → Taupo (1717 cal. yrs B.P.)
  Depth 674 – 570 = 104 cm
  1040 mm / 1693 yrs
  = 0.61 mm/yr

- Taupo (1717 cal. yrs B.P.) → Kaharoa (636 cal. yrs B.P.)
  Depth 565 – 513 = 52 cm
  520 mm / 1081 yrs
  = 0.48 mm/yr

- Kaharoa (636 cal. yrs B.P.) → Tarawera (64 cal. yrs B.P.)
  Depth 504 – 50 = 454 cm (45 Tw, 1 R1, 1 TgVC, 2 R2, 1 R3)
  4540 mm / 1250 yrs
  = 3.6 mm/yr

4.4.2 Variations in sedimentation rates

There are many variations in the sedimentation rate at site RU188 (Fig. 4.14). Between the Whakatane eruption (5530 ± 60 cal. yr BP) and Waimihia eruption (3410 ± 40 cal. years BP) sedimentation rates averaged 0.12 mm yr^{-1}. A marked increase to 0.61 mm yr^{-1} followed the Waimihia eruption, then sedimentation dropped slightly after the 1717 ± 13 cal. years B.P. eruption of Taupo to 0.48 mm yr^{-1}.

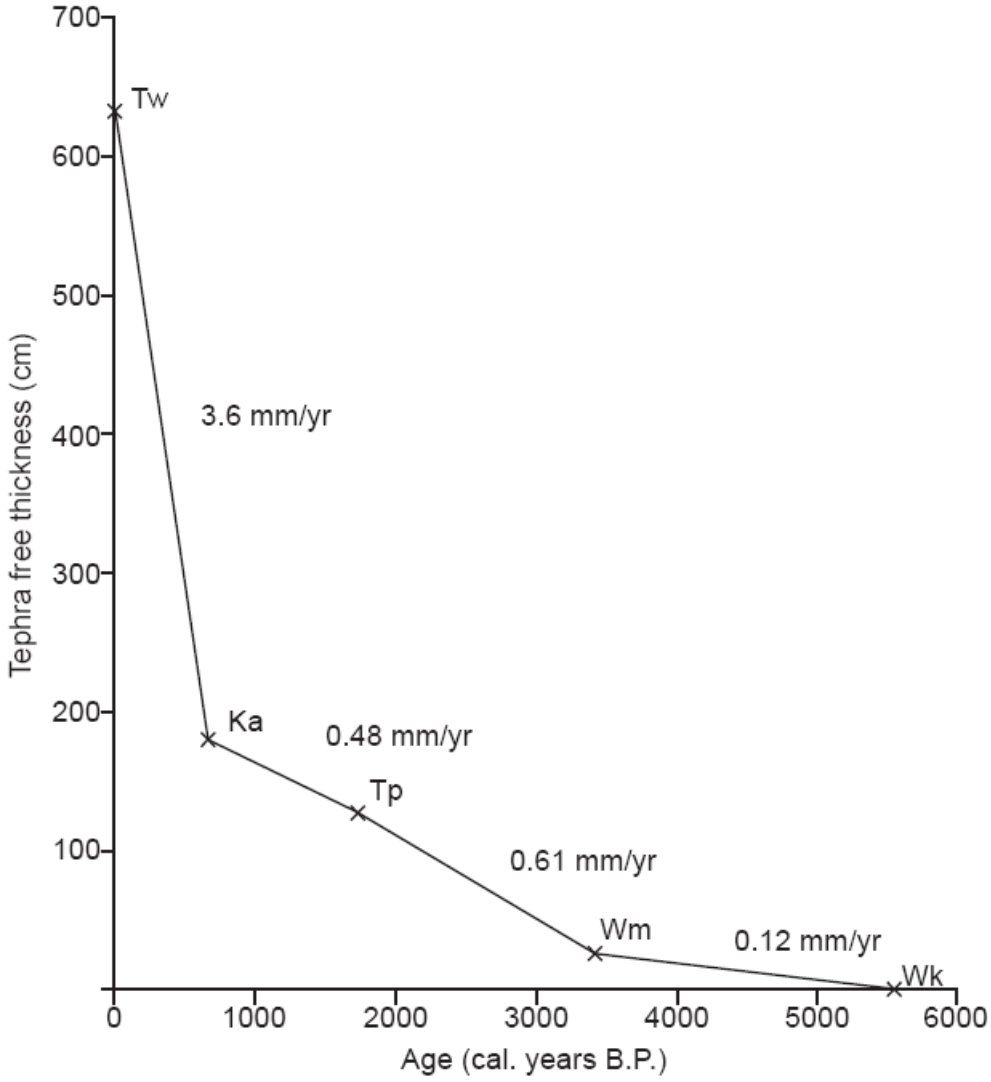

Figure 4.14: Mean sedimentation rate based on dated tephra ages (cal. yr B.P.)

The most substantial increase in sedimentation rate occurs immediately after the Kaharoa eruption (636 ± 12 cal. years B.P) and before the Tarawera (1886 A.D.) eruption at 3.6 mm yr^{-1}. The cause of this ten-fold increase initially may have been the consequence of the impact on forest within the catchment caused by fallout from the Kaharoa eruption. Also implicated, however, are impacts coincident with Polynesian settlement who arrived at around this time (e.g. Newnham et al., 1998b; Hogg et al., 2003). Pollen studies have been carried out in Holden's Bay, Lake Rotorua (McGlone, 1983a). This study covers the last ~ 9,500 years and shows a marked decrease in Nothofagus and other forest species, an increase in herbs (including *Pteridium* or bracken fern), and an influx of microscopic charcoal particles

immediately after the Kaharoa eruption, indicating Polynesian settlement and the start of deforestation by burning. Pollen records from elsewhere in the North Island consistently show a distinctive and abrupt environmental transformation at around the time of the Kaharoa eruption (e.g. McGlone, 1989; Newnham et al., 1998b; McGlone and Wilmshurst, 1999; Lowe et al., 2000a). This distinctive pollen signal consists of a sustained rise in curves for *Pteridium*, grasses and several other taxa, together with a decline in tall forest taxa, and a continuous flux of abundant charcoal (Newnham et al., 1998b).

4.4.3 Radiocarbon dating

The radiocarbon dating of this core proved to be of little value because the ^{14}C ages were all too old in the basis of the tephrochronology. Such old ^{14}C ages may relate to a number of reasons but it is thought primarily to be the result of the introduction of old carbon into the sediment system via the release of methane from the lake floor. As well, CO_2 discharge from geothermal vents may have introduced old carbon into the sediments. Hence, any future radiocarbon dating of bulk lake sediments from Lake Rotorua alone may prove unreliable. However, the age differences between bulk carbon and dated tephra may yield valuable information about the fluxes of old carbon into the lake.

4.5 Summary

The sediment of RU188 is made up primarily of fine grained, slightly sticky, diatomaceous ooze. There are subtle colour changes throughout the entire core ranging from olive to dark olive grey. Distinct laminations occur only after Kaharoa Tephra was deposited and possibly represent annual or quasi-annual inwash events associated with storms, extended periods of precipitation, or arising from human activities in the catchment (or all of these).

The age of the sediments are constrained between two OVC derived tephras, giving the core an age ranging from 5530 ± 60 cal. years B.P. at the base to 1886 A.D. at the top. There are 5 marker bed tephras throughout the core that provide the primary framework. These beds are derived primarily from the OVC and TVC (Fig. 4.15).

These beds were first identified by visual stratigraphic changes and their presence was reinforced by magnetic susceptibility analysis.

Since 5,500 cal. yrs B.P. the sedimentation rate has varied considerably from 0.12 mm yr^{-1} to 3.6 mm yr^{-1}. A large increase after the eruption of Kaharoa (636 ± 12 cal. years B.P.) is thought to have been initially caused by the forest disturbance arising from tephra fallout but was closely followed and sustained by the subsequent clearing of bush by early Polynesian settlers.

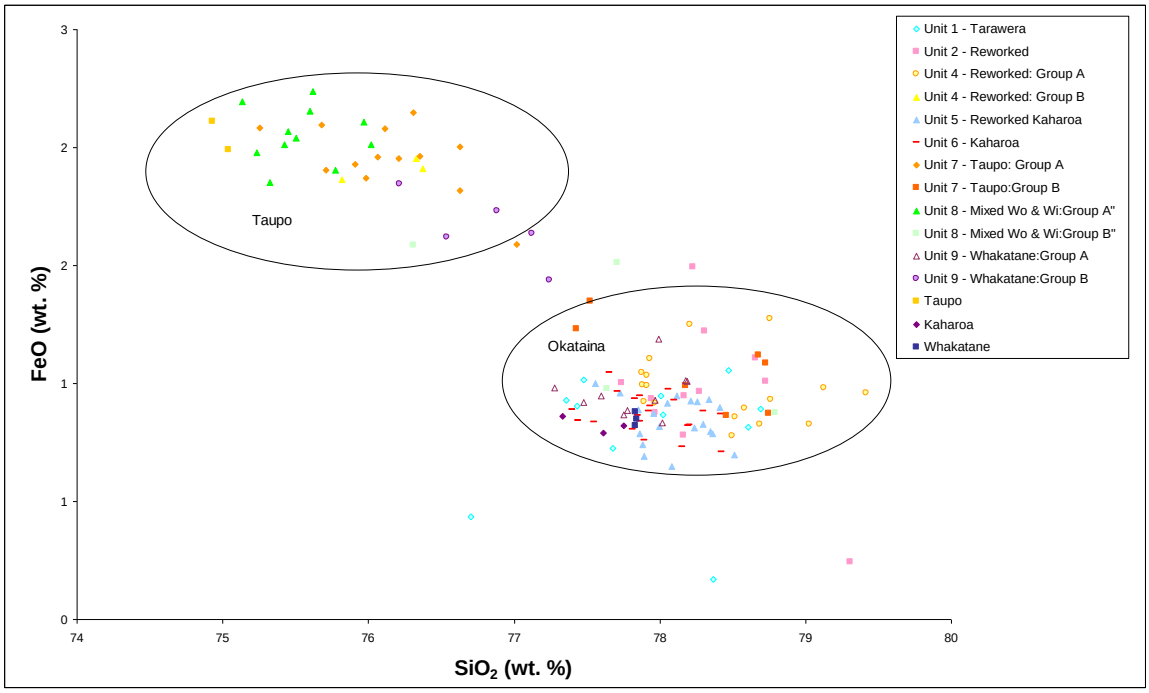

Figure 4.15: Plot showing rhyolitic glass data; these data indicate two separate sources – TVC and OVC, compared with data from Shane (2000) and Lowe et al. (2008).

Chapter Five

Physical Characteristics: sediment structure and composition



Chapter Five – Physical Characteristics: Sediment structure and composition

5.0 INTRODUCTION

Palaeolimnology is based on the analysis of the sediment which accumulates over time on lake beds. These sediments are derived both from within the lake and from its catchment. The layers of sediment or laminations provide the highest potential resolution from the sedimentary record, but at the same time pose the challenge of how to extract this information. From the lake come various inorganic chemical compounds such as nitrogen and phosphorus, and the end products of decomposition processes such as organic compounds (e.g. lipids, pigments), and bits and pieces of plant and animals which remain in the bottom muds as microfossils (e.g. diatoms, chydorids, chironomids). From the surrounding catchment come various inorganic minerals eroded from rock and soil materials (deposited as sand, silt, or clay particles), chemicals leached from the soil, and organic matter from both soil and vegetation (e.g. humus, leaf remains, pollen). The sediments accumulate gradually and lock away information on the catchment and the lake (Green and Lowe, 1992a).

Studies of lakes and their many layers of silt and sediment can tell us a great deal, from centuries-old deforestation to climate changes over thousands of years. New Zealand palaeolimnology has given us a greater understanding of the geological and climatological processes which have formed our landscape as well as the effects of both Maori and European settlement on it.

This chapter covers the physical characteristics obtained from RU188 and provides a record of the bedding and structures hidden within.

5.1 Photography

Digital images were taken in 20 cm sections of core to record as much detail as possible. These were then stitched together to form images of both the core sections and one of the full core. These images record the colour, thickness, laminations, and positions of tephra deposits in the stratigraphic sequence. The images displayed in Figure 5.1 give examples of these characteristics found in the core.

5.2 X radiography

Most primary structures in sedimentary cores result from physical processes operating at the time of deposition and therefore provide important information concerning geological processes and sedimentary environments. In most cores some structural detail can generally be recognised, either by colour changes between each unit or by variations in texture and composition, so the sediment appears to be structureless and homogeneous. Such sediments are typically described simply as “thick-bedded”, “massive”, or “structureless”.

The X-radiographic images of the core provide an almost continuous record of the past ~ 5500 cal. years of sedimentation, distinguishing massive and laminated olive, fine-grained sediment from more dense, coarse-grained clastic inputs or ashfall units. These images revealed a range of grey tones. These were found (through SEM imaging and grain size analysis) to be predominantly related to density differences controlled by variations in sediment composition (the amount of terrigenous matter versus autochthonous derived) rather than changes in the type of diatom frustules.

Coloured laminated intervals that were evident in the photographs show up clearly on the X-rays (Fig 5.1). These rhythmnites are probably produced by variability in sediment inputs from waters draining into Lake Rotorua. In the absence of terrigenous sediment input changes in the composition of inflowing water, such as algal blooms, may produce rhythmic deposits in the lake basin (Pickrill et al., 1991). A record of correlated photographic and X-radiographic images along the entire length of RU188-07 can be found deposited in jpeg format on the Appendix I - CD.

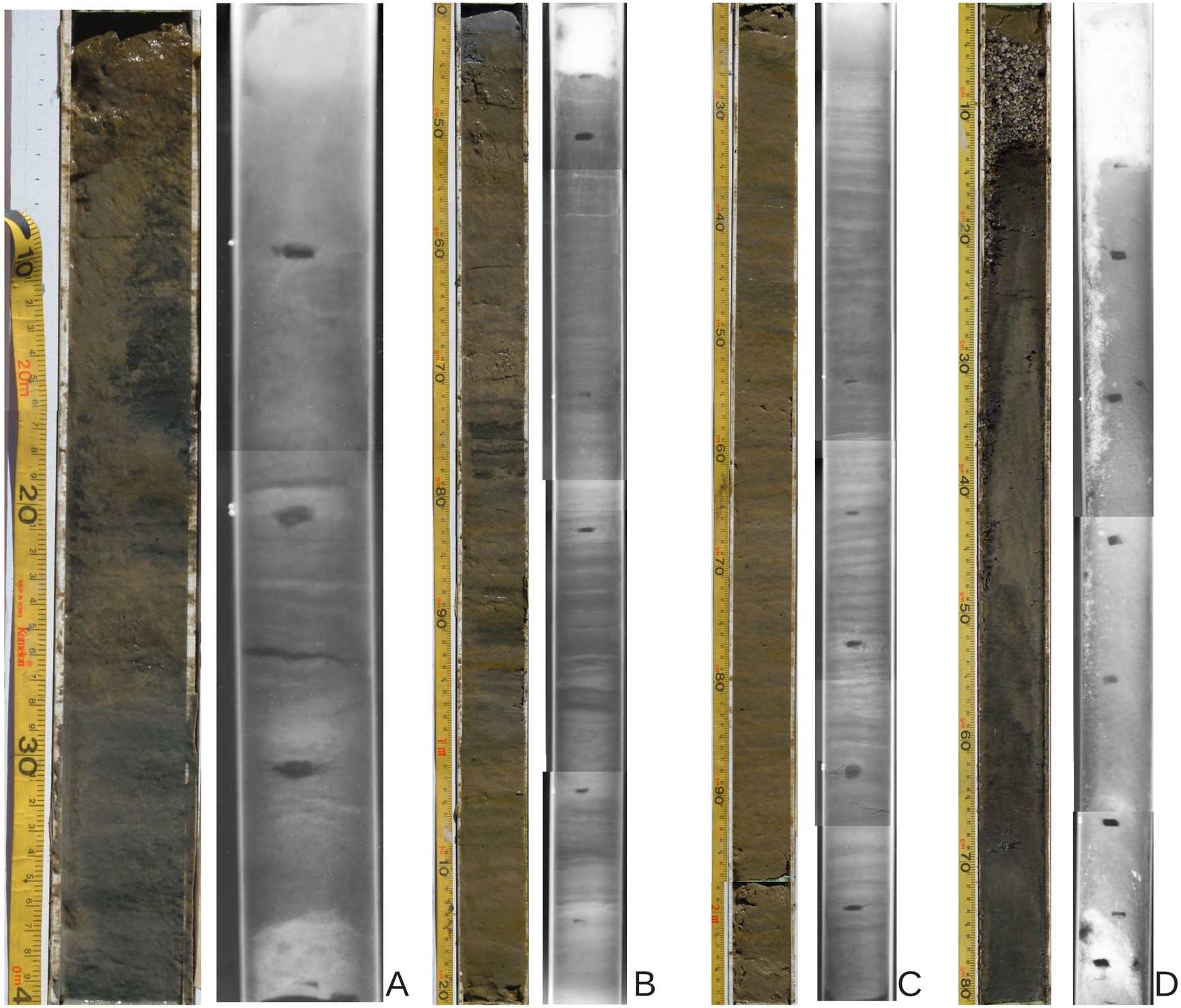

Figure 5.1: Photographs and x-radiographic images of four lengths of core - showing evidence of the laminations, oxidation and tephras. Left to right A 0-40 cm, B 40-121 cm, C 121-207 cm, D 502-579 cm

5.3 Colour reflection

High-resolution records have lately become keywords in palaeolimnology because of the recent development in attempts to sample and analyse lake records in extreme detail. One way of obtaining high-resolution data from lake sediments is the use of digital sediment colour analyses. The advantage of the method is its high-resolution capacity and consequently the close spacing of the data points. The spacing is much denser than would ever be possible with, for example, traditional chemical analyses (Christensen and Biorck, 2001).

5.3.1 Colour

Colour is reported using the L*a*b* system. It can be visualized as a cylindrical coordinate system in which the axis of the cylinder is the lightness component L*, ranging from 0% to 100%, and the radii are the chromaticity components a* and b*. Component a* is the green (negative) to red (positive) axis, and component b* is the blue (negative) to yellow (positive) axis. In suitable lakes, the lightness (L*) component can be used as a proxy for carbonate vs. terrigenous content, the green-red component (a*) can be used as a proxy for clay and glauconite concentration/variation within sediments, and the blue-yellow component (b*) has been shown to be a proxy for diatom-detritus content.

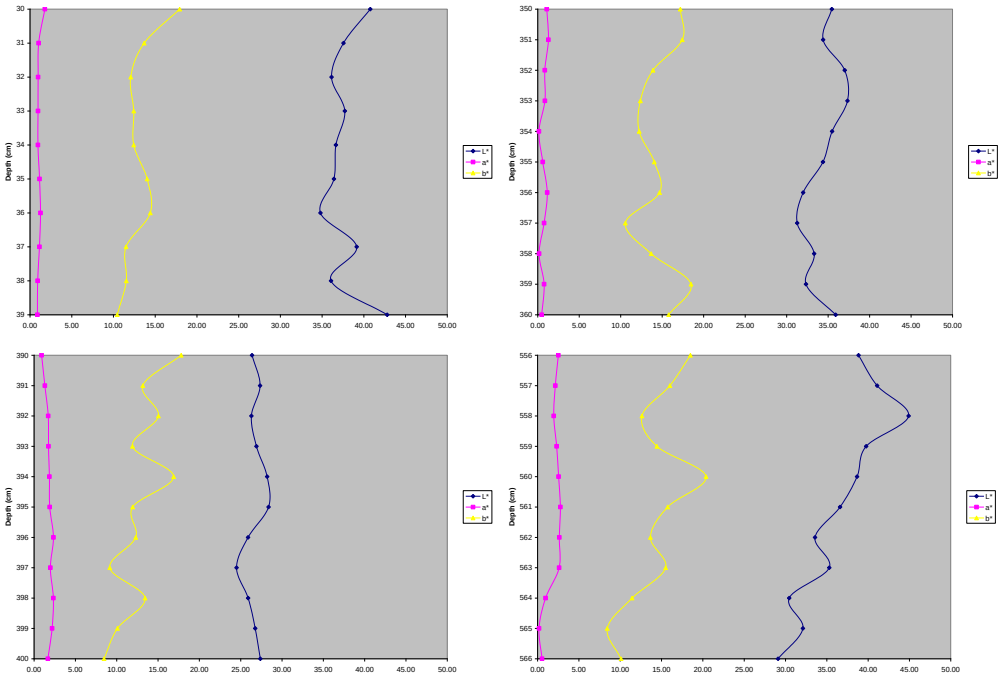

Figure 5.2: Combination plots of L*, a* and b*, for four representative core segments (30-39, 350-360, 390-400, 556-566).

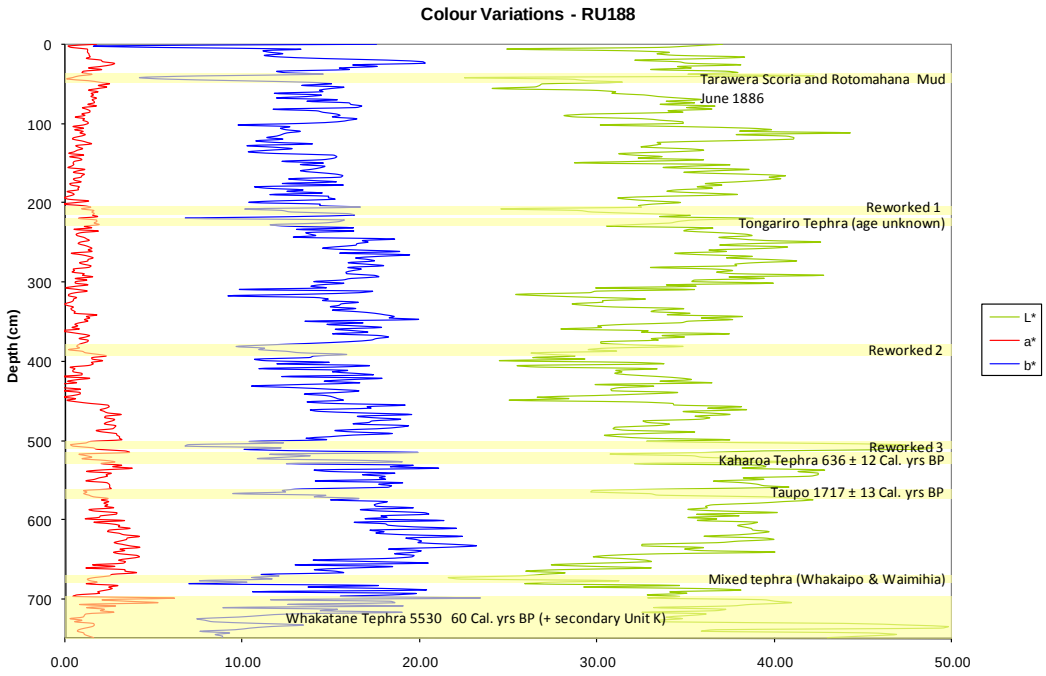

Figure 5.3: Whole core multi-plot of L*, a* and b*, yellow bands indicate tephra layers

L* represents lightness, where black is zero and white is 100, and this fluctuates considerably between 20 – 50%. Decreases in this variable represent terrigenous sediment inputs and are generally mirrored by decreases in the b* variable (tending towards the blue variable) on a wider timescale (Fig. 5.3). This same trend is not as evident in the more closely sampled sections (Figs. 5.2 A-D).

a* shows little variation (Fig. 5.3), but as there is no carbonate in these sediment, this shifting is hence concluded to be due to varying amounts of clay particles. This inference is supported by the representative grain size analysis, where clay size particles increase in the lower sections of the core (Figs. 5.20 and 5.2 D).

Debret et al. (2006) have shown in a recent study that b* variations can be used to indicate changes in sediment input where light-coloured laminae are diatom-rich and tend towards yellow (high b* values), and darker laminae rich in detrital material tend towards blue (low b* values). These findings are evident in this study. When there is a known input of clastic detrital material through tephra deposition the b* parameter drops considerably but then recovers rapidly following this event (Fig. 5.4). The other substantial drops may be due to

seasonal influxes of winter wash-in or stronger winds causing reworking in shallower waters.

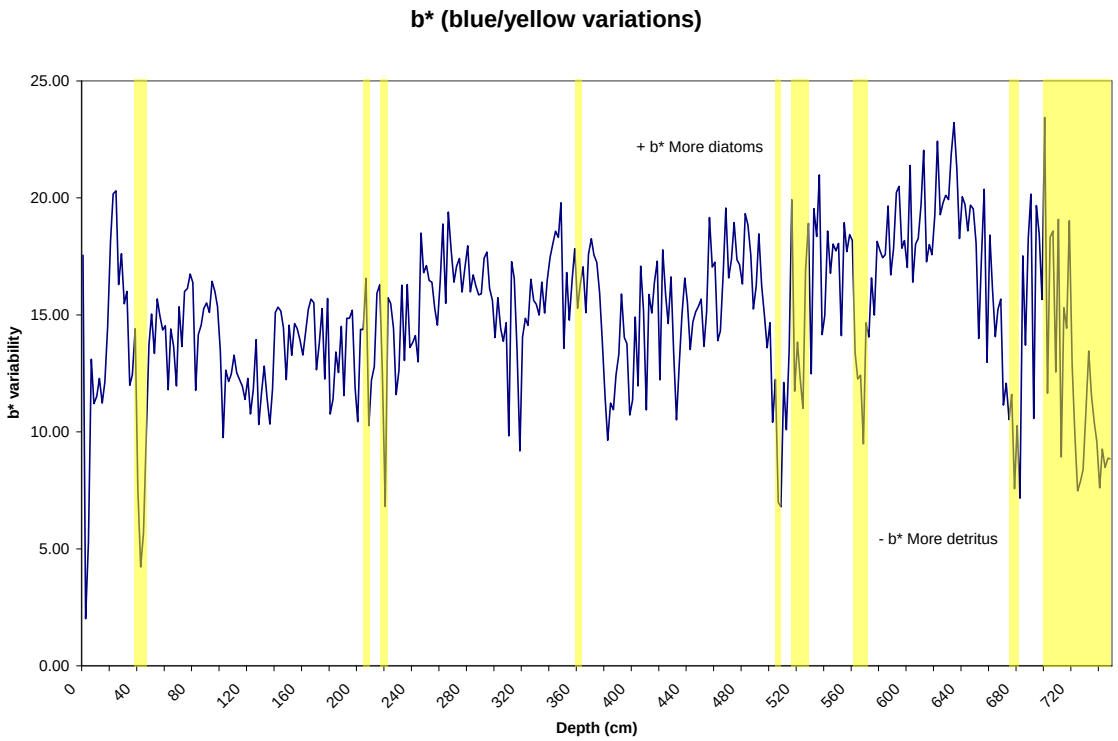

Figure 5.4: Whole core plot of b* variable, where a higher b* value represents sediment consisting of more diatoms and a lower b* value indicates more detritus or clastic material. Yellow bands indicate tephra layers.

5.3.2 Spectrophotometry reflectance

According to previous lacustrine and marine sediments studies (Deaton and Balsam, 1991; Balsam and Deaton, 1996; Debret et al., 2006; Chapron et al., 2007), spectral data can be used as a proxy to estimate the abundance of certain minerals and the presence of organic matter. For example, reflectance values at 555, 565, 575 nm wavelengths can be used as a proxy for the abundance of iron oxide minerals, and values between 605 and 695 nm indicates different amounts of organic components of the sediment and other inorganic materials – in particular clay minerals (illite, montmorillonite and chlorite), and calcite.

Reflectance at 560 nm in RU188 is indicative of changes in iron oxide minerals and varies considerably between 4 and 19% (Fig. 5.5 A). These minerals probably originated from the tephra layers and the erosion of these materials from the catchment. Most high concentrations correlate with the tephras and all the other peaks are hence likely to be indicative of erosion events.

Variations in organic matter in particular can be seen at c. 660 nm, and correspond strongly with variations in b* signal. In this case the reflectance value alters only a small amount throughout the core but enough to indicate possible seasonal fluctuations especially in the upper core (Fig 5.5 B).

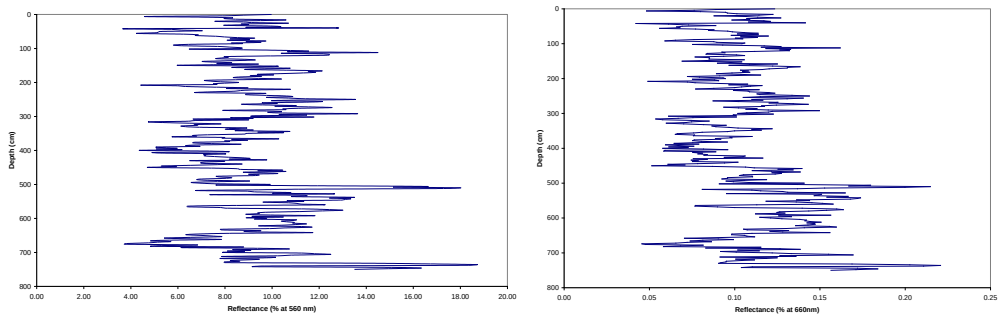

Figure 5.5: A) Reflective data from 560 nm are indicative of specific sediment components in particular iron oxide minerals (555, 565, 575 nm). B) Reflective data from 660 nm are indicative of organic matter

First derivative values of reflectance data (Fig. 5.6) indicate high values particularly at wavelengths over 600 nm. These values indicate changes in organic material, as discussed above. Organic matter is common throughout the core, but where the values change towards blue (at wavelengths > 600 nm), these values correspond in most cases to tephra layers, with the exception of Kaharoa and Whakatane which are orange. This anomaly is probably an error in the reflectance relating to the coarse grain sizes of these two tephras. There are two changes, at ~ 320 cm depth (c. 400 cal. years B.P.) and ~ 450 cm depth (c. 560 cal. years B.P.), which do not correspond to tephra layers and which are possibly associated with non-tephra-derived clastic deposition. The organic matter appears to be highest following the Taupo eruption, with high values also following the Waimihia eruption and again at around 200-300 cm depth (c. 220-380 cal. years B.P.) in the core.

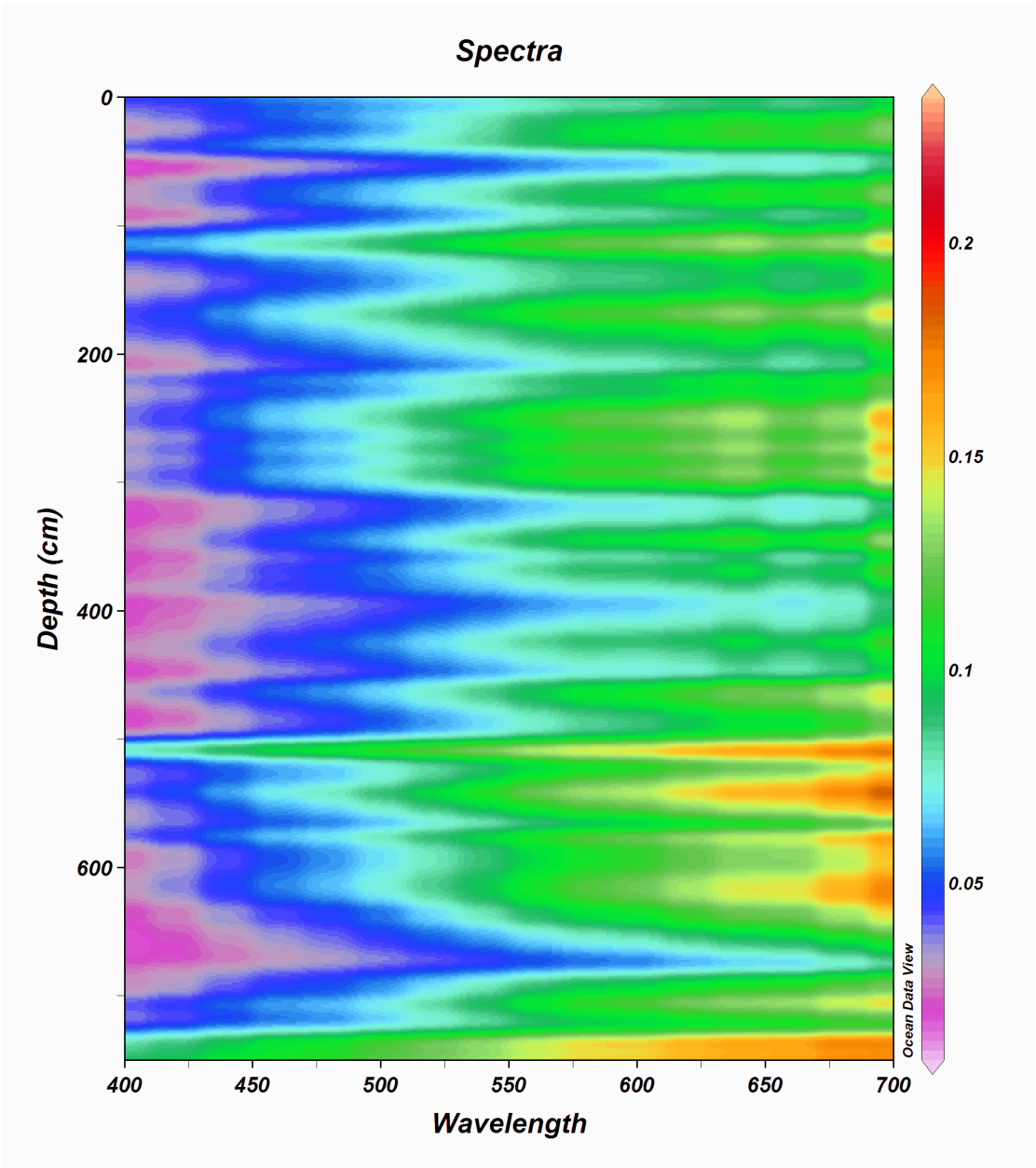

Figure 5.6: Down-core changes of first derivative values. The first derivative of all 6000 spectra has been plotted on this 3D diagram. The X axis represents the different wave lengths, Y is depth in cm, and Z the derivative value for the corresponding wavelength expressed by a code of colour. The higher the first derivative the more the colour tends towards the red; the lower its value the more it tends towards blue/purple.

5.4 Scanning electron microscopy

Lake sediments contain the remains of a variety of organisms such as cyanobacteria, chrysophytes, chironomid larvae, terrestrial vegetation (pollen and spores), sponges, occasionally blue and green algae, and most commonly diatoms (Rawlence, 1984; Harper et al., 1986; Cassie-Cooper, 1996). These organisms can show changes in lake environments that may or may not be directly related to climatic change. Climatic influences on lake organisms generally occur by means of indirect mechanisms such as changes in evaporation and runoff (hence lake-level changes) or catchment vegetational type (Brugam, 1984). Studies from Lake Poukawa, Hawke's Bay, have shown that diatoms increase in abundance following the deposition of tephra due to its fertilizing effect. However, because of time restraints in this project, this possible relationship was not able to be proved in Rotorua's case. Nevertheless, we can give windows of insight into the sediment's make up. Diatom productivity is dependent on the season, and the largest populations are commonly found in autumn to early spring (Cassie-Cooper, 1996). Fossils of diatoms provide a means of reconstructing past lake history. These algae are especially well suited for palaeolimnological studies because their siliceous cell walls are more or less well preserved in lake sediment. The scanning electron microscope (SEM) allows for pictures to be taken of diatom cells, or frustules, which can then generally be identified by species. Diatoms are useful palaeoenvironmental indicators because they inhabit lakes of all types and because some species prefer particular environmental conditions.

In the Lake Rotorua sediments, most of the organic component of organisms decomposes and leaves little evidence of the biota. Diatom frustules remain largely intact to dominate the accumulating sediment. The abundance is the result of the large amount of volcanic material deposited in Lake Rotorua. The discharge of silica-laden geothermal waters and groundwaters high in silica from the ignimbrite aquifers have also maintained moderate levels of soluble silicic acid, preventing the diatom frustules from dissolving (Rawlence, 1984; Harper et al., 1986). Samples were taken from the top (30 and 32 cm), and two middle (350-359 and 390-400 cm) sections of the core (Fig. 5.7). These were examined under the SEM to identify the make up of the different coloured laminae – diatom species and other materials present in the sediment. As with many lakes in New

Zealand, *Aulacoseira* is widespread and the most abundant planktonic taxa, followed by *Cyclotella*.

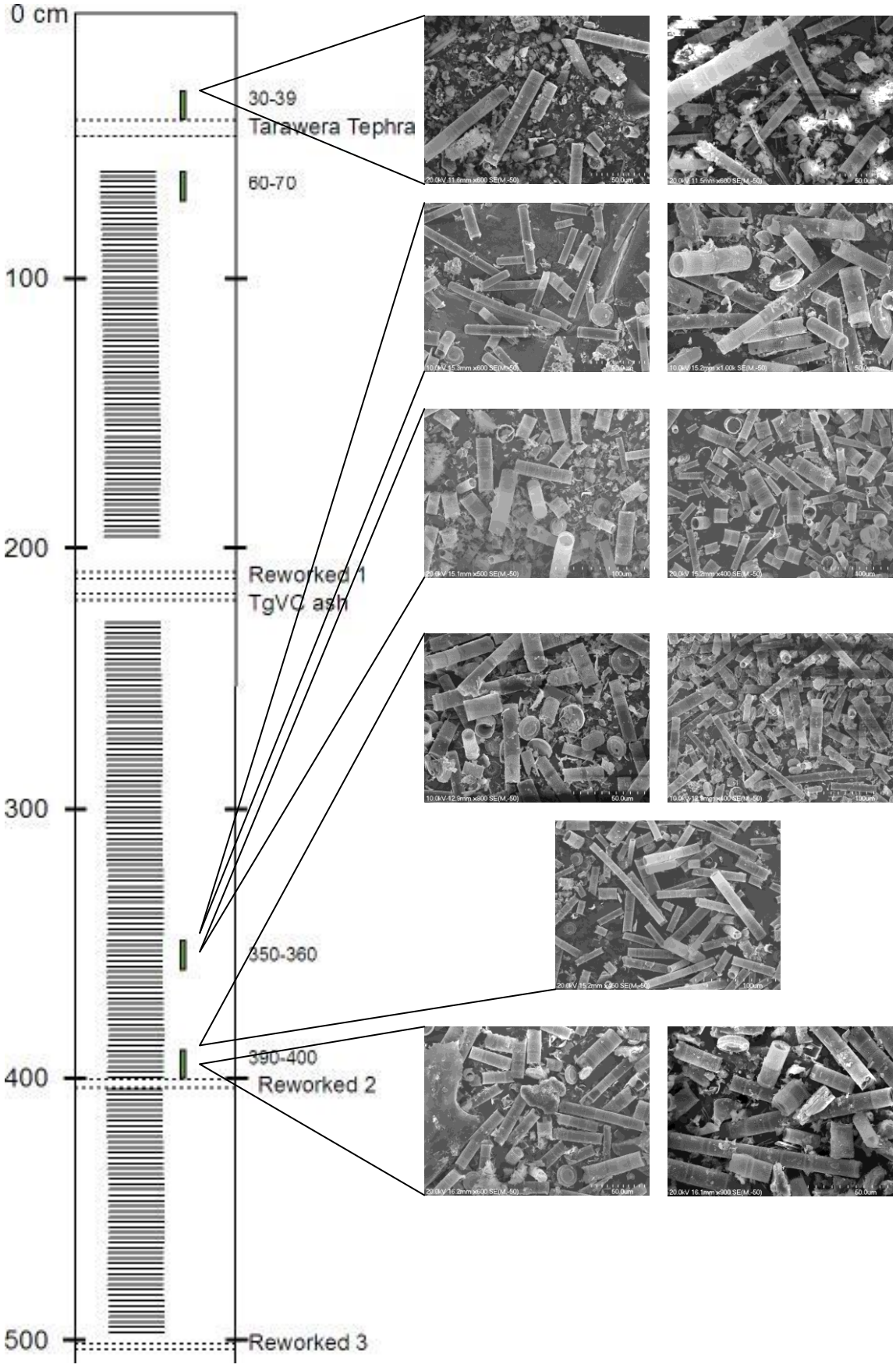

Figure 5.7: Representative SEM images from RU188 at depth ranges as noted (in cm).

Identification of diatom species present was made using taxonomic guides and scanning electron photographs from Cassie (1984), Round et al. (1990), Cassie-Cooper (1996), and with assistance from Dr Vivienne Cassie-Cooper.

5.4.1 Diatom record

A total of 20 diatom taxa were identified in the SEM images from the representative samples. The most abundant diatoms were the planktonic taxa *Aulacoseira granulata v. angustissima, Aulacoseira islandia, Cyclotella stelligera and Stephanodiscus sp.* Benthic taxa were less common with the most common being *Achnanthes sp. Cocconeis sp., Epithemia sorex, Eunotia sp.,* and *Rhopalodia sp.* (Fig. 5.8).

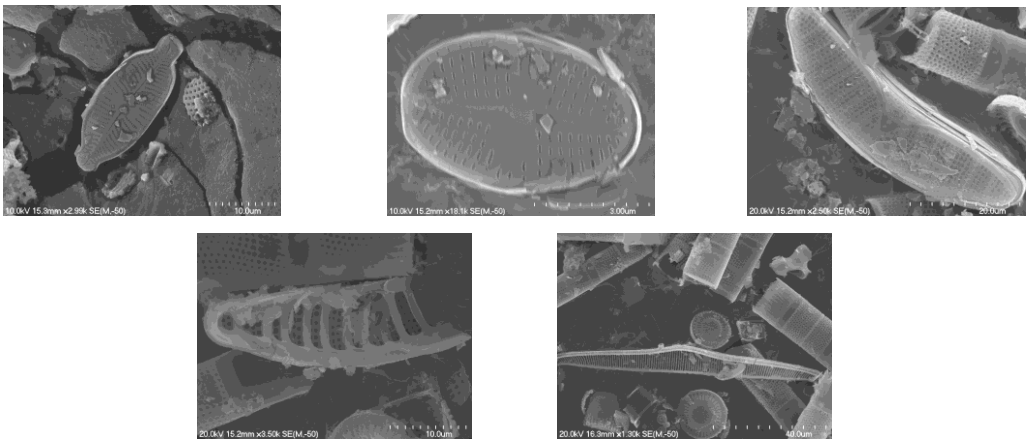

Figure 5.8: Examples of benthic taxa (l-r) – *Achnanthes sp. Cocconeis sp., Epithemia sorex, Eunotia sp.,* and *Rhopalodia sp.*

Three zones of diatom assemblages were identified and based on these identifications pH and water conditions inferred. These samples are dominated by planktonic taxons which are typically associated with alkaliphilous conditions.

5.4.1.1 30-32 cm (c. 58-64 cal. years B.P.)

The first zone includes the uppermost samples from 30 and 32 cm depths (Figs. 5.9 & 5.10). The typically eutrophic *Aulacoseira granulate* is abundant in these samples, although this species is thought to tolerate a wide range of trophic conditions. Also found were various other species including *A. islandia, Achnanthes sp., Cocconeis placentula, Fragilaria construens, Nitzschia sigmoidea, Pinnularia microstauron,* and *Synedra sp.* These freshwater species all prefer high pH and tolerate some salt, apart from *Achnanthes sp.,* which is

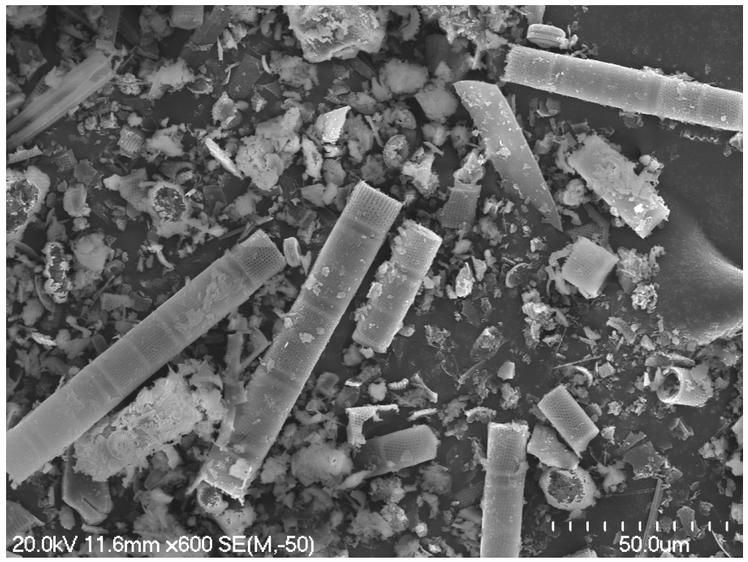



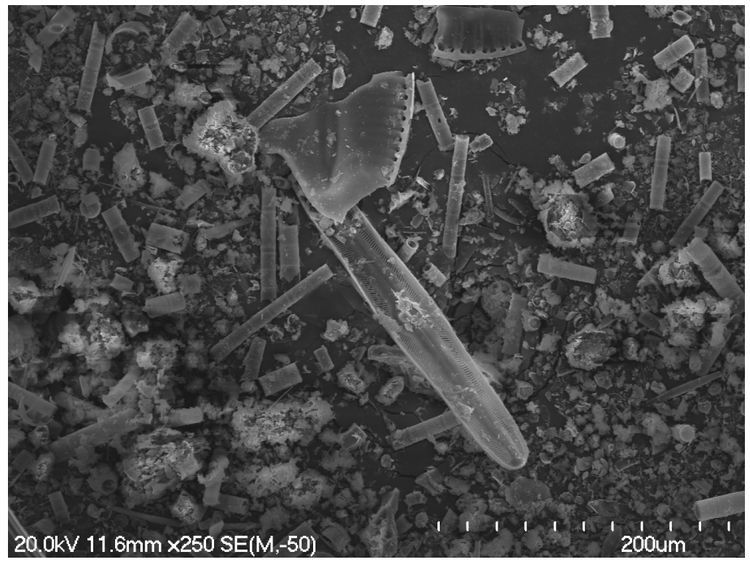

Complex of Aulacoseira granulata/islandia & Pinnularia microstauron

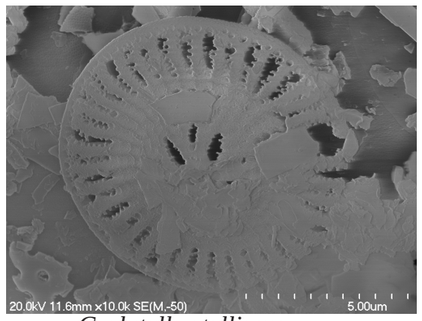

Cyclotella stelligera





Achnanthes sp.

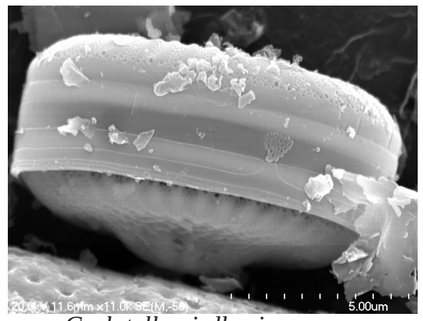

Cyclotella girdle view

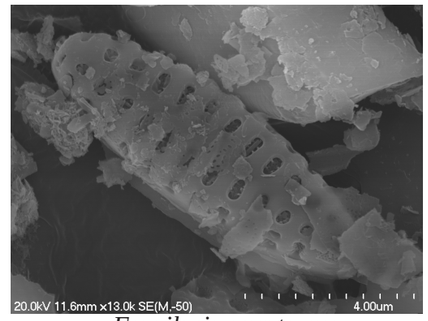

Fragilaria construens

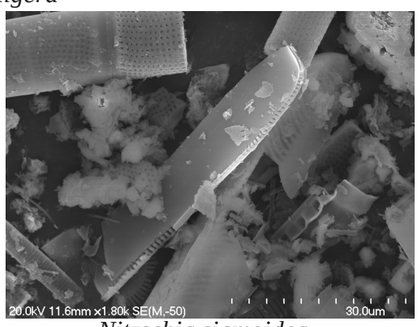

Nitzschia sigmoidea



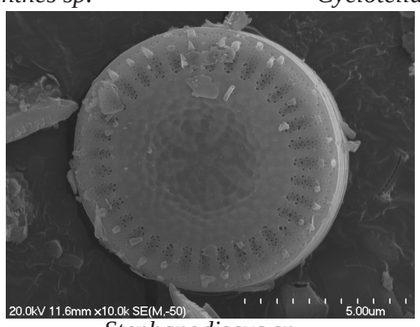

Stephanodiscus sp.

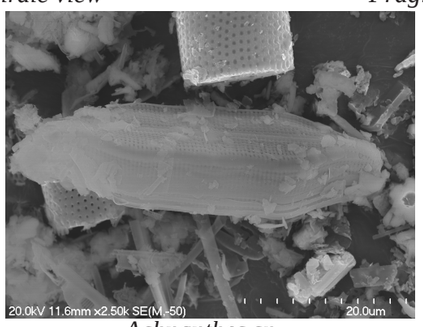

Achnanthes sp.

Figure 5.9: Diatoms from sample at 30 cm depth.

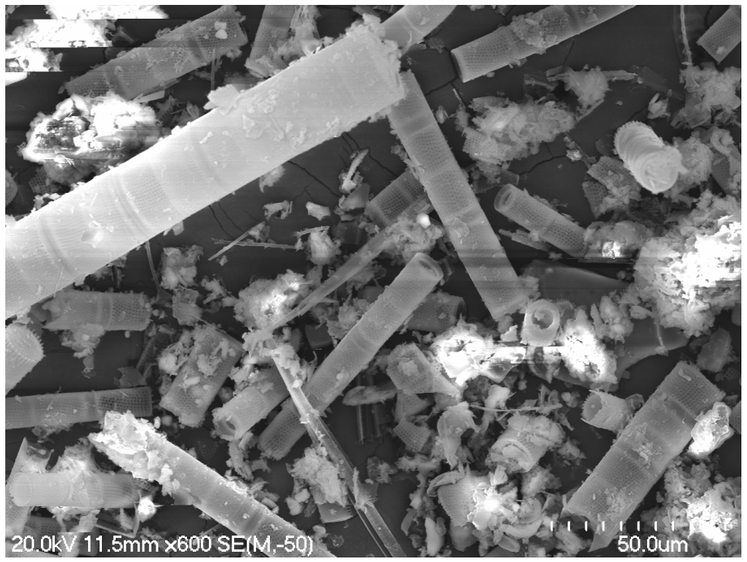

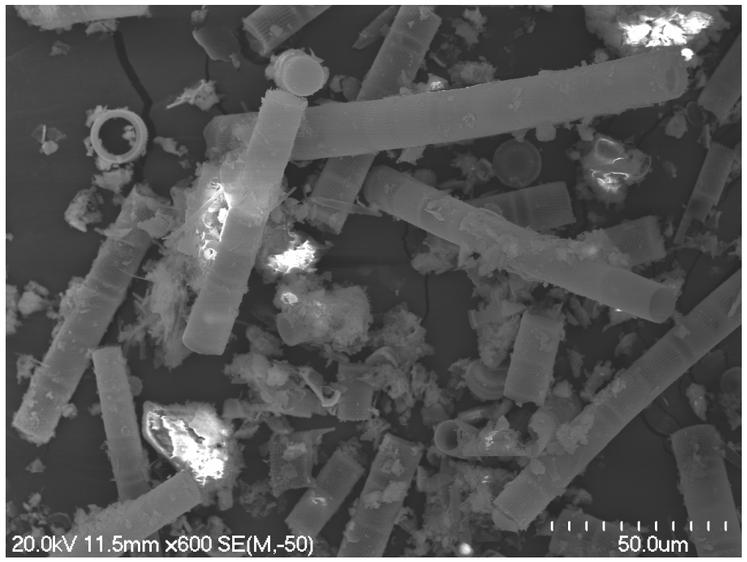

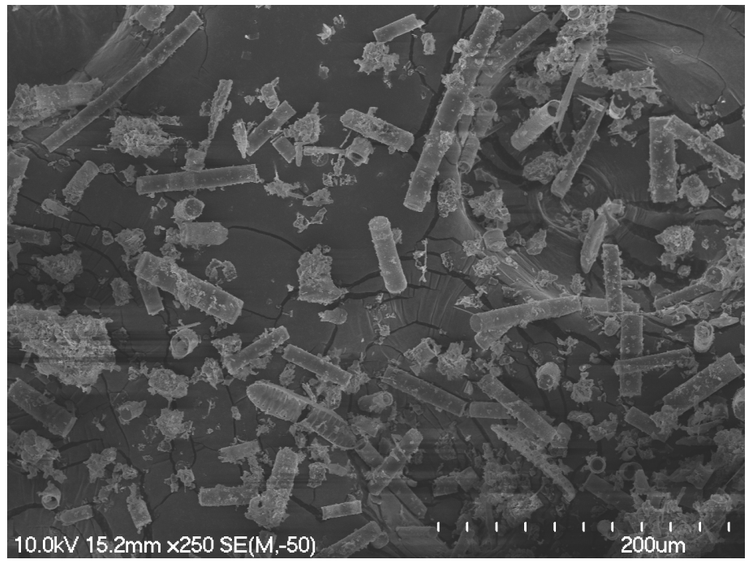



Aulacoseira granulata

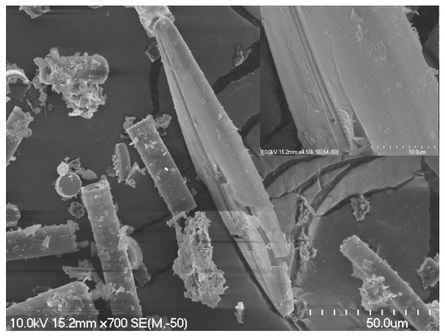

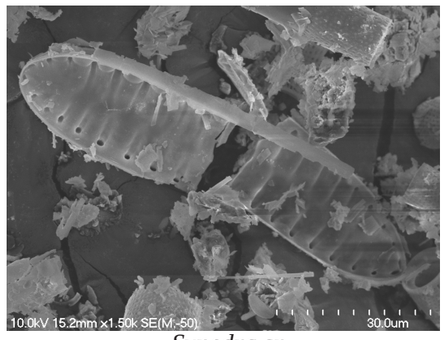

Synedra sp.



Cyclotella stelligera



Stephanodiscus sp.

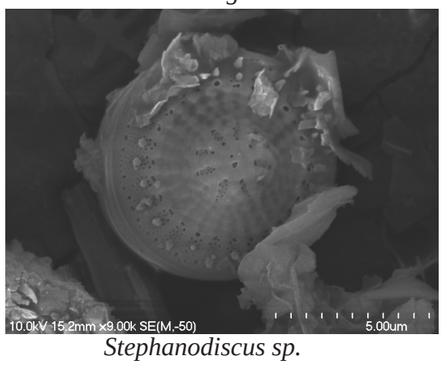

Stephanodiscus sp.

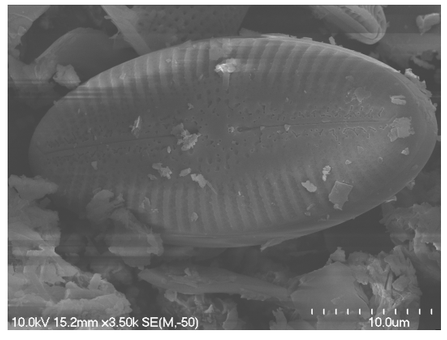

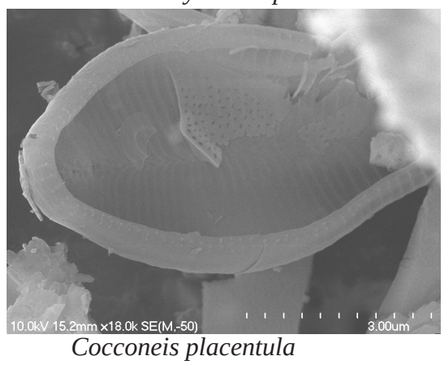

Cocconeis placentula

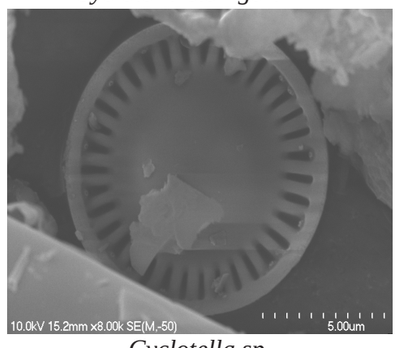

Cyclotella sp.

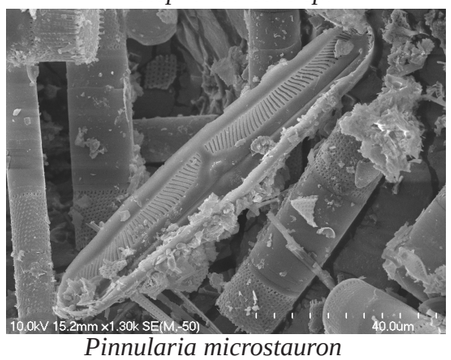

Pinnularia microstauron

Figure 5.10: Diatoms from at sample 32 cm depth

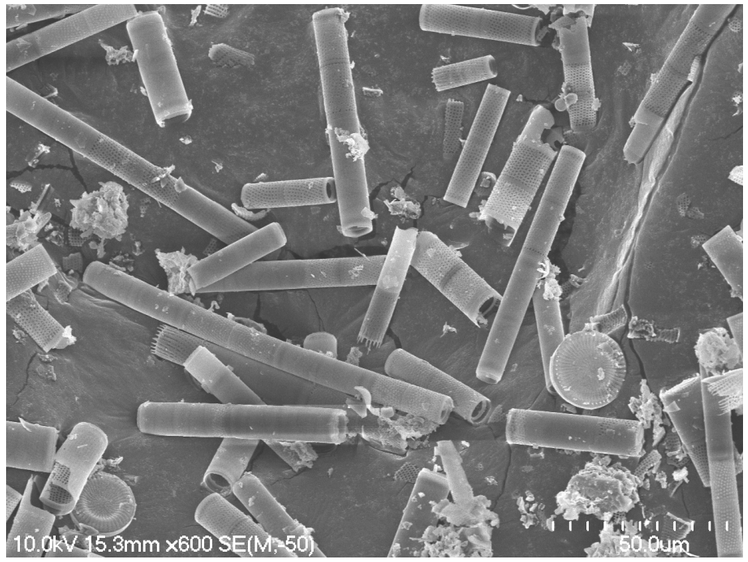

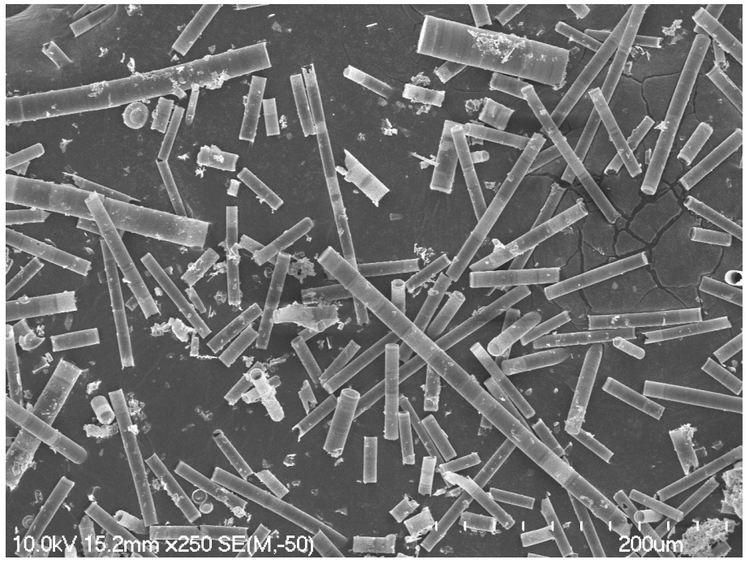

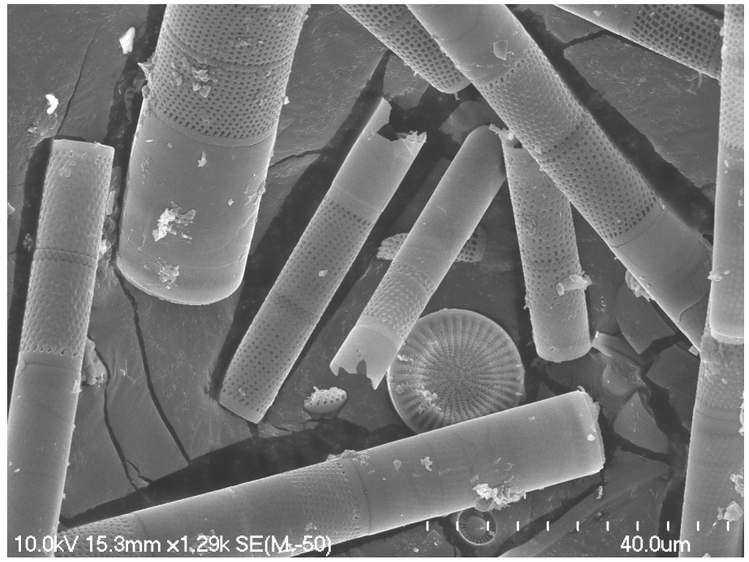

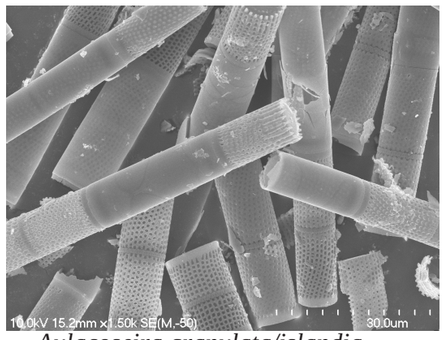

Aulacoseira granulata/islandia

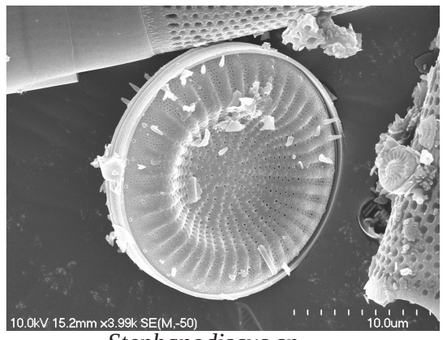

Stephanodiscus sp.



Cyclotella stelligera

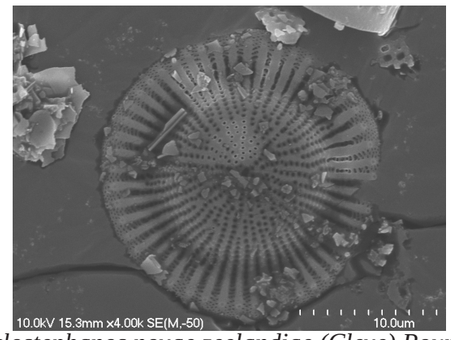

Cyclostephanos novae zeelandiae (Cleve) Round

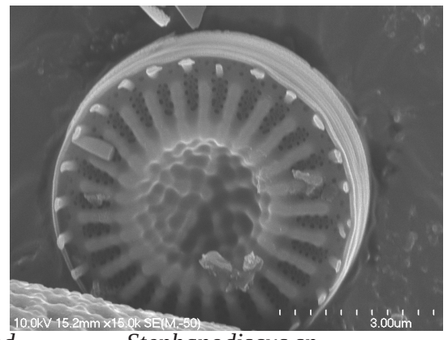

Stephanodiscus sp.

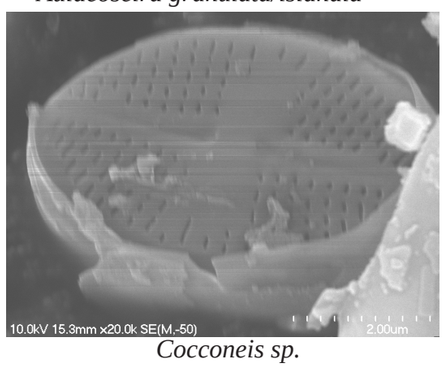

Cocconeis sp.

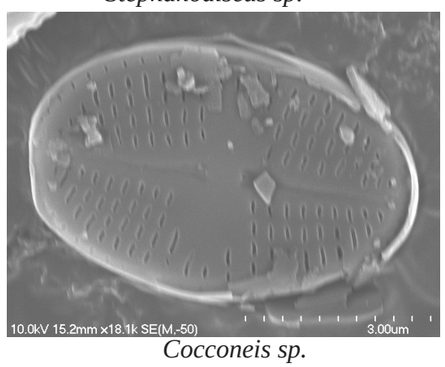

Cocconeis sp.

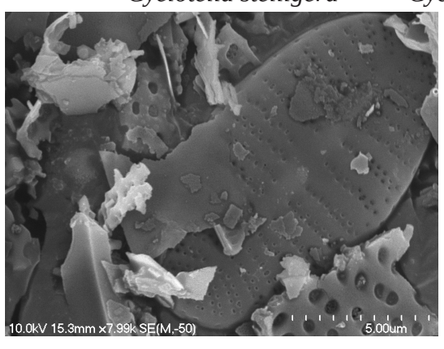

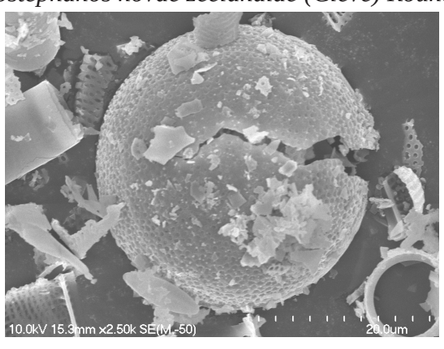

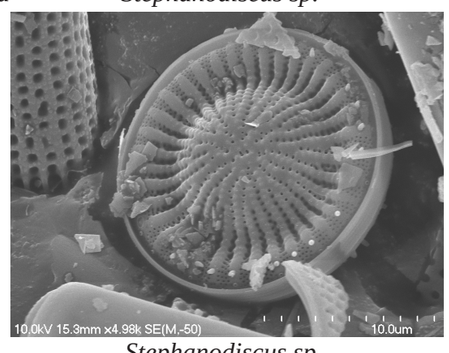

Stephanodiscus sp.

Figure 5.11: Diatoms from sample at 350 cm depth

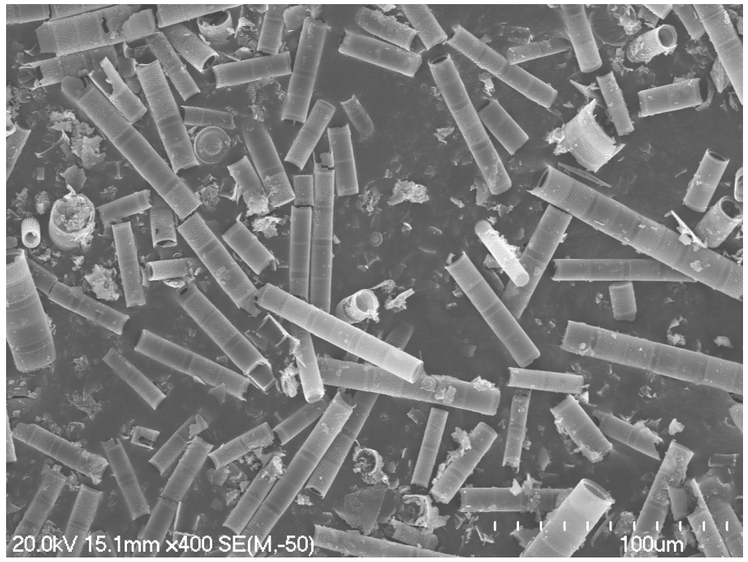



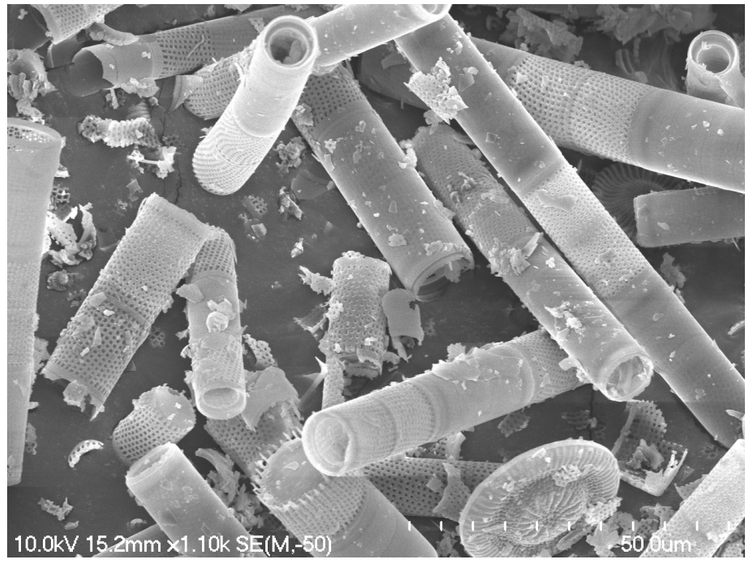

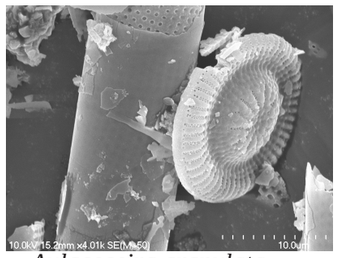

Aulacoseira granulata

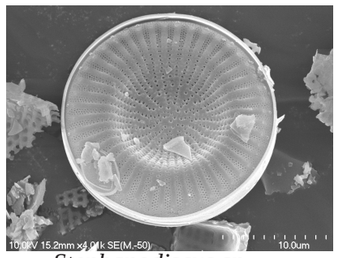

Stephanodiscus sp.

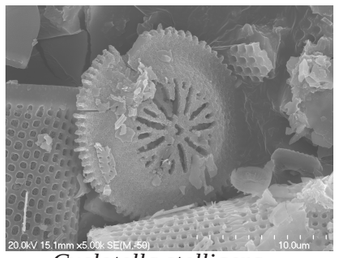

Cyclotella stelligera

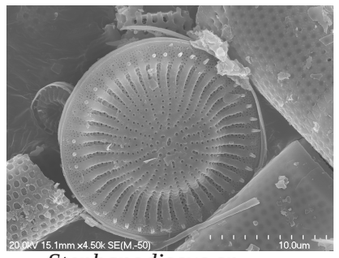

Stephanodiscus sp.

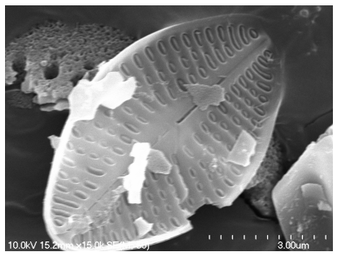





Achnanthes lanceolata

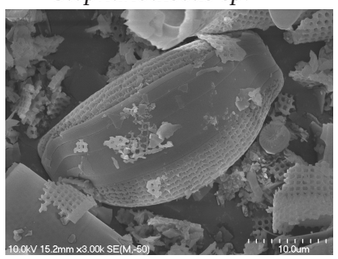



Achnanthes sp.

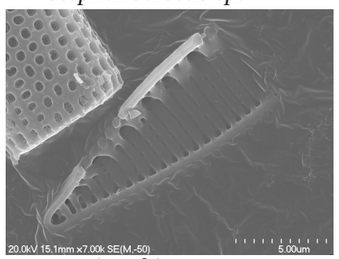

Nitzschia sp.

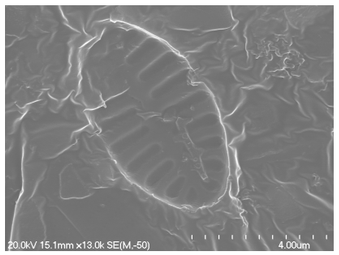

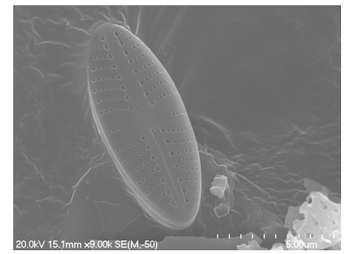

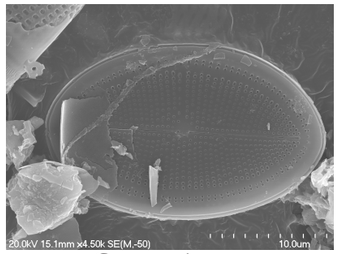

Cocconeis sp.

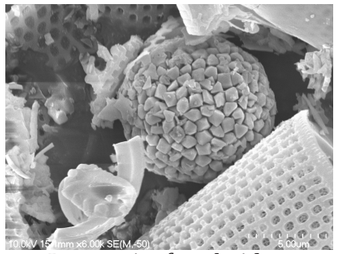

Iron pyrite framboid

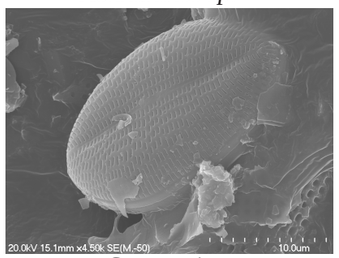

Cocconeis sp.

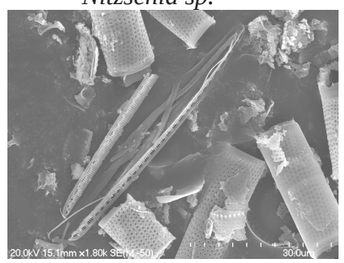

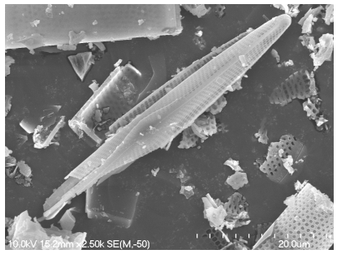

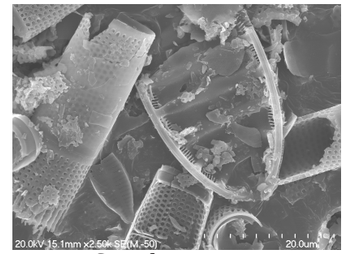

Synedra sp.

Figure 5.12: Diatoms from sample at 351 cm depth

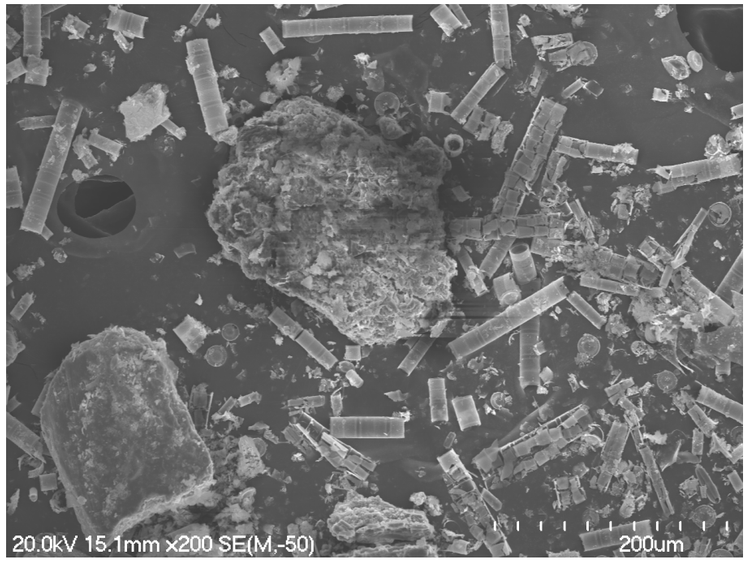

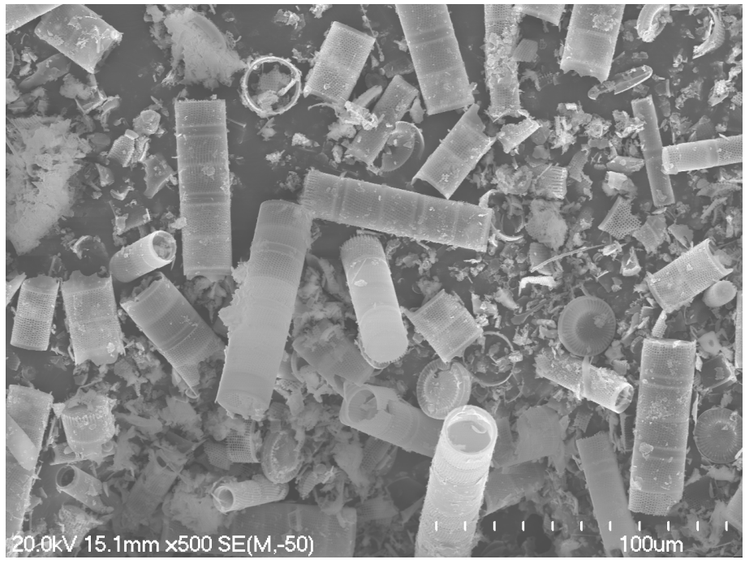

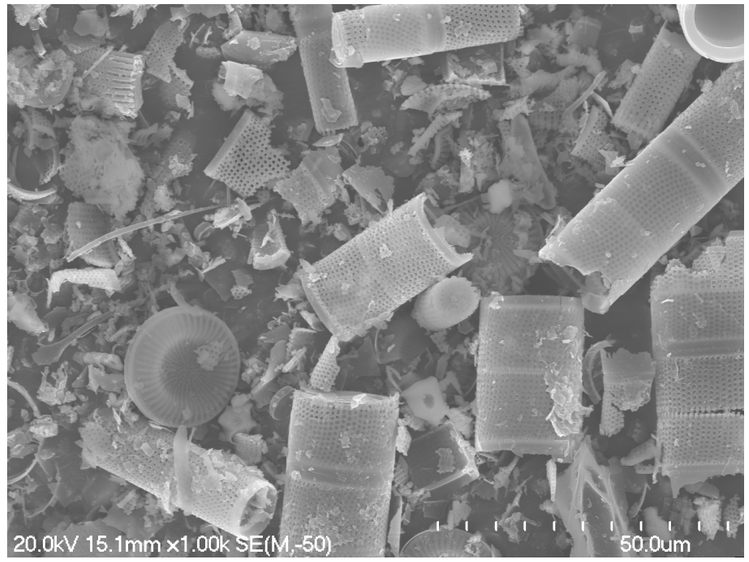

Large clasts of debris with *Aluacoseira sp.*

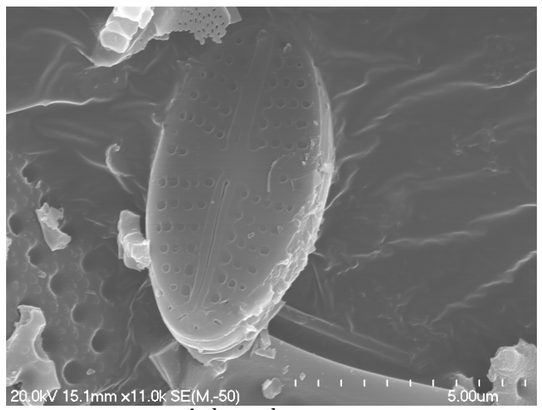

Achnanthes sp.

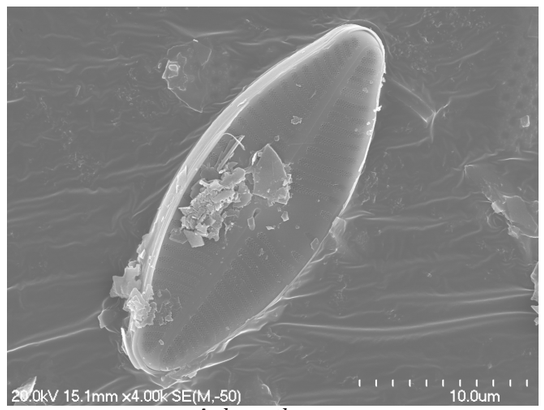

Achnanthes sp.

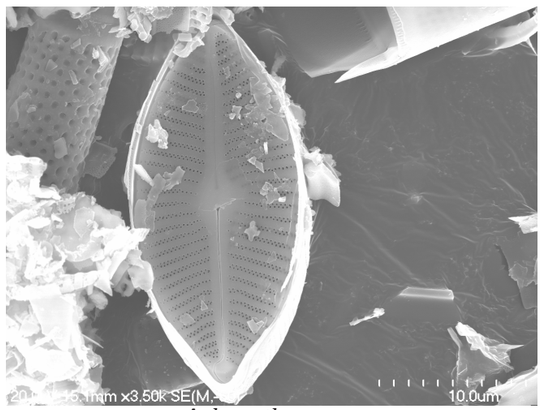

Achnanthes sp.

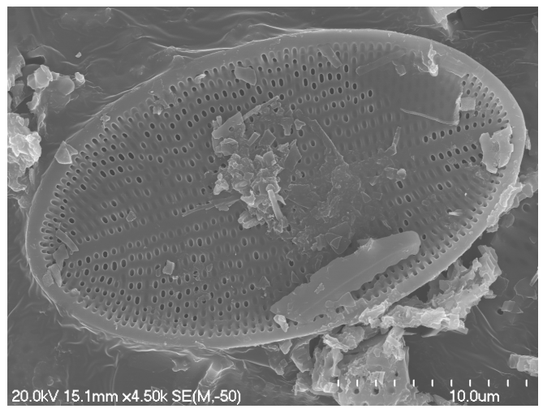

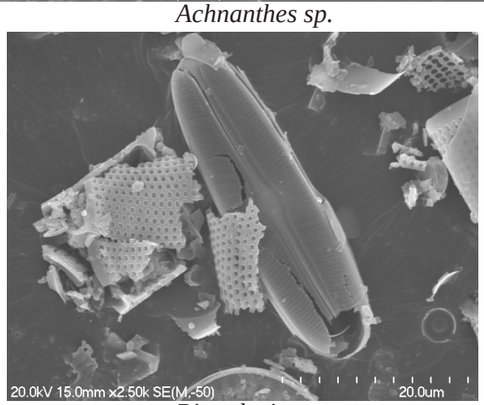

Pinnularia sp.

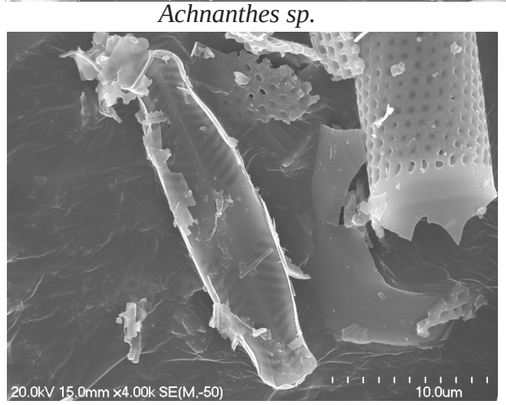

Figure 5.13: Diatoms from sample at 358 cm depth

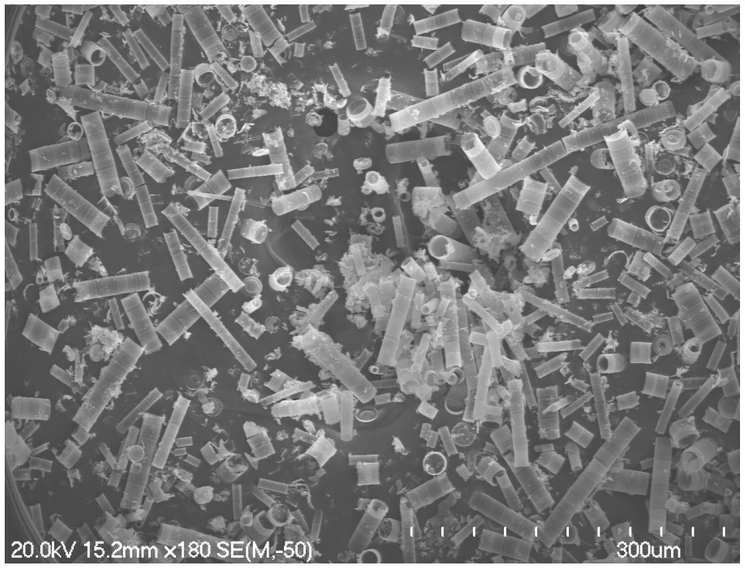

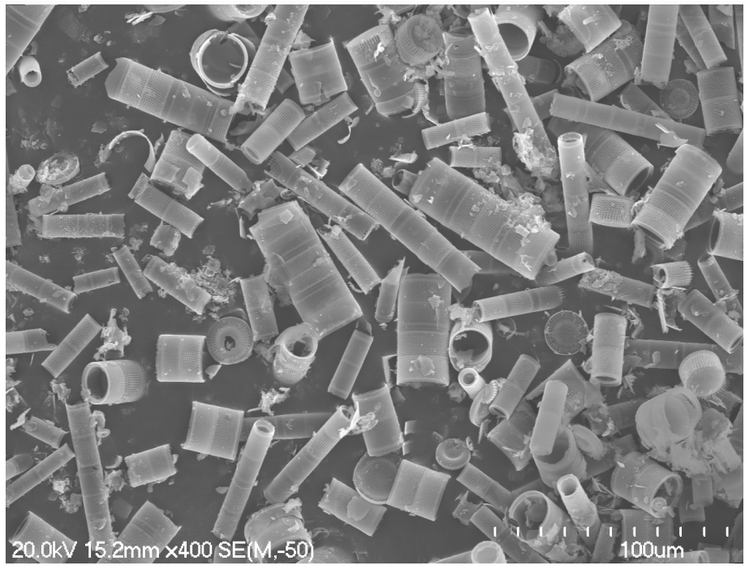

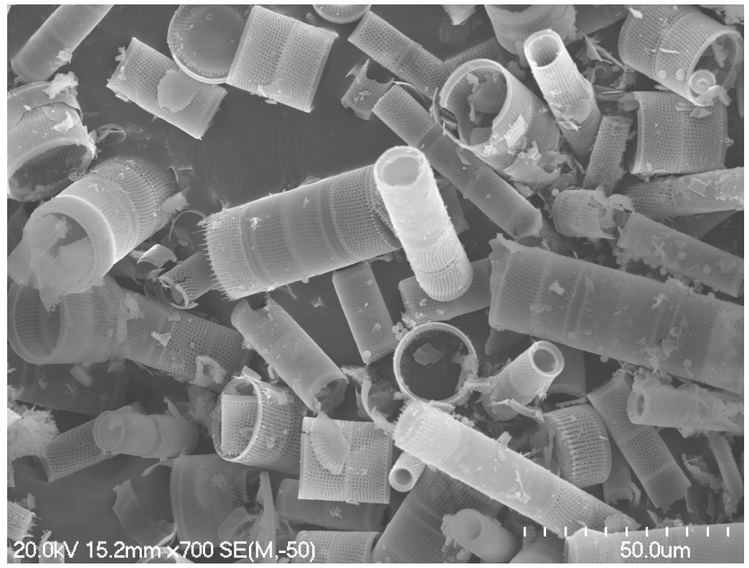

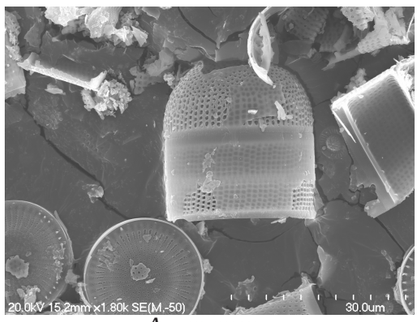

Auxospore

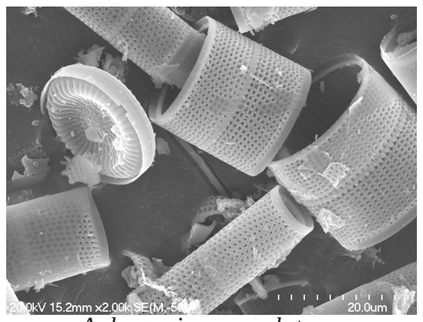

Aulacoseira granulata

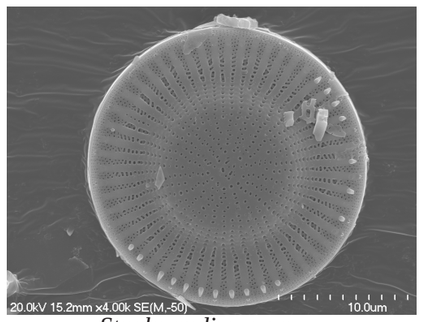

Stephanodiscus sp.

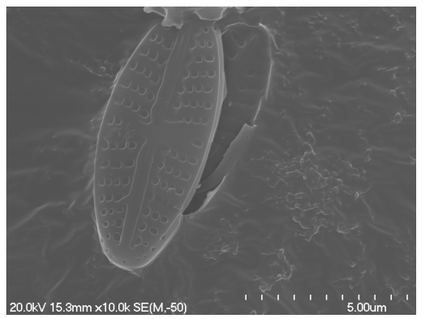

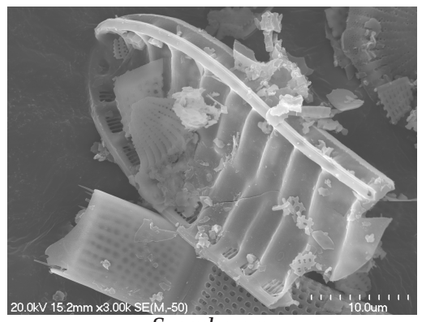

Synedra sp.

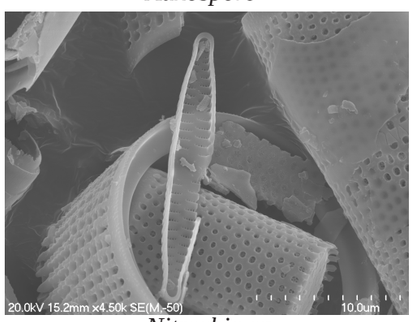

Nitzschia sp.

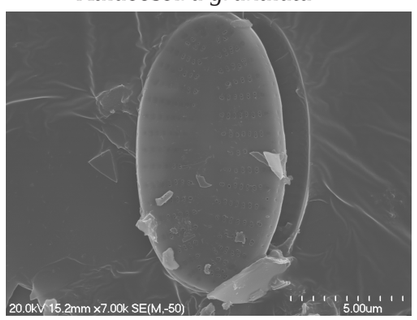

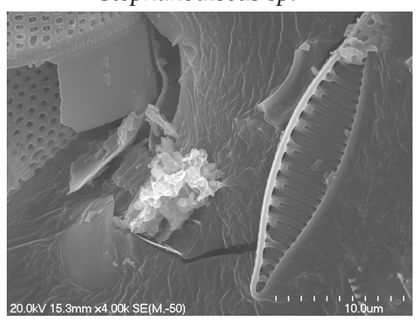

Nitzschia sp.

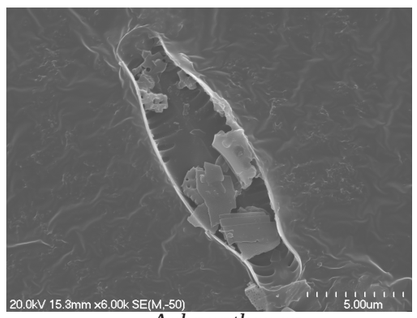

Achnanthes sp.

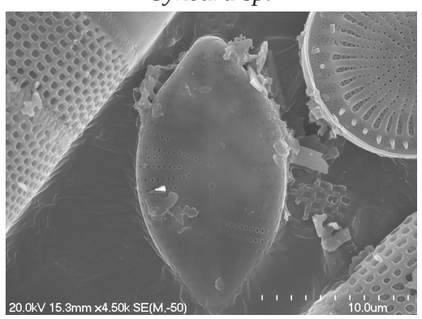

Figure 5.14: Diatoms from sample at 359 cm depth

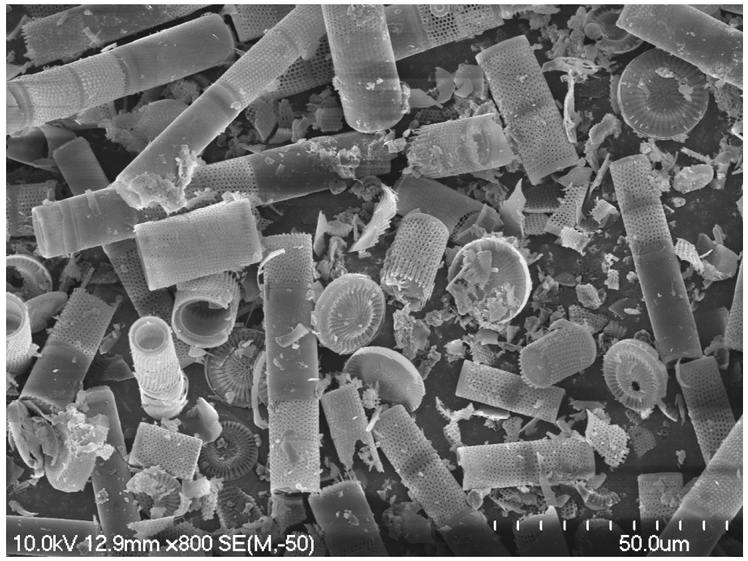

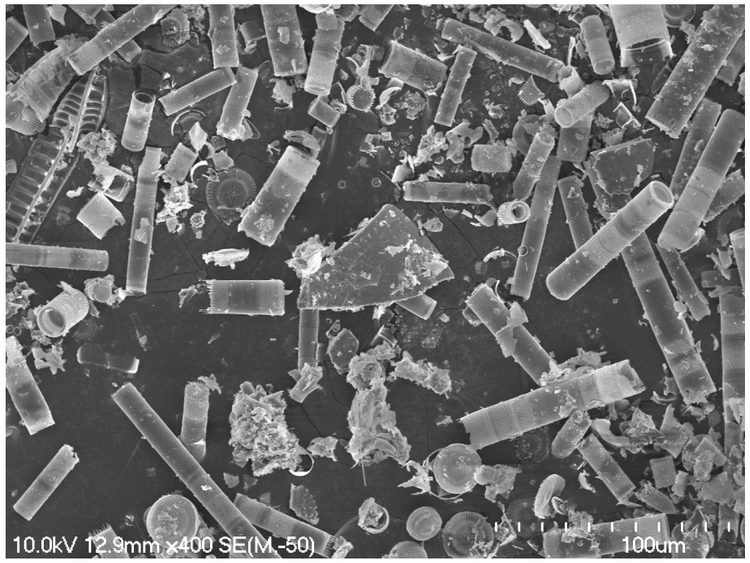

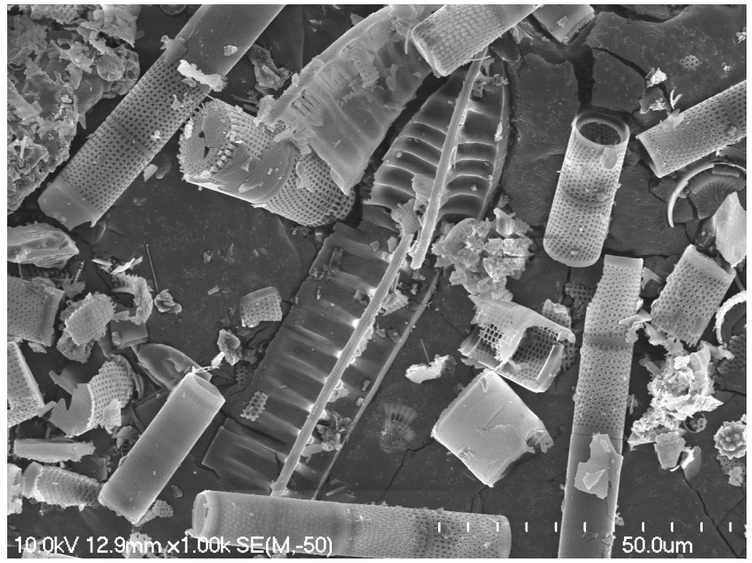

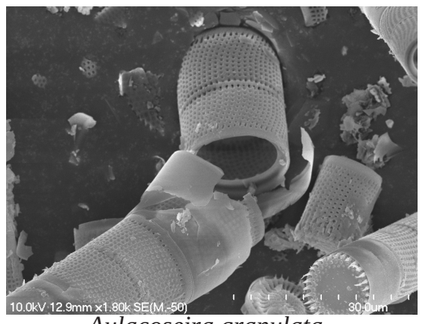

Aulacoseira granulata

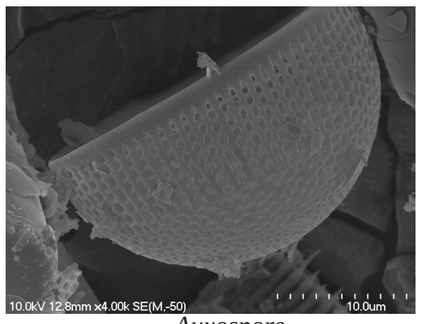

Auxospore

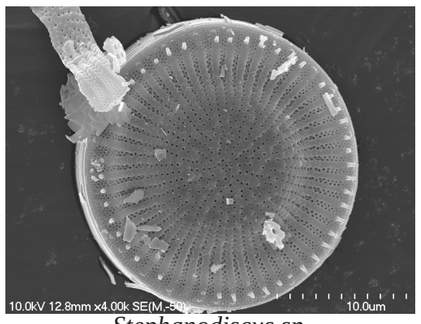

Stephanodiscus sp.

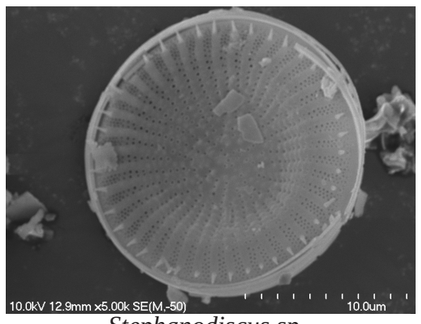

Stephanodiscus sp.

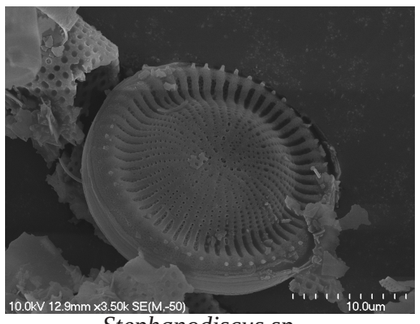

Stephanodiscus sp.

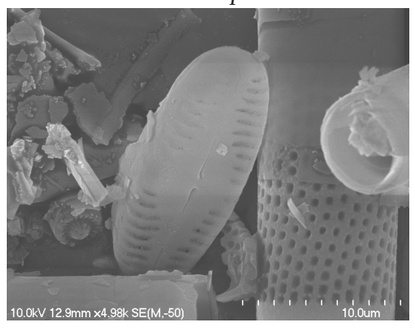

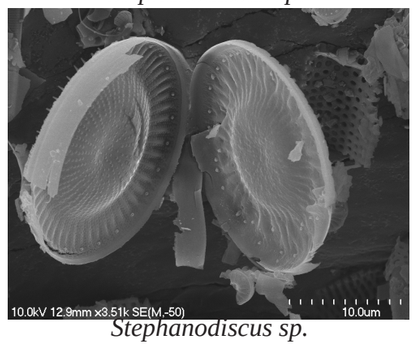

Stephanodiscus sp.

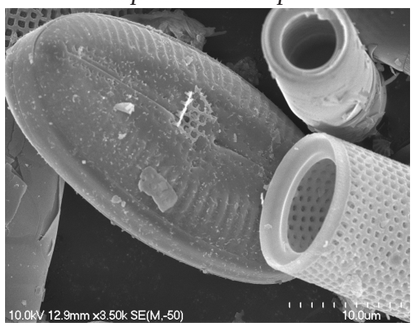

Figure 5.15: Diatoms from sample at 390 cm depth

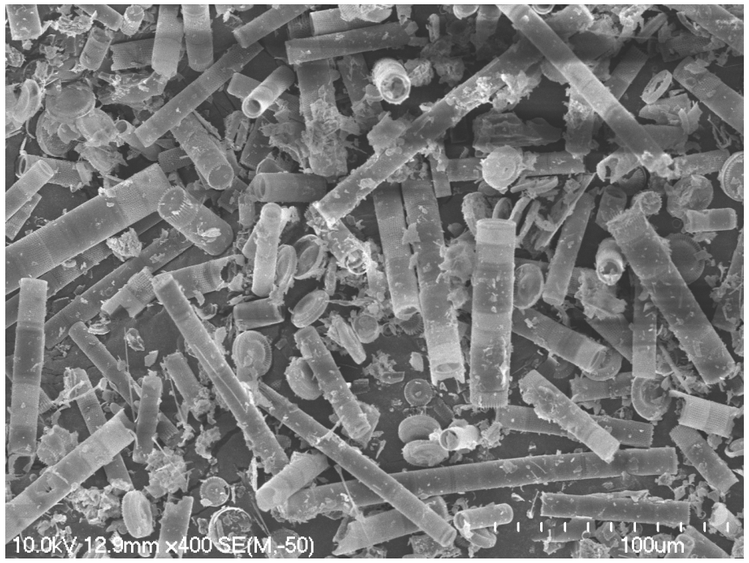





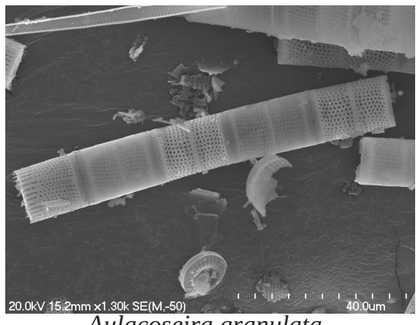

Aulacoseira granulata

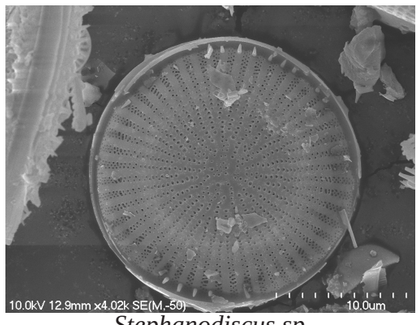

Stephanodiscus sp.

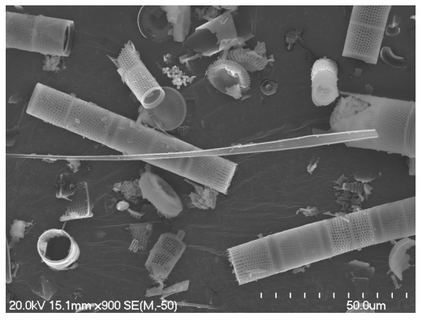

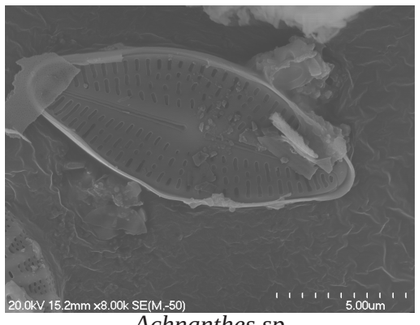

Achnanthes sp.

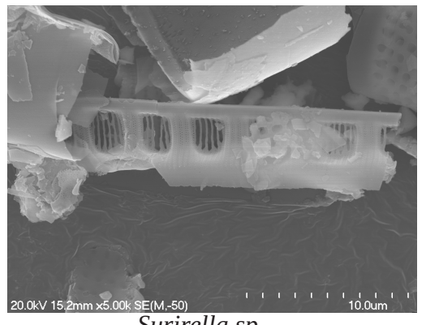

Surirella sp.

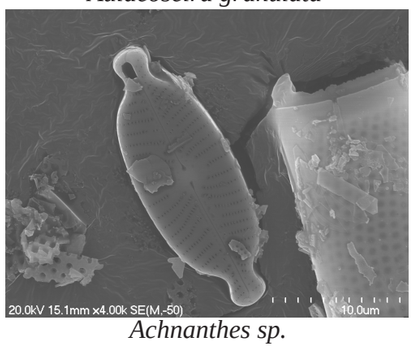

Achnanthes sp.



Staurosirella sp.

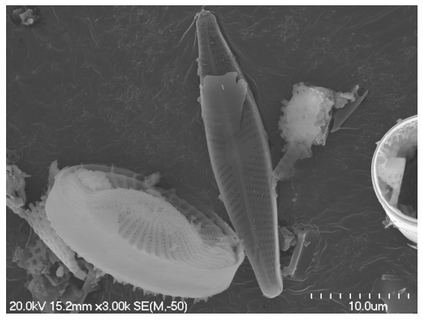

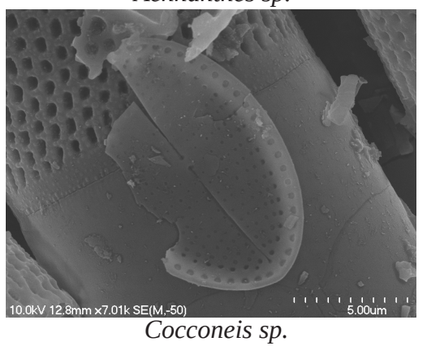

Cocconeis sp.

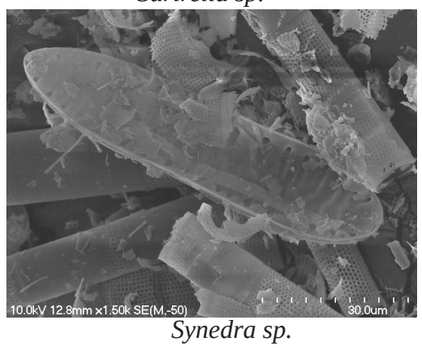

Synedra sp.

Figure 5.16: Diatoms from sample at 391 cm depth

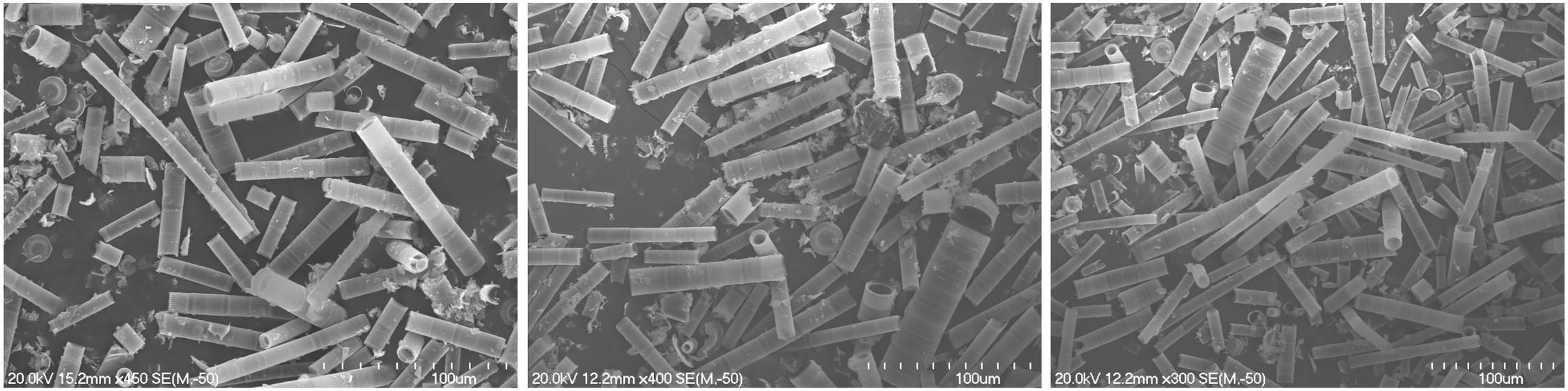

Aulacoseira granulata with auxospores *Aulacoseira granulata* *Stephanodiscus alpinus* *Stephanodiscus alpinus* *Navicula sp.* *Achnanthes lanceolata*

Part of Surirella *Frustulia sp.* *Achnanthes sp.* *Surirella sp.* *Cocconeis pediculus* *Cocconeis placentula*

Cocconeis placentula *Pollen spores* *Aulacoseira with pollen spores*

Figure 5.17: Diatoms from sample at 392 cm depth

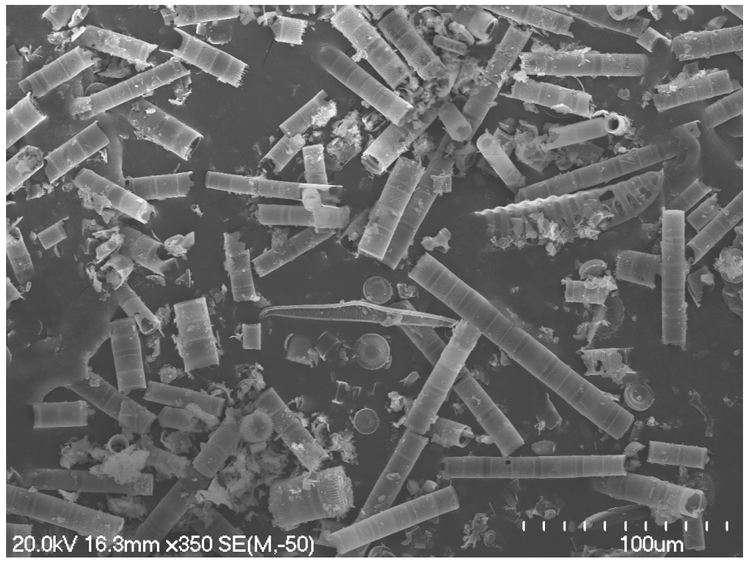

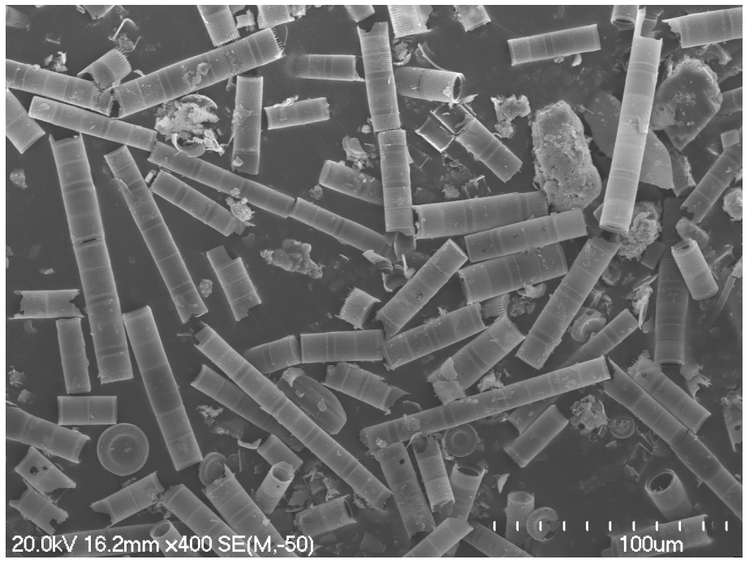

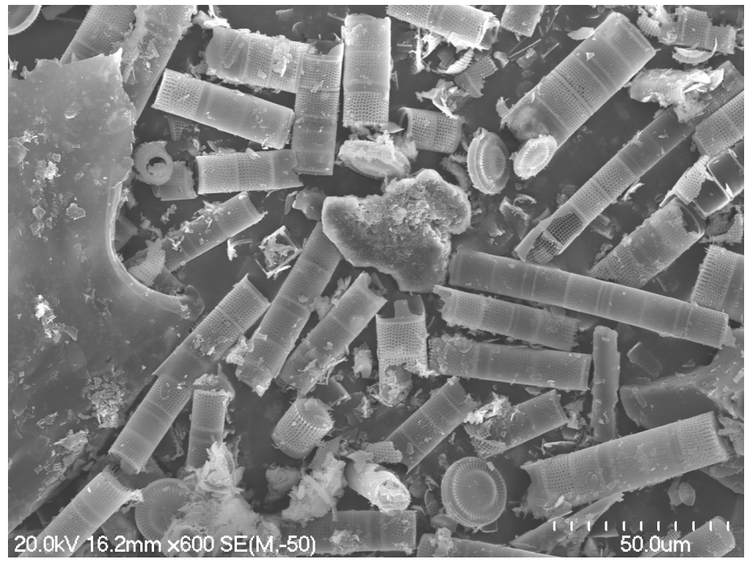

Aulacoseira granulata and debris

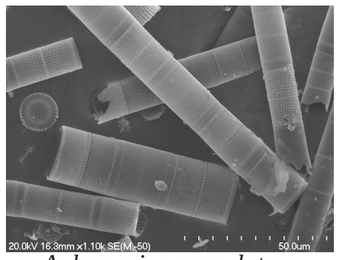

Aulacoseira granulata

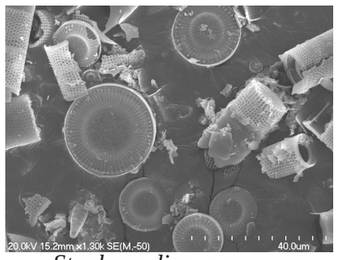

Stephanodiscus sp.



Cyclotella sp.



Stephanodiscus sp.

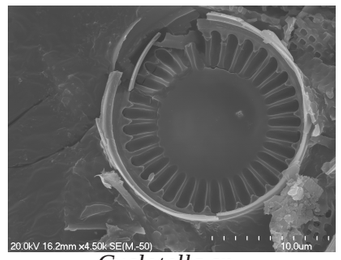

Cyclotella sp.

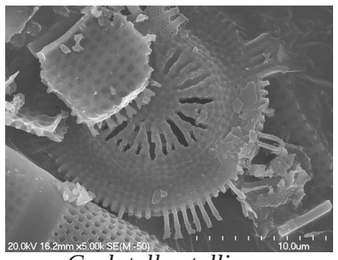

Cyclotella stelligera

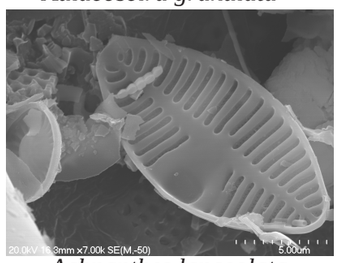

Achnanthes lanceolata

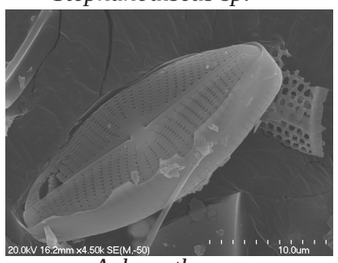

Achnanthes sp.

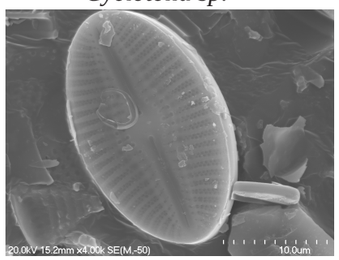

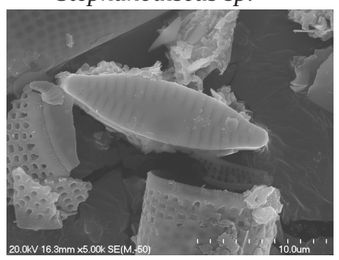

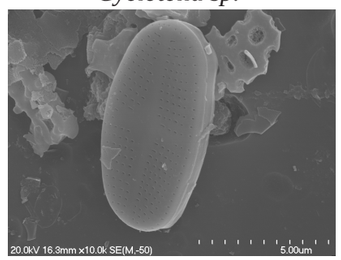



Pinnularia microstauron

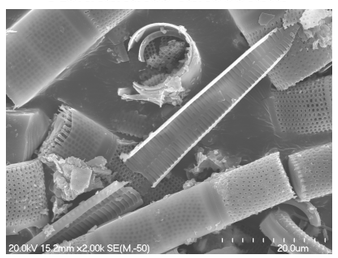

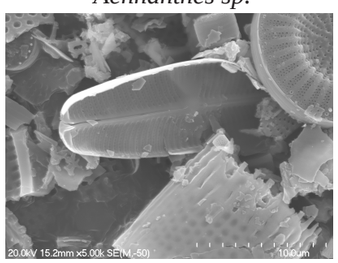

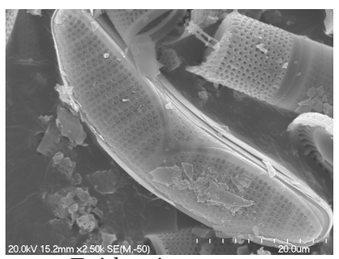

Epithemia sorex



Synedra sp.

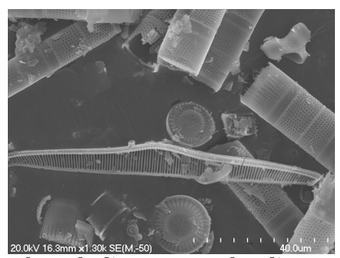

Rhopalodia novae-zelandiae

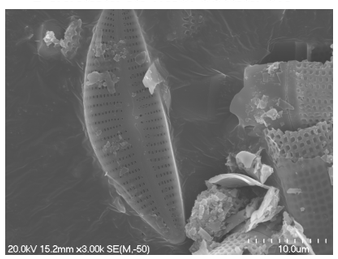

Figure 5.18: Diatoms from sample at 396 cm depth



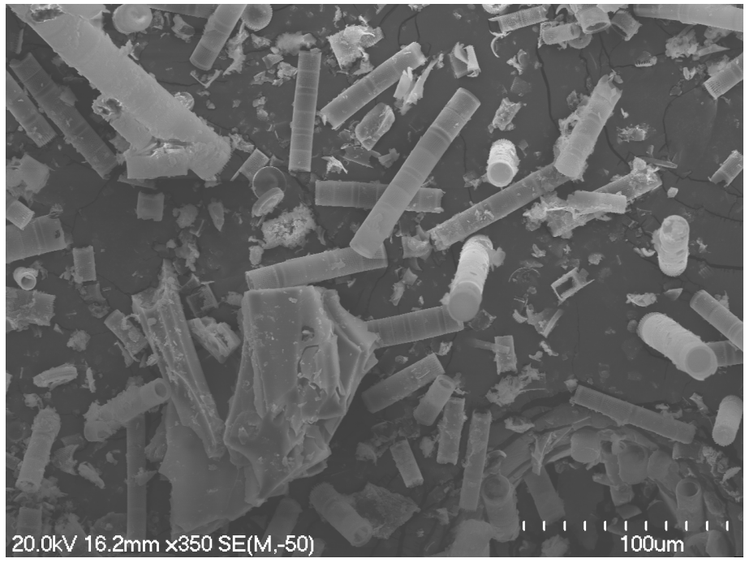

Aulacoseira granulata/islandia and debris

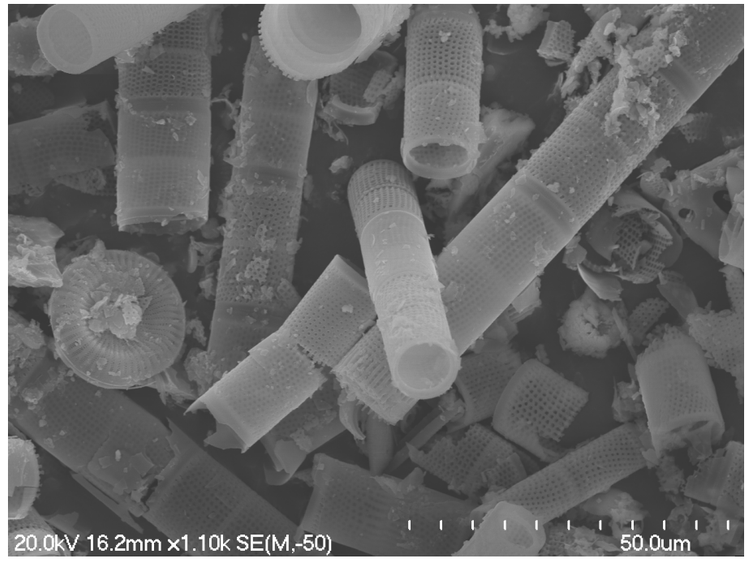

Aulacoseira granulata/islandia and *Cyclotella stelligera*

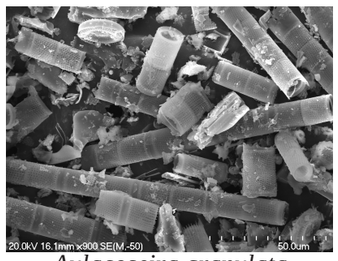

Aulacoseira granulata

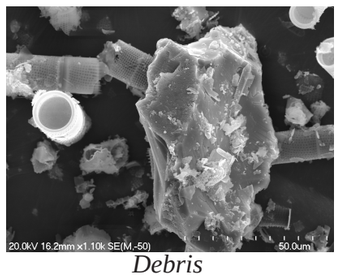

Debris

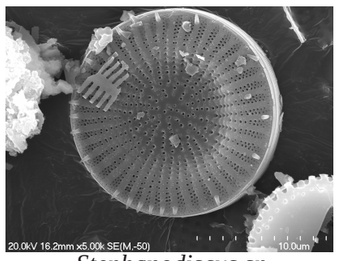

Stephanodiscus sp.

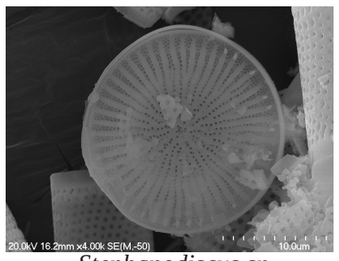

Stephanodiscus sp.

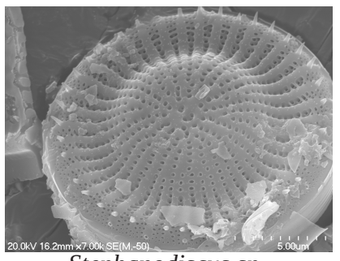

Stephanodiscus sp.





Cocconeis disculus

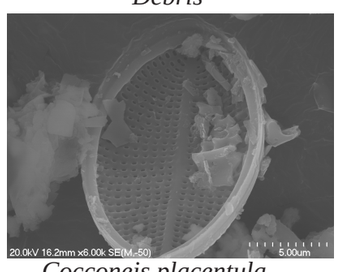

Cocconeis placentula

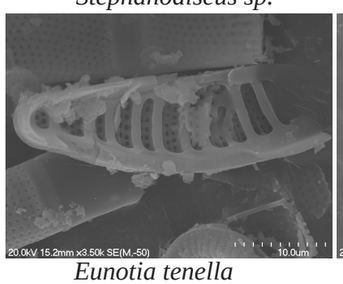

Eunotia tenella

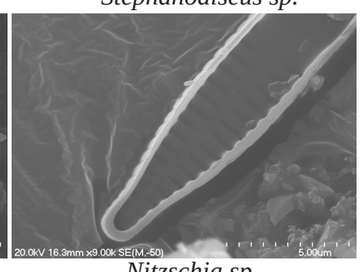

Nitzschia sp.

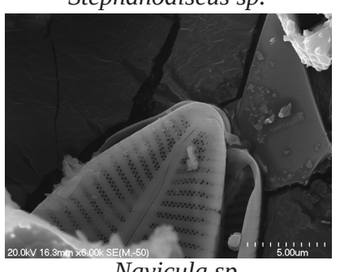

Navicula sp.

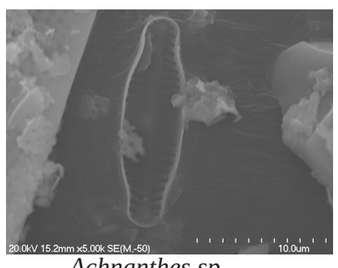

Achnanthes sp.



Navicula sp.

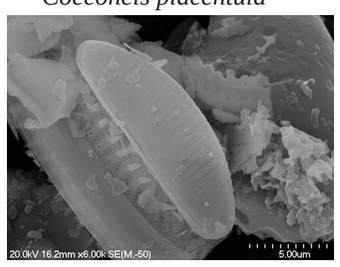

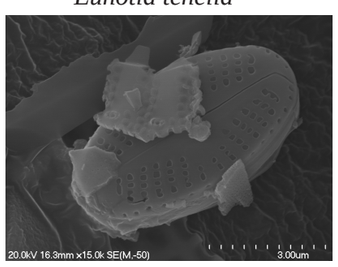

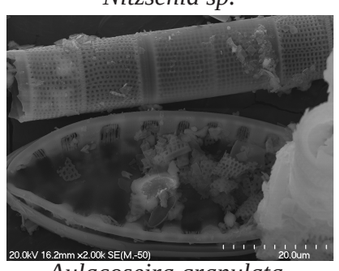

Aulacoseira granulata with Surirella sp.

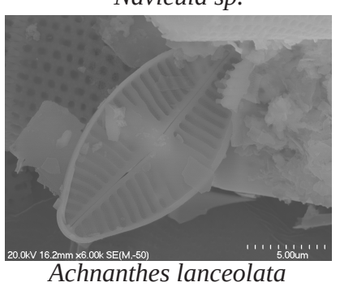

Achnanthes lanceolata

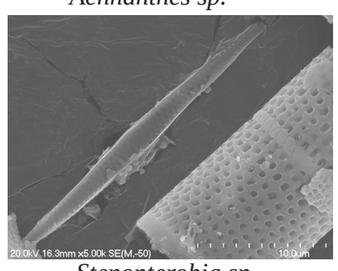

Stenopterobia sp.

Figure 5.19: Diatoms from sample at 400 cm depth

acidophilous (6.4-6.6) and which prefers oligotrophic conditions (Cassie, 1989). Reconstructed values for pH indicate a smaller range but similar water conditions as inferred from values for underlying samples.

5.4.1.2 350-359 cm (c. 450-475 cal. years B.P.)

This zone incorporates the four sediment samples taken from between 350 and 359 cm (Figs. 5.11-5.14). These samples are dominated by planktonic species *Aulacoseira granulate* and *A. islandia.* The planktonic taxa *Cyclotella stelligera, Nitzschia sp., Stephanodiscus sp.,* and *Cyclostephanos novae zeelandiae (Cleve) Round* are also relatively abundant though this period. The only benthic taxon identified is *Cocconeis sp.* These taxa are typical of alkaliphilous conditions, preferring a high pH, and some salt. Also seen was an iron pyrite framboid (Fig. 5.12).

5.4.1.3 390-400 cm (c. 510-520 cal. years B.P.)

This deepest zone consists of five samples taken between 390 and 400 cm (Figs. 5.15-5.19). These samples are dominated by planktonic species *Aulacoseira granulate* and *A. islandia, Cyclotella sp.* (including *Cyclotella stelligera*), and *Stephanodiscus sp.* (including *Stephanodiscus alpinus).* Benthic taxons include *Achnanthes sp.* (including *Achnanthes lanceolata*), *Cocconeis sp.* (including *Cocconeis disculus*, *Cocconeis pediculus* and *Cocconeis placentula*), *Eunotia tenella, Rhopalodia novae-zealandiae, Stenopterobia sp.* These species prefer some salt (oligohalobous) and a high pH but *Eunotia tenella* is intolerant of salt and is typically indicative of oligotrophic waters. Also found are various other species which prefer a silt dominated habitat including *Frustulia sp., Navicula sp., Nitzschia sp., Surirella sp., Pinnularia microstauron,* and *Staurosirella sp*. All of these silt species prefer fresh or slightly brackish water of high pH. *Nitzschia sp.* in particular prefers a pH of (6.5-8.4) and eutrophic waters. *Navicula, Pinnularia microstauron, Rhopalodia novae-zealandiae, Stephanodiscus,* and *Surirella* species generally only like water with little salt. Hence reconstructed values for pH indicate a high pH probably ranging between 6.5-8.4, lower tolerances of salt than overlying layers, and mixed water conditions ranging from slightly brackish water near the water-sediment interface with possibly the majority of the lake water oligotrophic. The SEM images also found a number of pollen spores attached to one of the *Aulacoseira granulate*.

The SEM images taken from individual laminae of different colours showed that darker laminae are primarily the result of greater amount of clastic (detrital) material, whereas the paler laminae are mainly biogenic material.

5.5 Grain-size analysis

Although chemical or biological evidence provide useful insights into former environmental conditions, lithologic records provide a substantial amount of information regarding environmental change within the catchment basin. Grain size distribution is generally controlled by the source material and the energy of the transport medium. Furthermore, grain size commonly demonstrates a decreasing trend from the margin to deepest point in a basin (Yum et al., 2003).

Grain size and texture play an important role in determining the proportion of particles washed in from the surrounding catchment. The interpretation gives clues to the source, mechanisms for transport, and past physical and chemical environmental and limnological conditions in the basin at the time of deposition. The most important aspect of grain size is its influence on other key properties within the sediment. In general, we consider any grain over 32 μm as clastic sediment – that means that it has generally been sourced from the surrounding catchment. Those grains over 63 μm are sand sized and probably originate from the reworking of coarse terrigenous sediment in the shallower (< 10 m) waters of the lake, and from tephra deposition.

The sediment in the core falls into two main types – mixed and silt. The coarser mixed sediments are typically poorly sorted, and occur over a range of depths. These deposits are usually dominated by volcanic fragments. Clastic grain size analysis was carried out on eight representative samples in the core from depths 30-39 cm, 60-70 cm, 350-360 cm, 390-400 cm, 530-540 cm, 556-566 cm, 600-610 cm, and 640-650 cm.

Silt-dominated sediment predominates over coarser sand-dominated sediments in the core (Fig. 5.20). The silt is composed predominantly of diatom frustules, especially species of *Aulacoseira granulata* and *Aulacoseira islandia* but also *Cyclotella stelligera* and *Stephanodiscus sp*. This silt fraction also contains a large proportion of clastic material. The clay-size fraction makes up a small (<

10%) proportion of the sediment but two significant changes are evident in the core. Above the 1886 A.D. Tarawera deposit the clay fraction makes up between 15-20% of the clastic derived sediment. Clay decreases below this deposit to ~ 10% and remains fairly consistent until ~ 5 m in depth. Below 5 m, the clay proportion increases to between 20-30 %. These two increases in clay are both associated with non-laminated sediments and possibly indicate background levels of deposition in the lake. The amount of clay material changes inversely with the sand (> 63 µm) fraction, hence where the sediment is laminated there is a larger amount of clastic material which hence effectively "dilutes" the background clay portion.

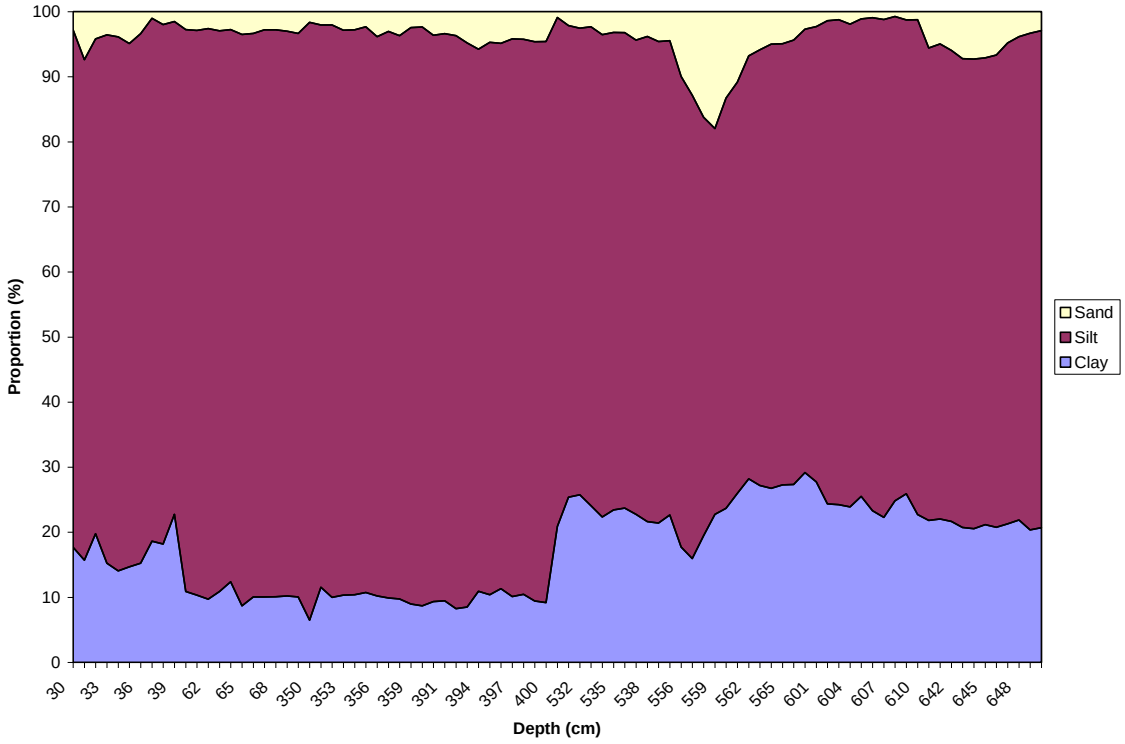

Figure 5.20: Grain size analysis of representative samples stacked on top of one another to get an overall down-core trend.

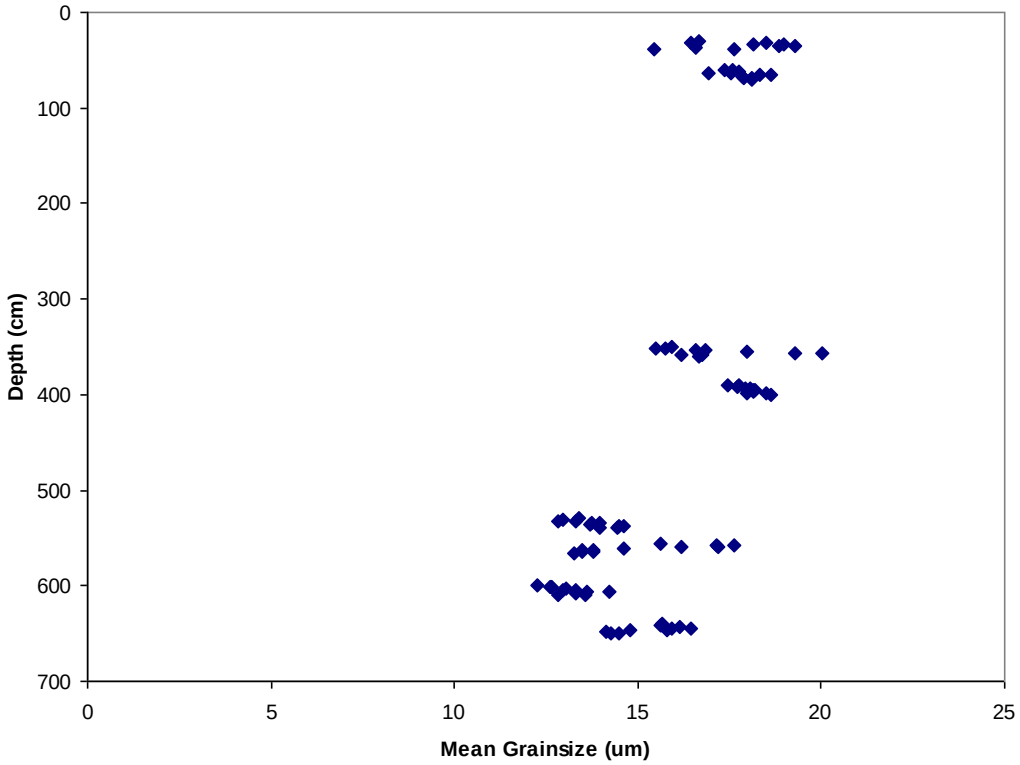

Figure 5.21: Mean grain size of representative samples from RU188

The representative analyses provided an overall trend with mean grain sizes generally fining downwards. These means range from 20 to 12 µm, with minima occurring at 600 cm depth (Fig. 5.21).

The percentage of grains > 32 µm (clastic derived fraction) remains above 10% throughout the core, fluctuating up to 30% in some samples. The percentage of grains > 63 µm (sand size fraction) remains at below 10% throughout the core, increasing to > 10% in the tephra layers. Some of the fluctuations may be related to erosion from the catchment or to reworking of sediment in the lake basin.

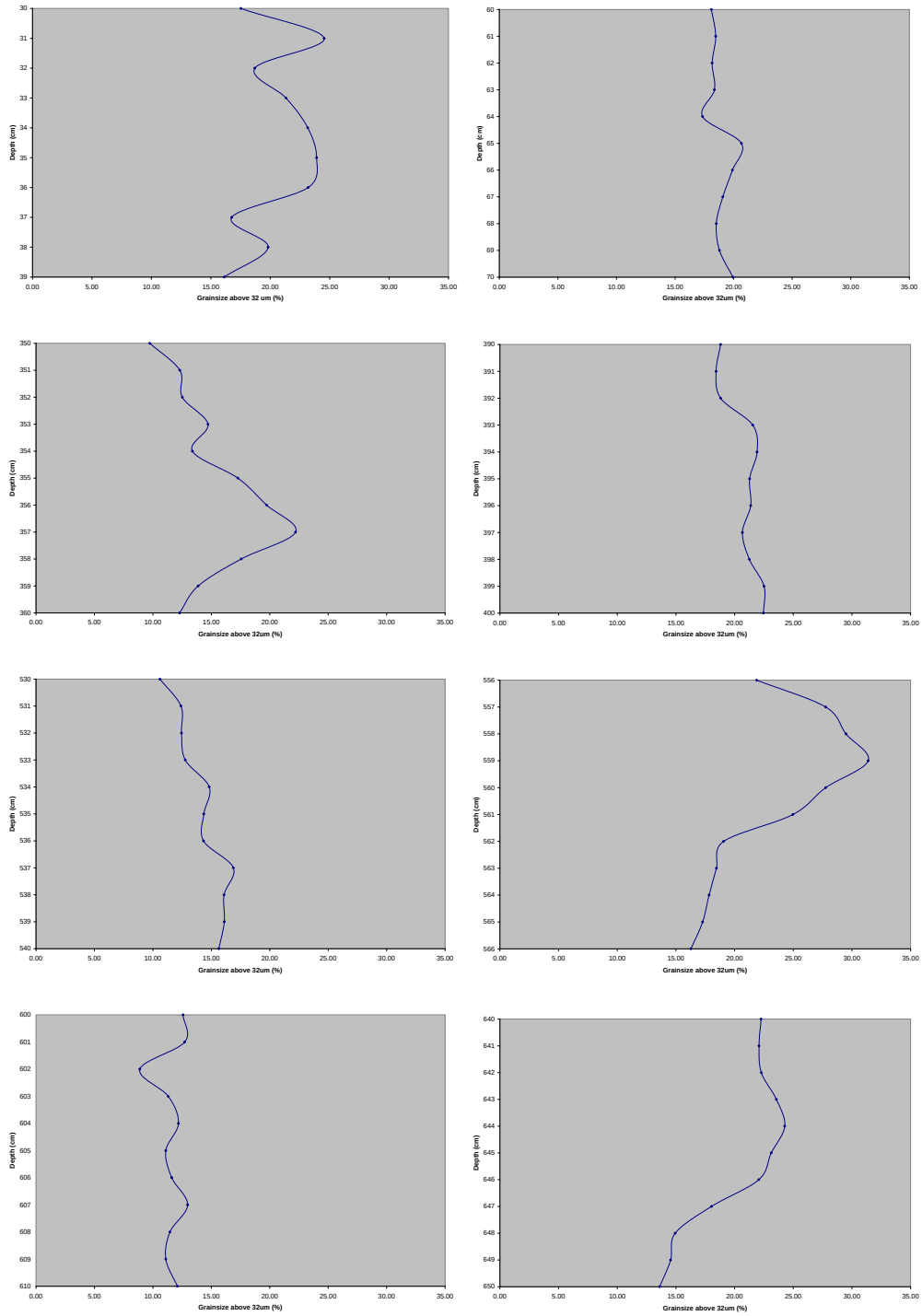

Figure 5.22: Representative samples showing percentage of grains > 32 µm – indicative of clastic (detrital) sediment.

At depth 30-39 cm (c. 58 – 64 cal. years B.P.; Fig 5.22 A), the percentage of grains > 32 µm ranges between 15 and 25%, and peaks in three places to > 20%. This pattern is mirrored in the > 63 µm samples (Fig. 5.23 A) where sand increases considerably just after the Tarawera deposit from ~ 1% to over 7%. These fluctuations may indicate a period of land clearing within the catchment

first by natural erosion of volcanic debris and second by people returning to the area some years after the eruption.

Samples from depths 60-70, 390-400 and 600-610 cm (c. 64 – 58, c. 510 – 520, c. 2200 – 2350 cal. years B.P., respectively) (Figs. 5.22 B, D, G and 5.23 B, D, G) indicate relatively constant proportions for both grain size fractions, with only small scale fluctuations. This consistency is indicative of stable conditions in the lake with possibly just small amounts of erosion in the surrounding catchment.

The > 32 µm fraction at depths 350-360 cm (c. 450 – 475 cal. years B.P.; Fig. 5.22 C) shows one substantial peak of > 20%. However, this peak does not correlate with > 63 µm (Fig. 5.23 C) portion and may indicate a plume of finer material from a large, one-off erosion event in the catchment without the reworking of coarser grained material, indicating that this may have been due prolonged rainfall rather than to stormy weather.

Samples from 530-540 cm depth (c. 1100 – 1300 cal. years B.P.) show a constant decrease in the proportions of grains > 32 µm with two small fluctuations. This decreasing trend is also reflected in the data from the > 63 µm fraction (Figs. 5.22 E and 5.23 E). These small fluctuations are inferred to be due to natural fluxes of sediment to the lake.

A considerable spike occurs in the grain size samples from 556-566 cm depth (c. 1500 – 1700 cal. years B.P.). This group of samples is from sediment deposited following the Taupo eruption, hence the peaks in both the > 32 µm and > 63 µm fractions (Figs. 5.22 F and 5.23 F) are inferred to be due to the coarser grained lapilli and ash being reworked from shallower areas of the lake after this event.

The sample from 640-650 cm depth (c. 2800 – 3050 cal. years B.P.) shows a marked increase in the proportion of grains > 32 µm and > 63 µm, to > 20% and > 6%, respectively (Figs. 5.22 H and 5.23 H). At ~ 646 cm depth, a large broad change indicates a change in the surrounding catchment and may be due to an accelerated rate of erosion.

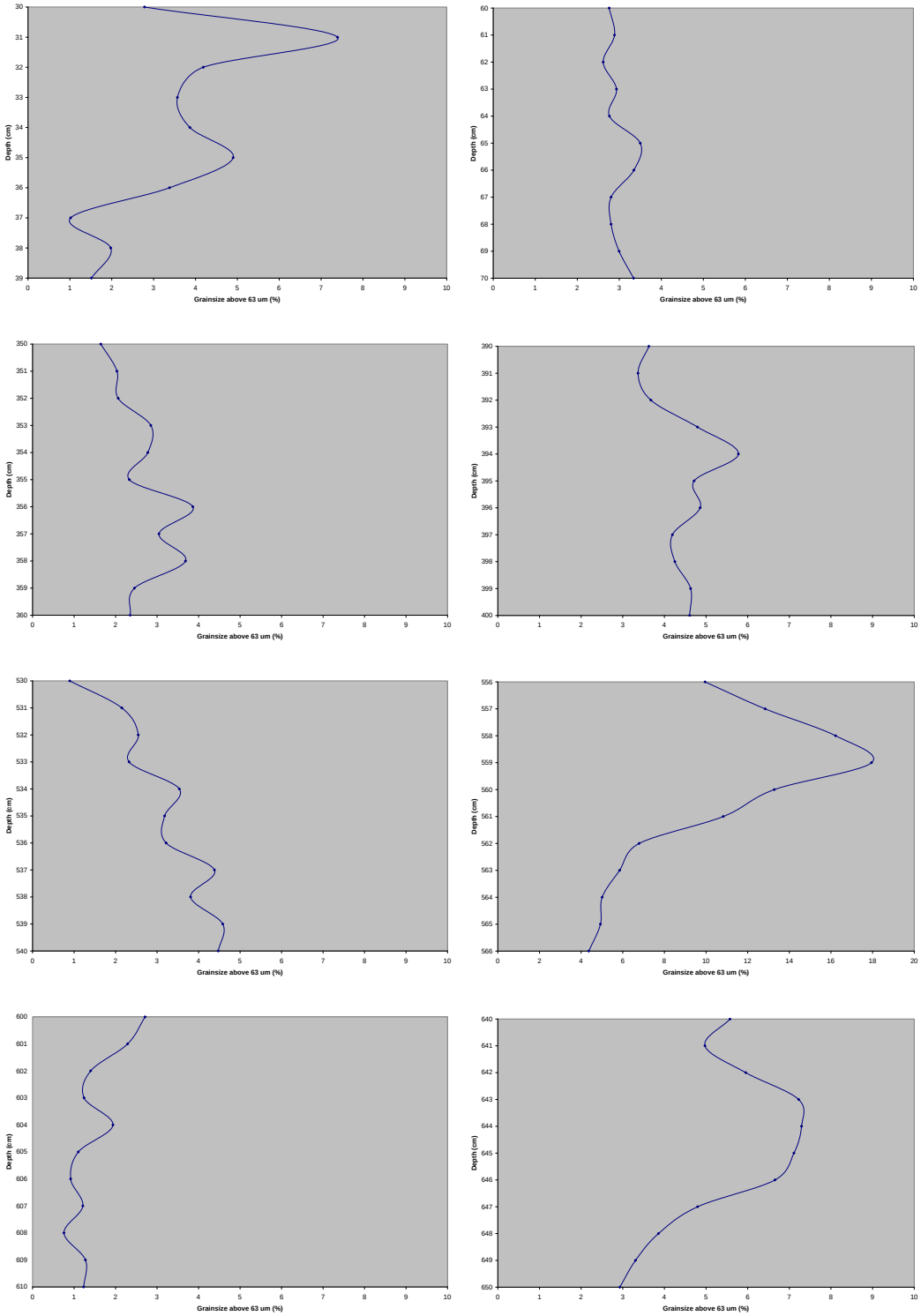

Figure 5.23: Representative samples showing percentage of grains > 63 µm – indicative of clastic (detrital) sediment.

5.6 Summary

The images generated by X-radiography indicated the laminations evident in the photographs relate primarily to changes in the physical make up and density of the sediments. SEM images revealed mainly that the darker laminae contained a large proportion of terrigenous detrital matter whereas the paler laminae are composed mainly of diatoms. These images also provided a record of changes in diatom species. *A. granulate, A. islandia, Stephanodiscus sp.* and *C. stelligera* dominate planktic taxa throughout the three sampling depths. There are also significant amounts of benthic species, which indicate the presence of plants and sufficient nutrients to support them. Salinity reconstructions, inferred from the presence of various species of diatom, indicate that the lake-level has been constantly dropping since c. 5500 cal. years B.P. This inference is consistent with previous lake-level reconstructions (Kennedy et al., 1978).

Colour reflection data, in particular b*, provide a quantitative tool for examining the make up of the sediment. a*, a proxy for clay particles, shows increased clay particles below 450 cm (c. 560 cal. years B.P.) and above the Tarawera Tephra, corresponding to the same trend evident in grain size analysis. These clay particles possibly represent background levels of clay deposition but which are effectively diluted with occasional clastic input, i.e. where there are laminae.

The variations in debris and diatoms can also be seen in the b* parameter (Fig. 5.2 C). b* shows variations in the make up of the sediments. Many of these fluxes correspond to slight changes in grain size. Grain size and SEM images have confirmed that these fluctuations are due to changes in algal production and inputs of terrigenous sediments.

Changes in the proportions of clastic material may be due to two factors. The percentage of grains > 32 µm, commonly used as an indicator of erosion of terrigenous matter, fluctuates between 10 – 30%. In contrast, the percentage of grains > 63 µm (sand size fraction) displays no strong trend and varies between 1 to 15%. Some of these fluctuations are due to the input of tephra, and others possibly represent increases in windiness and therefore wave action in the shallow waters feeding coarse, reworked material into deeper water, or alternatively these

fluctuations may be related to lake-level changes and therefore increases in impact of wind related processes.

The three zones of diatoms analysed all indicate similar water conditions with mainly species which prefer a high pH and which are tolerant of some salt. However, trophic conditions were difficult to firmly establish as many of the species found show tolerance to a wide range of conditions. The upper two zones contained only a few species, dominated by planktics. These species indicate alkaliphilous conditions with some salts present. The salts could indicate a small change in the size of the lake (i.e. lake level fall) concentrating more salt in the waters, possibly associated with warmer climate and coinciding with the MWP (approx. 850 – 1150 cal. years B.P.). The lowest zone contained the most diverse range of species, all of which preferred a high pH (the same as in the upper zones), but many of the species showed lower salt tolerances indicating that the lake may have been slightly larger at this time (c. 510 – 520 cal. years B.P.). The number of species found and the size of the lake may be related to higher rainfall and erosion inferred during this time from many East Coast records (Lorrey et al., 2008). These conditions are indicated by the significant amount of coarser grains found in the samples and the reworked tephra-derived sediment that underlies these samples. This deposition (from erosion in the catchment) would have generated large amounts of nutrients required for diatom growth and may be responsible for the diversity of species present at this time interval. Water conditions have been inferred to be mixed with slightly brackish waters near the sediment-water interface but the overlying water clear possibly oligotrophic at c. 510 to 520 cal. years B.P.

Chapter Six

Geochemical Characteristics



Chapter Six – Geochemical Characteristics

6.0 INTRODUCTION

Chemical composition of lake sediments provide another method for interpreting changes that have occurred within a lake and its surrounding catchment. Studies such as Mackereth's (1966) work on the geochemistry of lake sediments in England and Scotland, and more recently Meyer's (1997) and Meyer's and Lallier-Vegre's (1999) work using organic sediment geochemistry as a proxy for reconstructing palaeolimnologic and palaeoclimatic processes, and investigations by Boudreau (1999) and Dean (1999) on biochemical, carbon cycles, and metal dynamics, have meant that the geochemistry of lake sediments is becoming better understood. This work along with that of many others has meant that sediment geochemistry has become incorporated into the standard parameters measured during lake sediment studies. However, even with the large amount of research in this field, the geochemistry of lake sediments still have a level of uncertainty associated with many elements, mainly around origin and changes through diagenesis. The chemical composition of the sediments is investigated in this chapter by looking at a number of major and trace elements, and organic matter constituents – total organic carbon, total nitrogen and biogenic silica.

6.1 Chemical composition

An important aim in the study of lake-sediment chemistry has been to develop a suitable chemical index of lake trophic status (Brugam, 1984). The trophic status of lakes in New Zealand is, on average, low compared with those in more densely populated areas of the globe. Despite this, trends towards eutrophication are currently widespread due mainly to agriculture (Reid, 2005).

Sediment chemistry can also be used to as a proxy for inferring climatic changes. Changes in climate influence the type of vegetation growing in the catchment. This in turn affects the chemistry and the amount of clastic sediment contained in the runoff waters. Hence changes should be reflected in changing lake conditions and recorded in the sediments (Brugam, 1984).

Pearson (2007) used the major element chemistry (phosphorus, iron, manganese, arsenic, lead and sulfur) to summarise variations in the top 20 cm of sediments of Lake Rotorua. In longer cores she found that the concentrations of all these elements decreased with depth, but showed a peak in concentration in the tephra layers (Tarawera and Kaharoa).

- Phosphorus, in the centre of the lake, reached concentrations of 2500 µg/g in the top 2 cm but declined rapidly to 800 µg/g by 20 cm depth. Iron and manganese concentrations, which are dependent on the availability of the element and the sedimentation rate of diatom frustules, are controlled predominantly by redox conditions of the sediment, and have an average concentration of approximately 8000 µg/g and 300-400 µg/g, respectively.
- Arsenic was found to be highly dependent on water depth, with general concentrations between 50-100 µg/g. Lead concentrations are typically low below 15 µg/g. Both of these elements are highly correlated with iron and manganese in the sediment and mimic the concentration profiles.
- Sulfur concentrations were typically higher towards the centre of the lake.
- Concentrations of carbon and nitrogen in the surface sediment were typically c. 5 % and 0.7 %, and decline with depth to < 2 % and 0.4 %, respectively. Pearson (2007) found that the rapid decrease in carbon and nitrogen concentrations showed that most of the remineralisation and recycling through diagenesis takes place mostly within the top 10 cm but can be as deep as 50 cm.

For this study sediment was digested using reverse aqua regia, then analysed using an inductively coupled plasma mass spectrometer (ICP-MS). This method allows for a large number of elements to be determined for each sample, in this case: lithium (Li), sodium (Na), potassium (K), magnesium (Mg), calcium (Ca), strontium (Sr), barium (Ba), phosphorus (P), sulfur (S), selenium (Se), boron (B), silicon (Si), arsenic (As), aluminium (Al), thallium (Tl), lead (Pb), bismuth (Bi), chromium (Cr), manganese (Mg), iron (Fe), cobalt (Co), nickel (Ni), copper (Cu), zinc (Zn), silver (Ag), cadmium (Cd), mercury (Hg), and uranium (U). Organic matter was measured indirectly using carbon, nitrogen and biogenic silica determinations.

6.1.2 Sediment elemental geochemistry

The majority of the sediment in RU188 consists of diatomaceous ooze, hence its elemental chemistry is composed predominantly of the element silicon. Diatoms require a number of elements including carbon, hydrogen, oxygen, phosphorus, nitrogen, silicon and trace elements to grow. These are all extracted from the surrounding waters.

Lake Rotorua is well mixed, but occasionally during calm periods thermal stratification can occur when warm well-mixed surface waters (the epilimnion) overlie colder bottom waters (the hypolimnion). Oxygen consumption in the isolated bottom waters then leads to anoxic conditions, which, as discussed in chapter two, effect the availability of certain elements.

The palaeolimnological significance of many of the elements determined in this study is unknown and therefore the interpretation of the chemical history can be problematic for specific elements. Despite this, valuable information can be derived from the sediment chemistry of Lake Rotorua.

6.1.2.1 Phosphorus (P)

Primary productivity is closely linked with phosphorus, and because sediments are an effective sink, the phosphorus content of lake sediments is often used as a proxy for palaeoproduction. The phosphorous concentration in Lake Rotorua has varied considerably over the last ~ 5500 years. Peak concentrations are associated with tephra layers, and reach as high as 15,000 µg/g in the Whakatane Tephra (Fig 6.1). Not all the phosphorus peaks correlate with tephra layers, however, and can be linked with other element influxes and possible increases in palaeoproduction and changes in trophic status. In the diatomaceous sediment the concentration of phosphorus ranges from as low as 110 µg/g to nearly 4000 µg/g.

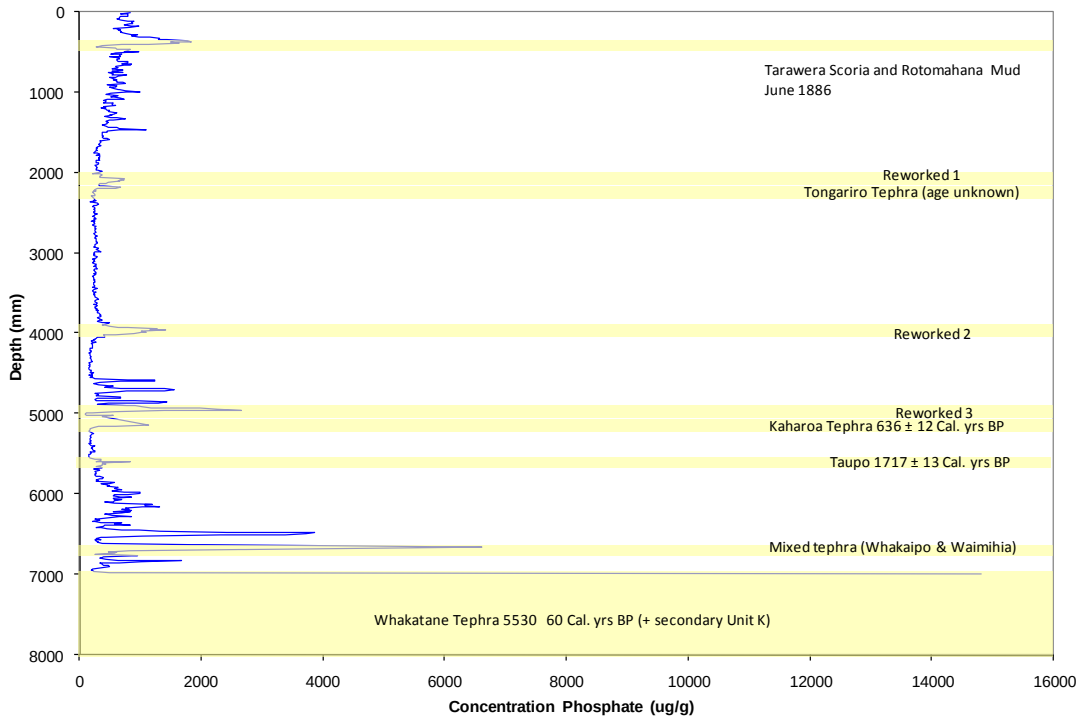

Figure 6.1: Phosphorus concentration for RU188, where yellow bands indicate tephra layers.

The concentration of phosphorus in the diatomaceous sediment fluctuates significantly in the lower sediments. These fluctuations were followed by a uniform period of low concentrations directly after the Taupo eruption. A phase of higher concentrations directly following the Kaharoa eruption corresponds to an influx of dark, clastic, erosion-derived sediment. This sediment is probably associated with large scale erosion relating to damage to vegetation in the catchment following the Kaharoa eruption. Concentrations then return to relatively low post-Taupo-like conditions (456-414 and 400-220 cm). In the upper 200 cm, the fluctuations begin again – but these fluctuations are smaller in magnitude than in the earlier series, and can be linked by other elements to increases in clastic sediment deposition probably related to vegetation clearing for hunting, settlement and horticulture by early Polynesians.

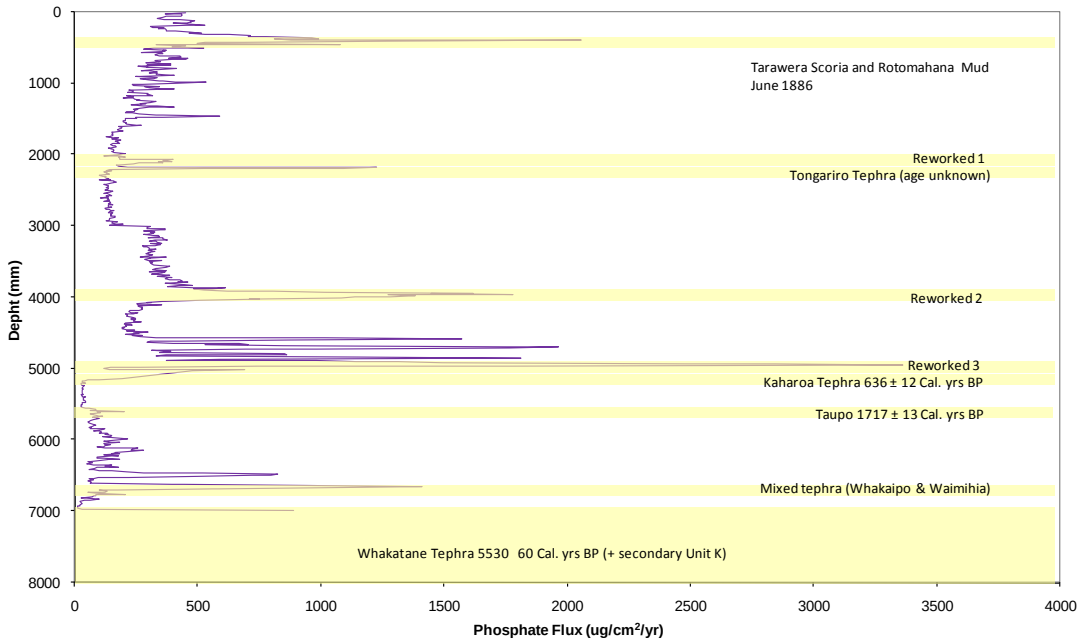

Figure 6.2: Phosphorus flux in the sediments, where yellow bands indicate tephra layers.

The flux of phosphate to the sediment has been derived from the concentration by multiplying by the density (which increases down-core) and the accumulation rate (which increases up-core). The phosphate flux (Fig 6.2) shows the same overall pattern of phosphate concentration due to the low density at the surface but reduces the apparent peaks of the accumulating phosphate in the upper 200 cm. The step change at 300 cm is due to a change in the value for density used in the flux calculation. Because of compression during core extraction, the density could not be measured directly on RU188, so assumptions were made for density using the numbers generated by Pearson (2007). Density was assumed to be 0.5 gm/cm^3 for tephra layers, 0.15 gm/cm^3 for sediment above 300 cm, and 0.35 gm/cm^3 for sediment below 300 cm.

6.1.2.2 Iron (Fe)

Iron and magnesium are related to reduction-oxidation (redox) conditions in the lake. The iron concentrations in Lake Rotorua are principally dependent on iron absorption by diatoms and the erosion of clay and other minerals from the surrounding catchment.

Peaks in the tephra layers are possibly due to the weathering of iron from glass shards or from ferromagnesian minerals, or both. The highest peak of iron occurs in the Whakatane Tephra at nearly 30,000 µg/g; the peaks in the other ash layers range between 9,000 and 17,000 µg/g (Fig. 6.3).

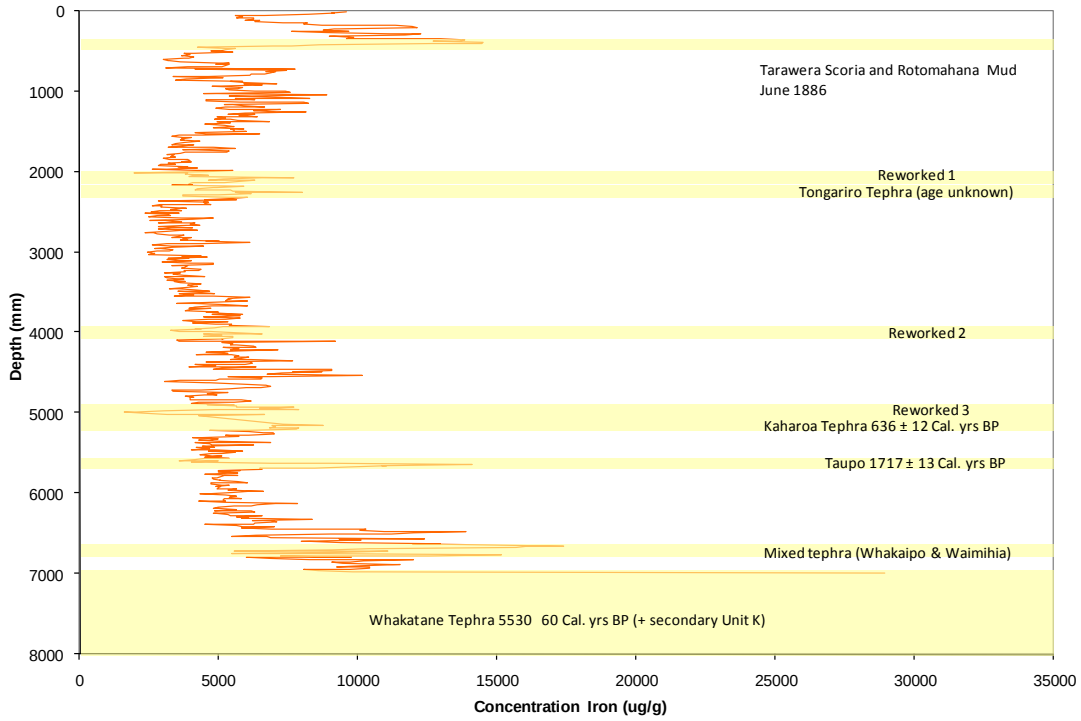

Figure 6.3: Iron concentration for RU188, where yellow bands indicate tephra layers.

Iron also fluctuates in the sediments between the tephra layers from 2,000-14,000 µg/g. This fluctuation shows a gradual decreasing trend up until the TgVC ash unit (informally named "Tongariro Tephra"), above which it steadily increases until the Tarawera deposit. After the Tarawera deposit the iron decreases up until 8 cm depth where it increases to 9,500 µg/g.

6.1.2.3 Manganese (Mn)

Manganese concentrations follow the same trends as other elements affected by redox conditions – peaking again in some of the tephra layers, with the largest "spike" in the Whakatane Tephra (3,000 µg/g).

In the sediment the concentration of manganese ranges between 80 µg/g and 500 µg/g (Fig. 6.4). The trends in the diatomaceous sediment are similar to the trends exhibited by phosphorus – Mn values fluctuate a lot in the lower samples, and then, following the Taupo eruption, a period of low concentrations persists up until 220 cm. In the upper 200 cm the fluctuations begin again increasing not only in periodicity but also in concentration. These are higher following the Tarawera eruption but occur less often.

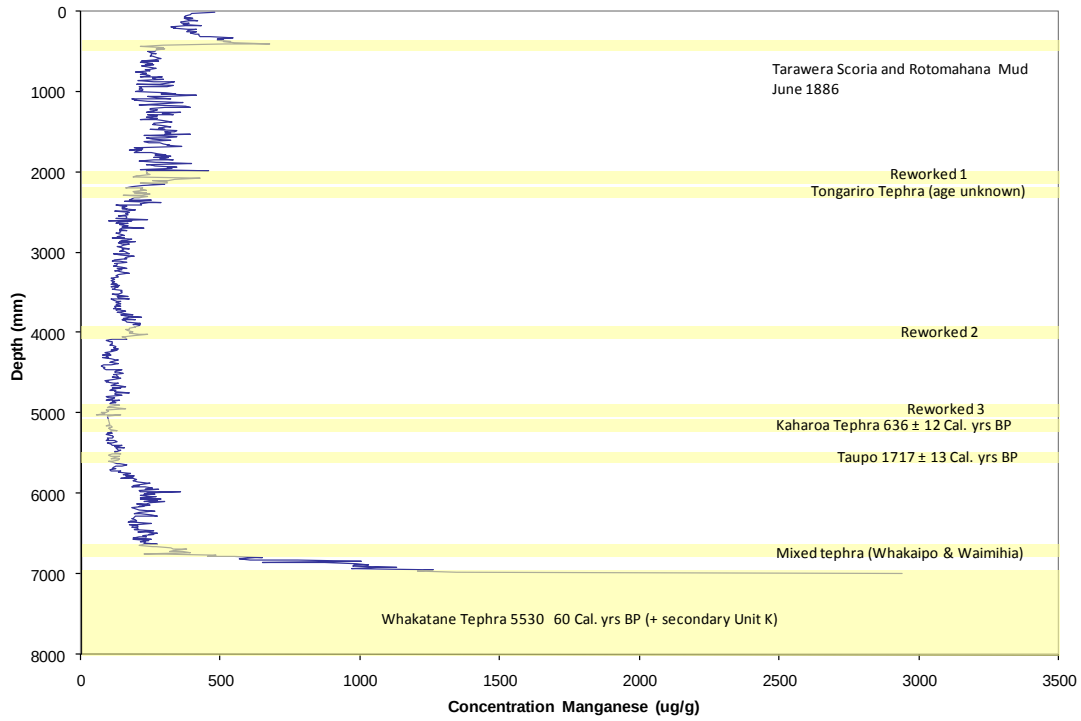

Figure 6.4: Manganese concentration for RU188, where yellow bands indicate tephra layers.

6.1.2.4 Arsenic (As)

Arsenic shows a slightly different trend from those of the other elements. There are two periods of high concentrations observed since the Whakatane eruption (Fig. 6.5). The first occurred around the time of the Waimihia eruption (1,100 µg/g). Arsenic then decreased until the Taupo eruption and then the second phase of higher concentrations began around and following the Kaharoa eruption (412 µg/g). Low arsenic concentrations in the Tarawera Tephra and TgVC ash unit ("Tongariro Tephra") discount them as sources, but arsenic spikes in the Kaharoa Tephra, Taupo Tephra, and the mixed Whakaipo/Waimihia layer indicate they are likely to be temporary sources.

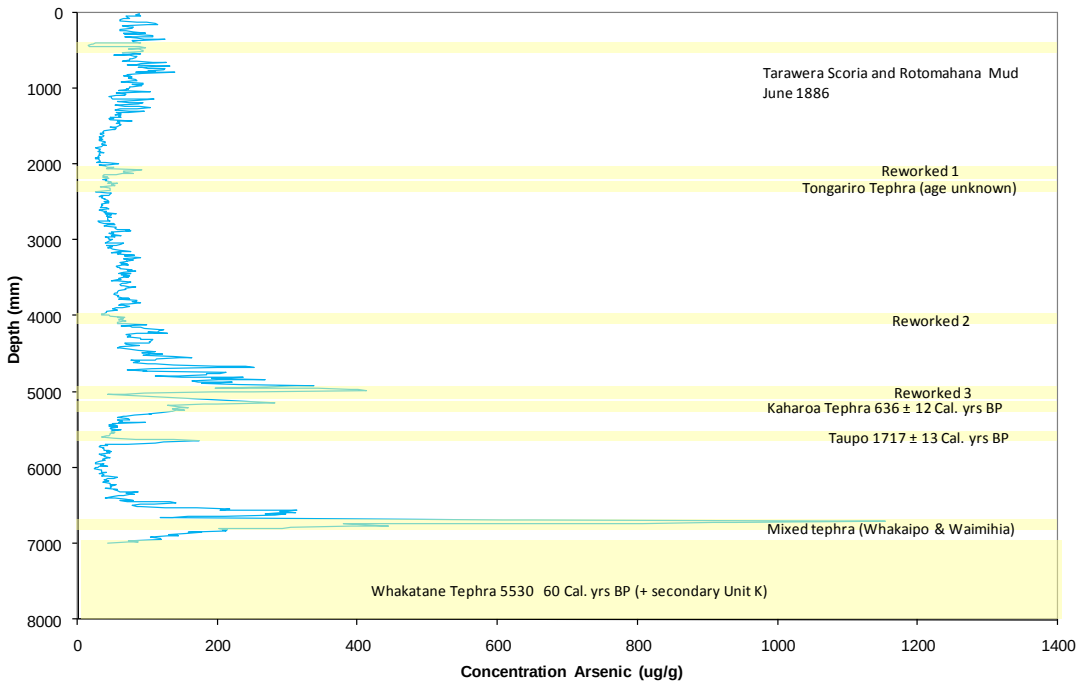

Figure 6.5: Arsenic concentration for RU188, where yellow bands indicate tephra layers.

Isolated peaks of arsenic within the sediment suggest it has periodically been incorporated into the sediments from the water column rather than from seepage of fluids from under and around the lake bed. Both the Rotorua and Tikitere geothermal waters contain elevated levels (< 10 mg/m^3) of arsenic (Smith, 1986), and both feed directly into the lake waters hence the elevated levels observed in the sediments are likely to be directly related to increases in activity of these geothermal systems. There is also a series of minor fluctuations in the top 150 cm of the core that may also be related to changes in geothermal inputs both before and after the Tarawera eruption.

6.1.2.5 Sulfur (S)

Most of the sulfur entering Lake Rotorua is of geothermal origin and enters the lake as sulfate in solution or elemental sulfur in suspension. Increases are likely to indicate periods of increased geothermal activity.

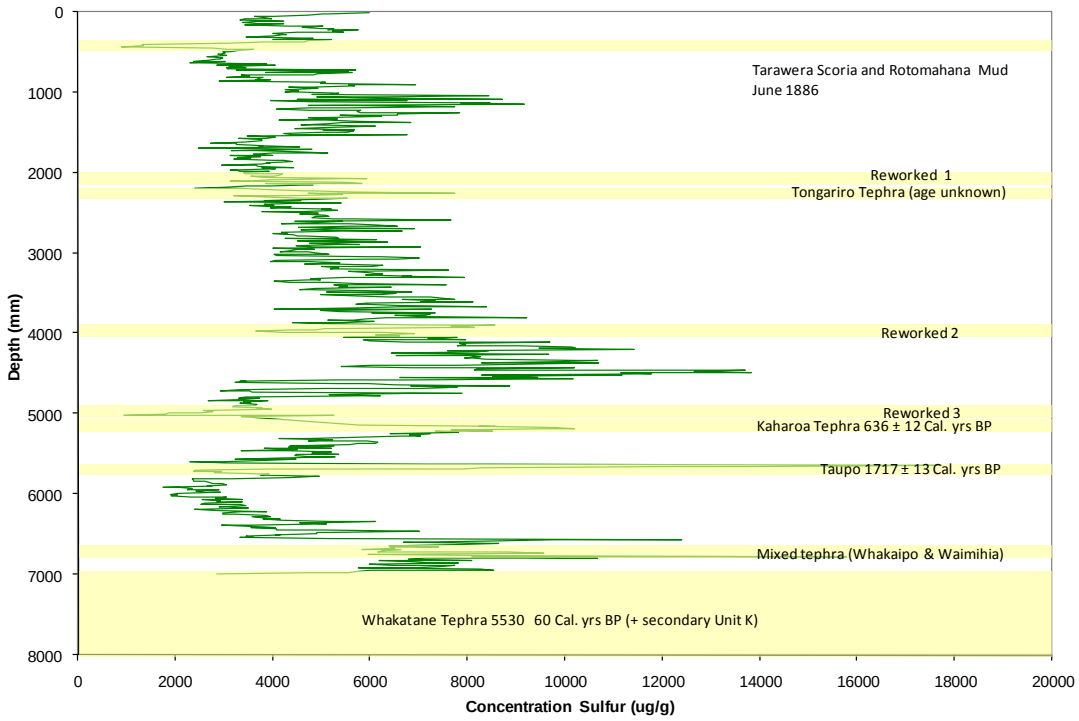

Figure 6.6: Sulfur concentration for RU188, where yellow bands indicate tephra layers.

Unlike many of the other elements analysed, sulfur shows low values in the tephra layers, and fluctuates throughout the diatomaceous sediments (1,700 – 14,000 µg/g; Fig. 6.6). Sulfur shows a period of decreasing concentrations following the Whakatane and Waimihia eruptions. It then increases prior to the Kaharoa eruption (10,000 µg/g), drops rapidly (950 µg/g) immediately following the eruption and then increases steadily for a short time. The sulfur concentrations then gradually decline until just before the Tarawera eruption.

6.1.2.6 Trace elements

Trace elements Cd, Co, Cr, Ni, Pb, and Zn are all contained in New Zealand subsoils and increases could be related to increased erosion in the catchment because of the clearing of vegetation and the development of agricultural processes (Smith, 1986), although Pb often shows industrial inputs with its widespread use as an antiknocking agent in automobile fuels.

Heavy metals (Cd, Co, Cu, Fe, Hg, Mn, Pb, and Zn) originate from a number of sources. Some are primarily supplied to the lake by the natural flux of elements eroded

from the catchment soils. Others such as copper (Cu), zinc (Zn), mercury (Hg), and lead (Pb) come predominantly from hydrothermal inflows in the form of insoluble sulfides (C. Hendy, pers. comm. 2008). Geothermal fields in the TVZ include a distinctive suite of minerals, in particular high levels of arsenic and mercury. As discussed in Chapter two, Lake Rotorua is influenced by two geothermal fields the Rotorua City system to the south and the Tikitere field to the east.

The heavy metals Pb, Zn, Hg and Cu vary throughout the core with the values for each increasing particularly over the upper 200 cm of the sediment record (Fig. 6.7). Lead (Pb) levels remain relatively low until 200 cm depth after which levels increase to peaks of around 3.5 µg/g below the Tarawera Tephra (39 – 42 cm). These peaks possibly relate to increases in geothermal activity and erosion in the catchment just before the Tarawera eruption. Above the Tarawera Tephra, lead increases to a maximum of 14 µg/g just below the top of the core. This last increase in lead concentration is significantly above the background levels. These higher-than-background concentrations supports an anthropogenic source and are probably related to the introduction of leaded petrol in New Zealand in the mid 1920s and the development of roads in the catchment at that time, with runoff from the slopes and roads flowing into the lake. New Zealand had one of the highest levels of Pb in petrol in the world (0.84 g/l) prior to 1986, when it was reduced to 0.45 g/l (Pickrill et al., 1991), and eliminated completely by 1994.

Zinc (Zn) increases gradually from the base of the core with markedly higher concentrations occurring after the Kaharoa eruption. This increase could possibly reflect zinc's greater mobility than other heavy metals. Unlike many of the other elements analysed, zinc does not peak in the tephra layers. Zn concentrations remain variable from ~ 500 cm depth. This trend is punctuated by two Zn concentration lows at 431 and 302 cm depths in the core. Zn concentrations peak at 137 µg/g at 88 cm and near the top of the core to 123 µg/g. This last peak may be related to urbanisation in the catchment and to the introduction of galvanised iron roofing in building. The degradation and rusting of Zn-plated roofing iron is an important source of Zn pollution. Zn is also found in pesticides and fertilisers and may be a

significant component of Zn influx to the lake (Pickrill et al., 1991), after the Tarawera eruption.

Mercury (Hg) varies mainly in the lower half of the core below 350 cm, and concentrations oscillate from 0.12 up to 2.7 µg/g in the diatomaceous sediments. Above 350 cm depth, the concentrations are relatively low (~ 0.1 µg/g) with very small fluctuations occurring up until prior to the Tarawera eruption. Here the concentrations steadily increase to 0.33 µg/g until the eruption, then they suddenly drop away. The concentrations then gradually increase in the top 25 cm. Mercury peaks only in the Waimihia, Taupo and Kaharoa tephra layers.

Copper (Cu) concentrations are generally low at less than 10 µg/g, although there is an increasing trend after the Tarawera eruption at around 21 cm depth increasing to a maximum of 19 µg/g at 12 cm depth. There are spikes at 623, 503 and 239 cm depths. These peaks could be related to increased geothermal activity around the times of volcanic activity in the TVZ. One of the highest concentrations (12 µg/g) encountered in these sediments occurred at the very top of the core and could be related to inputs from anthropogenic sources (Fig. 6.7).

The alkali elements (Li, Na and K) are generally found in volcanic-derived rocks and sediments and in tephra, hence they probably originate from weathering in the surrounding catchment, but can also have high concentrations in geothermal waters. These elements all show similar trends (Fig 6.8). A study was carried out in the mid 1980s by Timperley and Vigor-Brown. They looked at pumice as a possible source of major ions, and found that in the case of Lake Taupo large fluxes of sodium were derived from pumice and helped explain differences in the mass major ion budget (Timperley and Vigor-Brown, 1985). Volcanic glass, particularly rhyolite, has a tendency to dissolve in the presence of water. Hence it is probable that in the case of Rotorua, pumice from the surrounding ignimbrites and other pyroclastic material undergoes some degree of dissolution and could possible lead to fluxes of dissolved ions into the lake, particularly following periods of intense rainfall causing accelerated weathering and transport. This dissolution supplies large amounts of silica and possible fluxes of some trace elements, in particular sodium.

Lithium (Li) shows small fluctuations in concentration (1.5-3 µg/g) below 500 cm. Following the Kaharoa eruption these fluctuations become slightly larger until they peak at around 400 cm. The following phase (400-220 cm) shows a constant decrease from 5 µg/g to 1.5 µg/g. The latest phase (above 200 cm) shows a steady increase from 1.5 µg/g to ~ 6 µg/g. Sodium (Na) shows the same trend but with much larger fluctuations that vary between 200 and 680 µg/g. Potassium (K) again shows the same trend as lithium with smaller oscillations that range between 130 and 280 µg/g. Potassium peaks in all the tephra layers, except the TgVC ash ("Tongariro Tephra"), reaching as high as 980 µg/g in the Tarawera Tephra. The majority of the K in the lake sediments is probably derived from the dissolution of minerals and glass found in the tephra layers.

The alkali earth elements (Mg, Ca, and Sr) are common constituents of silicate minerals and typically have low concentrations in geothermal waters. These elements all show similar abundance trends to one another and to the alkali elements discussed above (Fig 6.8).

Magnesium (Mg) peaks in the tephra layers with the highest value occurring in the Tarawera Tephra (~ 4,000 µg/g). Concentrations of magnesium remain relatively constant below 430 cm where they vary between 180 – 340 µg/g. At 400 cm, Mg peaks at ~ 650 µg/g. Between 300 – 400 cm the concentration slowly drops back to become relatively steady for a short period at ~ 200 µg/g. Above 200 cm, magnesium concentrations increase from ~ 200 µg/g to more than 800 µg/g.

Calcium's (Ca) maximum value also occurs in the Tarawera Tephra (1,400 µg/g). However, in the diatomaceous sediments, the maximum value (642 µg/g) occurs in the lowest section of RU188 at 654 cm. Above this depth, values then drop back to fluctuate between 320 and 520 µg/g until the Taupo eruption. Following this eruption the fluctuations become smaller (270-370 µg/g) until the Kaharoa eruption, and the concentrations then increase with fluctuations varying up to 200 µg/g. After the deposition of the Tongariro-derived tephra, these fluctuations increase even more to vary more than 400 µg/g. In the top 39 cm of the core, magnesium drops from ~ 1000 µg/g to 550 µg/g.

Strontium (Sr) has five very high (> 15 µg/g) spikes throughout RU188. Three peaks coincide with tephra layers, but two occur within the diatomaceous sediment. The maximum value in the sediment (20 µg/g) coincides with that of calcium at 654 cm, then drops to fluctuate between 5.5 µg/g and 9 µg/g. Between 550 cm and 220 cm strontium's concentration fluctuates very little (c. 2 µg/g), whereas above 200 cm these fluctuations increase to 10 µg/g. In the upper 39 cm, strontium drops from ~ 17 µg/g to ~ 7 µg/g.

Both aluminium (Al) and beryllium (Be) originate purely from the erosion of soils and catchment rocks and hence are the best indicators of erosion in the catchment (Fig 6.8). Both elements show similar trends with a phase of high concentrations (1880-3500 µg/g and 70-190 µg/g, respectively) between the Waimihia and Taupo eruptions, followed by a phase of lower concentrations (~ 2,500 µg/g and ~ 50 µg/g, respectively) punctuated with minor fluctuations up until the Tongariro-derived tephra. The upper 250 cm of the core shows a steady increase in the concentration of both Al and Be (2500-7000 µg/g and 40-300 µg/g, respectively).

There is a significant peak in Al, K, and Ca concentration between 12-17 cm, which coincides with a peak that Rawlence (1984) found when carrying out pigment studies on another core from Lake Rotorua (Fig. 6.8). This peak was thought to be caused by the development of farms (~ 1914) within the catchment, presumably following extensive bush clearance and associated accelerated erosion.

Boron (B) is very soluble in water so there is little trace of it left in the sediments. That present tends to fluctuate considerably (1.5-50 µg/g). B shows an overall increase towards the top of the core (Fig. 6.9).

Other elements analysed show slightly different trends (Fig. 6.9). Chromium, nickel, selenium, silver, thallium, bismuth and uranium have very low concentrations (< 5 µg/g). Only four of these elements have a definite source. Selenium and thallium are from geothermal waters and exhibit similar patterns to those observed in many of the other trace elements. Chromium and nickel are contained within the

subsoils and increases could be related to increased erosion in the catchment, due in part to the clearing of vegetation and the development of agriculture.

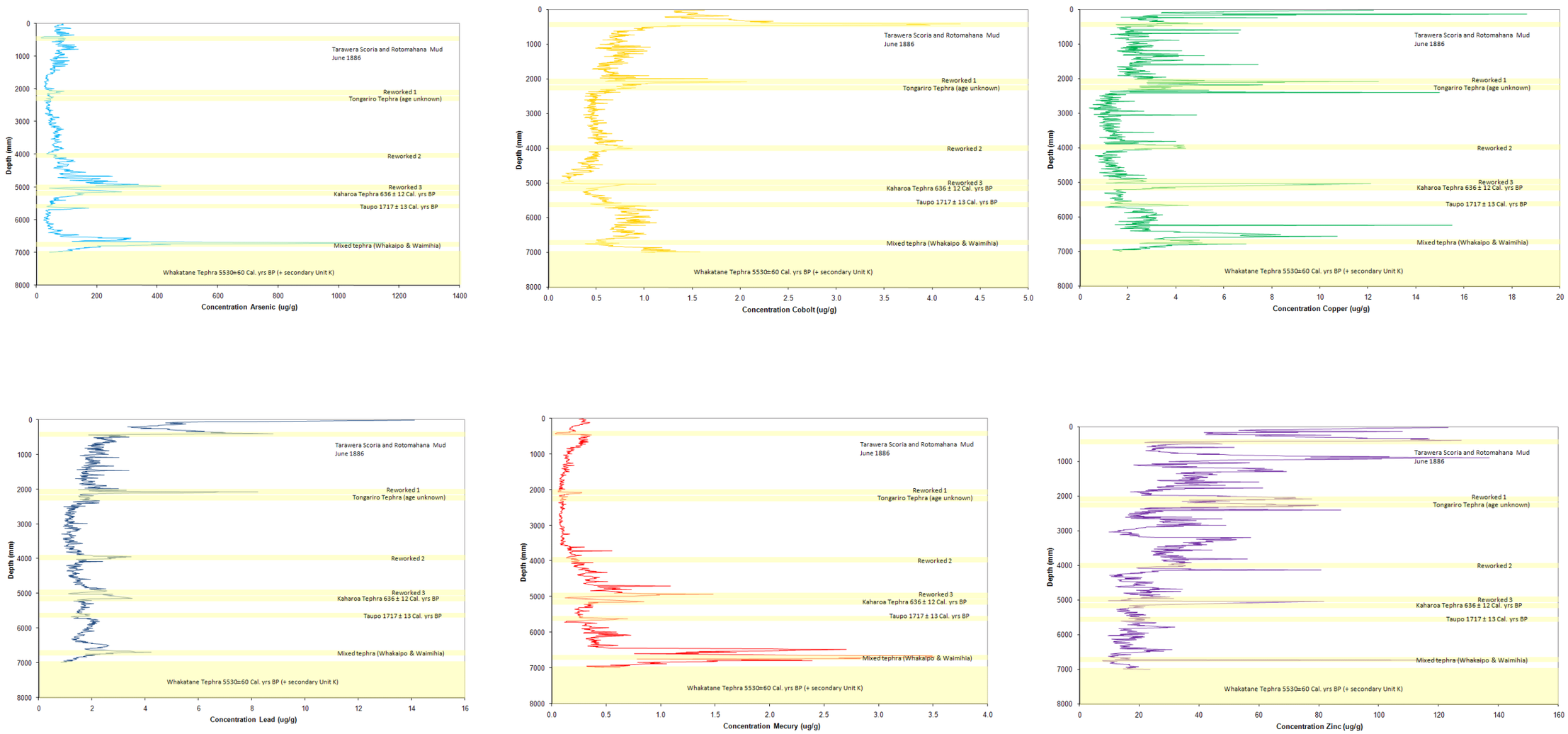

Figure 6.7: Plots of heavy metal elements - arsenic, colbolt, copper, lead, mecury, and zinc

Alkali elements (Li, K & Na)

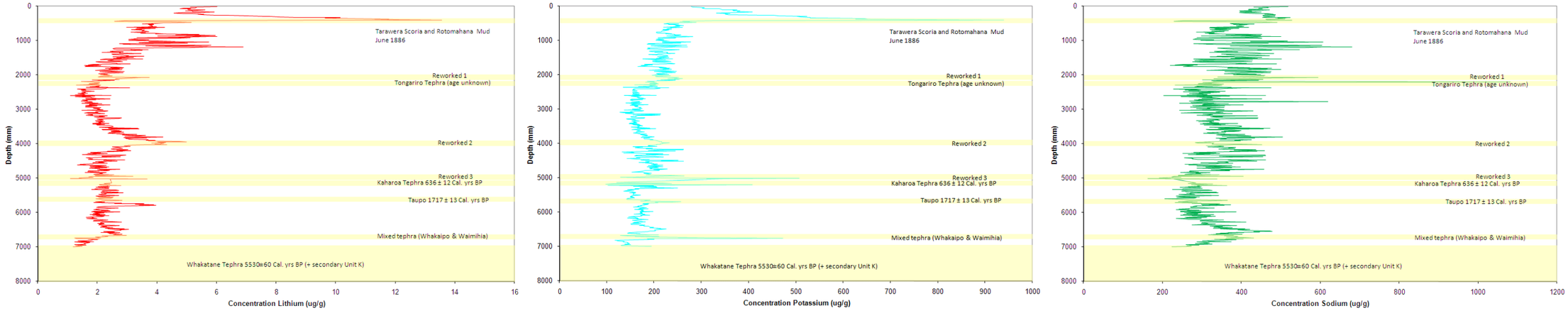

Alkali earth elements (Mg, Ca & Sr)

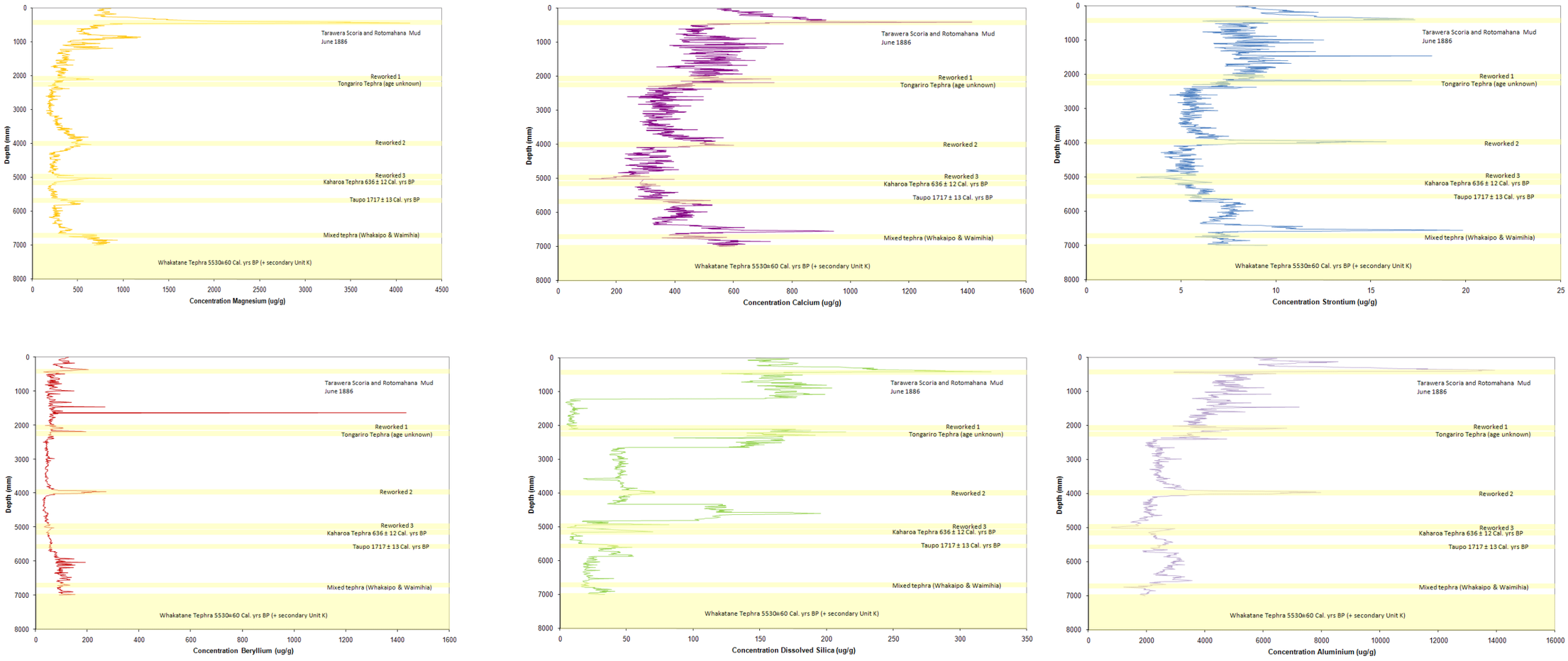

Figure 6.8: Plots of alkali and alkali earth elements - lithium, potassium, sodium, magnesium, calcium, strontium, beryllium, dissolved silica, and aluminium

Other trace elements

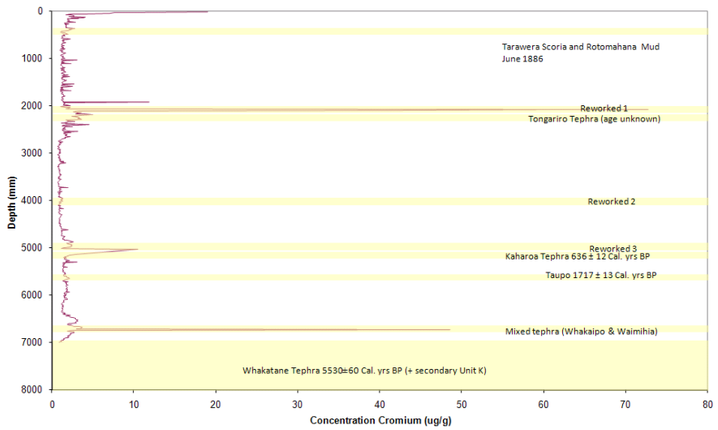

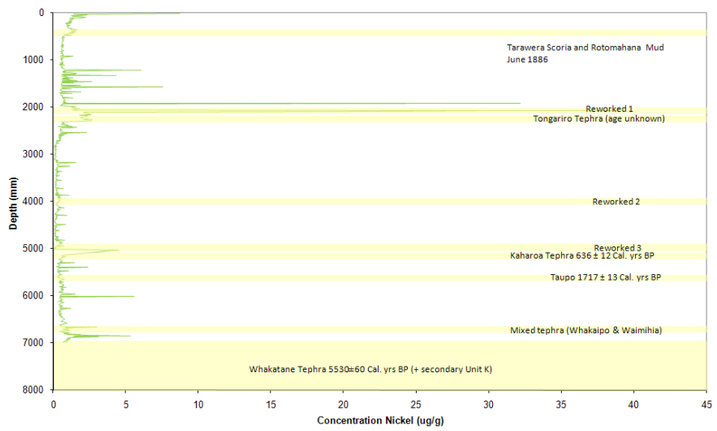

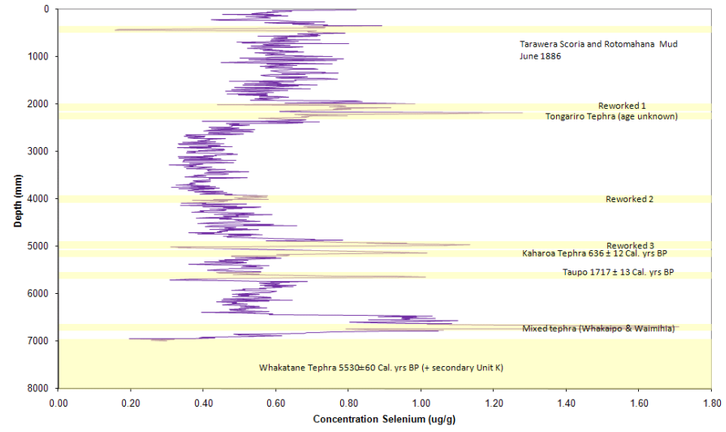

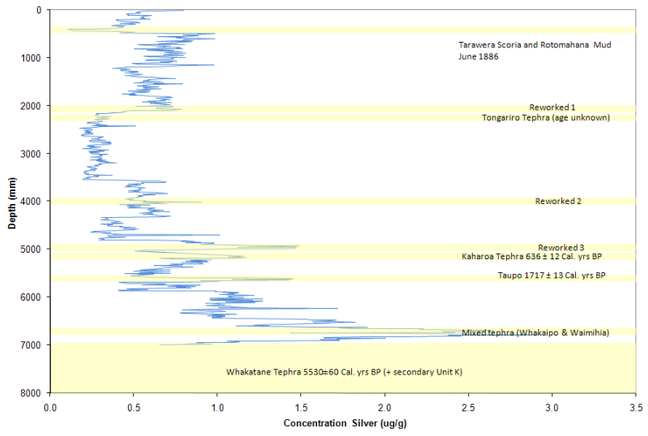

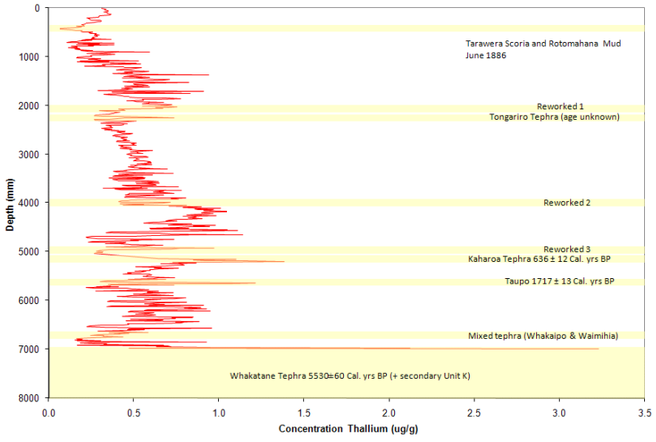

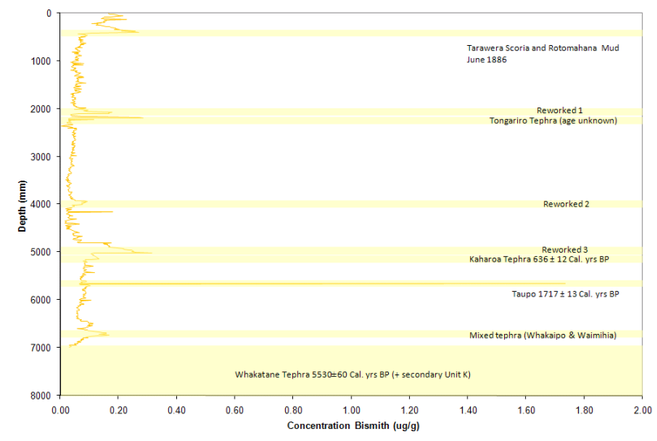

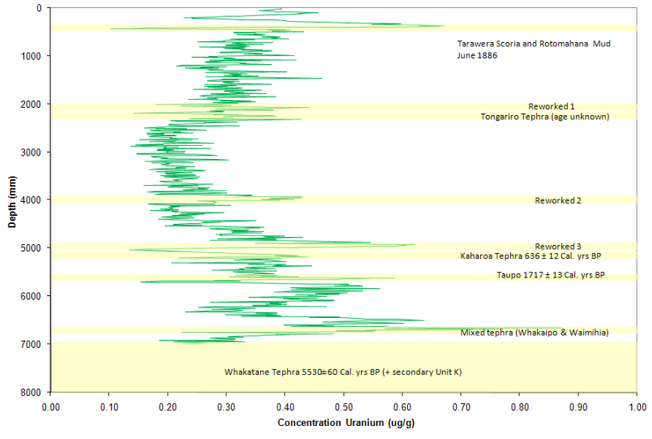

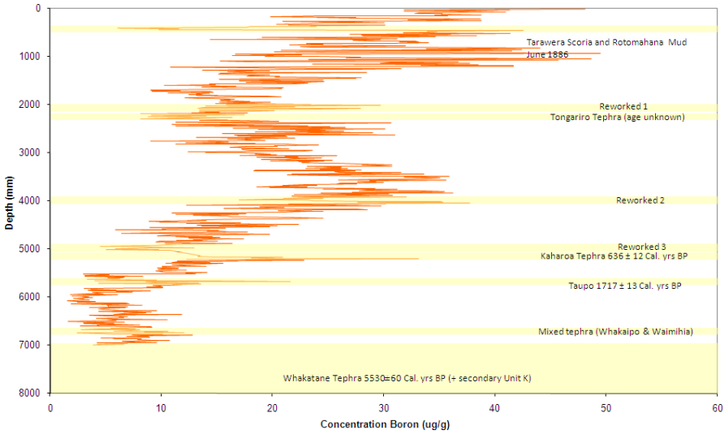

Figure 6.9: Plots of other trace elements - chromium, nickel, selenium, silver, thallium, bismith, uranium, and boron

6.1.2.7 Effect of volcanic ash

The nearby volcanoes in the OVC and TVC have supplied substantial quantities of tephra to the Rotorua region. These tephra layers have in turn supplied a number of elements to the lake sediments and the soils of the catchment. All the elements were examined in the sediment both before and after each tephra layer, but there were no trends evident with either increases or decreases of elements before and after each eruption (Fig 6.10).

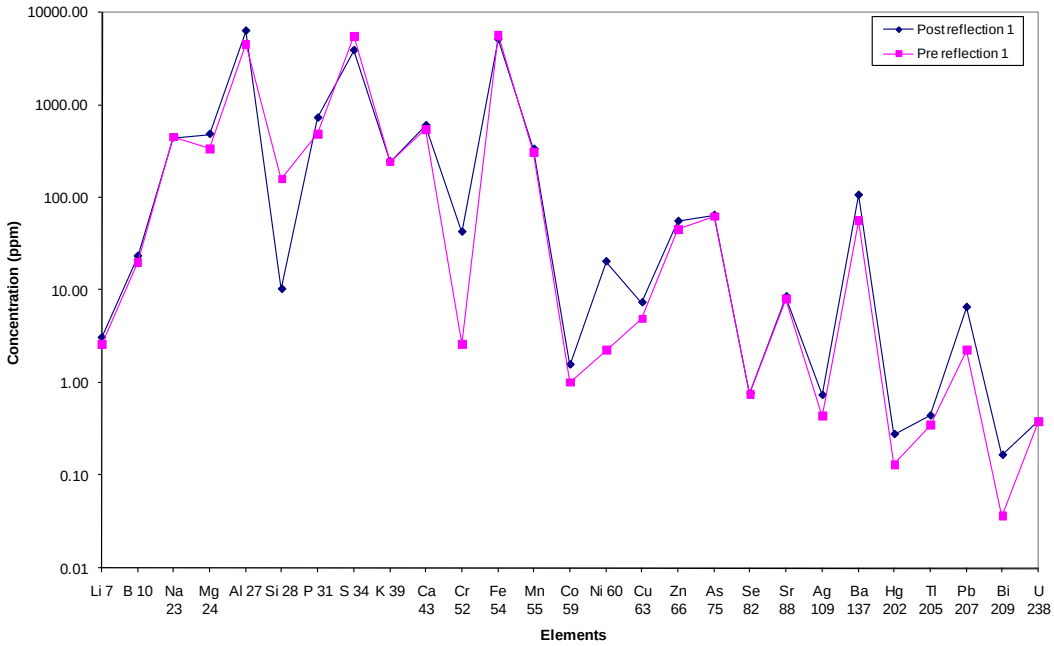

Figure 6.10: An example of element comparisons made from sediment samples before and after the tephra layers.

6.2 Organic matter elemental geochemistry

Organic matter constitutes a minor but important fraction of lake sediments. It originates from the complex mixture of lipids, carbohydrates, proteins, and other bio-chemicals produced by organisms that have lived in the lake and its catchment (Meyers and Lallier-Verges, 1999). Identification of the sources of organic matter in sedimentary records provides important paleolimnologic information. As the types and abundances of plant life in and around lakes change, the composition and amount of organic matter delivered to the lakes sediment also changes.

6.2.1 Biogenic silica

An attempt was made to determine the concentrations of biogenic silica using the techniques of Mortlock and Froelich (1989) as described in Chapter 3. Samples were taken at 1 cm intervals between 30-39, 350-360, 390-400, and 556-566 cm depth. The concentrations determined were very high, consistent with the SEM evidence that most of the sediment consisted of diatoms and fell within the range of 4 to 11% Si. As these results are lower than would be expected from the SEM imagery and there was a wide scatter between samples it seems likely that the digestion process described by (Mortlock and Froelich, 1989) may not be recovering all of the biogenic silica (Fig. 6.11). This investigation was not pursued further due to time constraints, but may be worth further research.

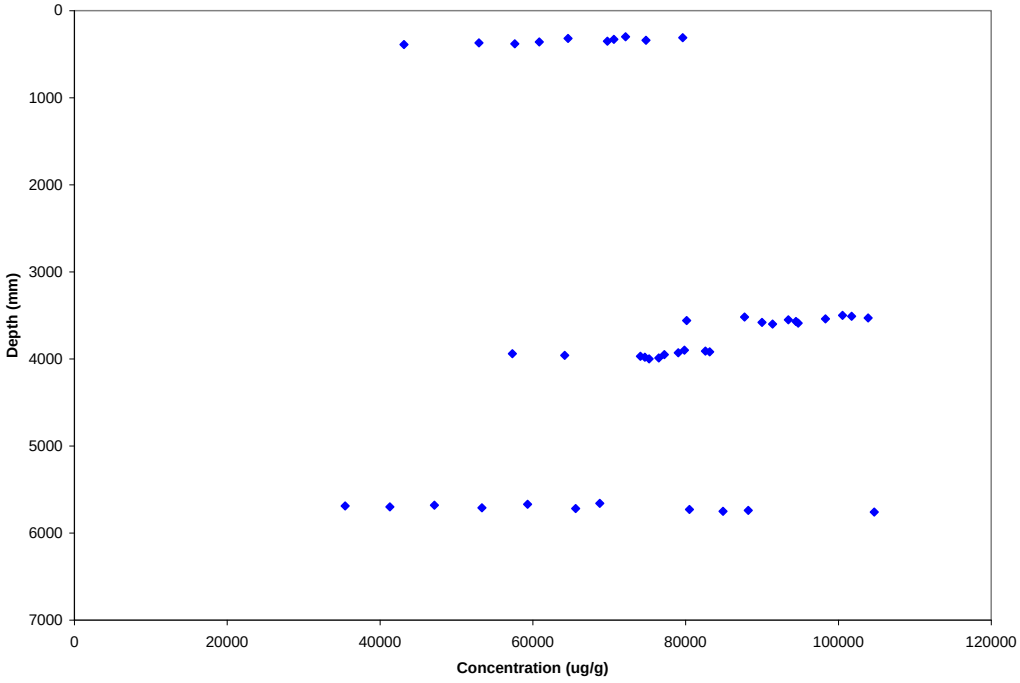

Figure 6.11: Biogenic silica concentrations as measured by ICP-MS.

6.2.2 Total organic carbon and total nitrogen

The proportion of sedimentary organic matter derived from terrestrial plants and that derived from within a lake can be identified from the difference between TOC/TN ratios of vascular land plants and algae (Fig. 6.12; Meyers 1994). Increased influx of land-plant-derived organic matter is recorded as increased TOC/TN ratios, because vascular land plants have TOC/TN ratios > 20 whilst algae typically have TOC/TN ratios between 4 and 10. Values between 10 and 20 usually relate to a

mixed terrestrial-aquatic source for the organic matter. This difference is likely to be a consequence of the absence of cellulose in algae and its abundance in vascular plants (Meyers 1994; Meyers and Lallier-Verges 1999). The concentration of total organic carbon (TOC) is a fundamental parameter for describing the abundance of organic matter in sediments. TOC concentrations are generally expressed in weight/weight ratios and are therefore influenced by other sediment components. TOC concentration is a bulk value that represents the fraction of organic matter that escaped remineralization during sedimentation (Meyers and Lallier-Verges, 1999).

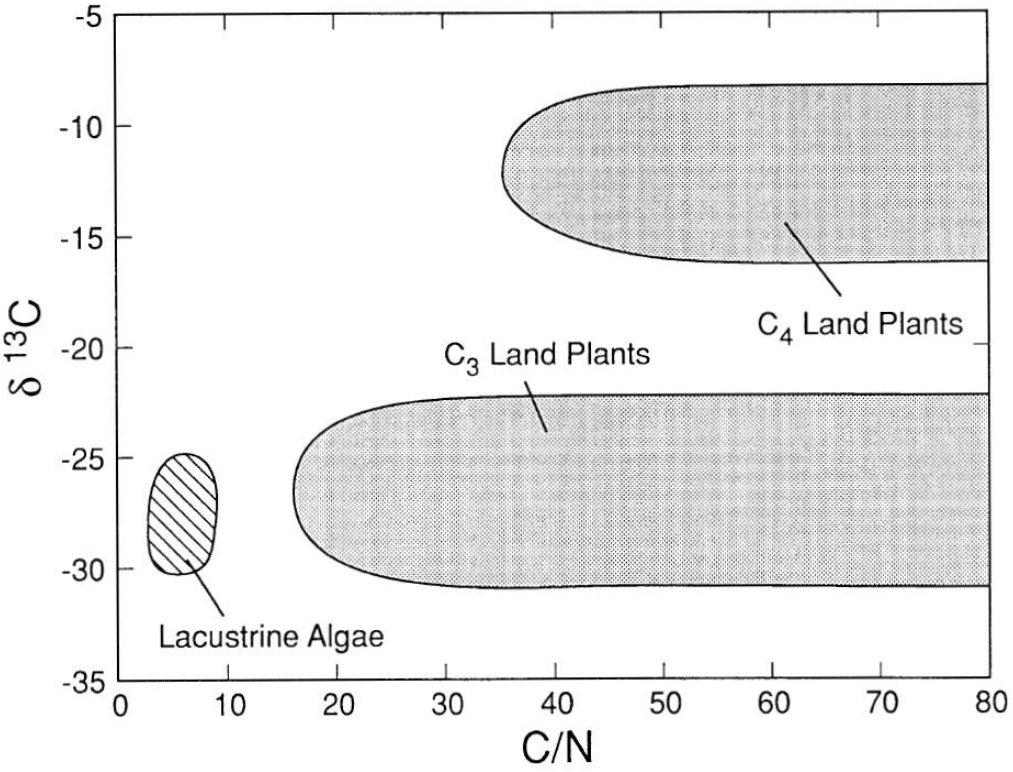

Figure 6.12: Representative elemental and carbon isotopic compositions of organic matter from lacustrine algae, C_3 land plants, and C_4 land plants that use CO_2 as their source of carbon during photosynthesis. Deviations from these generalized patterns occur and provide paleolimnologic information. Atomic C/N ratios and organic $\delta^{13}C$ values for individual plant samples (Meyers and Lallier-Verges 1999).

The organic matter total organic carbon (TOC) and total nitrogen (TN) geochemistry varies considerably down core (Fig. 6.13). The TOC values reflect changes in in-situ lacustrine and terrestrial organic matter biomass. Peak values for TOC occur at a number of depths 1, 118, 172, 207, 449, 497, 652 and 671 cm (vary between 3.0 – 7.6 %), and a minimum value of 0.2% occurs at 117 and 171 cm (Fig. 6.13). The lower TOC percentages indicate the increased dominance of algal production and are possibly associated with seasonal algal blooms.

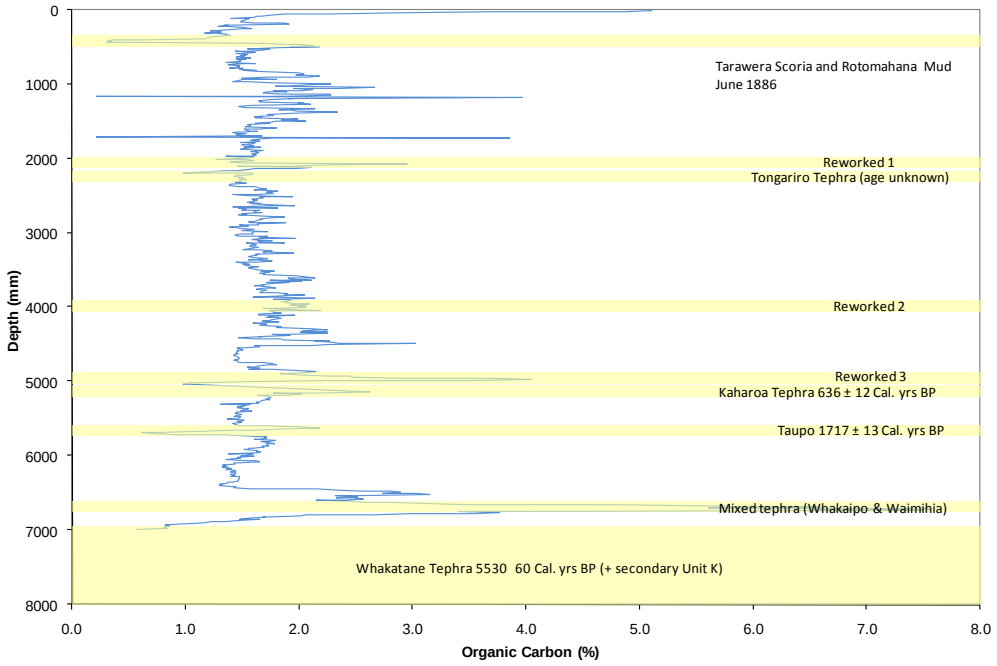

Figure 6.13: Organic carbon content of the sediment in Lake Rotorua, where the yellow bands indicate tephra layers.

Total nitrogen remains fairly constant at around 0.5% but shows a major decrease to minima at 117 (0%) and 171 (0.1%) cm (Fig. 6.14). It also shows a marked decline around the time of the Tarawera Tephra to 0.2% at 44 cm.

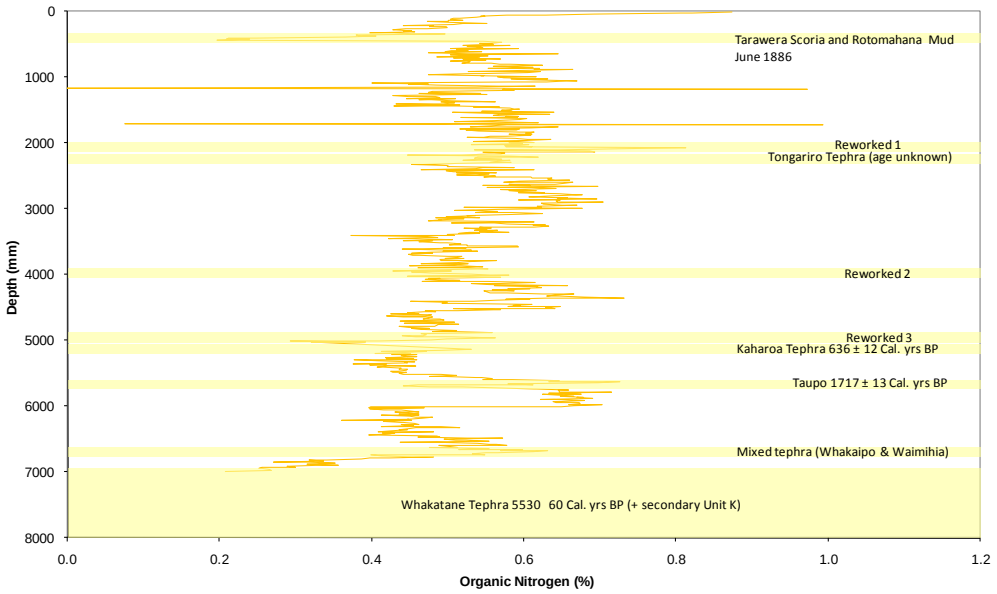

Figure 6.14: Organic nitrogen content of the sediment in Lake Rotorua, where the yellow bands indicate tephra layers.

The TOC/TN ratio closely follows the TOC trend (Fig. 6.15), with minima of 1.53, 0 and 1.37 at 44, 117 and 569 cm depths, respectively. The TOC/TN peak at various points throughout the core vary from 13.75 – 3.63 % with similar spacing to the TOC peaks. The low TOC/TN ratio indicates that the type of organic matter delivered to the lake sediments has remained predominantly algal in origin, possibly associated with long-term lake eutrophication. The spike of TOC/TN values of between 10 and 14 at 673 cm depth indicates the only mixed terrestrial/aquatic source, and could possibly be due to a seed casing which was found in the lower sediments during sampling. This peak corresponds to inferred wash-in after the Whakatane and Waimihia eruptions. Enhanced erosion probably occurred close to this time causing an increase in the proportion of land-derived organic matter.

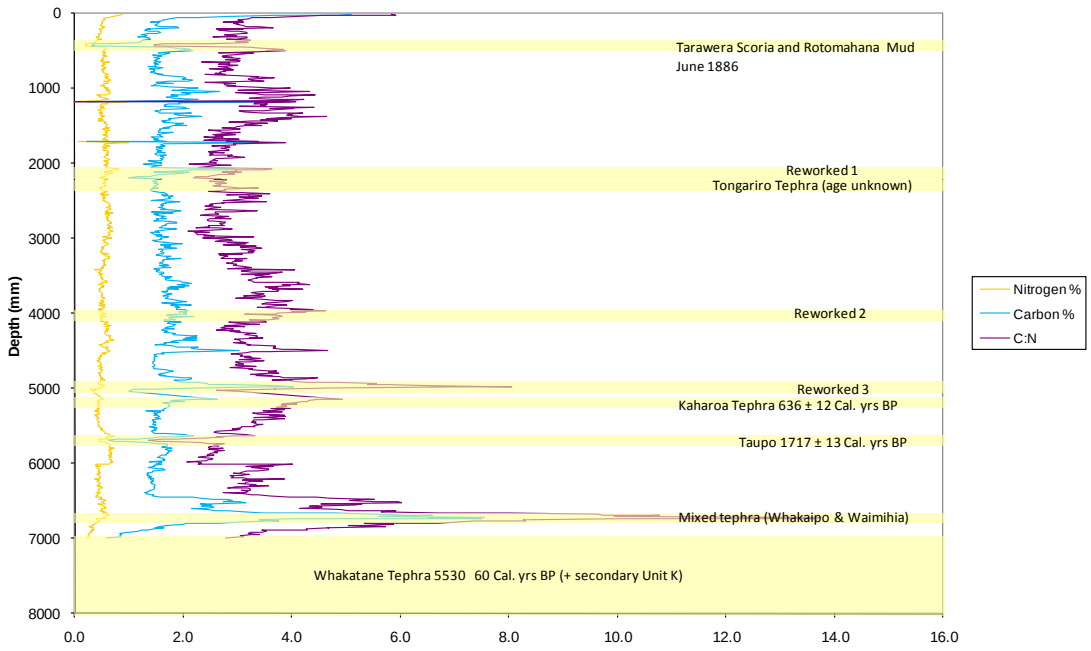

Figure 6.15: Plot showing percentage carbon, nitrogen, and the ratio of carbon: nitrogen for RU188, where yellow bands indicate tephra layers.

6.3 Summary

The significant variations in sediment geochemistry can be explained by the three principal processes: diatoms derived from within the lake water, erosion of rocks and soils from the catchment, and from distal tephra fall or dust. Geothermal fluids may also contribute some of the elements such as sulfur, arsenic and mercury.

In the sediments, diatomaceous ooze is interrupted by episodic deposition of tephra. The tephras have distinct mineralogical and elemental signatures allowing the influence of each to be traced throughout the sediment column. There are three reworked layers of tephra above the Kaharoa Tephra, in most cases normally indicative of slope failure and redeposition of lake sediments. However, in this case these layers are probably derived from erosion within the catchment, either due to large storms triggering instability or long/extended periods of rainfall.

Venting of gas and fluids from pockmarks was evident during the seismic survey, and on a calm day bubbles of gas could be seen on the lake surface. Concentrations of some of the trace elements, e.g. chromium, selenium, silver, thallium, bismuth, in the sediments may be related to this episodic venting into the water column and the subsequent accumulation in the sediments.

Concentrations of carbon and nitrogen in the surface sediment are c. 5 % and 0.9 %, respectively. Carbon decreases steadily down the upper 30 cm of the core, and then fluctuates between 4% and 0.2% below 30 cm depth. These fluctuations are possibly associated with seasonal algal blooms. Nitrogen declines steeply below 30 cm and then remains constant at ~ 0.5 % throughout the core. This rapid decrease in carbon and nitrogen concentration with depth in the sediment shows that most of the remineralisation and recycling through diagenesis takes place within the top 30 cm, but mostly within the top 10 cm. The TOC/TN ratio oscillates considerably throughout but the constant low TOC/TN ratio indicates a dominance of autochthonous algal-derived organic matter, which possibly indicates a long-term trend in the lake towards eutrophication.

All the elements associated with soils and the dissolution of minerals show similar trends with erosion after the Kaharoa eruption, then a long sequence of low concentrations (inferred to be quiet, stable conditions), followed by a series of steadily increasing concentrations. McGlone's (1983a) pollen study showed Polynesian settlement and deforestation in south-eastern Lake Rotorua directly following the Kaharoa eruption. The erosion signal in RU188 does not agree with this inferred large scale deforestation and erosion. Instead, the erosion signal indicates that at least for the north-eastern section of the catchment, large scale deforestation is not evident until around 220 cm (c. 300 cal. years B.P.) suggesting that widespread clearing of the land in this area did not occur until much later, possibly beginning with the clearing of tracks and paths, followed by considerably clearing for farms, housing and later roads.

Some elements are recycled within the sediments, in particular Fe, Mn, P and S. Fe, Mn, and P react to changing organic productivity in the lake. As algal sedimentation increases the sediments become chemically reduced allowing Fe, Mn and P to migrate back into the lake, only for the Fe and Mn to be reprecipitated. Although Fe and Mn are driven by the same processes, there is a separation. Above c. 220 cm (after c. 300 cal. years B.P.), Fe and P are linked indicating they are being contributed to the sediment by erosion. Below c. 220 cm (before c. 300 cal. years B.P.), Mn and P are linked because the Mn is more readily reduced making it more mobile than the Fe and allowing the P to bind to it (Fig 6.16). Sulfur from the lake water is also chemically reduced, reacting with iron to form iron sulfide minerals, e.g. iron pyrite frambiodes found in the 351 cm sample (Fig. 5.12).

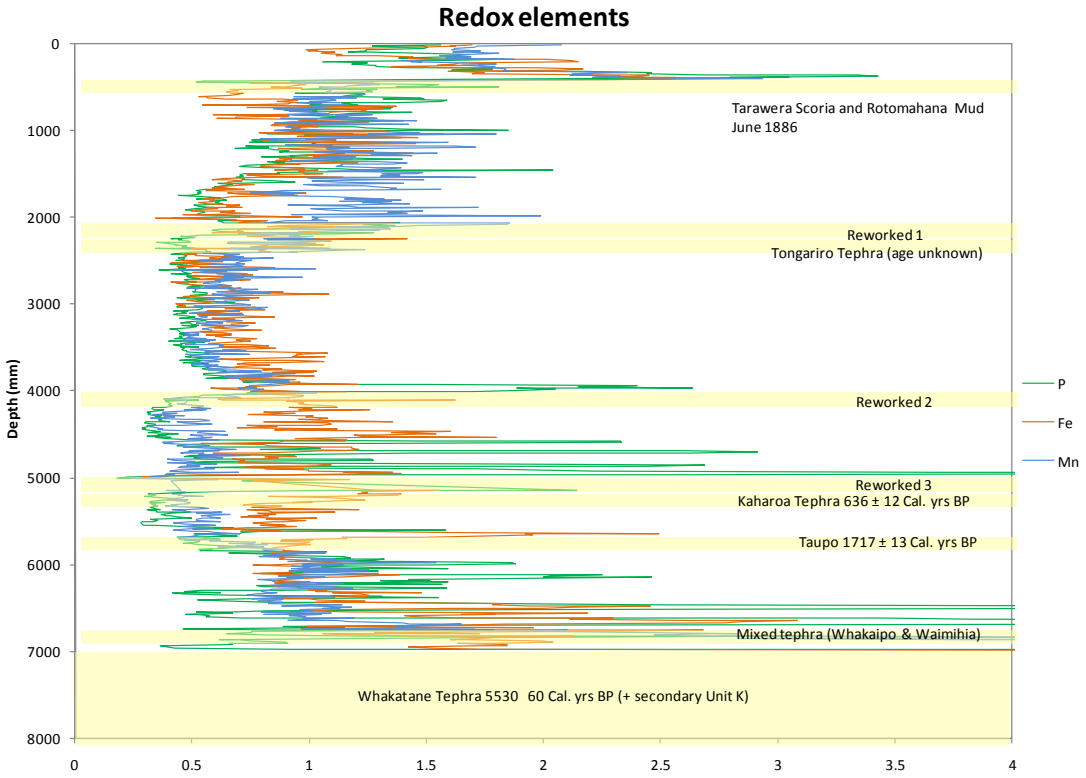

Figure 6.16: Plot of redox related elements – Fe, Mn and P, with yellow bands indicating tephra layers

Chapter Seven

Palaeoenvironmental Interpretation



7.0 INTRODUCTION

Investigations carried out on the sediment from Lake Rotorua provide a number of proxies from which inferences have been made. The aim of this chapter is to summarise the findings and provide an overall palaeolimnological history for Lake Rotorua during the mid-late Holocene period. This c. 5,500 year-long inferred history has then been compared with palaeoclimate records from nearby regions.

7.1 Chronological model – tephrostratigraphy

The magnetic susceptibility survey, as well as visual stratigraphy, helped to confirm the location of tephra beds within the core and from this we were able to erect a stratigraphic framework for the Lake Rotorua sequence by identifying five key rhyolitic tephra beds. Identifications were based on physical character, glass major element chemistry, mineralogy and stratigraphic order, and by comparison with tephra beds recognised in nearby cores previously collected at Lake Rotorua (Pearson, 2007). We compared the geochemical signature of the Lake Rotorua tephras with those of reference samples from proximal TVZ sites. The five key beds are Tarawera Tephra (1886 A.D.), Kaharoa Tephra (636 ± 12 cal. years B.P.; 1314 ± 12 A.D.), Taupo Tephra (1717 ± 13 cal. years B.P.; 233 ± 13 A.D.), Waimihia Tephra (3410 ± 40 cal. years B.P.), and Whakatane (5530 ± 60 cal. yr B.P.) (all the quoted ages follow Lowe et al., 2008). Also present is an andesitic bed ("TgVC ash") from the Tongariro Volcanic Centre, possibly a member of the Tufa Trig Formation, and three beds of reworked tephras which are thought to have originated from reworking in the shallow water during storm events.

Radiocarbon dating was also carried out on four bulk sediment samples, but the ages generated proved to be "too old" on the basis of the tephrochronology. The excess ages are thought to be caused by the introduction of old carbon through geothermal and methane rich waters. A study from Lake Taupo suggested that geothermal venting transfers depleted carbon to lake waters which can effect the age of the water, the sediment, and plants and animals that live in and around the lake.

Ages on modern plant and animal material from near Tokaanu can be > 2,000 years older than expected (Beaven-Athfield et al., 2001).

7.2 Geochemical changes

There are significant variations within some of the 28 elements analysed. These can generally be explained by where the elements originate. In Lake Rotorua's case there are four principal sources: diatoms derived from within the lake water, erosion of the rocks and soils from the catchment, distal tephra fallout or dust, and geothermal and ground water inputs.

Alkali elements such as Al, Mg, Li, K, and Ca, and in some cases other elements including P and Pb, are largely associated with clastic (detrital) inputs. Increased concentrations of these elements can be indicative of erosion in the catchment, and very high concentrations have been inferred to be associated with either high intensity storms or prolonged rainfall events, or both. Increases around 200-300 cal. years B.P. (upper c. 240 cm of the core) have been inferred to be largely human induced – through the repeated burning and removal of forest vegetation (Figs. 7.1 and 7.2). The presence of humans in the area has been inferred from a pollen diagram for Holden's Bay (McGlone, 1983a). In particular, there is a peak in Al, K, and Ca that occurs between 12-17 cm, which coincides with a peak in pigments found in a previous study (Rawlence, 1984). This peak is thought to be caused by the initial development of European farms (~ 1914) within the catchment, presumably following extensive bush clearance and associated accelerated erosion.

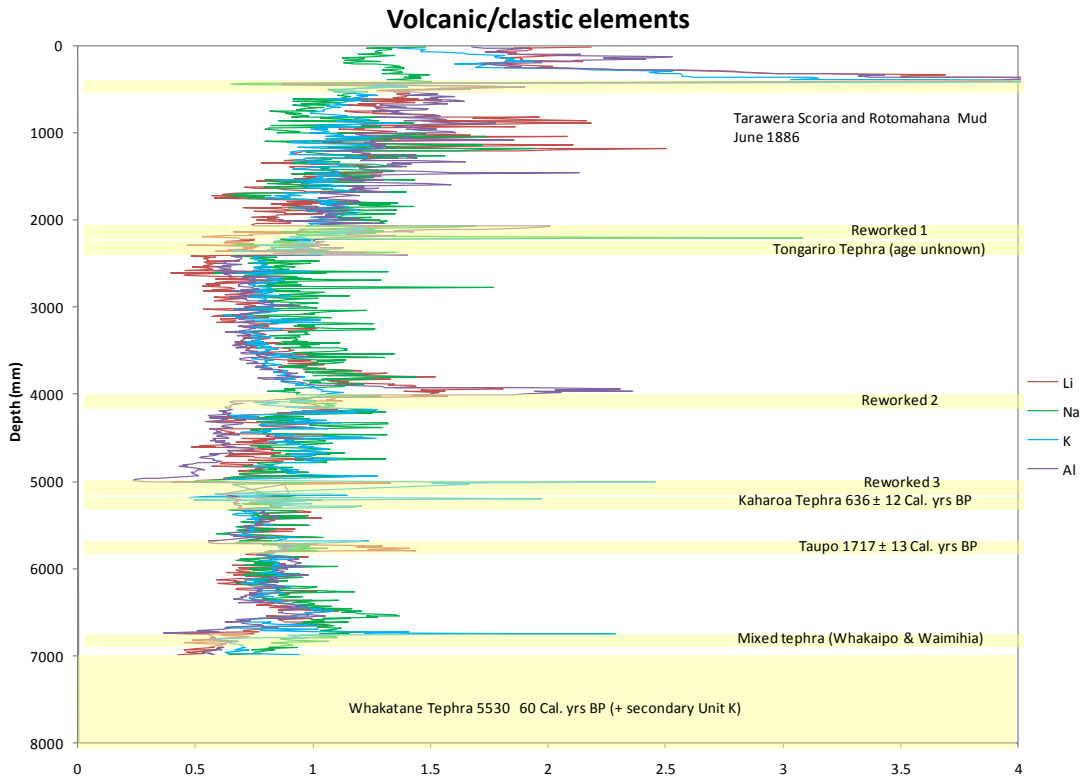

Figure 7.1: Plot of elements related to the dissolution of volcanic derived rocks and tephra, with yellow bands indicating tephra layers

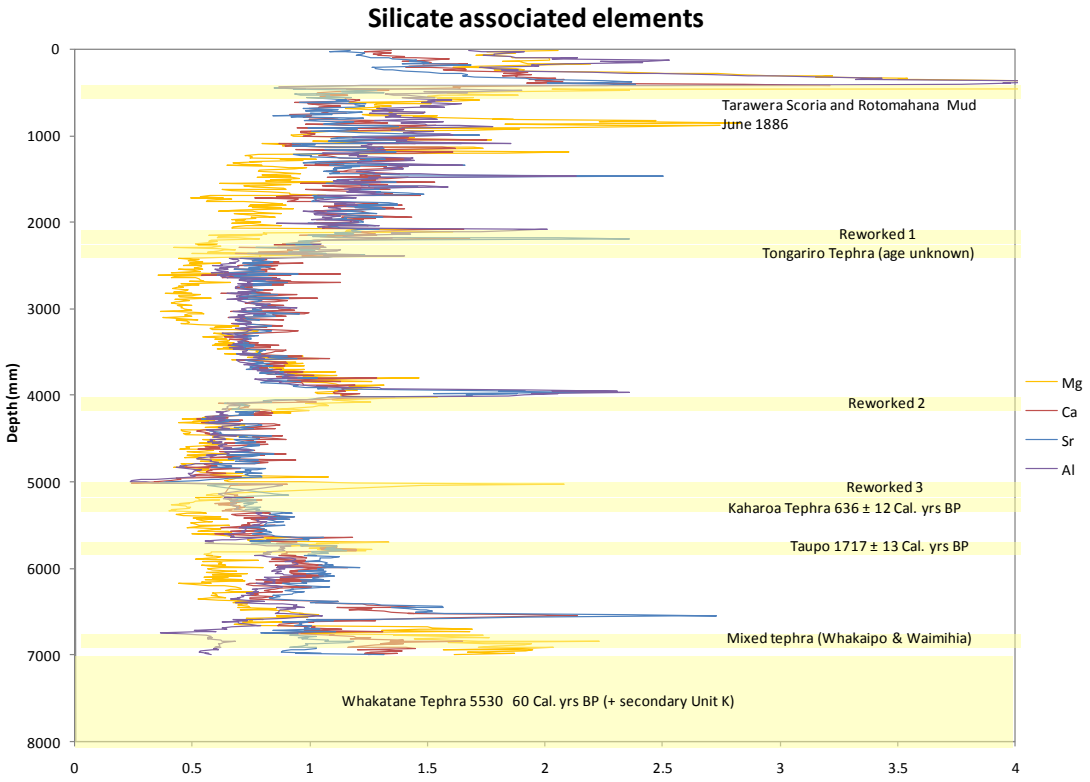

Figure 7.2: Plot of elements related to silicate mineral inputs (inwash), with yellow bands indicating tephra layers.

Heavy metals do not show the same trends as those elements that are typically clastic derived, confirming that they are probably not derived by deposition following erosion of subsoils in the catchment (Fig. 7.4). Some heavy metals (e.g. As and Hg) and sulfur were introduced to the lake predominantly from hydrothermal inflows (Fig. 7.3). These elements generally enter the lake waters in the form of insoluble sulfides and can therefore be used as a proxy for geothermal activity at both Tikitere and Rotorua City geothermal fields. Arsenic and sulfur have been used to infer changes in the intensity of activity in these two fields over the last c. 5,500 years, but as Tikitere feeds directly into the area of the lake where the core was retrieved it is likely that these reconstructions are probably limited to this field alone. Arsenic in particular is very high in the waters from this field compared with concentrations in many others in the TVZ (Smith, 1986). The concentrations reflect three periods of increased activity – the first occurring around the time of the eruption of the Waimihia Tephra (3410 ± 40 cal. years B.P.), the second following the eruption of Kaharoa Tephra (636 ± 12 cal. years B.P.; 1314 ± 12 A.D.), and the last preceding the 1886 A.D. Tarawera eruption. Sulfur is fed into the lake from both geothermal fields and some small streams on the south-eastern side of the lake meaning that much of the lake water contains high levels of sulfur both in solution and suspension; some of the increases in sulfur coincide with increases in arsenic, linked to the Tikitere Geothermal Field, but other fluctuations are evident and may be related to increased intensity of activity in the Rotorua City Geothermal Field.

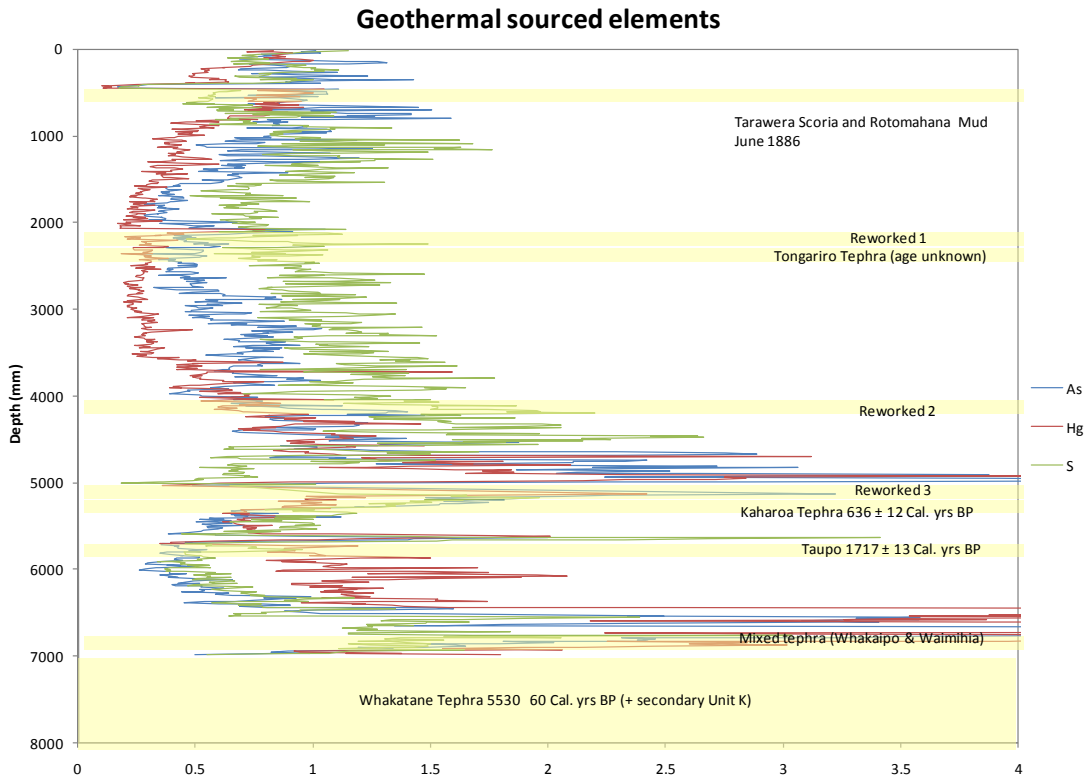

Figure 7.3: Plot of elements related to geothermal inputs, with yellow bands indicating tephra layers

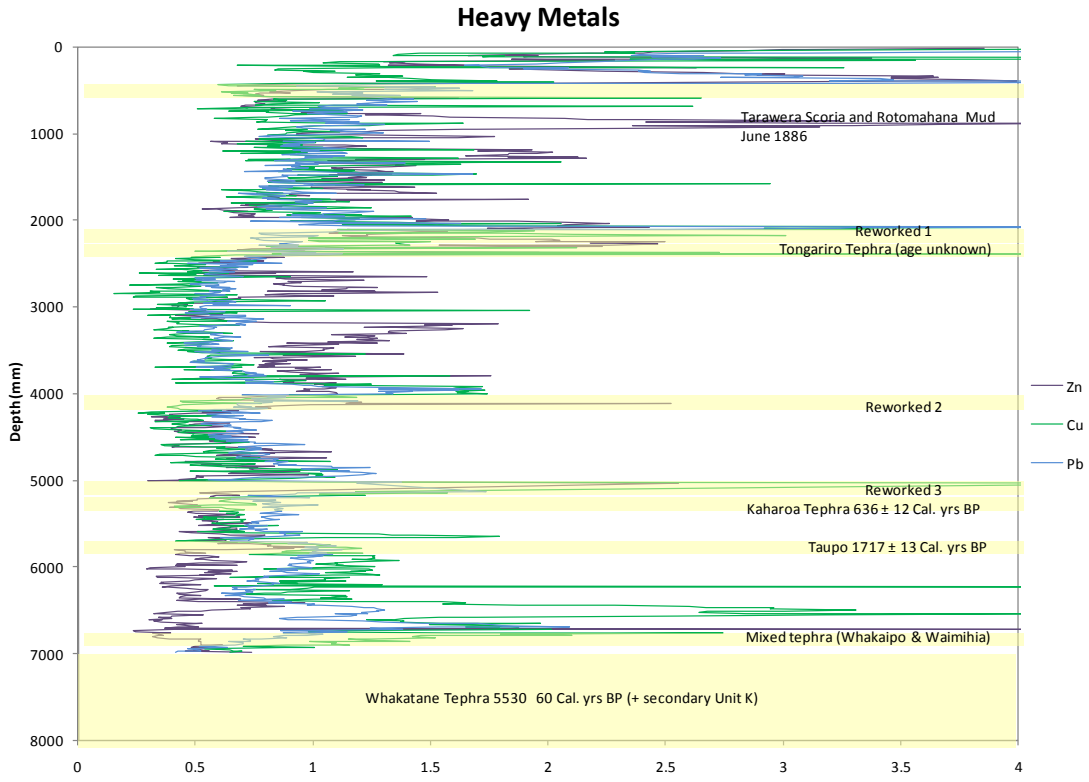

Figure 7.4: Plot of heavy metal element trends, with yellow bands indicating tephra layers

Many of the major and trace elements peak in the tephra layers suggesting that some of these layers have supplied a number of elements to the lake sediments and the soils of the catchment. However, when the concentrations in the sediment were analysed pre- and post eruption, no trend for the input of elements was evident.

Phosphorus has been closely linked in many studies to primary productivity and hence is often used as a proxy for palaeoproduction. Peaks are commonly associated with tephra layers and clastic inputs indicating that the fresh input of elements may lead to an increase in essential elements and therefore algal production. The proportion of sedimentary organic matter derived from terrestrial plants and that derived from within a lake can be identified from the difference between TOC/TN ratios of vascular land plants and algae. In the case of Lake Rotorua, the TOC/TN ratios fluctuate throughout the last 5,500 years but are consistently low (< 10), indicating a dominance of autochthonous algal-derived organic matter and possible long-term lake eutrophication. There is a rapid decrease in carbon and nitrogen concentration from surface sediment down to around 30 cm, indicating that most of the carbon and nitrogen is being subject to recycling and remineralisation through diagenesis. Previous studies have shown that the majority of this diagenesis takes place within the top 50 cm, but is more commonly confined to the top 10 cm.

7.3 Human disturbance in the catchment

New Zealand has a relatively short history of human occupation. The Polynesian people arrived in New Zealand from eastern Polynesia between about 1250 and 1300 A.D., approximately coincident with the Kaharoa eruption (c. 1314 A.D.; Lowe et al., 1998; Newnham et al., 1998b; Ogden et al., 1998; Lowe et al., 2000a, 2002; also see Wilmshurst et al., 2008). Pollen studies have been carried out on numerous sites around New Zealand (e.g., McGlone, 1983a; McGlone et al. 1995; Newnham, et al., 1995a, 1995b, 1998a; McGlone and Wilmshurst, 1999; Horrocks et al. 1999, 2002, 2005), and indicated that this first wave of human colonizers significantly reduced the area of native forest cover. Many sites along the north-eastern North Island record sustained increases in *Pteridium* (bracken) around the time of Kaharoa Tephra deposition (Fig 7.5), all within a few millimetres depth and an estimated maximum of ± 100 ^{14}C years of deposition of the tephra. This sustained increase has been inferred

to be due primarily to human deforestation. Examples of the sites include coastal records from the Bay of Plenty and Hauraki plains (e.g. Waihi Beach, Matakana Island, Papamoa, Kohika, the Rangitaiki Plains, and Kopouatai Bog) and lake records from Holden's Bay, Lake Rotorua, Lake Repongaere on the Gisborne Plains, and Lake Waikaremoana (Newnham et al, 1998a). Most of these sites have easy access to food resources and are likely to have been settled early in New Zealand's human history. Many authors (e.g. McGlone, 1983a, 1983b; McGlone et al., 1994; Scott, 1999) have suggested that the Maori people used fire as a means of land clearance for hunting moa and later for horticulture, and the deforestation encouraged the growth of bracken (*Pteridium esculentum*). Consequently, a Maori disturbance signal in the pollen record can be inferred by a decline in canopy tree pollen, a major increase in the quantity of *P. esculentum* spores, an influx of charcoal particles, followed by the appearance of pollen from colonizing species such as *Coriaria spp*. (McGlone and Wilmshurst 1999). It has been suggested that as much as a third of the pre-Maori forest cover was destroyed prior to the arrival of Europeans (Soons et al., 2002).

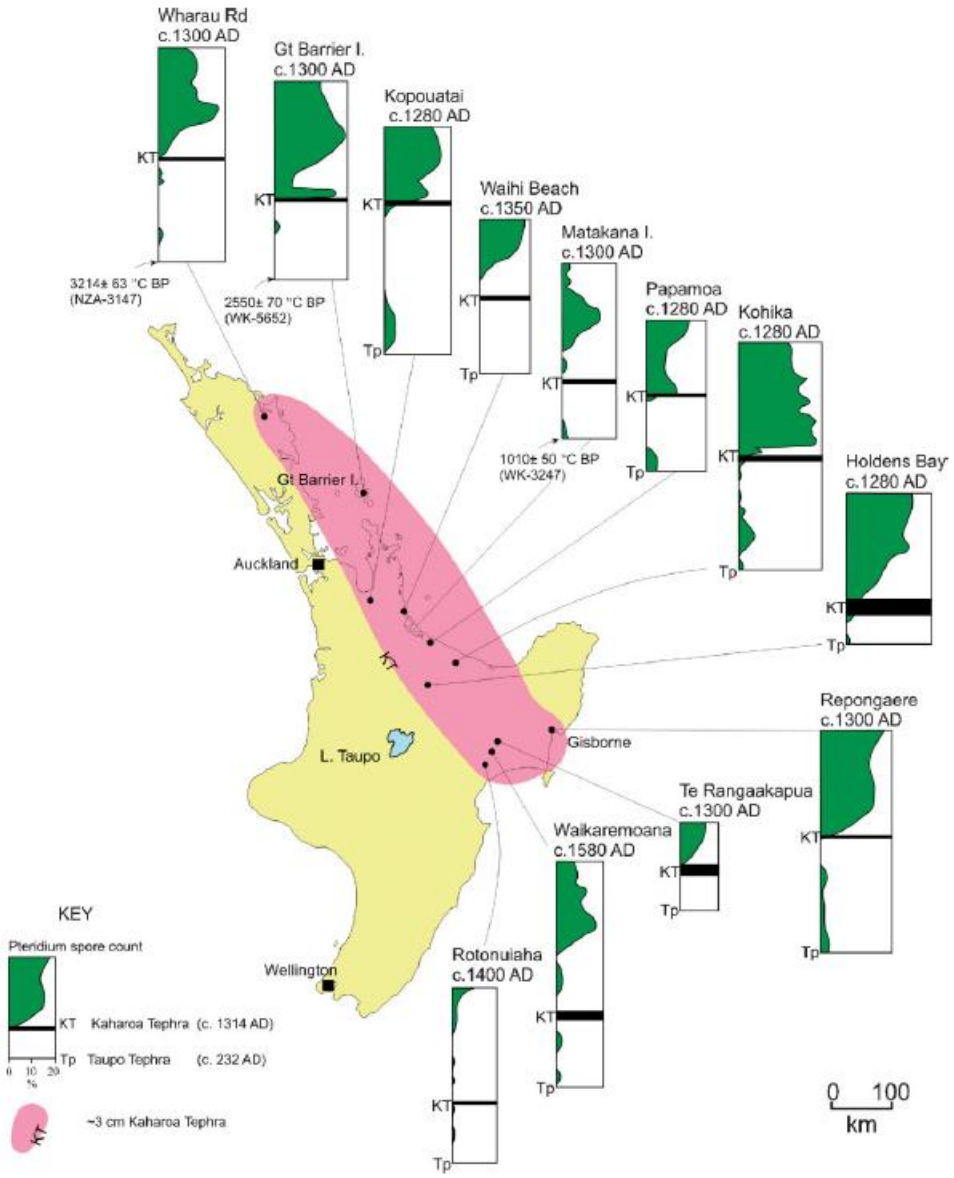

Figure 7.5: *Pteridium* (bracken) spore profiles, North Island, New Zealand, containing the *c*. 1314 A.D. Kaharoa Tephra. In most profiles, deforestation,marked by the dramatic increase in Pteridium and charcoal, occurs shortly after the deposition of Kaharoa Tephra. Ages shown at the top of each profile are estimates of the timing of the earliest human-induced deforestation impacts, based on major changes in *Pteridium* spore counts and pollen spectra with respect to the Kaharoa Tephra datum. The Taupo Tephra provides a pre-deforestation pre-impact datum in most profiles (Newnham et al., 1998b; Alloway et al., 2007b).

Pollen studies were not undertaken during this study making it is difficult to identify the exact timing of Maori arrival in the Rotorua region. However, McGlone carried out pollen analysis on sediment from Holden's Bay, Rotorua in 1983. This record has being examined in conjunction with the results from this current study. McGlone's (1983a) pollen analysis concluded that there has been little major change

in the composition of the forests since c. 9,000 cal. B.P. The largest event in the Holocene was the deforestation directly following the arrival of Maori in the region. Prior to the settlement of Maori in the region, the Rotorua Basin was completely covered by forest, dominated by forest taxa such as *Nothofagus* and *Dacrydium* which persisted in the catchment until ~ 600 cal. years B.P. Within a few centuries the Maori had eliminated much of the forest in the Rotorua Basin. This large scale deforestation must have had a substantial effect on the land and soils. It is inferred from erosion element profiles that for the north-east section of the catchment that, although there may have been some early clearing in that area for tracks or buildings, large-scale clearing and subsequent settlement probably did not occur until later at around c. 300 cal. years B.P (Fig 7.6). This timing coincides closely with dates Horrocks et al. (2007) have suggested for the occupation of the lake shore around Hamurana.

Europeans were present in the region prior to the 1886 eruption of Mt Tarawera. European influence on the catchment is thought to have commenced in the mid 1800s, but had little impact on the lake until about the turn of the century (Rawlence, 1984). These early European settlers noted that the Maori inhabitants maintained the vegetation – predominantly fern, tussock and scrub – by continual burning. Rawlence (1984) identified a peak in pigments from Holden's Bay, immediately after the Tarawera eruption, lasting ~ 3 years. This was followed by a long stable period until ~ 1914 when another increase has been identified. This same trend is evident in some of the elements in core RU188 indicative of erosion, the second peak pointing towards land clearing associated with the development of farming and local settlements. Increases in lead at the top of the Lake Rotorua core may be related to the introduction of the motor car in New Zealand and the development of roads around the lake in the 1920s – 1930s. This same increase has been found in cores from Rotoiti, Okataina, and Taupo (C. Hendy pers. comm., 2008).

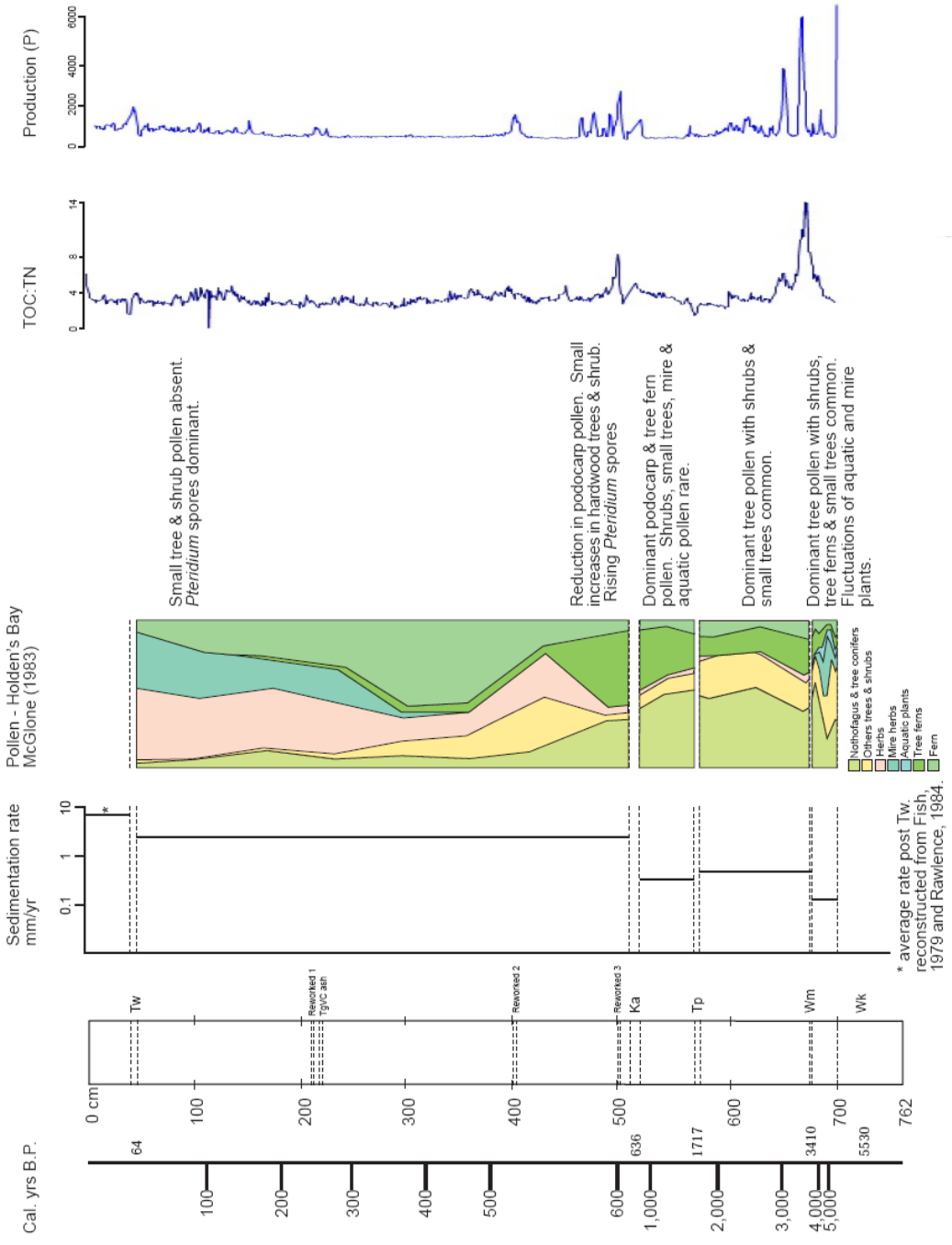

Figure 7.6: Composite diagram illustrating changes in pollen, sedimentation and production from Lake Rotorua over the last c. 5,500 years

7.4 Identification and descriptions of facies within RU188

A series of facies has been defined to summarise overall trends and infer changes with relation to palaeolimnology and climate. The core is characterized by seven facies (F1 to F7; Fig. 7.7) defined by broadly similar zones and significant fluctuations in sediment chemistry, and changes in sediment colour and reflectance spectra. Facies F1, F2, F3, F6 and F7 exhibit characteristics associated with increased inputs from erosion, whereas facies F4 and F5 are distinctly different and indicate inferred periods of 'quiet' or stability in the catchment. Facies F4 and F5 occur following the Taupo eruption (1717 ± 13 cal. years B.P.) and between c. 580 to c. 300 cal. years B.P.

7.4.1 Facies 1, 2, 3, 6, and 7 (disturbed)

The pre-Taupo period is characterised by a relatively stable catchment with well established vegetation. The catchment was only subject to occasional changes by natural events such as volcanic eruptions, storms, and sporadic fires caused by lightning strikes (Froggatt and Lowe, 1990; McGlone and Wilmshurst, 1999).

7.4.1.1 Facies 1 (5530 ± 60 to 3410 ± 40 cal. years B.P.)

Facies 1 shows a substantial change in vegetation and the introduction of aquatic and mire plants indicating a change in lake levels resulting from greater rainfall between c. 8,000 – 4,000 cal. years B.P., as inferred by McGlone (1983a). The dark sediment colour and the presence of seed casings indicate an increase in clastic or detrital sediment input following the Whakatane eruption (5530 ± 60 cal. years B.P.). There is a peak in production and phosphate, probably associated with the increase in clastic material, around 5,000 cal. years B.P.

7.4.1.2 Facies 2 (c. 3200 – c. 1700 cal. years B.P.)

Facies 2 consists of sediment that has undergone high degree of sulfide reduction which makes it difficult to see any changes, although there are a couple of small changes in texture. Changes in diatom vs. detritus are evident in the b* fluctuations, where there are two negative peaks which correspond to similar peaks in magnetic susceptibility and textural changes, possibly indicating another two minor episodes of reworking. The sediment chemistry shows significant fluctuations in many elements,

e.g. higher P concentrations, stepped changes in TOC: TN ratios, and variations in Al and K. These variations along with the textural changes possibly indicate a period of instability in the lake and the catchment.

7.4.1.3 Facies 3

Facies 3 is related to single, short-lived, climate phenomenon and consists of reworked tephra (F3; c. 520 and c. 220 cal. years B.P.) and sediment which contains increased amounts of clastic in-wash detritus (F3 a and b). Major storms generate considerable amounts of precipitation and strong winds. On Lake Rotorua the winds form waves, which rework the coarse sediment in shallow (< 10 m) waters, and the increased rainfall on the catchment can cause increased clastic inwash both of which produce a recognizable signal in the depositional record. There are three inferred storm events evident in the sediment record, one of which interrupts F5.

Following the Waimihia eruption, erosional elements, b*, phosphate and TOC: TN ratios indicate substantial amounts of clastic derived sediment – facies 3a (c. 3400 – c. 3200 cal. years B.P.; 660-640 cm). After the Kaharoa eruption, tall podocarp forest taxa declined overall and several tree fern and shrub taxa increased, and the pollen (*Pteridium*) spectra suggests the once dominant forest had been destroyed by the eruption (McGlone, 1983a). The disruption of the vegetation cover increased the susceptibility of the catchment to erosion, and following this eruption there is an ~ 10 cm thick section of dark predominantly clastic-derived inwash – facies 3b (c. 580 – c. 630 cal. years B.P.; 493-503 cm).

7.4.1.4 Facies 6 (c. 300 – c. 60 cal. years B.P.)

The transition from a natural environment to one affected by anthropogenic activities occurred in the Rotorua region c. 560 cal. years B.P. As discussed above, Maori routinely used fire to clear ground and encourage the growth of bracken (*Pteridium)*, and hence a substantial increase in erosional elements is inferred to be due to anthropogenic clearing. But at the site of RU188 the depositional erosion signal (Al), inferred to be due to the clearing of forest in the north-eastern section of the catchment, does not occur until much later, beginning around 300 cal. years B.P (Fig. 7.7). Facies 6 (300 – 64 cal. years B.P.) is characterised by sediment that

consists of distinctly different coloured laminations which have been linked with an increase in clastic material. The erosion signal fluctuates but shows a marked increase away from background levels and steadily increases until the Tarawera eruption, presumably as a result of increased deforestation and clearing, and later settlement development. There are also increases in the concentration of many other elements including phosphate and potassium.

7.4.1.4 Facies 7 (post 1886 A.D. – ? c. 1920)

Facies 7 corresponds to the time of increasing European settlement in the Rotorua region, following the Tarawera eruption (Fig. 7.7). The laminae present in the sediment after the Kaharoa eruption are no longer evident, and the proportion of clay particles increases because it is no longer masked by the significant proportion of larger clastic derived sediment. The b* parameter indicates an increase in the amount of diatoms in the sediment (7a). There is a rapid shift towards darker clastic material near the very top of the core (7b), as indicated by the sharp change in the b* parameter. This increase may be related to further development in the catchment and is possibly associated with the construction of roads in the region as indicated by the peak in lead (c. 1920s).

7.4.2 Facies 4 and 5 (stable or 'quiet')

Facies 4 and 5 have been inferred to be related to relatively 'quiet' periods in Lake Rotorua's history, with very little change in sediment geochemistry during these times.

7.4.2.1 Facies 4 (c. 1700 – c. 630 cal. years B.P.)

Facies 4 between the Taupo (1717 ± 13 cal. years B.P.) and Kaharoa (636 ± 12 cal. years B.P.) eruptions is an inferred period of stability in the lake and its catchment. There is a slight decrease in the average sedimentation rate and constant TOC: TN ratio. Spectra indicate a very high amount of organic derived material during this time, possibly related to a time of increased productivity in the lake. The sediment chemistry for this period of time indicates little variation especially evident in phosphate and potassium. Pollen from Holden's Bay indicates the catchment at this time is dominated by large trees but the record shows a slight decrease in large trees

c. 1200 cal. years B.P., and it also shows an increased amount of tree fern pollen compared with that of earlier forest (McGlone, 1983a).

7.4.2.2 Facies 5 (c. 580 to c. 300 cal. years B.P.)

Facies 5 also indicates a time of relative stability in the lake and surrounding catchment, interrupted by only one episode of reworking (F3) at ~ 520 cal. years B.P. This facies contains laminations not present in facies 4, which are thought to be due only to the increase in proportion of clastic inputs. b* and Al show occasional small increases in clastic material but the majority of the sediment is dominated by diatoms. During this period the catchment has been inferred to be under the influence of humans (McGlone, 1983a), but their presence only seems to influence the sedimentation rates (through increased diatom production) and not the erosional input characterised by increases in coarse sediment. The pollen record from Holden's Bay indicates an increasing amount of ferns and the introduction of mire plants c. 450 cal. years B.P., possible indicating a period of increased precipitation leading to higher lake levels or the development of swamp-like conditions in lowland areas around the lake (McGlone, 1983a).

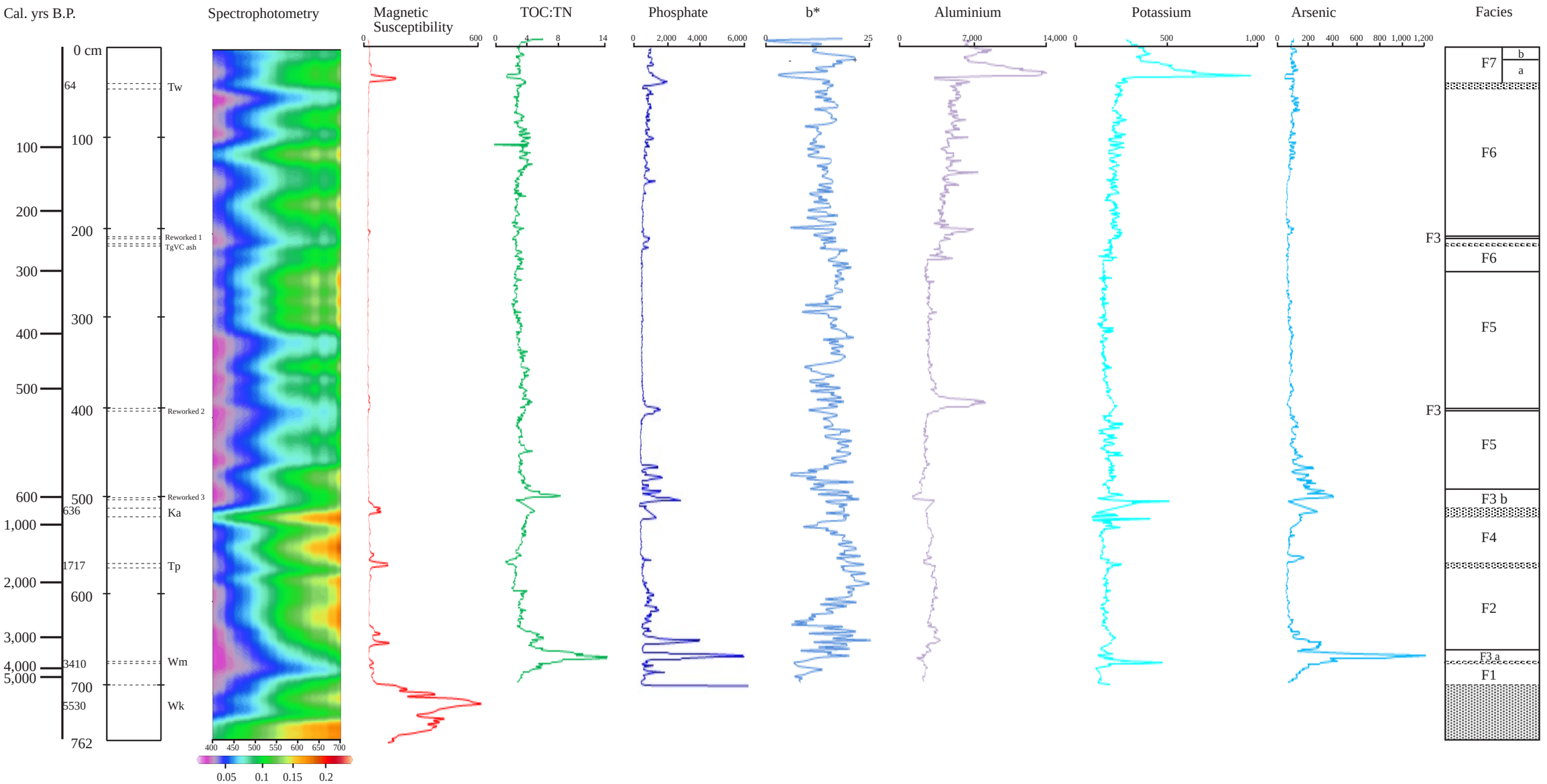

Figure 7.7: Multi proxy core summary. Downcore changes in first derivative values of sediment reflectance spectra measured by spectrophotometry are plotted on a 3D diagram where the X axis represents the different wavelengths, Y is the depth in core and Z the derivative value for the corresponding wavelength (in nm) expressed by a code of colour. The higher the first derivative the more the colour tends towards the red; the lower its value the more it tends towards blue/purple. High magnetic susceptibiliy values are indicative of the tephra layers. Total organic carbon: total nitrogen and phosphate indicate productivity. b* is used as an indicator of diatom vs. detritus, where a negative (lower value) indicates detritus. Al and K are erosion indicators (ug/g). Arsenic is an indicator of geothermal input (ug/g).

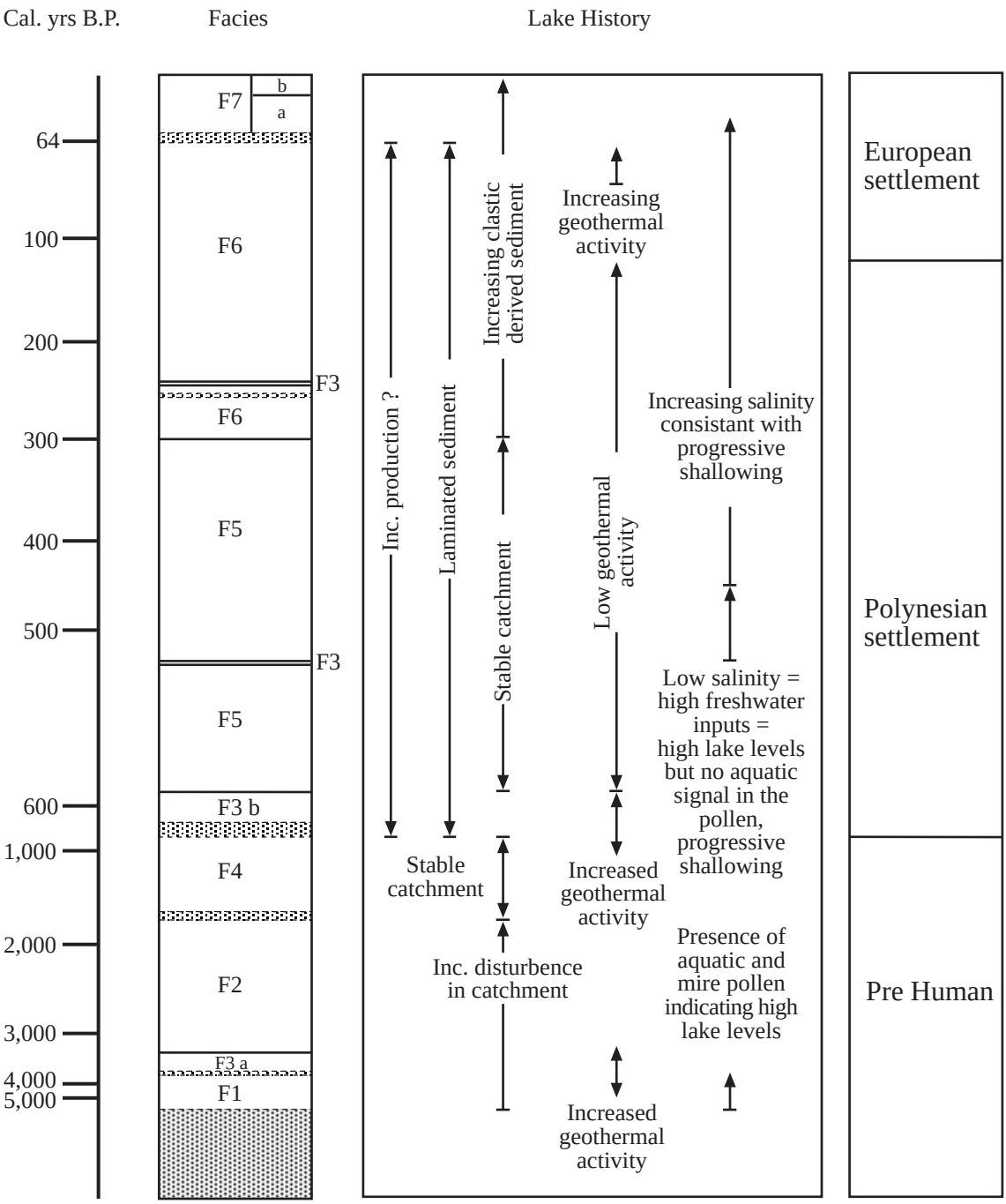

Figure 7.8: Summary of the development history of Lake Rotorua using combined information from sediment chemistry, pollen and sedimentation rates.

7.5 Lake history

The major factors influencing Lake Rotorua over the c. 5,500 cal. years B.P. analysed are likely to be changes in climate affecting the supply of nutrients and clastic material to the lake, and volcanic eruptions which can have significant effects on the landscape and drainage pathways. In the upper core, anthropogenic influences mask the affects of climate and major changes in sedimentation have been attributed largely to the effects of deforestation and increased nutrients available for primary productivity.

7.5.1 Pre-human occupation

In the pre-Kaharoa period, the landscape and vegetation cover of the Rotorua Basin was relatively stable and subject only to occasional disturbance by natural events such as fire (caused by lightning strikes), storms, minor distant volcanic eruptions, and seismic activity (Froggatt and Lowe, 1990; McGlone and Wilmshurst, 1999). The presence of a well-developed canopy and root network would have prevented soil loss, except during large events which caused local disturbances in vegetation cover and in turn erosion. Following each of the volcanic eruptions there is an increase in the amount of dark clastic derived sediment in the core. However, the intensity of this initial surface erosion declines quickly as the tephra mantled catchment then stabilized and vegetation became re-established (Gomez et al., 2007). The early lake history indicates a very disturbed catchment with a significant amount of coarse clastic or detrital input from erosion initially caused by the likely widespread devastation resulting from the Whakatane eruption (5,530 ± 60 cal. years B.P.). The presence of aquatic pollen indicates that the lake level was higher at this time, possibly due to blocking of drainage pathways by eruptives, but could also be due to increased rainfall. There is a significant amount of clastic deposition following the Waimihia eruption (3410 ± 40 cal. years B.P.) and the catchment continues to indicate a period of instability (F2). There also is a phase of increased geothermal activity around the time of this eruption. The period between the Taupo eruption and the Kaharoa eruption (c. 1700 to c. 600 cal. years B.P.) indicates the catchment was unusually stable with little erosion and a possible increase in organic productivity within the lake (F4) (Fig. 7.8).

7.5.2 Post-human occupation

Polynesian settlement probably occurred in the Rotorua region at around the time of the Kaharoa eruption as noted previously (McGlone, 1983a; Newnham et al., 1998b). This colonisation complicates the interpretation of the palaeoenvironmental history of Lake Rotorua making it difficult to distinguish changes in the climatic influences after the Kaharoa eruption. For example, it makes determining the cause of increased erosion difficult to identify – whether due to increased rainfall, or natural or anthropogenic deforestation, or both. In the core, the timing of human settlement in the region can be identified as coinciding with a substantial increase in the average sedimentation rate, but this increase does not correspond to a more substantial erosional signal until c. 300 cal. years B.P. (F6). Three storms are inferred to have occurred in this time (F3), each large enough to have reworked the coarse tephras in shallow waters and redeposit them in deeper waters. These Lake Rotorua events correspond to inferred storm events in the eastern North Island (Fig. 7.9). Another period of inferred environmental stability occurs between 600 to c. 520 cal. years B.P. and again from c. 510 to 300 cal. years B.P. These periods have very high rates of sedimentation, although this is thought to be associated more with high production within the lake rather than increased erosional input. There is another phase of increased geothermal activity around the time of the Kaharoa eruption. There is a slightly elevated level of geothermal activity building up to the Tarawera eruption, and again following the eruption. Diatom salinity reconstructions indicate that the salinity has increased, suggesting that the proportion of fresh water to geothermal water entering the lake have changed, and hence less fresh water input may lead to a progressively shallower lake. This interpretation (falling lake levels) fits in with previous tephrochronologically mapped palaeo-shorelines (Kennedy et al., 1978; Fig. 7.9 b and c; also see Figs. 2.6 and 2.7), possibly caused by decreased rainfall or the downcutting of the Ohau outlet (Green and Lowe, 1992b). These mapped shorelines indicate that the lake has dropped ~ 10 m over around 5,500 years to reach its present day level at 280 m.a.s.l.

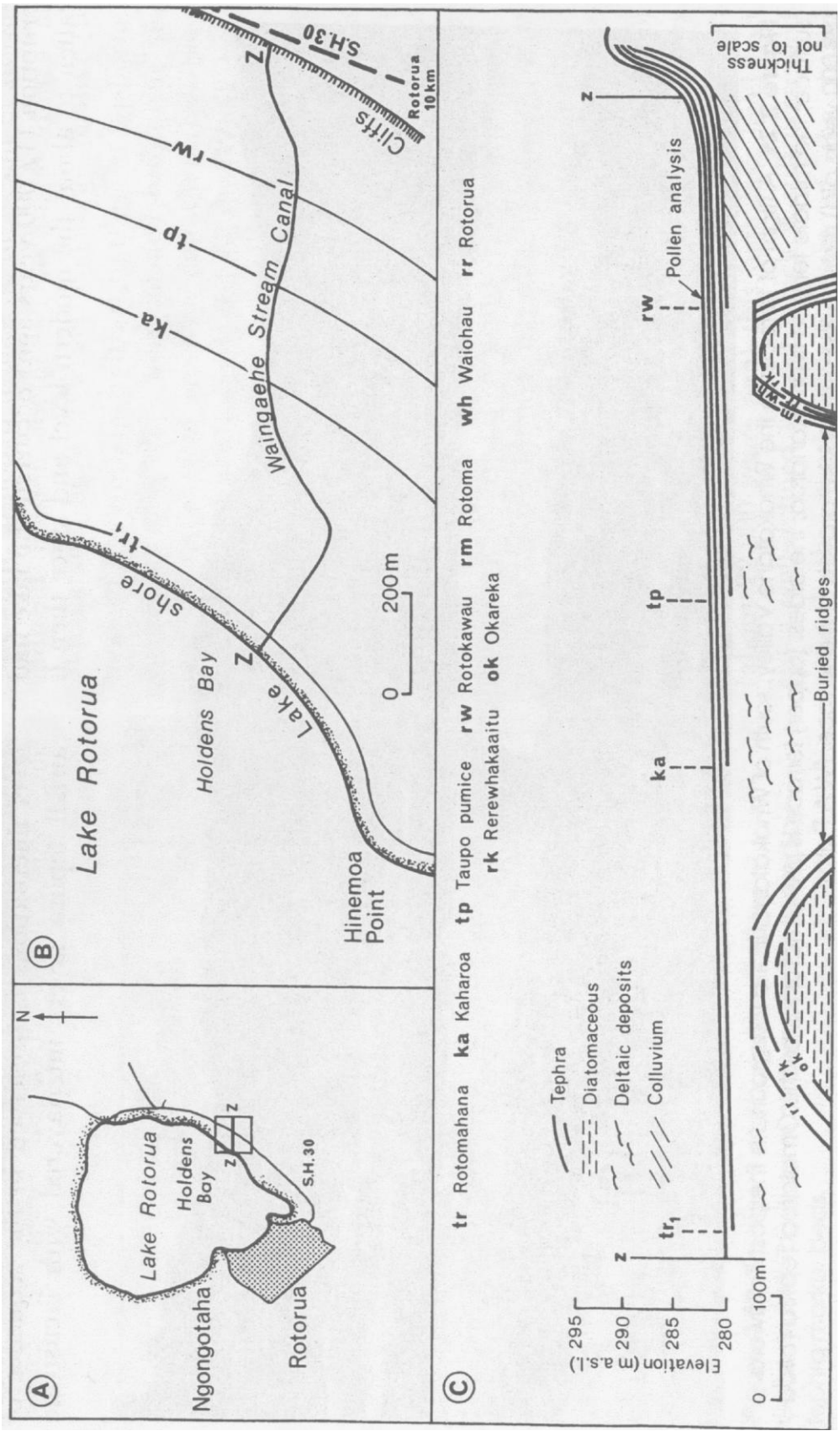

Figure 7.9: A sketch of tephra layers at Holden's Bay, Rotorua, which indicate the position of former lake shorelines (after Kennedy et al., 1978; sourced from Pillans et al., 1992, p. 54).

7.6 Palaeoclimatic reconstruction

The accumulation record of every lake is unique, yet studies of many different lakes have produced generalizations about the factors that control and modify the organic matter contents of lacustrine sediments. Lake systems respond physically, chemically and biologically to changes in climate and these responses are registered in various ways in lake sediment records.

New Zealand is a country of marked local and regional environmental variability. The complex terrain of mountainous topography and lowlands surrounded by extensive areas of ocean produce rapid changes of climate over relatively short distances (Sturman et al., 1999). This means that regional-scale climate, in particular precipitation, is extremely sensitive to changes in prevailing wind direction and circulation strength (Lorrey et al., 2007). The prevailing regional climate regime is dominated by the El Niño Southern Oscillation (ENSO). This regime became established ca. 4 cal. ka, and the climate has changed relatively little since (McGlone et al., 1993; Gomez et al., 2004, 2007; Lorrey et al., 2007). This ENSO regime brings periodic storms to the New Zealand region and one or two cyclonic storms pass within 100 km of the country every year (Gomez et al., 2007).

During El Niño events, a weakening of easterly trade winds occurs and stronger than normal south-westerly airflow develops across New Zealand. This airflow causes drier conditions for northeast areas and wetter conditions in the southwest of the country. Annual temperatures are also lower than normal and there is less precipitation. During La Niña events, warm north-easterly circulation is more prominent, and this is accompanied by more low pressure systems and wetter conditions particularly in northern and eastern regions (Gomez et al., 2004; Lorrey et al., 2007). These events are also associated with higher annual temperatures being caused by increased tropical airflows and weakened westerly and south-westerly airflows (V. Pickett pers. comm., 2008). The middle-late Holocene changes in climate for Lake Rotorua are inferred from various terrestrial records from the central North Island (as described below; Fig. 7.10).

7.6.1 Multi-record of the eastern North Island

Composite records of lake, speleothem, and marine core data have been obtained from the eastern North Island (Lorrey et al., 2007, 2008; Gomez et al., 2007). The speleothem data provide a record of wet and dry climate with inferences about the type of climatic regime dominate at that time, and a proxy record of storm activity and vegetation disturbance has been obtained from Lake Tutira, Hawke's Bay. Storm activity in the Lake Tutira catchment is linked to land-sliding events and clastic sediment deposition between organic-rich lacustrine deposits, and the disturbance history has been revealed from the relative abundances of several taxa (Wilmshurst et al., 1997; Eden and Page, 1998; Gomez et al., 2007).

7.6.2 Waitomo speleothem record

Speleothems are commonly used in palaeoclimate reconstructions because the oxygen isotopes contained within the calcite are closely related to temperature and small changes can therefore be used as a reconstruction proxy. Williams et al. (2004) presented a speleothem record from the western central North Island covering the mid-late Holocene. Inferences indicate that the mid-Holocene time interval was generally cool punctuated by some relatively mild peaks. Relatively high $\delta^{18}O$ values suggest that these occurred at 5.1, 4.9, 4.4, 3.9, and 3.2 cal. ka. This mid-Holocene period was followed by a long period of warmer temperatures only interrupted by a short period of cooling c. 325 cal. B.P.

Around 5 ka, $\delta^{18}O$ values, although oscillating, generally become more negative until about 3 cal. ka. This trend implies cooling, an interpretation that is supported by pollen records, which indicate cooling to have occurred after 6.3 cal. ka (McGlone, 1988; Newnham et al., 1989). The oscillating decline in δ-values also mirrors the cooling trend identified from Lake Maratoto records. From 3.6 to 1 cal. ka the droughty summers identified from Lake Maratoto and Waikato pollen records were probably associated with increasing average warmth, judging by the upwards trend in $\delta^{18}O$ values. This trend culminated in a late-Holocene $\delta^{18}O$ peak from 0.9 to 0.6 cal. ka coinciding closely with the 'Medieval Warm Period'. In New Zealand, this warming coincided approximately with a period of Polynesian settlement (McGlone and Wilmshurst, 1999). Temperatures, as implied by falling $\delta^{18}O$ values,

subsequently cooled rapidly to a trough about 325 cal. years ago, although at Waitomo $\delta^{18}O$ values were only marginally below present levels. The implied temperature depression at Waitomo about 325 years ago corresponds closely in timing of the 'Little Ice Age' (see also Newnham et al., 1998a). Delta ^{18}O values and hence temperatures have since increased to present day levels (Williams et al., 2004).

7.6.3 Dendrochronology – **Libocedrus bidwillii** *(NZ cedar)*

Tree rings have been used extensively to reconstruct past climates. Long tree-ring chronologies are valuable for providing information on the frequency of extreme events, long-term fluctuations in mean and variance, and in placing modern climatic data in a longer term context (Xiong and Palmer, 2000). Few tree ring-based climate reconstructions exist for New Zealand. There are currently around 100 chronologies looking at nine different species, but most only cover the last 500 years (Palmer and Xiong, 2004). The oldest record is from a New Zealand cedar, *Libocedrus bidwillii*, and stretches back to 1140 A.D. Tree rings have been successfully used to reconstruct a range of past climatic variables in New Zealand including four temperature series (e.g. Xiong and Palmer, 2000), one precipitation series, one river-flow series and a series of zonal and meridional flow indices (Palmer and Xiong, 2004). Some chronologies have been linked to ENSO, the dominate climatic force in New Zealand, with increased growth occurring in kauri, *Agathis australis*, during cold, dry El Niño phases and decreased growth during warmer, wet La Nina phases (Buckley 2000; Fowler et al., 2000; 2007). For the purpose of this study the temperature reconstruction from Palmer and Xiong (2004) has been used. It shows four cold periods and seven warm periods stretching back until 487 cal. yrs. B.P. (1463 A.D.; Table 7.1).

Interval	Mean	Standard deviation	Departure values
Cold periods			
1623–1647	15.756	0.282	–0.127
1678–1702	15.788	0.293	–0.095
1940–1964	15.808	0.209	–0.075
1881–1905	15.809	0.297	–0.074
1796–1820	15.809	0.297	–0.074
Warm periods			
1463–1487	15.996	0.289	+0.113
1728–1752	15.991	0.387	+0.108
1593–1617	15.956	0.263	+0.073
1763–1787	15.952	0.215	+0.069
1519–1543	15.952	0.264	+0.069

Table 7.1: A list of the five coldest and warmest 25-year intervals as indicated by the temperature reconstruction of *Libocedrus bidwillii* (Palmer and Xiong, 2004).

7.6.4 Lake Maratoto

Lake Maratoto is a small peat lake in the middle Waikato basin and provides a record from which wetting and drying events have been inferred. Changes in the growth rate of the peat where the fastest growth rate corresponds to the highest net precipitation rates. At Lake Maratoto the fastest growth rate occurred over the period 7,000-2,000 cal. years ago, corresponding to high rainfall and hence high lake level. Lake level then declined c. 2,000 cal. years B.P. indicating a drier climate (Green and Lowe, 1985).

7.6.5 Lake Rotorua

The early history of RU188 is difficult to determine as there is a substantial amount of compaction lower in the core making it difficult to link changes in sediment with abrupt changes in climate, but general longer term trends are evident. Pollen records from 5530-3410 cal. years B.P. indicate that the Rotorua region was significantly wetter during this period than in the following periods. The fluctuations in TOC: TN ratios, phosphate, b* and erosional elements indicate ongoing disturbances in the catchment up until around 3000 cal. years B.P. (Fig. 7.10). These fluctuations are likely to be associated with a fluctuating climate. This phase corresponds to around the time ENSO was becoming established as the dominant force controlling New

Zealand climate, and was possibly a time of variable weather patterns. Records from the eastern North Island indicate a mixed regime and a high storm index and the Lake Maratoto record indicates a wetter climate.

The stable period following the Taupo eruption does not match with the inferred wet, stormy climate from the eastern North Island records and tends to indicate a period of calm weather, and possibly drying as indicated in the Lake Maratoto record.

As stated above, pollen studies indicate the presence of humans in the Rotorua catchment at close to the time of the Kaharoa eruption. The sedimentation rate following this eruption increases ten-fold meaning that there must have been a significant change in the catchment. Thus changes recorded in the lake sediments are probably not related directly to climate. Diatom identification indicates that whilst the pH has changed little over the last ~ 550 cal. years, salinity has increased indicating that there has been a change in the amount of fresh water input to the lake possibly indicating a lake level drop significant enough to cause a response in the diatom populations. The diatom samples from 390-400 cm depths (c. 510-520 cal. years B.P.) correspond to an inferred very wet period on the east coast of the North Island (Fig. 7.10; Lorrey et al., 2007). In contrast, the faunal species in samples from 350-360 cm depths (c. 450-475 cal. years B.P.) indicate a higher tolerance of salinity and possibly indicate lower lakes levels consistent with a drier climate. The samples from 30-32 cm depth also indicate lower lake level consistent with a drier climate between c. 450 cal. years B.P. and c. 55 cal. years B.P.

There are two storm events identified from the reworking of tephra layers (F3; Fig. 7.10). These two events, dated approximately to 220 and to 520 cal. years B.P., roughly coincide with inferred storm events from Lake Tutira and Lake Rotonuiaha, and correspond to a phase dominated by the La Niña phase of ENSO when storms are more common. But chemical signatures from the sediments either side of these events indicate a relatively stable time in the catchment, possibly indicating a regime more like that of the present day when El Niño/La Niña cycles range from around 5 to 7 years with only the very largest storms being strong enough to travel that far inland and leave a perceivable layer. The reworked tephra above the Kaharoa Tephra

may represent another storm flux but it is interspersed within predominantly clastic sediment, some of which may be associated with inwash from prolonged rain events causing increased erosion on an already unstable landscape.

There is no significant change in the proxies indicating the presence of an abnormal warming event more commonly known as the Medieval Warm Period. But evidence for a delayed counterpart to this event occurring in New Zealand has been provided by tree ring, speleothem and glacial records from New Zealand and proxy climatic records from elsewhere in the Southern Hemisphere (e.g. Broecker, 2001; Soon & Baliunas, 2003; Goosse et al., 2004; Winker, 2004; Williams et al., 2005). The Little Ice Age (LIA) is another major climate event that has been recognised in climate records from around the world and has been previously positively identified in New Zealand, but cannot be positively identified in RU188 (e.g. Mayewski et al., 2004; Winker, 2004; Williams et al., 2004; Thompson et al., 2006; Gomez et al., 2007).

7.7 Summary

It is assumed that prior to the arrival of humans in the Rotorua region, volcanic eruptions, severe storms and the occasional fire, ignited by lightning, periodically disturbed the forest cover and caused relatively minor increases in clastic deposition. There have been at least three very large storms since the Kaharoa eruption, as evident by the reworking of tephra in the shallow water by waves then redeposited in the deeper waters towards the centre of the lake. Each of these inferred storm events corresponds to storms inferred from records from Lake Tutira and Lake Rotonuiaha (dated approximately to 220 and to 520 cal. years B.P.).

The single-most notable feature of the record from Lake Rotorua is the apparent environmental stability of the region directly after the Taupo eruption, between 600 to c. 520 cal. years B.P., and again from c. 510 to 300 cal. years B.P.

Cultural activities, involving land clearance by fire, impacted the native vegetation and lake sedimentation from c. 650 cal. years B.P., when Polynesian first arrived in the Rotorua region, but large scale removal of the forest cover and subsequent erosion did not occur in the north-eastern sector of the lake until c. 300 cal. yrs B.P. and

increased further with the arrival of European colonists and the development of roads around the lake.

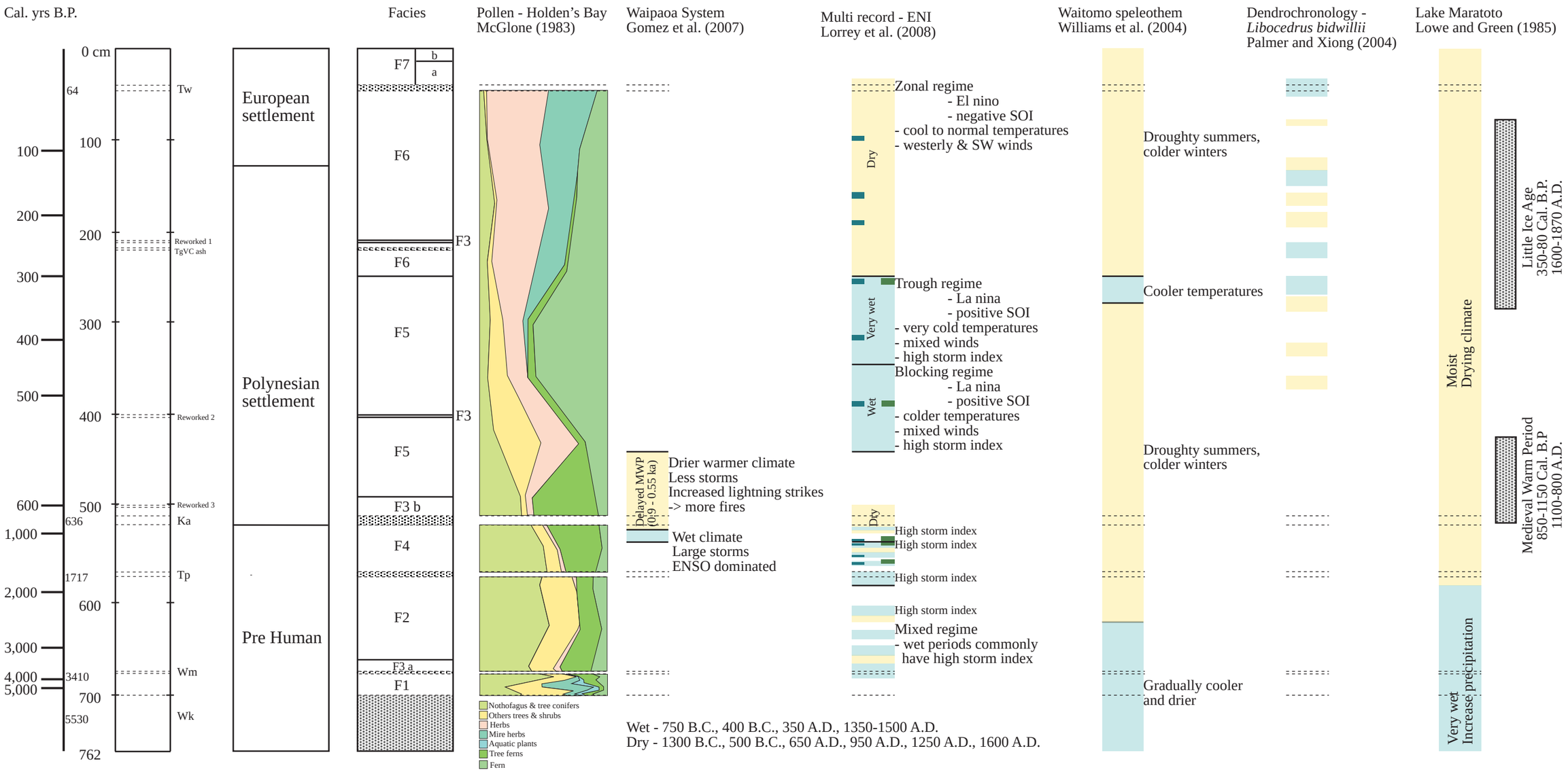

Figure 7.10: Comparison of lake facies and pollen changes with regional climate records from the upper North Island and anthropogenic history. From left to right: RU188 core summary, human settlement summary, sedimentary facies, pollen summary of McGlone (1983a), and palaeoclimate reconstructions from - the Waipaoa system (Gomez et al., 2007), eastern North Island composite record (including data from Hawke's Bay speleothem, Lake Tutira - right dark green storm index, Lake Poukawa, Round Lake and Lake Rotonuiaha - left dark blue storm index; where light blue indicates wet periods {at ~ 2700, ~ 2350, ~ 1650, ~ 900-750, ~ 550-450, and ~ 450-300 cal. years B.P} and yellow represents dry periods {at ~ 3250, ~ 2450, ~ 1300, ~ 1000, ~ 700-600, and ~ 300-50 cal. years B.P.}; Lorrey et al., 2008), Waikato (composite record from Waitomo caves and Lake Maratoto where blue is cooler and yellow is warmer), dendrochronology of *Libocedrus bidwillii* (NZ Cedar) where blue represents cold periods and yellow represents warm periods (Palmer and Xiong, 2004), and Lake Maratoto (Green and Lowe, 1985).

Chapter Eight

Conclusions

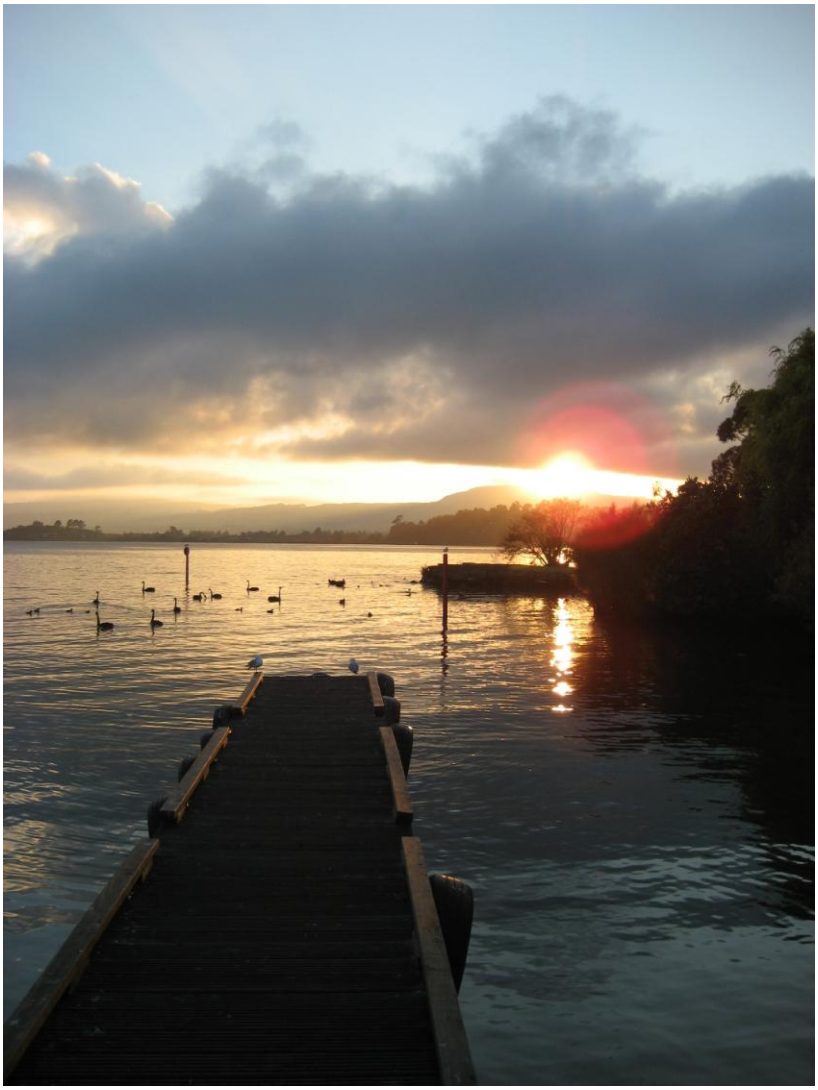

8.1 Conclusions

The principle aim of this study was to establish a partial palaeolimnologic history for Lake Rotorua, providing a palaeoclimate reconstruction for the middle to late Holocene.

- A stratigraphic framework and an age model were constructed using tephrostratigraphy. Five key rhyolitic tephra beds provided the primary timescale which extends back to c. 5,500 calendar (cal.) years ago, spanning the middle to late Holocene.

- The sediment in core RU188 is made up predominantly of olive and grey-olive diatomaceous ooze. It is interspersed with tephra layers, the deposition of which caused major changes to the landscape, and provided increased inputs of clastic (detrital) sediment to the lake shortly after each event until the landscape returned to equilibrium. The differences in relative abundances of clastic sediments and diatoms are responsible for the laminations evident in the core between the Kaharoa and Tarawera eruptives. The subsequent increase in clastic sediment is probably due to human impacts in the catchment, in particular deforestation and associated accelerated erosion.

- Contained within the sediments are layers of reworked glass shards. These reworked layers are inferred to be caused by the reworking of coarse grained tephra in shallow water, which is then deposited in the deeper lake basin, and are likely to be the result of large storms. Each of these storm-induced layers coincides approximately with similar events in other lake records from the east coast of the North Island.

- The sediment geochemistry has provided a proxy from which inferences about clastic erosion from the catchment and changes in geothermal activity

have been made. Phosphate and total organic carbon: total nitrogen ratios provided information about palaeoproductivity. They indicate that productivity has varied predominantly coincident with clastic inputs, as these inputs bring with them nutrients needed for growth. TOC: TN ratios indicate that there have been few periods when carbon has not been derived from within the lake.

- Sediment colour spectrophotometry, widely used in palaeoceanography, has been applied to the Lake Rotorua sediment as a way of permanently recording the visual colour changes and to investigate down-core variations in sediment composition. The b* parameter of this technique has been used as another proxy for both productivity and diatom content. This parameter matches major changes in clastic inputs and shows an especially interesting pattern of cyclicity possibly indicating seasonal changes in productivity and clastic inputs.

- Diatom identification has provided proxies of pH and salinity. These identifications indicate the lake has become increasingly saltier signifying a change in the ratio of freshwater to geothermal inputs, possibly related to falling lake levels over the mid-late Holocene.

- The determination of trophic status proved more difficult to evaluate because no suitable diatom assemblage was identified, and requires further investigation. However, major changes in phosphate concentrations in the sediments do support changes in trophic status. One possible avenue to determine this would be to undertake diatom counts, and with the development of a more robust diatom transfer function this is an option for future studies.

- Pollen counts (McGlone, 1989a) indicate the first human settlement in the Rotorua region occurred around the time of the Kaharoa eruption. The increase in diatom-related sedimentation is inferred to be due to an increase

in nutrients derived as a result of initial deforestation and erosion in the entire lake catchment. However, an increase in clastic derived elements does not occur in the core until c. 300 cal. years B.P., indicating that the initial Polynesian settlers did not have a significant impact in clearing the north-eastern region of the lake catchment until much later. This clastic-derived sedimentation rapidly increases until the Tarawera eruption and then fluctuates after the eruption reflecting changes in the catchment that probably relate to the development of modern settlements and roads.

8.2 Areas of future study

- Diatom counts and identification of samples from the entire length of the core may possibly be used in conjunction with recently developed transfer functions – providing a more sound estimate of pH and salinity through time, and possibly assisting interpretations of lake trophic status. Also of interest would be the influence tephra deposition has had on the diatom populations.
- A new pollen study from the northern sector of the lake would provide further evidence about the development in this section of the catchment, and test inferences made in this study.
- High-resolution grain size determination and the identification of the proportion of clastic sediment would help to develop a clastic sediment flux and disturbance proxy from which further palaeoclimate inferences may be made, in particular storm events, and cycles of El Niño/La Niña. The amount of reworked glass grains may also help create a proxy from which palaeowind inferences may be made.
- Further investigation into the causes of the discrepancies in the radiocarbon ages.
- Isotope and compositional analysis of the fluids being expelled from the vents on the lake bed – both methane and geothermal.

References



References

Adams, C.J., Graham, I.J., Seward, D. & Skinner, D.N.B., 1994. Geochronological and geochemical evolution of late Cenozoic volcanism in the Coromandel Peninsula, New Zealand *New Zealand Journal of Geology and Geophysics*, 37: 359-379.

Alloway, B., Neall, V.E., & Vucetich, C.G., 1995. Late Quaternary (post 28,000 year B.P.) tephrostratigraphy of northeast and central Taranaki, New Zealand. *Journal of the Royal Society of New Zealand*, 25(4): 385-458.

Alloway, B.V., Larsen, G., Lowe, D.J., Shane, P.A.R. & Westgate, J.A., 2007a. Tephrochronology. In: Elias, S.A. (ed.) *Encyclopaedia of Quaternary Science*. London, Elsevier.

Alloway, B.V.; Lowe, D.J.; Barrell, D.J.A.; Newnham, R.M..; Almond, P.C.; Augustinus, P.C.; Bertler, N.A.; Carter, L.; Litchfield, N.J.; McGlone, M.S.; Shulmeister, J.; Vandergoes, M.J.; Williams, P.W. & NZ-INTIMATE members 2007b. Towards a climate event stratigraphy for New Zealand over the past 30,000 years (NZ-INTIMATE project). *Journal of Quaternary Science*, 22: 9-35.

Anderson, A.J., 1991. The chronology of colonisation in New Zealand. *Antiquity*, 65: 767-795.

Augustinus, P., Reid, M., Andersson, S., Deng, Y. & Horrocks, M., 2006. Biological and geochemical record of anthropogenic impacts in recent sediments from Lake Pupuke, Auckland City, New Zealand. *Journal of Paleolimnology*, 35: 789-805.

Augustinus, P., Bleakley, N., Deng, Y., Shane, P., & Cochran, U., 2008. Rapid change in early Holocene environments inferred from Lake Pupuke, Auckland City, New Zealand. *Journal of Quaternary Science*, 23(5): 435-447.

Ballance, P.F., 1981. Geology and landforms of Rotorua Lakes Area. In: Chapman, V. J. (ed.) *Handbook of the Rotorua Lakes District*. Rotorua, The Guardians of the Rotorua Lakes.

Balsam, W.L., & Deaton, B.C., 1996. Determining the composition of Late Quaternary marine sediments from NUV, VIS, and NIR diffuse reflectance spectra. *Marine Geology*, 134(1-2): 31-55.

Battarbee, R.W., 2000. Palaeolimnological approaches to climate change, with special regard to the biological record. *Quaternary Science Reviews*, 19: 107-124.

Bailey, R.A. and Carr, R.G., 1994. Physical geology and eruptive history of the Matahina Ignimbrite, Taupo Volcanic Zone, North Island, New Zealand. *New Zealand Journal of Geology and Geophysics,* 37: 319-344.

Bauer, M., & Blodau, C., 2006. Mobilization of arsenic by dissolved organic matter from iron oxides, soils and sediments. *Science of the Total Environment,* 354(2-3): 179-190.

Beanland, S., & Houghton, B., 1991. Rotokawau Tephra: Basaltic maars in Okataina Volcanic Centre, Taupo Volcanic Centre. *New Zealand Geological Survey Record,* 43: 37-43.

Beavan-Athfield, N.R., Mcfadgen, B.G., & Sparks R.J., 2001. Environmental influences on dietary carbon and ^{14}C ages in modern rats and other species. *Radiocarbon*, 43: 7-14.

Bibby, H.M., Risk, G.F. and Caldwell, T.G. 2002. Long offset tensor apparent resistivity surveys of the Taupo Volcanic Zone, New Zealand. *Journal of Applied Physics,* 49: 17-32.

Black, T.M., Shane, P.A.R., Westgate, J.A., & Froggatt, P.C., 1996. Chronology and paleomagnetic constraints on widespread ignimbrites of the Taupo volcanic zone, New Zealand. *Bulletin of Volcanology*, 58: 226-238.

Boggs, S.J., 2001. *Principles of Sedimentology and Stratigraphy*. 3rd ed. New Jersey, Prentice-Hall Inc.

Boudreau, B.P., 1999. Metals and models: Diagenetic modelling in freshwater lacustrine sediments. *Journal of Paleolimnology*, 22: 227-251.

Bowyer, D.A., 2001. Evolution of Okataina, Rotorua and Kapenga Rhyolite Lavas, Taupo Volcanic Zone, New Zealand. Ph.D Thesis, University of Waikato, Hamilton.

Broecker, W.S., 2001. Was the Medieval Warm Period Global? *Science,* 291: 1497-1499.

Bronk Ramsey, C., 2001. Development of the radiocarbon calibration program OxCal. *Radiocarbon,* 43: 355-363.

Brugman, R.B. 1984. Holocene Paleolimnology. In: Wright, M.E. (ed.). *Late Quaternary Environments of the United States: The Holocene* Vol. 2. University of Minnesota Press, Minneapolis, USA.

Bryant, C.L., Farmer, J.G., MacKenzie, A.B., Bailey-Watts, A.E., & Kirika, A., 1997. Manganese behavior in the sediments of diverse Scottish freshwater lochs. *Limnology and Oceanography*, 42(5): 918-929.

Buckley, B., Ogden, J., Palmer, J., Fowler, A., & Salinger, J., 2000. Dendroclimatic interpretation of tree-rings in *Agathis australis* (kauri). 1. Climate correlation functions and master chronology. *Journal of The Royal Society of New Zealand*, 30(3): 263-276.

Burger, D.F. 2006. Dynamics of internal nutrient loading in a eutrophic, polymictic lake (Lake Rotorua, New Zealand). Ph.D Thesis. University of Waikato, Hamilton.

Burger, D.F., Hamilton, D.P., Pilditch, C.A., & Gibbs, M.M. 2007. Benthic nutrient fluxes in a eutrophic, polymictic lake (Lake Rotorua, New Zealand). *Hydrobiologica*, 584: 13-25.

Burnet, A.M.R. & Davis, J.M., 1980. Primary production in Lakes Rotorua, Rerewhakaaitu, and Rotoiti, North Island, New Zealand, 1973-78. *New Zealand Journal of Marine & Freshwater Research*, 14(3): 229-236.

Bussell, M.R., 1988. Mid and late Holocene pollen diagrams and Polynesian deforestation, Wanganui district, New Zealand. *New Zealand Journal of Botany*, 26: 431-451.

Byrami, M., Ogden, J., Horrocks, M., Deng, Y., Shane, P., & Palmer, J., 2002. A palynological study of Polynesian and European effects on vegetation in Coromandel, NZ, showing the variability between four records from a single swamp (Kaharoa Tephra). *Journal of The Royal Society of New Zealand*, 32: 507-531.

Carroll, L.D., Gamble, J.A., Houghton, B.F., Thordarson, T., & Higham, T.F.G., 1997. A radiocarbon age determination for Mt Edgecumbe (Putauaki) volcano, Bay of Plenty, New Zealand. *New Zealand Journal of Geology and Geophysics*, 40: 559-562.

Carter, L., Nelson, C.S., Neil, H.L., & Froggatt P.C., 1995. Correlation, dispersal, and preservation of the Kawakawa Tephra and other late Quaternary tephra layers in the Southwest Pacific Ocean. *New Zealand Journal of Geology and Geophysics*, 38: 29-46.

Carter, J.A., 2002. Phytolith analysis and paleoenvironmental reconstruction from Lake Poukawa Core, Hawkes Bay, New Zealand. *Global and Planetary Change*, 33: 257-267.

Carter, R.M., 2005. A New Zealand climatic template back to c. 3.9 Ma: ODP Site 1119, Canterbury Bight, south-west Pacific Ocean, and it relationship to onland successions. *Journal of the Royal Society of New Zealand,* 35: 9-42.

Carman, R., Edlund, G., & Damberg, C., 2000. Distribution of organic and inorganic phosphorus compounds in marine and lacustrine sediments: a ^{31}P NMR study. *Chemical Geology,* 163(1-4): 101-114.

Cassie, V., 1984. *Checklist of the Freshwater Diatoms of New Zealand.* Bibliotheca Diatomologica Band 4. Vaduz, Cramer, pp. 125.

Cassie, V., 1989. A contribution to the study of New Zealand diatoms. J. Cramer, Berlin, pp. 266.

Cassie-Cooper, V., 1996. *Microalgae: Microscopic Marvels.* Riverside Books. Hamilton, New Zealand, pp. 164.

Chapron, E., Fain, X., Magand, O., Charlet, L., Debret, M., & Melieres, M.A. 2007. Reconstructing recent environmental changes from proglacial lake sediments in the Western Alps (Lake Blanc Huez, 2543 m a.s.l., Grandes Rousses Massif, France). *Palaeogeography, Palaeoclimatology, Palaeoecology,* 252: 586-600.

Christensen, J.Q., & Bjorck, S., 2001. Digital sediment colour analyses, DSCA, of lake sediments – pitfalls and potentials. *Journal of Paleolimnology,* 25: 531-538.

Cohen, A. S., 2003. *Paleolimnology - The history and evolution of lake systems*. New York, Oxford University Press Inc.

Cole, J.W., 1978. Andesites of the Tongariro Volcanic Centre, North Island, New Zealand. *Journal of Volcanology and Geothermal Research,* 3: 121-153.

Cole, J.W., 1981. Genesis of lavas of the Taupo Volcanic Zone, North Island, New Zealand. *Journal of Volcanology and Geothermal Research,* 10: 317-337.

Cole, J.W., Graham, I.J., Hackett, W.R., & Houghton, B.F., 1986. Volcanology and petrology of Quaternary composite volcanoes of Tongariro Volcanic Centre, Taupo Volcanic Zone. *Journal of The Royal Society of New Zealand,* 23: 224-250.

Cole, J.W., Milner, D.M., & Spinks, K.D. 2005. Calderas and caldera structures: a review. *Earth-Science Reviews,* 69: 1-26.

Cotton, C.A. 1922. *Geomorphology of New Zealand*. Government printer, Wellington.

D'Arrigo, R.D., Cook, E.R., Salinger, M.J., Palmer, J., Krusic, P.J., Buckley, B.M., & Villalba, R., 1998. Tree-ring records from New Zealand: long-term context for recent warming trend. *Climate Dynamics,* 14: 191-199

Davis, W.J., 1985. Geochemistry and petrology of the Rotoiti and Earthquake Flat pyroclastic deposits. Unpublished MSc Thesis, University of Auckland, Auckland, 142 pp.

Davison, W., 1993. Iron and manganese in lakes. *Earth-Science Reviews,* 34: 119-163.

Davy, B.W., & Caldwell, T.G., 1997. Gravity, magnetic and seismic surveys of the caldera complex, Lake Taupo, North Island, New Zealand. *Journal of Volcanology and Geothermal Research,* 81: 69-89.

Dean, W.E., 1999. The carbon cycle and biogeochemical dynamics in lake sediments. *Journal of Paleolimnology,* 21: 375-393.

Deaton, B.C., & Balsam, W.L., 1991. Visible spectroscopy – a rapid method for determining hematite and goethite concentration in geological materials. *Journal of Sedimentary Petrology,* 61: 628-632.

Debret, M., Desmet, M., Balsam, W., Copard, Y., Francus, P., & Laj, C. 2006. Spectrophotometer analysis of Holocene sediments from an anoxic fjord: Saanich Inlet, British Columbia, Canada. *Marine Geology,* 229: 15-28.

Donoghue, S.L., Neall, V.E. & Palmer, A.S., 1995. Stratigraphy and chronology of late Quaternary andesitic tephra deposits, Tongariro Volcanic Centre, New Zealand. *Journal of the Royal Society of New Zealand,* 25: 115-206.

Donoghue, S.L., & Neall, V.E., 1996. Tephrostratigraphic Studies at Tongariro Volcanic Centre, New Zealand: An Overview. *Quaternary International,* 34-36: 13-20.

Donoghue, S.L., Neall, V.E., Palmer, A.S. & Stewart, R.B., 1997. The volcanic history of Ruapehu during the past 2 millennia based on the record of Tufa Trig tephras. *Bulletin of Volcanology,* 59: 136-146.

Donoghue, S.L., Vallance, J., Smith, I.E.M., & Stewart, R.B., 2007. Using geochemistry as a tool for correlating proximal andesitic tephras: case studies from Mt Rainier (USA) and Mt Ruapehu (New Zealand). *Journal of Quaternary Science,* 22: 395-410.

Dravitzki, D.N.R., 1999. The volcanic history and lake sediment characteristics of Paradise Valley, Rotorua. MSc. Thesis Earth Science Department, University of Waikato, Hamilton.

Eden, D.N., Froggatt, P.C., Trustrum, N.A., & Page, M.J., 1993. A multiple-source Holocene tephra sequence from Lake Tutira, Hawke's Bay, New Zealand. *New Zealand Journal of Geology and Geophysics*, 36: 233-242.

Eden, D.N. & Froggatt, P.C., 1996. A 6500-year-old history of tephra deposition recorded in the sediments of Lake Tutira, eastern North Island, New Zealand. *Quaternary International*, 34-36: 55-64.

Eden, D.N. & Page, M.J., 1998. Palaeoclimatic implications of a storm erosion record from late Holocene lake sediments, North Island, New Zealand. *Palaeogeography, Palaeoclimatology, Palaeoecology*, 139: 37-58.

Esler, W.R. 2006. An introduction to the Rotorua Basin. In: Lowe, D.J. (ed.) *Guidebook for 'Land and Lakes' Fieldtrip, New Zealand Society of Soil Science Biannial Conference*. Rotorua, New Zealand Society of Soil Science, Lincoln.

Ewart, A., 1963: Petrology and petrogenesis of the Quaternary pumice ash in the Taupo area. New Zealand. *Journal of petrology,* 4: 392-431.

Ewart, A., 1968: The petrology of the central North Island rhyolitic lavas. Part 2 – Regional petrology including notes on associated ash-flow pumice deposits. *New Zealand Journal of Geology and Geophysics,* 11: 478-545.

Ewart, A., 1971: Notes on the chemistry of ferromagnesian phenocrysts from selected volcanic rocks, Central Volcanic Region. *New Zealand Journal of Geology and Geophysics,* 14: 322-340.

Fish, G.R., 1975. A Nutrient Budget for Lake Rotorua. In: Jolly, V.H. and Brown, J.M.A. (eds), *New Zealand Lakes.* Auckland/Oxford University Press.

Fish, G.R., 1976. Nitrogen and phosphorus analysis of rainfall at Rotorua, New Zealand. *New Zealand Journal of Hydrology*, 15: 17-26.

Fish, G.R., 1979. Recent stratigraphy of sediments in Lake Rotorua. *New Zealand Journal of Marine and Freshwater Research*, 13(4): 529-532.

Fish, G.R., & Chapman, M.A., 1969. Synoptic surveys of lakes Rotorua and Rotoiti. *New Zealand Journal of Marine & Freshwater Research,* 3: 571-584.

Fish, G.R., & Andrew, I.A., 1980. Nitrogen and phosphorus in the sediments of Lake Rotorua. *New Zealand Journal of Marine and Freshwater Research,* 14(2): 121-128.

Fleming, C. A. 1959. *Geology of New Zealand*. Wellington, R. E. Owen Government Printer.

Foged, N., 1979. *Diatoms in New Zealand, the North Island*. Vaduz Cramer, Germany, pp. 224.

Fowler, A., Palmer, J., Salinger, J., & Ogden J., 2000. Dendroclimatic interpretation of tree-rings in *Agathis australis* (kauri): 2. Evidence of a significant relationship with ENSO. *Journal of The Royal Society of New Zealand,* 30(3): 277-292.

Fowler, A., & Boswijk, G., 2007. Five centuries of ENSO history recorded in *Agathis australis* (kauri) tree rings. *PAGES News,* 15(2): 20-21.

Froggatt, P.C., 1983. Toward a comprehensive Upper Quaternary tephra and ignimbrite stratigraphy of New Zealand using electron microprobe analysis of glass shards. *Quaternary Research,* 19: 188-200.

Froggatt, P.C., & Lowe, D.J., 1990. A review of late Quaternary silicic and some other tephra formations from New Zealand: their stratigraphy, nomenclature, distribution, volume and age. *New Zealand Journal of Geology and Geophysics,* 33: 89-109.

Gay, A., Lopez, M., Cochonat, P., Se´ranne, M., Levache´, D., & Sermondadaz. G. 2006a. Isolated seafloor pockmarks linked to BSRs, fluid chimneys, polygonal faults and stacked Oligocene–Miocene turbiditic palaeochannels in the Lower Congo Basin. *Marine Geology,* 226: 25-40.

Gay, A., Lopez, M., Ondreas, H., Charlou, J.-L., Sermondadaz, G., & Cochonat, P. 2006b. Seafloor facies related to upward methane flux within a Giant Pockmark of the Lower Congo Basin. *Marine Geology,* 226: 81-95.

Gehrels, M.J., Newnham, R.M., Lowe, D.J., Wynne, S., Hazell, Z.J., & Caseldine, C., 2008. Towards rapid assay of cryptotephra in peat cores: Review and evaluation of selected methods. *Quaternary International,* 178: 68-84.

Glover, R.B. & Mroczek, E.K., 1998. Changes in silica chemistry and hydrology across the Rotorua geothermal field, New Zealand. *Geothermics*, 27: 183-196.

Gomez, B., Carter, L., Trustrum, N.A., Palmer, A.S., & Roberts, A.P. 2004. El Niño–Southern Oscillation signal associated with middle Holocene climate change in intercorrelated terrestrial and marine sediment cores, North Island, New Zealand. *Geology,* 32: 653-656.

Gomez, B., Carter, L., & Trustrum, N.A., 2007. A 2400 yr record of natural events and anthropogenic impacts in intercorrelated terrestrial and marine sediment cores: Waipaoa sedimentary system, New Zealand. *Geological Society of America Bulletin,* 119: 1415-1432.

Goodwin, R.G., 1984. *Neoglacial lacustrine sedimentation and ice advance, Glacier Bay, Alaska.* Institute of Polar Studies Report No. 79. Columbus, Ohio, Institute of Polar Studies and Department of Geology and Mineralogy, Ohio State University.

Goosse, H., Masson-Delmotte, V., Renssen, H., Delmotte, M., Fichefet, T., Morgan, V., van Ommen, T., Khim, B.K., & Stenni, B., 2004. A late medieval warm period in the Southern Ocean as a delayed response to external forcing?. *Geophysical Research Letters,* 31.

Grange, L.I., 1929. A classification of soils of Rotorua County. *New Zealand Journal of Science and Technology,* 11:219-228.

Grange, L.I., 1931. Volcanic ash showers. *N.Z. Journal of Science and Technology,* 12: 228-240.

Grange, L.I., & Taylor, N.H., 1932. The distribution and field characteristics of bush-sick soils. Part 2A. In Bush Sickness, pp. 21 -35. N.Z. *Department of Scientific and Industrial Research,* Bulletin No. 32.

Grange, L.I., Taylor, N.H., Sutherland, C.F., Dixon, J.K., Hodgson, L., Seelye, F.T., Kidson, E., Cranwell, L.M., & Smallfield, P.W., 1939. Soils and agriculture of part of Waipa County. *New Zealand Department of Scientific and Industrial Research*, Bulletin 76.

Grange, L.I. 1937. The geology of the Rotorua-Taupo subdivision: Rotorua and Kaimanawa divisions. *New Zealand Geological Survey Bulletin*, No. 37, 132p.

Green, J.D., 1979. Palaeolomnological studies on Lake Maratoto, North Island, New Zealand. *Paleolimnology of Lake Biwa and the Japanese Pleistocene*, 7: 416-438.

Green, J.D., & Lowe, D.J., 1985. Stratigraphy and development of c. 17 000 year old Lake Maratoto, North Island, New Zealand, with some inferences about postglacial climatic change. *New Zealand Journal of Geology and Geophysics*, 28: 675-699.

Green, J.D., & Lowe, D.J., 1992a. Palaeolimnology in New Zealand. *Quaternary Australasia,* 10: 25-34.

Green, J.D., & Lowe, D.J., 1992b. Lakes. In: J.M. Soons, M.J. Selby (eds). *Landforms of New Zealand* 2nd Ed. Longman Paul, Auckland

Green, J.D., & Lowe, D.J. 1992c. The Lore of Lakes. *New Zealand Science Monthly,* 3: 8-9.

Green, J.D., & Lowe, D.J., 1994. Origins and development. In: Clayton, J.S.; de Winton, M.D. (eds) *"Lake Rotoroa: Change in an Urban Lake".* National Institute of Water & Atmospheric Research Ecosystems Publication, 9: 13-23.

Green M.R., 1994. The Holocene palaeolimnology and developmental history of Lake Taharoa (Kawhia), North Island, New Zealand. MSc Thesis. University of Waikato, Hamilton.

Hajdas, I., Lowe D.J., Newnham, R.M., & Bonani, G., 2006. Timing of the late-glacial climate reversal in the Southern Hemisphere using high-resolution radiocarbon chronology for Kaipo bog, New Zealand. *Quaternary Research*, 65: 340-345.

Harper, M.A., Howorth, R., & Mcleod, M., 1986. Late Holocene diatoms in Lake Poukawa: effects of airfall and changes in depth. *New Zealand Journal of Marine and Freshwater Research,* 20: 107-118.

Harper, M.A., & Collen, J.D., 2002. Glaciations, interglaciations and reworked microfossils in Poukawa Basin, New Zealand. *Global and Planetary Change,* 33(3-4):243-256.

Hatherton, T., Davey, F.J. & Hunt, T.M., 1979. Geophysical anomalies and igneous bodies off the west coast, North Island. *Journal of The Royal Society of New Zealand,* 9: 13-28.

Healy, J., 1962. Structure and Volcanism in the Taupo Volcanic Zone, New Zealand. *American Geophysical Union Geophysical Monographs*, 6: 151-157.

Healy, J., 1964. Volcanic mechanisms in Taupo Volcanic Zone, New Zealand. *New Zealand Journal of Geology and Geophysics*, 7: 6-23.

Hellstrom, J., McCulloch, M., & Stone, J., 1998. A detailed 31,000-year record of climate and vegetation change, from the isotope geochemistry of two New Zealand speleothems. *Quaternary Research,* 50: 167-178.

Henderson, J., 1924. The structure of the Taupo-Rotorua Region. *New Zealand Journal of Science and Technology,* 6: 270-278.

Higham, T.F.G. & Hogg, A.G., 1997. Evidence for late Polynesian colonisation of New Zealand: University of Waikato radiocarbon measurements. *Radiocarbon,* 39: 149-192.

Higham, T.F.G., Anderson, A.J., & Jacomb, C., 1999. Dating the first New Zealanders: the chronology of Wairau Bar. *Antiquity,* 73: 420-427.

Hoare, R.A., 1978. *Particulate matter in tributaries of Lake Rotorua.* Proceedings of the 25th Anniversary Conference on 'Erosion assessment and control in New Zealand'. New Zealand Association of Soil Conservators. pp 244-51.

Hoare R.A., 1984. Nitrogen and phosphorus in Rotorua urban streams. *New Zealand Journal of Marine and Freshwater Research*, 18: 451-454.

Hobden, B.J., Houghton, B.F., Lanphere, M.A., & Nairn, I.A., 1996. Growth of the Tongariro volcanic complex: new evidence from K-Ar age determinations. *New Zealand Journal of Geology and Geophysics*, 39: 151-154.

Hobden, B.J., Houghton, B.F., Davidson, J.P., & Weaver, S.D., 1999. Small and short-lived magma batches at composite volcanoes: time windows at Tongariro volcano, New Zealand. *Journal of the Geological Society*, 156: 865-868.

Hochstetter, F. V. 1864a. *Lectures by Dr. F. Hochstetter,* Auckland, T. Delattre.

Hochstetter, F. V. 1864b. *Voyage of the Austrian Frigate Novara: Geological Part,* Vienna, Imperial and Royal Court and Government Printing Offices.

Hochstetter, F. von. 1864c. *Geology of New Zealand: Contributions to the Geology of the provinces of Auckland and Nelson.* Translated from german and edited by C.A. Fleming. 1959. R.E. Owen, Government printer, Wellington. 319p.

Hodgson, K. A., & Nairn, I. A., 2005. The c. AD 1315 syn-eruption and AD 1904 post-eruption breakout floods from Lake Tarawera, Haroharo caldera, North Island, New Zealand. *New Zealand Journal of Geology & Geophysics*, 48: 491-506.

Hogg, A.G., Higham, T.F.G., Lowe, D.J., Palmer, J., Reimer, P., & Newnham, R.M., 2003. A wiggle-match date for Polynesian settlement of New Zealand. *Antiquity*, 77: 116-125.

Horrocks, M.J., Ogden, J., Nichol, S.L., Alloway, B.V., & Sutton, D.G., 1999. A late Quaternary palynological and sedimentological record from two coastal swamps at southern Kaitoke, Great Barrier Island, New Zealand. *Journal of the Royal Society of New Zealand*, 30: 49-68.

Horrocks, M., Deng, Y., Nichol, S.L., Shane, P.A., & Ogden, J., 2002. A palaeoenvironmental record of natural and human change from the Auckland Isthmus, New Zealand, during the late Holocene. *Journal of the Royal Society of New Zealand*, 32: 337-353.

Horrocks, M., Augustinus, P., Deng, Y., Shane, P., & Andersson, S., 2005. Holocene vegetation, environment, and tephra recorded from Lake Pupuke, Auckland, New Zealand. *New Zealand Journal of Geology and Geophysics*, 48: 85-94.

Horrocks, M., Campbell M., & Gumbley, W., 2007. A short note on starch and xylem of *Ipomoea batatas* (sweet potato) in archaeological deposits from northern New Zealand *Journal of Archaeological Science*, 34: 1441-1448.

Horwell, C.J., Patterson, J.E., Gamble, J.A., & Allen, A.G., 2005. Monitoring and mapping of hydrogen sulphide emissions across an active geothermal field: Rotorua, New Zealand. *Journal of Volcanology and Geothermal Research*, 139(3-4): 259-269.

Houghton, B. & Scott, B., 1982. *Geyserland: a guide to the volcanoes and geothermal areas of Rotorua.* Geological Society of New Zealand, Levin, Graphic Press and Packaging Ltd.

Houghton, B. & Scott, B., 2002. *Geyserland: a guide to the volcanoes and geothermal areas of Rotorua.* Levin, Graphic Press and Packaging Ltd.

Houghton, B.F., Wilson, C.J.N., McWilliams, M.O., Lanphere, M.A., Weaver, S.D., Briggs, R.M., & Pringle, M.S., 1995. Chronology and dynamics of a large silicic magmatic system: Central Taupo Volcanic Zone, New Zealand. *Geology*, 23: 13-16.

IPCC, 2007. *Climate Change 2007: Synthesis Report. Contribution of Working Groups I, II and III to the Fourth Assessment Report of the Intergovernmental Panel on Climate Change*. [Core Writing Team, Pachauri, R.K and Reisinger, A. (eds.)]. IPCC, Geneva, Switzerland, pp.104.

Jurado-Chichay, Z. & Walker, G.P.L., 2000. Stratigraphy and dispersal of the Mangoane Subgroup deposits, Okataina Volcanic Centre, New Zealand. *Journal of Volcanology and Geothermal Research*, 104(1-4): 319-380.

Jurado-Chichay, Z. & Walker, G.P.L., 2001a. The intensity and magnitude of the Mangoane Subgroup plinian eruptions from Okataina Volcanic Centre, New Zealand. *Journal of Volcanology and Geothermal Research*, 111: 219-237.

Jurado-Chichay, Z. & Walker, G.P.L., 2001b. Variability of plinian fall deposits: examples from Okataina Volcanic Centre, New Zealand. *Journal of Volcanology and Geothermal Research*, 111: 239-263.

Katesv, S., Tsandev, I., L'Heureux, I., & Rancourt, D.G., 2006. Factors controlling long-term phosphorus efflux from lake sediments: Exploratory reactive-transport modelling. *Chemical Geology*, 234: 127-147.

Keam, R.J., 1988. *Tarawera: The volcanic eruption of 1886.* R.F. Keam. Auckland. pp 472.

Kennedy, N.M., Pullar, W.A. & Pain, C.A., 1978. Late Quaternary land surfaces and geomorphic changes in the Rotorua basin, North Island, New Zealand. *New Zealand Journal of Science*, 21: 249-264.

Kennedy, N.M. & Pullar, W.A., 1981. Landscape features and deposits in the Lake Rotorua Basin. In: Chapman, V. J. (ed.) *Handbook of the Rotorua Lakes District.* Rotorua, The Guardians of the Rotorua Lakes.

King, L.H. & MacLean, B., 1970. Pockmarks on the Scotian Shelf. *Geological Society of America Bulletin*, 81: 3141-3148.

Kissling, W.M., and Weir, G.J., 2005. The spatial distribution of the geothermal fields in the Taupo Volcanic Zone, New Zealand. *Journal of Volcanology and Geothermal Research,* 145: 136-150.

Knox, G.J., 1982. Taranaki Basin, structural style and tectonic setting. *New Zealand Journal of Geology and Geophysics,* 25: 125-140.

Kohn, B. P. 1973: Studies of New Zealand Quaternary pyroclastic rocks. Unpublished Ph.D. Thesis, Victoria University of Wellington, Wellington.

LECO Corporation. 2006. *TruSpec CN Carbon/Nitrogen Determinator*, Instruction Manual. LECO Corporation. United States.

Leonard, G.S., Cole, J.W., Nairn, I.A., & Self, S., 2002. Basalt triggering of the c. AD 1305 Kaharoa rhyolite eruption, Tarawera Volcanic Complex, New Zealand. *Journal of Volcanology and Geothermal Research,* 115: 461-486.

Lipman, P.W., 2000. Calderas. In: Sigurdsson, H. (ed.), *Encyclopaedia of Volcanoes.* Academic Press, San Francisco, pp. 643-662.

Locke, C.A., & Cassidy, J., 1997. Egmont Volcano, New Zealand: three-dimensional structure and its implications for evolution. *Journal of Volcanology and Geothermal Research,* 76: 149-161.

Lorrey, A., Fowler, A.M., & Salinger, J., 2007. Regional climate regime classification as a qualitative tool for interpreting multi-proxy palaeoclimate data spatial patterns: A New Zealand case study. *Palaeogeography, Palaeoclimatology, Palaeoecology,* 253: 407-433.

Lorrey, A., Williams, P., Salinger, J., Martin, T., Palmer, J., Fowler, A., Zhao, J., & Neil, H., 2008. Speleothem stable isotope records interpreted within a multi-proxy framework and implications for New Zealand palaeoclimate reconstruction. *Quaternary International,* 187: 52-75.

Lowe, D.J., 1988. Stratigraphy, age, composition, and correlation of late Quaternary tephras interbedded with organic sediments in Waikato lakes, North Island, New Zealand. *New Zealand Journal of Geology and Geophysics,* 31: 125-165.

Lowe, D.J., 1990. Tephra Studies in New Zealand: an historical review. *Journal of the Royal Society of New Zealand,* 20: 119-150.

Lowe, D.J., Hogg, A.G., & Hendy, C.H., 1981. Detection of thin tephra deposits in peat and organic lake sediments by rapid X-radiography and X-ray fluorescence techniques. In: *Proceedings of the Tephra Workshop, June 30–July 1 1980*, Victoria University of Wellington, Vol. 20. Geology Department, Victoria University of Wellington Publication, pp. 74–77.

Lowe, D.J. & Green, J.D., 1985. Stratigraphy and development of c 17000 year old lake Maratoto, North Island, New Zealand, with some inferences about postglacial climatic change. *New Zealand Journal of Geology and Geophysics,* 28: 695-699.

Lowe, D.J. & Green, J.D., 1992. Lakes. In: Soons, J.M.; Selby, M.J. (eds) *Landforms of New Zealand* 2nd Ed. Auckland, Longman Paul, pp. 107-143.

Lowe, D.J., Green, J.D., Northcote, T.G., & Hall, K.J., 1997. Holocene Fluctuations of a Meromictic Lake in Southern British Columbia. *Quaternary Research,* 48(1): 100-113.

Lowe, D.J., McFadgen, B.G., Higham, T.F.G., Hogg, A.G., Froggatt, P.C. & Nairn, I.A., 1998. Radiocarbon age of the Kaharoa Tephra, a key marker for late-Holocene stratigraphy and archaeology in New Zealand. *The Holocene,* 8: 499-507.

Lowe, D.J., & Newnham, R.M., 1999. Advances in Quaternary tephrostratigraphy and tephrochronology in New Zealand. *Quaternary Australasia,* 17: 12-19.

Lowe, D.J., Newnham, R.M., McFadgen, B.G., & Higham, T.F.G., 2000a. Tephras and New Zealand archaeology. *Journal of Archaeological Science,* 27: 859-870.

Lowe, D.J., & de Lange, W.P. 2000b. Volcano-meteorological tsunamis, the *c.* AD 200 Taupo eruption (New Zealand) and the possibility of a global tsunami. *The Holocene,* 10: 401-407.

Lowe, D.J., & Hunt, J.B., 2001. A summary of terminology used in tephra-related studies. *Les Dossiers de l'Archeo-Logis* 1: 17-22.

Lowe, D.J., Newnham, R.M., & McCraw, J.D., 2002. Volcanism and early Maori society in New Zealand. In: Torrence, R., & Grattan, J. (eds) *Natural Disasters and Cultural Change*. Routledge, London, pp. 126-161.

Lowe, D.J., & Newnham, R.M., 2004. Role of Tephra in Dating Polynesian Settlement and Impact, New Zealand. In: Hall, V.A., Alloway, B.V., Kull, C., Christen, L., (eds) *"Tephra".* PAGES (Past Global Changes) News 12 (No. 3): 5-7.

Lowe, D.J., & Palmer, D.J., 2005. Andisols of New Zealand and Australia. *Journal of Integrated Field Science,* 2: 39-65.

Lowe, D.J., Shane, P.A.R., Alloway, B.V., & Newnham, R.M., 2008. Fingerprints and age models for widespread New Zealand tephra marker beds erupted since 30,000 years ago: a framework for NZ-INTIMATE. *Quaternary Science Reviews,* 27: 95-126.

Lyle, M., & Lyle, A.O., 2002. Determination of biogenic opal in pelagic marine sediments: a simple method revisited. In: Wilson, P.A., & Janecek, T.R., (eds) *Proceedings of the Ocean Drilling Program, Initial Reports,* 199.

Mackereth, F.J.H., 1965. Chemical investigation of lake sediments and their interpretation. *Proceedings of the Royal Society,* 161: 295-309.

Mackereth, F.J.H., 1966. Some Chemical Observations on Post-Glacial Lake Sediments. *Philosophical Transactions of the Royal Society of London,* 250: 165-213.

Manighetti, B., Palmer, A., Eden, D., & Elliot, M., 2003. An occurrence of Tuhua Tephra in deep-sea sediments offshore eastern North Island, New Zealand. *New Zealand Journal of Geology & Geophysics,* 46: 581–590.

Marshall, P., 1905. *The geography of New Zealand,* Wellington, Whitcombe and Tombs Ltd.

Marshall, P., 1912a. *Geology of New Zealand,* Wellington, John Mackay Government Printer.

Marshall, P., 1912b. *New Zealand and adjacent islands,* Heidelberg, Carl Winter's Universitatsbuchhandlung.

Marwick, J., Fyfe, H.E., & Grange, L.I., 1937. Chapter 2: Physiography and Structure. In: Grange, L.I., (ed), The geology of the Rotorua-Taupo Subdivision. *New Zealand Geological Survey Bulletin,* 37: 15-22.

Marx, R.S., 2004. The Evolution of Lake Rotorua. M.Sc. Thesis. University of Otago, Dunedin, New Zealand.

Matthews, R.J., 1979. Chemical analysis of Lake Rotorua sediments. M.Sc. Thesis. University of Waikato, Hamilton, New Zealand.

Mayewski P.A., Rohling, E.E., Stager, J.C., Karlen, W., Maasch, K.A., Meeker, L.D., Meyerson, E.A., Gasse, F., van Kreveld, S. Holmgren, K., Lee-Thorp, J., Rosqvist, G., Rack, F., Staubwasser, M., Schneider, R.R., & Steig, E.J., 2004. Holocene climate variability. *Quaternary Research,* 62: 243-255.

McCormac, F.G., Hogg, A.G., Blackwell, P.G., Buck, C.E., Higham, T.F.G., & Reimer, P.J., 2004. SHCal04 Southern Hemisphere calibration, 0-11.0 cal KYR B.P. *Radiocarbon,* 46: 1087-1092.

McGlone M.S. 1983a. Holocene pollen diagrams, Lake Rotorua, North Island, New Zealand. *Journal of the Royal Society of NZ,* 13: 53-65.

McGlone M.S. 1983b. Polynesian deforestation of New Zealand: a preliminary synthesis. *Archaeology in Oceania,* 18: 1-10.

McGlone, M.S., 1988. History of the New Zealand vegetation. In: Huntley, B., & Webb III, T. (eds.), *Vegetation History*. Kluwer Academic Publishing, Dordrecht, pp. 557– 599.

McGlone, M.S., 1989. The Polynesian settlement of New Zealand in relation to environmental and biotic changes. *New Zealand Journal of Ecology (Supplement),* 12: 115-129.

McGlone, M.S., 2002. A Holocene and latest Pleistocene pollen record from Lake Poukawa, Hawke's Bay, New Zealand. *Global and Planetary Change,* 33: 283-299.

McGlone, M.S., Salinger, M.J., & Moar, N.T., 1993. Paleovegetation studies of New Zealand's climate since the Last Glacial Maximum. In: Wright, H.E., et al., (eds.). *Global Climates since the Last Glacial Maximum*. Minneapolis, University of Minnesota Press, pp. 294–317.

McGlone, M.S., Anderson, A.J. & Holdaway, R.N., 1994. An ecological approach to the Polynesian settlement of New Zealand. In: D.G., Sutton, (ed.), *Origins of the First New Zealanders*. Auckland: Auckland University Press, pp.136-163.

McGlone, M.S, Mark, A.F., & Bell, D., 1995. Late Pleistocene and Holocene vegetation history, Central Otago, South Island, New Zealand. *Journal of The Royal Society of New Zealand,* 25(1): 1-22.

McGlone, M.S., & Wilmshurst, J.M., 1999. Dating initial Maori environmental impact in New Zealand. *Quaternary International,* 59: 5-16.

McGlone, M.S., Wilmshurst, J.M., & Leach, H.M., 2005. An ecological and historical review of bracken (*Pteridium esculentum*) in New Zealand, and its cultural significance. *New Zealand Journal of Ecology*, 29(2): 165-184.

Meyers P.A., 1994. Preservation of source identification of sedimentary organic matter during and after deposition. *Chemical Geology*, 144: 289-302.

Meyers P.A., 1997. Organic geochemical proxies of paleoceanographic, paleolimnologic, and paleoclimatic processes. *Organic geochemistry*, 27: 213-250.

Meyers, P.A., & Lallier-Verges, E., 1999. Lacustrine sedimentary organic matter records of Late Quaternary paleoclimates. *Journal of Paleolimnology,* 21: 345-372.

Milner, D.M., Cole, J.W., & Wood, C.P., 2002. Asymmetric, multiple block collapse at Rotorua Caldera, Taupo Volcanic Zone, New Zealand. *Bulletin of Volcanology,* 64: 134-149.

Milner, D.M., Cole, J.W., & Wood, C.P., 2003. Mamaku Ignimbrite: a caldera-forming ignimbrite erupted from a compositionally zoned magma chamber in Taupo Volcanic Zone, New Zealand. *Journal of Volcanology and Geothermal Research,* 122: 243-264.

Modriniak, N., & Studt, F.E., 1959. Geological structure and volcanism of the Taupo-Tarawera District. *New Zealand Journal of Geology and Geophysics*, 2: 654-684.

Mortlock, R.A., & Froelich, P.N., 1989. A simple method for the rapid determination of biogenic opal in pelagic marine sediments. *Deep Sea Research,* 36: 1415–1426.

Munro, A.J., 1994. Holocene evolution and palaeolimnology of a barrier spit, north western Matakana Island, Bay of Plenty, New Zealand. MSc Thesis, University of Waikato, Hamilton

Munsell Soil Colour Charts, 1967 2nd Edition.

Nairn, I.A., 1989. Sheet V16AC Tarawera – Geological Map of New Zealand 1:50 000. New Zealand Department of Scientific and Industrial Research,Wellington.

Nairn, I.A., 1992. The Te Rere and Okareka eruptive episodes – Okataina Volcanic Centre, Taupo Volcanic Zone, New Zealand. *New Zealand Journal of Geology and Geophysics,* 35: 93-108.

Nairn, I.A., 2002. Geology of the Okataina Volcanic Centre, scale 1:50 000. Institute of Geological and Nuclear Sciences geological map 25. 1 sheet + 156 p. Institute of Geological and Nuclear Sciences Ltd, Lower Hutt, New Zealand.

Nairn, I.A., & Cole, J.W., 1981. Basalt dikes in the 1886 Tarawera Rift. *New Zealand Journal of Geology and Geophysics,* 24: 585-592.

Nairn, I.A., Kobayashi T., & Nakagawa, M., 1998. The ~ 10 ka multiple vent pyroclastic eruption sequence at Tongariro Volcanic Centre, Taupo Volcanic Zone, New Zealand: Part 1. Eruptive processes during regional extension. *Journal of Volcanology and Geothermal Research,* 86: 19-44.

Nairn, I.A., Self, S., Cole, J.W., Leonard, G.S. & Scutter, C., 2001. Distribution, stratigraphy, and history of proximal deposits from the c. AD 1305 Kaharoa eruptive episode at Tarawera Volcano, New Zealand. *New Zealand Journal of Geology and Geophysics,* 44: 467-484.

Nairn, I.A., Shane, P.R., Cole, J.W., Leonard, G.J., Self, S., & Pearson. N., 2004. Rhyolite magma processes of the ~AD 1315 Kaharoa eruption episode, Tarawera volcano, New Zealand. *Journal of Volcanology and Geothermal Research,* 131: 265-294.

Neall, V.E., & Alloway, B.V., 1991: Volcanic hazards at Egmont Volcano. *Ministry of Civil Defence volcanic hazards information series 1.*

Nelson, C.S., 1983. Bottom sediments of Lake Rotoma. New *Zealand Journal of Marine and Freshwater Research,* 11: 185-204.

Newnham, R.M., Lowe, D.J., & Green, J.D., 1989. Palynology, vegetation, and climate of the Waikato lowlands, North Island, New Zealand, since c. 18 000 years ago. *Journal of the Royal Society of New Zealand,* 19: 127-150.

Newnham, R.M. & Lowe, D.J., 1991. Holocene vegetation and volcanic activity, Auckland Isthmus, New Zealand. *Journal of Quaternary Science,* 6: 177-193.

Newnham, R.M. de Lange, P.J., & Lowe, D.J., 1995a. Holocene vegetation, climate, and history of a raised bog complex, northern New Zealand, based on

palynology, plant macrofossils and tephrochronology. *The Holocene*, 5: 267-282.

Newnham, R.M., Lowe, D.J., & Wigley, G.N.A., 1995b. Late Holocene palynology and palaeovegetation of tephra-bearing mires at Papamoa and Waihi Beach, western Bay of Plenty, North Island, New Zealand. *Journal of the Royal Society of New Zealand*, 25: 283-300.

Newnham, R.M., Lowe, D.J. & Matthews, B.W., 1998a. A late Holocene and prehistoric record of environmental change from Lake Waikaremoana, New Zealand. *The Holocene*, 8: 443-454.

Newnham, R.M., Lowe, D.J., McGlone, M.S., Wilmshurst, J.M. & Higham, T.F.G., 1998b. The Kaharoa Tephra as a critical datum for earliest human impact in northern New Zealand. *Journal of Archaeological Science* 25: 533-544.

Newnham, R.M., Lowe, D.J., & Williams, P.W., 1999. Quaternary environmental change in New Zealand: a review. *Progress in Physical Geography*, 23: 567-610.

Newnham, R.M., & Lowe, D.J., 2000. Fine-resolution pollen record of late-glacial climate reversal from New Zealand. *Geology*, 28(8): 759-762.

Newnham, R.M., Eden, D.N., Lowe, D.J., Hendy, C.H., 2003. Rerewhakaaitu Tephra, a land–sea marker for the Last Termination in New Zealand, with implications for global climate change. *Quaternary Science Reviews*, 22: 289-308.

Newnham, R.M., Lowe, D.J., Giles, T., Alloway, B.V., 2007a. Vegetation and climate of Auckland, New Zealand, since ca 32,000 cal yr ago: support for an extended LGM. *Journal of Quaternary Science*, 22: 517–534.

Newnham, R.M., Vandergoes, M.J., Hendy, C.H., Lowe, D.J., Preusser, F., 2007b. A terrestrial palynological record for the last two glacial cycles from southwestern New Zealand. *Quaternary Science Reviews*, 26: 517-535.

Nichols, G., 1999. Chapter 10 - Lacustrine environments: fresh and saline lakes. In: Sedimentology and Stratigraphy. UK, Blackwell Science Ltd.

Ogden, J., Basher, L.R. & McGlone, M.S., 1998. Fire, forest regeneration and links with early human habitation: evidence from New Zealand. *Annals of Botany*, 81: 687-696.

Palmer, B.A., & Neall, V.E., 1991. Contrasting lithofacies architecture in ring-plain deposits related to edifice construction and destruction, the Quaternary

Stratford and Opunake Formations, Egmont Volcano, New Zealand. *Sedimentary Geology*, 74: 71-88.

Palmer, J.G. & Xiong, L., 2004. New Zealand climate over the last 500 years reconstructed from *Libocedrus bidwillii* Hook. f. tree-ring chronologies. *The Holocene*, 14, 282-289.

Park, J., 1910. *The Geology of New Zealand: an introduction to the historical, structural and economic geology,* Wellington, Whitcombe and Tombs Ltd.

Pearson, L., 2007. The nature, composition and distribution of sediment in Lake Rotorua, New Zealand. MSc Thesis. University of Waikato, Hamilton

Pickrill, R.A., Nelson, C.S., Stoffers, P., & Craig, G.G.P., 1991. Influence of Late Holocene pyroclastic eruptions on the sedimentary geochemistry of Lake Rotoiti, North Island, New Zealand. *Journal of Paleolimnology,* 6: 173-192.

Pickrill, R.A., 1993. Shallow seismic stratigraphy and pockmarks of a hydrothermally influenced lake, Lake Rotoiti, New Zealand. *Sedimentology,* 40(5): 813-828.

Pillans, B.J., Pullar, W.A., Selby, M.J., & Soons, J.M., 1992. The age and development of the New Zealand landscape. In: Soons, J.M., & Selby, M.J., (eds), *Landforms of New Zealand 2nd Ed.*, Longman Paul, Auckland. pp. 31-62.

Platt, N.H. & Wright, V.P., 1991. Lacustrine carbonates: facies models, facies distribution and hydrocrabon aspects. *Special Publication - International Association of Sedimentologists,* 13: 57-74.

Platz, T., Cronin, S.J., Smith, I.E.M., Turner, M.B., & Stewart, R.B., 2007. Improving the reliability of microprobe based analyses of andesitic glasses for tephra correlation. *The Holocene* 17(5): 573-583.

Pullar, W.A. & Kennedy, N.M., 1981. Tephra Deposits in the Rotorua Lakes District. In: Chapman, V.J. (ed), *Handbook of the Rotorua Lakes District.* The Guardians of the Rotorua Lakes.

Rawlence, D.J., 1984. A study of pigment and diatoms in a core from Lake Rotorua, North Island, New Zealand, with an emphasis on recent history. *Journal of the Royal Society of New Zealand,* 14(2): 119-132.

Reid, M., 2005. Diatom-based models for reconstructing past water quality and productivity in New Zealand lakes. *Journal of Paleolimnology,* 33: 13-38.

Reimer, P.J., Baillie, M.G.L., Bard, E., Bayliss, A., Beck, J.W., Bertrand, C.J.H., Blackwell, P.G., Buck, C.E., Burr, G.S., Cutler, K.B., Damon, P.E., Edwards,

R.L., Fairbanks, R.G., Friedrich, M., Guilderson, T.P., Hogg, A.G., Hughen, K.A., Kromer, B., McCormac, F.G., Manning, S., Bronk Ramsey, C., Reimer, R.W., Remmele, S., Southon, J.R., Stuiver, M., Talamo, S., Taylor, F.W., van der Plicht, J., Weyhenmeyer, C.E., 2004. IntCal04 terrestrial radiocarbon age calibration, 0–26 cal kyr BP. *Radiocarbon,* 46: 1029-1058.

Rodgers, J.N., Kelley, J.T., Belknap, D.F., Gontz, A. and Barnhardt, W.A., 2006. Shallow-water pockmark formation in temperate estuaries: A consideration of origins in the western gulf of Maine with special focus on Belfast Bay. *Marine Geology*, 225: 45-62.

Round, F. E., Crawford, R. M. & Mann, D. G., 1990. *The Diatoms: Biology and Morphology of the Genera.* Cambridge University Press, Cambridge, pp. 747.

Rowland, J.V., & Sibson, R.H., 2004. Structural controls on hydrothermal flow in a segmented rift system, Taupo Volcanic Zone, New Zealand. *Geofluids,* 4: 259-283.

Sandiford, A., Alloway, B., Shane, P., 2001. A 28,000-6,600 cal yr record of local and distal volcanism preserved in a paleo-lake, Auckland, NZ. *New Zealand Journal of Geology & Geophysics,* 44: 323-336.

Sandgren, P., & Snowball, I., 2001. Chapter 8: Last, W.M., & Smol, J.P., (eds), *Tracking Environmental Change Using Lake Sediments. Physical and Geochemical Methods.* Kluwer Academic Publishers, London, pp. 217-237.

Schaller, T., Christoph Moor, H., & Wehrli, B., 1997. Sedimentary profiles of Fe, Mn, V, Cr, As and Mo as indicators of benthic redox conditions in Baldeggersee. *Aquatic Sciences,* 59: 345-361.

Self, S., 1993. Large scale silicic phreatomagmatic volcanism: a case study from New Zealand. *Journal of Volcanology and Geothermal Research,* 17: 433-469.

Shulmeister, J., Shane, P., Lian, O.B., Okuda, M., Carter, J.A., Harper, M., Dickinson, W., Augustinus, P., & Heijnis, H., 2001. A long late Quaternary record from Lake Poukawa, Hawke's Bay, New Zealand. *Palaeogeography, Palaeoclimatology, Palaeoecology,* 176: 81-107.

Shane, P., 1998. Correlation of rhyolitic pyroclastic eruptive units from the Taupo volcanic zone by Fe–Ti oxide compositional data. *Bulletin of Volcanology*, 60: 224-238.

Shane, P., 2000. Tephrochronology: a New Zealand case study. *Earth-Science Reviews,* 49: 223-259.

Shane, P., Black, T., & Westgate, J., 1994. Isothermal plateau fission track age for the paleomagnetic excursion in the Mamaku Ignimbrite, New Zealand, and implications for late Quaternary stratigraphy. *Geophysical Research Letters*, 21: 1695-1698.

Shane, P., Lian, O.B., Okuda, M., Augustinus, P., Robert, C., & Heijnis, H. 2002. Tephrostratigraphy and geochronology of a ca. 120 ka terrestrial record at Lake Poukawa, North Island, New Zealand. *Global and Planetary Change*, 33: 221-242.

Shane, P., Smith, V., Lowe, D.J., & Nairn, I., 2003. Re-identification of c. 15,700 cal yr BP tephra bed at Kaipo Bog, eastern North Island: implications for the dispersal of Rotorua and Puketarata tephra beds. *New Zealand Journal of Geology and Geophysics*, 46: 591-596.

Shane, P., Nairn, I.A., & Smith, V.C., 2005. Magma mingling in the ~50 ka Rotoiti eruption from Okataina Volcanic Centre: implications for geochemical diversity and chronology of large volume rhyolites. *Journal of Volcanology and Geothermal Research*, 139: 295-313.

Shane, P., Sikes, E.L., & Guilderson, T.P., 2006. Tephra beds in deep-sea cores off northern New Zealand: implications for the history of Taupo Volcanic Zone, Mayor Island and White Island volcanoes. *Journal of Volcanology and Geothermal Research*, 154: 276-290.

Shane, P., Martin, S.B., Smith, V.C., Beggs, K.F., Darragh, M.B., Cole, J.W., Nairn, I.A., 2007. Multiple rhyolite magmas and basalt injection in the 17.7 ka Rerewhakaaitu eruption episode from Tarawera volcanic complex, New Zealand. *Journal of Volcanology and Geothermal Research*, 164: 1-26.

Shane, P., Nairn, I.A., Martin, S.B. & Smith, V.C. 2008. Compositional heterogeneity in tephra deposits resulting from the eruption of multiple magma bodies: Implications for tephrochronology. *Quaternary International*, 178(1): 44-53.

Sherburn, S., Bannister, S., & Bibby, H., 2003. Seismic velocity structure of the central Taupo Volcanic Zone, New Zealand, from local earthquake tomography. *Journal of Volcanology and Geothermal Research*, 122: 69-88.

Smith, D.G., 1986. *Heavy metals in the New Zealand Aquatic Environment: A Review*. Water and Soils Miscellaneous Publication No. 100, Wellington, New Zealand.

Smith, R.T., Houghton, B.F., 1995. Vent migration and changing eruptive style during the 1800 ka Taupo eruption: new evidence from the Hatepe and Rotongaio phreatoplinian ashes. *Bulletin of Volcanology,* 57: 432-439.

Smith, V.C., 2001. The stratigraphy and geochemistry of the Mangaone Subgroup tephra beds, Okataina Volcanic Centre, New Zealand. M.Sc. Thesis. University of Auckland, Auckland.

Smith, V.C., Shane, P. & Smith, I.A. 2002. Tephrastratigraphy and geochemical fingerprinting of the Mangaone Subgroups Tephra beds, Okataina Volcanic Centre, New Zealand. *New Zealand Journal of Geology and Geophysics,* 45: 207-219.

Smith, V.C., Shane, P., & Nairn, I.A., 2004. Reactivation of a rhyolite magma body by new rhyolite intrusion before the 15.8 ka Rotorua eruptive episode: implications for magma storage in the Okataina Volcanic Centre, New Zealand. *Journal of the Geological Society,* London, 161: 757-772.

Smith, V.C., Shane, P., & Nairn, I.A., 2005. Trends in rhyolite geochemistry, mineralogy, and magma storage during the last 50 kyr at Okataina and Taupo volcanic centres, Taupo Volcanic Zone, New Zealand. *Journal of Volcanology and Geothermal Research,* 148: 372-406.

Smith, V.C., Shane, P., Nairn, I.A., Williams, C.M., 2006. Geochemistry and magmatic properties of eruption episodes from Haroharo Linear Vent Zone, Okataina Volcanic Centre, New Zealand during the last 10 kyr. *Bulletin of Volcanology,* 69: 57-88.

Soengkono, S., 1995. A magnetic model for deep plutonic bodies beneath the central Taupo Volcanic Zone, North Island, New Zealand. *Journal of Volcanology and Geothermal Research,* 68: 193-207.

Soons, J.M., 1998. Recent coastal change in Canterbury – the case study of Lake Forsyth/Te Wairewa. *New Zealand Geography,* 54: 7-14.

Soons, J.M., Moar, N.T., Shulmeister, J., Wilson, H.D., & Carter, J., 2002. Vegetation and climate change on Banks Peninsula, South Island, New Zealand. *Global and Planetary Change,* 33: 301-314.

Soon, W., & Baliunas, S., 2003. Proxy climatic and environmental changes of the past 1000 years. *Climate Research,* 23: 89-110.

Sparks, R.J., Melhuish, W.H., McKee, J.W.A., Ogden, J., & Palmer, J.G., 1995. ^{14}C calibration in the Southern Hemisphere and the date of the last Taupo eruption: evidence from tree-ring sequences. *Radiocarbon,* 37: 155-163.

Sparks, R.J., Graham, I.J., & Morgenstern, U., 2008. Cosmic chronometers. In: Graham, I.J. (Chief ed.), "A Continent on the Move: New Zealand Geoscience Into the 21st Century". *Geological Society of New Zealand Miscellaneous Publication,* 25: 64-68.

Speirs D.A., 1995. The palaeolimnology of Lake Rotoroa (Hamilton Lake), North Island, New Zealand: sedimentology, fossil pigments, Cladocera, and Chironomidae. MSc Thesis. University of Waikato, Hamilton.

Spinks, K.D., Acocella, V., Cole, J.W., & Bassett, K.N., 2005. Structural control of volcanism and caldera development in the transtensional Taupo Volcanic Zone, New Zealand. *Journal of Volcanology and Geothermal Research*, 144: 7-22.

Steiner, A., 1958. Petrogenetic Implications of the 1954 Ngauruhoe Lava and its Xenoliths. *New Zealand Journal of Geology and Geophysics,* 1: 325-263.

Stokes, S., Lowe, D.J., & Froggatt, P.C., 1992. Discriminant function analysis and correlation of late Quaternary tephra deposits from Taupo and Okataina volcanoes, New Zealand, using glass shard major element compositions. *Quaternary International,* 13/14: 103-120.

Sturman, A.P., McGowan, H.A., & Spronken-Smith, R.A., 1999. Mesoscale and local climates in New Zealand. *Progress in Physical Geography,* 23(4): 611-635.

Suggate, R.P., Stevens, G.R., & Te Punga, M.T., (ed.), 1978. *The geology of New Zealand.* Wellington, Government Printer.

Sutton, A.N., Blake, S., & Wilson, C.J.N., 1995. An outline geochemistry of rhyolite eruptives from Taupo volcanic centre, New Zealand. *Journal of Volcanology and Geothermal Research,* 68: 153-175.

Sutton, A.N., Blake, S. Wilson, C.J.N., Charlier, B.L.A., 2000. Late Quaternary evolution of a hyperactive rhyolite magmatic system: Taupo volcanic centre, New Zealand. *Journal of the Geological Society,* 157: 537-552.

Svoboda, J., 2004. *Magnetic Techniques for the Treatment of Materials.* Secaucus, NJ, USA: Kluwer Academic Publishers, pg 141-142.

Taylor, N.H., 1930. The relation of geology to sheep sickness in Mairoa district. *N.Z. Journal of Science and Technology*, 12: 1-10.

Taylor, N.H., 1933. Soil processes in volcanic ash-beds. *N.Z. Journal of Science and Technology* 14: 193-202, 338-352.

Taylor, N.H., 1953. The ecological significance of the central North Island ash showers - the soil pattern. *Proceedings of the N.Z. Ecological Society*, 1: 1 1-12.

Thomas, A.P.W., 1888. *Report on the Eruption of Tarawera and Rotomahana, New Zealand.* Wellington: Government Printer.

Thompson, B.N. 1964. Quaternary volcanism of the Central Volcanic Region. *New Zealand Journal of Geology and Geophysics*, 7: 45-65.

Thompson, L.G., Mosley-Thompson E., Brecher H., Davis M., Leoń B., Les D., Lin P., Mashiotta T., & Mountain, K., 2006. Abrupt tropical climate change: Past and present. *Proceedings of the National Academy of Sciences,* 103: 10536–10543.

Timperley, M.H., & Vigor-Brown, R.J. 1985. Weathering of pumice in the sediments as a possible source of major ions for the waters of Lake Taupo, New Zealand. *Chemical Geology,* 49: 43-52.

Timperley, M.H., & Vigor-Brown, R.J. 1986. Water chemistry of lakes in the Taupo Volcanic Zone, New Zealand. *New Zealand Journal of Marine and Freshwater Research,* 20: 173-183.

Turney, C.S.M. & Lowe, J.J., 2001. Tephrochronology. In: Last, W.M. & Smol, J.P. (eds.) *Tracking environmental change using lake sediments. Volume 1: Basin Analysis, coring and chronological techniques.* Dordrecht, The Netherlands, Kluwer Academic Publishers.

Vandergoes, M.J., & Fitzsimons, S.J., 2003. The Last Glacial–Interglacial Transition (LGIT) in south Westland, New Zealand: paleoecological insight into mid-latitude Southern Hemisphere climate change. *Quaternary Science Reviews,* 22: 1461-1476.

Vandergoes, M.J., Newnham, R.M., Preusser, F., Hendy, C.H., Lowell, T.V., Fitzsimons, S.J., Hogg, A.G., Kasper, H.U., & Schluchter, C., 2005. Regional insolation forcing of late Quaternary climate change in the Southern Hemisphere. *Nature,* 436: 242-244.

Vucetich, C.G., & Howorth, R., 1976. Late Pleistocene Tephrostratigraphy in the Taupo District, New Zealand. *New Zealand Journal of Geology and Geophysics,* 19: 51-69.

Werner, C. & Cardellini, C., 2006. Comparison of carbon dioxide emissions with fluid upflow, chemistry, and geologic structures at the Rotorua geothermal system, New Zealand. *Geothermics,* 35: 221-238.

White, E., Don, B.J., Downes, M.T., Kemp, L.J., MacKenzie, A.L. & Payne, G.W., 1978. Sediments of Lake Rotorua as sources and sinks for plant nutrients. *New Zealand Journal of Marine and Freshwater Research,* 12(2): 121-130.

Whittaker, T., submitted 2008. High-Resolution Speleothem-Based Palaeoclimate Records from New Zealand reveal robust teleconnection to North Atlantic during MIS 1-4. Ph.D. Thesis, University of Waikato, Hamilton.

Williams, H., 1941. Calderas and their origin. *Bulletin of the Department of Geological Sciences, University of California, Berkeley*, 25:239-346.

Williams P.W., 1996. A 230 ka record of glacial and interglacial events from Aurora Cave, Fiordland, New Zealand. *New Zealand Journal of Geology and Geophysics,* 39: 225-241.

Williams P.W., King D.N.T., Zhao J-X, & Collerson K.D., 2004. Speleothem master chronologies: combined Holocene ^{18}O and ^{13}C records from the North Island of New Zealand and their palaeoenvironmental interpretation. *The Holocene,* 14: 194-208.

Williams P.W., King D.N.T., Zhao J-X, & Collerson K.D., 2005. Late Pleistocene to Holocene composite speleothem ^{18}O and ^{13}C chronologies from South Island, New Zealand—did a global Younger Dryas really exist? *Earth and Planetary Science Letters,* 230: 301-317.

Wilmshurst, J.M. & McGlone, M.S., 1996. Forest disturbance in the central North Island, New Zealand, following the 1850 BP Taupo eruption. *The Holocene,* 6(4): 399-411.

Wilmshurst, J.M. 1997. The impact of human settlement on vegetation and soil stability in Hawke's Bay, New Zealand. *New Zealand Journal of Botany,* 35: 97-111.

Wilmshurst, J.M., McGlone, M.S. & Partridge, T.R., 1997. A late Holocene history of natural disturbance in lowland podocarp/hardwood forest, Hawke's Bay, New Zealand. *New Zealand Journal of Botany,* 35: 79-96.

Wilmshurst, J.M., Eden, D.N. & Froggatt, P.C., 1999. Late Holocene forest disturbance in Gisborne, New Zealand: a comparison of terrestrial and marine pollen records. *New Zealand Journal of Botany,* 37: 523-540.

Wilmshurst, J.M., & Higham, T.F.G., 2004. Using rat-gnawed seeds to independently date the arrival of Pacific rats and humans to New Zealand. *The Holocene,* 14: 801-806.

Wilmshurst, J.M., Anderson, A.J., Higham, T.F.G., & Worthy, T.H., 2008. Dating the late prehistoric dispersal of Polynesians to New Zealand using the commensal Pacific rat. *Proceedings of the Natural Academy of Science of the United States of America,* 105(22): 7676-7680.

Wilmshurst, J.M., McGlone, M.S., Leathwick, J.R., & Newnham, R.M., 2007. A pre-deforestation pollen-climate calibration model for New Zealand and quantitative temperature reconstructions for the past 18000 years. *Journal of Quaternary Science*, 22: 535-547.

Wilson, C.J.N., 1991. Ignimbrite morphology and the effects of erosion: a New Zealand case study. *Bulletin of Volcanology,* 53: 635-644.

Wilson, C.J.N., 1993. Stratigraphy, chronology, styles and dynamics of Late Quaternary eruptions from Taupo volcano, New Zealand. Philosophical Transactions of the Royal Society of London A343, 205-306.

Wilson, C.J.N., 2001. The 26.5 ka Oruanui eruption, New Zealand: an introduction and overview. *Journal of Volcanology and Geothermal Research*, 112(1-4): 133-174.

Wilson, C.J.N., Rogan, M.A., Smith, I.E.M., Northey, D.J., Nairn, I.E., Houghton, B.F., 1984. Caldera volcanoes of the Taupo Volcanic Zone, New Zealand. *Journal of Geophysical Research,* 89: 8463-8484.

Wilson, C.J.N. & Walker, G.P.L., 1985. The Taupo eruption, New Zealand. I. General aspects. Philosophical Transactions of the Royal Society, London A314, 199-228.

Wilson, C.J.N., Houghton, B.F., Lanphere, M.A., & Weaver, S.D., 1992. A new radiometric age estimate for the Rotoehu Ash from Mayor Island volcano, New Zealand. *New Zealand Journal of Geology and Geophysics, 1992,* 35: 371-374.

Wilson, C.J.N., Houghton, B.F., McWilliams, M.O., Lanphere, M.A., Weaver, S.D., & Briggs, R.M., 1995a. Volcanic and structural evolution of the Taupo Volcanic Zone, New Zealand: a review. *Journal of Volcanology and Geothermal Research,* 68: 1-28.

Wilson, C.J.N., Houghton, B.F., Pillans, B.J., & Weaver, S.D., 1995b. Taupo Volcanic Zone talc-alkaline tephras on the peralkaline Mayor Island volcano, New Zealand: identification and uses as marker horizons. *Journal of Volcanology and Geothermal Research*, 69: 303-311.

Wilson, C.J.N., Blake, S., Charlier, B.L.A., & Sutton, A.N., 2006. The 26.5 Ka Oruanui Eruption, Taupo Volcano, New Zealand: Development, Characteristics and Evacuation of a Large Rhyolitic Magma Body. *Journal of Petrology*, 47: 35-69.

Winkler, S., 2004. Lichenometric dating of the 'Little Ice Age' maximum in Mt Cook National Park, Southern Alps, New Zealand. *The Holocene,* 14(6): 911-920.

Wood, C.P., 1992. Geology of the Rotorua geothermal system. *Geothermics*, 21: 25-41.

Woodward, C.A. & Shulmeister, J., 2005. A Holocene record of human induced and natural environmental change from Lake Forsyth (Te Wairewa), New Zealand. *Journal of Paleolimnology*, 34: 481-501.

Woodward, C.A. & Shulmeister, J., 2006. New Zealand chironomids as proxies for human induced and natural environmental change: transfer functions for temperature and lake production (chlorophyll *a*). *Journal of Paleolimnology*, 36: 407-429.

Xiong, L., & Palmer, J.G., 2000. Reconstruction of New Zealand temperatures back to Ad 1720 Using *Libocedrus Bidwillii* Tree-Rings. *Climatic Change* 45: 339-359.

Yum, J.G., Takemura, K., Tokuoka, T., & Yu, K.M., 2003. Holocene environmental changes of the Hwajinpo Lagoon on the eastern coast of Korea. *Journal of Paleolimnology*, 29: 155-166.

Appendices



Date collected: 19/04/2007
GPS coordinates: 38 04í32.9î S
176 17í69.9î E

Rotorua Cores

Site: RU 188-07 Section I

Length: 0-400 mm

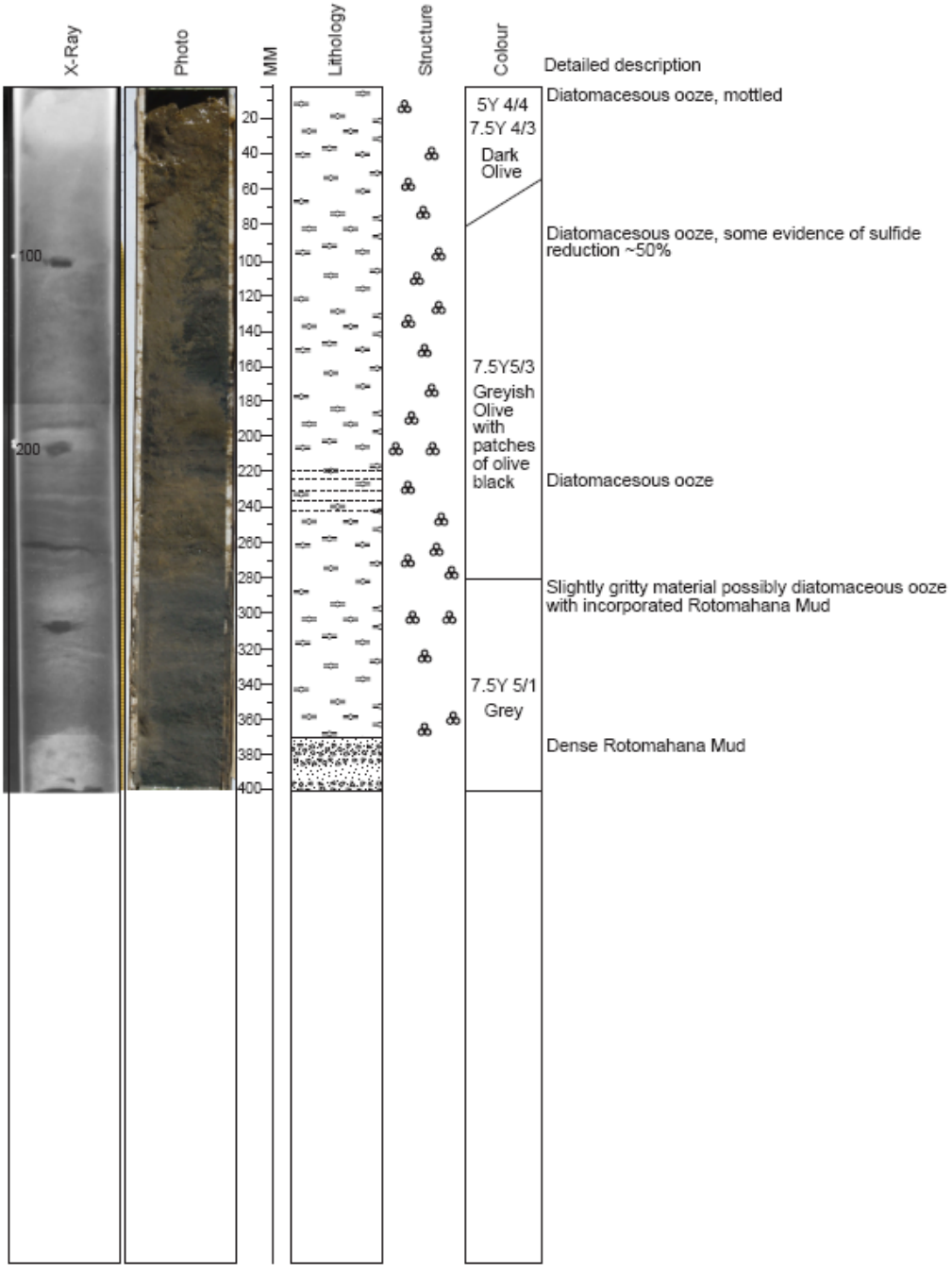

Date collected: 19/04/2007
GPS coordinates: 38 04ĺ32.9ĺ S
176 17ĺ69.9ĺ E

Rotorua Cores

Site: RU 188-07 Section II

Length: 400-1210 mm

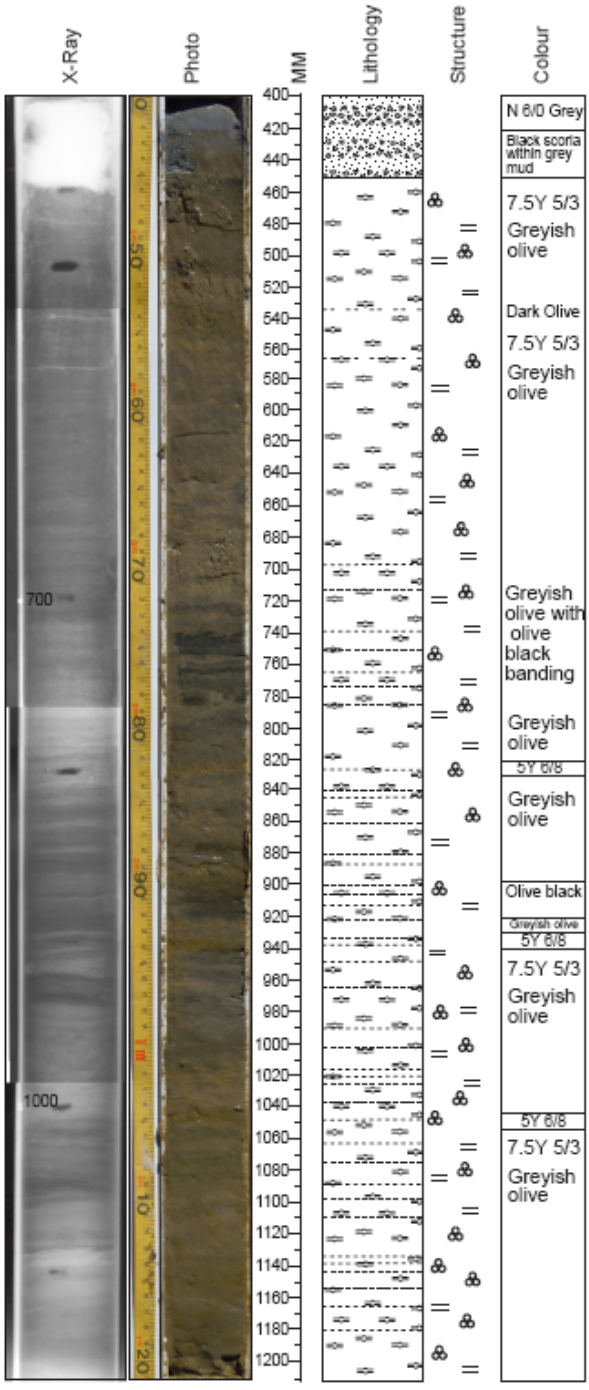

Detailed description

Rotomahana Mud
Tarawera Scoria, mainly concentrated on the left hand side, possibly caused by infilling of a hole or disruption during coring process
Diatomacesous ooze, some fine olive-dark olive banding evident - indicated by dashed lines

Diatomacesous ooze, coarse sulfide reduction banding

Diatomacesous ooze

Diatomacesous ooze, olive banding evident
Diatomacesous ooze, fine sulfide reduction banding

Diatomacesous ooze, olive banding

Diatomacesous ooze, sulfide reduction evident

Diatomacesous ooze
Diatomacesous ooze, olive band
Diatomacesous ooze, medium sulfide reduction banding

Diatomacesous ooze, olive band
Diatomacesous ooze, fine greyish bands towards the top

Date collected: 19/04/2007
GPS coordinates: 38 04í32.9î S
176 17í69.9î E

Rotorua Cores

Site: RU 188-07 Section III

Length: 1210-2070 mm

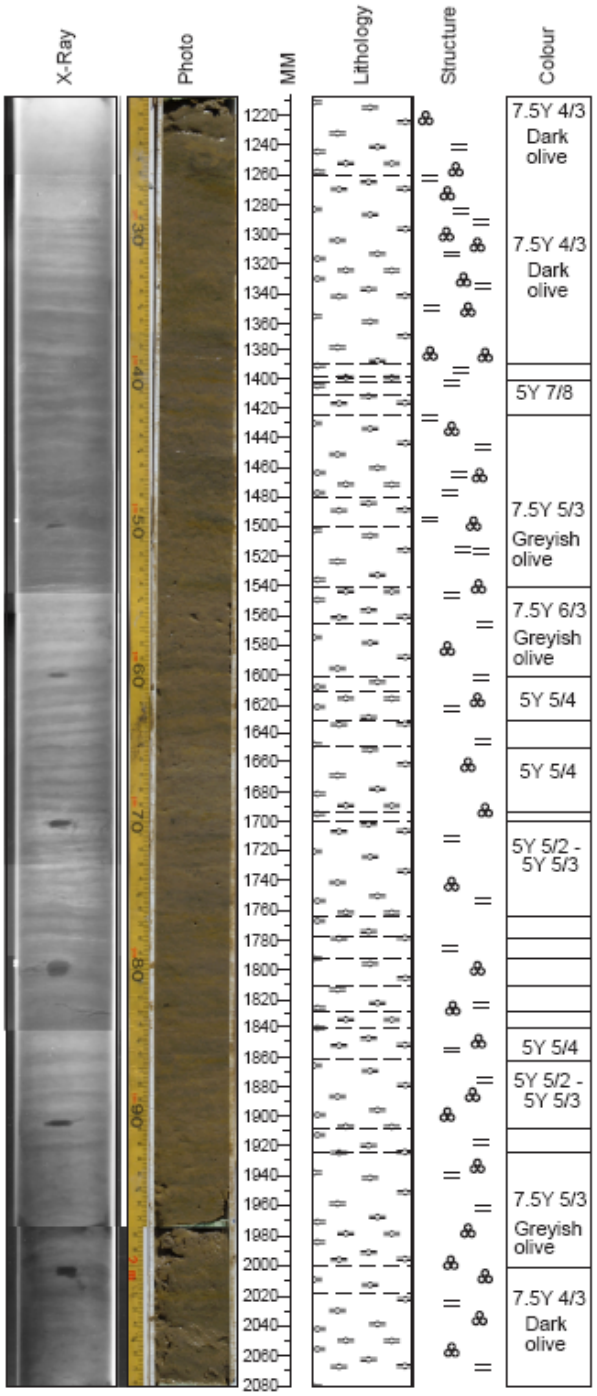

Detailed description

Diatomacesous ooze, fine olive banding evident throughout, most bands are ~ 4 mm in thickness and vary from an intense orangy gold to a slightly lighter olive than standard diatomaceous ooze. Bands are evident as marked by the dashed lines.

Diatomacesous ooze, fine orangy gold bands

Date collected: 19/04/2007
GPS coordinates: 38 04ί32.9î S
176 17ί69.9î E

Rotorua Cores

Site: RU 188-07 Section IV

Length: 2070-2315 mm

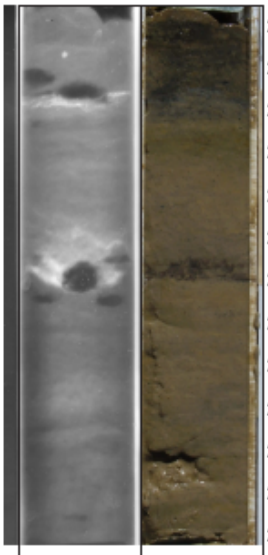

Detailed description

Diatomacesous ooze, with medium sulfide reduction banding

Very fine band of light grey ash (~ 16 mm thick)

Diatomacesous ooze

Fine reddish ash, not evident as a definite bed, spread out/slightly diffused (~10 mm total thickness, 2-4 mm in places)

Diatomacesous ooze, has undergone some expansion below 2320 mm

Date collected: 19/04/2007
GPS coordinates: 38 04í32.9î S
176 17í69.9î E

Rotorua Cores

Site: RU 188-07 Section V

Length: 2260-3160 mm

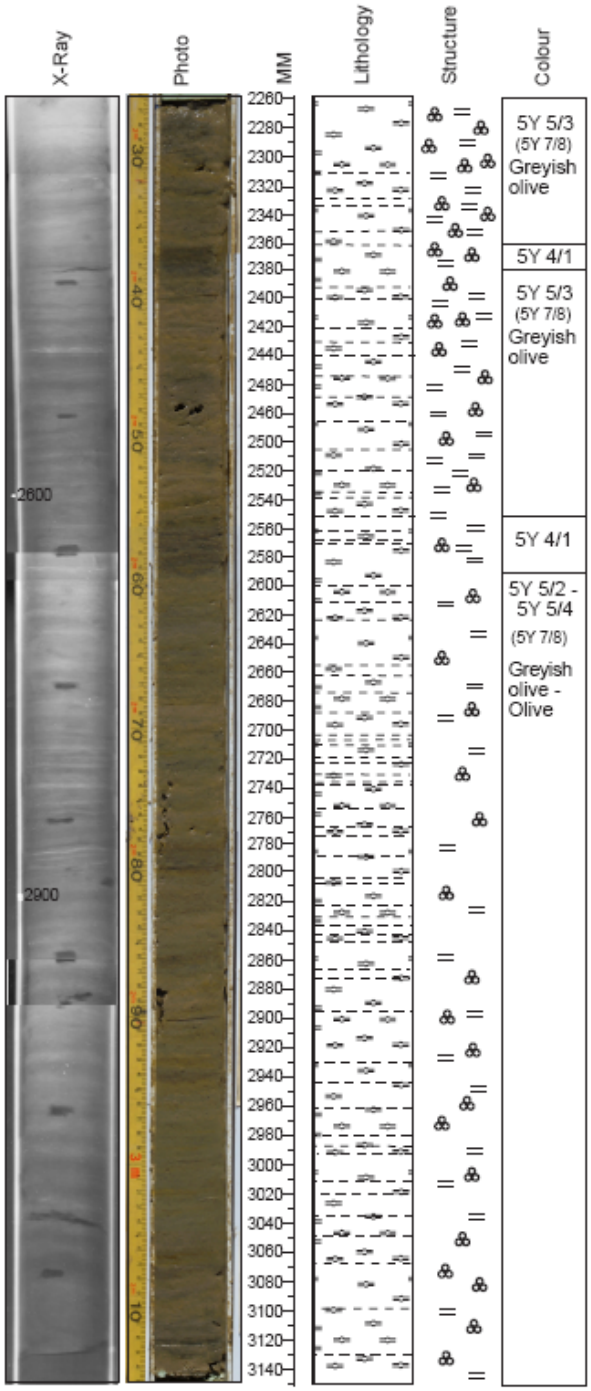

Colour	Detailed description
5Y 5/3 (5Y 7/8) Greyish olive	Diatomacesous ooze, some gas bubbles evident, with gold/olive banding occurs ~ every 10 mm, however some bands are very difficult to distinguish due to there light colour
5Y 4/1	Diatomacesous ooze, sulfide reduction
5Y 5/3 (5Y 7/8) Greyish olive	Diatomacesous ooze, gold/olive banding occuring ~10 mm apart
5Y 4/1	Diatomacesous ooze, sulfide reduction
5Y 5/2 - 5Y 5/4 (5Y 7/8) Greyish olive - Olive	Diatomacesous ooze, gold/olive banding occuring ~10 mm apart

Date collected: 19/04/2007
GPS coordinates: 38 04í32.9î S
176 17í69.9î E

Rotorua Cores

Site: RU 188-07 Section VI

Length: 3160-4080 mm

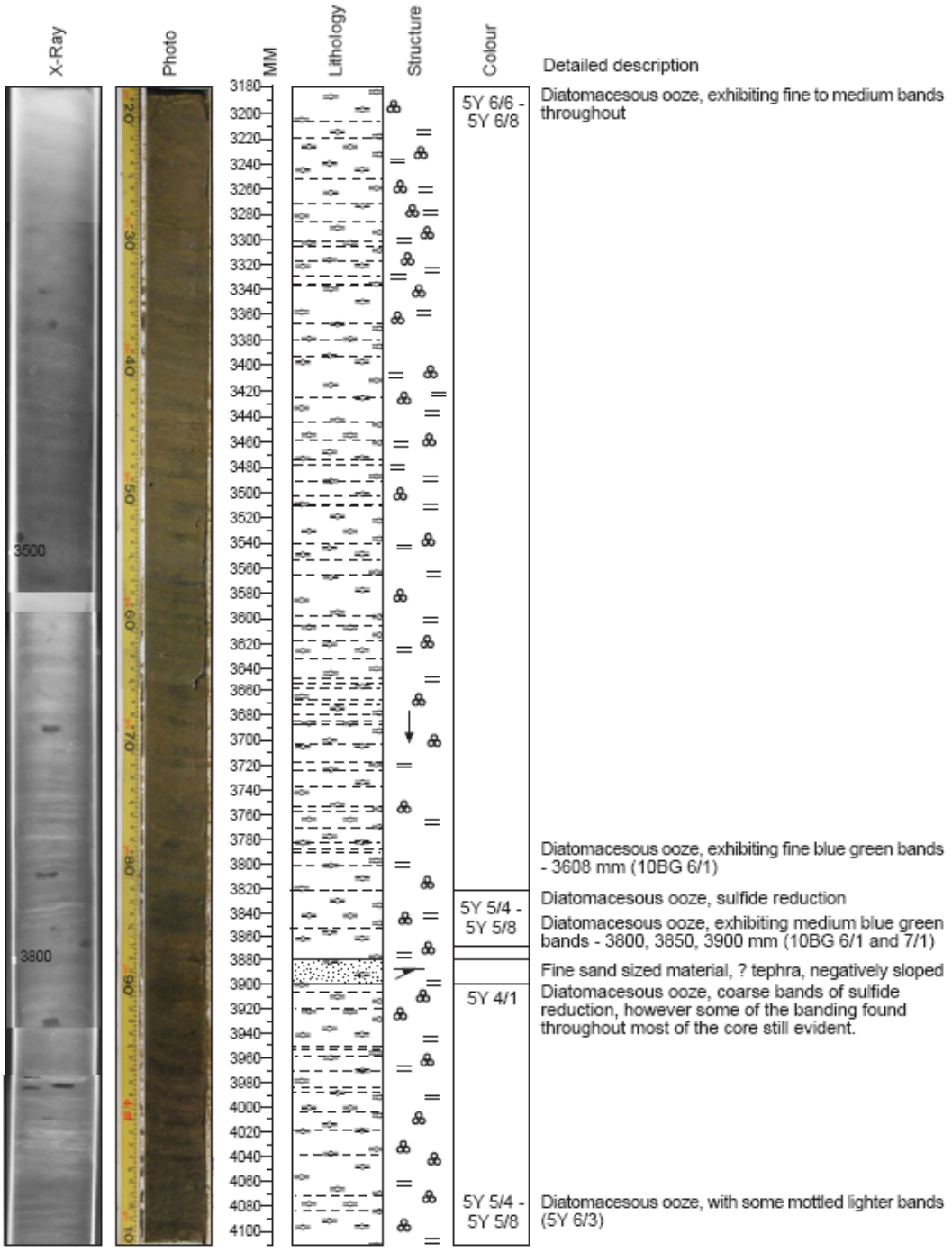

Date collected: 19/04/2007
GPS coordinates: 38 04í32.9î S
176 17í69.9î E

Rotorua Cores

Site: RU 188-07 Section VII

Length: 4080-5020 mm

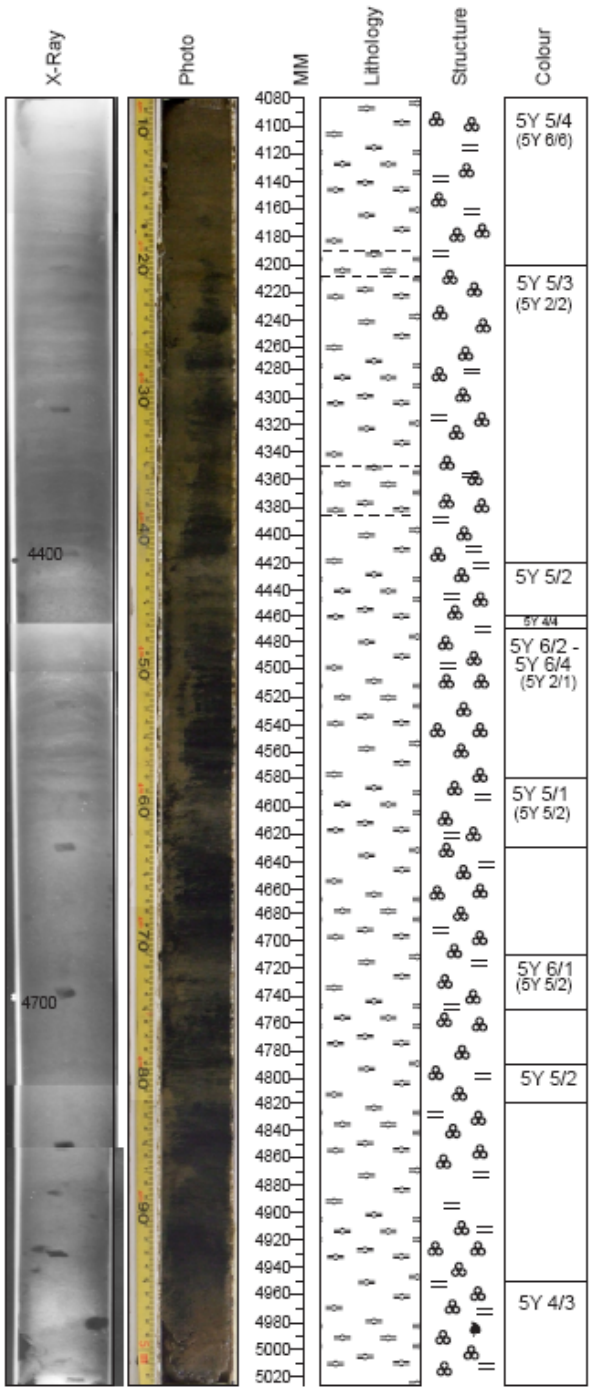

Colour	Detailed description
5Y 5/4 (5Y 8/6)	Diatomacesous ooze, exhibiting some medium banding throughout
5Y 5/3 (5Y 2/2)	Diatomacesous ooze, medium sized blocks of strong sulfide reduction
5Y 5/2	Diatomacesous ooze
5Y 4/4	Diatomacesous ooze
5Y 6/2 - 5Y 6/4 (5Y 2/1)	Diatomacesous ooze, strong sulfide reduction
5Y 5/1 (5Y 5/2)	Diatomacesous ooze, very fine sulfide reduction banding
	Diatomacesous ooze, strong blocks of sulfide reduction
5Y 6/1 (5Y 5/2)	Diatomacesous ooze, fine sulfide reduction banding
	Diatomacesous ooze, strong blocky sulfide reduction
5Y 5/2	Diatomacesous ooze, with sulfide reduction banding
	Diatomacesous ooze, strong blocky sulfide reduction
5Y 4/3	Sediment becomes coarser grading from very fine sand to sand sized material Plant material removed from 4998

Date collected: 19/04/2007
GPS coordinates: 38 04í32.9î S
176 17í69.9î E

Rotorua Cores

Site: RU 188-07 Section VIII

Length: 5020-5790 mm

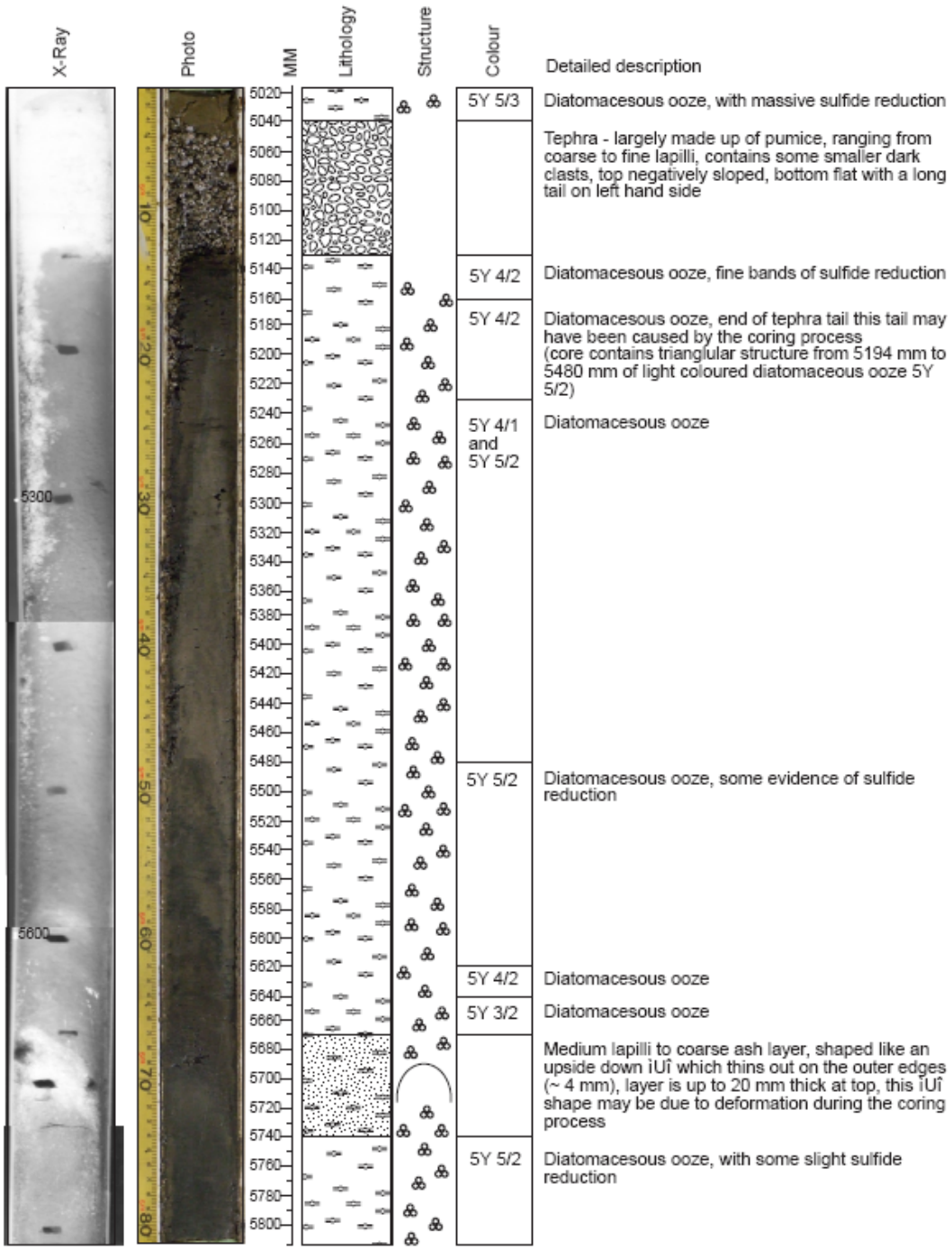

Date collected: 19/04/2007
GPS coordinates: 38 04í32.9î S
176 17í69.9î E

Rotorua Cores

Site: RU 188-07 Section IX

Length: 5790-6650 mm

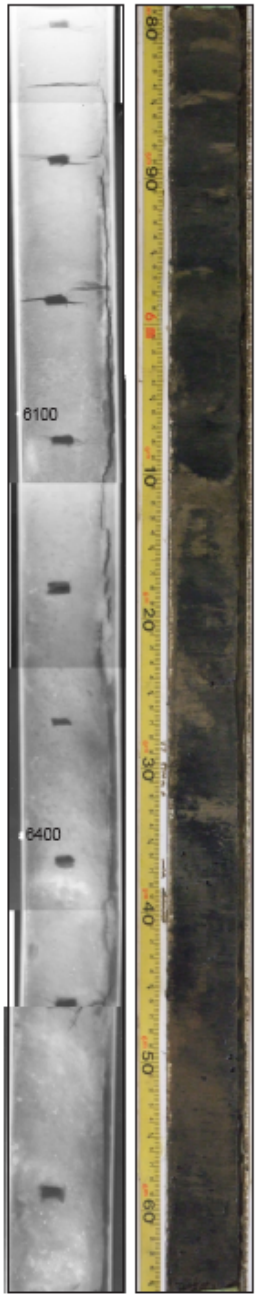

MM	Lithology	Structure	Colour	Detailed description
5790–6100			5Y 4/1	Diatomacesous ooze, with massive sulfide reduction
6100–6120			5Y 5/3	Diatomacesous ooze, change in texture to fine sand sized material, plant material recovered
6120–6460			5Y 4/1 - 5Y 5/3	Diatomacesous ooze, medium blocky sulfide reduction
6460–6600			5Y 4/2	Diatomacesous ooze, plant sample taken at 6510
6600–6650			5Y 3/2	Diatomacesous ooze, massive sulfide reduction but with the occasional fine structure

Date collected: 19/04/2007
GPS coordinates: 38 04í32.9î S
176 17í69.9î E

Rotorua Cores

Site: RU 188-07 Section X

Length: 6650-7950 mm





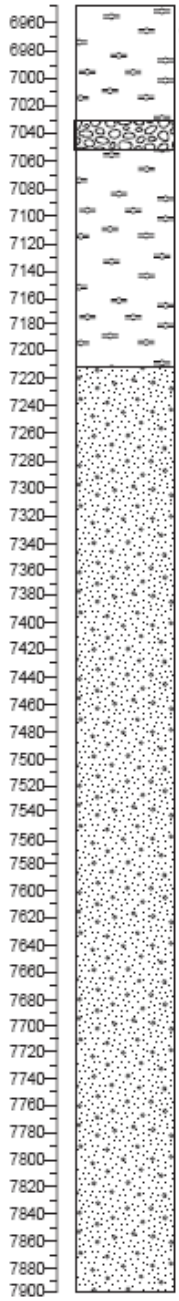

Colour	Detailed description
5Y 3/2	Diatomacesous ooze, with plant material recovered from 6990 mm
	Change in texture to coarse lapilli sized pumice material
5Y 5/3	Diatomacesous ooze, fine bedding structures
5Y 4/1	Diatomacesous ooze, sulfide reduction
10BG 4/1	Coarse sand sized material
10BG 3/1	Medium sand sized material, some larger green coloured clasts found within at 7400, 7450, 7510 and 7530 mm
5BG 6/1	Coarse sand sized material, some fine bedding structures evident, some medium lapilli sized pumice, no apparent grading
	Coarse lapilli sized clasts ~ 10 mm in size, these appear green in colour

Appendix B: Radiocarbon dating

	Depth (mm)	Wk	δ C^{13} (‰)	% Modern	^{14}C ages (± 1σ)	Calibrated ages (cal. yrs B.P. (2 σ) *
Sample 3, Core 8	5415-5420	23218	-24.6 ± 0.2	62.0 ± 0.1	3835 ± 30 BP	4290-4070 (87.8%) 4050-3990 (7.6%)
Sample 4, Core 9	6215-6220	23219	-18.7 ± 0.2	55.2 ± 0.1	4776 ± 34 BP	5590-5440 (54.7%) 5420-5320 (40.7%)
Sample 1, Core 10	6705-6710	23216	-31.8 ± 0.2	55.3 ± 0.1	4763 ± 30 BP	5490-5320 (70.6%) 5590-5500 (24.8%)
Sample 2, Core 10	6945-6950	23217	-27.7 ± 0.2	52.5 ± 0.1	5181 ± 30 BP	5940-5740 (95.4%)

Report on Radiocarbon Age Determination for Wk- 23216

(AMS measurement)

Submitter	R Pickett
Submitter's Code	Sample 1, Core 10
Site & Location	Ru188: North side of Mokia Island, Lake Rotorua, New Zealand
Sample Material	Diatomaceous ooze
Physical Pretreatment	None.
Chemical Pretreatment	Sample washed in hot HCl, filtered, rinsed and dried.

$\delta^{13}C$	-31.8 ± 0.2	‰
$D^{14}C$	-447.3 ± 1.2	‰
$F^{14}C$%	55.3 ± 0.1	%
Result	**4763 ± 30 BP**	

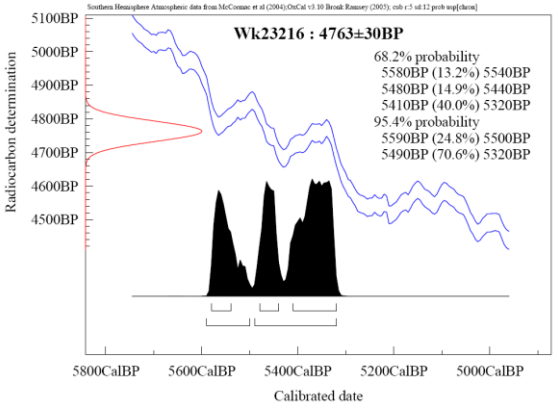

Report on Radiocarbon Age Determination for Wk- 23217

(AMS measurement)

Submitter	R Pickett
Submitter's Code	Sample 2, Core 10
Site & Location	Ru188: North side of Mokia Island, Lake Rotorua, New Zealand
Sample Material	Diatomaceous ooze
Physical Pretreatment	None.
Chemical Pretreatment	Sample washed in hot HCl, filtered, rinsed and dried.

$\delta^{13}C$	-27.7 ± 0.2	‰
$D^{14}C$	-475.3 ± 1.1	‰
$F^{14}C$%	52.5 ± 0.1	%
Result	**5181 ± 30 BP**	

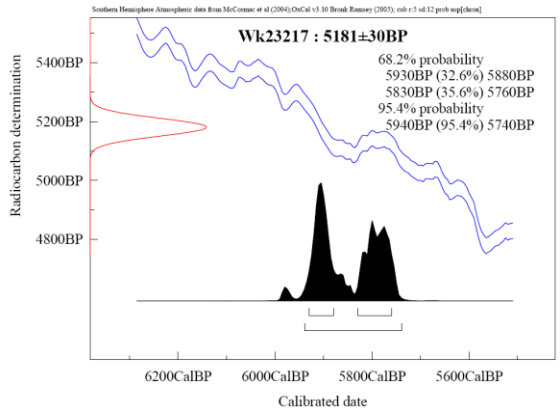

Report on Radiocarbon Age Determination for Wk- 23218

(AMS measurement)

Submitter	R Pickett
Submitter's Code	Sample 3, Core 8
Site & Location	Ru188: North side of Mokia Island, Lake Rotorua, New Zealand
Sample Material	Diatomaceous ooze
Physical Pretreatment	None.
Chemical Pretreatment	Sample washed in hot HCl, filtered, rinsed and dried.

$\delta^{13}C$	-24.6 ± 0.2	‰
$D^{14}C$	-379.6 ± 1.4	‰
$F^{14}C$%	62.0 ± 0.1	%

Result **3835 ± 30 BP**

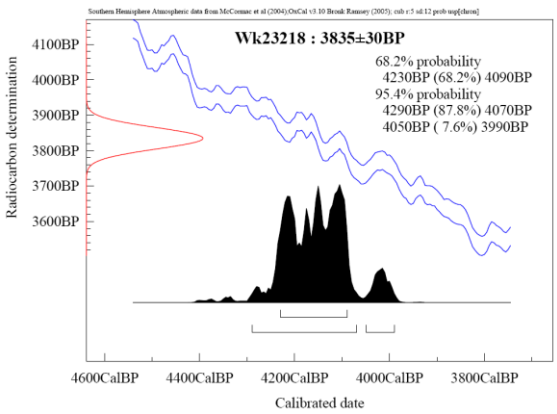

Report on Radiocarbon Age Determination for Wk- 23219

(AMS measurement)

Submitter	R Pickett
Submitter's Code	Sample 4, Core 9
Site & Location	Ru188: North side of Mokia Island, Lake Rotorua, New Zealand
Sample Material	Diatomaceous ooze
Physical Pretreatment	None.
Chemical Pretreatment	Sample washed in hot HCl, filtered, rinsed and dried.

$\delta^{13}C$	-18.7 ± 0.2	‰
$D^{14}C$	-448.2 ± 1.4	‰
$F^{14}C$%	55.2 ± 0.1	%

Result **4776 ± 34 BP**

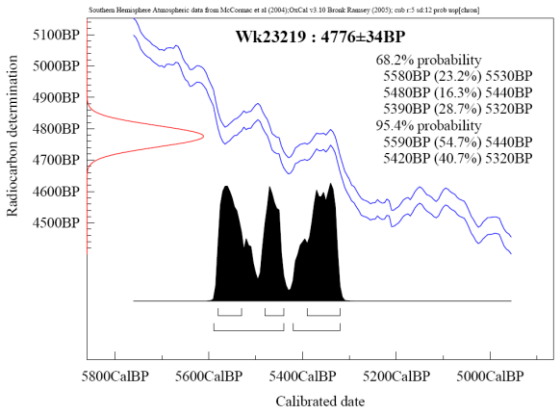

Appendix C – Magnetic Susceptibility

Position (cm)	Depth (mm)	Value
0	0	1.0
2	20	3.0
4	40	7.0
6	60	6.0
8	80	6.0
10	100	9.0
12	120	9.0
14	140	8.0
16	160	12.0
18	180	9.0
20	200	7.0
22	220	9.0
24	240	6.0
26	260	9.0
28	280	19.0
30	300	16.0
32	320	17.0
34	340	14.0
36	360	15.0
38	380	17.0
40	400	74.0
42	420	147.8
44	440	113.7
46	460	10.5
48	480	6.9
50	500	7.0
52	520	4.0
54	540	7.0
56	560	7.0
58	580	3.0
60	600	4.0
62	620	4.0
64	640	4.0
66	660	6.0
68	680	5.0
70	700	3.0
72	720	3.0
74	740	4.0
76	760	6.0
78	780	2.0
80	800	4.0
82	820	3.8
84	840	1.8
86	860	2.7
88	880	1.6
90	900	2.5
92	920	3.4
94	940	2.3
96	960	4.3
98	980	4.2
100	1000	2.1
102	1020	-1.0
104	1040	0.0
106	1060	0.0
108	1080	1.0
110	1100	1.0
112	1120	2.0
114	1140	0.0
116	1160	1.0
118	1180	1.0
120	1200	0.0
122	1220	2.9
124	1240	-0.2
126	1260	0.8
128	1280	1.7
130	1300	2.6
132	1320	1.4
134	1340	0.3
136	1360	0.2
138	1380	0.2
140	1400	0.0
142	1420	0.0
144	1440	0.0
146	1460	3.0
148	1480	0.0
150	1500	0.0
152	1520	0.0
154	1540	2.0
156	1560	1.0
158	1580	2.0
160	1600	0.0
162	1620	0.0
164	1640	0.0
166	1660	0.0
168	1680	0.0
170	1700	1.0
172	1720	1.0
174	1740	3.0
176	1760	1.0
178	1780	4.0
180	1800	0.0
182	1820	-1.2
184	1840	-0.3
186	1860	-0.3
188	1880	1.6
190	1900	-0.5
192	1920	-1.5
194	1940	-0.6
196	1960	-0.6
198	1980	1.3
200	2000	-0.5
202	2020	1.4
204	2040	0.4
206	2060	0.4
208	2080	13.3
210	2100	8.3
212	2120	3.2
214	2140	1.2
216	2160	1.1
218	2180	5.1
220	2200	3.5
222	2220	3.4
224	2240	2.3
226	2260	3.2
228	2280	1.2
230	2300	1.1
232	2320	0.7
234	2340	3.6
236	2360	2.5
238	2380	1.3
240	2400	0.2
242	2420	0.2
244	2440	-0.8
246	2460	0.3
248	2480	0.4
250	2500	3.5
252	2520	-0.4
254	2540	0.6
256	2560	0.7
258	2580	1.8
260	2600	0.0
262	2620	1.0
264	2640	1.0
266	2660	2.0
268	2680	0.0
270	2700	-1.0
272	2720	-1.0
274	2740	0.0
276	2760	0.0
278	2780	0.0
280	2800	1.0
282	2820	3.8
284	2840	-0.3
286	2860	0.7
288	2880	2.5
290	2900	-0.5
292	2920	-0.6
294	2940	0.3
296	2960	-0.8
298	2980	2.2
300	3000	0.1
302	3020	0.0
304	3040	-1.0
306	3060	0.0
308	3080	-1.0
310	3100	1.0
312	3120	0.0
314	3140	0.0
316	3160	3.0
318	3180	2.0
320	3200	0.0
322	3220	1.2
324	3240	0.2
326	3260	1.2
328	3280	0.2
330	3300	1.1
332	3320	1.1
334	3340	1.1
336	3360	3.1
338	3380	2.1
340	3400	2.0
342	3420	0.8
344	3440	-0.2
346	3460	0.7
348	3480	0.6
350	3500	-0.5
352	3520	-0.5
354	3540	1.4
356	3560	5.3
358	3580	3.2
360	3600	1.0
362	3620	0.0
364	3640	0.0
366	3660	1.0
368	3680	2.0
370	3700	1.0
372	3720	2.0
374	3740	0.0
376	3760	4.0
378	3780	2.0
380	3800	2.0
382	3820	0.9
384	3840	1.8
386	3860	3.7
388	3880	10.7
390	3900	6.6
392	3920	3.5
394	3940	12.3
396	3960	13.2
398	3980	10.2
400	4000	10.1
402	4020	1.0
404	4040	4.0
406	4060	2.0
408	4080	2.0
410	4100	0.0
412	4120	1.0
414	4140	0.0
416	4160	1.0
418	4180	0.0
420	4200	1.0
422	4220	1.8
424	4240	1.8
426	4260	1.7
428	4280	1.6
430	4300	1.5
432	4320	1.4
434	4340	1.4
436	4360	0.3
438	4380	0.2
440	4400	3.1
442	4420	5.2
444	4440	4.2
446	4460	0.3
448	4480	2.4
450	4500	0.5
452	4520	2.6
454	4540	1.6
456	4560	2.7
458	4580	2.8
460	4600	3.9
462	4620	4.9
464	4640	1.8
466	4660	1.7
468	4680	0.6
470	4700	2.6
472	4720	2.5
474	4740	1.4
476	4760	2.3
478	4780	2.2
480	4800	2.1
482	4820	2.1
484	4840	3.2
486	4860	5.3
488	4880	5.4
490	4900	4.4
492	4920	7.5
494	4940	7.6
496	4960	6.7
498	4980	1.8
500	5000	3.9
502	5020	13.8
504	5040	26.7
506	5060	28.6
508	5080	66.6
510	5100	45.5
512	5120	69.4
514	5140	15.3
516	5160	4.3
518	5180	5.2
520	5200	4.1
522	5220	6.0
524	5240	7.0
526	5260	9.0
528	5280	7.0
530	5300	9.0
532	5320	13.0
534	5340	14.0
536	5360	10.0
538	5380	8.0
540	5400	7.0
542	5420	6.0
544	5440	7.0
546	5460	9.0
548	5480	13.0
550	5500	10.0
552	5520	9.0
554	5540	11.0
556	5560	16.0
558	5580	33.0
560	5600	23.0
562	5620	12.0
564	5640	7.0
566	5660	39.0
568	5680	105.0
570	5700	106.0
572	5720	24.0
574	5740	14.0
576	5760	11.0
578	5780	9.0
580	5800	10.0
582	5820	18.1
584	5840	15.1
586	5860	12.1
588	5880	9.1
590	5900	9.1
592	5920	11.1
594	5940	9.1
596	5960	9.0
598	5980	6.0
600	6000	7.0
602	6020	8.0
604	6040	7.0
606	6060	8.0
608	6080	11.0
610	6100	10.0
612	6120	8.0
614	6140	7.0
616	6160	6.0
618	6180	6.0
620	6200	6.0
622	6220	9.0
624	6240	6.0
626	6260	5.0
628	6280	6.0
630	6300	7.0
632	6320	7.0
634	6340	8.0
636	6360	17.0
638	6380	31.0
640	6400	32.0
642	6420	36.9
644	6440	65.8
646	6460	23.7
648	6480	24.6
650	6500	29.5
652	6520	43.5
654	6540	113.4
656	6560	33.3
658	6580	11.2
660	6600	5.1
662	6620	9.0
664	6640	5.0
666	6660	5.0
668	6680	5.0
670	6700	6.0
672	6720	11.0
674	6740	24.0
676	6760	30.0
678	6780	8.0
680	6800	10.0
682	6820	30.9
684	6840	29.8
686	6860	31.7
688	6880	20.6
690	6900	18.6
692	6920	26.4
694	6940	27.3
696	6960	37.3
698	6980	47.2
700	7000	142.0
702	7020	168.0
704	7040	207.0
706	7060	168.0
708	7080	325.0
710	7100	351.0
712	7120	207.0
714	7140	436.0
716	7160	522.0
718	7180	546.0
720	7200	592.0
722	7220	484.0
724	7240	422.0
726	7260	370.0
728	7280	352.0
730	7300	319.0
732	7320	255.0
734	7340	281.0
736	7360	400.0
738	7380	342.0
740	7400	375.0
742	7420	311.8
744	7440	360.7
746	7460	337.6
748	7480	332.6
750	7500	279.5
752	7520	230.4
754	7540	159.4
756	7560	150.3
758	7580	125.2
760	7600	138.2
762	7620	105.0

RU188

Sensor,"MS2E1"
Range,1
Units,"SI"
Drift Limit,1
Alignment,"Core axis"
Interval,2
IntervalUnits,"cm"

Appendix D – Spectrophotometry Data

Colour data

Ref. #	Depth (cm)	L*	a*	b*
344	0	37.07	1.73	17.57
345	2	35.37	0.15	2.01
346	4	33.37	0.31	5.28
347	6	24.90	1.20	13.10
348	8	31.21	1.23	11.20
349	10	34.01	1.22	11.52
350	12	33.37	1.30	12.28
351	14	34.46	1.32	11.23
352	16	38.27	1.37	12.13
353	18	36.34	1.18	14.54
354	20	32.14	1.98	18.15
355	22	34.54	2.08	20.17
356	24	35.13	2.74	20.30
357	26	38.10	2.55	16.29
358	28	34.58	1.96	17.61
359	30	35.28	1.28	15.47
360	32	33.04	2.03	16.00
361	34	37.21	1.01	11.99
362	36	37.91	0.92	12.44
363	38	35.21	1.48	14.40
364	40	41.93	0.74	7.55
365	42	22.98	0.40	4.22
366	44	28.37	0.08	5.68
367	46	29.41	1.26	9.62
368	48	31.36	1.91	13.72
369	50	26.92	2.47	15.03
370	52	26.76	1.83	13.35
371	54	26.45	2.31	15.68
372	56	24.15	1.79	14.96
373	58	29.53	1.28	14.35
374	60	31.03	1.82	14.53
375	62	30.84	1.44	11.80
376	64	32.63	1.56	14.39
377	66	33.41	1.42	13.65
378	68	34.66	1.73	11.96
379	70	35.86	1.49	15.34
380	72	33.89	1.59	13.64
381	74	35.49	1.60	16.00
382	76	33.55	1.24	16.12
383	78	36.62	1.73	16.74
384	80	35.04	0.96	16.38
385	82	36.46	1.16	11.77
386	84	33.99	1.36	14.15
387	86	34.77	1.33	14.55
388	88	29.85	0.91	15.27
389	90	28.14	1.07	15.51
390	92	28.89	0.53	15.10
391	94	32.51	1.04	16.43
392	96	33.56	0.96	16.00
393	98	34.82	1.21	15.35
394	100	34.84	1.26	13.44
395	102	30.17	0.98	9.75
396	104	34.68	0.40	12.63
397	106	38.50	1.00	12.15
398	108	39.83	0.50	12.46
399	110	38.16	0.97	13.27
400	112	44.27	0.80	12.52
401	114	37.92	1.10	12.23
402	116	40.63	0.87	11.94
403	118	41.09	0.45	11.38
404	120	41.04	0.39	12.28
405	122	37.19	0.87	10.76
406	124	33.40	1.19	11.81
407	126	33.59	1.43	13.94
408	128	33.07	0.58	10.31
409	130	32.53	0.71	11.70
410	132	35.03	0.95	12.81
411	134	35.99	0.64	11.43
412	136	34.16	0.46	10.33
413	138	31.30	0.18	11.82
414	140	32.01	1.01	15.10
415	142	33.66	0.22	15.33
416	144	32.36	0.75	15.16
417	146	36.00	0.90	14.45
418	148	32.35	0.49	12.23
419	150	28.84	0.41	14.56
420	152	37.25	0.45	13.27
421	154	35.29	0.32	14.63
422	156	33.83	0.14	14.41
423	158	38.50	1.06	13.91
424	160	36.50	0.67	13.28
425	162	34.92	0.44	14.21
426	164	38.13	1.03	15.23
427	166	40.58	0.91	15.67
428	168	39.69	0.85	15.52
429	170	40.35	0.44	12.65
430	172	39.30	0.52	13.78
431	174	37.76	0.86	15.27
432	176	36.10	0.24	12.25
433	178	37.03	0.31	15.70
434	180	35.64	0.75	10.76
435	182	36.47	0.68	11.40
436	184	34.49	0.70	13.41
437	186	33.96	0.08	12.53
438	188	35.94	0.36	14.51
439	190	37.86	0.46	11.55
440	192	33.98	0.16	14.85
441	194	31.23	-0.08	14.85
442	196	31.77	0.19	15.20
443	198	33.12	1.28	11.89

Ref. #	Depth (cm)	L*	a*	b*
444	200	34.70	0.60	10.43
445	202	33.15	-0.18	14.38
446	204	32.32	0.96	14.37
447	206	32.48	1.41	16.56
448	208	24.62	0.89	10.26
449	210	28.88	1.57	12.21
450	212	29.70	1.47	12.78
451	214	32.57	1.61	15.92
452	216	35.25	1.51	16.28
453	218	33.60	1.77	12.48
454	220	38.77	0.72	6.81
455	222	35.58	1.71	15.73
456	224	34.56	1.75	15.48
457	226	34.05	1.60	14.42
458	228	31.95	1.87	11.59
459	230	30.68	1.05	12.63
460	232	36.39	1.45	16.27
461	234	35.19	0.46	13.05
462	236	34.92	1.84	16.29
463	238	36.76	0.89	13.60
464	240	38.34	0.59	13.82
465	242	38.70	0.66	14.11
466	244	36.87	1.01	12.99
467	246	38.02	1.17	18.49
468	248	39.45	1.31	16.80
469	250	42.60	0.83	17.10
470	252	38.62	0.70	16.47
471	254	36.95	1.03	16.39
472	256	40.66	1.30	15.27
473	258	39.46	1.47	14.56
474	260	36.35	1.26	16.46
475	262	37.24	1.46	18.88
476	264	34.40	0.32	15.49
477	266	35.94	0.87	19.39
478	268	38.73	1.29	17.77
479	270	37.29	1.54	16.40
480	272	39.64	1.26	17.09
481	274	41.24	1.23	17.41
482	276	38.95	0.78	15.97
483	278	37.76	0.99	17.02
484	280	37.85	1.42	17.95
485	282	33.00	1.29	15.98
486	284	36.48	0.43	16.71
487	286	37.64	0.49	16.24
488	288	36.73	0.37	15.85
489	290	37.78	1.03	15.90
490	292	42.77	0.95	17.42
491	294	37.51	1.51	17.68
492	296	39.39	0.53	16.13
493	298	35.51	1.19	15.62
494	300	35.36	0.56	14.03
495	302	39.93	0.55	15.73
496	304	34.01	1.25	14.40
497	306	35.48	0.52	13.87
498	308	29.91	0.00	14.66
499	310	35.49	0.69	9.83
500	312	29.98	1.21	17.27
501	314	29.55	0.54	16.56
502	316	25.47	0.18	13.45
503	318	27.13	0.17	9.18
504	320	29.89	0.60	14.05
505	322	32.72	0.44	14.85
506	324	30.31	0.42	14.55
507	326	30.32	0.26	16.52
508	328	28.61	-0.05	15.61
509	330	29.36	0.06	15.45
510	332	30.88	0.42	14.99
511	334	34.82	0.29	16.40
512	336	33.38	0.35	15.08
513	338	33.08	0.53	16.49
514	340	35.23	0.48	17.46
515	342	34.02	1.74	18.05
516	344	38.16	1.17	18.57
517	346	35.87	1.35	18.31
518	348	37.64	1.05	19.79
519	350	35.16	1.24	13.57
520	352	34.68	0.78	16.81
521	354	31.63	0.51	14.77
522	356	30.03	0.67	16.49
523	358	30.23	0.35	17.83
524	360	28.01	0.75	15.28
525	362	32.85	-0.27	16.29
526	364	32.52	0.22	17.05
527	366	37.45	0.82	15.09
528	368	33.72	1.33	17.60
529	370	34.92	1.12	18.25
530	372	33.05	0.75	17.55
531	374	33.42	1.25	17.24
532	376	30.22	1.22	15.93
533	378	30.22	0.92	13.89
534	380	32.09	0.69	11.48
535	382	34.83	0.62	9.64
536	384	30.65	0.75	11.23
537	386	29.49	0.15	10.94
538	388	31.02	0.91	12.43
539	390	26.39	1.12	13.32
540	392	27.39	1.84	15.89
541	394	28.74	2.28	14.03
542	396	26.37	1.48	13.76
543	398	29.30	1.50	10.72

Ref. #	Depth (cm)	L*	a*	b*
544	400	24.48	2.08	11.36
545	402	31.69	1.46	14.90
546	404	33.62	1.55	11.96
547	406	25.61	1.28	17.08
548	408	26.73	0.27	15.18
549	410	33.27	0.51	10.93
550	412	31.08	0.40	15.87
551	414	31.40	0.42	15.08
552	416	31.00	0.91	16.40
553	418	31.91	0.89	17.29
554	420	33.48	-0.25	12.22
555	422	34.73	1.33	17.78
556	424	35.27	0.61	15.89
557	426	33.55	0.10	14.63
558	428	36.39	0.59	16.62
559	430	29.93	-0.70	13.39
560	432	33.17	-0.56	10.51
561	434	31.27	-0.19	12.94
562	436	30.77	0.83	14.99
563	438	30.84	-0.10	16.57
564	440	34.50	0.78	15.53
565	442	32.63	0.81	13.51
566	444	29.91	0.40	14.70
567	446	26.63	-0.13	15.13
568	448	28.39	0.55	15.37
569	450	25.10	0.06	15.67
570	452	31.98	0.64	13.65
571	454	34.27	1.39	15.13
572	456	34.34	2.35	19.16
573	458	38.11	2.45	17.04
574	460	36.23	2.27	17.25
575	462	38.42	1.94	13.89
576	464	34.90	2.16	14.31
577	466	36.23	2.37	16.77
578	468	37.48	3.13	19.56
579	470	35.54	2.26	16.58
580	472	36.35	2.20	17.38
581	474	35.77	2.74	18.94
582	476	32.61	2.62	17.35
583	478	32.83	2.30	17.14
584	480	34.07	2.19	16.32
585	482	33.34	2.81	19.32
586	484	31.05	2.76	18.84
587	486	30.90	2.63	17.58
588	488	31.73	1.73	15.25
589	490	35.50	2.06	16.24
590	492	32.62	2.84	18.46
591	494	30.45	2.88	16.23
592	496	31.24	3.03	14.94
593	498	32.90	3.03	13.59
594	500	37.48	3.15	14.66
595	502	32.80	1.41	10.41
596	504	40.55	1.12	12.24
597	506	47.28	0.28	6.98
598	508	45.53	0.43	6.79
599	510	48.94	1.51	12.11
600	512	48.00	1.80	10.09
601	514	39.43	3.34	13.53
602	516	36.12	3.57	19.92
603	518	30.72	0.78	11.74
604	520	35.28	1.15	13.83
605	522	35.94	1.46	12.31
606	524	38.75	0.93	11.00
607	526	37.27	2.22	16.92
608	528	41.24	2.77	18.91
609	530	32.10	1.99	12.48
610	532	39.21	3.14	19.54
611	534	39.51	2.66	18.35
612	536	38.27	3.75	20.98
613	538	42.75	2.06	14.15
614	540	41.32	1.18	14.97
615	542	42.44	2.54	18.58
616	544	42.45	2.28	16.78
617	546	41.94	2.34	18.03
618	548	38.30	1.89	17.73
619	550	39.37	1.61	18.05
620	552	36.58	1.15	14.11
621	554	38.08	2.28	18.93
622	556	38.99	2.44	17.70
623	558	39.42	2.48	18.42
624	560	40.67	2.47	18.18
625	562	34.54	2.55	13.38
626	564	29.76	1.02	12.25
627	566	29.65	1.19	12.42
628	568	32.96	1.01	9.48
629	570	33.50	1.32	14.66
630	572	39.42	1.56	14.05
631	574	41.24	2.38	16.58
632	576	42.15	2.01	14.99
633	578	40.52	2.42	18.14
634	580	39.05	2.15	17.77
635	582	36.56	2.37	17.44
636	584	36.11	2.21	17.57
637	586	36.19	2.68	19.65
638	588	35.12	1.33	16.71
639	590	37.05	1.64	17.82
640	592	40.15	2.87	20.23
641	594	35.63	2.84	20.49
642	596	38.00	1.97	17.85
643	598	35.13	1.88	18.17
644	600	36.74	1.13	17.03
645	602	35.70	3.32	21.38
646	604	39.00	1.60	16.40
647	606	38.69	2.49	18.03
648	608	37.93	3.03	18.26
649	610	38.25	2.98	19.70
650	612	38.69	3.62	22.03
651	614	38.79	2.47	17.27
652	616	39.69	2.36	18.00
653	618	39.03	2.99	17.57
654	620	37.97	3.29	19.24
655	622	36.04	4.16	22.42
656	624	39.33	3.48	19.28
657	626	39.95	3.42	19.80
658	628	37.98	3.04	20.11
659	630	36.72	2.73	19.93
660	632	32.55	3.17	21.84
661	634	32.53	3.62	23.21
662	636	35.93	4.17	21.23
663	638	34.93	3.08	18.26
664	640	35.87	3.32	20.05
665	642	40.01	2.70	19.72
666	644	33.56	3.04	18.59
667	646	30.73	3.99	19.68
668	648	29.79	4.15	19.53
669	650	31.43	3.57	18.06
670	652	32.69	2.98	13.99
671	654	33.02	3.37	17.56
672	656	29.85	3.21	20.37
673	658	27.41	1.51	12.97
674	660	29.86	2.77	18.41
675	662	33.03	1.13	16.11
676	664	28.09	3.32	14.07
677	666	25.97	3.34	15.23
678	668	28.18	3.98	15.67
679	670	26.90	2.63	11.14
680	672	25.65	2.46	12.07
681	674	21.62	1.64	10.52
682	676	22.36	1.22	11.60
683	678	31.12	1.36	7.57
684	680	27.28	1.77	10.26
685	682	26.07	1.18	7.16
686	684	34.64	2.90	17.52
687	686	29.24	2.43	13.70
688	688	35.97	2.62	18.29
689	690	38.08	2.25	20.16
690	692	34.16	1.80	10.57
691	694	35.04	1.89	19.67
692	696	32.82	0.62	18.45
693	698	34.65	0.42	15.65
694	700	32.98	6.14	23.44
695	702	39.24	2.13	11.65
696	704	40.02	3.45	18.31
697	706	40.92	5.14	18.58
698	708	38.66	0.83	12.56
699	710	37.47	2.81	19.08
700	712	33.18	1.18	8.92
701	714	37.20	2.16	15.30
702	716	36.61	1.96	14.43
703	718	32.52	2.70	19.02
704	720	36.13	1.16	12.84
705	724	33.92	0.97	9.77
706	726	34.80	0.23	7.47
707	728	33.47	0.91	7.88
708	730	33.51	0.51	8.38
709	732	43.90	1.54	10.87
710	734	47.33	1.61	13.45
711	736	49.80	1.49	11.60
712	738	49.36	1.08	10.42
713	740	36.69	0.73	9.58
714	742	35.92	0.66	7.60
715	744	45.24	1.00	9.26
716	746	46.88	1.05	8.47
717	748	45.06	1.29	8.87
718	750	42.98	1.57	8.84
Min		22.98	-0.08	2.01
Max		44.27	2.74	20.30
Median		34.62	0.98	13.69
Average		34.38	1.02	13.39

First derivative reflectance data

Depth (cm)	[400nm]	[420nm]	[440nm]	[460nm]	[480nm]	[500nm]	[520nm]	[540nm]	[560nm]	[580nm]	[600nm]	[620nm]	[640nm]	[660nm]	[680nm]	[700nm]
0	0.0274	0.0332	0.0440	0.0541	0.0605	0.0695	0.0794	0.0884	0.0998	0.1083	0.1112	0.1200	0.1275	0.1234	0.1312	0.1482
2	0.0790	0.0781	0.0798	0.0825	0.0816	0.0842	0.0851	0.0851	0.0880	0.0888	0.0876	0.0904	0.0912	0.0890	0.0909	0.0924
4	0.0584	0.0585	0.0614	0.0652	0.0662	0.0694	0.0723	0.0741	0.0791	0.0824	0.0811	0.0838	0.0852	0.0762	0.0775	0.0859
6	0.0158	0.0169	0.0210	0.0248	0.0279	0.0318	0.0362	0.0401	0.0459	0.0506	0.0512	0.0542	0.0575	0.0483	0.0502	0.0631
8	0.0324	0.0340	0.0396	0.0451	0.0488	0.0539	0.0585	0.0630	0.0694	0.0748	0.0758	0.0806	0.0848	0.0799	0.0839	0.0954
10	0.0396	0.0417	0.0481	0.0543	0.0580	0.0642	0.0699	0.0750	0.0829	0.0885	0.0898	0.0952	0.0997	0.0947	0.0981	0.1100
12	0.0331	0.0368	0.0440	0.0506	0.0550	0.0616	0.0666	0.0720	0.0795	0.0851	0.0868	0.0928	0.0976	0.0958	0.1015	0.1102
14	0.0405	0.0437	0.0500	0.0567	0.0607	0.0669	0.0723	0.0771	0.0845	0.0901	0.0917	0.0981	0.1027	0.1013	0.1068	0.1155
16	0.0518	0.0549	0.0629	0.0700	0.0744	0.0824	0.0895	0.0962	0.1057	0.1127	0.1145	0.1215	0.1265	0.1224	0.1277	0.1391
18	0.0353	0.0394	0.0485	0.0572	0.0628	0.0714	0.0788	0.0857	0.0952	0.1022	0.1040	0.1116	0.1166	0.1142	0.1200	0.1301
20	0.0191	0.0225	0.0297	0.0365	0.0403	0.0468	0.0565	0.0655	0.0758	0.0835	0.0853	0.0912	0.0960	0.0879	0.0912	0.1066
22	0.0182	0.0231	0.0323	0.0405	0.0451	0.0533	0.0651	0.0760	0.0879	0.0964	0.0989	0.1063	0.1124	0.1066	0.1126	0.1273
24	0.0212	0.0262	0.0343	0.0418	0.0455	0.0531	0.0656	0.0785	0.0914	0.1005	0.1036	0.1110	0.1173	0.1135	0.1196	0.1329
26	0.0410	0.0446	0.0529	0.0597	0.0623	0.0698	0.0819	0.0941	0.1070	0.1164	0.1185	0.1261	0.1332	0.1270	0.1317	0.1489
28	0.0238	0.0289	0.0373	0.0448	0.0492	0.0568	0.0672	0.0767	0.0872	0.0950	0.0976	0.1046	0.1103	0.1071	0.1131	0.1254
30	0.0272	0.0333	0.0434	0.0517	0.0565	0.0641	0.0730	0.0807	0.0900	0.0971	0.0993	0.1055	0.1103	0.1088	0.1140	0.1217
32	0.0231	0.0285	0.0366	0.0428	0.0455	0.0522	0.0615	0.0699	0.0796	0.0864	0.0886	0.0947	0.0990	0.0984	0.1037	0.1099
34	0.0432	0.0488	0.0585	0.0663	0.0713	0.0792	0.0850	0.0907	0.0994	0.1058	0.1072	0.1139	0.1181	0.1171	0.1233	0.1291
36	0.0449	0.0503	0.0600	0.0681	0.0737	0.0816	0.0883	0.0946	0.1036	0.1100	0.1118	0.1181	0.1229	0.1209	0.1262	0.1340
38	0.0306	0.0362	0.0460	0.0532	0.0576	0.0652	0.0729	0.0801	0.0895	0.0963	0.0986	0.1048	0.1096	0.1081	0.1132	0.1209
40	0.0818	0.0864	0.0943	0.1013	0.1042	0.1111	0.1152	0.1195	0.1272	0.1322	0.1324	0.1388	0.1424	0.1415	0.1469	0.1513
42	0.0255	0.0273	0.0304	0.0321	0.0327	0.0344	0.0356	0.0365	0.0387	0.0400	0.0398	0.0418	0.0420	0.0421	0.0437	0.0431
44	0.0361	0.0381	0.0426	0.0458	0.0473	0.0503	0.0525	0.0541	0.0572	0.0593	0.0590	0.0614	0.0620	0.0613	0.0629	0.0637
46	0.0293	0.0327	0.0377	0.0421	0.0448	0.0490	0.0528	0.0564	0.0614	0.0656	0.0669	0.0712	0.0746	0.0730	0.0764	0.0828
48	0.0244	0.0286	0.0352	0.0413	0.0453	0.0514	0.0571	0.0627	0.0702	0.0761	0.0788	0.0847	0.0904	0.0889	0.0939	0.1042
50	0.0144	0.0173	0.0225	0.0272	0.0304	0.0352	0.0406	0.0459	0.0524	0.0579	0.0604	0.0661	0.0712	0.0692	0.0739	0.0847
52	0.0161	0.0194	0.0243	0.0291	0.0324	0.0369	0.0416	0.0459	0.0517	0.0565	0.0584	0.0633	0.0677	0.0659	0.0694	0.0791
54	0.0112	0.0147	0.0207	0.0253	0.0289	0.0337	0.0393	0.0444	0.0507	0.0560	0.0587	0.0640	0.0690	0.0679	0.0726	0.0825
56	0.0088	0.0120	0.0168	0.0213	0.0252	0.0296	0.0337	0.0376	0.0427	0.0472	0.0493	0.0538	0.0583	0.0560	0.0597	0.0697
58	0.0185	0.0222	0.0286	0.0352	0.0397	0.0457	0.0509	0.0559	0.0625	0.0679	0.0696	0.0750	0.0803	0.0771	0.0812	0.0933
60	0.0216	0.0255	0.0325	0.0389	0.0439	0.0505	0.0557	0.0610	0.0687	0.0747	0.0773	0.0837	0.0900	0.0878	0.0920	0.1052
62	0.0270	0.0312	0.0373	0.0428	0.0469	0.0524	0.0570	0.0613	0.0675	0.0725	0.0743	0.0798	0.0851	0.0847	0.0900	0.0984
64	0.0251	0.0295	0.0370	0.0443	0.0496	0.0561	0.0624	0.0682	0.0760	0.0822	0.0846	0.0911	0.0973	0.0959	0.1015	0.1139
66	0.0295	0.0331	0.0410	0.0483	0.0533	0.0599	0.0662	0.0718	0.0798	0.0856	0.0878	0.0943	0.1004	0.0987	0.1051	0.1171
68	0.0382	0.0418	0.0492	0.0559	0.0602	0.0668	0.0722	0.0773	0.0853	0.0917	0.0937	0.1009	0.1070	0.1056	0.1114	0.1236
70	0.0303	0.0358	0.0446	0.0539	0.0602	0.0684	0.0755	0.0827	0.0926	0.0999	0.1024	0.1099	0.1171	0.1137	0.1175	0.1341
72	0.0309	0.0350	0.0427	0.0499	0.0547	0.0613	0.0679	0.0739	0.0821	0.0884	0.0909	0.0973	0.1032	0.1016	0.1073	0.1186
74	0.0273	0.0324	0.0423	0.0513	0.0575	0.0659	0.0735	0.0808	0.0906	0.0980	0.1007	0.1086	0.1161	0.1138	0.1204	0.1358
76	0.0226	0.0272	0.0359	0.0445	0.0505	0.0580	0.0654	0.0720	0.0810	0.0881	0.0899	0.0961	0.1030	0.0980	0.1027	0.1196
78	0.0292	0.0345	0.0450	0.0538	0.0593	0.0683	0.0777	0.0864	0.0973	0.1053	0.1079	0.1162	0.1234	0.1197	0.1270	0.1431
80	0.0247	0.0291	0.0393	0.0493	0.0565	0.0645	0.0719	0.0787	0.0889	0.0959	0.0978	0.1043	0.1114	0.1036	0.1091	0.1279
82	0.0451	0.0484	0.0558	0.0636	0.0681	0.0756	0.0812	0.0869	0.0952	0.1013	0.1025	0.1093	0.1151	0.1133	0.1195	0.1301
84	0.0300	0.0335	0.0418	0.0493	0.0546	0.0617	0.0682	0.0744	0.0827	0.0894	0.0912	0.0976	0.1038	0.1004	0.1060	0.1195
86	0.0311	0.0349	0.0431	0.0513	0.0570	0.0645	0.0712	0.0778	0.0870	0.0937	0.0954	0.1023	0.1088	0.1047	0.1103	0.1249
88	0.0177	0.0209	0.0278	0.0346	0.0398	0.0460	0.0517	0.0571	0.0646	0.0699	0.0711	0.0758	0.0812	0.0761	0.0801	0.0939
90	0.0141	0.0175	0.0240	0.0299	0.0338	0.0386	0.0454	0.0509	0.0581	0.0634	0.0644	0.0680	0.0729	0.0652	0.0677	0.0831
92	0.0175	0.0194	0.0260	0.0325	0.0366	0.0421	0.0481	0.0533	0.0614	0.0675	0.0670	0.0696	0.0749	0.0591	0.0613	0.0847
94	0.0203	0.0239	0.0324	0.0410	0.0463	0.0532	0.0608	0.0675	0.0768	0.0834	0.0846	0.0900	0.0961	0.0877	0.0919	0.1102
96	0.0240	0.0277	0.0361	0.0449	0.0505	0.0580	0.0650	0.0717	0.0821	0.0892	0.0899	0.0950	0.1013	0.0896	0.0932	0.1147
98	0.0268	0.0320	0.0415	0.0502	0.0562	0.0639	0.0714	0.0781	0.0873	0.0941	0.0962	0.1029	0.1091	0.1059	0.1116	0.1249
100	0.0339	0.0382	0.0460	0.0540	0.0585	0.0655	0.0724	0.0787	0.0872	0.0935	0.0950	0.1017	0.1071	0.1042	0.1100	0.1221

Depth (cm)	[400nm]	[420nm]	[440nm]	[460nm]	[480nm]	[500nm]	[520nm]	[540nm]	[560nm]	[580nm]	[600nm]	[620nm]	[640nm]	[660nm]	[680nm]	[700nm]
102	0.0331	0.0343	0.0393	0.0444	0.0475	0.0520	0.0561	0.0593	0.0647	0.0687	0.0696	0.0741	0.0782	0.0753	0.0790	0.0890
104	0.0382	0.0406	0.0479	0.0546	0.0585	0.0647	0.0725	0.0794	0.0877	0.0930	0.0922	0.0964	0.1016	0.0930	0.0970	0.1119
106	0.0539	0.0564	0.0632	0.0713	0.0755	0.0827	0.0906	0.0981	0.1078	0.1149	0.1150	0.1211	0.1271	0.1173	0.1211	0.1401
108	0.0566	0.0587	0.0676	0.0769	0.0821	0.0907	0.0989	0.1060	0.1157	0.1228	0.1220	0.1282	0.1360	0.1271	0.1324	0.1508
110	0.0504	0.0525	0.0604	0.0668	0.0694	0.0766	0.0870	0.0970	0.1075	0.1145	0.1136	0.1175	0.1251	0.1156	0.1195	0.1389
112	0.0777	0.0791	0.0883	0.0992	0.1050	0.1148	0.1247	0.1337	0.1451	0.1532	0.1535	0.1615	0.1697	0.1619	0.1688	0.1877
114	0.0525	0.0543	0.0615	0.0683	0.0716	0.0785	0.0877	0.0955	0.1045	0.1109	0.1116	0.1170	0.1236	0.1183	0.1228	0.1378
116	0.0660	0.0672	0.0739	0.0815	0.0844	0.0920	0.1018	0.1114	0.1219	0.1285	0.1276	0.1326	0.1403	0.1328	0.1384	0.1539
118	0.0689	0.0690	0.0771	0.0857	0.0897	0.0975	0.1060	0.1137	0.1245	0.1315	0.1299	0.1349	0.1412	0.1265	0.1309	0.1526
120	0.0620	0.0646	0.0736	0.0831	0.0884	0.0964	0.1056	0.1137	0.1237	0.1307	0.1299	0.1352	0.1434	0.1321	0.1370	0.1587
122	0.0515	0.0540	0.0615	0.0691	0.0733	0.0800	0.0859	0.0914	0.0993	0.1051	0.1056	0.1117	0.1177	0.1117	0.1173	0.1318
124	0.0352	0.0382	0.0453	0.0517	0.0556	0.0616	0.0672	0.0725	0.0798	0.0852	0.0863	0.0924	0.0973	0.0925	0.0977	0.1101
126	0.0308	0.0346	0.0415	0.0483	0.0518	0.0581	0.0662	0.0730	0.0815	0.0877	0.0890	0.0952	0.1005	0.0943	0.0999	0.1145
128	0.0396	0.0415	0.0475	0.0535	0.0567	0.0618	0.0673	0.0719	0.0784	0.0835	0.0828	0.0869	0.0921	0.0839	0.0878	0.1027
130	0.0347	0.0366	0.0431	0.0487	0.0517	0.0572	0.0640	0.0694	0.0763	0.0814	0.0812	0.0855	0.0904	0.0832	0.0866	0.1005
132	0.0374	0.0406	0.0482	0.0557	0.0605	0.0671	0.0738	0.0801	0.0885	0.0942	0.0953	0.1010	0.1065	0.1010	0.1060	0.1191
134	0.0434	0.0469	0.0550	0.0625	0.0671	0.0739	0.0799	0.0856	0.0928	0.0983	0.0990	0.1046	0.1096	0.1058	0.1106	0.1228
136	0.0411	0.0443	0.0511	0.0576	0.0611	0.0673	0.0726	0.0770	0.0834	0.0880	0.0880	0.0926	0.0975	0.0935	0.0976	0.1078
138	0.0292	0.0315	0.0384	0.0447	0.0484	0.0538	0.0599	0.0645	0.0706	0.0750	0.0748	0.0784	0.0827	0.0768	0.0805	0.0913
140	0.0236	0.0273	0.0346	0.0412	0.0447	0.0511	0.0593	0.0665	0.0748	0.0805	0.0811	0.0861	0.0909	0.0850	0.0902	0.1022
142	0.0269	0.0300	0.0383	0.0461	0.0513	0.0581	0.0667	0.0742	0.0830	0.0891	0.0888	0.0928	0.0979	0.0852	0.0898	0.1095
144	0.0249	0.0281	0.0356	0.0420	0.0458	0.0522	0.0607	0.0685	0.0768	0.0822	0.0823	0.0869	0.0923	0.0850	0.0904	0.1045
146	0.0354	0.0396	0.0480	0.0559	0.0609	0.0683	0.0770	0.0848	0.0943	0.1010	0.1017	0.1073	0.1135	0.1056	0.1113	0.1285
148	0.0322	0.0345	0.0405	0.0472	0.0516	0.0573	0.0633	0.0686	0.0753	0.0805	0.0801	0.0840	0.0906	0.0850	0.0889	0.1043
150	0.0167	0.0198	0.0269	0.0330	0.0373	0.0429	0.0492	0.0543	0.0605	0.0653	0.0655	0.0691	0.0744	0.0692	0.0740	0.0857
152	0.0453	0.0474	0.0555	0.0635	0.0678	0.0747	0.0841	0.0919	0.1015	0.1085	0.1075	0.1119	0.1176	0.1041	0.1090	0.1287
154	0.0336	0.0366	0.0451	0.0529	0.0582	0.0654	0.0745	0.0821	0.0910	0.0971	0.0968	0.1013	0.1076	0.0974	0.1036	0.1219
156	0.0310	0.0337	0.0408	0.0481	0.0528	0.0596	0.0683	0.0756	0.0836	0.0892	0.0883	0.0918	0.0989	0.0899	0.0950	0.1126
158	0.0452	0.0488	0.0579	0.0673	0.0735	0.0820	0.0898	0.0976	0.1074	0.1147	0.1162	0.1239	0.1304	0.1250	0.1325	0.1477
160	0.0414	0.0446	0.0526	0.0602	0.0650	0.0725	0.0809	0.0878	0.0969	0.1024	0.1033	0.1089	0.1142	0.1086	0.1141	0.1275
162	0.0332	0.0363	0.0443	0.0526	0.0581	0.0651	0.0730	0.0798	0.0886	0.0946	0.0949	0.0997	0.1052	0.0967	0.1019	0.1182
164	0.0391	0.0436	0.0532	0.0627	0.0693	0.0779	0.0869	0.0953	0.1060	0.1134	0.1148	0.1220	0.1296	0.1223	0.1301	0.1491
166	0.0447	0.0500	0.0612	0.0726	0.0797	0.0894	0.0997	0.1092	0.1211	0.1291	0.1307	0.1388	0.1463	0.1383	0.1467	0.1663
168	0.0420	0.0469	0.0583	0.0689	0.0759	0.0853	0.0951	0.1040	0.1154	0.1234	0.1248	0.1320	0.1397	0.1310	0.1378	0.1591
170	0.0556	0.0587	0.0690	0.0789	0.0855	0.0936	0.1017	0.1092	0.1187	0.1256	0.1259	0.1324	0.1388	0.1307	0.1377	0.1550
172	0.0478	0.0512	0.0616	0.0715	0.0773	0.0854	0.0944	0.1023	0.1134	0.1207	0.1204	0.1263	0.1328	0.1202	0.1273	0.1478
174	0.0363	0.0405	0.0513	0.0617	0.0684	0.0770	0.0851	0.0929	0.1038	0.1116	0.1126	0.1193	0.1264	0.1162	0.1237	0.1432
176	0.0403	0.0438	0.0529	0.0615	0.0669	0.0739	0.0806	0.0861	0.0939	0.0994	0.0997	0.1048	0.1097	0.1034	0.1094	0.1212
178	0.0347	0.0385	0.0479	0.0577	0.0638	0.0716	0.0820	0.0905	0.1006	0.1077	0.1073	0.1125	0.1196	0.1080	0.1138	0.1350
180	0.0451	0.0479	0.0552	0.0627	0.0669	0.0734	0.0787	0.0837	0.0908	0.0960	0.0966	0.1023	0.1078	0.1046	0.1113	0.1224
182	0.0466	0.0491	0.0570	0.0643	0.0693	0.0759	0.0823	0.0879	0.0955	0.1010	0.1017	0.1073	0.1129	0.1088	0.1154	0.1268
184	0.0344	0.0372	0.0447	0.0526	0.0578	0.0643	0.0716	0.0778	0.0858	0.0914	0.0921	0.0976	0.1035	0.0984	0.1051	0.1188
186	0.0362	0.0379	0.0453	0.0523	0.0568	0.0633	0.0701	0.0763	0.0837	0.0888	0.0878	0.0917	0.0970	0.0893	0.0945	0.1083
188	0.0369	0.0393	0.0475	0.0553	0.0610	0.0686	0.0778	0.0854	0.0941	0.1001	0.1004	0.1051	0.1118	0.1037	0.1094	0.1265
190	0.0511	0.0549	0.0621	0.0698	0.0746	0.0818	0.0893	0.0957	0.1038	0.1093	0.1095	0.1147	0.1206	0.1152	0.1216	0.1344
192	0.0300	0.0322	0.0405	0.0477	0.0532	0.0598	0.0687	0.0761	0.0844	0.0900	0.0895	0.0932	0.1000	0.0912	0.0973	0.1142
194	0.0221	0.0247	0.0321	0.0394	0.0444	0.0502	0.0576	0.0639	0.0715	0.0768	0.0761	0.0789	0.0842	0.0723	0.0761	0.0956
196	0.0218	0.0250	0.0329	0.0405	0.0454	0.0521	0.0595	0.0658	0.0737	0.0791	0.0788	0.0828	0.0884	0.0794	0.0839	0.1008
198	0.0335	0.0366	0.0437	0.0507	0.0552	0.0610	0.0661	0.0709	0.0780	0.0835	0.0852	0.0913	0.0968	0.0932	0.0990	0.1112
200	0.0441	0.0455	0.0527	0.0596	0.0635	0.0692	0.0750	0.0792	0.0859	0.0911	0.0914	0.0964	0.1011	0.0945	0.1000	0.1133

Depth (cm)	[400nm]	[420nm]	[440nm]	[460nm]	[480nm]	[500nm]	[520nm]	[540nm]	[560nm]	[580nm]	[600nm]	[620nm]	[640nm]	[660nm]	[680nm]	[700nm]
202	0.0261	0.0284	0.0376	0.0470	0.0528	0.0586	0.0658	0.0713	0.0799	0.0868	0.0851	0.0884	0.0944	0.0752	0.0802	0.1074
204	0.0238	0.0276	0.0361	0.0435	0.0490	0.0556	0.0618	0.0673	0.0749	0.0808	0.0823	0.0879	0.0938	0.0881	0.0936	0.1083
206	0.0205	0.0246	0.0331	0.0401	0.0449	0.0515	0.0602	0.0678	0.0765	0.0832	0.0850	0.0908	0.0968	0.0906	0.0959	0.1119
208	0.0183	0.0205	0.0242	0.0280	0.0304	0.0339	0.0372	0.0400	0.0445	0.0479	0.0485	0.0515	0.0540	0.0491	0.0511	0.0595
210	0.0233	0.0259	0.0314	0.0361	0.0398	0.0448	0.0491	0.0534	0.0599	0.0646	0.0662	0.0712	0.0758	0.0723	0.0768	0.0876
212	0.0237	0.0261	0.0323	0.0380	0.0416	0.0466	0.0519	0.0567	0.0632	0.0683	0.0698	0.0750	0.0800	0.0768	0.0811	0.0927
214	0.0224	0.0260	0.0340	0.0417	0.0465	0.0533	0.0607	0.0677	0.0764	0.0834	0.0852	0.0919	0.0981	0.0912	0.0972	0.1145
216	0.0272	0.0318	0.0410	0.0499	0.0557	0.0635	0.0721	0.0799	0.0897	0.0974	0.0997	0.1070	0.1138	0.1076	0.1138	0.1316
218	0.0364	0.0387	0.0453	0.0508	0.0536	0.0595	0.0666	0.0730	0.0811	0.0872	0.0890	0.0948	0.0997	0.0966	0.1014	0.1118
220	0.0737	0.0756	0.0808	0.0864	0.0881	0.0938	0.0977	0.1009	0.1077	0.1120	0.1114	0.1170	0.1202	0.1160	0.1211	0.1281
222	0.0316	0.0356	0.0443	0.0519	0.0558	0.0635	0.0732	0.0820	0.0920	0.0994	0.1012	0.1086	0.1152	0.1092	0.1166	0.1330
224	0.0290	0.0330	0.0415	0.0489	0.0527	0.0598	0.0690	0.0770	0.0866	0.0934	0.0954	0.1027	0.1090	0.1040	0.1118	0.1265
226	0.0302	0.0340	0.0421	0.0491	0.0527	0.0592	0.0676	0.0750	0.0838	0.0901	0.0920	0.0984	0.1042	0.0999	0.1074	0.1206
228	0.0336	0.0358	0.0417	0.0468	0.0495	0.0547	0.0605	0.0657	0.0727	0.0784	0.0800	0.0862	0.0910	0.0877	0.0935	0.1035
230	0.0253	0.0283	0.0352	0.0413	0.0449	0.0502	0.0557	0.0609	0.0678	0.0727	0.0737	0.0786	0.0828	0.0771	0.0821	0.0939
232	0.0300	0.0351	0.0451	0.0540	0.0593	0.0678	0.0768	0.0856	0.0966	0.1039	0.1059	0.1132	0.1201	0.1143	0.1220	0.1380
234	0.0342	0.0382	0.0475	0.0565	0.0619	0.0689	0.0753	0.0811	0.0889	0.0951	0.0958	0.1007	0.1065	0.0993	0.1045	0.1195
236	0.0276	0.0320	0.0410	0.0486	0.0526	0.0600	0.0697	0.0785	0.0888	0.0959	0.0980	0.1052	0.1123	0.1079	0.1157	0.1317
238	0.0391	0.0424	0.0523	0.0613	0.0664	0.0735	0.0816	0.0884	0.0977	0.1047	0.1056	0.1116	0.1180	0.1087	0.1154	0.1351
240	0.0416	0.0457	0.0568	0.0675	0.0746	0.0832	0.0902	0.0966	0.1062	0.1136	0.1143	0.1210	0.1291	0.1201	0.1274	0.1482
242	0.0425	0.0468	0.0577	0.0681	0.0753	0.0839	0.0915	0.0988	0.1086	0.1160	0.1167	0.1237	0.1321	0.1235	0.1312	0.1514
244	0.0401	0.0437	0.0536	0.0632	0.0692	0.0767	0.0827	0.0885	0.0975	0.1043	0.1055	0.1128	0.1201	0.1131	0.1209	0.1387
246	0.0304	0.0348	0.0457	0.0557	0.0611	0.0701	0.0830	0.0942	0.1071	0.1164	0.1170	0.1237	0.1315	0.1148	0.1224	0.1509
248	0.0371	0.0426	0.0542	0.0652	0.0715	0.0811	0.0922	0.1020	0.1143	0.1228	0.1243	0.1331	0.1423	0.1336	0.1434	0.1655
250	0.0483	0.0528	0.0654	0.0787	0.0862	0.0968	0.1097	0.1209	0.1354	0.1457	0.1459	0.1542	0.1633	0.1438	0.1536	0.1855
252	0.0358	0.0400	0.0512	0.0626	0.0701	0.0789	0.0889	0.0973	0.1093	0.1182	0.1186	0.1254	0.1339	0.1150	0.1222	0.1539
254	0.0336	0.0369	0.0465	0.0559	0.0615	0.0694	0.0796	0.0887	0.1000	0.1088	0.1093	0.1150	0.1224	0.1050	0.1107	0.1400
256	0.0469	0.0512	0.0629	0.0739	0.0809	0.0904	0.0998	0.1090	0.1210	0.1298	0.1314	0.1403	0.1495	0.1402	0.1503	0.1730
258	0.0496	0.0528	0.0615	0.0698	0.0732	0.0812	0.0928	0.1033	0.1145	0.1225	0.1233	0.1303	0.1383	0.1307	0.1386	0.1574
260	0.0294	0.0338	0.0442	0.0536	0.0596	0.0680	0.0772	0.0853	0.0961	0.1040	0.1056	0.1127	0.1205	0.1101	0.1182	0.1395
262	0.0259	0.0311	0.0420	0.0519	0.0583	0.0673	0.0791	0.0895	0.1021	0.1109	0.1128	0.1202	0.1291	0.1165	0.1260	0.1510
264	0.0286	0.0320	0.0402	0.0484	0.0535	0.0597	0.0692	0.0774	0.0871	0.0938	0.0933	0.0963	0.1023	0.0873	0.0909	0.1138
266	0.0220	0.0267	0.0368	0.0466	0.0526	0.0610	0.0730	0.0836	0.0959	0.1042	0.1045	0.1100	0.1179	0.1021	0.1083	0.1360
268	0.0316	0.0374	0.0491	0.0601	0.0670	0.0762	0.0877	0.0976	0.1103	0.1191	0.1212	0.1289	0.1379	0.1253	0.1347	0.1616
270	0.0330	0.0376	0.0477	0.0572	0.0628	0.0716	0.0812	0.0901	0.1012	0.1093	0.1115	0.1192	0.1274	0.1202	0.1287	0.1497
272	0.0360	0.0423	0.0543	0.0651	0.0719	0.0818	0.0930	0.1031	0.1154	0.1241	0.1262	0.1344	0.1433	0.1343	0.1434	0.1660
274	0.0405	0.0460	0.0587	0.0717	0.0797	0.0904	0.1015	0.1116	0.1255	0.1353	0.1371	0.1464	0.1565	0.1431	0.1527	0.1811
276	0.0391	0.0435	0.0545	0.0648	0.0712	0.0803	0.0909	0.1000	0.1114	0.1195	0.1200	0.1267	0.1352	0.1244	0.1318	0.1538
278	0.0323	0.0369	0.0472	0.0579	0.0644	0.0733	0.0837	0.0927	0.1045	0.1132	0.1138	0.1206	0.1293	0.1158	0.1240	0.1500
280	0.0312	0.0361	0.0465	0.0560	0.0612	0.0699	0.0824	0.0932	0.1058	0.1146	0.1160	0.1231	0.1309	0.1174	0.1257	0.1502
282	0.0230	0.0266	0.0354	0.0430	0.0475	0.0544	0.0630	0.0700	0.0791	0.0854	0.0869	0.0927	0.0994	0.0936	0.1005	0.1167
284	0.0294	0.0334	0.0436	0.0538	0.0602	0.0682	0.0785	0.0867	0.0977	0.1055	0.1052	0.1102	0.1184	0.1023	0.1086	0.1374
286	0.0351	0.0398	0.0488	0.0587	0.0650	0.0734	0.0845	0.0933	0.1042	0.1115	0.1118	0.1172	0.1249	0.1130	0.1190	0.1422
288	0.0311	0.0352	0.0461	0.0565	0.0635	0.0721	0.0807	0.0882	0.0981	0.1057	0.1060	0.1118	0.1188	0.1066	0.1146	0.1355
290	0.0349	0.0403	0.0506	0.0600	0.0659	0.0744	0.0846	0.0935	0.1044	0.1120	0.1131	0.1196	0.1282	0.1197	0.1264	0.1482
292	0.0465	0.0520	0.0655	0.0786	0.0863	0.0972	0.1104	0.1220	0.1365	0.1467	0.1477	0.1561	0.1656	0.1497	0.1596	0.1897
294	0.0309	0.0361	0.0461	0.0551	0.0602	0.0689	0.0809	0.0917	0.1035	0.1119	0.1136	0.1205	0.1286	0.1220	0.1294	0.1482
296	0.0398	0.0442	0.0552	0.0667	0.0730	0.0821	0.0932	0.1023	0.1145	0.1230	0.1228	0.1289	0.1373	0.1197	0.1269	0.1562
298	0.0294	0.0339	0.0432	0.0521	0.0579	0.0655	0.0741	0.0815	0.0914	0.0983	0.1000	0.1067	0.1138	0.1071	0.1144	0.1329
300	0.0347	0.0380	0.0463	0.0547	0.0599	0.0671	0.0749	0.0820	0.0910	0.0969	0.0968	0.1021	0.1090	0.1018	0.1085	0.1249

Depth (cm)	[400nm]	[420nm]	[440nm]	[460nm]	[480nm]	[500nm]	[520nm]	[540nm]	[560nm]	[580nm]	[600nm]	[620nm]	[640nm]	[660nm]	[680nm]	[700nm]
302	0.0439	0.0481	0.0586	0.0695	0.0762	0.0849	0.0961	0.1056	0.1178	0.1263	0.1263	0.1321	0.1400	0.1226	0.1292	0.1587
304	0.0284	0.0328	0.0411	0.0492	0.0544	0.0610	0.0680	0.0747	0.0832	0.0897	0.0912	0.0973	0.1039	0.0992	0.1053	0.1215
306	0.0355	0.0393	0.0475	0.0553	0.0599	0.0671	0.0753	0.0830	0.0917	0.0978	0.0975	0.1017	0.1094	0.1008	0.1067	0.1260
308	0.0217	0.0235	0.0297	0.0355	0.0395	0.0443	0.0520	0.0584	0.0664	0.0722	0.0706	0.0718	0.0765	0.0612	0.0633	0.0853
310	0.0484	0.0506	0.0574	0.0639	0.0677	0.0736	0.0785	0.0831	0.0902	0.0949	0.0951	0.1001	0.1053	0.1010	0.1068	0.1174
312	0.0171	0.0203	0.0265	0.0319	0.0342	0.0397	0.0496	0.0585	0.0673	0.0729	0.0727	0.0759	0.0821	0.0755	0.0808	0.0953
314	0.0148	0.0180	0.0254	0.0322	0.0364	0.0419	0.0501	0.0563	0.0644	0.0702	0.0701	0.0736	0.0788	0.0668	0.0709	0.0907
316	0.0124	0.0151	0.0211	0.0262	0.0300	0.0342	0.0392	0.0429	0.0479	0.0516	0.0517	0.0543	0.0585	0.0537	0.0573	0.0676
318	0.0248	0.0269	0.0319	0.0363	0.0388	0.0426	0.0461	0.0491	0.0533	0.0561	0.0559	0.0586	0.0617	0.0578	0.0608	0.0687
320	0.0206	0.0238	0.0304	0.0366	0.0407	0.0460	0.0527	0.0583	0.0651	0.0697	0.0700	0.0741	0.0789	0.0744	0.0798	0.0906
322	0.0270	0.0298	0.0366	0.0439	0.0480	0.0544	0.0631	0.0701	0.0784	0.0838	0.0836	0.0877	0.0932	0.0850	0.0903	0.1056
324	0.0216	0.0243	0.0305	0.0369	0.0413	0.0469	0.0540	0.0601	0.0670	0.0721	0.0722	0.0755	0.0806	0.0747	0.0795	0.0923
326	0.0183	0.0209	0.0279	0.0338	0.0378	0.0435	0.0527	0.0603	0.0684	0.0736	0.0729	0.0756	0.0809	0.0715	0.0760	0.0922
328	0.0161	0.0192	0.0251	0.0307	0.0344	0.0394	0.0471	0.0540	0.0614	0.0660	0.0648	0.0667	0.0711	0.0599	0.0628	0.0793
330	0.0157	0.0192	0.0263	0.0333	0.0380	0.0439	0.0506	0.0565	0.0632	0.0680	0.0677	0.0709	0.0762	0.0701	0.0746	0.0872
332	0.0195	0.0235	0.0312	0.0381	0.0427	0.0491	0.0561	0.0626	0.0692	0.0744	0.0744	0.0784	0.0851	0.0818	0.0873	0.0995
334	0.0264	0.0302	0.0395	0.0483	0.0538	0.0613	0.0711	0.0795	0.0890	0.0959	0.0954	0.0993	0.1066	0.0950	0.1012	0.1223
336	0.0270	0.0299	0.0381	0.0457	0.0504	0.0569	0.0656	0.0730	0.0815	0.0874	0.0871	0.0907	0.0973	0.0867	0.0921	0.1115
338	0.0220	0.0256	0.0345	0.0423	0.0473	0.0545	0.0635	0.0711	0.0803	0.0862	0.0865	0.0911	0.0969	0.0890	0.0952	0.1108
340	0.0249	0.0296	0.0388	0.0477	0.0527	0.0607	0.0717	0.0811	0.0919	0.0988	0.0986	0.1031	0.1099	0.0967	0.1039	0.1264
342	0.0214	0.0263	0.0349	0.0422	0.0468	0.0540	0.0649	0.0745	0.0847	0.0921	0.0942	0.1006	0.1074	0.1020	0.1097	0.1259
344	0.0288	0.0342	0.0456	0.0561	0.0625	0.0716	0.0840	0.0952	0.1075	0.1164	0.1177	0.1247	0.1335	0.1219	0.1311	0.1549
346	0.0222	0.0278	0.0387	0.0485	0.0547	0.0630	0.0737	0.0829	0.0939	0.1020	0.1041	0.1114	0.1190	0.1101	0.1188	0.1401
348	0.0232	0.0288	0.0408	0.0521	0.0590	0.0683	0.0809	0.0919	0.1048	0.1141	0.1151	0.1221	0.1310	0.1156	0.1259	0.1536
350	0.0369	0.0394	0.0474	0.0547	0.0587	0.0649	0.0732	0.0806	0.0894	0.0962	0.0970	0.1028	0.1089	0.0999	0.1065	0.1247
352	0.0254	0.0292	0.0385	0.0470	0.0521	0.0597	0.0697	0.0782	0.0881	0.0952	0.0957	0.1009	0.1078	0.0957	0.1020	0.1247
354	0.0218	0.0257	0.0333	0.0408	0.0456	0.0520	0.0589	0.0649	0.0726	0.0782	0.0785	0.0827	0.0883	0.0809	0.0863	0.1017
356	0.0152	0.0191	0.0268	0.0334	0.0378	0.0438	0.0519	0.0586	0.0662	0.0714	0.0720	0.0761	0.0816	0.0759	0.0811	0.0949
358	0.0140	0.0173	0.0247	0.0322	0.0370	0.0430	0.0516	0.0588	0.0678	0.0745	0.0736	0.0765	0.0825	0.0664	0.0711	0.0961
360	0.0159	0.0183	0.0244	0.0296	0.0331	0.0380	0.0453	0.0513	0.0578	0.0628	0.0628	0.0660	0.0715	0.0652	0.0701	0.0837
362	0.0221	0.0252	0.0338	0.0421	0.0475	0.0539	0.0631	0.0706	0.0799	0.0863	0.0843	0.0868	0.0932	0.0765	0.0814	0.1066
364	0.0208	0.0239	0.0322	0.0397	0.0440	0.0503	0.0603	0.0687	0.0788	0.0857	0.0838	0.0864	0.0927	0.0758	0.0809	0.1060
366	0.0388	0.0425	0.0517	0.0604	0.0651	0.0731	0.0834	0.0922	0.1028	0.1104	0.1105	0.1161	0.1229	0.1102	0.1172	0.1399
368	0.0204	0.0253	0.0344	0.0425	0.0471	0.0545	0.0645	0.0732	0.0832	0.0903	0.0916	0.0974	0.1046	0.0972	0.1052	0.1232
370	0.0210	0.0259	0.0363	0.0454	0.0509	0.0586	0.0692	0.0785	0.0895	0.0978	0.0984	0.1040	0.1118	0.0984	0.1062	0.1314
372	0.0179	0.0223	0.0319	0.0409	0.0465	0.0534	0.0627	0.0704	0.0799	0.0868	0.0874	0.0924	0.0994	0.0887	0.0959	0.1168
374	0.0216	0.0259	0.0341	0.0421	0.0468	0.0536	0.0635	0.0718	0.0818	0.0889	0.0899	0.0955	0.1021	0.0918	0.0982	0.1198
376	0.0174	0.0211	0.0284	0.0347	0.0386	0.0441	0.0521	0.0587	0.0668	0.0726	0.0736	0.0780	0.0836	0.0763	0.0813	0.0978
378	0.0225	0.0254	0.0315	0.0379	0.0415	0.0466	0.0535	0.0593	0.0663	0.0715	0.0720	0.0762	0.0812	0.0753	0.0801	0.0936
380	0.0333	0.0358	0.0417	0.0479	0.0509	0.0562	0.0622	0.0673	0.0744	0.0791	0.0792	0.0830	0.0879	0.0804	0.0845	0.1003
382	0.0469	0.0492	0.0554	0.0618	0.0647	0.0702	0.0756	0.0803	0.0868	0.0916	0.0913	0.0956	0.1012	0.0957	0.1009	0.1136
384	0.0291	0.0319	0.0379	0.0435	0.0468	0.0516	0.0567	0.0613	0.0677	0.0722	0.0723	0.0761	0.0809	0.0754	0.0800	0.0928
386	0.0281	0.0295	0.0349	0.0405	0.0437	0.0478	0.0530	0.0573	0.0632	0.0672	0.0666	0.0688	0.0732	0.0645	0.0679	0.0831
388	0.0277	0.0304	0.0364	0.0426	0.0462	0.0516	0.0575	0.0625	0.0691	0.0743	0.0749	0.0789	0.0848	0.0789	0.0844	0.0989
390	0.0161	0.0183	0.0236	0.0284	0.0313	0.0358	0.0408	0.0452	0.0511	0.0555	0.0560	0.0593	0.0646	0.0594	0.0634	0.0770
392	0.0130	0.0166	0.0224	0.0273	0.0304	0.0353	0.0420	0.0479	0.0551	0.0605	0.0620	0.0665	0.0716	0.0668	0.0722	0.0855
394	0.0190	0.0225	0.0282	0.0332	0.0362	0.0412	0.0468	0.0523	0.0597	0.0650	0.0673	0.0728	0.0783	0.0760	0.0823	0.0947
396	0.0144	0.0173	0.0227	0.0278	0.0313	0.0357	0.0404	0.0447	0.0507	0.0551	0.0567	0.0610	0.0656	0.0614	0.0663	0.0800
398	0.0282	0.0306	0.0356	0.0397	0.0423	0.0468	0.0513	0.0554	0.0617	0.0660	0.0672	0.0714	0.0759	0.0727	0.0776	0.0895
400	0.0158	0.0181	0.0228	0.0263	0.0284	0.0318	0.0356	0.0388	0.0437	0.0476	0.0491	0.0535	0.0575	0.0578	0.0635	0.0714

Depth (cm)	[400nm]	[420nm]	[440nm]	[460nm]	[480nm]	[500nm]	[520nm]	[540nm]	[560nm]	[580nm]	[600nm]	[620nm]	[640nm]	[660nm]	[680nm]	[700nm]
402	0.0252	0.0277	0.0344	0.0405	0.0434	0.0487	0.0572	0.0648	0.0734	0.0796	0.0803	0.0848	0.0906	0.0817	0.0873	0.1059
404	0.0367	0.0398	0.0461	0.0520	0.0551	0.0608	0.0673	0.0733	0.0812	0.0867	0.0882	0.0938	0.0993	0.0959	0.1027	0.1152
406	0.0086	0.0119	0.0176	0.0221	0.0246	0.0293	0.0365	0.0429	0.0495	0.0540	0.0546	0.0581	0.0621	0.0591	0.0635	0.0724
408	0.0125	0.0159	0.0214	0.0271	0.0301	0.0351	0.0416	0.0472	0.0533	0.0573	0.0573	0.0599	0.0636	0.0584	0.0619	0.0718
410	0.0374	0.0401	0.0470	0.0529	0.0563	0.0620	0.0678	0.0730	0.0798	0.0839	0.0842	0.0882	0.0926	0.0889	0.0933	0.1026
412	0.0190	0.0224	0.0304	0.0372	0.0418	0.0480	0.0558	0.0628	0.0710	0.0766	0.0764	0.0797	0.0857	0.0754	0.0802	0.0987
414	0.0215	0.0250	0.0324	0.0395	0.0440	0.0501	0.0580	0.0646	0.0719	0.0770	0.0772	0.0813	0.0868	0.0811	0.0867	0.0992
416	0.0214	0.0240	0.0302	0.0357	0.0387	0.0445	0.0543	0.0630	0.0712	0.0769	0.0767	0.0802	0.0860	0.0784	0.0839	0.0983
418	0.0201	0.0239	0.0308	0.0371	0.0404	0.0468	0.0575	0.0666	0.0755	0.0813	0.0816	0.0855	0.0913	0.0839	0.0894	0.1037
420	0.0340	0.0373	0.0444	0.0513	0.0554	0.0613	0.0687	0.0744	0.0816	0.0863	0.0852	0.0880	0.0921	0.0820	0.0860	0.1000
422	0.0229	0.0282	0.0370	0.0452	0.0502	0.0578	0.0688	0.0782	0.0885	0.0954	0.0971	0.1029	0.1109	0.1061	0.1136	0.1295
424	0.0286	0.0332	0.0417	0.0509	0.0561	0.0640	0.0735	0.0817	0.0905	0.0975	0.0972	0.1023	0.1118	0.1048	0.1118	0.1310
426	0.0268	0.0309	0.0394	0.0472	0.0518	0.0592	0.0676	0.0744	0.0819	0.0872	0.0864	0.0904	0.0983	0.0939	0.1003	0.1132
428	0.0312	0.0355	0.0447	0.0532	0.0576	0.0658	0.0781	0.0882	0.0975	0.1041	0.1032	0.1077	0.1196	0.1165	0.1246	0.1409
430	0.0213	0.0244	0.0315	0.0377	0.0420	0.0482	0.0548	0.0604	0.0653	0.0694	0.0667	0.0680	0.0790	0.0757	0.0811	0.0947
432	0.0394	0.0409	0.0474	0.0535	0.0565	0.0621	0.0690	0.0742	0.0798	0.0836	0.0810	0.0827	0.0897	0.0839	0.0882	0.1010
434	0.0286	0.0308	0.0364	0.0425	0.0454	0.0507	0.0588	0.0651	0.0720	0.0763	0.0744	0.0761	0.0823	0.0745	0.0783	0.0927
436	0.0225	0.0250	0.0317	0.0375	0.0409	0.0462	0.0547	0.0619	0.0696	0.0748	0.0746	0.0777	0.0855	0.0786	0.0845	0.1010
438	0.0180	0.0211	0.0283	0.0356	0.0399	0.0465	0.0554	0.0625	0.0703	0.0759	0.0742	0.0765	0.0848	0.0752	0.0798	0.0993
440	0.0289	0.0325	0.0411	0.0485	0.0525	0.0600	0.0697	0.0781	0.0872	0.0933	0.0928	0.0974	0.1068	0.1019	0.1087	0.1248
442	0.0275	0.0315	0.0391	0.0460	0.0500	0.0565	0.0637	0.0696	0.0767	0.0817	0.0824	0.0874	0.0936	0.0940	0.1003	0.1084
444	0.0193	0.0229	0.0294	0.0357	0.0394	0.0458	0.0528	0.0589	0.0652	0.0699	0.0698	0.0731	0.0797	0.0783	0.0835	0.0930
446	0.0130	0.0159	0.0218	0.0265	0.0296	0.0347	0.0419	0.0477	0.0530	0.0569	0.0556	0.0566	0.0648	0.0609	0.0650	0.0771
448	0.0152	0.0189	0.0251	0.0305	0.0339	0.0391	0.0469	0.0532	0.0594	0.0639	0.0637	0.0666	0.0732	0.0708	0.0764	0.0860
450	0.0091	0.0116	0.0175	0.0230	0.0264	0.0307	0.0370	0.0420	0.0473	0.0515	0.0508	0.0527	0.0588	0.0514	0.0552	0.0691
452	0.0274	0.0310	0.0373	0.0433	0.0467	0.0530	0.0608	0.0673	0.0743	0.0794	0.0790	0.0826	0.0904	0.0870	0.0923	0.1048
454	0.0292	0.0340	0.0416	0.0481	0.0518	0.0589	0.0684	0.0767	0.0854	0.0916	0.0923	0.0980	0.1065	0.1064	0.1144	0.1252
456	0.0206	0.0255	0.0340	0.0412	0.0454	0.0530	0.0648	0.0754	0.0865	0.0941	0.0972	0.1047	0.1120	0.1115	0.1205	0.1322
458	0.0324	0.0391	0.0488	0.0585	0.0655	0.0755	0.0842	0.0929	0.1045	0.1136	0.1183	0.1290	0.1381	0.1394	0.1512	0.1635
460	0.0260	0.0322	0.0420	0.0512	0.0581	0.0672	0.0756	0.0835	0.0939	0.1026	0.1070	0.1163	0.1246	0.1254	0.1357	0.1494
462	0.0440	0.0488	0.0578	0.0671	0.0727	0.0812	0.0888	0.0958	0.1059	0.1139	0.1170	0.1266	0.1341	0.1342	0.1447	0.1563
464	0.0351	0.0386	0.0455	0.0518	0.0551	0.0620	0.0705	0.0784	0.0880	0.0947	0.0973	0.1045	0.1105	0.1103	0.1182	0.1281
466	0.0322	0.0369	0.0449	0.0517	0.0551	0.0626	0.0740	0.0849	0.0962	0.1036	0.1070	0.1146	0.1207	0.1215	0.1297	0.1381
468	0.0267	0.0328	0.0427	0.0504	0.0562	0.0654	0.0778	0.0893	0.1023	0.1122	0.1176	0.1279	0.1367	0.1384	0.1493	0.1621
470	0.0271	0.0329	0.0413	0.0499	0.0562	0.0652	0.0730	0.0802	0.0902	0.0982	0.1023	0.1115	0.1192	0.1219	0.1319	0.1421
472	0.0261	0.0321	0.0420	0.0512	0.0586	0.0680	0.0762	0.0841	0.0946	0.1031	0.1073	0.1171	0.1256	0.1274	0.1376	0.1501
474	0.0238	0.0290	0.0382	0.0462	0.0513	0.0597	0.0710	0.0813	0.0929	0.1017	0.1060	0.1150	0.1234	0.1237	0.1338	0.1478
476	0.0193	0.0244	0.0322	0.0389	0.0437	0.0510	0.0595	0.0670	0.0764	0.0835	0.0873	0.0956	0.1029	0.1052	0.1141	0.1243
478	0.0219	0.0255	0.0333	0.0400	0.0443	0.0512	0.0605	0.0686	0.0778	0.0850	0.0880	0.0951	0.1023	0.1028	0.1113	0.1232
480	0.0251	0.0294	0.0376	0.0454	0.0510	0.0588	0.0666	0.0737	0.0829	0.0904	0.0939	0.1021	0.1095	0.1102	0.1195	0.1310
482	0.0172	0.0221	0.0308	0.0380	0.0427	0.0505	0.0607	0.0699	0.0806	0.0884	0.0923	0.1011	0.1088	0.1105	0.1203	0.1320
484	0.0138	0.0186	0.0258	0.0326	0.0367	0.0436	0.0524	0.0605	0.0699	0.0770	0.0807	0.0882	0.0952	0.0958	0.1042	0.1146
486	0.0149	0.0200	0.0268	0.0337	0.0394	0.0464	0.0533	0.0595	0.0680	0.0750	0.0792	0.0870	0.0943	0.0958	0.1044	0.1150
488	0.0229	0.0265	0.0334	0.0398	0.0441	0.0504	0.0581	0.0646	0.0724	0.0785	0.0805	0.0869	0.0931	0.0925	0.0996	0.1103
490	0.0291	0.0337	0.0423	0.0503	0.0561	0.0645	0.0730	0.0807	0.0904	0.0981	0.1016	0.1098	0.1179	0.1187	0.1280	0.1404
492	0.0188	0.0235	0.0304	0.0370	0.0414	0.0486	0.0582	0.0670	0.0768	0.0845	0.0886	0.0966	0.1030	0.1055	0.1138	0.1214
494	0.0176	0.0223	0.0281	0.0344	0.0393	0.0459	0.0518	0.0579	0.0659	0.0723	0.0765	0.0847	0.0912	0.0950	0.1039	0.1121
496	0.0235	0.0268	0.0328	0.0385	0.0430	0.0494	0.0552	0.0611	0.0690	0.0756	0.0799	0.0882	0.0949	0.0993	0.1091	0.1182
498	0.0338	0.0346	0.0397	0.0461	0.0508	0.0574	0.0624	0.0680	0.0762	0.0828	0.0869	0.0965	0.1041	0.1083	0.1198	0.1340
500	0.0411	0.0445	0.0523	0.0610	0.0673	0.0757	0.0822	0.0892	0.0993	0.1079	0.1136	0.1257	0.1351	0.1407	0.1545	0.1694

Depth (cm)	[400nm]	[420nm]	[440nm]	[460nm]	[480nm]	[500nm]	[520nm]	[540nm]	[560nm]	[580nm]	[600nm]	[620nm]	[640nm]	[660nm]	[680nm]	[700nm]
502	0.0380	0.0409	0.0466	0.0523	0.0549	0.0602	0.0653	0.0700	0.0765	0.0815	0.0829	0.0885	0.0926	0.0910	0.0959	0.1035
504	0.0575	0.0622	0.0717	0.0808	0.0860	0.0941	0.1026	0.1096	0.1192	0.1265	0.1284	0.1362	0.1423	0.1368	0.1436	0.1573
506	0.1109	0.1175	0.1278	0.1375	0.1402	0.1489	0.1529	0.1573	0.1654	0.1705	0.1696	0.1771	0.1799	0.1797	0.1860	0.1867
508	0.1015	0.1076	0.1174	0.1264	0.1293	0.1370	0.1402	0.1442	0.1518	0.1566	0.1563	0.1636	0.1666	0.1669	0.1728	0.1733
510	0.0940	0.1032	0.1170	0.1293	0.1355	0.1471	0.1563	0.1664	0.1801	0.1892	0.1926	0.2044	0.2117	0.2147	0.2253	0.2292
512	0.1068	0.1112	0.1207	0.1300	0.1321	0.1411	0.1498	0.1595	0.1729	0.1814	0.1832	0.1932	0.1983	0.1998	0.2085	0.2100
514	0.0538	0.0569	0.0638	0.0716	0.0762	0.0842	0.0922	0.0999	0.1111	0.1202	0.1255	0.1376	0.1471	0.1527	0.1668	0.1800
516	0.0250	0.0290	0.0377	0.0455	0.0498	0.0586	0.0713	0.0825	0.0944	0.1037	0.1092	0.1207	0.1300	0.1368	0.1514	0.1645
518	0.0268	0.0303	0.0370	0.0430	0.0465	0.0516	0.0572	0.0618	0.0676	0.0719	0.0730	0.0774	0.0808	0.0810	0.0864	0.0912
520	0.0329	0.0379	0.0464	0.0551	0.0597	0.0671	0.0746	0.0811	0.0895	0.0954	0.0976	0.1041	0.1093	0.1101	0.1172	0.1246
522	0.0407	0.0447	0.0530	0.0603	0.0648	0.0713	0.0782	0.0844	0.0925	0.0981	0.1007	0.1074	0.1130	0.1153	0.1238	0.1314
524	0.0541	0.0580	0.0674	0.0757	0.0801	0.0878	0.0941	0.0999	0.1079	0.1136	0.1149	0.1224	0.1273	0.1282	0.1361	0.1442
526	0.0313	0.0371	0.0473	0.0557	0.0606	0.0691	0.0802	0.0898	0.1008	0.1090	0.1126	0.1217	0.1293	0.1311	0.1419	0.1550
528	0.0406	0.0468	0.0573	0.0669	0.0718	0.0822	0.0974	0.1114	0.1260	0.1362	0.1409	0.1523	0.1616	0.1648	0.1776	0.1921
530	0.0302	0.0337	0.0402	0.0460	0.0487	0.0544	0.0606	0.0663	0.0737	0.0789	0.0811	0.0879	0.0928	0.0952	0.1029	0.1101
532	0.0333	0.0388	0.0487	0.0574	0.0613	0.0707	0.0853	0.0993	0.1136	0.1235	0.1283	0.1391	0.1478	0.1509	0.1636	0.1774
534	0.0369	0.0428	0.0525	0.0610	0.0651	0.0744	0.0887	0.1019	0.1150	0.1244	0.1287	0.1385	0.1468	0.1494	0.1611	0.1742
536	0.0289	0.0337	0.0429	0.0509	0.0542	0.0625	0.0780	0.0931	0.1089	0.1195	0.1247	0.1348	0.1429	0.1466	0.1589	0.1715
538	0.0615	0.0669	0.0769	0.0863	0.0905	0.1005	0.1112	0.1220	0.1347	0.1434	0.1466	0.1570	0.1641	0.1665	0.1775	0.1878
540	0.0459	0.0529	0.0662	0.0780	0.0856	0.0960	0.1051	0.1132	0.1243	0.1324	0.1354	0.1452	0.1523	0.1541	0.1647	0.1757
542	0.0415	0.0489	0.0621	0.0738	0.0799	0.0917	0.1054	0.1182	0.1332	0.1439	0.1489	0.1614	0.1708	0.1738	0.1874	0.2022
544	0.0461	0.0531	0.0658	0.0783	0.0868	0.0984	0.1084	0.1178	0.1312	0.1420	0.1470	0.1598	0.1699	0.1720	0.1862	0.2031
546	0.0411	0.0486	0.0611	0.0727	0.0797	0.0910	0.1035	0.1153	0.1292	0.1398	0.1446	0.1562	0.1659	0.1677	0.1806	0.1972
548	0.0302	0.0370	0.0483	0.0583	0.0640	0.0736	0.0851	0.0953	0.1068	0.1157	0.1192	0.1280	0.1356	0.1363	0.1466	0.1593
550	0.0304	0.0379	0.0506	0.0621	0.0694	0.0799	0.0910	0.1010	0.1133	0.1219	0.1256	0.1353	0.1432	0.1439	0.1547	0.1679
552	0.0351	0.0407	0.0503	0.0592	0.0650	0.0729	0.0805	0.0874	0.0962	0.1027	0.1052	0.1121	0.1178	0.1184	0.1265	0.1354
554	0.0291	0.0353	0.0457	0.0546	0.0592	0.0689	0.0817	0.0938	0.1069	0.1157	0.1193	0.1283	0.1351	0.1361	0.1462	0.1576
556	0.0340	0.0403	0.0508	0.0608	0.0669	0.0767	0.0879	0.0981	0.1106	0.1199	0.1245	0.1350	0.1435	0.1453	0.1571	0.1712
558	0.0315	0.0386	0.0500	0.0612	0.0683	0.0790	0.0897	0.1001	0.1127	0.1225	0.1277	0.1391	0.1485	0.1514	0.1643	0.1792
560	0.0384	0.0452	0.0562	0.0664	0.0726	0.0832	0.0959	0.1077	0.1215	0.1315	0.1361	0.1472	0.1558	0.1577	0.1700	0.1828
562	0.0354	0.0388	0.0460	0.0525	0.0563	0.0628	0.0698	0.0762	0.0848	0.0916	0.0951	0.1034	0.1108	0.1129	0.1233	0.1363
564	0.0248	0.0278	0.0338	0.0389	0.0417	0.0469	0.0528	0.0579	0.0640	0.0680	0.0692	0.0735	0.0770	0.0772	0.0823	0.0875
566	0.0242	0.0280	0.0333	0.0385	0.0404	0.0453	0.0517	0.0575	0.0640	0.0681	0.0690	0.0733	0.0763	0.0767	0.0817	0.0841
568	0.0417	0.0447	0.0499	0.0544	0.0562	0.0609	0.0665	0.0719	0.0780	0.0817	0.0826	0.0870	0.0893	0.0899	0.0940	0.0957
570	0.0254	0.0312	0.0400	0.0467	0.0506	0.0576	0.0657	0.0729	0.0810	0.0869	0.0892	0.0949	0.0987	0.1000	0.1057	0.1086
572	0.0454	0.0517	0.0621	0.0708	0.0761	0.0855	0.0943	0.1022	0.1125	0.1200	0.1231	0.1316	0.1379	0.1396	0.1491	0.1577
574	0.0461	0.0525	0.0631	0.0725	0.0780	0.0884	0.1006	0.1116	0.1245	0.1343	0.1389	0.1492	0.1579	0.1598	0.1720	0.1860
576	0.0553	0.0608	0.0711	0.0809	0.0867	0.0972	0.1079	0.1177	0.1301	0.1393	0.1431	0.1535	0.1615	0.1637	0.1758	0.1887
578	0.0408	0.0468	0.0562	0.0656	0.0706	0.0807	0.0944	0.1073	0.1214	0.1313	0.1355	0.1446	0.1525	0.1538	0.1654	0.1779
580	0.0346	0.0405	0.0511	0.0609	0.0664	0.0765	0.0883	0.0990	0.1115	0.1207	0.1241	0.1340	0.1422	0.1434	0.1550	0.1684
582	0.0296	0.0345	0.0438	0.0519	0.0566	0.0650	0.0760	0.0859	0.0971	0.1054	0.1093	0.1177	0.1248	0.1264	0.1371	0.1493
584	0.0257	0.0312	0.0413	0.0502	0.0564	0.0654	0.0747	0.0831	0.0939	0.1022	0.1061	0.1154	0.1228	0.1248	0.1354	0.1475
586	0.0197	0.0263	0.0374	0.0467	0.0531	0.0628	0.0731	0.0826	0.0946	0.1040	0.1090	0.1185	0.1273	0.1294	0.1407	0.1550
588	0.0237	0.0296	0.0401	0.0484	0.0545	0.0632	0.0720	0.0796	0.0889	0.0960	0.0990	0.1058	0.1119	0.1122	0.1204	0.1305
590	0.0262	0.0327	0.0436	0.0531	0.0599	0.0700	0.0795	0.0885	0.0994	0.1080	0.1112	0.1195	0.1267	0.1268	0.1367	0.1496
592	0.0307	0.0375	0.0490	0.0596	0.0669	0.0786	0.0911	0.1030	0.1182	0.1298	0.1352	0.1467	0.1564	0.1563	0.1687	0.1848
594	0.0182	0.0246	0.0342	0.0429	0.0496	0.0594	0.0698	0.0796	0.0917	0.1014	0.1065	0.1161	0.1244	0.1258	0.1364	0.1499
596	0.0314	0.0367	0.0471	0.0562	0.0627	0.0731	0.0834	0.0929	0.1049	0.1142	0.1180	0.1266	0.1335	0.1333	0.1419	0.1537
598	0.0214	0.0277	0.0373	0.0454	0.0516	0.0610	0.0701	0.0787	0.0891	0.0975	0.1009	0.1085	0.1148	0.1147	0.1226	0.1327
600	0.0274	0.0335	0.0441	0.0534	0.0609	0.0704	0.0793	0.0876	0.0977	0.1055	0.1080	0.1153	0.1219	0.1211	0.1298	0.1423

Depth (cm)	[400nm]	[420nm]	[440nm]	[460nm]	[480nm]	[500nm]	[520nm]	[540nm]	[560nm]	[580nm]	[600nm]	[620nm]	[640nm]	[660nm]	[680nm]	[700nm]
602	0.0178	0.0239	0.0334	0.0417	0.0470	0.0561	0.0681	0.0799	0.0929	0.1030	0.1084	0.1179	0.1260	0.1277	0.1380	0.1505
604	0.0364	0.0434	0.0539	0.0632	0.0704	0.0809	0.0903	0.0990	0.1103	0.1190	0.1224	0.1311	0.1384	0.1383	0.1477	0.1589
606	0.0316	0.0382	0.0491	0.0588	0.0650	0.0753	0.0858	0.0959	0.1089	0.1187	0.1230	0.1333	0.1416	0.1420	0.1533	0.1680
608	0.0302	0.0359	0.0461	0.0553	0.0612	0.0710	0.0812	0.0910	0.1040	0.1143	0.1193	0.1298	0.1390	0.1412	0.1529	0.1676
610	0.0264	0.0333	0.0441	0.0532	0.0600	0.0705	0.0820	0.0928	0.1061	0.1167	0.1225	0.1332	0.1421	0.1443	0.1550	0.1684
612	0.0229	0.0297	0.0405	0.0504	0.0570	0.0677	0.0810	0.0939	0.1095	0.1218	0.1281	0.1397	0.1496	0.1506	0.1628	0.1782
614	0.0339	0.0403	0.0513	0.0605	0.0674	0.0772	0.0872	0.0964	0.1088	0.1187	0.1233	0.1334	0.1416	0.1424	0.1529	0.1660
616	0.0353	0.0417	0.0525	0.0627	0.0697	0.0803	0.0914	0.1015	0.1147	0.1249	0.1296	0.1398	0.1490	0.1469	0.1578	0.1746
618	0.0353	0.0416	0.0515	0.0608	0.0672	0.0773	0.0873	0.0971	0.1101	0.1206	0.1261	0.1371	0.1465	0.1471	0.1585	0.1741
620	0.0277	0.0340	0.0441	0.0531	0.0597	0.0702	0.0804	0.0906	0.1042	0.1149	0.1209	0.1321	0.1416	0.1429	0.1544	0.1687
622	0.0174	0.0229	0.0328	0.0408	0.0461	0.0553	0.0678	0.0802	0.0944	0.1057	0.1123	0.1234	0.1328	0.1357	0.1481	0.1622
624	0.0327	0.0382	0.0488	0.0586	0.0643	0.0741	0.0867	0.0983	0.1126	0.1236	0.1298	0.1418	0.1525	0.1555	0.1698	0.1873
626	0.0340	0.0391	0.0501	0.0598	0.0652	0.0755	0.0892	0.1022	0.1169	0.1281	0.1342	0.1464	0.1566	0.1596	0.1735	0.1908
628	0.0264	0.0323	0.0424	0.0519	0.0572	0.0670	0.0798	0.0917	0.1055	0.1158	0.1207	0.1313	0.1407	0.1408	0.1535	0.1712
630	0.0238	0.0292	0.0395	0.0476	0.0524	0.0613	0.0742	0.0861	0.0989	0.1081	0.1123	0.1212	0.1293	0.1303	0.1411	0.1547
632	0.0134	0.0175	0.0252	0.0321	0.0356	0.0427	0.0549	0.0664	0.0781	0.0866	0.0905	0.0978	0.1047	0.1052	0.1142	0.1270
634	0.0124	0.0165	0.0238	0.0296	0.0329	0.0399	0.0532	0.0659	0.0788	0.0873	0.0915	0.0992	0.1065	0.1074	0.1168	0.1288
636	0.0227	0.0275	0.0356	0.0423	0.0455	0.0531	0.0667	0.0807	0.0951	0.1056	0.1108	0.1207	0.1293	0.1316	0.1433	0.1563
638	0.0235	0.0285	0.0371	0.0447	0.0494	0.0573	0.0674	0.0767	0.0880	0.0967	0.1013	0.1107	0.1183	0.1207	0.1312	0.1425
640	0.0222	0.0276	0.0369	0.0444	0.0489	0.0572	0.0696	0.0812	0.0937	0.1033	0.1084	0.1180	0.1258	0.1282	0.1390	0.1511
642	0.0305	0.0378	0.0497	0.0604	0.0674	0.0781	0.0910	0.1032	0.1172	0.1279	0.1335	0.1446	0.1537	0.1558	0.1681	0.1817
644	0.0204	0.0252	0.0332	0.0397	0.0435	0.0505	0.0608	0.0709	0.0820	0.0903	0.0941	0.1021	0.1082	0.1101	0.1187	0.1273
646	0.0149	0.0183	0.0244	0.0300	0.0338	0.0405	0.0491	0.0577	0.0681	0.0767	0.0812	0.0898	0.0975	0.0984	0.1082	0.1200
648	0.0113	0.0159	0.0222	0.0278	0.0326	0.0392	0.0466	0.0536	0.0633	0.0714	0.0766	0.0858	0.0935	0.0982	0.1089	0.1185
650	0.0163	0.0209	0.0277	0.0342	0.0397	0.0469	0.0539	0.0608	0.0698	0.0779	0.0831	0.0924	0.1006	0.1058	0.1168	0.1272
652	0.0285	0.0324	0.0384	0.0447	0.0495	0.0558	0.0617	0.0670	0.0751	0.0820	0.0865	0.0952	0.1025	0.1072	0.1178	0.1279
654	0.0221	0.0263	0.0334	0.0397	0.0435	0.0503	0.0596	0.0684	0.0783	0.0862	0.0908	0.0997	0.1068	0.1117	0.1224	0.1310
656	0.0105	0.0145	0.0216	0.0272	0.0307	0.0371	0.0465	0.0556	0.0652	0.0723	0.0762	0.0834	0.0891	0.0925	0.1009	0.1081
658	0.0181	0.0209	0.0262	0.0314	0.0348	0.0396	0.0443	0.0484	0.0541	0.0584	0.0604	0.0649	0.0690	0.0705	0.0762	0.0804
660	0.0126	0.0164	0.0235	0.0301	0.0346	0.0410	0.0486	0.0556	0.0643	0.0710	0.0747	0.0820	0.0887	0.0904	0.0996	0.1124
662	0.0210	0.0254	0.0345	0.0429	0.0489	0.0565	0.0638	0.0702	0.0784	0.0845	0.0870	0.0933	0.0991	0.0993	0.1071	0.1167
664	0.0190	0.0217	0.0270	0.0311	0.0340	0.0389	0.0440	0.0492	0.0563	0.0621	0.0656	0.0724	0.0783	0.0813	0.0896	0.0984
666	0.0119	0.0154	0.0203	0.0246	0.0283	0.0330	0.0375	0.0419	0.0483	0.0537	0.0575	0.0640	0.0700	0.0739	0.0824	0.0909
668	0.0179	0.0203	0.0246	0.0290	0.0322	0.0370	0.0426	0.0488	0.0570	0.0633	0.0672	0.0749	0.0817	0.0864	0.0972	0.1078
670	0.0235	0.0246	0.0286	0.0321	0.0347	0.0388	0.0425	0.0462	0.0513	0.0559	0.0584	0.0641	0.0694	0.0721	0.0804	0.0895
672	0.0189	0.0206	0.0240	0.0278	0.0305	0.0346	0.0385	0.0420	0.0474	0.0515	0.0538	0.0593	0.0641	0.0655	0.0738	0.0835
674	0.0138	0.0153	0.0181	0.0210	0.0229	0.0257	0.0289	0.0315	0.0349	0.0381	0.0392	0.0425	0.0453	0.0456	0.0508	0.0567
676	0.0122	0.0143	0.0177	0.0215	0.0242	0.0275	0.0307	0.0334	0.0373	0.0404	0.0414	0.0449	0.0478	0.0478	0.0526	0.0588
678	0.0442	0.0444	0.0474	0.0513	0.0532	0.0574	0.0604	0.0635	0.0681	0.0720	0.0728	0.0776	0.0814	0.0815	0.0882	0.0956
680	0.0255	0.0270	0.0306	0.0347	0.0372	0.0411	0.0450	0.0482	0.0529	0.0571	0.0589	0.0634	0.0673	0.0683	0.0748	0.0820
682	0.0299	0.0305	0.0331	0.0360	0.0373	0.0405	0.0427	0.0451	0.0488	0.0515	0.0520	0.0555	0.0578	0.0582	0.0623	0.0659
684	0.0280	0.0315	0.0385	0.0447	0.0479	0.0549	0.0657	0.0763	0.0877	0.0955	0.0994	0.1068	0.1125	0.1153	0.1242	0.1313
686	0.0225	0.0250	0.0299	0.0349	0.0380	0.0432	0.0488	0.0543	0.0613	0.0665	0.0693	0.0755	0.0805	0.0830	0.0906	0.0979
688	0.0257	0.0308	0.0400	0.0483	0.0530	0.0620	0.0725	0.0824	0.0938	0.1025	0.1062	0.1158	0.1229	0.1266	0.1374	0.1461
690	0.0253	0.0320	0.0429	0.0523	0.0571	0.0667	0.0811	0.0939	0.1072	0.1162	0.1201	0.1290	0.1355	0.1384	0.1484	0.1562
692	0.0445	0.0464	0.0519	0.0565	0.0584	0.0636	0.0703	0.0760	0.0837	0.0887	0.0903	0.0963	0.1004	0.1018	0.1087	0.1141
694	0.0191	0.0251	0.0351	0.0430	0.0465	0.0553	0.0675	0.0791	0.0911	0.0983	0.1011	0.1079	0.1125	0.1144	0.1216	0.1259
696	0.0173	0.0224	0.0317	0.0381	0.0409	0.0486	0.0602	0.0710	0.0809	0.0860	0.0867	0.0905	0.0927	0.0917	0.0961	0.0982
698	0.0271	0.0325	0.0415	0.0490	0.0523	0.0598	0.0705	0.0796	0.0885	0.0936	0.0944	0.0987	0.1012	0.1009	0.1056	0.1082
700	0.0167	0.0192	0.0253	0.0299	0.0325	0.0391	0.0509	0.0643	0.0798	0.0914	0.0983	0.1091	0.1177	0.1220	0.1344	0.1458

Depth (cm)	[400nm]	[420nm]	[440nm]	[460nm]	[480nm]	[500nm]	[520nm]	[540nm]	[560nm]	[580nm]	[600nm]	[620nm]	[640nm]	[660nm]	[680nm]	[700nm]
702	0.0615	0.0650	0.0699	0.0750	0.0760	0.0828	0.0925	0.1019	0.1126	0.1197	0.1217	0.1283	0.1318	0.1332	0.1403	0.1426
704	0.0397	0.0457	0.0550	0.0629	0.0665	0.0760	0.0893	0.1028	0.1181	0.1292	0.1348	0.1451	0.1512	0.1550	0.1648	0.1697
706	0.0497	0.0529	0.0593	0.0652	0.0667	0.0739	0.0889	0.1059	0.1247	0.1380	0.1449	0.1562	0.1643	0.1694	0.1827	0.1935
708	0.0469	0.0529	0.0629	0.0715	0.0759	0.0840	0.0918	0.0994	0.1084	0.1149	0.1164	0.1223	0.1255	0.1265	0.1332	0.1358
710	0.0274	0.0334	0.0433	0.0519	0.0570	0.0663	0.0781	0.0896	0.1024	0.1124	0.1170	0.1264	0.1329	0.1359	0.1465	0.1542
712	0.0453	0.0471	0.0519	0.0563	0.0582	0.0631	0.0681	0.0724	0.0784	0.0826	0.0835	0.0884	0.0911	0.0914	0.0966	0.1003
714	0.0395	0.0439	0.0514	0.0583	0.0616	0.0697	0.0795	0.0898	0.1011	0.1090	0.1120	0.1190	0.1229	0.1249	0.1321	0.1351
716	0.0408	0.0443	0.0516	0.0578	0.0605	0.0681	0.0778	0.0873	0.0977	0.1051	0.1076	0.1139	0.1173	0.1185	0.1247	0.1265
718	0.0185	0.0228	0.0299	0.0360	0.0390	0.0461	0.0564	0.0668	0.0778	0.0855	0.0889	0.0953	0.0989	0.1006	0.1069	0.1096
720	0.0404	0.0449	0.0533	0.0597	0.0627	0.0702	0.0783	0.0859	0.0946	0.1005	0.1022	0.1078	0.1104	0.1116	0.1167	0.1175
724	0.0426	0.0466	0.0524	0.0576	0.0596	0.0655	0.0707	0.0757	0.0825	0.0867	0.0878	0.0924	0.0943	0.0951	0.0990	0.0988
726	0.0513	0.0548	0.0615	0.0666	0.0681	0.0734	0.0779	0.0812	0.0863	0.0892	0.0894	0.0932	0.0946	0.0949	0.0985	0.0976
728	0.0462	0.0497	0.0555	0.0600	0.0614	0.0662	0.0704	0.0742	0.0796	0.0832	0.0839	0.0883	0.0905	0.0919	0.0961	0.0963
730	0.0434	0.0478	0.0542	0.0591	0.0611	0.0665	0.0709	0.0747	0.0799	0.0834	0.0840	0.0880	0.0898	0.0906	0.0941	0.0940
732	0.0784	0.0841	0.0934	0.1018	0.1061	0.1155	0.1226	0.1306	0.1412	0.1487	0.1513	0.1605	0.1655	0.1688	0.1774	0.1797
734	0.0827	0.0903	0.1021	0.1140	0.1201	0.1329	0.1431	0.1535	0.1673	0.1776	0.1806	0.1925	0.1988	0.2027	0.2136	0.2157
736	0.1056	0.1139	0.1253	0.1360	0.1413	0.1538	0.1635	0.1736	0.1872	0.1968	0.1997	0.2109	0.2170	0.2207	0.2316	0.2341
738	0.1082	0.1157	0.1274	0.1377	0.1423	0.1540	0.1624	0.1712	0.1833	0.1916	0.1932	0.2033	0.2081	0.2107	0.2204	0.2212
740	0.0528	0.0563	0.0636	0.0695	0.0719	0.0784	0.0844	0.0898	0.0966	0.1012	0.1019	0.1072	0.1093	0.1103	0.1151	0.1152
742	0.0555	0.0601	0.0658	0.0706	0.0728	0.0785	0.0823	0.0862	0.0918	0.0954	0.0960	0.1008	0.1028	0.1039	0.1081	0.1082
744	0.0942	0.0984	0.1069	0.1149	0.1179	0.1273	0.1340	0.1412	0.1509	0.1572	0.1584	0.1664	0.1699	0.1720	0.1794	0.1799
746	0.1071	0.1129	0.1203	0.1278	0.1299	0.1396	0.1460	0.1530	0.1635	0.1696	0.1702	0.1785	0.1819	0.1839	0.1915	0.1916
748	0.0956	0.1001	0.1077	0.1150	0.1172	0.1260	0.1324	0.1394	0.1496	0.1562	0.1574	0.1653	0.1688	0.1711	0.1789	0.1797
750	0.0864	0.0896	0.0965	0.1027	0.1043	0.1121	0.1183	0.1250	0.1350	0.1415	0.1429	0.1503	0.1537	0.1564	0.1648	0.1669

Appendix E: Grain-size data

Averaged data

Depth (cm)	>32um (%)	>63um (%)	Clay	Silt	Sand
30	17.53	2.78	17.69	79.52	2.78
31	24.53	7.39	15.70	76.91	7.39
32	18.71	4.19	19.77	76.05	4.19
33	21.33	3.57	15.22	81.21	3.57
34	23.16	3.87	14.05	82.08	3.87
35	23.90	4.90	14.67	80.43	4.90
36	23.20	3.38	15.24	81.38	3.38
37	16.76	1.02	18.60	80.38	1.02
38	19.82	1.98	18.18	79.84	1.98
39	16.12	1.52	22.74	75.74	1.52
60	18.10	2.76	10.88	86.36	2.76
61	18.47	2.89	10.34	86.78	2.89
62	18.17	2.62	9.71	87.67	2.62
63	18.36	2.93	10.88	86.19	2.93
64	17.35	2.77	12.37	84.87	2.77
65	20.67	3.50	8.68	87.83	3.50
66	19.90	3.35	10.04	86.61	3.35
67	19.08	2.80	10.05	87.15	2.80
68	18.52	2.81	10.09	87.11	2.81
69	18.79	2.99	10.19	86.81	2.99
70	19.94	3.34	10.05	86.61	3.34
350	9.74	1.64	6.48	91.88	1.64
351	12.31	2.03	11.53	86.43	2.03
352	12.52	2.06	9.99	87.94	2.06
353	14.72	2.85	10.33	86.82	2.85
354	13.39	2.78	10.40	86.83	2.78
355	17.28	2.33	10.72	86.95	2.33
356	19.73	3.86	10.20	85.94	3.86
357	22.21	3.05	9.91	87.05	3.05
358	17.55	3.69	9.76	86.56	3.69
359	13.87	2.46	8.96	88.58	2.46
360	12.28	2.35	8.67	88.98	2.35
390	18.81	3.63	9.34	87.03	3.63
391	18.42	3.37	9.47	87.16	3.37
392	18.81	3.68	8.26	88.07	3.68
393	21.54	4.80	8.49	86.71	4.80
394	21.92	5.78	10.91	83.31	5.78
395	21.28	4.71	10.41	84.88	4.71
396	21.37	4.86	11.33	83.81	4.86
397	20.67	4.19	10.12	85.69	4.19
398	21.26	4.25	10.46	85.28	4.25
399	22.51	4.63	9.44	85.93	4.63
400	22.46	4.61	9.18	86.22	4.61
530	10.61	0.90	20.89	78.21	0.90
531	12.40	2.15	25.37	72.47	2.15
532	12.45	2.55	25.74	71.71	2.55
533	12.77	2.33	24.07	73.60	2.33
534	14.82	3.54	22.33	74.13	3.54
535	14.36	3.18	23.42	73.40	3.18
536	14.33	3.22	23.70	73.08	3.22
537	16.88	4.38	22.74	72.88	4.38
538	16.09	3.81	21.62	74.57	3.81
539	16.11	4.58	21.42	74.00	4.58
540	15.64	4.47	22.64	72.89	4.47
556	21.88	9.95	17.72	72.33	9.95
557	27.77	12.84	15.94	71.22	12.84
558	29.50	16.22	19.47	64.31	16.22
559	31.38	17.95	22.75	59.30	17.95
560	27.76	13.28	23.67	63.05	13.28
561	24.97	10.83	25.98	63.19	10.83
562	19.06	6.79	28.20	65.02	6.79
563	18.45	5.85	27.18	66.97	5.85
564	17.83	5.01	26.75	68.24	5.01
565	17.28	4.93	27.29	67.79	4.93
566	16.28	4.37	27.33	68.30	4.37
600	12.58	2.71	29.16	68.13	2.71
601	12.72	2.29	27.72	69.99	2.29
602	8.88	1.40	24.36	74.24	1.40
603	11.31	1.24	24.25	74.51	1.24
604	12.19	1.94	23.90	74.16	1.94
605	11.10	1.10	25.49	73.41	1.10
606	11.61	0.92	23.31	75.77	0.92
607	12.97	1.21	22.26	76.53	1.21
608	11.46	0.76	24.82	74.43	0.76
609	11.10	1.27	25.90	72.82	1.27
610	12.10	1.23	22.72	76.05	1.23
640	22.25	5.58	21.80	72.62	5.58
641	22.08	4.97	22.02	73.01	4.97
642	22.28	5.95	21.66	72.39	5.95
643	23.56	7.22	20.73	72.05	7.22
644	24.27	7.29	20.53	72.18	7.29
645	23.12	7.11	21.17	71.72	7.11
646	22.06	6.66	20.75	72.60	6.66
647	18.03	4.80	21.28	73.92	4.80
648	14.94	3.86	21.88	74.26	3.86
649	14.55	3.31	20.36	76.34	3.31
650	13.61	2.93	20.71	76.36	2.93

Sed.size (um)	0.05	0.06	0.12	0.24	0.49	0.7	0.98	1	2	3	3.9	7	7.8	15.6	20	31	37	44	53	60	63	74	88	105	125	149	177	210	250	300	350	420	500	590	710	840	1000
RU188 - 30	0	0	0	0.167061	0.783731	0.932236	0.953267	2.402499	2.62119	2.262468	7.062223	1.902397	21.99577	11.71963	20.75366	7.052341	5.710749	4.729815	2.373874	0.779454	2.043518	1.486795	1.040868	0.763166	0.52461	0.468048	0.197014	0	0	0	0	0	0	0	0	0	0
RU188 - 30	0	0	0	0.114279	0.624907	0.772631	0.946664	2.07412	2.467222	2.191053	7.076449	2.033734	25.55424	14.03365	23.24187	6.879572	4.916203	3.435494	1.427984	0.413821	0.932426	0.538665	0.340349	0.291118	0.28419	0.227938	0.079515	0	0	0	0	0	0	0	0	0	0
RU188 - 30	0	0	0	0.11801	0.659878	0.832011	0.950988	2.318616	2.721237	2.387884	7.765351	2.245722	27.65542	14.60444	22.77087	6.153969	4.080999	2.588493	0.968876	0.263319	0.559771	0.316712	0.238898	0.247085	0.258265	0.173661	0.023482	0	0	0	0	0	0	0	0	0	0
RU188 - 30	0	0	0	0.122171	0.703802	0.908256	0.958641	2.637586	3.030529	2.610544	8.523256	2.477261	29.57862	14.81353	21.57402	5.316784	3.310404	1.981258	0.732531	0.206593	0.492263	0.271943	0.318466	0.201548	0.031693	0	0	0	0	0	0	0	0	0	0	0	0
RU188 - 30	0	0	0	0.129241	0.737852	0.924193	0.96779	2.703945	3.141266	2.676524	8.703293	2.528946	29.9144	14.84469	21.39501	5.098911	3.12213	1.842145	0.685787	0.19742	0.484553	0.268239	0.346822	0.203876	0.03049	0	0	0	0	0	0	0	0	0	0	0	0
RU188 - 30	0	0	0	0.145913	0.751027	0.937514	0.973579	2.744457	3.241151	2.726731	8.881553	2.579647	30.23711	15.02713	21.34122	5.001731	3.023211	1.802722	0.637588	0.183422	0.475295	0.275918	0.374644	0.214744	0.034722	0.569465	0.344749	0.265785	0.160658	0.12785	0.020313	0	0	0	0	0	0
RU188 - 31	0	0	0	0.154943	0.752287	0.932023	0.963972	2.480626	2.856916	2.340256	8.269203	2.541286	29.50588	13.27719	21.42349	6.258921	4.546461	3.370961	1.574186	0.507263	1.350855	1.096091	0.911098	0.766111	0.640838	0.496108	0.381824	0.308578	0.257657	0.156439	0.053595	0	0	0	0	0	0
RU188 - 31	0	0	0	0.152576	0.752862	0.901543	0.953487	2.539025	2.898756	2.377022	8.880486	2.948383	24.74085	13.16272	20.8563	5.956503	4.268704	3.156203	1.50086	0.500144	1.403192	1.254883	1.114134	0.930657	0.728293	0.520666	0.398851	0.35631	0.245388	0.224681	0.07713	0	0	0	0	0	0
RU188 - 31	0	0	0	0.15319	0.77127	0.923776	0.956866	2.633444	3.992305	2.454868	8.343117	2.657845	25.46894	13.31186	20.723	5.780869	4.069215	2.940616	1.378205	0.452261	1.236467	1.136492	1.02607	0.871716	0.660964	0.496359	0.380031	0.331202	0.237424	0.138542	0.035983	0	0	0	0	0	0
RU188 - 32	0	0	0	0.167505	0.78706	1.10073	0.969732	3.386179	3.674912	2.794481	7.087976	1.910186	24.80952	13.27133	20.07365	5.952842	4.286431	3.15952	1.462731	0.466082	1.210089	0.915325	0.692673	0.542635	0.443201	0.336792	0.242391	0.165131	0.070095	0	0	0	0	0	0	0	0
RU188 - 32	0	0	0	0.19078	0.909822	1.141075	0.972589	3.487965	3.720617	2.82767	7.241611	1.957372	25.24358	13.42199	20.94209	5.876434	4.162084	3.00067	1.381638	0.430376	1.11579	0.857254	0.666909	0.523549	0.398671	0.259467	0.139897	0.065107	0	0	0	0	0	0	0	0	0
RU188 - 32	0	0	0	0.19047	0.925442	1.173299	0.975028	3.586334	3.762399	2.850785	7.399091	2.014407	25.63301	13.42452	20.66691	5.710084	4.000702	2.841966	1.266189	0.394987	1.009723	0.751797	0.573851	0.452153	0.360834	0.26691	0.197552	0.162968	0.154331	0.114442	0.042213	0	0	0	0	0	0
RU188 - 32	0	0	0	0.195657	0.963439	1.234745	0.979225	3.734919	3.854853	2.931331	7.116892	2.11455	26.40736	13.60554	20.42797	5.426371	3.89353	2.564021	1.140983	0.361492	0.959987	0.779125	0.690019	0.502673	0.384318	0.224776	0.068281	0	0	0	0	0	0	0	0	0	0
RU188 - 33	0	0	0	0.141857	0.677327	0.876573	0.945119	2.606572	2.802403	2.143078	5.941466	1.709472	23.73778	13.5155659	23.00702	7.185344	5.452542	4.176938	1.940468	0.605678	1.486155	0.940901	0.550302	0.332858	0.240761	0.192625	0.163485	0.140509	0.119223	0.035077	0	0	0	0	0	0	0
RU188 - 33	0	0	0	0.145258	0.698039	0.798636	0.947125	2.616278	2.734606	2.238554	6.204248	1.790393	24.75917	13.96337	23.1801	6.992104	5.149657	3.789065	1.681652	0.509192	1.203995	0.723547	0.403291	0.329398	0.22603	0.19461	0.158278	0.111994	0.055428	0	0	0	0	0	0	0	0
RU188 - 33	0	0	0	0.147295	0.723073	0.842084	0.950258	2.388801	2.914336	2.372951	6.634092	1.922001	26.11176	14.3796	23.06714	6.598561	4.641317	3.205101	1.320985	0.380499	0.848464	0.470326	0.271035	0.206198	0.187103	0.152086	0.105363	0.062368	0	0	0	0	0	0	0	0	0
RU188 - 33	0	0	0	0.150015	0.741186	0.868843	0.95219	2.494134	3.022324	2.465742	6.99886	2.017324	26.88103	14.52406	22.80384	6.321884	4.327255	2.872832	1.226821	0.313258	0.870315	0.589419	0.298858	0.231174	0.206349	0.168343	0.112787	0	0	0	0	0	0	0	0	0	0
RU188 - 34	0	0	0	0.139577	0.773457	0.894555	0.956023	2.577214	3.144595	2.701715	7.127877	2.079231	27.54455	14.41181	22.45577	6.27021	4.435744	2.975064	1.292847	0.344618	0.914497	0.627384	0.317172	0.379148	0.238554	0.178667	0.118966	0	0	0	0	0	0	0	0	0	0
RU188 - 34	0	0	0	0.139647	0.667738	0.756354	0.944226	2.065135	2.585209	2.112619	5.645259	1.613913	23.67022	13.97089	23.88791	7.388303	5.517201	4.121797	1.859849	0.569782	1.368813	0.923085	0.623085	0.328374	0.228021	0.221787	0.217723	0.199258	0.178273	0.169405	0.142226	0.117354	0.069727	0	0	0	0
RU188 - 35	0	0	0	0.145775	0.72183	0.848423	0.950798	2.364361	2.906421	2.441733	6.519662	1.793184	24.09033	14.1745	23.84621	7.020223	4.955498	3.388576	1.359778	0.38097	0.809024	0.395084	0.209058	0.198213	0.249218	0.272002	0.256547	0.222019	0.184583	0.122401	0.11277	0.016816	0	0	0	0	0
RU188 - 35	0	0	0	0.118904	0.606596	0.73636	0.944827	2.154689	2.70475	2.309601	6.406375	1.753541	24.55184	14.48107	24.21516	7.002708	4.840889	3.199031	1.224635	0.330739	0.69911	0.304302	0.183322	0.220957	0.29125	0.304977	0.267282	0.214301	0.177781	0.138643	0.170781	0.165737	0.13387	0.076176	0	0
RU188 - 35	0	0	0	0.126998	0.62153	0.719775	0.940894	2.048507	2.607122	2.090752	6.070352	1.641021	24.14522	14.54622	24.98427	7.617167	5.029211	3.525677	1.561208	0.391849	0.761539	0.270709	0.167523	0.192048	0.125122	0.2045	0.300784	0.237283	0.198468	0.134586	0.121844	0.130486	0.116992	0.090238	0.04976	0	0
RU188 - 36	0	0	0	0.135951	0.70704	0.828375	0.947022	2.211817	2.729727	2.286454	6.545253	1.784623	23.75099	14.27067	24.70477	7.577107	5.076027	3.562211	1.577155	0.398557	0.818364	0.274844	0.168903	0.211795	0.14282	0.272005	0.311535	0.26823	0.211441	0.159681	0.145489	0.15686	0	0	0	0	0
RU188 - 36	0	0	0	0.116282	0.743258	0.863119	0.951179	2.172762	2.419922	2.029312	5.926109	1.656963	21.96739	12.86984	23.09452	7.648968	6.011032	4.777973	2.293447	0.72829	1.814064	1.167318	0.644201	0.537968	0.202226	0.146111	0.123444	0.104145	0.045658	0	0	0	0	0	0	0	0
RU188 - 36	0	0	0	0.165792	0.769143	0.899259	0.953611	2.557006	2.955101	2.412978	6.218352	1.743192	23.02601	12.93784	23.33454	7.513163	5.721264	4.346257	1.974559	0.602768	1.422014	0.815311	0.384565	0.177198	0.114844	0.103176	0.099158	0.063674	0	0	0	0	0	0	0	0	0
RU188 - 36	0	0	0	0.169164	0.787431	0.924931	0.955376	2.393191	2.652804	2.204821	6.440088	1.810638	23.78889	13.63673	23.56184	7.341131	5.454101	3.997428	1.734925	0.511426	1.145685	0.577831	0.21781	0.084795	0.082473	0.11563	0.135141	0.123833	0.052079	0	0	0	0	0	0	0	0
RU188 - 36	0	0	0	0.172109	0.807297	0.953878	0.957356	2.495453	2.75728	2.285626	6.701734	1.888603	24.59077	13.92068	23.65933	7.19377	5.231819	3.720129	1.554648	0.445574	0.958255	0.440711	0.139699	0.025384	0	0	0	0	0	0	0	0	0	0	0	0	0
RU188 - 36	0	0	0	0.174022	0.820397	0.974255	0.958823	2.577214	2.841623	2.350437	6.927975	1.953897	25.30823	14.1352	23.99986	6.991954	4.971851	3.422559	1.37172	0.379148	0.780667	0.294526	0.059836	0	0.173973	0	0.135077	0.06094	0	0	0	0	0	0	0	0	0
RU188 - 37	0	0	0	0.176172	0.844757	0.97139	0.960722	2.617444	2.870294	2.419978	7.013092	1.973579	25.60446	14.25135	24.01466	7.115957	5.121258	3.610986	1.402755	0.387647	0.797109	0.302766	0.149525	0.199603	0.175683	0.165637	0.13507	0	0	0	0	0	0	0	0	0	0
RU188 - 37	0	0	0	0.179672	0.859467	1.044267	0.964041	2.800174	2.974643	2.4659	7.47775	2.081054	25.15535	13.63998	22.93852	6.932601	4.991338	3.479443	1.405251	0.388647	0.795108	0.282766	0.049535	0	0	0	0	0	0	0	0	0	0	0	0	0	0
RU188 - 37	0	0	0	0.179774	0.872194	1.069168	0.965951	2.913302	3.091888	2.55234	7.747683	2.163086	26.00704	13.90503	22.85354	6.657121	4.644934	3.086824	1.189421	0.305943	0.580407	0.134345	0	0	0	0	0	0	0	0	0	0	0	0	0	0	0
RU188 - 37	0	0	0	0.180035	0.881323	1.086585	0.967278	2.990998	3.172975	2.614065	7.946437	2.221999	26.55338	14.03407	22.70151	6.464244	4.422447	2.852131	1.029511	0.266224	0.427451	0.087345	0	0	0	0	0	0	0	0	0	0	0	0	0	0	0
RU188 - 37	0	0	0	0.180321	0.894089	1.112197	0.969257	3.013369	3.278966	2.697733	8.2465	2.307454	27.20798	14.13617	22.42886	6.216401	4.154438	2.930454	0.879839	0.222202	0.281968	0	0	0	0	0	0	0	0	0	0	0	0	0	0	0	0
RU188 - 37	0	0	0	0.181418	0.903829	1.128974	0.970604	3.045123	3.169599	2.745219	8.423246	2.359832	27.61248	14.1839	22.21288	6.047388	3.960677	2.818486	0.794225	0.190552	0.238682	0	0	0	0	0	0	0	0	0	0	0	0	0	0	0	0
RU188 - 38	0	0	0	0.182531	0.904525	1.129693	0.971015	3.056445	3.182358	2.751778	8.437573	2.361418	27.70781	14.19282	22.09677	6.027153	3.941019	2.804274	0.780115	0.187984	0.231589	0.077158	0	0	0	0	0	0	0	0	0	0	0	0	0	0	0
RU188 - 38	0	0	0	0.153254	0.770779	0.941528	0.957717	2.599235	2.625962	2.553581	7.129733	1.850691	25.56238	13.94073	21.96729	5.970236	4.198255	3.115869	1.658169	0.559971	1.300616	0.727295	0.34115	0.168866	0.118594	0.105936	0.07539	0	0	0	0	0	0	0	0	0	0
RU188 - 38	0	0	0	0.1568	0.797797	0.982723	0.960556	2.740484	3.106459	2.645703	7.58694	1.962863	23.72506	13.40338	23.19599	7.148906	5.218943	3.714486	1.550126	0.443587	0.952192	0.437513	0.14282	0.026971	0	0	0	0	0	0	0	0	0	0	0	0	0
RU188 - 38	0	0	0	0.158574	0.815123	1.011076	0.962549	2.837035	3.206765	2.733369	7.831659	2.04377	24.48481	13.64505	23.16336	6.92816	4.922027	3.363985	1.53007	0.363295	0.73398	0.26415	0.059926	0	0	0	0	0	0	0	0	0	0	0	0	0	0
RU188 - 38	0	0	0	0.161471	0.833631	1.038491	0.964434	2.931409	3.304833	2.814682	8.149206	2.119162	25.18172	13.83246	23.02581	6.694503	4.641004	3.059052	1.550211	0.299693	0.656937	0.131304	0	0	0	0	0	0	0	0	0	0	0	0	0	0	0
RU188 - 38	0	0	0	0.162826	0.847035	1.061935	0.96614	3.016274	3.385399	2.882578	8.400692	2.190582	25.74353	13.93727	22.93518	6.491364	4.808973	2.813484	1.003758	0.257415	0.410434	0.083349	0	0	0	0	0	0	0	0	0	0	0	0	0	0	0
RU188 - 39	0	0	0	0.167251	0.867022	1.085722	0.967211	3.057243	3.426387	2.949135	8.621485	2.261911	26.29581	14.11195	22.79988	6.289154	4.706153	3.328547	1.447253	0.372973	0.763552	0.314417	0.157469	0.132954	0.114018	0.097599	0.062169	0	0	0	0	0	0	0	0	0	0
RU188 - 39	0	0	0	0.171981	0.88102	1.107242	0.969102	3.098723	3.475135	2.984705	8.824015	2.311918	26.73882	14.29681	22.60745	6.091549	4.566151	3.208147	1.403963	0.385175	0.745172	0.305178	0.136232	0.160101	0.175257	0.157196	0.118475	0	0	0	0	0	0	0	0	0	0
RU188 - 39	0	0	0	0.176535	0.893275	1.123835	0.970344	3.136383	3.573688	3.025597	9.027861	2.362453	27.38555	14.47905	22.41195	5.893549	4.426153	3.088141	1.348259	0.365175	0.726178	0.295409	0.129435	0.151675	0.166514	0.136232	0.114875	0.104698	0	0	0	0	0	0	0	0	0	0
RU188 - 39	0	0	0	0.180742	0.90283	1.139753	0.971762	3.175795	3.621444	3.065844	9.229077	2.413482	27.98663	14.65928	22.21983	5.693594	4.285111	2.967722	1.292665	0.344812	0.706243	0.284887	0.123422	0.146111	0.157825	0.14469	0.109936	0.097599	0	0	0	0	0	0	0	0	0
RU188 - 39	0	0	0	0.183021	0.910369	1.154187	0.972896	3.215797	3.670552	3.105439	9.430853	2.464527	28.58043	14.84082	22.02971	5.494253	4.144128	2.847901	1.237267	0.325449	0.687239	0.275112	0.116241	0.137397	0.150318	0.130473	0.104698	0.094466	0	0	0	0	0	0	0	0	0
RU188 - 39	0	0	0	0.185418	0.917693	1.168944	0.973845	3.255499	3.719865	3.145233	9.632084	2.515686	29.17934	15.02963	21.84403	5.294901	4.046219	2.730383	1.183235	0.306148	0.669318	0.263744	0.109163	0.128221	0.144018	0.125122	0.100101	0.091909	0.086143	0.061277	0	0	0	0	0	0	0
RU188 - 39	0	0	0	0.187431	0.924955	1.183644	0.974543	3.295844	3.768043	3.185064	9.834984	2.566682	29.37934	15.20179	21.69153	5.094528	3.947043	2.638277	1.129977	0.296911	0.652422	0.252044	0.101195	0.118611	0.13622	0.115135	0.095815	0.086143	0.061277	0	0	0	0	0	0	0	0
RU188 - 39	0	0	0	0.190842	0.933236	1.203957	0.975433	3.336598	3.816644	3.266504	10.04026	2.618089	29.92977	15.38637	21.56968	4.895745	3.851448	2.530743	1.075506	0.286051	0.638772	0.240144	0.093833	0.110425	0.123442	0.106446	0.088275	0.079644	0.056861	0.042099	0	0	0	0	0	0	0
RU188 - 39	0	0	0	0.196494	0.942453	1.219835	0.977344	3.432384	3.736388	3.325997	9.973891	2.665627	30.47345	15.55409	21.27667	4.696753	3.813235	2.429201	1.026243	0.272969	0.614031	0.229448	0.085146	0.100121	0.111945	0.096733	0.080144	0.072167	0.051575	0.038503	0	0	0	0	0	0	0
RU188 - 39	0	0	0	0.202521	1.001086	1.238891	0.979161	3.568147	3.858088	3.326818	10.10692	2.756784	31.29148	15.89498	20.94526	4.513445	3.686234	2.329277	0.996849	0.259272	0.597242	0.218051	0.081445	0.095815	0.106446	0.092271	0.077644	0.062223	0.044139	0.032863	0	0	0	0	0	0	0
RU188 - 39	0	0	0	0.207156	1.020022	1.262453	0.981644	3.691753	3.965844	3.413484	10.44026	2.660682	32.26093	16.42963	20.17934	4.581931	3.579043	2.382877	0.944619	0.245934	0.548121	0.075506	0	0	0	0	0	0	0	0	0	0	0	0	0	0	0
RU188 - 39	0	0	0	0.20942	1.03971	1.326555	0.984137	3.812299	4.075745	3.551418	10.80171	2.751089	27.41097	12.92645	19.79855	5.336526	3.514174	2.157016	0.733549	0.180589	0.276453	0.053846	0	0	0	0	0	0	0	0	0	0	0	0	0	0	0

Sed size (um)	0.05	0.06	0.12	0.24	0.49	0.7	0.98	1	2	3	3.9	7	7.8	15.6	20	31	37	44	53	60	63	74	88	105	125	149	177	210	250	300	350	420	500	590	710	840	1000
RU188 - 60	0	0	0	0.078579	0.465941	0.522286	0.910701	1.650183	1.867146	1.202333	4.266023	1.906412	2.91299	5.117265	22.97214	6.336016	4.640129	3.515583	1.674186	0.539858	1.403862	1.025116	0.698665	0.462717	0.304547	0.163609	0.095141	0	0	0	0	0	0	0	0	0	0
RU188 - 60	0	0	0	0.078727	0.466001	0.522589	0.910757	1.650183	1.867146	1.202333	4.266023	1.906412	2.91299	5.117265	22.97214	6.336016	4.640129	3.515583	1.674186	0.539858	1.403862	1.025116	0.698665	0.462717	0.304547	0.163609	0.095141	0	0	0	0	0	0	0	0	0	0
RU188 - 60	0	0	0	0.078728	0.47369	0.542768	0.93219	1.764568	2.029286	1.304987	4.549666	1.965156	30.30496	15.5442	23.0106	6.243597	4.378118	3.111469	1.361667	0.41648	1.008035	0.651321	0.404357	0.268999	0.200654	0.149551	0.101952	0.060035	0	0	0	0	0	0	0	0	0
RU188 - 60	0	0	0	0.080599	0.480579	0.551955	0.932846	1.802444	2.066753	1.358607	4.68003	2.02367	30.60938	15.69889	23.17098	6.209929	4.280236	2.950357	1.241191	0.365951	0.846367	0.501974	0.294291	0.207109	0.179076	0.153179	0.121138	0.06547	0	0	0	0	0	0	0	0	0
RU188 - 60	0	0	0	0.081043	0.485228	0.558956	0.933365	1.84356	2.14224	1.39958	4.789148	2.054358	30.99334	15.84843	23.21137	6.121801	4.1496	2.78573	1.130987	0.324496	0.722805	0.39816	0.222769	0.167579	0.16449	0.156606	0.134149	0.080214	0	0	0	0	0	0	0	0	0
RU188 - 60	0	0	0	0.081206	0.489026	0.565531	0.933856	1.876836	2.185095	1.433693	4.893252	2.07823	31.25097	15.94962	23.28206	6.073414	4.065214	2.666061	1.043802	0.290372	0.617438	0.307322	0.163359	0.159754	0.163355	0.141787	0.082817	0	0	0	0	0	0	0	0	0	0
RU188 - 61	0	0	0	0.077649	0.447115	0.496284	0.928594	1.535571	1.784111	1.128605	4.006479	1.847623	29.12765	15.20507	22.82378	6.387154	4.657709	3.540115	1.699286	0.561961	1.451269	1.083707	0.756703	0.518007	0.346358	0.219643	0.138673	0.097266	0.044833	0	0	0	0	0	0	0	0
RU188 - 61	0	0	0	0.078156	0.457697	0.51743	0.930101	1.640748	1.943784	1.245594	4.314435	1.935965	30.21096	15.62827	23.2701	6.328776	4.451526	3.184554	1.410178	0.451666	1.048758	0.668947	0.396519	0.244163	0.17112	0.12837	0.101413	0.063138	0	0	0	0	0	0	0	0	0
RU188 - 61	0	0	0	0.080459	0.468048	0.524043	0.930613	1.687125	2.00122	1.296007	4.443742	1.964935	30.49945	15.82173	23.39195	6.275831	4.341569	3.019854	1.289008	0.384469	0.903128	0.549821	0.332438	0.215889	0.172651	0.140037	0.110794	0.064193	0	0	0	0	0	0	0	0	0
RU188 - 61	0	0	0	0.081145	0.47349	0.535433	0.931125	1.725654	2.056167	1.338679	4.551273	1.995167	30.87901	15.95833	23.5009	6.21981	4.223536	2.86287	1.173354	0.338814	0.759773	0.420385	0.229285	0.161743	0.148596	0.123567	0.107832	0.062604	0	0	0	0	0	0	0	0	0
RU188 - 61	0	0	0	0.081186	0.477394	0.538425	0.931641	1.758775	2.100918	1.378724	4.666036	2.021818	31.11928	16.07983	23.55401	6.168458	4.141614	2.733619	1.081313	0.36335	0.652166	0.329356	0.169127	0.13327	0.144311	0.142455	0.121968	0.070989	0	0	0	0	0	0	0	0	0
RU188 - 62	0	0	0	0.077492	0.430516	0.470042	0.926964	1.503556	1.789605	1.079315	3.952982	1.714982	28.81446	15.4994	23.57082	6.627106	4.808316	3.603183	1.169156	0.540123	1.186883	0.991214	0.664659	0.444514	0.312941	0.216105	0.146151	0.071011	0	0	0	0	0	0	0	0	0
RU188 - 62	0	0	0	0.077641	0.441862	0.492597	0.927479	1.608319	1.852284	1.135482	3.978211	1.771498	29.09513	15.68345	23.72523	6.596251	4.662227	3.352248	1.245644	0.496238	1.268368	0.945201	0.617234	0.410734	0.300619	0.201051	0.145859	0.084657	0	0	0	0	0	0	0	0	0
RU188 - 62	0	0	0	0.077563	0.45356	0.500726	0.929062	1.65174	1.91233	1.23825	3.9647	1.845403	30.4276	16.22218	24.15024	6.424319	4.358733	2.918301	1.176016	0.33474	0.734656	0.387791	0.206426	0.162394	0.181218	0.191964	0.183997	0.139483	0.042696	0	0	0	0	0	0	0	0
RU188 - 62	0	0	0	0.079124	0.460414	0.509171	0.929537	1.697545	2.054525	1.280795	4.071601	1.882932	30.95978	16.44	24.20933	6.291127	4.166085	2.687738	1.032643	0.283878	0.596593	0.394904	0.164103	0.152481	0.181941	0.193263	0.17571	0.104693	0	0	0	0	0	0	0	0	0
RU188 - 62	0	0	0	0.080087	0.465428	0.515031	0.930009	1.724512	2.069783	1.318375	4.173022	1.909638	31.2713	16.65694	24.24402	6.207045	4.040221	2.530997	0.993006	0.246746	0.491221	0.216359	0.121496	0.139715	0.186657	0.220428	0.183131	0.106797	0	0	0	0	0	0	0	0	0
RU188 - 63	0	0	0	0.080472	0.460941	0.517021	0.930321	1.678131	1.992131	1.287705	4.022891	1.793079	28.72737	15.17534	22.69719	6.413454	4.673155	3.540814	1.690419	0.546698	1.428774	1.05609	0.733663	0.500981	0.348059	0.227315	0.143772	0.074896	0	0	0	0	0	0	0	0	0
RU188 - 63	0	0	0	0.081391	0.46947	0.529755	0.931216	1.736398	2.063456	1.329273	4.189665	1.841078	29.34324	15.45617	23.14723	6.374317	4.542528	3.318561	1.529826	0.47156	1.17843	0.804187	0.505067	0.364943	0.259033	0.185674	0.133711	0.103837	0.054804	0	0	0	0	0	0	0	0
RU188 - 63	0	0	0	0.081969	0.480597	0.547955	0.93253	1.822815	2.181762	1.424312	4.463753	1.909175	30.09033	15.78322	23.38185	6.247669	4.291064	2.94714	1.23797	0.365282	0.848752	0.515037	0.321199	0.241755	0.231027	0.20767	0.169014	0.123069	0.045813	0	0	0	0	0	0	0	0
RU188 - 63	0	0	0	0.08139	0.484892	0.552479	0.933139	1.843145	2.169234	1.438242	4.594731	1.931211	30.59833	15.93218	23.71498	6.296751	4.396257	3.052148	1.281644	0.496227	1.075231	0.756238	0.496453	0.351244	0.306689	0.21961	0.174259	0.126144	0.06457	0	0	0	0	0	0	0	0
RU188 - 63	0	0	0	0.077053	0.45356	0.500726	0.929062	1.651774	1.91233	1.23825	3.9647	1.845403	30.4276	16.22218	24.15024	6.424319	4.358733	2.918301	1.176016	0.33474	0.734656	0.387791	0.206426	0.162394	0.181218	0.191964	0.183997	0.139483	0.042696	0	0	0	0	0	0	0	0
RU188 - 63	0	0	0	0.079124	0.460414	0.509171	0.929537	1.697545	2.054525	1.280795	4.071601	1.882932	30.95978	16.44	24.20933	6.291127	4.166085	2.687738	1.032643	0.283878	0.596593	0.394904	0.164103	0.152481	0.181941	0.193263	0.17571	0.104693	0	0	0	0	0	0	0	0	0
RU188 - 63	0	0	0	0.080472	0.460941	0.517021	0.930321	1.678131	1.992131	1.287705	4.022891	1.793079	28.72737	15.17534	22.69719	6.413454	4.673155	3.540814	1.690419	0.546698	1.428774	1.05609	0.733663	0.500981	0.348059	0.227315	0.143772	0.074896	0	0	0	0	0	0	0	0	0
RU188 - 63	0	0	0	0.081391	0.46947	0.529755	0.931216	1.736398	2.063456	1.329273	4.189665	1.841078	29.34324	15.45617	23.14723	6.374317	4.542528	3.318561	1.529826	0.47156	1.17843	0.804187	0.505067	0.364943	0.259033	0.185674	0.133711	0.103837	0.054804	0	0	0	0	0	0	0	0
RU188 - 63	0	0	0	0.081969	0.480597	0.547955	0.93253	1.822815	2.181762	1.424312	4.463753	1.909175	30.09033	15.78322	23.38185	6.247669	4.291064	2.94714	1.23797	0.365282	0.848752	0.515037	0.321199	0.241755	0.231027	0.20767	0.169014	0.123069	0.045813	0	0	0	0	0	0	0	0
RU188 - 63	0	0	0	0.0838	0.489749	0.559986	0.933337	1.873289	2.248694	1.478691	4.611567	1.948967	30.55146	15.97893	23.90555	6.176948	4.163944	2.774545	1.118096	0.31959	0.710585	0.395091	0.231758	0.185576	0.184828	0.169517	0.133541	0.072161	0	0	0	0	0	0	0	0	0
RU188 - 63	0	0	0	0.084131	0.494957	0.567706	0.933873	1.907699	2.296629	1.520474	4.731175	1.979556	30.86807	16.01457	23.97786	6.121083	4.063337	2.633726	1.016349	0.280124	0.589534	0.389947	0.15782	0.14348	0.16591	0.164832	0.134706	0.073449	0	0	0	0	0	0	0	0	0
RU188 - 64	0	0	0	0.077691	0.473728	0.553102	0.932855	1.845609	1.948038	1.37325	5.041889	2.031176	28.92421	14577.76	21.77715	6.144542	4.540497	3.522295	1.731306	0.570806	1.527297	1.172422	0.838641	0.576767	0.393615	0.248611	0.151329	0.075511	0	0	0	0	0	0	0	0	0
RU188 - 64	0	0	0	0.079696	0.489142	0.572484	0.934138	1.783057	2.069458	1.468933	5.305866	2.107632	29.86182	14956.28	22.17039	6.09222	4.366403	3.226797	1.491742	0.471158	1.19146	0.824944	0.531185	0.34076	0.229731	0.151871	0.101063	0.052773	0	0	0	0	0	0	0	0	0
RU188 - 64	0	0	0	0.078727	0.473728	0.553102	0.932855	1.845609	1.948038	1.37325	5.041889	2.031176	28.92421	14577.76	21.77715	6.144542	4.540497	3.522295	1.731306	0.570806	1.527297	1.172422	0.838641	0.576767	0.393615	0.248611	0.151329	0.075511	0	0	0	0	0	0	0	0	0
RU188 - 64	0	0	0	0.079696	0.489142	0.572484	0.934138	1.783057	2.069458	1.468933	5.305866	2.107632	29.86182	14956.28	22.17039	6.09222	4.366403	3.226797	1.491742	0.471158	1.19146	0.824944	0.531185	0.34076	0.229731	0.151871	0.101063	0.052773	0	0	0	0	0	0	0	0	0
RU188 - 64	0	0	0	0.083006	0.512713	0.605422	0.936432	1.94379	2.295226	1.654752	5.798288	2.23446	31.28581	15.60518	22.54113	5.827369	3.882996	2.540721	0.998169	0.278047	0.595942	0.305584	0.172164	0.15362	0.174417	0.175875	0.151272	0.111257	0.040356	0	0	0	0	0	0	0	0
RU188 - 64	0	0	0	0.080408	0.520722	0.618814	0.937229	1.999093	2.374212	1.722448	5.987755	2.281764	31.73871	15.75716	22.54901	5.704325	3.704409	2.315288	0.945772	0.221996	0.433147	0.181009	0.106508	0.142496	0.198173	0.209603	0.175041	0.095167	0	0	0	0	0	0	0	0	0
RU188 - 65	0	0	0	0.076586	0.417305	0.44321	0.924903	1.37723	1.669332	0.973781	2.839114	1.473152	27.02964	15.20777	23.78213	6.935327	5.208492	4.111382	2.053921	0.683594	1.847398	1.434677	1.026866	0.68991	0.463883	0.228292	0.09221	0	0	0	0	0	0	0	0	0	0
RU188 - 65	0	0	0	0.079845	0.427181	0.45457	0.925604	1.423818	1.737855	1.028941	2.996017	1.521951	27.70773	15.56074	24.19707	6.927653	5.076188	3.842316	1.818905	0.582382	1.497279	1.065296	0.702476	0.457279	0.313839	0.217796	0.159948	0.124115	0.055575	0	0	0	0	0	0	0	0
RU188 - 65	0	0	0	0.079963	0.441447	0.470359	0.926445	1.470709	1.761491	1.062151	3.096821	1.567537	28.3873	15.61404	24.39717	6.69254	4.767601	3.525731	1.662539	0.494492	1.093569	0.707032	0.48413	0.325448	0.222852	0.154313	0.11574	0.13851	0.045359	0	0	0	0	0	0	0	0
RU188 - 65	0	0	0	0.080218	0.451898	0.486673	0.927691	1.559931	1.940838	1.199827	3.441362	1.643574	29.39749	16.42316	25.03207	6.758211	4.604534	3.08907	1.2464	0.355498	0.785827	0.429953	0.248146	0.199337	0.200907	0.185732	0.14747	0.090386	0	0	0	0	0	0	0	0	0
RU188 - 65	0	0	0	0.082866	0.457803	0.49456	0.928216	1.593713	1.983279	1.240891	3.553346	1.673639	29.74471	16.65719	25.13305	6.679028	4.464109	2.897617	1.115199	0.306325	0.642611	0.31872	0.183758	0.175855	0.202792	0.197174	0.156887	0.083566	0	0	0	0	0	0	0	0	0
RU188 - 66	0	0	0	0.08263	0.452145	0.492821	0.928185	1.543874	1.94525	1.272033	3.458774	1.51323	27.00181	15.34452	23.95655	6.831746	4.984565	3.763669	1.785709	0.575052	1.495886	1.100813	0.769883	0.540563	0.39675	0.281743	0.196721	0.130917	0.054163	0	0	0	0	0	0	0	0
RU188 - 66	0	0	0	0.08434	0.461406	0.503679	0.928874	1.593444	2.019399	1.329061	3.594407	1.553008	27.58144	15.63348	24.24606	6.810847	4.876088	3.575635	1.635001	0.513191	1.232348	0.900217	0.601995	0.41614	0.30827	0.220191	0.149435	0.077044	0	0	0	0	0	0	0	0	0
RU188 - 66	0	0	0	0.085447	0.468619	0.513766	0.929561	1.630294	2.017874	1.379232	3.71732	1.5817	27.93048	15.80861	24.40815	6.796939	4.759919	3.591402	1.682614	0.464715	1.115528	0.734478	0.477941	0.344035	0.281115	0.225901	0.170567	0.11649	0.04898	0	0	0	0	0	0	0	0
RU188 - 66	0	0	0	0.086441	0.474759	0.525275	0.930161	1.675779	2.017874	1.379232	3.71732	1.5817	27.93048	15.80861	24.40815	6.796939	4.759919	3.591402	1.682614	0.464715	1.115528	0.734478	0.477941	0.344035	0.281115	0.225901	0.170567	0.11649	0.04898	0	0	0	0	0	0	0	0
RU188 - 66	0	0	0	0.08731	0.483102	0.533275	0.931081	1.721925	2.197196	1.476067	3.966359	1.648002	28.76083	16.1804	24.63521	6.605389	4.685928	3.014648	1.621389	0.355162	0.810899	0.467534	0.287435	0.230028	0.226219	0.213931	0.18124	0.132555	0.047567	0	0	0	0	0	0	0	0
RU188 - 66	0	0	0	0.08844	0.48897	0.54154	0.931429	1.755101	2.246612	1.520022	4.079446	1.675779	29.11356	16.35473	24.77242	6.54715	4.366251	2.841113	1.110496	0.307227	0.659	0.346186	0.2073	0.189167	0.210826	0.20882	0.176055	0.125177	0.042723	0	0	0	0	0	0	0	0
RU188 - 67	0	0	0	0.076785	0.440984	0.488549	0.929077	1.469966	1.703971	1.089174	3.874951	1.774114	28.31636	15.50457	24.16028	6.553798	4.857708	3.774225	1.854998	0.611273	1.632939	1.246253	0.879929	0.593064	0.391106	0.241176	0.099014	0	0	0	0	0	0	0	0	0	0
RU188 - 67	0	0	0	0.079258	0.454598	0.504868	0.929107	1.533699	1.798725	1.157115	4.086696	1.836393	29.11602	15.84946	24.48274	6.619965	4.812786	3.606901	1.685119	0.534353	1.334392	0.929072	0.600957	0.300718	0.044158	0	0	0	0	0	0	0	0	0	0	0	0
RU188 - 67	0	0	0	0.080515	0.4609	0.512412	0.929604	1.572777	1.853347	1.211937	4.207864	1.865536	29.46179	15.62561	23.94811	6.554274	4.661386	3.467125	1.498767	0.458894	1.138993	0.886203	0.603161	0.402558	0.302718	0.241602	0.174653	0.104738	0.059948	0	0	0	0	0	0	0	0
RU188 - 67	0	0	0	0.079258	0.454598	0.504868	0.929107	1.533699	1.798725	1.157115	4.086696	1.836393	29.11602	15.84946	24.48274	6.619965	4.812786	3.606901	1.685119	0.534353	1.334392	0.929072	0.600957	0.300718	0.044158	0	0	0	0	0	0	0	0	0	0	0	0
RU188 - 67	0	0	0	0.079258	0.454598	0.504868	0.929107	1.533699	1.798725	1.157115	4.086696	1.836393	29.11602	15.84946	24.48274	6.619965	4.812786	3.606901	1.685119	0.534353	1.334392	0.929072	0.600957	0.300718	0.044158	0	0	0	0	0	0	0	0	0	0	0	0
RU188 - 67	0	0	0	0.080515	0.4609	0.512412	0.929604	1.572777	1.853347	1.211937	4.207864	1.865536	29.46179	15.62561	23.94811	6.554274	4.661386	3.467125	1.498767	0.458894	1.138993	0.886203	0.603161	0.402558	0.302718	0.241602	0.174653	0.104738	0.059948	0	0	0	0	0	0	0	0
RU188 - 67	0	0	0	0.080515	0.4609	0.512412	0.929604	1.572777	1.853347	1.211937	4.207864	1.865536	29.46179	15.62561	23.94811	6.554274	4.661386	3.467125	1.498767	0.458894	1.138993	0.886203	0.603161	0.402558	0.302718	0.241602	0.174653	0.104738	0.059948	0	0	0	0	0	0	0	0
RU188 - 67	0	0	0	0.080226	0.473634	0.530237	0.930737	1.653486	1.972158	1.310963	4.163023	1.861753	29.78764	16.03036	23.98028	6.439226	4.408663	2.990958	1.222398	0.350978	0.761604	0.407685	0.196788	0.127824	0.11718	0.111753	0.081555	0	0	0	0	0	0	0	0	0	0
RU188 - 67	0	0	0	0.082955	0.478712	0.536503	0.931232	1.685753	2.021589	1.353817	4.575234	1.959595	30.62934	16.16879	24.94054	6.362933	4.279905	2.812498	1.095558	0.301699	0.62425	0.275194	0.107913	0.084334	0.118826	0.144348	0.139192	0.085295	0	0	0	0	0	0	0	0	0
RU188 - 67	0	0	0	0.079603	0.45529	0.502239	0.928804	1.545445	1.892644	1.252117	3.985827	1.751327	28.93382	15.78287	24.01406	6.586297	4.619142	3.283923	1.450171	0.445604	1.098139	0.74793	0.504156	0.360627	0.275723	0.199487	0.135287	0.069481	0	0	0	0	0	0	0	0	0
RU188 - 67	0	0	0	0.079946	0.441933	0.486628	0.927805	1.475512	1.791636	1.173606	3.791297	1.695169	28.13621	15.53678	23.54132	6.596778	4.762685	3.564971	1.689101	0.546314	1.438805	1.096068	0.802722	0.579954	0.418336	0.272703	0.158728	0.096972	0	0	0	0	0	0	0	0	0
RU188 - 68	0	0	0	0.079603	0.45529	0.502239	0.928804	1.545445	1.892644	1.252117	3.985827	1.751327	28.93382	15.78287	24.01406	6.586297	4.619142	3.283923	1.450171	0.445604	1.098139	0.74793	0.504156	0.360627	0.275723	0.199487	0.135287	0.069481	0	0	0	0	0	0	0	0	0
RU188 - 68	0	0	0	0.080833	0.461452	0.510289	0.929345	1.582928	1.948473	1.286904	4.100314	1.772227	29.28373	15.96998	24.23481	6.577328	4.540797	3.28196	1.432424	0.322095	0.78196	0.567908	0.39598	0.261158	0.223884	0.180762	0.15042	0.096314	0	0	0	0	0	0	0	0	0
RU188 - 68	0	0	0	0.082833	0.47451	0.528013	0.930519	1.655248	1.983316	1.345477	4.29822	1.832353	30.02644	16.12267	24.49598	6.450635	4.295238	2.785456	1.078443	0.327199	0.802204	0.521209	0.386004	0.267231	0.230211	0.196727	0.154556	0.098314	0	0	0	0	0	0	0	0	0
RU188 - 68	0	0	0	0.083355	0.478469	0.532514	0.930827	1.683494	2.095184	1.418396	4.383692	1.85077	30.2483	16.44015	24.97057	6.399921	4.202873	2.657555	0.986804	0.263297	0.529559	0.240019	0.136238	0.147828	0.185218	0.189059	0.158023	0.087807	0	0	0	0	0	0	0	0	0
RU188 - 69	0	0	0	0.075945	0.438433	0.479425	0.927389	1.486373	1.867662	1.239698	3.628476	1.579402	27.32109	15.53892	24.0206	6.821839	4.934362	3.666545	1.704591	0.541738	1.389042	1.005374	0.706403	0.51414	0.401153	0.305964	0.228537	0.161301	0.069376	0	0	0	0	0	0	0	0
RU188 - 69	0	0	0	0.077717	0.44712	0.493085	0.928274	1.542227	1.944953	1.308698	3.798883	1.62276	27.89158	15.66895	24.3392	6.783064	4.789125	3.418105	1.509406	0.463023	1.138069	0.775922	0.537511	0.411303	0.344178	0.271747	0.197097	0.129721	0.043787	0	0	0	0	0	0	0	0
RU188 - 69	0	0	0	0.079878	0.457056	0.504872	0.929026	1.594572	2.028353	1.371102	3.94405	1.661844	28.44054	15.95629	24.55551	6.715337	4.640948	3.199974	1.344682	0.397509	0.929414	0.680035	0.383095	0.307227	0.28176	0.240914	0.185335	0.128108	0.045771	0	0	0	0	0	0	0	0
RU188 - 69	0	0	0	0.078678	0.457056	0.504872	0.929026	1.594572	2.028353	1.371102	3.94405	1.661844	28.44054	15.95629	24.55551	6.715337	4.640948	3.199974	1.344682	0.397509	0.929414	0.680035	0.383095	0.307227	0.28176	0.240914	0.185335	0.128108	0.045771	0	0	0	0	0	0	0	0
RU188 - 69	0	0	0	0.082201	0.49112	0.539075	0.929828	1.653937	2.115661	1.414875	4.218819	1.760894	29.50795	16.23522	24.76547	6.634045	4.615156	2.80114	1.13227	0.315342	0.678878	0.36977	0.237239	0.206783	0.234572	0.214533	0.194177	0.134141	0.052268	0	0	0	0	0	0	0	0
RU188 - 69	0	0	0	0.082201	0.49112	0.539075	0.929828	1.653937	2.115661	1.414875	4.218819	1.760894	29.50795	16.23522	24.76547	6.634045	4.615156	2.80114	1.13227	0.315342	0.678878	0.36977	0.237239	0.206783	0.234572	0.214533	0.194177	0.134141	0.052268	0	0	0	0	0	0	0	0
RU188 - 70	0	0	0	0.075164	0.442006	0.491381	0.928364	1.581263	1.933052	1.288466	4.005797	1.766328	29.60254	16.44089	25.14376	6.640409	4.766227	3.486493	1.576832	0.488847	1.202938	0.873655	0.478803	0.296295	0.201331	0.133955	0.100268	0.079121	0	0	0	0	0	0	0	0	0
RU188 - 70	0	0	0	0.078437	0.45074	0.501586	0.929217	1.631265	2.005276	1.325375	4.198747	1.809434	29.18204	15.73282	23.94515	6.600064	4.633807	3.270636	1.412883	0.423924	1.000857	0.612154	0.399082	0.238206	0.19118	0.159707	0.129744	0.078915	0	0	0	0	0	0	0	0	0

Sed size (um)	0.05	0.06	0.12	0.24	0.49	0.7	0.98	1	2	3	3.9	7	7.8	15.6	20	31	37	44	53	60	63	74	88	105	125	149	177	210	250	300	350	420	500	590	710	840	1000
RU188_350	0	0	0	0.00286	0.19279	0.219198	0.013504	0.992215	0.994365	0.307239	2539765	1.986554	35.46221	17.20252	22.8007	5.572111	3.785936	2.772583	1.280569	0.417714	1.124954	0.686773	0.67452	0.460062	0.272162	0.075645	0.000613	0	0	0	0	0	0	0	0	0	0
RU188_350	0	0	0	0.038371	0.257305	0.291631	0.017945	1.30561	1.335144	0.474633	3.118181	2.952994	38.54294	18.13861	22.85249	4.94751	2.92649	1.687416	0.605235	0.166322	0.376397	0.250656	0.192379	0.141726	0.07635	0.003667	0	0	0	0	0	0	0	0	0	0	0
RU188_350	0	0	0	0.041321	0.269841	0.304836	0.016794	1.384596	1.460205	0.558005	3.303913	2.809956	39.38901	18.51506	22.97373	4.720759	2.599481	1.305241	0.37.3586	0.085054	0.151532	0.081057	0.070696	0.071774	0.011557	0	0	0	0	0	0	0	0	0	0	0	0
RU188_350	0	0	0	0.040515	0.304711	0.341174	0.01584	1.579024	1.722883	0.619726	3.609691	3.1.3.2	40.82142	19.17206	23.89389	4.534946	2.45.3.9	1.3.9.9	0.0.5.4	0.0.5.4	0.0.5.4	0.0.5.4	0.0.5.4	0.0.5.4	0.0.5.4	0.0.5.4	0.0.5.4	0.0.5.4	0.0.5.4	0.0.5.4	0.0.5.4	0.0.5.4	0.0.5.4	0.0.5.4	0.0.5.4	0.0.5.4	0.0.5.4	0.0.5.4
RU188_350	0	0	0	0.049524	0.308673	0.346069	0.021434	1.619906	1.796883	0.758741	3.661839	2.415728	40.85995	18.99449	22.77621	4.276794	2.025697	0.989169	0	0	0	0	0	0	0	0	0	0	0	0	0	0	0	0	0	0	0	0
RU188_351	0	0	0	0.084708	0.46312	0.532928	0.033355	2.0136	1.876322	0.835028	4.516586	2.48771	34.32569	15.10623	19.96648	5.085313	3.642526	2.833103	1.44313	0.492873	1.387118	1.164026	0.876757	0.574523	0.244501	0.016177	0	0	0	0	0	0	0	0	0	0	0
RU188_351	0	0	0	0.090754	0.493315	0.574328	0.036286	2.20413	2.002998	1.000265	4.974742	2.618288	35.75578	15.68479	20.36003	4.869216	3.213516	2.189789	0.958087	0.298044	0.760255	0.565159	0.419688	0.315751	0.240304	0.1698	0.102325	0	0	0	0	0	0	0	0	0	0
RU188_351	0	0	0	0.095671	0.5136	0.598865	0.03807	2.331335	2.273131	1.131684	5.257433	2.683582	36.47072	15.9684	20.46383	4.693485	2.930102	1.808052	0.690111	0.195024	0.447841	0.302231	0.249811	0.23961	0.229315	0.189163	0.134477	0.063656	0	0	0	0	0	0	0	0	0
RU188_351	0	0	0	0.078997	0.427245	0.512853	0.03211	2.110725	2.171475	1.141481	5.196569	2.621696	36.84469	16.47115	21.29938	4.797909	2.973047	1.618365	0.621796	0.127546	0.237529	0.124675	0.13925	0.195287	0.231253	0.21261	0.157349	0.076082	0	0	0	0	0	0	0	0	0
RU188_351	0	0	0	0.084761	0.4.1.4	0.5.1.4	0.0.1.4	1.9.1.4	1.9.1.4	0.9.1.4	4.6.1.4	2.3.1.4	3.1.1.4	1.4.1.4	1.8.1.4	4.1.1.4	2.6.1.4	1.9.1.4	0.8.1.4	0.2.1.4	0.4.1.4	0.3.1.4	0.2.1.4	0.1.1.4	0.1.1.4	0.1.1.4	0.1.1.4	0.1.1.4	0.1.1.4	0.1.1.4	0.1.1.4	0.1.1.4	0.1.1.4	0.1.1.4	0.1.1.4	0.1.1.4	0.1.1.4	0.1.1.4	0.1.1.4
RU188_351	0	0	0	0.081006	0.429228	0.517495	0.03381	2.195794	2.25322	1.289769	5.374875	2.65714	37.49157	16.98176	21.70941	4.672373	2.620351	1.272588	0.539453	0.012759	0	0	0	0	0	0	0	0	0	0	0	0	0	0	0	0	0	0
RU188_352	0	0	0	0.006838	0.398174	0.44862	0.027966	1.784354	1.992773	0.551492	3.883461	2.411344	34.02915	15.51682	20.55899	5.432013	3.965501	3.116543	1.587438	0.539261	1.501945	1.227912	0.905166	0.596506	0.259536	0.017003	0	0	0	0	0	0	0	0	0	0	0
RU188_352	0	0	0	0.07178	0.423102	0.494559	0.03051	1.960243	1.7938	0.689595	4.32909	2.563485	35.79189	15.90216	21.18058	5.23813	3.497758	2.368268	1.003286	0.302073	0.733481	0.499266	0.349894	0.264627	0.209606	0.153633	0.105602	0.053491	0	0	0	0	0	0	0	0	0
RU188_352	0	0	0	0.075807	0.440783	0.506321	0.032029	2.070237	1.946859	0.7987	4.594513	2.641072	36.77445	16.31818	21.48893	5.09415	3.200605	1.924613	0.673904	0.172173	0.328038	0.139799	0.098353	0.133339	0.172894	0.17337	0.143129	0.081571	0	0	0	0	0	0	0	0	0
RU188_352	0	0	0	0.078393	0.454194	0.523899	0.033267	2.173656	2.015818	0.888209	4.800277	2.702974	37.54297	16.65794	21.78317	5.000893	3.012191	1.850922	0.486514	0.074005	0.108212	0	0	0	0	0	0	0	0	0	0	0	0	0	0	0	0	0
RU188_352	0	0	0	0.081631	0.4.1.4	0.5.1.4	0.0.1.4	1.9.1.4	1.9.1.4	0.9.1.4	4.6.1.4	2.3.1.4	3.1.1.4	1.4.1.4	1.8.1.4	4.1.1.4	2.6.1.4	1.9.1.4	0.8.1.4	0.2.1.4	0.4.1.4	0.3.1.4	0.2.1.4	0.1.1.4	0.1.1.4	0.1.1.4	0.1.1.4	0.1.1.4	0.1.1.4	0.1.1.4	0.1.1.4	0.1.1.4	0.1.1.4	0.1.1.4	0.1.1.4	0.1.1.4	0.1.1.4	0.1.1.4	0.1.1.4
RU188_352	0	0	0	0.083631	0.47324	0.545769	0.034639	2.315014	2.288153	1.040604	5.020758	2.758374	38.07535	16.90435	21.75894	4.788883	2.669196	1.259901	0	0	0	0	0	0	0	0	0	0	0	0	0	0	0	0	0	0	0	0
RU188_353	0	0	0	0.089035	0.433132	0.501486	0.032132	1.603761	1.785406	0.905909	3.447148	1.918325	30.50564	15.10171	21.34047	5.714392	4.207213	3.399276	1.816061	0.639861	1.87234	1.664672	1.339851	0.949026	0.597288	0.198763	0.001692	0	0	0	0	0	0	0	0	0	0
RU188_353	0	0	0	0.093221	0.465782	0.543136	0.029915	1.77981	2.008074	1.08029	3.962445	2.064385	32.30912	15.92709	22.16231	5.604238	3.816277	2.717096	1.258568	0.407965	1.096737	0.886068	0.69309	0.514043	0.35264	0.199743	0.078965	0	0	0	0	0	0	0	0	0	0
RU188_353	0	0	0	0.097968	0.488749	0.521992	0.030858	1.912422	2.192266	1.028809	4.342234	2.162111	33.44625	16.43723	22.56	5.448293	3.483372	2.215236	0.882004	0.258069	0.621207	0.447763	0.363516	0.315104	0.263524	0.185508	0.095521	0	0	0	0	0	0	0	0	0	0
RU188_353	0	0	0	0.102916	0.507904	0.543214	0.032229	2.012619	2.341246	1.047987	4.60962	2.223367	34.16418	16.76131	22.78068	5.317137	3.231569	1.850575	0.615708	0.15379	0.298163	0.196085	0.17011	0.218949	0.239963	0.199532	0.112188	0	0	0	0	0	0	0	0	0	0
RU188_353	0	0	0	0.107095	0.534306	0.574023	0.034246	2.116073	2.376945	1.545396	4.990703	2.286704	34.9572	17.20068	23.15837	5.717451	3.92854	1.490043	0.313924	0.012357	0.109112	0	0	0	0	0	0	0	0	0	0	0	0	0	0	0	0	0
RU188_354	0	0	0	0.097265	0.453521	0.503521	0.032481	1.507257	1.97857	1.207287	3.251771	1.567929	28.21441	15.50631	23.07044	6.230854	4.458961	3.412968	1.720986	0.588683	1.681595	1.476039	1.214353	0.917814	0.62485	0.341042	0.001406	0	0	0	0	0	0	0	0	0	0
RU188_354	0	0	0	0.107798	0.500346	0.570579	0.032826	1.763797	2.327445	1.468475	3.88646	1.75274	30.73408	16.6902	24.03463	5.933777	3.789205	2.390014	0.944736	0.276798	0.676341	0.515629	0.450139	0.408562	0.351466	0.25241	0.149385	0.060466	0	0	0	0	0	0	0	0	0	0
RU188_354	0	0	0	0.112599	0.520389	0.530118	0.030129	1.892478	2.519612	1.614704	4.172832	1.81879	31.66402	17.12403	24.26693	5.726476	3.437825	1.915656	0.614988	0.150944	0.29774	0.197097	0.238206	0.303401	0.324625	0.269855	0.178628	0.078446	0	0	0	0	0	0	0	0	0	0
RU188_354	0	0	0	0.086935	0.433132	0.501486	0.032132	1.603761	1.785406	0.905909	3.447148	1.918325	30.50564	15.10171	21.34047	5.714392	4.207213	3.399276	1.816061	0.639861	1.87234	1.664672	1.339851	0.949026	0.597288	0.198763	0.001692	0	0	0	0	0	0	0	0	0	0
RU188_354	0	0	0	0.124651	0.568787	0.588173	0.034292	2.195317	2.97261	1.963247	4.745111	1.913427	33.13947	17.89177	24.94569	5.330042	2.783984	1.103653	0	0	0	0	0	0	0	0	0	0	0	0	0	0	0	0	0	0	0	0
RU188_354	0	0	0	0.102376	0.478448	0.484358	0.02647	1.445512	1.943093	1.316526	3.395539	1.434089	26.59271	15.57491	24.32122	6.762991	4.816596	3.565599	1.694599	0.554261	1.496052	1.207256	0.943057	0.710237	0.517659	0.335786	0.196301	0.083963	0	0	0	0	0	0	0	0	0	0
RU188_355	0	0	0	0.107798	0.504856	0.516584	0.028567	1.579707	2.135386	1.480247	3.821598	1.537475	27.76436	16.12762	24.94936	6.662823	4.523161	3.075637	1.302541	0.392832	0.982348	0.680874	0.516215	0.429692	0.374566	0.299171	0.215853	0.110546	0	0	0	0	0	0	0	0	0	0
RU188_355	0	0	0	0.112302	0.523009	0.537138	0.029866	1.669412	2.276707	1.599399	4.083578	1.594185	28.49598	16.43233	25.12524	6.539517	4.277891	2.772679	1.049326	0.294436	0.658807	0.41179	0.318397	0.308841	0.307479	0.268023	0.201089	0.10357	0	0	0	0	0	0	0	0	0	0
RU188_355	0	0	0	0.115726	0.536791	0.552476	0.031827	1.739538	2.392179	1.699127	4.231111	1.653369	29.38239	16.74784	25.32282	6.844062	4.494483	2.857004	1.362938	0.417795	0.917647	0.572191	0.445048	0.417347	0.381331	0.152384	0.204061	0.264475	0.255864	0.213258	0.14419	0.050312	0	0	0	0	0	0
RU188_355	0	0	0	0.122307	0.562351	0.580601	0.03254	1.814949	2.485618	1.90754	4.645249	1.90754	33.09127	17.8.1.9	25.66146	5.409585	2.889044	1.429178	0.413741	0.093203	0.070209	0.051502	0.043741	0.038943	0.033242	0.026911	0.020773	0.012565	0	0	0	0	0	0	0	0	0	0
RU188_355	0	0	0	0.122297	0.56367	0.582256	0.0327	1.871553	2.608	1.880797	4.641791	1.696254	29.91842	17.28814	25.82664	6.33071	3.813424	2.044991	0.57.473	0.083578	0.117298	0	0	0	0	0	0	0	0	0	0	0	0	0	0	0	0	0
RU188_356	0	0	0	0.082832	0.422884	0.43153	0.022774	1.119686	1.686049	1.299415	2.82111	0.986097	22.03359	15.23227	26.40253	7.843238	5.665423	4.173911	1.947731	0.629307	1.684645	1.377347	1.145244	0.956061	0.789	0.586536	0.400493	0.209753	0.050543	0	0	0	0	0	0	0	0	0
RU188_356	0	0	0	0.093019	0.465961	0.478644	0.025643	1.310803	1.995777	1.566026	3.424675	1.123799	23.99864	16.23265	27.35282	7.586943	5.054966	3.237086	1.242758	0.348512	0.792659	0.551143	0.515838	0.564589	0.594322	0.528736	0.40773	0.274459	0.139686	0.030958	0	0	0	0	0	0	0	0
RU188_356	0	0	0	0.124651	0.568787	0.588173	0.034292	2.195317	2.97261	1.963247	4.745111	1.913427	33.13947	17.89177	24.94569	5.330042	2.783984	1.103653	0	0	0	0	0	0	0	0	0	0	0	0	0	0	0	0	0	0	0	0
RU188_356	0	0	0	0.103861	0.507931	0.522297	0.028256	1.499585	2.334411	1.862842	3.982474	1.421486	25.41204	17.12493	27.91094	7.208963	4.38951	2.849596	0.942878	0.125805	0.302042	0.017906	0.205772	0.429934	0.575766	0.563485	0.450009	0.239494	0.111256	0	0	0	0	0	0	0	0	0
RU188_356	0	0	0	0.107095	0.534306	0.574023	0.034246	2.116073	2.376945	1.545396	4.990703	2.286704	34.9572	17.20068	23.15837	5.717451	3.92854	1.490043	0.313924	0.012357	0.109112	0	0	0	0	0	0	0	0	0	0	0	0	0	0	0	0	0
RU188_357	0	0	0	0.109366	0.526759	0.541866	0.029483	1.599007	2.513091	2.015036	4.223854	1.241306	25.88143	17.40376	27.89626	6.911643	3.993409	1.88605	0.383476	0.102534	0.023521	0	0	0	0	0	0	0	0	0	0	0	0	0	0	0	0	0
RU188_357	0	0	0	0.106483	0.385991	0.451413	0.024073	1.089586	1.378808	1.119039	3.498279	1.190812	19.85701	13.28169	25.33484	8.524493	6.669951	5.385314	2.656433	0.882003	2.393631	1.920849	1.482538	1.116864	0.798299	0.470618	0.15195	0	0	0	0	0	0	0	0	0	0
RU188_357	0	0	0	0.070252	0.41642	0.464813	0.026141	1.229028	1.587472	1.28353	3.865426	1.290329	21.49458	14.24434	26.46183	8.480449	6.297541	4.626968	2.059586	0.63074	1.542972	1.950888	0.74743	0.600818	0.523376	0.421765	0.309198	0.19822	0.076885	0	0	0	0	0	0	0	0	0
RU188_357	0	0	0	0.076401	0.441342	0.490901	0.027711	1.34015	1.768577	1.429142	4.166577	1.365247	22.7705	15.00074	27.28046	8.392288	5.955792	4.04.46	1.600941	0.444053	0.938321	0.476266	0.299969	0.316327	0.379267	0.379083	0.316091	0.215831	0.084322	0	0	0	0	0	0	0	0	0
RU188_357	0	0	0	0.090213	0.492886	0.542921	0.030644	1.723546	2.150949	1.403901	4.170256	1.463071	25.18627	16.53907	28.46385	8.01125	5.156054	3.918962	0.944047	0.109256	0.122559	0	0	0	0	0	0	0	0	0	0	0	0	0	0	0	0	0
RU188_357	0	0	0	0.093328	0.503498	0.553797	0.031539	1.634645	2.040055	1.787951	4.79601	1.513351	25.5927	16.61679	28.51285	7.84351	4.921901	2.643987	0.685318	0.028777	0	0	0	0	0	0	0	0	0	0	0	0	0	0	0	0	0	0
RU188_358	0	0	0	0.00631	0.375378	0.439045	0.027547	1.664008	1.454241	0.509095	3.618869	2.201264	31.20771	14.3603	20.80957	5.848162	4.452666	3.646722	1.922295	0.665469	1.896622	1.619742	1.275949	0.927984	0.636442	0.383892	0.212019	0.090694	0	0	0	0	0	0	0	0	0	0
RU188_358	0	0	0	0.006688	0.399395	0.472309	0.02985	1.804986	1.595269	0.63181	4.039808	2.335943	32.66806	14.97399	21.23585	5.796142	4.198957	3.17393	1.520098	0.494583	1.310188	1.005449	0.739842	0.537142	0.393254	0.270144	0.182856	0.129653	0.054996	0	0	0	0	0	0	0	0	0
RU188_358	0	0	0	0.006969	0.415607	0.493656	0.031304	1.886576	1.719028	0.733769	4.32894	2.412989	33.47972	15.13171	21.49872	5.68794	3.962288	2.865146	1.234829	0.379042	0.936173	0.690592	0.496728	0.377491	0.324219	0.273592	0.224548	0.180569	0.131947	0.03796	0	0	0	0	0	0	0	0
RU188_358	0	0	0	0.007049	0.429472	0.501113	0.032442	1.902643	1.825259	0.866515	4.711115	2.507331	34.58201	15.60116	22.19255	5.875535	4.098513	3.282114	1.274853	0.394211	0.967455	0.713168	0.513165	0.390715	0.335497	0.282711	0.230773	0.185751	0.135241	0.04773	0	0	0	0	0	0	0	0
RU188_358	0	0	0	0.072045	0.446906	0.523869	0.03897	2.069231	1.995164	0.958435	4.854253	2.53298	34.8163	15.91273	21.88719	5.414213	3.456978	2.094389	0.731526	0.186122	0.356617	0.173301	0.165779	0.236849	0.296215	0.288576	0.234986	0.165368	0.070201	0	0	0	0	0	0	0	0
RU188_359	0	0	0	0.074291	0.392177	0.413142	0.024722	1.634208	1.532916	0.456784	3.03064	2.188094	33.71714	15.48123	20.8788	5.454291	3.978842	3.157248	1.639024	0.565194	1.608409	1.369831	1.070587	0.746428	0.456847	0.128122	0.001037	0	0	0	0	0	0	0	0	0	0
RU188_359	0	0	0	0.079727	0.421262	0.450903	0.02728	1.798563	1.736293	0.615986	3.564549	2.385521	35.49125	16.17748	21.43781	5.275206	3.555912	2.485449	1.115871	0.352666	0.916284	0.700913	0.529476	0.392389	0.27715	0.166553	0.075528	0	0	0	0	0	0	0	0	0	0
RU188_359	0	0	0	0.082832	0.437457	0.471635	0.029876	1.8905	1.816185	0.719695	3.861493	2.435251	36.26397	16.64554	21.83447	5.147121	3.310707	2.127908	0.852894	0.249133	0.593485	0.409774	0.318504	0.273792	0.235066	0.175379	0.103895	0	0	0	0	0	0	0	0	0	0
RU188_359	0	0	0	0.085482	0.446826	0.481591	0.029609	1.961285	1.863194	0.783788	4.054747	2.481735	36.84294	16.67245	22.01901	5.33213	3.122497	1.872809	0.670001	0.177916	0.373414	0.22067	0.192221	0.214643	0.22561	0.19125	0.132486	0.059015	0	0	0	0	0	0	0	0	0
RU188_359	0	0	0	0.069755	0.362046	0.406067	0.02353	1.763	1.910784	0.879402	4.15606	2.454374	37.38018	17.4487	22.93909	5.184916	3.029366	1.557536	0.415363	0.018009	0	0	0	0	0	0	0	0	0	0	0	0	0	0	0	0	0	0
RU188_360	0	0	0	0.092837	0.434838	0.425471	0.023519	1.523659	1.883715	0.946074	2.654824	1.659247	31.10598	16.50828	23.25196	5.859758	4.000326	2.906048	1.402268	0.469747	1.317929	1.134464	0.921175	0.683135	0.45465	0.245016	0.095284	0	0	0	0	0	0	0	0	0	0
RU188_360	0	0	0	0.099727	0.464785	0.45841	0.025589	1.667642	2.084471	1.096949	3.077386	1.77974	32.90637	17.62649	23.74048	5.618477	3.547179	2.259528	0.927735	0.281545	0.661142	0.110029	0	0	0	0	0	0	0	0	0	0	0	0	0	0	0	0
RU188_360	0	0	0	0.081591	0.388384	0.393561	0.022449	1.51838	1.985762	1.108917	3.172954	1.792877	33.40008	17.90747	24.73832	5.682427	3.377237	1.888859	0.624239	0.159523	0.335144	0.231592	0.242651	0.269133	0.261008	0.204065	0.140093	0.077301	0	0	0	0	0	0	0	0	0	0
RU188_360	0	0	0	0.081699	0.385462	0.395112	0.022874	1.596536	2.072102	1.186638	3.358528	1.841675	34.44163	18.49659	25.74048	5.618477	3.547179	1.151722	1.563225	0.412584	0.066142	0.110029	0	0	0	0	0	0	0	0	0	0	0	0	0	0	0	0
RU188_360	0	0	0	0.093827	0.4.1.4	0.5.1.4	0.0.1.4	1.9.1.4	1.9.1.4	0.9.1.4	4.6.1.4	2.3.1.4	3.1.1.4	1.4.1.4	1.8.1.4	4.1.1.4	2.6.1.4	1.9.1.4	0.8.1.4	0.2.1.4	0.4.1.4	0.3.1.4	0.2.1.4	0.1.1.4	0.1.1.4	0.1.1.4	0.1.1.4	0.1.1.4	0.1.1.4	0.1.1.4	0.1.1.4	0.1.1.4	0.1.1.4	0.1.1.4	0.1.1.4	0.1.1.4	0.1.1.4	0.1.1.4	0.1.1.4
RU188_360	0	0	0	0.114471	0.522231	0.520275	0.02957	1.960927	2.544749	1.456115	3.85287	1.995389	35.61468	18.45787	24.2524	4.999173	2.565357	1.014668	0.484945	0.00682	0	0	0	0	0	0	0	0	0	0	0	0	0	0	0	0	0	0
RU188_360	0	0	0	0.117079	0.531389	0.530713	0.030206	2.017258	2.625252	1.821399	3.959706	2.010895	35.83115	18.54638	24.18214	4.866435	2.398243	0.831754	0	0	0	0	0	0	0	0	0	0	0	0	0	0	0	0	0	0	0	0

Sed size (um)	.005	.06	.12	.24	.49	.7	.98	1	2	3	3.9	7	7.8	15.6	20	31	37	44	53	60	63	74	88	105	125	149	177	210	250	300	350	420	500	590	710	840	1000
RU188 - 390		0	0	0.085959	0.421653	0.428859	0.023832	1.353783	1.537774	0.790409	2.842838	1.663184	28.04218	1.485145	22.31207	6.37089	4.845104	4.003347	2.152083	0.756376	2.196383	1.923188	1.524329	1.062924	0.653595	0.188309	0.001537	0	0	0	0	0	0	0	0	0	0	0
RU188 - 390		0	0	0.091064	0.451405	0.466119	0.026234	1.499916	1.723646	0.944929	3.334264	1.776391	29.67825	1.553285	23.09618	6.332861	4.57014	3.468705	1.689228	0.568283	1.511083	1.196284	0.887371	0.61119	0.426015	0.120011	0.001006	0	0	0	0	0	0	0	0	0	0	0
RU188 - 390		0	0	0.093386	0.481511	0.5073	0.028958	1.671047	1.902572	1.045275	3.939772	1.965048	31.44917	1.613957	24.73422	6.673047	4.982396	3.715761	1.814798	0.63765	1.686071	1.344183	0.969148	0.729451	0.477514	0.129496	0.001158	0	0	0	0	0	0	0	0	0	0	0
RU188 - 390		0	0	0.100599	0.495151	0.517216	0.029496	1.714277	2.043037	1.214539	4.080488	1.974531	31.84667	1.640629	23.82564	5.978181	3.91985	2.540589	1.010964	0.290382	0.670673	0.430061	0.310714	0.260521	0.223431	0.164734	0.093373	0	0	0	0	0	0	0	0	0	0	0
RU188 - 390		0	0	0.102741	0.503608	0.526559	0.030086	1.754075	2.100359	1.261762	4.207381	2.007665	32.20048	16.595	23.67246	5.904617	3.807129	2.397596	0.915524	0.255304	0.56517	0.340612	0.24462	0.213489	0.188608	0.134474	0.07088	0	0	0	0	0	0	0	0	0	0	0
RU188 - 391		0	0	0.083838	0.434563	0.460964	0.026309	1.463386	1.494912	0.759095	3.378786	1.864481	29.36473	1.483457	21.8698	6.173238	4.665805	3.818063	2.025631	0.705035	2.019691	1.722998	1.325062	0.899671	0.530172	0.108169	0.000766	0	0	0	0	0	0	0	0	0	0	0
RU188 - 391		0	0	0.088593	0.460067	0.49191	0.026321	1.565218	1.665319	0.888199	3.756289	1.983175	30.82928	1.550182	23.58284	6.154466	4.446516	3.380252	1.842168	0.54001	1.445311	1.109806	0.779034	0.549091	0.361231	0.115359	0.001242	0	0	0	0	0	0	0	0	0	0	0
RU188 - 391		0	0	0.091161	0.473733	0.502849	0.02947	1.609726	1.796854	0.941065	3.896834	2.064221	31.53413	1.602647	23.92098	6.095329	4.295335	3.452791	1.867921	0.547094	1.467201	1.126024	0.790778	0.557116	0.366298	0.11459	0.001254	0	0	0	0	0	0	0	0	0	0	0
RU188 - 391		0	0	0.093725	0.492722	0.522969	0.030647	1.677172	1.872136	0.980754	4.060705	2.150998	32.84165	1.663047	24.73115	6.350267	4.474772	3.594855	1.945704	0.569234	1.527891	1.172611	0.823731	0.579778	0.381288	0.119519	0.001305	0.071564	0.128743	0.069834	0	0	0	0	0	0	0	0
RU188 - 391		0	0	0.096996	0.493734	0.53191	0.031024	1.739533	1.907624	1.000222	4.267344	2.125513	32.48779	16.20637	24.08489	5.908412	3.942126	2.616118	1.062848	0.307749	0.704396	0.424562	0.270669	0.207369	0.180299	0.147238	0.112812	0.063669	0	0	0	0	0	0	0	0	0	0
RU188 - 392		0	0	0.087567	0.438694	0.456778	0.029323	1.450613	1.49581	0.662596	2.834398	1.791962	30.32381	1.562696	22.7569	6.184489	4.500179	3.506905	1.777205	0.603919	1.659844	1.406289	1.072555	0.763731	0.448527	0.119397	0.000949	0	0	0	0	0	0	0	0	0	0	0
RU188 - 392		0	0	0.091708	0.459795	0.484252	0.027604	1.502695	1.612561	0.767398	3.159515	1.836099	31.50049	1.613899	23.19633	6.138553	4.461247	3.463846	1.838853	0.46346	1.213926	0.92446	0.669776	0.447795	0.291315	0.166853	0.084902	0	0	0	0	0	0	0	0	0	0	0
RU188 - 392		0	0	0.093521	0.470302	0.495151	0.028776	1.556477	1.670045	0.829074	3.506727	1.914151	30.96873	1.594577	23.01015	6.091715	4.427531	3.438965	1.824707	0.579039	1.502178	1.252755	0.945757	0.663224	0.443198	0.14877	0.001671	0.064902	0	0	0	0	0	0	0	0	0	0
RU188 - 392		0	0	0.094522	0.47397	0.500464	0.02876	1.622207	1.72086	0.8454	3.401856	1.963741	32.30227	16.4551	23.41125	5.982837	4.034562	2.770189	1.198599	0.36635	0.930843	0.621287	0.419811	0.292263	0.212147	0.146777	0.10329	0.083109	0.042922	0	0	0	0	0	0	0	0	0
RU188 - 392		0	0	0.096401	0.482534	0.510386	0.029371	1.658209	1.768173	0.883992	3.513526	1.997011	32.70865	16.62971	23.91945	5.911229	3.905548	2.594455	1.077052	0.320567	0.769645	0.516859	0.361714	0.275946	0.218955	0.156931	0.093689	0	0	0	0	0	0	0	0	0	0	0
RU188 - 393		0	0	0.087762	0.434418	0.450906	0.025486	1.449757	0.656271	0.823414	1.744716	0.929848	4.220866	2.324329	0.822474	2.38626	2.054182	1.575501	1.062678	0.620065	0.511838	0.33838	0.240446	0.175702	0.127677	0.093711	0.001222	0	0	0	0	0	0	0	0	0	0	0
RU188 - 393		0	0	0.090827	0.4535	0.475995	0.027153	1.504186	1.563509	0.739738	3.122381	1.841475	29.80206	1.498198	21.99506	6.267469	4.782458	3.923375	2.056376	0.70504	1.967063	1.587886	1.137178	0.718087	0.243033	0.014352	0	0	0	0	0	0	0	0	0	0	0	0
RU188 - 393		0	0	0.088887	0.459494	0.471042	0.026828	1.504101	1.565454	0.717561	2.999451	1.844363	30.99199	1.593213	23.05033	6.154591	4.385186	3.306617	1.610839	0.533843	1.451111	1.152683	0.84597	0.561973	0.344013	0.010578	0	0	0	0	0	0	0	0	0	0	0	0
RU188 - 393		0	0	0.091708	0.469795	0.482832	0.027604	1.502695	1.612561	0.767398	3.159515	1.836099	31.50049	1.613899	23.19633	6.138553	4.461247	3.463846	1.838853	0.46346	1.213926	0.92446	0.669776	0.447795	0.291315	0.166853	0.084902	0	0	0	0	0	0	0	0	0	0	0
RU188 - 393		0	0	0.093521	0.470302	0.495151	0.028776	1.556477	1.670045	0.829074	3.506727	1.914151	30.96873	1.594577	23.01015	6.091715	4.427531	3.438965	1.824707	0.579039	1.502178	1.252755	0.945757	0.663224	0.443198	0.14877	0.001671	0.064902	0	0	0	0	0	0	0	0	0	0
RU188 - 393		0	0	0.094522	0.47397	0.500464	0.02876	1.622207	1.72086	0.8454	3.401856	1.963741	32.30227	16.4551	23.41125	5.982837	4.034562	2.770189	1.198599	0.36635	0.930843	0.621287	0.419811	0.292263	0.212147	0.146777	0.10329	0.083109	0.042922	0	0	0	0	0	0	0	0	0
RU188 - 393		0	0	0.096401	0.482534	0.510386	0.029371	1.658209	1.768173	0.883992	3.513526	1.997011	32.70865	16.62971	23.91945	5.911229	3.905548	2.594455	1.077052	0.320567	0.769645	0.516859	0.361714	0.275946	0.218955	0.156931	0.093689	0	0	0	0	0	0	0	0	0	0	0
RU188 - 393		0	0	0.090827	0.4535	0.475995	0.027153	1.504186	1.563509	0.739738	3.122381	1.841475	29.80206	1.498198	21.99506	6.267469	4.782458	3.923375	2.056376	0.70504	1.967063	1.587886	1.137178	0.718087	0.243033	0.014352	0	0	0	0	0	0	0	0	0	0	0	0
RU188 - 393		0	0	0.088887	0.459494	0.471042	0.026828	1.504101	1.565454	0.717561	2.999451	1.844363	30.99199	1.593213	23.05033	6.154591	4.385186	3.306617	1.610839	0.533843	1.451111	1.152683	0.84597	0.561973	0.344013	0.010578	0	0	0	0	0	0	0	0	0	0	0	0
RU188 - 393		0	0	0.091708	0.469795	0.482832	0.027604	1.502695	1.612561	0.767398	3.159515	1.836099	31.50049	1.613899	23.19633	6.138553	4.461247	3.463846	1.838853	0.46346	1.213926	0.92446	0.669776	0.447795	0.291315	0.166853	0.084902	0	0	0	0	0	0	0	0	0	0	0
RU188 - 394		0	0	0.112359	0.546309	0.605666	0.035942	1.818856	1.932558	1.165406	3.981832	1.826224	28.2345	14.43998	21.5138	6.133413	4.648866	3.788996	1.986172	0.684166	1.932333	1.615286	1.238139	0.875801	0.580305	0.330849	0.001222	0	0	0	0	0	0	0	0	0	0	0
RU188 - 394		0	0	0.114811	0.560701	0.628907	0.036995	1.869727	2.027769	1.251651	4.261889	1.898847	28.9712	14.65157	21.60945	6.027461	4.668582	3.533297	1.796156	0.608105	1.687196	1.380327	1.047791	0.743113	0.502277	0.297826	0.102696	0	0	0	0	0	0	0	0	0	0	0
RU188 - 394		0	0	0.113757	0.557846	0.627642	0.036911	1.866557	2.023774	1.249722	4.252374	1.894277	29.00748	14.66721	21.66882	5.772951	4.094261	3.651379	1.845231	0.615945	1.682586	1.378155	1.045434	0.741307	0.500238	0.274691	0.151502	0.062523	0	0	0	0	0	0	0	0	0	0
RU188 - 394		0	0	0.119808	0.591348	0.669064	0.039988	2.072759	2.248716	1.442081	4.883018	2.063752	30.3025	15.08927	21.63801	5.693997	3.9806	2.905806	1.36484	0.443147	1.185405	0.94488	0.739283	0.572018	0.437825	0.299937	0.185034	0.08619	0	0	0	0	0	0	0	0	0	0
RU188 - 395		0	0	0.10207	0.48374	0.503177	0.02831	1.542216	1.869451	1.131146	3.093024	1.484258	26.44125	14.53836	22.33436	6.544968	5.066451	4.248063	2.292362	0.802748	2.305744	1.961714	1.499948	1.011498	0.596554	0.121724	0.000863	0	0	0	0	0	0	0	0	0	0	0
RU188 - 395		0	0	0.104056	0.501319	0.529183	0.030076	1.639578	1.992883	1.242389	3.448452	1.577744	27.33262	14.87917	22.60486	6.466648	4.875057	3.83231	2.03496	0.694911	1.940113	1.584111	1.170739	0.774785	0.479767	0.163059	0.001395	0	0	0	0	0	0	0	0	0	0	0
RU188 - 395		0	0	0.106306	0.516633	0.549915	0.03144	1.717375	2.098863	1.334365	3.736064	1.656233	28.13339	15.191	22.83934	6.390041	4.703689	3.66204	1.82086	0.606336	1.84295	1.579886	1.208161	0.958634	0.382738	0.12664	0.00109	0	0	0	0	0	0	0	0	0	0	0
RU188 - 395		0	0	0.108112	0.527716	0.559812	0.032368	1.785146	2.183124	1.408254	3.917077	1.763208	28.77913	15.5143	23.29231	6.537014	4.946825	3.823198	1.849985	0.615803	1.872945	1.602181	1.229691	0.97647	0.647254	0.21706	0.001258	0	0	0	0	0	0	0	0	0	0	0
RU188 - 395		0	0	0.110645	0.537231	0.570115	0.03354	1.827403	2.235143	1.440874	4.007977	1.817355	29.70695	15.87531	23.97373	6.691045	5.062308	4.029185	2.029118	0.654965	1.997258	1.708754	1.310761	1.041871	0.690258	0.231768	0.001778	0.109676	0.062076	0	0	0	0	0	0	0	0	0
RU188 - 395		0	0	0.11086	0.545996	0.590834	0.034215	1.876009	2.298797	1.514732	4.336345	1.914978	29.62246	15.67689	22.98581	6.088338	4.231116	3.024174	1.364	0.427175	1.079569	0.761512	0.513006	0.349338	0.253046	0.185528	0.144953	0.122406	0.05982	0	0	0	0	0	0	0	0	0
RU188 - 395		0	0	0.112417	0.555069	0.602928	0.035016	1.924517	2.362429	1.570465	4.52502	1.872985	30.12326	15.83111	22.96274	5.959288	4.048202	2.795605	1.21235	0.370855	0.916776	0.637423	0.445158	0.32987	0.262	0.202717	0.156884	0.129932	0.059885	0	0	0	0	0	0	0	0	0
RU188 - 396		0	0	0.106272	0.514916	0.557687	0.032652	1.644749	1.925453	1.235688	3.459958	1.505511	25.62213	14.18279	22.16604	6.591305	5.131732	4.324335	2.345242	0.824224	2.380482	2.048364	1.588597	1.080008	0.626793	0.134028	0.000722	0	0	0	0	0	0	0	0	0	0	0
RU188 - 396		0	0	0.108888	0.545969	0.604033	0.03523	1.820438	2.133907	1.424144	4.072308	1.66594	27.19637	14.77146	22.60309	6.430406	4.771118	3.745365	1.8792	0.629856	1.723042	1.570965	1.003128	0.684149	0.439609	0.253564	0.080745	0	0	0	0	0	0	0	0	0	0	0
RU188 - 396		0	0	0.111173	0.559587	0.604029	0.03589	1.862628	2.227527	1.504344	4.34316	1.736744	27.81346	14.95205	22.85602	6.360909	4.62419	3.512102	1.69738	0.565602	1.478899	1.303966	0.906505	0.651028	0.396772	0.22546	0.091039	0	0	0	0	0	0	0	0	0	0	0
RU188 - 396		0	0	0.113757	0.570825	0.627642	0.036911	1.866557	2.023774	1.249722	4.252374	1.894277	29.00748	15.87531	23.97373	6.691045	5.062308	4.029185	2.029118	0.654965	1.997258	1.708754	1.310761	1.041871	0.690258	0.231768	0.001778	0.109676	0.062076	0	0	0	0	0	0	0	0	0
RU188 - 396		0	0	0.114788	0.578825	0.652753	0.03851	2.005501	2.363366	1.623584	4.731292	1.844528	28.84323	15.3338	22.80646	6.100312	4.253311	3.046676	1.385921	0.438938	1.134929	0.850266	0.623753	0.455948	0.332297	0.219858	0.13729	0.070836	0	0	0	0	0	0	0	0	0	0
RU188 - 396		0	0	0.117596	0.59281	0.69312	0.039638	2.069105	2.442896	1.686007	4.936648	1.903196	29.37925	15.4918	22.79253	5.977088	4.072742	2.829113	1.245158	0.387039	0.983973	0.728496	0.543196	0.411612	0.309884	0.207875	0.12574	0.057539	0	0	0	0	0	0	0	0	0	0
RU188 - 397		0	0	0.102708	0.490026	0.514804	0.029066	1.527988	1.766526	1.046239	3.167173	1.548252	26.78695	14.65399	22.59381	6.572242	5.018393	4.129389	2.192561	0.762319	2.176525	1.849513	1.416093	0.961855	0.570173	0.122508	0.000891	0	0	0	0	0	0	0	0	0	0	0
RU188 - 397		0	0	0.105621	0.510895	0.543966	0.031027	1.644045	1.903956	1.161706	3.541136	1.660647	27.99154	15.12696	22.96338	6.478831	4.790174	3.760507	1.895523	0.638184	1.756345	1.406792	1.024515	0.668968	0.38757	0.111457	0	0	0	0	0	0	0	0	0	0	0	0
RU188 - 397		0	0	0.108137	0.525951	0.563861	0.032341	1.714146	1.968168	1.244893	3.817833	1.738045	28.7514	15.41469	23.18235	6.386657	4.600523	3.469621	1.670142	0.546255	1.454393	1.109069	0.77804	0.499762	0.30721	0.110735	0.000885	0	0	0	0	0	0	0	0	0	0	0
RU188 - 397		0	0	0.110704	0.545027	0.594394	0.034403	1.83301	2.141763	1.367467	4.249022	1.864529	29.95207	15.8143	23.34053	6.620578	4.295726	3.037968	1.349612	0.418095	1.042018	0.716941	0.495337	0.304308	0.198201	0.107978	0.001017	0	0	0	0	0	0	0	0	0	0	0
RU188 - 397		0	0	0.112065	0.556139	0.606588	0.03524	1.878384	2.196561	1.417345	4.428116	1.91508	30.40693	15.95943	23.37628	6.119161	4.160284	3.077205	1.422533	0.370167	0.894427	0.58527	0.371739	0.245524	0.17113	0.108376	0.001041	0	0	0	0	0	0	0	0	0	0	0
RU188 - 398		0	0	0.095612	0.476423	0.51121	0.029344	1.555859	1.725996	0.999695	3.397048	1.669638	26.97845	14.09423	21.64554	6.516227	5.161405	4.414691	2.404818	0.842307	2.403994	2.020342	1.506288	0.982254	0.550522	0.135898	0.000695	0	0	0	0	0	0	0	0	0	0	0
RU188 - 398		0	0	0.097703	0.496629	0.546848	0.031794	1.698511	1.883255	1.134761	3.862148	1.804867	28.32086	14.61041	22.09726	6.433735	4.913245	3.982091	2.041955	0.688701	1.880923	1.463125	1.016213	0.619814	0.369526	0.011643	0	0	0	0	0	0	0	0	0	0	0	0
RU188 - 398		0	0	0.099693	0.514121	0.56743	0.033186	1.766098	1.985351	1.226795	4.169698	1.886437	29.09061	14.90312	22.33561	6.385415	4.745389	3.709363	1.824374	0.598885	1.581348	1.1833	0.758766	0.469274	0.194176	0.012828	0	0	0	0	0	0	0	0	0	0	0	0
RU188 - 398		0	0	0.102776	0.537552	0.600158	0.035458	1.896358	2.146202	1.373074	4.670349	2.025392	30.34809	15.32971	23.51803	6.159097	4.38775	3.203545	1.453961	0.452577	1.132149	0.741822	0.486539	0.350116	0.138121	0.009609	0	0	0	0	0	0	0	0	0	0	0	0
RU188 - 398		0	0	0.104297	0.546626	0.613571	0.036298	1.940356	2.197847	1.418952	4.834067	2.070181	30.72135	15.44027	22.95038	6.086674	4.276854	3.056529	1.350202	0.412234	0.995628	0.729753	0.364539	0.224387	0.111398	0.007757	0	0	0	0	0	0	0	0	0	0	0	0
RU188 - 399		0	0	0.103522	0.480005	0.494619	0.02759	1.440672	1.621007	0.886784	2.917762	1.547529	26.6044	14.26363	22.08694	6.684304	5.314842	4.568924	2.49924	0.877261	2.511	2.100092	1.551349	0.972425	0.424481	0.009618	0	0	0	0	0	0	0	0	0	0	0	0
RU188 - 399		0	0	0.105413	0.499095	0.523759	0.029612	1.554724	1.754224	1.011682	3.30523	1.665952	27.71769	14.7019	22.50564	6.639291	5.130559	4.226735	2.203818	0.750369	2.069028	1.629125	1.139822	0.682506	0.162062	0.007163	0	0	0	0	0	0	0	0	0	0	0	0
RU188 - 399		0	0	0.107682	0.514349	0.544814	0.031026	1.638854	1.852699	1.092609	3.57142	1.739134	29.5634	15.03481	22.76619	6.561918	4.948945	3.937366	1.975153	0.656221	1.759947	1.314112	0.865123	0.491339	0.039909	0	0	0	0	0	0	0	0	0	0	0	0	0
RU188 - 399		0	0	0.110138	0.552446	0.578993	0.03375	1.698435	1.901478	1.129489	3.772564	1.787501	28.96727	15.41618	22.69982	6.501792	4.832225	3.785283	2.018903	0.695732	1.824868	1.497241	1.07695	0.714041	0.470825	0.194761	0.070491	0.010711	0	0	0	0	0	0	0	0	0	0
RU188 - 399		0	0	0.110566	0.540134	0.58439	0.03378	1.789197	2.039209	1.262259	4.165355	1.900591	29.98827	15.51767	23.00722	6.324555	4.523566	3.816809	1.503831	0.468989	1.154996	0.749117	0.439055	0.249226	0.155379	0.103854	0.070491	0	0	0	0	0	0	0	0	0	0	0
RU188 - 400		0	0	0.098904	0.496132	0.525648	0.032128	1.768691	1.997793	1.285522	2.747078	2.747078	26.40213	14.4458	22.41735	6.711978	5.285555	4.565128	2.454625	0.861917	2.475499	2.092807	1.571928	1.029437	0.582575	0.216965	0	0	0	0	0	0	0	0	0	0	0	0
RU188 - 400		0	0	0.099357	0.475845	0.492765	0.027495	1.465576	1.711922	0.998017	3.505811	1.561635	27.26034	14.79954	22.77151	6.690643	5.147499	4.232193	2.213014	0.756607	2.101779	1.680046	1.191552	0.74004	0.424003	0.091149	0.000661	0	0	0	0	0	0	0	0	0	0	0
RU188 - 400		0	0	0.100055	0.491175	0.512486	0.028788	1.543874	1.82113	1.06178	3.312236	1.634978	28.0582	15.1218	23.05785	6.648655	5.011389	3.994094	2.013992	0.672353	1.812002	1.375751	0.915759	0.562089	0.213186	0.013313	0	0	0	0	0	0	0	0	0	0	0	0
RU188 - 400		0	0	0.103967	0.501336	0.525779	0.029663	1.599265	1.893878	1.140888	3.489664	1.663071	28.53412	15.30006	23.17963	6.594145	4.898943	3.820236	1.877952	0.61621	1.623584	1.18979	0.762161	0.452654	0.166782	0.010176	0	0	0	0	0	0	0	0	0	0	0	0
RU188 - 400		0	0	0.101726	0.493102	0.516107	0.029243	1.581755	1.852707	1.102454	3.441959	1.659763	28.06829	15.07214	23.00292	6.452323	4.657284	3.441959	1.594679	0.504298	1.288896	0.852707	0.506304	0.275338	0.044624	0	0	0	0	0	0	0	0	0	0	0	0	0
RU188 - 400		0	0	0.107296	0.520006	0.550489	0.031352	1.703207	2.027468	1.250749	3.820763	1.779619	29.51473	15.67714	23.40092	6.452523	4.657284	3.441959	1.594679	0.504298	1.288896	0.852707	0.506304	0.275338	0.044624	0	0	0	0	0	0	0	0	0	0	0	0	0
RU188 - 400		0	0	0.108014	0.526004	0.556238	0.032049	1.740672	2.071024	1.292342	3.970305	1.813674	29.75644	15.7213	23.3763	6.388121	4.538212	4.538212	2.288976	1.485978	0.458886	1.118205	0.704813	0.387689	0.203458	0.119772	0.088375	0.087679	0.097004	0.055366	0	0	0	0	0	0	0	0

Sed size (um)	0.05	0.06	0.12	0.24	0.49	0.7	0.98	1	2	3	3.9	7	7.8	15.6	20	31	37	44	53	60	63	74	88	105	125	149	177	210	250	300	350	420	500	590	710	840	1000
RU188 - 530	0	0	0	0.125679	0.622553	0.749762	0.945848	2.237043	2.883442	2.799525	10.60815	3.001076	28.72879	12.35233	18.77727	5.647573	4.36214	3.53108	1.690876	0.517953	1.096174	0.222732	0	0	0	0	0	0	0	0	0	0	0	0	0	0	0
RU188 - 530		0	0	0.129437	0.648553	0.7962	0.949474	2.486375	3.193168	3.055856	11.35132	3.179884	30.06571	12.62693	18.42714	5.199562	3.81504	2.901912	1.248938	0.354153	0.471361	0	0	0	0	0	0	0	0	0	0	0	0	0	0	0	0	0
RU188 - 530			0	0.115426	0.662209	0.814587	0.949916	2.568947	3.375096	3.258692	12.62793	3.53178	31.13498	16.83123	4.171137	2.757038	1.648947	0.456305	0.019375	0	0	0	0	0	0	0	0	0	0	0	0	0	0	0	0	0	0	0
RU188 - 530			0	0.09131	0.538704	0.68683	0.04309	2.344975	3.268179	3.211211	12.27056	3.541739	33.89373	13502844	17.95434	4.196905	2.749117	1.63731	0.421584	0.016969	0	0	0	0	0	0	0	0	0	0	0	0	0	0	0	0	0	0
RU188 - 530			0	0.093317	0.555174	0.715342	0.045272	2.490185	3.462223	3.381687	13.25858	3.648683	34.47316	13540893	17.9434	4.302903	2.862399	1.0045468	0	0	0	0	0	0	0	0	0	0	0	0	0	0	0	0	0	0	0	0
RU188 - 531			0	0.159046	0.7417	0.927559	0.058414	2.647145	3.581167	3.4755	13.56358	3.741988	35.59537	14.0273	18.57084	4.392093	2.913194	0.9972148	0	0	0	0	0	0	0	0	0	0	0	0	0	0	0	0	0	0	0	0
RU188 - 531			0	0.153227	0.770358	0.913508	0.0551	2.68745	3.353098	3.152415	11.42259	3.138764	28.74153	11.73947	17.10972	4.910329	3.661124	2.815721	1.342291	0.430433	1.106714	0.79414	0.547387	0.393225	0.30519	0.226704	0.154362	0.074846	0	0	0	0	0	0	0	0	0	0
RU188 - 531			0	0.158235	0.810007	0.976205	0.060383	3.0076	3.728105	3.44015	12.17453	3.314928	30.0955	12.03445	16.80934	4.483976	3.132858	2.199699	0.943115	0.28188	0.667697	0.429649	0.299954	0.256611	0.246264	0.213137	0.156581	0.077134	0	0	0	0	0	0	0	0	0	0
RU188 - 531			0	0.162029	0.838453	1.022697	0.063799	3.228387	3.981715	3.639147	12.68702	3.422239	30.67755	12.02425	16.33652	4.181118	2.827586	1.904839	0.782018	0.227814	0.527165	0.336378	0.249755	0.231151	0.22943	0.199411	0.14717	0.074356	0	0	0	0	0	0	0	0	0	0
RU188 - 531			0	0.166002	0.85985	1.060337	0.066875	3.415526	4.189213	3.791561	13.03744	3.490316	31.00483	11.98037	15.97141	3.976357	2.636685	1.732421	0.692982	0.198769	0.453218	0.286156	0.216585	0.205221	0.203796	0.174969	0.127129	0.060189	0	0	0	0	0	0	0	0	0	0
RU188 - 531			0	0.168677	0.874899	1.065577	0.068663	3.551091	4.34741	3.913419	13.31162	3.516591	31.12899	11.90145	15.88924	3.853888	2.528896	1.642052	0.647304	0.18378	0.414057	0.257467	0.195312	0.185433	0.19401	0.159038	0.110961	0.05823	0	0	0	0	0	0	0	0	0	0
RU188 - 532			0	0.173869	0.903482	1.082381	0.070114	3.683482	4.509728	4.061523	13.81478	3.637627	32.29205	11.84078	15.90729	3.814584	2.494773	1.597476	0.662728	0.174504	0.384773	0.239174	0.171265	0.162254	0.168958	0.138594	0.096253	0.043556	0	0	0	0	0	0	0	0	0	0
RU188 - 532			0	0.175069	0.849742	1.021568	0.063452	3.617624	3.802161	3.40891	12.01977	3.313163	30.26388	12.00075	16.52491	4.337175	3.007069	2.106622	0.91114	0.275905	0.670998	0.461735	0.345832	0.301155	0.28542	0.251578	0.205232	0.152353	0.066798	0	0	0	0	0	0	0	0	0
RU188 - 532			0	0.177659	0.868222	1.035534	0.065948	3.434241	3.997102	3.558887	12.41241	3.395455	30.68578	11.97249	16.13961	4.109501	2.785236	1.897582	0.798019	0.237866	0.570753	0.391209	0.301731	0.271881	0.231118	0.203923	0.191425	0.150301	0.111931	0.027579	0	0	0	0	0	0	0	0
RU188 - 532			0	0.181245	0.88919	1.087046	0.068434	3.487677	4.152759	3.690048	12.75778	3.462495	30.94648	11.91332	15.83282	3.95304	2.638905	1.782162	0.724851	0.213219	0.505767	0.345945	0.274028	0.255254	0.241122	0.206835	0.164197	0.125233	0.096245	0.026607	0	0	0	0	0	0	0	0
RU188 - 532			0	0.183793	0.907231	1.119236	0.070964	3.648035	4.327737	3.827707	13.10292	3.526154	31.11888	11.77682	15.40903	3.771982	2.495693	1.662618	0.676376	0.196612	0.482238	0.329617	0.270085	0.253235	0.239062	0.202135	0.16923	0.126544	0.1006	0.027012	0	0	0	0	0	0	0	0
RU188 - 532			0	0.186356	0.925941	1.150777	0.073149	3.808411	4.503255	3.963723	13.38977	3.595021	31.93705	11.63245	15.0145	3.587241	2.447023	1.628214	0.649849	0.188746	0.461446	0.314744	0.257109	0.241555	0.227962	0.192235	0.160731	0.120671	0.095672	0.026723	0	0	0	0	0	0	0	0
RU188 - 533			0	0.160356	0.769353	0.900078	0.054709	2.673628	3.235252	2.925415	10.65804	3.032698	28.7971	11.93762	17.42852	5.019835	3.762928	3.020948	1.408675	0.455388	1.182006	0.858908	0.590424	0.410785	0.302255	0.215344	0.148909	0.102268	0.040922	0	0	0	0	0	0	0	0	0
RU188 - 533			0	0.169105	0.835961	1.008971	0.062907	3.204215	3.83777	3.399713	11.99915	3.353466	31.07486	12.31808	16.67618	4.24202	2.859763	1.923769	0.790879	0.230892	0.553656	0.340367	0.244535	0.216316	0.208416	0.180274	0.139474	0.102714	0.044547	0	0	0	0	0	0	0	0	0
RU188 - 533			0	0.171079	0.857938	1.050411	0.066168	3.410515	4.069771	3.58556	12.48806	3.451604	31.48307	12.01245	16.13505	3.972211	2.6203	1.722746	0.695972	0.202024	0.469644	0.305291	0.229013	0.199064	0.186297	0.156886	0.120771	0.09245	0.043556	0	0	0	0	0	0	0	0	0
RU188 - 533			0	0.173435	0.874117	1.071111	0.067403	3.474497	4.252764	3.691077	12.85938	3.551295	32.01245	12.06496	16.20214	4.289446	2.885241	1.744296	0.702284	0.204962	0.475131	0.309446	0.232135	0.201982	0.188531	0.158414	0.122016	0.093131	0.04085	0	0	0	0	0	0	0	0	0
RU188 - 533			0	0.150638	0.763557	0.890226	0.05429	2.682253	2.721073	2.852215	10.7404	3.075684	29.57313	12.08236	17.56758	4.841603	3.485303	2.566655	1.174079	0.36842	0.791739	0.237503	0.579447	0.413061	0.324874	0.284326	0.256137	0.212537	0.168993	0.138495	0.123832	0.100346	0.111257	0.086375	0.00637	0	0
RU188 - 534			0	0.153867	0.779666	0.929226	0.057228	2.843256	3.950719	3.191798	11.52048	3.293117	31.37194	12.61067	16.94673	4.228487	2.812454	1.880116	0.785458	0.233848	0.58125	0.431207	0.360501	0.330106	0.307276	0.261016	0.212295	0.175058	0.151135	0.109	0.104797	0.01595	0	0	0	0	0
RU188 - 534			0	0.129801	0.669784	0.816622	0.05283	2.373614	3.493788	3.304779	11.8106	3.144928	31.44657	12.45843	16.97959	4.095214	2.797731	1.801851	0.746896	0.223871	0.534446	0.401939	0.332035	0.301752	0.276111	0.225394	0.173766	0.135021	0.12744	0.115017	0.147289	0.134757	0.094507	0.046941	0	0	0
RU188 - 534			0	0.171079	0.857938	1.050411	0.066168	3.410515	4.069771	3.58556	12.48806	3.451604	31.48307	12.01245	16.13505	3.972211	2.6203	1.722746	0.695972	0.202024	0.469644	0.305291	0.229013	0.199064	0.186297	0.156886	0.120771	0.09245	0.043556	0	0	0	0	0	0	0	0	0
RU188 - 535			0	0.176328	0.844181	1.01513	0.063637	3.309004	3.918239	3.347649	11.99015	3.220085	30.51791	12.33245	16.77978	4.288909	2.914531	1.995915	0.846875	0.254205	0.615995	0.428471	0.331623	0.29887	0.2916	0.266514	0.228894	0.181661	0.129746	0.090187	0	0	0	0	0	0	0	0
RU188 - 535			0	0.177874	0.857948	1.040909	0.065662	3.429836	4.041568	3.446513	11.68268	3.263148	30.75031	12.26517	16.50266	4.161371	2.796986	1.887499	0.78832	0.234758	0.566521	0.399135	0.321137	0.296335	0.284376	0.247482	0.199872	0.152248	0.111401	0.028259	0	0	0	0	0	0	0	0
RU188 - 535			0	0.177616	0.856552	1.061785	0.067413	3.536062	4.138129	3.516674	11.89896	3.313944	30.95187	12.21924	16.21624	4.028038	2.679971	1.788628	0.742389	0.221281	0.537469	0.386834	0.316394	0.290076	0.275654	0.24293	0.205844	0.171139	0.130739	0.103437	0	0	0	0	0	0	0	0
RU188 - 536			0	0.175339	0.828257	0.983129	0.061033	3.138247	3.742364	3.219834	11.01681	3.106216	29.93062	12.23741	17.18423	4.535585	3.151823	2.220105	0.971158	0.29729	0.735404	0.522008	0.395107	0.333732	0.301249	0.256435	0.210788	0.17227	0.13977	0.043803	0	0	0	0	0	0	0	0
RU188 - 536			0	0.171079	0.857938	1.050411	0.066168	3.410515	4.069771	3.58556	12.48806	3.451604	31.48307	12.01245	16.13505	3.972211	2.6203	1.722746	0.695972	0.202024	0.469644	0.305291	0.229013	0.199064	0.186297	0.156886	0.120771	0.09245	0.043556	0	0	0	0	0	0	0	0	0
RU188 - 536			0	0.174874	0.857948	1.040909	0.065662	3.429836	4.041568	3.446513	11.68268	3.263148	30.75031	12.26517	16.50266	4.161371	2.796986	1.887499	0.78832	0.234758	0.566521	0.399135	0.321137	0.296335	0.284376	0.247482	0.199872	0.152248	0.111401	0.028259	0	0	0	0	0	0	0	0
RU188 - 536			0	0.176328	0.844181	1.01513	0.063637	3.309004	3.918239	3.347649	11.99015	3.220085	30.51791	12.33245	16.77978	4.288909	2.914531	1.995915	0.846875	0.254205	0.615995	0.428471	0.331623	0.29887	0.2916	0.266514	0.228894	0.181661	0.129746	0.090187	0	0	0	0	0	0	0	0
RU188 - 536			0	0.1751	0.820759	0.970746	0.0602	3.1051	3.713262	3.181023	10.74645	3.013935	29.20205	12.20429	17.37178	4.722966	3.355175	2.457538	1.016894	0.347698	0.887258	0.657454	0.50701	0.406002	0.343654	0.270618	0.201687	0.13947	0.06104	0	0	0	0	0	0	0	0	0
RU188 - 536			0	0.176618	0.839516	0.999814	0.062479	3.246257	3.856562	3.288363	11.0872	3.104084	29.79574	12.24511	17.06143	4.50832	3.137373	2.221667	0.982092	0.303536	0.761976	0.556461	0.430616	0.364009	0.321769	0.261539	0.197124	0.138643	0.058494	0	0	0	0	0	0	0	0	0
RU188 - 536			0	0.177453	0.847378	1.021319	0.064208	3.35504	3.966712	3.369783	11.32451	3.1617	30.10855	12.21617	17.16566	4.331574	2.96815	2.062139	0.895396	0.274297	0.684932	0.503767	0.402879	0.354564	0.32532	0.275784	0.221084	0.169654	0.127428	0.033842	0	0	0	0	0	0	0	0
RU188 - 536			0	0.17848	0.865932	1.044765	0.066064	3.467605	4.079426	3.456062	11.58401	3.223703	30.45134	12.21383	16.55117	4.213076	2.854281	1.953471	0.833727	0.252476	0.621519	0.44611	0.349455	0.304471	0.277986	0.235247	0.189273	0.147736	0.114087	0.031125	0	0	0	0	0	0	0	0
RU188 - 536			0	0.178597	0.866514	1.060751	0.067386	3.501055	4.162288	3.519593	11.77074	3.262477	30.57808	12.21323	16.72978	4.101158	2.760844	1.87434	0.792573	0.238608	0.594384	0.420358	0.338858	0.311742	0.29673	0.265441	0.222286	0.180009	0.138445	0.040718	0	0	0	0	0	0	0	0
RU188 - 536			0	0.178597	0.866514	1.060751	0.067386	3.501055	4.162288	3.519593	11.77074	3.262477	30.57808	12.21323	16.72978	4.101158	2.760844	1.87434	0.792573	0.238608	0.594384	0.420358	0.338858	0.311742	0.29673	0.265441	0.222286	0.180009	0.138445	0.040718	0	0	0	0	0	0	0	0
RU188 - 537			0	0.170965	0.807427	0.968084	0.060986	3.260853	3.868183	3.191693	10.22761	2.848192	28.2778	12.10166	17.50115	4.845223	3.495594	2.592151	1.20403	0.383616	0.995245	0.757603	0.591896	0.490721	0.423876	0.338838	0.255521	0.180629	0.124809	0.032534	0	0	0	0	0	0	0	0
RU188 - 537			0	0.170965	0.807427	0.968084	0.060986	3.260853	3.868183	3.191693	10.22761	2.848192	28.2778	12.10166	17.50115	4.845223	3.495594	2.592151	1.20403	0.383616	0.995245	0.757603	0.591896	0.490721	0.423876	0.338838	0.255521	0.180629	0.124809	0.032534	0	0	0	0	0	0	0	0
RU188 - 537			0	0.172019	0.824012	1.000203	0.063532	3.418443	4.026079	3.312051	10.62739	2.965112	29.01425	12.11929	17.21742	4.608112	3.23859	2.322711	1.041951	0.325263	0.827139	0.618827	0.491366	0.425047	0.38425	0.319725	0.246806	0.176247	0.121155	0.029463	0	0	0	0	0	0	0	0
RU188 - 537			0	0.171721	0.83314	1.021156	0.065213	3.512215	4.115432	3.386338	10.88448	3.013824	29.32534	12.1503	16.9072	4.451359	3.103039	2.21503	0.995095	0.311905	0.776917	0.605234	0.479571	0.404904	0.353393	0.28427	0.215273	0.159097	0.120412	0.082506	0.028887	0	0	0	0	0	0	0
RU188 - 537			0	0.171721	0.844591	1.041348	0.066773	3.605444	4.026079	3.312051	10.62739	2.965112	29.01425	12.11944	17.21742	4.608112	3.23859	2.322711	1.041951	0.325263	0.827139	0.618827	0.491366	0.425047	0.38425	0.319725	0.246806	0.176247	0.121155	0.029463	0	0	0	0	0	0	0	0
RU188 - 538			0	0.153088	0.697118	0.852413	0.055243	2.962041	3.346822	2.882851	9.726018	2.526525	24.98405	11.34978	18.38765	5.625965	4.07733	3.30414	1.643956	0.622552	1.097244	0.837455	0.599149	0.490491	0.368107	0.268249	0.188288	0.140825	0.102314	0.040916	0	0	0	0	0	0	0	0
RU188 - 538			0	0.156117	0.759972	0.929891	0.058982	2.956587	3.567951	2.995496	10.02593	2.882765	29.23786	12.60655	18.09734	4.893905	3.430514	2.428096	1.064195	0.326181	0.81048	0.588564	0.470099	0.427574	0.409955	0.314803	0.242228	0.178324	0.132225	0.075637	0	0	0	0	0	0	0	0
RU188 - 538			0	0.157173	0.777089	0.935592	0.05876	3.144781	3.71148	3.152009	10.49823	3.000789	29.97944	12.64569	18.78578	4.611975	3.141654	2.140993	0.900271	0.269142	0.653445	0.469039	0.390503	0.37511	0.373137	0.332406	0.266835	0.189153	0.079522	0	0	0	0	0	0	0	0	0
RU188 - 538			0	0.158046	0.791718	0.964509	0.061049	3.280137	3.901934	3.254067	10.83865	3.084326	30.38579	12.60094	17.35946	4.450591	2.996662	2.010326	0.828358	0.24386	0.580242	0.404689	0.337947	0.334323	0.340755	0.306535	0.244828	0.170085	0.070277	0	0	0	0	0	0	0	0	0
RU188 - 538			0	0.158451	0.802872	0.987339	0.062859	3.388956	4.010653	3.351597	11.12097	3.144278	30.67957	12.59383	17.1536	4.319414	2.860326	1.871953	0.749171	0.216687	0.508535	0.357538	0.314477	0.322341	0.326448	0.282536	0.212318	0.138637	0.056347	0	0	0	0	0	0	0	0	0
RU188 - 539			0	0.138272	0.676865	0.828697	0.048374	2.429154	2.846452	2.411398	8.760011	2.630647	24.29594	11.98711	18.07399	5.386229	4.149598	3.357098	1.714941	0.579303	1.690168	1.341693	1.089446	0.878991	0.718769	0.536511	0.365243	0.213568	0.069848	0	0	0	0	0	0	0	0	0
RU188 - 539			0	0.141711	0.701463	0.852413	0.049773	2.490185	2.929262	2.469833	9.012048	2.707241	25.01425	12.04569	18.15625	5.477441	4.126525	3.284117	1.692966	0.622552	1.097244	0.837455	0.599149	0.490491	0.368107	0.268249	0.188288	0.140825	0.102314	0.040916	0.09047	0.027012	0	0	0	0	0	0
RU188 - 539			0	0.144221	0.74241	0.903829	0.056709	2.952633	3.452786	2.903863	10.19352	3.001926	30.03228	12.56094	17.47291	4.58387	3.167689	2.223472	0.981037	0.304958	0.784823	0.626572	0.559882	0.538942	0.518991	0.443786	0.343167	0.243611	0.155799	0.088221	0.026855	0	0	0	0	0	0	0
RU188 - 539			0	0.146611	0.760065	0.934504	0.059016	3.089842	3.611889	3.042637	10.5985	3.087237	30.44385	12.55304	17.15206	4.39324	2.882174	2.051713	0.891358	0.276277	0.714029	0.581732	0.528835	0.505918	0.476003	0.395368	0.297649	0.207724	0.134849	0.080959	0.026425	0	0	0	0	0	0	0
RU188 - 539			0	0.146801	0.771897	0.957899	0.060865	3.205454	3.749048	3.162068	10.91933	3.145186	30.60299	12.4453	16.84925	4.247659	2.845006	1.920007	0.815264	0.249174	0.636527	0.51935	0.487872	0.486415	0.474057	0.40554	0.31438	0.227868	0.159118	0.093455	0.08823	0.01399	0	0	0	0	0	0
RU188 - 539			0	0.153029	0.718426	0.88265	0.049967	2.611132	2.974709	2.460868	9.396921	2.719209	27.3487	11.54358	17.24294	5.185664	4.05429	3.853328	1.751191	0.599214	1.618841	1.146941	1.046542	0.841138	0.687872	0.514703	0.350145	0.204828	0.066848	0	0	0	0	0	0	0	0	0
RU188 - 539			0	0.139239	0.676434	0.826091	0.048275	2.421775	2.837205	2.401084	8.731475	2.617409	24.25403	11.96725	18.04084	5.368229	4.140958	3.350913	1.711041	0.577468	1.687524	1.336512	1.086446	0.877891	0.717377	0.535017	0.364717	0.213274	0.069574	0	0	0	0	0	0	0	0	0
RU188 - 540			0	0.141257	0.756967	0.923997	0.058982	2.956587	3.567951	2.995496	10.02593	2.882765	29.23786	12.60655	18.09734	4.893905	3.430514	2.428096	1.064195	0.326181	0.81048	0.588564	0.470099	0.427574	0.409955	0.314803	0.242228	0.178324	0.132225	0.075637	0	0	0	0	0	0	0	0
RU188 - 540			0	0.139239	0.716426	0.88265	0.049967	2.611132	2.974709	2.460868	9.396921	2.719209	27.3487	11.54358	17.24294	5.185664	4.05429	3.853328	1.751191	0.599214	1.618841	1.146941	1.046542	0.841138	0.687872	0.514703	0.350145	0.204828	0.066848	0	0	0	0	0	0	0	0	0
RU188 - 540			0	0.141711	0.721465	0.868418	0.049274	2.429154	2.846452	2.411398	8.760011	2.630647	24.29594	11.98711	18.07399	5.386229	4.149598	3.357098	1.714941	0.579303	1.690168	1.341693	1.089446	0.878991	0.718769	0.536511	0.365243	0.213568	0.069848	0	0	0	0	0	0	0	0	0
RU188 - 540			0	0.139239	0.716426	0.88265	0.049967	2.611132	2.974709	2.460868	9.396921	2.719209	27.3487	11.54358	17.24294	5.185664	4.05429	3.853328	1.751191	0.599214	1.618841	1.146941	1.046542	0.841138	0.687872	0.514703	0.350145	0.204828	0.066848	0	0	0	0	0	0	0	0	0
RU188 - 540			0	0.141711	0.721465	0.868418	0.049274	2.429154	2.846452	2.411398	8.760011	2.630647	24.29594	11.98711	18.07399	5.386229	4.149598	3.357098	1.714941	0.579303	1.690168	1.341693	1.089446	0.878991	0.718769	0.536511	0.365243	0.213568	0.069848	0	0	0	0	0	0	0	0	0
RU188 - 540			0	0.141257	0.756967	0.923997	0.058982	2.956587	3.567951	2.995496	10.02593	2.882765	29.23786	12.60655	18.09734	4.893905	3.430514	2.428096	1.064195	0.326181	0.81048	0.588564	0.470099	0.427574	0.409955	0.314803	0.242228	0.178324	0.132225	0.075637

Sed size (um)	0.05	0.06	0.12	0.24	0.49	0.7	0.98	1	2	3	3.9	7	7.8	15.6	20	31	37	44	53	60	63	74	88	105	125	149	177	210	250	300	350	420	500	590	710	840	1000
RU188 - 556	0	0	0	0.092871	0.544967	0.671317	0.04142	1.961453	2.035607	1.710152	7.703589	2.623626	27.68454	11.80218	17.13776	4.967863	3.831487	3.19255	1.73194	0.618477	1.848834	1.784568	1.685594	1.540155	1.383573	1.144694	0.90267	0.678792	0.471245	0.172293	0.040637	0	0	0	0	0	0
RU188 - 556	0	0	0	0.095338	0.578883	0.727796	0.045445	2.179917	2.294607	1.953279	8.538869	2.828132	28.98041	11.98552	16.75544	4.590044	3.39428	2.70971	1.432027	0.505741	1.52262	1.502272	1.4605	1.338518	1.219181	0.991292	0.764198	0.57675	0.426855	0.255704	0.207002	0.110445	0.008312	0	0	0	0
RU188 - 556	0	0	0	0.098689	0.605139	0.758678	0.048325	2.337494	2.490306	2.140761	9.144309	2.961962	29.67668	12.00935	16.39573	4.353938	3.163111	2.493685	1.313999	0.46625	1.413732	1.41092	1.379811	1.280088	1.138668	0.913066	0.693505	0.515135	0.376254	0.222246	0.16333	0.024857	0	0	0	0	0
RU188 - 556	0	0	0	0.101866	0.623255	0.785518	0.050215	2.444353	2.629782	2.276814	9.54321	3.034731	29.884	11.92474	16.08636	4.206561	3.022852	2.389887	1.239035	0.440391	1.343622	1.360721	1.352236	1.270346	1.136084	0.917546	0.696505	0.513376	0.367478	0.210089	0.144732	0.021408	0	0	0	0	0
RU188 - 556	0	0	0	0.104992	0.641732	0.811824	0.052115	2.544183	2.739262	2.417489	9.943251	3.125911	29.98205	11.83727	15.77502	4.021485	2.885687	2.265457	1.164713	0.373222	1.274193	1.309253	1.324611	1.261438	1.133278	0.921139	0.697413	0.510998	0.358339	0.204455	0.132728	0.034629	0.002401	0	0	0	0
RU188 - 556	0	0	0	0.108245	0.656973	0.839432	0.053813	2.633351	2.837968	2.553422	10.15752	3.212642	29.94009	11.70735	15.57378	4.015942	2.787495	2.253243	1.13704	0.425342	1.230125	1.337608	1.306536	1.186108	1.029586	0.804925	0.61338	0.475501	0.349431	0.214364	0.136532	0.036241	0.002601	0	0	0	0
RU188 - 556	0	0	0	0.110575	0.582058	0.707785	0.049301	1.945136	2.126096	1.9307	8.17789	2.565744	25.69956	10.9636	16.63956	5.13081	4.114031	3.557842	1.981175	0.71249	2.15126	2.08155	1.957605	1.775519	1.576779	1.277513	0.974367	0.699983	0.475638	0.088729	0	0	0	0	0	0	0
RU188 - 557	0	0	0	0.102464	0.581321	0.709391	0.043164	1.955596	2.141103	1.945777	8.230992	2.578498	25.7551	10.99397	16.64464	5.10103	4.062694	3.481074	1.921554	0.688096	2.070697	2.000951	1.887401	1.71749	1.525293	1.239774	0.941387	0.676661	0.467416	0.255162	0.191538	0.097998	0.007332	0	0	0	0
RU188 - 557	0	0	0	0.102279	0.586502	0.717993	0.043751	1.980386	2.191285	2.000052	8.431875	2.629514	26.15812	11.12421	16.72196	5.052468	3.968996	3.338704	1.90684	0.639955	1.90661	1.827773	1.732122	1.609962	1.456644	1.215764	0.96723	0.747548	0.554055	0.315811	0.156179	0.017909	0	0	0	0	0
RU188 - 557	0	0	0	0.102215	0.587005	0.718963	0.043907	1.992214	2.193902	2.009411	8.467213	2.641218	26.31184	11.08653	16.62368	4.998532	3.915874	3.357371	1.780616	0.61544	1.884845	1.807386	1.712621	1.583765	1.44178	1.21223	0.972592	0.750021	0.557857	0.343092	0.216162	0.127948	0.009338	0	0	0	0
RU188 - 557	0	0	0	0.101551	0.583901	0.714744	0.043597	1.979433	2.179844	2.000135	8.419707	2.627182	26.17007	11.03747	16.55243	4.973127	3.896112	3.339227	1.773252	0.613284	1.876255	1.800242	1.706131	1.578021	1.437178	1.207268	0.967253	0.744515	0.554766	0.341414	0.215378	0.126855	0.010026	0	0	0	0
RU188 - 558	0	0	0	0.134113	0.712207	0.894711	0.055543	2.58928	2.770919	2.426945	8.947566	2.556717	23.9434	9.860174	14.65992	4.445343	3.575958	3.181352	1.86878	0.700745	2.240321	2.374155	2.411234	2.302507	2.1096	1.73932	1.336405	0.966543	0.644609	0.344707	0.18547	0.02256	0	0	0	0	0
RU188 - 558	0	0	0	0.148189	0.738516	0.923012	0.058217	2.731642	2.932802	2.562863	9.283483	2.612909	24.30705	9.91625	14.52569	4.312549	3.428605	3.031657	1.785366	0.67263	2.167096	2.324956	2.383142	2.286673	2.099407	1.732134	1.329788	0.951739	0.632725	0.314708	0	0	0	0	0	0	0
RU188 - 558	0	0	0	0.155422	0.776706	0.961021	0.062262	2.947822	3.171345	2.76011	9.970107	2.767987	24.71218	9.904054	14.27583	4.168125	3.292833	2.907134	1.716065	0.647634	2.097994	2.231495	2.260021	2.162696	1.992498	1.652768	1.336081	0.930255	0.629412	0.279711	0.148037	0.017752	0	0	0	0	0
RU188 - 558	0	0	0	0.161442	0.807405	0.998215	0.064775	3.060725	3.295727	2.873041	10.34148	2.870337	24.70927	9.847411	14.13663	4.129747	3.259611	2.879021	1.698258	0.641147	2.078111	2.209604	2.239727	2.141413	1.973707	1.636755	1.322474	0.921148	0.623744	0.276478	0.146312	0.017585	0	0	0	0	0
RU188 - 559	0	0	0	0.108584	0.676194	0.841522	0.051664	2.148808	2.958072	2.626444	2.581478	25.74031	10.97889	16.5705	5.042816	3.993456	3.403187	3.073383	1.670783	0.623987	1.963824	1.863229	1.700916	1.508803	1.210879	0.913376	0.666267	0.485314	0.305413	0.229524	0.225224	0.154669	0.074964	0	0	0	0
RU188 - 559	0	0	0	0.119274	0.776963	0.974307	0.060241	2.514218	2.711447	2.5262	2.398322	29.49832	12.14815	19.3415	6.521868	4.986532	4.013474	3.621731	1.780616	0.65144	1.884845	1.807386	1.712621	1.583765	1.44178	1.21223	0.972592	0.750021	0.557857	0.343092	0.216162	0.127948	0.009338

Sed size (um)	0.05	0.06	0.12	0.24	0.49	0.7	0.98	1	2	3	3.9	7	7.8	15.6	20	31	37	44	53	60	63	74	88	105	125	149	177	210	250	300	350	420	500	590	710	840	1000
RU188 - 600	0	0	0	0.225914	0.95222	1.097362	0.865846	3.671105	4.692001	4.107652	12.57016	3.113037	27.21791	11.0989	16.31273	4.604514	3.309307	2.384836	1.045935	0.316997	0.735541	0.504108	0.35309	0.295782	0.285044	0.266873	0.239774	0.206991	0.16475	0.096194	0.028496	0	0	0	0	0	0
RU188 - 600		0	0	0.229387	0.972959	1.146191	0.972129	3.910151	4.877367	4.218701	12.94659	3.226945	28.02487	11.18615	15.90436	4.305816	3.001379	2.079941	0.974585	0.259279	0.606686	0.396049	0.298371	0.281856	0.283459	0.278891	0.24172	0.194992	0.14622A	0.043944	0	0	0	0	0	0	0
RU188 - 600			0	0.22897	0.99289	1.196355	0.976336	4.142978	5.043289	4.318836	13.29476	3.323761	28.53038	11.10856	15.4492	4.068677	2.782281	1.883151	0.773289	0.225511	0.525497	0.346389	0.270549	0.260962	0.23999	0.206746	0.174044	0.145986	0.099628	0.033255	0	0	0	0	0	0	0
RU188 - 600			0	0.226358	1.011633	1.242563	0.980422	4.358719	5.194523	4.414196	13.80523	3.401272	28.81431	10.9749	14.96754	3.86551	2.615746	1.752891	0.715405	0.208697	0.491O1	0.338181	0.281548	0.276085	0.277324	0.248862	0.207131	0.166603	0.134219	0.092428	0.031783	0	0	0	0	0	0	0
RU188 - 600			0	0.223986	1.020895	1.238946	0.983495	4.511635	5.297967	4.490691	13.82389	3.452574	28.93898	11.05257	14.81728	3.738349	2.519957	1.667428	0.694653	0.205185	0.484225	0.355795	0.296895	0.274927	0.275131	0.247272	0.210788	0.183106	0.14089	0.10714	0.039388	0	0	0	0	0	0	0
RU188 - 601			0	0.219157	0.951994	1.107468	0.968661	3.602299	4.514297	3.986559	12.63551	3.210837	28.29224	11.45475	16.95683	4.566403	3.214806	2.240965	0.93564	0.27177	0.611438	0.343875	0.205175	0.172928	0.185166	0.186383	0.16963	0.141642	0.113563	0.03247	0	0	0	0	0	0	0
RU188 - 601			0	0.224624	0.977871	1.168352	0.973717	3.906773	4.774793	4.150989	13.1007	3.33081	29.02653	11.42682	16.88357	5.067858	3.823721	2.933269	1.37703	0.435594	1.100017	0.770054	0.533521	0.409025	0.349924	0.296118	0.239599	0.17401	0.077238	0	0	0	0	0	0	0	0
RU188 - 601			0	0.225989	1.000096	1.216661	0.977659	4.132725	4.963837	4.273386	13.43018	3.40713	29.38992	11.3735	15.5793	3.996436	2.664322	1.727114	0.661589	0.180982	0.379942	0.199912	0.143967	0.16278	0.1937	0.192481	0.165345	0.128762	0.101512	0.030185	0	0	0	0	0	0	0
RU188 - 601			0	0.180974	0.845664	1.008234	0.869787	3.828529	4.686908	4.088647	13.15362	3.392164	29.71289	11.67257	15.97327	4.092094	2.717619	1.792091	0.6656	0.181406	0.380881	0.205011	0.155268	0.175579	0.209392	0.206579	0.185831	0.138512	0.138898	0.104534	0.03865	0	0	0	0	0	0
RU188 - 602			0	0.109487	0.653838	0.859229	0.958357	3.13523	3.889396	3.371493	12.21553	3.587832	34.2051	13.12631	16.32745	3.57838	2.105318	1.172144	0.398257	0.107696	0.236205	0.23439	0.262096	0.252887	0.089134	0.004938	0	0	0	0	0	0	0	0	0	0	0	0
RU188 - 602			0	0.111906	0.672732	0.892348	0.958319	3.278649	4.045092	3.48925	12.44264	3.614538	34.19487	12.99795	15.8655	3.344822	1.906069	1.040717	0.37486	0.113256	0.332256	0.393692	0.44679	0.351428	0.031322	0	0	0	0	0	0	0	0	0	0	0	0	0
RU188 - 602			0	0.114734	0.690302	0.921856	0.960518	3.408444	4.189891	3.611869	12.84257	3.704435	33.82688	13.05479	15.43757	3.196991	1.833696	1.066571	0.445977	0.149753	0.470937	0.515299	0.477952	0.131228	0.00629	0	0	0	0	0	0	0	0	0	0	0	0	0
RU188 - 602			0	0.113906	0.685141	0.917127	0.960518	3.408444	4.189891	3.611869	12.84257	3.704435	33.82688	13.05479	15.43757	3.196991	1.833696	1.066571	0.445977	0.149753	0.470937	0.515299	0.477952	0.131228	0.00629	0	0	0	0	0	0	0	0	0	0	0	0	0
RU188 - 603			0	0.156754	0.779934	0.941617	0.958704	3.962636	4.838906	3.011025	11.09564	3.205618	30.10564	12.07049	17.44453	4.819252	3.430656	2.436071	1.041004	0.307403	0.706465	0.413541	0.255098	0.217662	0.237278	0.245941	0.227271	0.176272	0.073797	0	0	0	0	0	0	0	0
RU188 - 603			0	0.119228	0.817559	1.014027	0.964409	3.813196	4.805314	3.292312	11.87911	3.388463	31.2624	12.29147	16.80454	4.334283	2.906661	1.886925	0.712743	0.190234	0.375165	0.154581	0.087109	0.126182	0.202188	0.245827	0.248416	0.220822	0.166594	0.048245	0	0	0	0	0	0	0
RU188 - 603			0	0.129497	0.687192	0.885682	0.957516	3.070629	3.638231	3.202896	11.73183	3.371771	31.47711	12.51193	17.14955	4.403708	2.929472	1.874295	0.693161	0.181868	0.350731	0.141903	0.093993	0.151663	0.235138	0.279699	0.24138	0.178283	0.05035	0	0	0	0	0	0	0	0
RU188 - 603			0	0.128515	0.688512	0.90147	0.959128	3.1984	3.812288	3.36059	12.20143	3.475762	32.13757	12.65168	17.1736	4.349702	2.859217	1.795868	0.645216	0.168213	0.329794	0.093947	0	0	0	0	0	0	0	0	0	0	0	0	0	0	0	0
RU188 - 603			0	0.13154	0.709746	0.93191	0.961417	3.335143	3.974203	3.494339	12.48815	3.615189	32.20398	12.57327	16.89998	4.213052	2.793827	1.680091	0.589641	0.149388	0.253729	0.070357	0	0	0	0	0	0	0	0	0	0	0	0	0	0	0	0
RU188 - 603			0	0.135594	0.715583	0.937514	0.962454	3.446155	4.036538	3.547794	12.68583	3.671734	32.70128	12.74121	17.27527	4.318521	2.861755	1.721444	0.603705	0.153108	0.258375	0.107227	0.015477	0.015477	0.015477	0.015477	0.015477	0.015477	0.015477	0.015477	0.015477	0.015477	0.015477	0.015477	0.015477	0.015477	0.015477	0.015477
RU188 - 604			0	0.16739	0.822065	0.998217	0.975179	3.709078	3.673843	3.205218	11.48724	3.292811	31.2897	12.65006	17.40422	4.454601	2.954514	1.887563	0.699801	0.184591	0.369843	0.152718	0.097877	0.140334	0.206893	0.240522	0.241518	0.219773	0.182487	0.106049	0.036039	0	0	0	0	0	0	0
RU188 - 604			0	0.141226	0.722217	0.922182	0.95086	3.623195	3.831914	3.331947	11.82306	3.385983	31.44144	12.501	16.83906	4.256514	2.790044	1.755187	0.639686	0.166974	0.324295	0.14254	0.105356	0.152065	0.212125	0.235842	0.225747	0.19856	0.169631	0.118747	0.12471	0.105696	0.008317					
RU188 - 604			0	0.145161	0.744652	0.957529	0.962462	3.73373	3.868835	3.465624	12.12836	3.402361	31.44314	12.33342	16.49734	4.084719	2.845703	1.635653	0.580796	0.148143	0.276854	0.116824	0.099919	0.160089	0.224306	0.243693	0.227238	0.198597	0.176972	0.138072	0.161143	0.148382	0.01497	0.063583				
RU188 - 604			0	0.140867	0.72808	0.94926	0.962418	3.410106	3.696687	3.360144	12.43125	3.472838	32.05585	12.53845	16.8724	4.18763	2.701879	1.665502	0.584647	0.150771	0.267087	0.083868	0.0351	0.208383	0.20433	0.197533	0.178625	0.146079	0.067074	0	0	0	0	0	0	0	0
RU188 - 605			0	0.17622	0.867204	1.075547	0.97645	3.962636	4.138744	3.587794	13.20143	3.716727	34.9435	13.57527	17.27527	4.618521	3.061755	1.841013	0.645977	0.164115	0.284775	0.115477	0.015477	0.015477	0.015477	0.015477	0.015477	0.015477	0.015477	0.015477	0.015477	0.015477	0.015477	0.015477	0.015477	0.015477	0.015477
RU188 - 605			0	0.186806	0.914123	1.144021	0.973838	3.898053	4.439036	3.700002	12.28038	3.384054	31.36548	12.63988	16.61742	4.121473	2.678708	1.672209	0.602747	0.158649	0.285224	0.0881	0	0	0	0	0	0	0	0	0	0	0	0	0	0	0	0
RU188 - 605			0	0.18958	0.933239	1.176922	0.976306	4.032601	4.578295	3.813717	12.54876	3.423782	31.38323	12.72762	16.33137	4.007075	2.581874	1.592115	0.584691	0.146448	0.262313	0.082913	0	0	0	0	0	0	0	0	0	0	0	0	0	0	0	0
RU188 - 605			0	0.194076	0.967278	1.214817	0.974699	4.177248	4.726873	3.939983	12.86271	3.477375	31.40713	12.71432	16.02328	3.939929	2.488267	1.509397	0.518047	0.129999	0.214065	0.049884	0.241584	0.19471	0.198695	0.196709	0.181011	0.1551	0.12905	0.035754	0	0	0	0	0	0	0
RU188 - 606			0	0.133607	0.655743	0.805121	0.95116	2.769955	3.325758	2.802957	9.811975	2.92378	30.44707	13.29015	19.0643	5.073896	3.453782	2.28724	0.8893	0.243581	0.500825	0.226342	0.112704	0.113957	0.151274	0.17008	0.16743	0.157421	0.155624	0.11712	0.125913	0.021737					
RU188 - 606			0	0.171012	0.833676	1.012726	0.964154	3.389287	3.915737	3.227648	10.85982	3.130726	31.21564	13.0913	18.15456	4.642843	3.064718	1.936515	0.699678	0.183208	0.318681	0.089271	0	0	0	0	0	0	0	0	0	0	0	0	0	0	0	0
RU188 - 606			0	0.173856	0.854988	1.052693	0.967181	3.553748	4.087256	3.373318	11.23562	3.19269	31.32592	12.97452	17.81702	4.491368	2.923176	1.801387	0.623508	0.156609	0.245653	0.049498	0	0	0	0	0	0	0	0	0	0	0	0	0	0	0	0
RU188 - 606			0	0.176809	0.871751	1.079781	0.969189	3.670224	4.225143	3.491982	11.50784	3.229002	31.30746	12.86646	17.89387	4.4064	2.848396	1.733142	0.583934	0.149257	0.133359	0	0	0	0	0	0	0	0	0	0	0	0	0	0	0	0	0
RU188 - 606			0	0.17977	0.886883	1.102274	0.971458	3.792173	4.354941	3.601979	11.73654	3.259547	31.22443	12.74248	17.35449	4.328499	2.785693	1.678011	0.553334	0.135959	0.118437	0	0	0	0	0	0	0	0	0	0	0	0	0	0	0	0	0
RU188 - 607			0	0.181729	0.894597	1.100854	0.963305	3.941612	3.229366	3.324107	18.71749	4.843748	3.207379	2.032148	0.736906	0.193821	0.344317	0.102932	0	0	0	0	0	0	0	0	0	0	0	0	0	0	0	0	0	0	0	0
RU188 - 607			0	0.184936	0.867232	1.044368	0.965982	3.501318	4.101607	3.365301	10.79157	3.032645	30.57722	13.11019	18.40626	4.718983	3.095556	1.927134	0.678356	0.173253	0.289828	0.071155	0	0	0	0	0	0	0	0	0	0	0	0	0	0	0	0
RU188 - 607			0	0.18786	0.8772	1.078407	0.965842	3.646736	4.263703	3.501753	11.12301	3.083813	30.63147	12.99731	18.08694	4.586039	2.979826	1.822013	0.621588	0.153768	0.238736	0.049044	0	0	0	0	0	0	0	0	0	0	0	0	0	0	0	0
RU188 - 608			0	0.188233	0.872272	1.084229	0.967536	3.680446	4.314955	3.514662	11.46564	3.183022	31.08921	13.19642	18.28145	4.737287	3.081145	1.867156	0.633297	0.161753	0.247986	0.072919	0.047612	0.047612	0.047612	0.047612	0.047612	0.047612	0.047612	0.047612	0.047612	0.047612	0.047612	0.047612	0.047612	0.047612	0.047612	0.047612
RU188 - 608			0	0.191262	0.898204	1.090625	0.969015	3.577375	4.138709	3.472111	11.4427	3.169489	30.5806	12.74617	17.98296	4.589319	3.035302	1.901136	0.693075	0.161148	0.306841	0.077435	0	0	0	0	0	0	0	0	0	0	0	0	0	0	0	0
RU188 - 608			0	0.193438	0.915674	1.124766	0.97165	3.728763	4.293527	3.599043	11.77432	3.228926	30.7187	12.6319	17.46677	4.437105	2.902962	1.805795	0.634776	0.161881	0.259846	0.052966	0	0	0	0	0	0	0	0	0	0	0	0	0	0	0	0
RU188 - 608			0	0.196429	0.935601	1.158879	0.974082	3.862972	4.441908	3.719709	12.04321	3.256849	30.72757	12.52684	17.19318	4.320687	2.801017	1.719501	0.593576	0.148987	0.230144	0.042133	0	0	0	0	0	0	0	0	0	0	0	0	0	0	0	0
RU188 - 608			0	0.196233	0.961721	1.18351	0.976044	3.972068	4.553862	3.817058	12.28824	3.320959	30.7427	12.42851	17.04239	4.239418	2.731288	1.657505	0.558465	0.143001	0.185607	0	0	0	0	0	0	0	0	0	0	0	0	0	0	0	0	0
RU188 - 609			0	0.190274	0.862309	1.048468	0.966837	3.843855	4.362013	3.639462	11.98677	3.293482	30.16721	12.34629	16.89744	4.203583	3.155631	2.069944	0.612015	0.226482	0.414435	0.232776	0.138966	0.1477	0.185497	0.199044	0.180921	0.156791	0.119358	0.040928	0	0	0	0	0	0	0
RU188 - 609			0	0.187272	0.876552	1.085769	0.970277	3.915784	4.464752	3.714727	12.29875	3.345455	30.87813	12.44957	17.08453	4.252849	3.192372	2.094662	0.619722	0.229242	0.419002	0.235375	0.140795	0.149586	0.187551	0.201672	0.182575	0.158705	0.121154	0.041325	0	0	0	0	0	0	0
RU188 - 609			0	0.183124	0.851782	1.055753	0.963357	3.810924	4.414955	3.687781	12.16111	3.304645	30.61795	12.36627	17.15044	4.406821	2.910463	1.838839	0.669189	0.173823	0.330305	0.129405	0.080794	0.125611	0.191588	0.228769	0.235135	0.220092	0.188228	0.104651	0.034051	0	0	0	0	0	0	0
RU188 - 609			0	0.195643	0.955646	1.203129	0.977639	4.012751	4.542743	3.850932	12.78291	3.441677	30.95262	12.11488	16.40117	4.103196	2.662049	1.643658	0.57946	0.149344	0.258068	0.073288	0	0	0	0	0	0	0	0	0	0	0	0	0	0	0	0
RU188 - 609			0	0.198995	0.974868	1.235718	0.980093	4.148816	4.69236	3.971068	12.99743	3.45353	30.7689	11.98942	16.20614	4.041655	2.613019	1.604899	0.561857	0.143928	0.248878	0.069425	0	0	0	0	0	0	0	0	0	0	0	0	0	0	0	0
RU188 - 610			0	0.140524	0.730001	0.918861	0.964824	2.730444	3.129203	2.736106	10.35341	3.068508	29.77765	12.48627	18.25259	5.128943	3.677432	2.639237	1.147794	0.344429	0.812087	0.500876	0.312245	0.237063	0.226082	0.210487	0.187292	0.156365	0.071996	0	0	0	0	0	0	0	0
RU188 - 610			0	0.140489	0.734457	0.921436	0.96235	2.738901	3.141376	2.746149	10.38577	3.078295	29.91014	12.53203	18.32705	5.149662	3.693107	2.650754	1.152869	0.345662	0.815644	0.502876	0.313124	0.237883	0.226782	0.210987	0.187958	0.156705	0.072255	0.011124	0	0	0	0	0	0	0
RU188 - 610			0	0.138431	0.634357	0.811842	0.952835	2.706469	3.014901	2.697158	10.97019	3.247495	31.36381	13.29111	18.7278	5.294301	3.785945	2.705394	1.185243	0.356441	0.773084	0.479234	0.297434	0.215419	0.143502	0.12116	0.123379	0.127532	0.15739	0.171174	0.169392	0.158568	0.140198	0.045032	0	0	0
RU188 - 610			0	0.144971	0.644882	0.851782	0.955753	3.010924	3.598217	3.17549	11.68914	3.381391	32.00629	12.94244	17.89048	4.571371	2.995543	1.86113	0.65641	0.168378	0.294341	0.089187	0	0	0	0	0	0	0	0	0	0	0	0	0	0	0	0
RU188 - 610			0	0.117639	0.661509	0.875935	0.957596	3.129538	3.750298	3.305559	11.96463	3.413803	31.97255	12.83536	17.64847	4.479458	2.918311	1.793172	0.617436	0.154258	0.247168	0.057316	0	0	0	0	0	0	0	0	0	0	0	0	0	0	0	0

Sed size (um)	0.05	0.06	0.12	0.24	0.49	0.7	0.98	1	2	3	3.9	7	7.8	15.6	20	31	37	44	53	60	63	74	88	105	125	149	177	210	250	300	350	420	500	590	710	840	1000
RU188 -640		0	0	0	0.125447	0.679008	0.852163	0.952398	2.502043	2.865282	2.950388	3.277829	22.83175	0.135579	18.09383	6.479527	5.661962	4.969859	2.708977	0.934961	2.598267	2.095388	1.404315	0.871553	0.482916	0.254621	0.001162	0	0	0	0	0	0	0	0	0	0	0
RU188 -640		0	0	0	0.129755	0.679108	0.852163	0.952398	2.502043	2.865282	2.950388	3.277829	22.83175	0.135579	18.09383	6.479527	5.661962	4.969859	2.708977	0.934961	2.598267	2.095388	1.404315	0.871553	0.482916	0.254621	0.001162	0	0	0	0	0	0	0	0	0	0	0
RU188 -640		0	0	0	0.134905	0.760513	0.982778	0.962565	3.021469	3.394745	3.022872	3.842966	25.81948	0.182554	17.03715	5.484424	4.44705	3.770277	1.97341	0.667529	1.814167	1.385051	0.933357	0.564118	0.317067	0.147069	0.062929	0	0	0	0	0	0	0	0	0	0	0
RU188 -640		0	0	0	0.138396	0.784448	1.020742	0.965377	3.164898	3.560651	3.180987	11.04546	2.956727	26.40039	10.83726	16.66815	5.250787	4.20612	3.522062	1.823406	0.613055	1.654711	1.253553	0.842518	0.513468	0.294916	0.143585	0.067499	0	0	0	0	0	0	0	0	0	0
RU188 -640		0	0	0	0.140141	0.797383	1.041978	0.969818	3.248612	3.659617	3.274103	11.32791	3.013065	26.61032	10.77609	16.39876	5.102164	4.056405	3.370014	1.732488	0.580155	1.559016	1.169375	0.774419	0.462569	0.257475	0.136894	0.078996	0.077074	0.097063	0.090974	0.092067	0.013967	0	0	0	0	0
RU188 -640		0	0	0	0.14337	0.814369	1.066766	0.968653	3.341474	3.761843	3.373762	11.62034	3.070054	26.82129	10.97345	16.16778	4.973396	3.927429	3.241354	1.667546	0.553571	1.483355	1.107079	0.727332	0.427928	0.232706	0.117716	0.078814	0.090433	0.12362	0.117258	0.128077	0.021878	0	0	0	0	0
RU188 -641		0	0	0	0.130501	0.689211	0.895628	0.953311	2.492417	2.814253	2.525055	8.773184	2.375631	22.50592	10.26896	18.01061	6.493149	5.610832	4.658249	2.78379	0.966739	2.700171	2.140269	1.471948	0.881878	0.497687	0.007676	0	0	0	0	0	0	0	0	0	0	0
RU188 -641		0	0	0	0.132726	0.693541	0.902447	0.955311	2.502043	2.865282	2.950388	9.027854	2.447055	23.17283	10.57345	17.72157	5.753842	4.822295	3.994469	2.130313	0.728209	2.010737	1.533057	0.913751	0.513753	0.266173	0	0	0	0	0	0	0	0	0	0	0	0
RU188 -641		0	0	0	0.143078	0.777117	0.990447	0.96274	3.001759	3.390498	3.029606	10.47848	2.809745	25.54363	10.80763	17.22157	5.638942	4.632295	3.99469	2.130313	0.728209	2.010737	1.533057	0.913751	0.513753	0	0	0	0	0	0	0	0	0	0	0	0	0
RU188 -641		0	0	0	0.147179	0.805068	1.034068	0.965927	3.175192	3.584388	3.202992	11.03456	2.938541	26.25978	10.81625	16.73454	5.324283	4.318842	3.693821	1.963304	0.670775	1.850641	1.406201	0.850138	0.522672	0	0	0	0	0	0	0	0	0	0	0	0	0
RU188 -641		0	0.1501	0.825974	1.068151	0.968291	3.297854	3.72438	3.335701	11.45223	3.025464	26.66498	10.83007	16.5588	5.19524	4.176188	3.540499	1.868323	0.63891	1.739283	1.234129	0.560747	0.044711	0	0	0	0	0	0	0	0	0	0	0	0	0	0	0
RU188 -641		0	0	0	0.153168	0.843362	1.09589	0.970308	3.405053	3.840351	3.435004	11.71008	3.07052	26.76971	10.72219	16.16771	5.009932	4.009192	3.390392	1.787211	0.608259	1.644602	1.234129	0.020489	0	0	0	0	0	0	0	0	0	0	0	0	0	0
RU188 -642		0	0	0	0.127623	0.677946	0.883904	0.952072	2.451824	2.792558	2.494335	8.742451	2.384656	22.86505	10.37113	17.87283	6.346328	5.441396	4.869386	2.663143	0.921661	2.562271	2.027167	1.408798	0.881144	0.516781	0.275311	0.11472	0.103754	0.036171	0	0	0	0	0	0	0	0
RU188 -642		0	0	0	0.130614	0.754772	0.959718	0.960725	2.942988	3.351873	2.961715	10.37057	2.845131	25.41737	10.81564	17.89167	5.439001	4.413086	3.745914	1.938381	0.675161	1.854018	1.467485	1.007229	0.610946	0.329854	0.213014	0.101926	0	0	0	0	0	0	0	0	0	0
RU188 -642		0	0	0	0.14227	0.783211	1.002774	0.96374	3.107444	3.534393	3.142288	10.87785	2.931995	26.4841	10.87544	16.55171	5.142847	4.10012	3.456017	1.791708	0.606852	1.658592	1.289185	0.898445	0.576523	0.35603	0.206444	0.130388	0.103596	0.100693	0.07744	0.027752	0	0	0	0	0	0
RU188 -642		0	0	0	0.144725	0.799729	1.028921	0.96567	3.208939	3.653109	3.252701	11.21629	3.001999	26.78186	10.83809	16.28651	5.001759	3.96727	3.312457	1.723387	0.582987	1.59005	1.228282	0.845627	0.532612	0.321334	0.182486	0.115997	0.09723	0.103006	0.084909	0.032064	0	0	0	0	0	0
RU188 -642		0	0	0	0.147869	0.815511	1.052318	0.967311	3.294699	3.750208	3.358364	11.45562	3.047965	26.96921	10.81625	16.11665	4.896232	3.850827	3.180046	1.634771	0.548701	1.481797	1.12565	0.765176	0.486878	0.316259	0.216466	0.176815	0.164558	0.153181	0.100879	0.030404	0	0	0	0	0	0
RU188 -643		0	0	0	0.113833	0.640686	0.801062	0.949602	2.391094	2.766824	2.472683	8.630597	2.368194	22.63536	10.23336	17.95667	6.246747	5.389261	4.877653	2.707024	0.946834	2.675885	2.182786	1.588223	1.058488	0.676975	0.401879	0.245467	0.166296	0.123877	0.083553	0	0	0	0	0	0	0
RU188 -643		0	0	0	0.117265	0.67281	0.852541	0.936204	2.357243	2.679258	2.494335	8.742451	2.384656	22.86505	10.37113	17.87283	6.346328	5.441396	4.869386	2.663143	0.921661	2.562271	2.027167	1.408798	0.881144	0.516781	0.275311	0.11472	0.103754	0.036171	0	0	0	0	0	0	0	0
RU188 -643		0	0	0	0.130614	0.754772	0.959718	0.960725	2.942988	3.351873	2.961715	10.37057	2.845131	25.41737	10.81564	17.89167	5.439001	4.413086	3.745914	1.938381	0.675161	1.854018	1.467485	1.007229	0.610946	0.329854	0.213014	0.101926	0	0	0	0	0	0	0	0	0	0
RU188 -643		0	0	0	0.14227	0.783211	1.002774	0.96374	3.107444	3.534393	3.142288	10.87785	2.931995	26.4841	10.87544	16.55171	5.142847	4.10012	3.456017	1.791708	0.606852	1.658592	1.289185	0.898445	0.576523	0.35603	0.206444	0.130388	0.103596	0.100693	0.07744	0.027752	0	0	0	0	0	0
RU188 -643		0	0	0	0.124984	0.749293	0.978678	0.0627	3.1051	3.587508	3.199755	11.02593	2.964605	26.8106	10.96613	16.38457	4.931094	3.839632	3.142757	1.614227	0.544933	1.497398	1.203519	0.909673	0.668449	0.496947	0.354879	0.258089	0.198807	0.163439	0.109422	0.094176	0.012756	0	0	0	0	0
RU188 -644		0	0	0	0.144725	0.799729	1.028921	0.06567	3.208939	3.653109	3.252701	11.21629	3.001999	26.78186	10.83809	16.28651	5.001759	3.96727	3.312457	1.723387	0.582987	1.59005	1.228282	0.845627	0.532612	0.321334	0.182486	0.115997	0.09723	0.103006	0.084909	0.032064	0	0	0	0	0	0
RU188 -644		0	0	0	0.118407	0.672175	0.844654	0.952691	2.570312	3.012602	2.694957	9.241704	2.580551	23.62071	10.46034	17.31739	5.892539	4.952634	4.076622	2.387281	0.829209	2.334112	1.911032	1.42354	0.997682	0.691436	0.453891	0.299204	0.226934	0.169926	0.123484	0.023804	0	0	0	0	0	0
RU188 -644		0	0	0	0.125621	0.724148	0.925837	0.958592	2.678508	3.362369	2.997313	10.21687	2.749983	25.56039	10.91291	17.00463	5.361023	4.296383	3.626606	1.91243	0.653757	1.815627	1.470285	1.0181	0.790089	0.565858	0.383521	0.256599	0.196982	0.06294	0	0	0	0	0	0	0	0
RU188 -644		0	0	0	0.127385	0.739595	0.951313	0.960414	2.972662	3.465203	3.088906	10.51159	2.972673	25.98642	10.97273	16.87734	5.225473	4.135044	3.442396	1.794376	0.610329	1.688419	1.384156	1.025492	0.740294	0.534541	0.38631	0.251388	0.173894	0.076158	0	0	0	0	0	0	0	0
RU188 -645		0	0	0	0.129811	0.754178	0.972872	0.961936	3.056336	3.563871	3.173262	10.76008	2.874965	26.36838	11.03625	16.76564	5.103402	3.992277	3.276244	1.681634	0.566383	1.548273	1.228163	0.912723	0.663293	0.496894	0.363346	0.27282	0.208839	0.140153	0.037285	0	0	0	0	0	0	0
RU188 -645		0	0	0	0.138498	0.727491	0.913272	0.957454	2.727829	3.01266	2.616957	8.977734	2.466478	23.61695	10.47724	17.27069	5.869347	4.949556	4.403666	2.423832	0.846746	2.398308	1.980208	1.472663	1.01072	0.667649	0.406314	0.247311	0.162323	0.122083	0.035024	0	0	0	0	0	0	0
RU188 -645		0	0	0	0.141486	0.749282	0.948207	0.959776	2.861269	3.177195	2.755663	9.443085	2.590424	24.596	10.69734	17.09909	5.594127	4.610108	4.012348	2.174183	0.754366	2.172089	1.753011	1.314991	0.915935	0.62272	0.386766	0.236204	0.153072	0.115837	0.064887	0.031959	0	0	0	0	0	0
RU188 -645		0	0	0	0.145813	0.766509	0.964412	0.960922	3.009192	3.477847	3.092077	10.92956	2.925857	26.48637	10.96565	16.66526	5.167577	4.122431	3.470467	1.842563	0.632961	1.617132	1.270447	1.014645	0.706044	0.514874	0.373673	0.253126	0.184552	0.150559	0.104663	0.096531	0.014219	0	0	0	0	0
RU188 -645		0	0	0	0.140813	0.786606	1.003682	0.96385	3.087636	3.542169	3.063818	10.98271	2.774214	25.87129	10.88981	16.66526	5.167577	4.122431	3.470467	1.842563	0.632961	1.617132	1.270447	1.014645	0.706044	0.514874	0.373673	0.253126	0.184552	0.150559	0.104663	0.096531	0.014219	0	0	0	0	0
RU188 -645		0	0	0	0.140172	0.799854	1.022726	0.965168	3.158811	3.520393	3.065979	10.43283	2.82526	26.21076	10.95046	16.56561	5.064989	4.003796	3.348377	1.776373	0.602688	1.681707	1.377343	1.044709	0.753595	0.538035	0.361579	0.244813	0.177525	0.148845	0.096191	0.032416	0	0	0	0	0	0
RU188 -645		0	0	0	0.151569	0.810898	1.037889	0.966217	3.218222	3.594288	3.133113	10.63521	2.873729	26.46656	10.97236	16.45508	4.978122	3.907331	3.241406	1.691183	0.576552	1.601869	1.305236	0.987454	0.711277	0.506406	0.338959	0.229772	0.169966	0.140702	0.098024	0.088897	0.012736	0	0	0	0	0
RU188 -646		0	0	0	0.136339	0.706107	0.870162	0.954077	2.560606	2.895923	2.547516	8.886114	2.479757	24.20277	10.81341	17.98777	5.830131	4.831	4.226597	2.299028	0.799286	2.257874	1.86477	1.402234	0.986737	0.679913	0.438822	0.283029	0.190098	0.133122	0.038707	0	0	0	0	0	0	0
RU188 -646		0	0	0	0.139596	0.792773	0.967497	0.95672	2.717278	3.061866	2.703365	9.39094	2.617675	25.3692	11.11498	17.4615	5.52911	4.449525	3.786116	2.021076	0.697203	1.9618	1.623242	1.232916	0.87642	0.60307	0.380808	0.23689	0.156653	0.120005	0.035636	0	0	0	0	0	0	0
RU188 -646		0	0	0	0.144401	0.765051	0.964514	0.960661	2.972662	3.465203	3.088906	10.51159	2.972673	25.98642	10.97273	16.87734	5.225473	4.135044	3.442396	1.794376	0.610329	1.688419	1.384156	1.025492	0.740294	0.534541	0.38631	0.251388	0.173894	0.076158	0	0	0	0	0	0	0	0
RU188 -646		0	0	0	0.147026	0.779251	0.981496	0.962019	3.021353	3.433772	3.009606	10.39199	2.865728	27.01545	11.13198	16.61288	4.973755	3.83787	3.133267	1.619418	0.550753	1.530715	1.25301	0.953882	0.688595	0.488863	0.327479	0.226734	0.176515	0.154886	0.114555	0.112623	0.01751	0	0	0	0	0
RU188 -646		0	0	0	0.149427	0.794025	1.003879	0.963613	3.11227	3.541903	3.10487	10.69462	2.942377	27.44279	11.13765	16.68654	4.855453	3.704935	2.988331	1.528825	0.517418	1.432516	1.169944	0.892801	0.646756	0.459072	0.305044	0.206517	0.153198	0.123856	0.087593	0.029829	0	0	0	0	0	0
RU188 -647		0	0	0	0.121423	0.670358	0.828868	0.05133	2.451866	2.824709	2.51508	9.170241	2.6503	26.31719	11.15855	16.99511	5.589963	4.438594	3.716514	1.956104	0.670065	1.870212	1.52882	1.147493	0.803375	0.539387	0.323942	0.181393	0.054687	0	0	0	0	0	0	0	0	0
RU188 -647		0	0	0	0.12587	0.707506	0.886118	0.05432	2.705582	3.142201	2.787883	10.02796	2.882603	26.04832	11.19693	17.06181	5.092266	3.82693	3.01997	1.511025	0.505029	1.386314	1.109052	0.838	0.603433	0.423512	0.272993	0.174675	0.122278	0.100212	0.031152	0	0	0	0	0	0	0
RU188 -647		0	0	0	0.127677	0.722327	0.910063	0.057203	2.817903	3.271314	2.902137	10.38507	3.053103	28.00573	11.20702	17.40106	4.910667	3.628183	2.815417	1.580896	0.459475	1.243892	0.994784	0.734836	0.534099	0.389105	0.243955	0.16738	0.129831	0.114568	0.083836	0.029476	0	0	0	0	0	0
RU188 -647		0	0	0	0.129647	0.731053	0.919084	0.058654	2.847571	3.311373	2.937214	10.50755	3.090577	28.35375	11.34702	17.61045	4.972001	3.675211	2.851146	1.602707	0.465682	1.259688	1.007711	0.743904	0.541252	0.394611	0.247211	0.169554	0.131586	0.116068	0.085005	0.030122	0.013565	0	0	0	0	0
RU188 -648		0	0	0	0.123311	0.678152	0.826494	0.051248	2.607043	3.057008	2.58376	9.330565	2.861226	30.12287	13.14242	18.64624	4.928414	3.417585	2.429999	1.099447	0.348947	0.915249	0.723918	0.583573	0.475848	0.387893	0.2902	0.205557	0.136613	0.056514	0	0	0	0	0	0	0	0
RU188 -648		0	0	0	0.125257	0.697004	0.857242	0.0535	2.744677	3.222894	2.72576	9.774797	2.961157	30.89537	13.23626	18.32351	4.65892	3.129576	2.137317	0.93035	0.289719	0.795538	0.59366	0.495098	0.418173	0.350446	0.269219	0.19778	0.137931	0.056847	0	0	0	0	0	0	0	0
RU188 -648		0	0	0	0.128979	0.710148	0.880914	0.055643	2.844575	3.267113	2.78215	9.962453	2.917223	30.89537	13.23626	18.32351	4.65892	3.129576	2.137317	0.93035	0.289719	0.795538	0.59366	0.495098	0.418173	0.350446	0.269219	0.19778	0.137931	0.056847	0	0	0	0	0	0	0	0
RU188 -648		0	0	0	0.131971	0.707506	0.886118	0.05432	2.705582	3.142201	2.787883	10.02796	2.882603	26.04832	11.19693	17.06181	5.092266	3.82693	3.01997	1.511025	0.505029	1.386314	1.109052	0.838	0.603433	0.423512	0.272993	0.174675	0.122278	0.100212	0.031152	0	0	0	0	0	0	0
RU188 -648		0	0	0	0.134642	0.744852	0.913693	0.056879	2.796396	3.460324	2.989774	10.57395	3.075355	28.12966	11.42385	17.73473	5.004777	3.731483	2.873524	1.614202	0.751902	1.262724	1.014795	0.749213	0.545605	0.398535	0.250199	0.178541	0.132706	0.117013	0.086011	0.029834	0	0	0	0	0	0
RU188 -648		0	0	0	0.132449	0.729825	0.908846	0.057041	2.864294	3.333415	2.875354	10.18832	2.973649	29.82035	12.62042	17.67395	4.657095	3.25998	2.370799	1.107088	0.358842	0.96285	0.760566	0.628359	0.491577	0.375261	0.257858	0.169797	0.119131	0.099641	0.081442	0.088946	0.014867	0	0	0	0	0
RU188 -648		0	0	0	0.134642	0.744852	0.913693	0.056879	2.796396	3.460324	2.989774	10.57395	3.075355	28.12966	11.42385	17.73473	5.004777	3.731483	2.873524	1.614202	0.751902	1.262724	1.014795	0.749213	0.545605	0.398535	0.250199	0.178541	0.132706	0.117013	0.086011	0.029834	0	0	0	0	0	0
RU188 -648		0	0	0	0.132449	0.729825	0.908846	0.057041	2.864294	3.333415	2.875354	10.18832	2.973649	29.82035	12.62042	17.67395	4.657095	3.25998	2.370799	1.107088	0.358842	0.96285	0.760566	0.628359	0.491577	0.375261	0.257858	0.169797	0.119131	0.099641	0.081442	0.088946	0.014867	0	0	0	0	0
RU188 -648		0	0	0	0.137501	0.764519	0.963157	0.060973	3.062089	3.620987	3.138199	10.97746	3.133688	30.59315	12.57673	17.07688	4.293578	2.889104	1.903075	0.981513	0.277514	0.777631	0.586465	0.490132	0.410601	0.337021	0.251812	0.185407	0.14001	0.137071	0.110508	0.113836	0.018114	0	0	0	0	0
RU188 -648		0	0	0	0.13879	0.771803	0.971304	0.061788	3.147345	3.687559	3.196643	11.11988	3.162262	30.65264	12.52427	16.85405	4.183093	2.791453	1.915755	0.850865	0.270243	0.720947	0.601355	0.515518	0.433861	0.352351	0.258848	0.186275	0.145485	0.134982	0.111373	0.127425	0.101361	0.007576	0	0	0	0
RU188 -649		0	0	0	0.123449	0.658969	0.790037	0.049441	2.419118	2.823893	2.388651	8.701887	2.682355	28.80064	12.93011	19.13046	5.379828	3.911766	2.940359	1.396097	0.452672	1.200689	0.937126	0.718917	0.547301	0.421185	0.299599	0.199204	0.099357	0	0	0	0	0	0	0	0	0
RU188 -649		0	0	0	0.123331	0.678152	0.826494	0.051248	2.607043	3.057008	2.58376	9.330565	2.861226	30.12287	13.14242	18.64624	4.928414	3.417585	2.429999	1.099447	0.348947	0.915249	0.723918	0.583573	0.475848	0.387893	0.2902	0.205557	0.136613	0.056514	0	0	0	0	0	0	0	0
RU188 -649		0	0	0	0.125257	0.697004	0.857242	0.0535	2.744677	3.222894	2.72576	9.774797	2.961157	30.89537	13.23626	18.32351	4.65892	3.129576	2.137317	0.93035	0.289719	0.795538	0.59366	0.495098	0.418173	0.350446	0.269219	0.19778	0.137931	0.056847	0	0	0	0	0	0	0	0
RU188 -649		0	0	0	0.128979	0.710148	0.880914	0.055643	2.844575	3.267113	2.78215	9.962453	2.917223	30.89537	13.23626	18.32351	4.65892	3.129576	2.137317	0.93035	0.289719	0.795538	0.59366	0.495098	0.418173	0.350446	0.269219	0.19778	0.137931	0.056847	0	0	0	0	0	0	0	0
RU188 -649		0	0	0	0.132449	0.729825	0.908846	0.057041	2.864294	3.333415	2.875354	10.18832	2.973649	29.82035	12.62042	17.67395	4.657095	3.25998	2.370799	1.107088	0.358842	0.96285	0.760566	0.628359	0.491577	0.375261	0.257858	0.169797	0.119131	0.099641	0.081442	0.088946	0.014867	0	0	0	0	0
RU188 -649		0	0	0	0.134642	0.744852	0.913693	0.056879	2.796396	3.460324	2.989774	10.57395	3.075355	28.12966	11.42385	17.73473	5.004777	3.731483	2.873524	1.614202	0.751902	1.262724	1.014795	0.749213	0.545605	0.398535	0.250199	0.178541	0.132706	0.117013	0.086011	0.029834	0	0	0	0	0	0
RU188 -650		0	0	0	0.128323	0.731344	0.91702	0.057963	3.012318	3.557638	3.035817	10.70667	3.152908	31.69988	13.15177	17.57685	4.238856	2.720025	1.737285	0.696838	0.205718	0.504489	0.381811	0.330184	0.308526	0.294547	0.264756	0.231879	0.194907	0.17321	0.032459	0	0	0	0	0	0	0
RU188 -650		0	0	0	0.13879	0.771803	0.971304	0.061788	3.147345	3.687559	3.196643	11.11988	3.162262	30.65264	12.52427	16.85405	4.183093	2.791453	1.915755	0.850865	0.270243	0.720947	0.601355	0.515518	0.433861	0.352351	0.258848	0.186275	0.145485	0.134982	0.111373	0.127425	0.101361	0.007576	0	0	0	0
RU188 -650		0	0	0	0.135067	0.766181	0.97468	0.061835	3.097487	3.621646	3.200945	11.22806	3.136702	29.59351	12.06101	16.80737	4.778878	3.179213	2.348171	1.10558	0.357921	0.959324	0.744001	0.567337	0.426575	0.322224	0.233414	0.175078	0.147288	0.138529	0.104396	0.037179	0	0	0	0	0	0
RU188 -650		0	0	0	0.129854	0.712104	0.881734	0.055082	2.744177	3.184548	2.743998	9.773129	2.872403	29.14799	12.55391	18.0208	4.91897	3.528667	2.629725	1.246958	0.405339	1.081959	0.8567	0.6633	0.504717	0.379637	0.264651	0.186127	0.14675	0.133798	0.106435	0.109178	0.017367	0	0	0	0	0
RU188 -650		0	0	0	0.132449	0.729825	0.908846	0.057041	2.864294	3.333415	2.875354	10.18832	2.973649	29.82035	12.62042	17.67395	4.657095	3.25998	2.370799	1.107088	0.358842	0.96285	0.760566	0.628359	0.491577	0.375261	0.257858	0.169797	0.119131	0.099641	0.081442	0.088946	0.014867	0	0	0	0	0
RU188 -650		0	0	0	0.135067	0.766181	0.97468	0.061835	3.097487	3.621646	3.200945	11.22806	3.136702	29.59351	12.06101	16.80737	4.778878	3.179213	2.348171	1.10558	0.357921	0.959324	0.744001	0.567337	0.426575	0.322224	0.233414	0.175078	0.147288	0.138529	0.104396	0.037179	0	0	0	0	0	0
RU188 -650		0	0	0	0.129854	0.712104	0.881734	0.055082	2.744177	3.184548	2.743998	9.773129	2.872403	29.14799	12.55391	18.0208	4.91897	3.528667	2.629725	1.246958	0.405339	1.081959	0.8567	0.6633	0.504717	0.379637	0.264651	0.186127	0.14675	0.133798	0.106435	0.109178	0.017367	0	0	0	0	0
RU188 -650		0	0	0	0.13879	0.771803	0.971304	0.061788	3.147345	3.687559	3.196643	11.11988	3.162262	30.65264	12.52427	16.85405	4.183093	2.791453	1.915755	0.850865	0.270243	0.720947	0.601355	0.515518	0.433

Appendix F – Glass data

This chapter contains sample layout in EMPA disks (below), tables of raw data identifying glass (blue), plagioclase (yellow) and quartz (red), and backscattered images indicating the shards analysed.

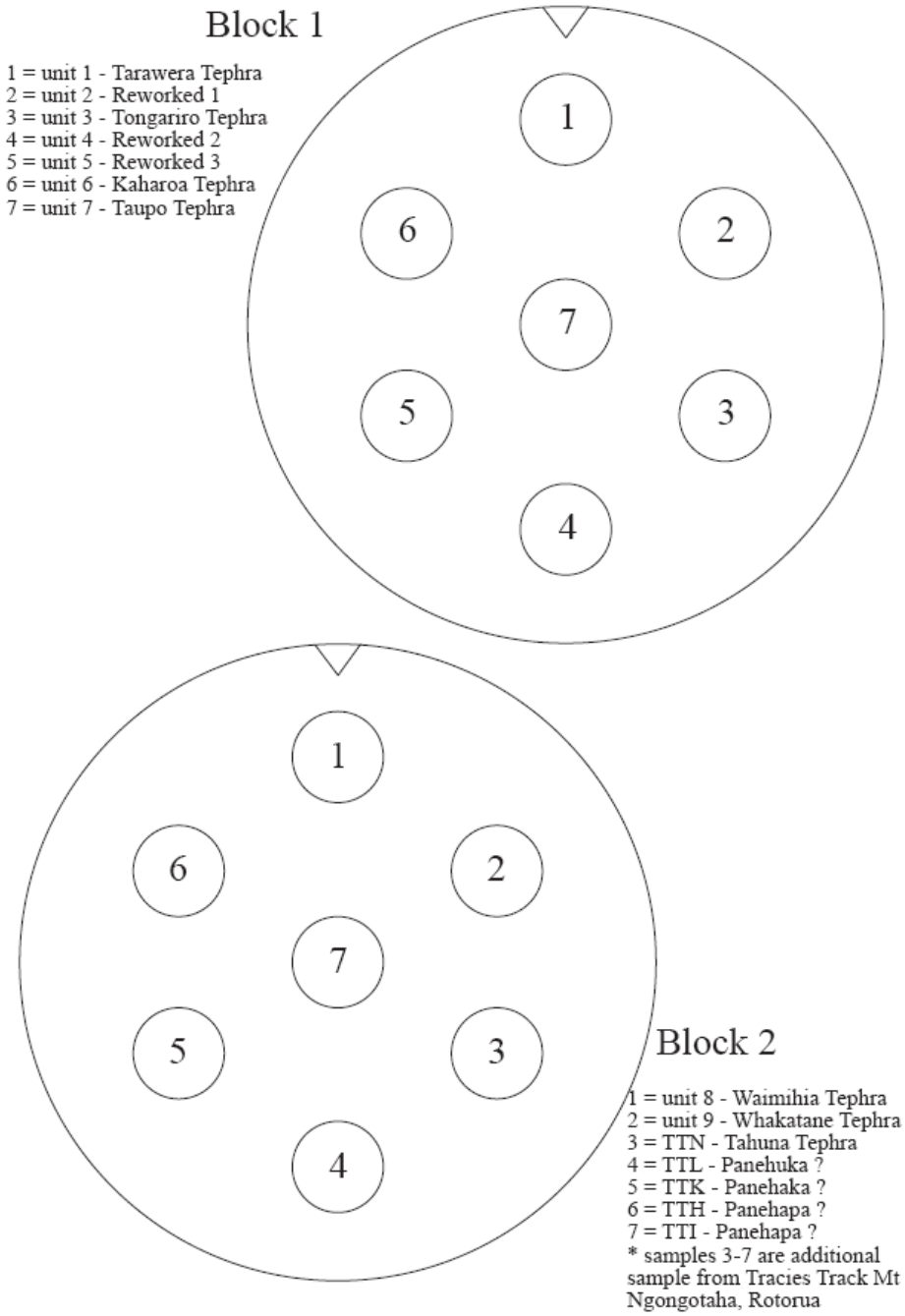

Sample 1	1	2	3	4	5	6	7	8	9	10	11	11b	12	13	14	15	16	17	18	19
SiO2	61.437	99.351	61.583	77.477	78.365	77.356	77.431	58.865	76.702	60.598	78.692	78.605	98.656	78.007	98.998	78.469	90.370	60.821	78.021	77.675
Al2O3	24.389	0.398	24.275	12.794	12.806	13.140	13.094	25.832	12.889	24.710	12.371	12.641	0.740	13.170	0.399	12.608	5.151	24.011	12.279	12.609
TiO2	0.000	0.097	0.029	0.144	0.161	0.105	0.080	0.054	0.118	0.056	0.103	0.152	0.060	0.135	0.183	0.160	0.103	0.030	0.073	0.156
FeO	0.214	0.000	0.227	1.014	0.171	0.929	0.905	0.235	0.437	0.243	0.892	0.816	0.112	0.948	0.208	1.057	0.435	0.277	0.866	0.726
MnO	0.027	0.035	0.005	0.096	0.000	0.127	0.141	0.000	0.185	0.168	0.117	0.141	0.054	0.166	0.045	0.010	0.055	0.106	0.020	0.232
MgO	0.026	0.004	0.016	0.111	0.056	0.098	0.048	0.013	0.032	0.012	0.109	0.067	0.028	0.142	0.000	0.152	0.007	0.009	0.070	0.062
CaO	5.416	0.088	5.702	0.807	0.778	0.633	0.635	7.350	0.345	5.990	0.784	0.644	0.089	0.928	0.028	1.115	0.402	6.422	0.791	0.463
Na2O	7.783	0.013	7.472	3.239	3.806	3.113	3.478	7.210	2.614	7.640	2.567	2.609	0.252	2.802	0.069	2.600	1.758	7.822	3.457	3.447
K2O	0.705	0.009	0.619	4.111	3.859	4.347	4.025	0.382	6.578	0.576	4.258	4.213	0.010	3.626	0.059	3.742	1.709	0.446	4.243	4.351
Cl	0.002	0.003	0.071	0.208	0.000	0.156	0.164	0.059	0.100	0.006	0.108	0.112	0.000	0.077	0.010	0.088	0.009	0.055	0.178	0.277
TOTAL	100	100	100	100	100	100	100	100	100	100	100	100	100	100	100	100	100	100	100	100

Sample 2	1	2	3	4	5	6	7	8	9	10	11	12	13	14	15	16	17	18	19	20	21
SiO2	60.121	78.726	99.808	77.967	98.763	77.940	77.739	60.757	78.270	78.657	78.227	78.163	60.132	60.946	78.166	58.175	79.307	96.154	60.239	78.308	57.619
Al2O3	24.575	12.333	0.008	13.048	0.593	12.954	12.327	24.460	12.363	12.368	12.013	12.913	25.379	24.391	12.475	25.792	12.402	2.280	24.640	12.407	26.628
TiO2	0.006	0.162	0.038	0.126	0.137	0.140	0.138	0.004	0.427	0.174	0.189	0.244	0.017	0.041	0.195	0.079	0.122	0.062	0.000	0.075	0.083
FeO	0.266	1.011	0.000	0.875	0.027	0.937	1.003	0.198	0.967	1.107	1.495	0.780	0.215	0.319	0.948	0.283	0.243	0.052	0.248	1.222	0.232
MnO	0.000	0.062	0.048	0.083	0.000	0.058	0.065	0.099	0.105	0.098	0.074	0.020	0.146	0.067	0.075	0.006	0.121	0.069	0.022	0.051	0.031
MgO	0.013	0.094	0.000	0.140	0.009	0.169	0.100	0.086	0.164	0.134	0.255	0.127	0.018	0.015	0.155	0.029	0.012	0.000	0.029	0.130	0.002
CaO	6.916	0.674	0.035	0.848	0.013	0.857	0.602	6.506	0.921	0.824	1.086	0.835	12.006	5.854	1.010	8.361	1.663	0.196	6.901	0.892	8.652
Na2O	7.481	3.452	0.007	3.697	0.247	3.629	3.502	7.422	3.513	3.444	2.691	3.575	1.948	7.719	3.643	6.913	5.229	1.096	7.491	3.494	6.429
K2O	0.583	3.349	0.008	3.141	0.166	3.196	4.301	0.467	3.138	3.091	3.806	3.159	0.059	0.624	3.197	0.310	0.805	0.075	0.414	3.288	0.304
Cl	0.040	0.140	0.047	0.073	0.044	0.119	0.222	0.000	0.133	0.102	0.162	0.186	0.081	0.023	0.145	0.052	0.094	0.017	0.014	0.134	0.022
TOTAL	100	100	100	100	100	100	100	100	100	100	100	100	100	100	100	100	100	100	100	100	100

Sample 3	1	2	3	4	5	6	7	8	9	10	11	12	13	14	15	16	17	17b	18	19	20	21a	21b	21c	22	23	24
SiO2	64.886	98.817	63.910	79.005	94.019	60.132	99.461	54.498	47.767	54.901	63.027	58.984	55.195	63.642	62.711	53.659	63.271	53.251	64.032	63.358	59.847	63.587	53.067	62.731	61.862	63.087	63.598
Al2O3	15.525	0.623	15.425	12.328	4.377	24.972	0.061	28.149	32.354	27.677	15.497	25.301	26.643	15.240	15.049	27.717	15.428	28.497	15.139	15.357	19.897	15.684	1.117	15.733	15.472	15.526	15.325
TiO2	1.115	0.012	1.024	0.072	0.068	0.007	0.097	0.144	0.069	0.067	1.062	0.010	0.186	1.014	1.052	0.109	0.992	0.141	0.892	1.072	0.613	0.980	0.362	1.048	1.102	1.093	1.023
FeO	5.445	0.105	6.403	1.016	0.338	0.177	0.022	0.631	0.696	0.654	6.765	0.384	1.445	6.795	7.190	1.121	6.692	0.808	6.645	6.311	4.587	6.635	18.242	6.838	6.786	6.963	6.624
MnO	0.170	0.151	0.121	0.014	0.027	0.019	0.062	0.116	0.009	0.086	0.184	0.034	0.062	0.138	0.220	0.086	0.114	0.039	0.041	0.214	0.114	0.161	0.467	0.211	0.148	0.132	0.177
MgO	1.946	0.069	2.042	0.106	0.578	0.077	0.049	0.038	0.125	0.061	2.276	0.055	0.325	2.160	2.305	0.297	2.279	0.221	2.107	2.220	1.322	1.918	24.436	2.063	2.331	2.072	2.091
CaO	4.433	0.071	4.882	0.851	0.133	6.463	0.016	11.379	16.506	10.942	4.967	7.687	11.099	4.641	5.269	11.945	4.885	11.869	5.182	5.399	7.585	4.516	2.181	5.158	5.783	4.913	4.853
Na2O	3.874	0.035	3.684	3.206	0.173	7.707	0.118	4.641	2.362	5.238	3.651	7.232	4.551	3.736	3.665	4.696	3.680	4.893	3.596	3.786	4.422	3.868	0.080	3.553	4.007	3.692	3.709
K2O	2.527	0.043	2.409	3.296	0.195	0.444	0.046	0.405	0.097	0.331	2.422	0.312	0.455	2.450	2.404	0.338	2.518	0.235	2.286	2.123	1.531	2.485	0.015	2.491	2.350	2.433	2.475
Cl	0.082	0.072	0.100	0.107	0.092	0.003	0.069	0.000	0.016	0.044	0.147	0.001	0.039	0.186	0.134	0.035	0.141	0.048	0.079	0.158	0.084	0.167	0.033	0.154	0.159	0.091	0.125
TOTAL	100	100	100	100	100	100	100	100	100	100	100	100	100	100	100	100	100	100	100	100	100	100	100	100	100	100	100

Sample 4	1	2	3	4	5	6	7	8	9	10	11	12	13	14	15	16	17	18	19	20	21
SiO2	77.879	77.933	79.027	78.761	76.328	78.495	58.836	77.911	77.878	78.583	77.965	77.891	78.208	78.688	77.913	79.125	78.518	75.819	78.754	79.418	76.372
Al2O3	12.243	12.378	12.456	12.466	13.479	12.523	25.499	12.520	12.742	12.842	12.683	12.538	13.001	12.658	12.432	13.009	12.562	14.085	12.605	12.585	13.356
TiO2	0.173	0.153	0.085	0.148	0.345	0.044	0.071	0.150	0.149	0.211	0.094	0.077	0.240	0.175	0.197	0.185	0.115	0.253	0.187	0.197	0.242
FeO	0.995	1.105	0.827	0.932	1.953	0.778	0.373	0.989	1.047	0.895	0.917	0.922	1.249	0.828	1.035	0.982	0.857	1.865	1.275	0.959	1.912
MnO	0.081	0.044	0.066	0.092	0.072	0.117	0.100	0.025	0.089	0.020	0.115	0.112	0.121	0.182	0.080	0.120	0.074	0.155	0.079	0.061	0.136
MgO	0.123	0.043	0.097	0.149	0.322	0.054	0.076	0.098	0.166	0.193	0.083	0.076	0.211	0.080	0.094	0.145	0.146	0.309	0.116	0.161	0.257
CaO	0.602	0.638	0.562	0.945	1.421	0.567	7.657	0.647	0.811	0.853	0.518	0.629	1.254	0.687	0.691	0.890	0.773	1.557	0.873	0.833	1.603
Na2O	3.186	3.247	3.054	2.988	3.134	3.511	7.072	3.273	3.410	3.154	3.483	3.562	2.982	3.082	3.096	2.333	3.368	3.193	2.818	2.563	3.332
K2O	4.435	4.147	3.668	3.269	2.726	3.779	0.298	4.142	3.568	3.040	3.982	3.963	2.572	3.416	4.271	3.024	3.468	2.568	3.093	3.010	2.651
Cl	0.166	0.313	0.158	0.249	0.219	0.132	0.020	0.246	0.140	0.211	0.161	0.229	0.161	0.204	0.192	0.187	0.118	0.196	0.201	0.214	0.138
TOTAL	100	100	100	100	100	100	100	100	100	100	100	100	100	100	100	100	100	100	100	100	100

Sample 5	1	2	3	4	5	6	7	8	9	10	11	12	13	14	15	16	17	18	19	20	21	22
SiO2	78.339	78.080	77.557	77.880	78.237	78.361	78.299	77.728	77.851	78.510	77.863	77.891	78.212	77.958	78.344	78.117	78.255	78.410	78.051	55.709	99.672	77.999
Al2O3	12.616	12.777	13.092	12.475	12.494	12.643	12.257	12.906	12.839	12.709	13.014	12.926	12.546	12.604	12.568	12.287	12.339	12.346	12.549	27.702	0.016	12.649
TiO2	0.057	0.157	0.071	0.144	0.131	0.108	0.106	0.119	0.122	0.140	0.073	0.101	0.178	0.113	0.102	0.177	0.171	0.132	0.165	0.075	0.036	0.047
FeO	0.931	0.647	1.000	0.741	0.810	0.788	0.827	0.959	0.889	0.697	0.787	0.693	0.927	0.874	0.796	0.947	0.922	0.897	0.918	0.308	0.055	0.817
MnO	0.099	0.199	0.124	0.041	0.113	0.057	0.112	0.177	0.145	0.072	0.077	0.140	0.085	0.160	0.055	0.202	0.185	0.104	0.071	0.020	0.031	0.157
MgO	0.109	0.060	0.100	0.086	0.059	0.078	0.160	0.118	0.107	0.058	0.067	0.086	0.081	0.068	0.074	0.079	0.092	0.070	0.148	0.011	0.033	0.116
CaO	0.503	0.539	0.690	0.610	0.614	0.616	0.623	0.541	0.590	0.607	0.608	0.608	0.631	0.638	0.600	0.569	0.626	0.532	0.844	9.883	0.026	0.695
Na2O	3.455	3.399	3.368	3.473	3.441	3.405	3.370	3.429	3.431	3.388	3.508	3.544	3.385	3.524	3.473	3.491	3.416	3.426	3.014	6.042	0.029	3.513
K2O	3.689	3.954	3.821	4.387	3.921	3.781	4.111	3.782	3.856	3.667	3.817	3.868	3.778	3.907	3.851	3.933	3.872	3.948	4.115	0.192	0.074	3.876
Cl	0.202	0.187	0.176	0.164	0.180	0.164	0.135	0.242	0.170	0.150	0.184	0.144	0.178	0.152	0.138	0.196	0.122	0.136	0.125	0.058	0.028	0.131
TOTAL	100	100	100	100	100	100	100	100	100	100	100	100	100	100	100	100	100	100	100	100	100	100

Sample 6	1	2	3	4	5	6	7	8	9	10	11	12	13	14	15	16	17	18	19	20	21
SiO2	78.189	77.708	78.055	78.296	78.422	77.848	77.435	77.650	77.828	77.934	78.199	77.889	78.152	77.922	77.862	77.399	77.545	77.812	77.864	78.094	78.414
Al2O3	12.606	12.739	12.537	12.321	12.573	12.658	13.066	12.711	12.726	12.660	12.462	12.639	12.664	12.412	12.757	12.779	12.670	12.665	12.536	12.768	12.405
TiO2	0.096	0.056	0.103	0.136	0.090	0.051	0.109	0.096	0.089	0.091	0.120	0.235	0.035	0.068	0.071	0.103	0.096	0.065	0.076	0.042	0.063
FeO	0.820	0.966	0.974	0.882	0.710	0.864	0.843	1.046	0.935	0.906	0.825	0.759	0.730	0.883	0.840	0.889	0.838	0.805	0.948	0.930	0.870
MnO	0.135	0.132	0.086	0.097	0.094	0.151	0.101	0.098	0.057	0.094	0.033	0.084	0.116	0.101	0.122	0.074	0.184	0.261	0.130	0.060	0.028
MgO	0.100	0.068	0.060	0.091	0.076	0.109	0.088	0.077	0.103	0.059	0.058	0.067	0.063	0.070	0.081	0.099	0.081	0.064	0.075	0.084	0.058
CaO	0.542	0.566	0.463	0.533	0.530	0.530	0.657	0.598	0.571	0.522	0.559	0.544	0.541	0.620	0.627	0.512	0.488	0.649	0.621	0.545	0.560
Na2O	3.434	3.579	3.561	3.522	3.458	3.464	3.441	3.488	3.578	3.566	3.562	3.447	3.589	3.426	3.474	3.610	3.506	3.463	3.535	3.222	3.488
K2O	3.955	3.981	4.016	3.946	3.856	4.175	4.085	4.064	3.947	3.929	4.006	4.124	3.976	4.304	4.013	4.379	4.387	4.060	4.043	4.143	3.938
Cl	0.123	0.205	0.146	0.174	0.192	0.151	0.173	0.172	0.167	0.239	0.175	0.211	0.135	0.195	0.153	0.156	0.206	0.156	0.172	0.113	0.175
TOTAL	100	100	100	100	100	100	100	100	100	100	100	100	100	100	100	100	100	100	100	100	100

Sample 7	1	2	3	4	5	6	7	8	9	10	11	12	13	14	15	16	17	18	19	20	21	22	23
SiO2	76.310	76.206	76.628	76.113	59.647	58.894	78.458	76.355	78.746	78.178	77.017	76.627	75.707	78.677	75.983	75.910	77.523	77.426	54.256	75.255	75.679	78.724	76.061
Al2O3	13.470	13.604	13.412	13.595	24.951	25.294	12.419	13.500	12.675	12.375	13.064	13.465	13.895	12.291	13.354	13.568	12.437	12.675	28.340	14.005	13.406	12.316	13.345
TiO2	0.336	0.238	0.237	0.318	0.079	0.014	0.111	0.343	0.149	0.067	0.186	0.272	0.286	0.096	0.183	0.263	0.193	0.141	0.041	0.226	0.255	0.188	0.407
FeO	2.147	1.954	2.004	2.080	0.390	0.379	0.865	1.963	0.874	0.992	1.589	1.818	1.903	1.119	1.870	1.928	1.349	1.230	0.663	2.085	2.095	1.088	1.959
MnO	0.097	0.114	0.094	0.150	0.051	0.122	0.097	0.127	0.121	0.028	0.101	0.121	0.206	0.067	0.223	0.130	0.181	0.000	0.001	0.186	0.146	0.178	0.188
MgO	0.267	0.317	0.271	0.270	0.038	0.049	0.192	0.245	0.102	0.109	0.255	0.271	0.308	0.107	0.254	0.342	0.143	0.132	0.069	0.314	0.297	0.156	0.304
CaO	1.452	1.672	1.583	1.358	7.136	7.953	0.688	1.569	0.992	0.591	1.341	1.460	1.597	1.027	1.498	1.554	0.691	1.164	10.652	1.588	1.605	0.948	1.499
Na2O	2.965	2.945	2.939	3.161	7.368	7.037	3.433	3.005	2.967	3.157	3.352	3.103	3.282	3.127	3.761	3.300	3.496	3.862	5.580	3.573	3.496	3.061	3.377
K2O	2.843	2.769	2.655	2.772	0.312	0.257	3.580	2.673	3.194	4.280	2.930	2.694	2.516	3.292	2.703	2.808	3.816	3.177	0.376	2.599	2.879	3.126	2.697
Cl	0.113	0.181	0.175	0.187	0.029	0.000	0.157	0.217	0.179	0.222	0.164	0.168	0.301	0.195	0.170	0.197	0.171	0.190	0.021	0.169	0.140	0.215	0.165
TOTAL	100	100	100	100	100	100	100	100	100	100	100	100	100	100	100	100	100	100	100	100	100	100	100

Sample 8	1	2	3	4	5	6	7	8	9	10	11	12	13	14	15	16
SiO2	75.448	77.708	78.790	75.971	75.232	75.322	57.453	75.505	77.635	75.598	75.774	75.616	75.422	76.016	76.306	75.132
Al2O3	13.754	12.800	12.665	13.222	13.909	13.843	26.627	13.644	12.953	13.737	14.129	13.959	14.192	13.982	14.211	14.147
TiO2	0.306	0.161	0.115	0.256	0.250	0.253	0.025	0.270	0.071	0.262	0.233	0.224	0.289	0.337	0.288	0.303
FeO	2.067	1.512	0.877	2.108	1.980	1.851	0.226	2.039	0.979	2.156	1.904	2.239	2.012	2.013	1.587	2.194
MnO	0.153	0.258	0.065	0.113	0.160	0.147	0.000	0.123	0.062	0.094	0.052	0.139	0.069	0.076	0.114	0.160
MgO	0.278	0.100	0.198	0.299	0.238	0.352	0.036	0.305	0.129	0.278	0.251	0.314	0.261	0.246	0.164	0.487
CaO	1.591	1.227	0.938	1.528	1.659	1.437	8.482	1.565	0.723	1.612	1.535	1.632	1.567	1.511	1.218	1.432
Na2O	3.400	3.137	2.992	3.610	3.656	3.742	6.874	3.500	3.704	3.415	2.836	2.808	2.990	2.738	2.998	3.143
K2O	2.866	2.917	3.193	2.705	2.777	2.855	0.247	2.862	3.551	2.692	3.194	2.896	2.977	2.918	2.969	2.809
Cl	0.138	0.182	0.164	0.187	0.138	0.197	0.028	0.190	0.194	0.159	0.093	0.175	0.221	0.163	0.145	0.192
TOTAL	100	100	100	100	100	100	100	100	100	100	100	100	100	100	100	100

Sample 9	1	2	3	4	5	6	7	8	9	10	11	12	13	14	15	16	17
SiO2	77.277	78.015	77.990	76.536	53.425	77.778	77.476	77.966	77.599	76.884	78.187	78.174	77.123	76.214	77.241	62.004	77.751
Al2O3	13.506	13.664	12.849	13.535	28.894	13.327	13.523	13.193	13.462	13.404	13.339	12.802	13.622	13.467	13.427	23.621	13.359
TiO2	0.130	0.190	0.181	0.279	0.090	0.174	0.093	0.149	0.170	0.170	0.228	0.183	0.142	0.201	0.188	0.030	0.151
FeO	0.980	0.832	1.187	1.622	0.556	0.886	0.919	0.928	0.949	1.732	1.009	1.013	1.635	1.846	1.439	0.155	0.866
MnO	0.174	0.046	0.136	0.140	0.000	0.092	0.107	0.053	0.099	0.124	0.135	0.119	0.168	0.162	0.095	0.044	0.085
MgO	0.156	0.183	0.134	0.220	0.056	0.108	0.154	0.154	0.115	0.196	0.135	0.149	0.195	0.159	0.167	0.000	0.161
CaO	0.890	0.986	0.931	1.392	11.631	0.680	0.886	0.969	0.639	1.103	0.709	1.120	1.320	1.404	1.124	4.321	0.771
Na2O	3.026	2.449	2.840	3.093	4.959	3.198	3.189	3.100	2.976	3.052	2.847	2.838	2.726	3.071	2.984	8.935	3.239
K2O	3.752	3.371	3.632	3.033	0.388	3.638	3.490	3.308	3.826	3.142	3.298	3.443	2.970	3.230	3.185	0.856	3.425
Cl	0.109	0.265	0.119	0.150	0.000	0.121	0.163	0.184	0.164	0.191	0.115	0.159	0.099	0.248	0.152	0.032	0.192
TOTAL	100	100	100	100	100	100	100	100	100	100	100	100	100	100	100	100	100

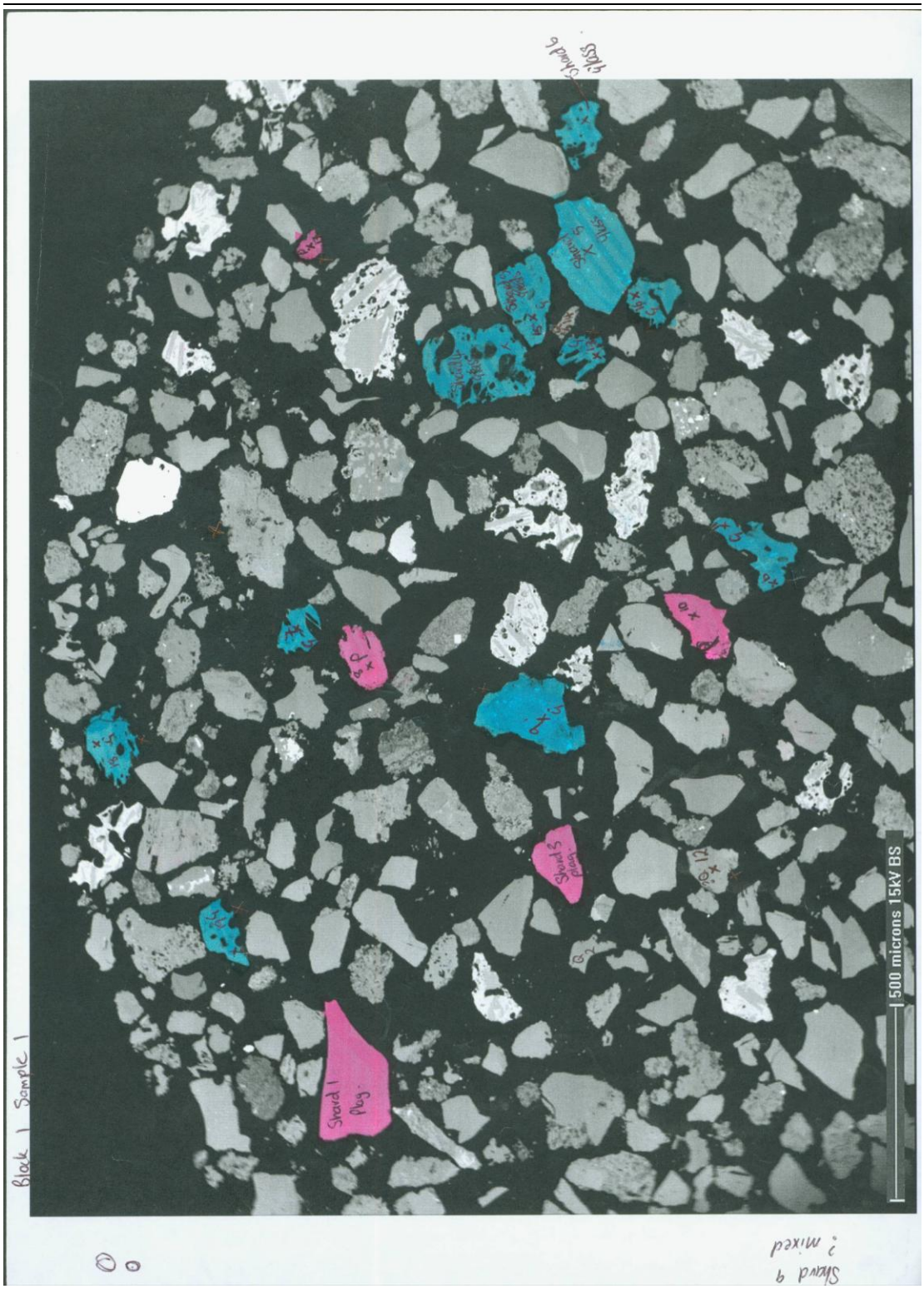
Black 1 Sample 1
Shard 1 Plag.
Shard 2 plag.
500 microns 15kV BS

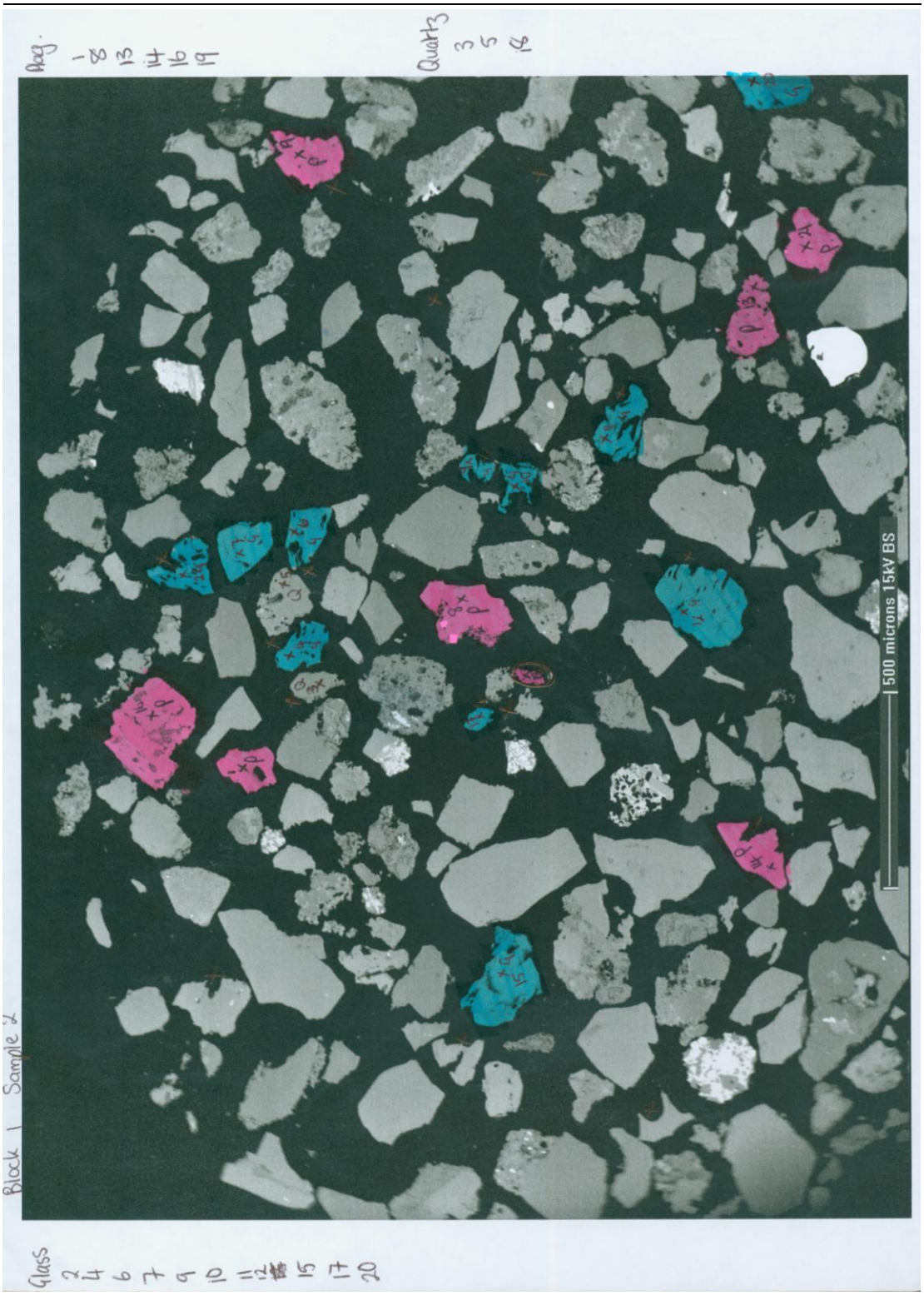
Agg.
1 8 13 14 16 19
Quartz
3 5 14
Block 1 Sample 2
Glass
2 4 6 7 9 10 11 15 17 20
500 microns 15kV BS

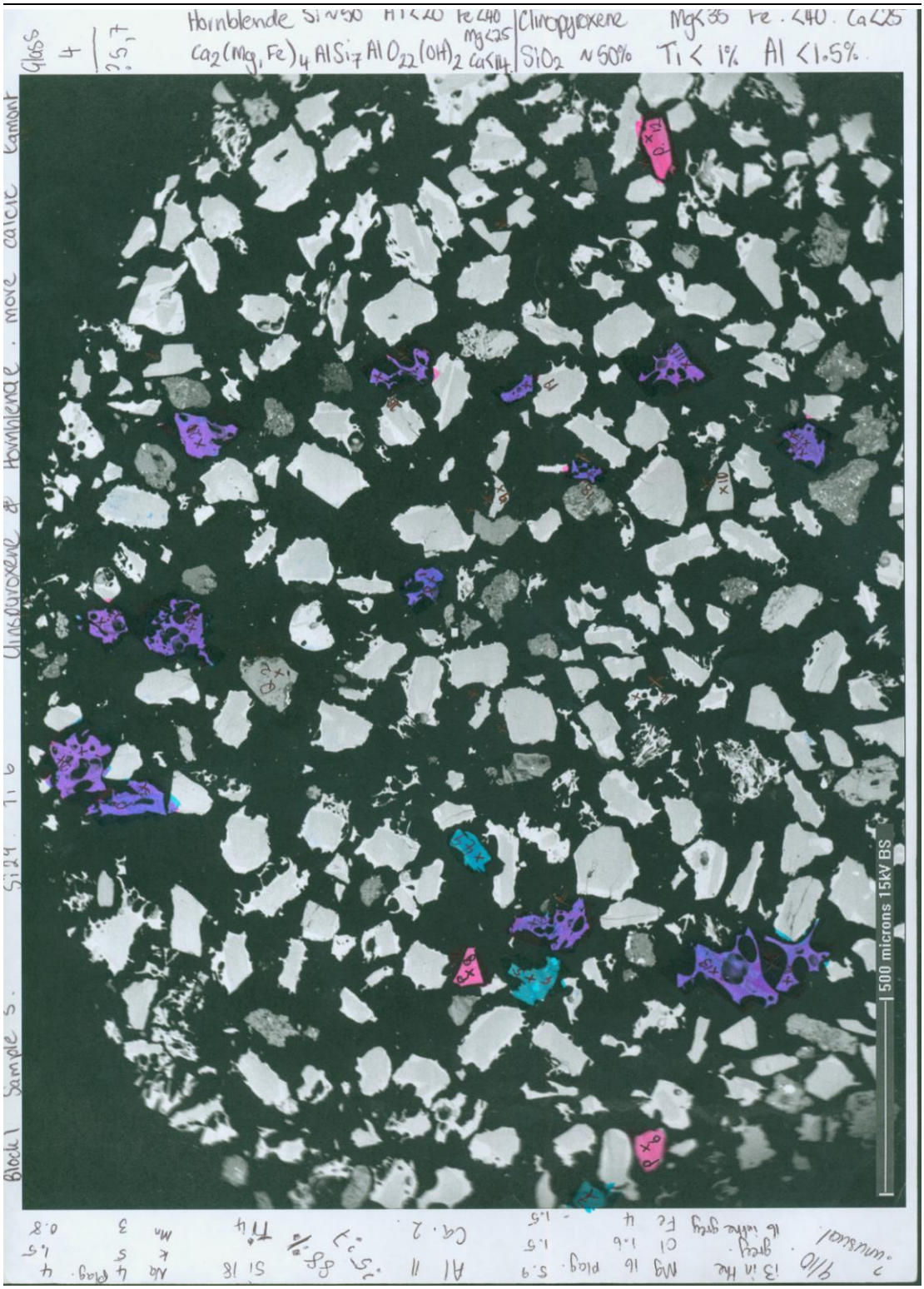
Hornblende Si ~50 Al<20 Fe<40 Mg<25
Ca2(Mg, Fe)4 AlSi7 AlO22(OH)2 Ca<14
Clinopyroxene Mg<35 Fe. <40. Ca<25
SiO2 ~50% Ti < 1% Al <1.5%
Glass 4
Block 1 Sample 5. Si29. Ti 6
Clinopyroxene & Hornblende. more calcic Kamont
500 microns 15kV BS

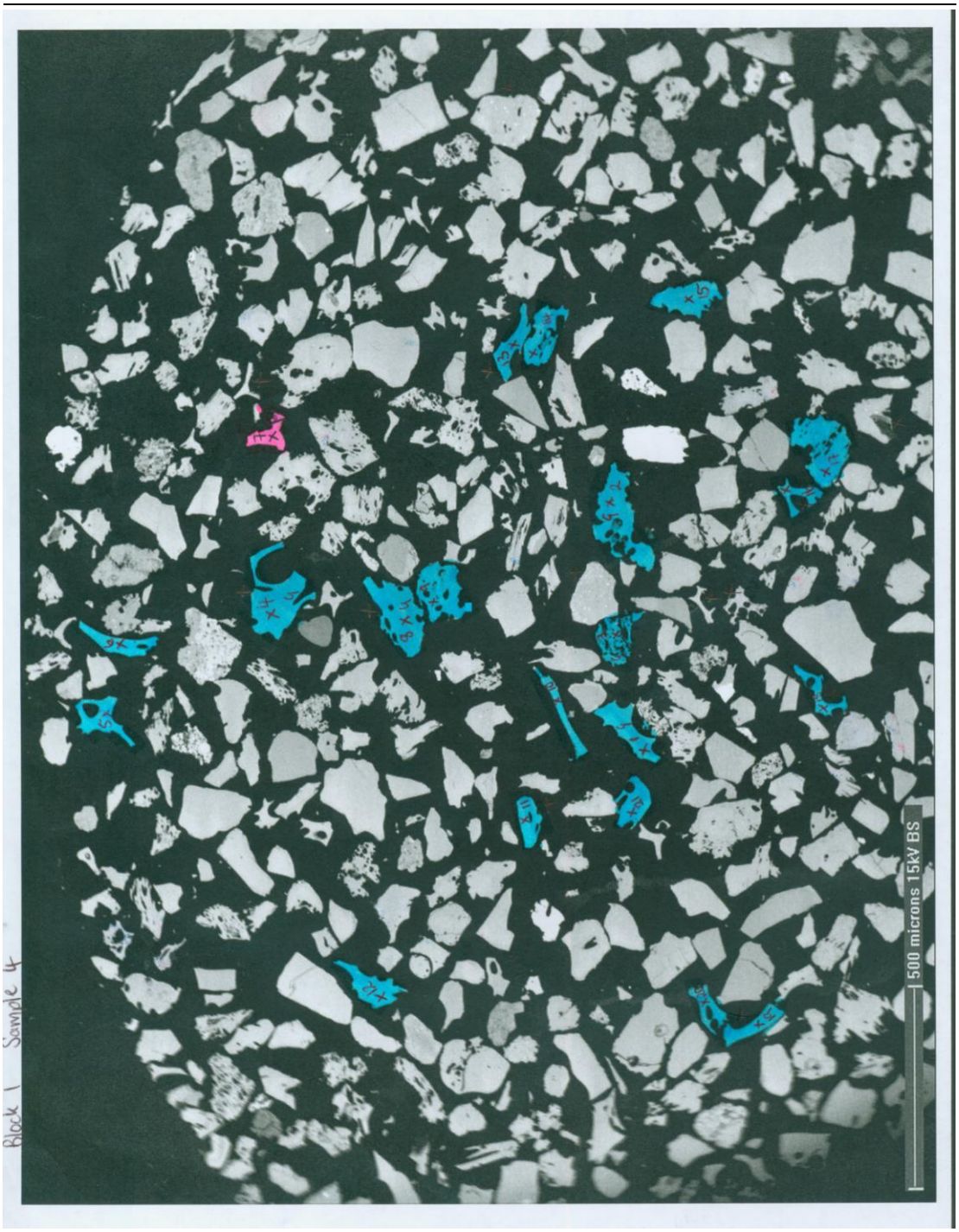
Block 1 Sample 4
500 microns 15kV BS

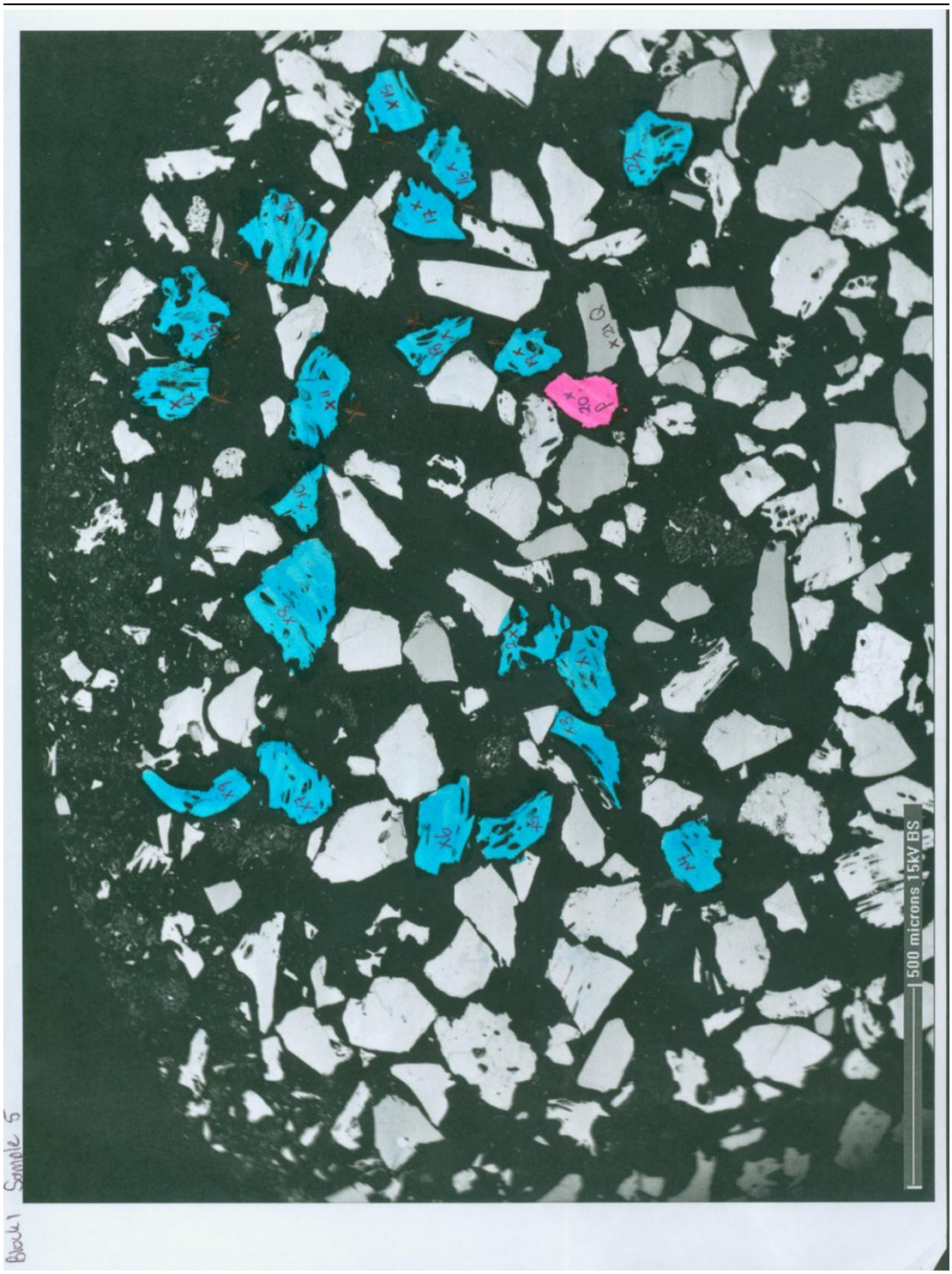
Block 1 Sample 5
500 microns 15kV BS

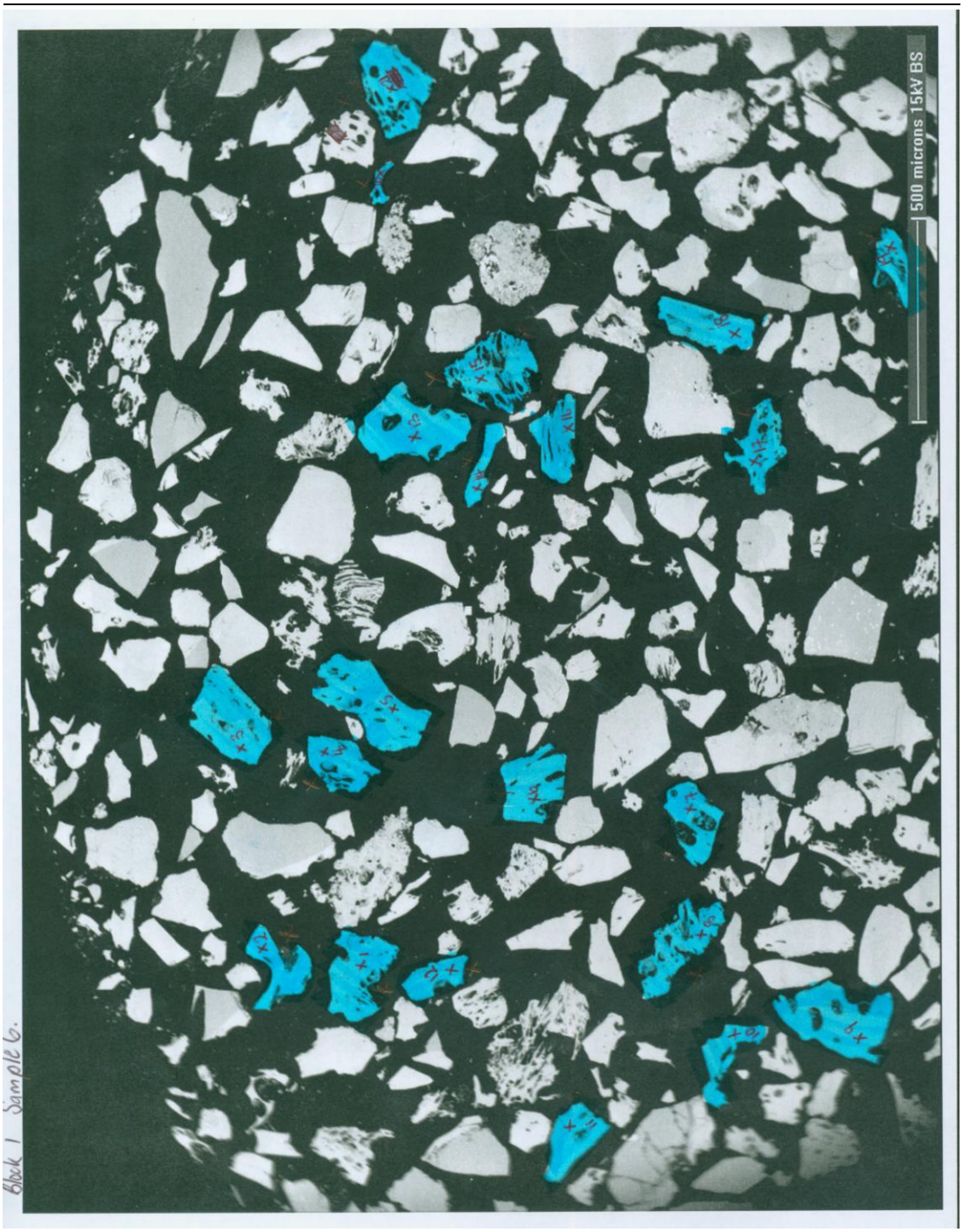
500 microns 15kV BS
Block 1 Sample 6.

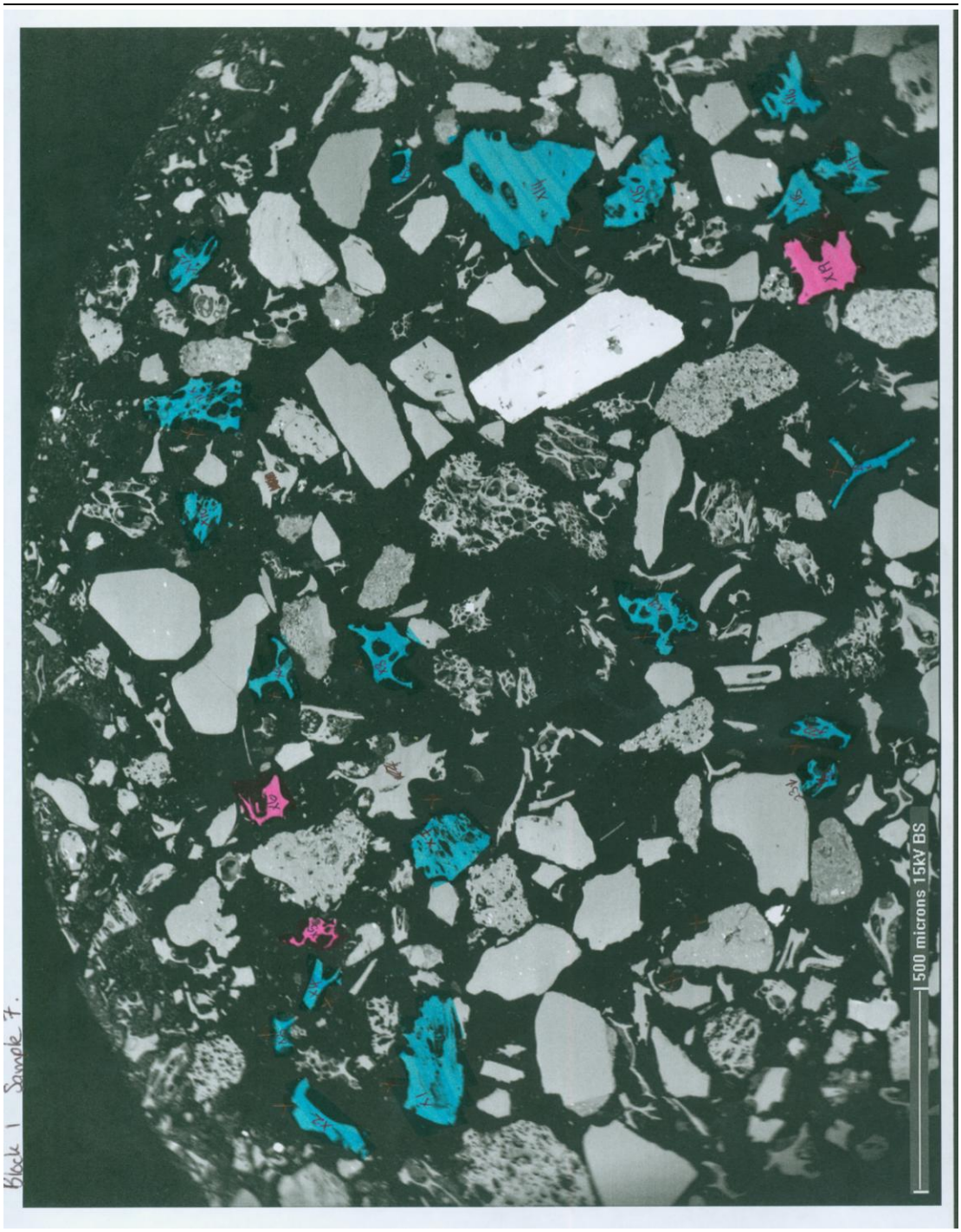
Block 1 Sample 7.
500 microns 15kV BS

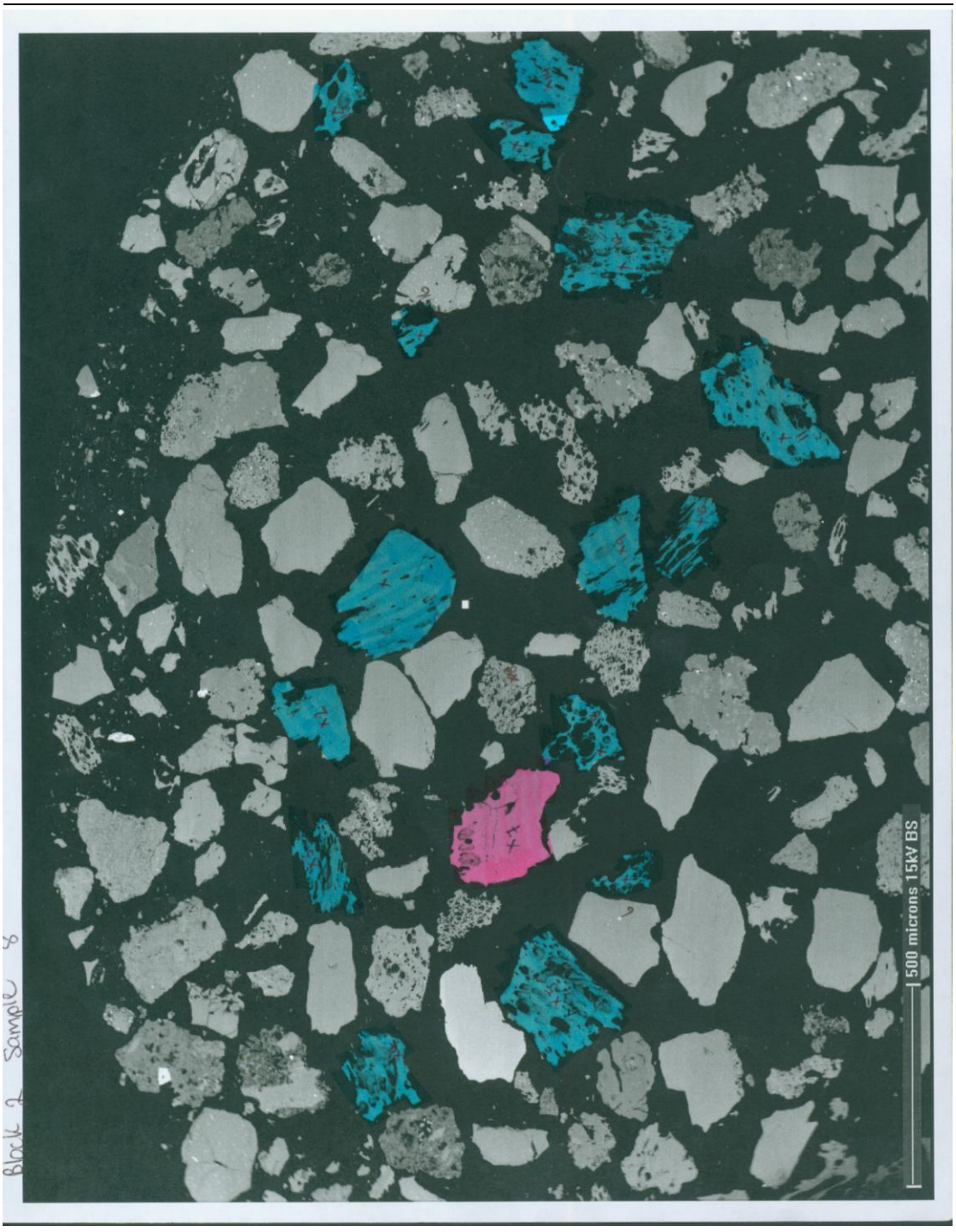
Block 2 Sample 6
500 microns 15kV BS

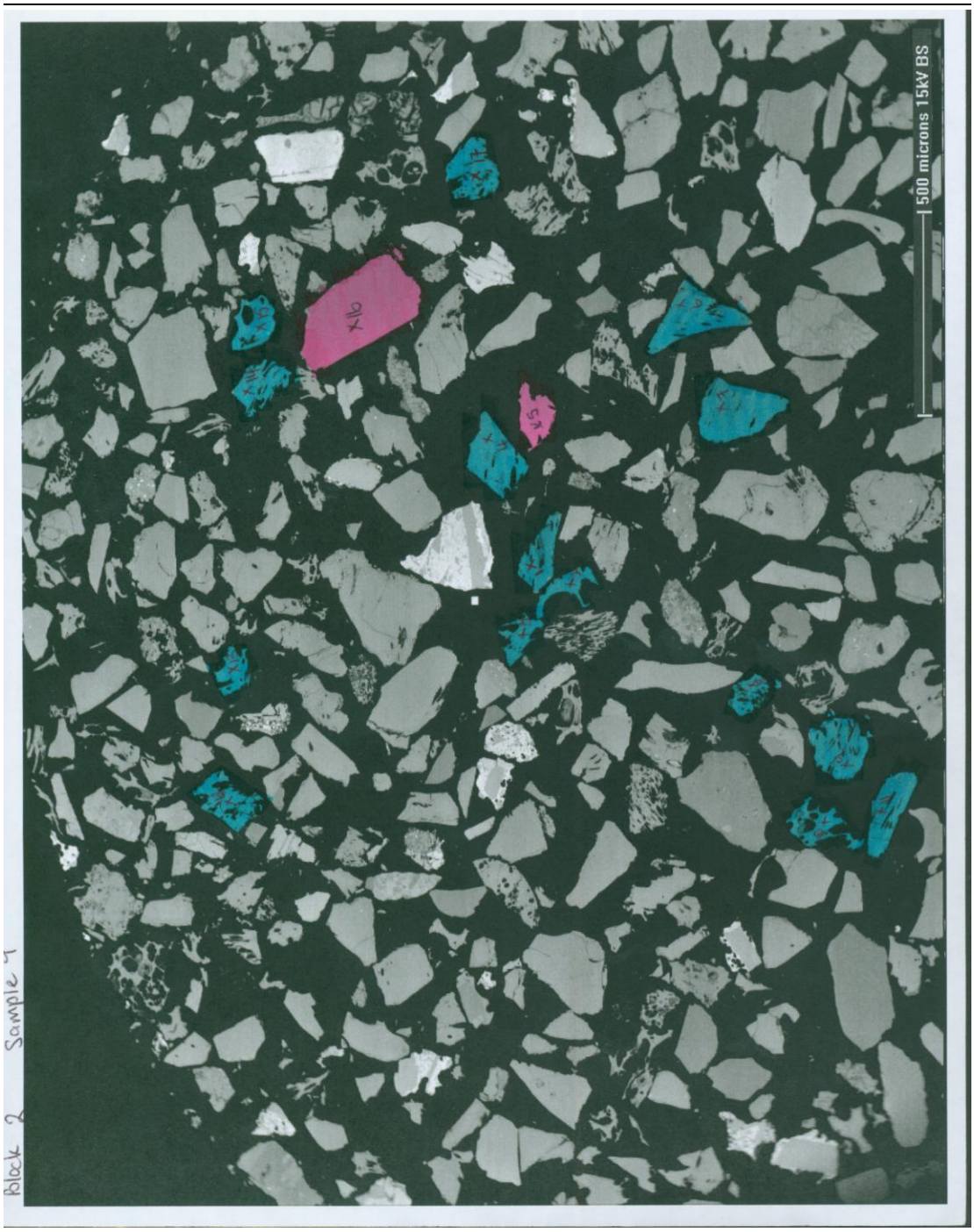
500 microns 15kV BS
Block 2 Sample 1

Appendix G: Sediment geochemistry data

	Depth (mm)	Sed. (ICPMS)	Li 7	B 10	Na 23	Mg 24	Al 27	Si 28	P 31	S 34	K 39	Ca 43	Cr 52	Fe 54	Mn 55	Co 59
Sample 1	10	0.1011	6.01	48.12	517.91	863.03	5676.27	146.82	835.36	5977.96	278.98	592.38	18.99	9582.13	476.87	1.63
Sample 2	20	0.1038	5.11	31.79	430.84	735.77	5867.12	161.57	678.93	5155.47	281.94	543.84	8.84	9036.08	395.07	1.33
Sample 3	30	0.1055	5.30	41.32	464.11	752.50	6469.16	171.73	794.85	5035.62	285.18	552.89	7.51	9152.37	393.38	1.31
Sample 4	40	0.1029	5.32	37.25	468.53	788.04	6244.87	164.79	804.25	4730.38	306.04	593.99	7.04	8224.61	390.93	1.39
Sample 5	50	0.1079	5.26	31.86	446.12	754.72	6031.37	153.94	795.86	4023.40	301.22	558.39	3.41	6631.99	370.97	1.33
Sample 6	60	0.1113	4.89	36.64	443.24	716.64	6031.40	140.96	684.13	3614.39	301.43	575.72	2.15	5573.04	371.12	1.31
Sample 7	70	0.1124	4.77	40.93	444.44	738.85	5885.12	141.21	665.03	3813.60	310.80	568.38	1.67	5844.00	369.00	1.34
Sample 8	80	0.1029	5.14	37.56	453.90	780.17	6276.44	157.93	663.18	3968.13	338.26	618.61	2.31	5634.53	397.31	1.42
Sample 09	90	0.121	5.03	33.16	418.85	781.37	6347.84	152.94	622.13	3416.10	342.38	595.79	2.71	6256.71	369.99	1.56
Sample 10	100	0.1428	5.09	32.78	418.13	847.06	7234.27	150.74	672.60	3312.66	344.83	637.59	2.64	6226.59	382.00	1.52
Sample 11	110	0.1124	5.61	35.29	472.00	848.12	6876.50	149.18	794.34	4221.22	375.25	701.41	2.01	5929.60	414.91	1.56
Sample 12	120	0.1038	5.33	35.23	441.39	847.96	8555.96	168.20	900.95	3735.66	366.36	660.94	4.02	6443.74	384.15	1.46
Sample 13	130	0.1038	4.95	38.77	394.80	765.04	8258.48	173.41	865.03	3384.32	368.79	613.39	3.81	6276.61	357.15	1.44
Sample 14	140	0.102	5.18	34.55	426.03	794.21	7563.97	174.20	877.31	3729.31	381.89	654.59	2.35	7288.18	357.55	1.49
Sample 15	150	0.1037	5.21	35.77	425.91	801.73	8180.16	178.66	844.97	4230.95	382.93	668.49	3.19	8155.71	387.30	1.67
Sample 16	160	0.1048	5.18	23.73	397.01	810.46	7166.02	177.87	738.79	3435.04	375.56	651.28	1.90	8021.02	363.06	1.64
Sample 17	170	0.1019	5.92	19.77	450.85	921.89	7086.24	177.51	865.30	4333.78	408.20	735.20	1.92	8679.19	430.35	1.88
Sample 18	180	0.1037	5.32	27.50	428.69	836.33	6581.39	166.15	980.48	5036.63	376.12	707.43	1.84	11340.47	371.29	1.66
Sample 19	190	0.1034	4.85	23.97	395.75	724.23	6690.88	174.66	838.44	4599.95	372.86	627.33	2.10	11965.19	319.05	1.41
Sample 20	200	0.117	4.56	27.87	411.94	675.83	5823.14	156.52	565.44	4987.07	331.57	619.51	2.04	12118.18	339.09	1.22
Sample 21	210	0.1029	4.95	38.71	442.71	706.22	5867.36	158.02	586.41	5257.88	360.80	664.48	1.83	12038.45	329.16	1.22
Sample 22	220	0.1097	5.21	36.71	467.95	788.25	6028.26	147.75	667.87	5134.36	356.61	731.73	2.23	9254.67	379.96	1.43
Sample 23	230	0.1016	5.57	35.01	481.22	803.38	6386.94	149.71	631.20	5761.04	352.28	733.76	2.87	9139.47	413.12	1.52
Sample 24	240	0.1064	5.38	32.19	458.40	749.51	6138.79	155.13	677.56	5222.78	349.72	690.52	1.95	8737.30	382.44	1.38
Sample 25	250	0.1045	5.53	38.75	486.11	769.82	6237.58	171.25	687.17	5456.82	357.15	728.02	1.51	8642.39	379.03	1.51
Sample 26	260	0.1032	6.01	24.57	485.57	986.85	7450.16	193.60	685.93	4504.28	437.78	848.93	1.58	7614.56	411.36	1.80
Sample 27	270	0.1018	6.41	20.92	454.56	1053.68	7973.62	209.70	757.36	4006.87	454.29	824.27	2.03	8873.36	391.71	1.91
Sample 28	280	0.1287	7.08	27.43	454.28	1148.09	8382.37	214.85	865.68	4269.81	463.17	803.10	1.58	11115.05	406.07	1.88
Sample 29	290	0.1242	7.69	30.02	478.43	1185.18	9196.95	221.55	953.59	4205.37	522.65	855.73	1.73	12239.02	422.58	1.97
Sample 30	300	0.1047	7.79	24.46	484.86	1248.23	9689.91	235.36	860.84	4013.62	502.47	800.52	1.77	11704.78	421.09	1.93
Sample 31	310	0.1204	8.12	23.21	457.91	1354.74	10074.15	226.92	980.18	3450.25	510.59	827.48	1.72	8978.64	426.14	2.04
Sample 32	320	0.1173	8.73	20.34	453.93	1324.50	10771.31	237.96	1159.22	3567.21	528.24	825.80	1.65	9156.50	458.33	2.06
Sample 33	330	0.1295	10.16	21.42	523.64	1487.91	11635.60	229.91	1316.38	4817.49	530.31	901.58	1.75	9858.95	541.29	2.34
Sample 34	340	0.1036	9.65	21.47	492.54	1471.92	11246.25	236.77	1306.12	4011.20	530.54	851.00	1.64	9567.57	487.01	2.25
Sample 35	350	0.107	9.65	30.10	511.18	1505.32	11414.33	234.15	1438.29	5208.31	541.73	915.81	1.66	12953.92	507.07	2.13
Sample 36	360	0.1027	10.65	23.37	486.09	1686.04	13557.25	274.36	1784.82	4711.38	645.35	863.52	2.75	13830.19	484.19	2.28
Sample 37	370	0.1164	11.79	23.90	510.64	1818.25	13929.96	288.66	1834.44	4660.66	650.86	914.59	2.02	13667.33	534.67	2.32
Sample 38	380	0.1614	11.30	17.94	461.30	1843.85	13378.83	265.81	1496.59	3856.99	626.00	846.43	2.39	12710.74	506.47	2.21
Sample 39	390	0.1174	12.13	17.68	464.66	2134.15	13480.84	295.55	1631.60	3098.02	750.07	867.44	2.12	14484.23	546.20	2.66
Sample 40	400	0.1134	13.57	6.07	507.34	3495.46	12772.37	323.27	1141.10	1431.47	939.35	1254.84	2.04	14463.63	673.58	4.29
Sample 41	410	0.1038	8.90	6.25	527.88	3249.34	8556.16	231.31	705.37	1316.64	874.49	1415.15	1.73	12639.64	514.34	3.82
Sample 42	420	0.168	4.08	11.52	306.49	3602.75	4102.64	182.65	384.22	1341.71	401.70	932.26	1.20	8596.53	292.72	3.73
Sample 43	430	0.1062	2.89	9.83	250.44	3700.74	2932.10	167.67	293.60	952.94	323.10	707.93	1.13	7594.26	217.93	3.92
Sample 44	440	0.1257	2.56	9.77	228.62	4149.98	2943.39	174.23	276.41	893.66	260.77	722.80	1.02	6923.04	210.38	3.98
Sample 45	450	0.1049	4.37	39.79	417.94	1183.57	4999.71	131.12	599.57	2772.34	275.47	585.61	1.33	4237.62	292.67	1.69
Sample 46	460	0.1054	4.49	42.53	439.72	853.33	5429.65	121.08	613.68	3056.48	254.19	509.69	1.57	5219.49	268.22	1.24
Sample 47	470	0.1045	5.15	33.88	491.32	991.72	6430.69	144.05	829.00	3599.01	288.85	587.87	1.82	5571.50	297.97	1.38
Sample 48	480	0.1019	4.26	34.77	416.76	792.44	5789.10	137.56	804.06	3280.38	255.44	500.47	2.00	5233.77	267.18	1.20
Sample 49	490	0.1179	4.18	34.55	403.60	783.19	5025.45	156.04	731.85	3119.74	232.36	491.73	1.32	5051.40	262.98	1.10
Sample 50	500	0.1223	3.90	31.75	371.57	665.13	5646.37	181.66	966.92	2970.78	229.41	454.61	1.48	4710.99	238.37	0.97
Sample 51	510	0.1048	3.50	41.37	378.74	697.51	4470.02	152.78	595.06	3029.61	220.59	452.52	1.59	5485.89	245.41	0.97
Sample 52	520	0.1029	3.88	40.07	432.45	792.22	4590.69	156.38	514.68	2914.42	251.63	512.39	1.26	4101.66	266.56	1.10
Sample 53	530	0.1053	3.70	26.94	380.50	652.46	4780.98	150.82	687.96	2869.62	230.34	476.21	1.20	3741.07	248.66	0.96
Sample 54	540	0.1129	3.89	36.00	414.52	630.67	4949.13	153.11	663.56	3043.61	239.77	459.06	1.19	3941.23	250.88	0.89
Sample 55	550	0.1038	3.74	27.98	395.70	659.57	5177.81	168.52	679.30	2694.40	249.43	500.16	1.33	3635.66	246.18	0.99
Sample 56	560	0.1013	3.84	38.39	393.97	712.60	4717.47	164.31	501.35	2648.65	262.82	507.49	1.17	3748.91	253.00	0.95
Sample 57	570	0.1017	3.84	28.14	386.40	647.11	4924.16	162.94	653.51	2983.43	245.39	506.13	1.35	4068.16	268.41	0.93
Sample 58	580	0.101	3.85	34.67	405.94	723.15	5430.91	150.70	661.21	2918.88	254.41	533.92	2.20	3925.58	284.17	1.01
Sample 59	590	0.108	3.70	29.07	394.65	675.07	5078.20	150.98	624.04	2860.81	241.58	521.95	1.64	3736.69	280.23	0.95
Sample 60	600	0.1117	3.99	19.06	388.28	644.49	5183.09	149.18	606.33	2670.21	246.33	501.09	1.29	2970.79	262.49	0.89
Sample 61	610	0.1134	2.98	25.39	320.15	490.76	4992.93	163.13	637.48	2383.72	219.78	412.66	1.45	3162.41	213.83	0.68
Sample 62	620	0.1049	4.25	25.78	418.70	636.36	5442.78	170.99	789.53	3015.50	260.47	527.01	1.28	3195.29	275.81	0.83
Sample 63	630	0.108	3.32	31.17	319.87	539.64	5564.49	173.68	796.65	2308.60	234.72	435.66	1.44	3605.82	212.89	0.72
Sample 64	640	0.1043	3.66	14.34	340.54	536.53	5340.73	167.43	702.24	3866.99	237.59	457.16	1.32	4980.60	249.05	0.82
Sample 65	650	0.1009	3.94	29.68	393.37	565.90	4967.19	161.29	849.01	3292.80	231.00	496.88	1.34	5365.01	254.86	0.72
Sample 66	660	0.1033	3.28	27.21	333.38	534.44	5329.99	158.14	836.16	2850.82	226.52	457.69	1.68	4860.59	229.45	0.72
Sample 67	670	0.1017	3.49	29.15	373.61	544.44	4924.32	155.76	732.39	4046.55	237.08	490.86	1.20	5382.25	259.46	0.74
Sample 68	680	0.1071	3.14	32.88	320.04	484.55	4346.23	142.27	605.17	3110.68	218.75	439.96	1.24	5228.31	217.22	0.66
Sample 69	690	0.1007	3.46	33.15	340.45	529.19	4524.39	143.58	625.51	3438.29	218.80	454.08	1.21	5114.85	241.58	0.68
Sample 70	700	0.1068	3.57	31.42	347.87	543.15	4725.18	144.61	643.97	3052.03	231.72	483.03	1.20	3884.54	242.78	0.66
Sample 71	710	0.1088	3.53	34.02	367.59	574.14	4273.03	135.97	535.06	3081.70	224.00	480.25	1.15	3064.46	265.73	0.73
Sample 72	720	0.1024	3.49	30.27	336.44	562.33	5038.31	148.67	697.01	5709.40	219.46	473.00	1.52	7743.89	240.33	0.90
Sample 73	730	0.1197	3.59	23.03	324.94	570.99	5001.43	181.39	726.03	3241.88	215.95	460.53	1.33	4147.53	228.60	0.72
Sample 74	740	0.1141	3.72	24.53	356.65	624.90	4244.49	158.47	541.63	5561.24	216.83	508.79	1.15	7417.22	244.33	0.83
Sample 75	750	0.1035	3.12	21.54	285.57	513.51	4628.90	183.65	720.75	3848.17	213.25	402.77	1.38	6696.33	193.50	0.64
Sample 76	760	0.105	3.23	24.39	306.58	528.82	4525.98	184.77	477.13	5639.67	204.93	416.67	1.20	7029.17	205.03	0.80
Sample 77	770	0.1127	3.62	31.96	332.02	648.63	4687.42	176.33	551.03	4933.75	205.30	442.63	1.41	6858.53	231.81	0.70
Sample 78	780	0.1055	3.45	25.11	308.23	603.66	4473.83	175.40	540.22	4820.04	207.86	426.56	1.09	6641.44	209.81	0.66
Sample 79	790	0.115	3.95	22.51	324.25	692.45	5136.23	185.33	767.94	3353.72	225.44	468.59	1.55	6151.41	229.47	0.64
Sample 80	800	0.1017	4.20	23.63	343.44	782.94	5217.11	199.88	629.23	3527.82	237.23	494.17	1.37	6119.28	246.09	0.64
Sample 81	810	0.101	3.95	31.85	318.36	748.14	4848.38	175.60	593.55	3044.13	224.54	438.61	1.39	4604.17	208.62	0.65
Sample 82	820	0.1068	5.40	44.08	452.13	1038.22	4305.92	147.93	497.01	3808.20	244.40	572.88	0.93	3329.51	290.37	0.71
Sample 83	830	0.1176	4.62	35.28	360.96	937.47	5127.82	168.84	560.56	3702.18	243.04	519.24	1.23	5154.67	255.30	0.71
Sample 84	840	0.1084	5.26	33.81	401.24	1016.19	5302.04	181.15	623.04	3657.32	256.87	528.91	1.31	3880.82	266.66	0.70
Sample 85	850	0.1031	5.95	42.38	448.94	1189.62	4695.84	161.81	559.24	3942.71	250.02	586.29	1.17	3836.77	295.86	0.77
Sample 86	860	0.1115	4.02	20.74	298.88	769.09	5045.23	175.45	618.07	2898.00	227.03	431.42	1.23	3418.28	201.05	0.57
Sample 87	870	0.1048	4.92	34.80	398.34	961.77	5077.79	173.02	608.82	5089.95	234.34	522.08	1.33	5839.03	261.03	0.67
Sample 88	880	0.1061	6.02	41.52	500.78	1153.43	5528.63	202.12	720.09	4996.30	282.63	676.43	1.67	5394.70	334.12	0.74
Sample 89	890	0.1042	5.64	29.20	451.74	1010.44	6028.41	204.02	749.40	4972.12	282.02	629.77	1.58	5951.53	313.55	0.74
Sample 90	900	0.1096	4.73	20.14	409.09	837.25	4990.14	173.43	491.16	6935.02	252.38	540.11	1.41	7074.59	282.81	0.82
Sample 91	910	0.1201	3.33	27.72	287.29	549.78	4709.77	157.47	454.19	5559.36	208.34	415.36	1.23	5873.70	195.60	0.71
Sample 92	920	0.103	5.12	36.15	441.71	795.38	4675.90	153.73	615.56	5688.93	247.01	618.57	1.12	6542.74	326.84	0.77
Sample 93	930	0.1025	4.71	49.49	451.53	713.64	4554.25	153.25	597.58	4808.09	244.27	596.58	1.05	4769.38	307.98	0.73
Sample 94	940	0.1219	3.23	21.87	282.90	450.37	4961.36	161.32	487.49	4326.89	208.03	423.10	1.18	4730.35	208.46	0.74
Sample 95	950	0.1263	3.36	16.67	285.34	452.95	5160.11	164.85	548.00	4923.74	219.34	444.11	1.39	5851.07	214.47	0.73
Sample 96	960	0.1293	3.05	22.61	277.63	419.77	4737.06	164.90	636.73	4351.54	204.68	422.77	1.28	5684.01	205.22	0.64
Sample 097	970	0.1195	3.46	16.39	303.74	416.11	4934.89	166.20	663.57	4243.51	215.76	449.03	1.19	5224.40	218.46	0.68
Sample 098	980	0.1082	3.73	20.05	330.92	424.65	5393.39	177.49	756.11	4536.19	221.09	450.28	1.38	5380.84	220.39	0.67
Sample 099	990	0.1127	3.30	19.31	297.05	386.01	5450.61	177.43	988.88	4250.07	210.14	442.20	1.55	6293.38	195.38	0.59
Sample 100	1000	0.1106	3.05	24.22	309.64	389.76	4832.82	176.83	770.99	4497.20	203.61	426.96	1.41	7388.48	196.70	0.54
Sample 101	1010	0.11	4.06	27.94	517.68	558.63	4002.63	161.56	506.73	5355.23	226.17	584.55	1.15	7568.89	303.04	0.74
Sample 102	1020	0.1113	4.60	26.58	482.66	606.72	4074.63	161.33	433.06	5150.19	233.05	623.73	1.14	4421.07	336.47	0.73
Sample 103	1030	0.108	3.72	31.88	422.78	549.82	4427.40	160.91	438.94	4800.45	217.88	567.82	3.02	4923.02	286.84	0.68
Sample 104	1040	0.1112	5.73	48.69	606.55	744.89	4743.31	182.40	634.75	8443.84	277.64	770.99	1.33	8882.32	412.69	0.96
Sample 105	1050	0.1107	4.13	27.67	459.07	557.38	4791.33	187.00	523.50	6343.16	235.73	593.35	1.36	6201.71	304.81	0.75
Sample 106	1060	0.1189	3.40	23.25	376.04	424.97	4630.93	183.15	563.65	4905.12	218.02	500.87	1.15	5366.44	236.50	0.66
Sample 107	1070	0.1179	3.80	45.69	423.09	477.72	5048.87	182.35	668.65	6150.06	232.72	532.52	1.22	7026.02	266.39	0.71
Sample 108	1080	0.1485	5.03	27.42	468.11	578.13	6279.33	198.74	743.56	8713.87	256.80	638.88	1.54	8264.95	319.66	1.06
Sample 109	1090	0.1234	2.74	15.27	279.12	335.31	4210.57	161.84	448.69	4501.18	188.12	381.67	1.15	5560.21	181.41	0.51
Sample 110	1100	0.1145	3.09	18.05	328.56	378.74	4273.46	161.13	403.81	6765.43	201.26	421.97	2.31	6294.95	197.69	0.66
Sample 111	1110	0.1058	2.87	36.68	310.36	371.50	4122.53	156.78	440.68	3958.45	185.86	394.61	1.14	4523.22	190.04	0.49
Sample 112	1120	0.1116	3.72	30.55	409.77	477.76	4281.20	165.95	428.01	4766.35	218.39	490.28	1.17	4542.13	235.68	0.65
Sample 113	1130	0.1074	5.81	29.70	588.14	712.65	4437.13	177.65	396.50	8468.99	269.07	687.87	1.07	5758.47	359.19	1.00
Sample 114	1140	0.1025	5.73	37.76	603.53	729.47	4214.10	160.86	551.39	7864.13	258.40	713.75	1.16	8021.96	365.45	0.92
Sample 115	1150	0.1091	4.76	32.20	489.68	592.92	4384.95	165.72	540.26	9158.85	238.37	585.14	1.23	8204.45	284.24	0.88
Sample 116	1160	0.1206	3.61	23.58	371.64	455.11	4281.86	164.68	556.39	4736.35	193.17	413.53	1.20	5200.39	205.66	0.61
Sample 117	1170	0.1012	4.50	38.50	466.43	583.72	4471.90	176.84	586.39	5503.43	221.47	488.24	1.31	5487.96	251.95	0.66
Sample 118	1180	0.1041	6.90	33.36	679.74	883.95	4140.94	153.85	388.65	7742.96	270.34	708.65	1.31	5879.97	372.11	0.92
Sample 119	1190	0.1068	5.66	41.64	601.10	765.26	3982.80	155.25	440.06	5496.91	243.78	636.33	1.61	6623.07	392.23	1.03
Sample 120	1200	0.1048	5.15	41.64	562.80	709.41	3561.21	152.91	364.91	4746.04	224.42	562.27	1.04	5213.45	298.17	0.86
Sample 121	1210	0.1204	2.63	11.02	348.77	327.03	4094.25	10.64	439.74	4086.58	193.14	488.28	1.38	4898.09	245.73	0.72
Sample 122	1220	0.1013	2.61	10.80	339.40	304.91	3941.34	11.01	451.77	4748.14	186.88	457.60	1.50	5381.56	247.47	0.76
Sample 123	1230	0.107	2.52	18.82	358.41	308.20	4203.34	8.17	487.97	5794.87	190.55	469.54	1.16	7200.59	272.27	0.79
Sample 124	1240	0.1022	2.58	24.41	381.84	317.37	4064.37	7.50	467.19	5727.68	185.63	486.66	1.13	6235.24	258.93	0.77
Sample 125	1250	0.1056	2.63	31.53	378.75	313.91	4867.61	8.47	600.12	5798.66	208.12	496.26	1.50	7076.87	234.23	0.72
Sample 126	1260	0.1005	3.71	26.91	547.34	431.99	4775.09	15.36	614.23	7847.20	234.72	630.27	1.37	8140.18	354.88	0.99
Sample 127	1270	0.112	3.12	22.85	441.39	367.92	4748.70	13.09	566.62	6552.51	253.64	533.44	1.49	5924.06	289.91	0.79
Sample 128	1280	0.1057	3.51	13.70	477.44	408.74	4893.73	8.81	491.59	6550.32	233.87	623.07	1.68	5302.54	329.62	0.84
Sample 129	1290	0.101	2.67	19.72	361.09	313.52	4377.98	7.00	533.56	5368.43	201.64	472.09	1.25	6263.57	239.07	0.69
Sample 130	1300	0.1018	2.65	18.22	377.94	334.24	4126.77	5.37	423.53	6242.17	198.97	532.32	1.34	5733.21	273.87	0.80
Sample 131	1310	0.1025	2.42	15.97	332.35	282.03	4075.24	4.14	518.74	4972.13	189.59	459.24	1.10	6349.61	234.98	0.68
Sample 132	1320	0.1109	2.54	18.01	347.51	297.13	4891.96	6.06	619.74	4723.34	198.12	449.68	1.50	4912.37	233.34	0.68
Sample 133	1330	0.1001	2.86	28.43	390.59	335.14	5590.88	6.91	746.16	5317.55	219.21	503.93	1.51	5209.51	271.50	0.84
Sample 134	1340	0.1023	2.15	15.28	318.75	271.11	4524.76	8.63	557.94	4118.97	201.88	429.61	1.39	4839.65	209.91	0.58
Sample 135	1350	0.1037	2.78	16.23	415.81	353.96	4801.86	7.91	492.39	5097.92	229.58	583.22	1.91	5384.18	268.54	0.75
Sample 136	1360	0.1017	2.74	15.11	440.80	382.11	4452.95	10.19	438.96	5701.21	227.19	578.63	1.25	5647.78	296.26	0.80
Sample 137	1370	0.1081	3.30	18.05	453.21	413.92	4542.68	5.72	476.57	5842.91	230.53	613.46	1.40	6810.16	325.57	0.89
Sample 138	1380	0.104	3.46	19.70	482.02	393.95	4728.60	7.06	451.99	5430.17	243.76	571.38	2.15	4911.43	310.44	0.80
Sample 139	1390	0.1022	2.48	17.84	349.95	330.06	4457.40	8.43	451.55	5116.64	208.78	513.48	1.23	5420.66	260.56	0.69
Sample 140	1400	0.107	2.53	17.69	374.22	328.05	4047.51	8.83	392.85	4573.36	204.36	501.46	1.31	4526.22	261.56	0.69
Sample 141	1410	0.104	2.53	20.63	361.44	328.27	4109.83	8.49	376.66	4938.45	188.97	470.48	1.10	4467.46	255.73	0.70
Sample 142	1420	0.1024	2.87	20.22	435.48	369.21	4311.92	8.19	432.11	6114.41	217.68	554.62	1.26	5201.24	294.42	0.75
Sample 143	1430	0.1024	2.90	27.99	468.77	403.93	4287.15	9.08	484.08	5177.33	222.02	609.14	1.19	5501.37	319.37	0.78
Sample 144	1440	0.1026	3.04	25.68	472.04	386.77	4967.72	8.94	609.71	5166.13	229.46	549.93	1.48	5544.96	303.77	0.76
Sample 145	1450	0.1032	2.95	27.49	338.49	334.99	5395.44	10.25	658.35	4452.54	226.52	533.67	1.45	4809.21	278.25	0.72
Sample 146	1460	0.1041	3.57	22.49	382.47	385.86	7225.22	10.98	1090.73	5668.96	228.93	573.24	1.73	5867.62	300.43	0.76
Sample 147	1470	0.1006	2.51	15.20	320.30	325.84	5278.55	10.01	658.72	5017.56	206.92	473.95	1.55	5396.38	246.65	0.69
Sample 148	1480	0.1027	2.99	22.33

	Depth (mm)	Sed. (ICPMS)	Ni 60	Cu 63	Zn 66	As 75	Se 82	Sr 88	Ag 109	Cd 111	Ba 137	Hg 202	Tl 205	Pb 207	Bi 209	U 238
Sample 1	10	0.1011	8.73	12.23	123.29	88.23	0.82	8.52	0.80	-0.08	126.83	0.29	0.31	14.11	0.17	0.39
Sample 2	20	0.1038	2.07	9.61	98.92	82.49	0.59	7.87	0.63	-0.11	115.64	0.25	0.33	12.07	0.17	0.39
Sample 3	30	0.1055	1.41	9.32	95.80	88.56	0.64	8.37	0.55	-0.11	116.74	0.29	0.33	11.57	0.19	0.39
Sample 4	40	0.1029	2.37	6.86	90.52	89.84	0.64	8.94	0.53	-0.12	115.02	0.32	0.33	9.55	0.20	0.38
Sample 5	50	0.1079	1.70	5.66	78.13	67.88	0.57	8.89	0.51	-0.12	113.93	0.30	0.34	7.74	0.20	0.36
Sample 6	60	0.1113	1.27	5.98	76.86	69.74	0.61	8.70	0.53	-0.11	101.00	0.29	0.35	6.24	0.22	0.36
Sample 7	70	0.1124	1.38	3.67	69.47	73.78	0.57	8.79	0.54	-0.11	92.46	0.29	0.35	5.20	0.19	0.38
Sample 8	80	0.1029	1.78	3.43	60.68	65.46	0.56	9.00	0.48	-0.11	89.86	0.31	0.32	4.85	0.17	0.39
Sample 09	90	0.121	2.25	3.38	53.10	59.88	0.53	9.16	0.45	-0.10	88.66	0.28	0.33	4.76	0.15	0.41
Sample 10	100	0.1428	2.07	4.57	62.59	59.72	0.59	9.71	0.47	-0.08	99.58	0.27	0.35	5.39	0.15	0.46
Sample 11	110	0.1124	1.18	4.34	60.59	59.67	0.45	9.82	0.46	-0.11	102.04	0.33	0.35	4.93	0.14	0.42
Sample 12	120	0.1038	1.44	18.62	107.89	83.72	0.61	10.56	0.60	-0.13	129.40	0.35	0.35	5.53	0.15	0.43
Sample 13	130	0.1038	1.34	12.26	90.76	99.08	0.57	10.32	0.56	-0.13	126.62	0.34	0.37	5.31	0.23	0.42
Sample 14	140	0.102	1.19	5.93	58.93	110.77	0.63	10.67	0.54	-0.15	124.85	0.32	0.36	5.02	0.15	0.38
Sample 15	150	0.1037	1.17	9.00	72.93	114.31	0.52	10.92	0.55	-0.14	131.06	0.29	0.36	4.76	0.16	0.37
Sample 16	160	0.1048	1.14	3.04	41.48	99.97	0.54	10.13	0.55	-0.14	104.51	0.27	0.30	4.49	0.16	0.34
Sample 17	170	0.1019	1.32	2.81	44.52	63.53	0.58	11.25	0.56	-0.14	114.28	0.29	0.29	4.49	0.15	0.32
Sample 18	180	0.1037	1.11	2.62	42.40	73.02	0.59	12.22	0.54	-0.15	150.79	0.26	0.30	4.16	0.15	0.30
Sample 19	190	0.1034	1.05	3.22	46.37	78.60	0.55	10.69	0.60	-0.14	114.69	0.26	0.29	3.95	0.15	0.28
Sample 20	200	0.117	1.29	3.24	52.60	77.40	0.52	9.17	0.39	-0.12	74.85	0.21	0.22	3.33	0.13	0.23
Sample 21	210	0.1029	0.89	1.71	42.18	76.48	0.46	9.27	0.39	-0.15	70.58	0.22	0.24	3.45	0.14	0.25
Sample 22	220	0.1097	1.24	3.03	63.54	60.28	0.42	9.30	0.40	-0.13	71.28	0.18	0.23	3.49	0.11	0.24
Sample 23	230	0.1016	1.04	8.23	84.11	59.54	0.45	9.54	0.40	-0.15	67.84	0.19	0.24	3.55	0.13	0.26
Sample 24	240	0.1064	0.91	3.39	64.12	69.28	0.61	9.82	0.42	-0.14	82.53	0.20	0.24	4.22	0.13	0.31
Sample 25	250	0.1045	1.01	2.14	58.71	79.53	0.63	10.13	0.52	-0.15	79.00	0.19	0.25	3.84	0.13	0.33
Sample 26	260	0.1032	0.95	2.11	65.24	95.95	0.66	10.92	0.52	-0.16	84.98	0.19	0.30	4.83	0.14	0.39
Sample 27	270	0.1018	1.16	2.75	71.86	64.45	0.73	11.31	0.53	-0.16	92.28	0.17	0.31	4.92	0.15	0.40
Sample 28	280	0.1287	0.96	2.41	72.12	67.55	0.57	11.93	0.42	-0.13	101.96	0.17	0.30	4.82	0.16	0.41
Sample 29	290	0.1242	1.03	2.52	85.10	82.09	0.61	12.13	0.47	-0.14	105.99	0.17	0.29	4.88	0.17	0.41
Sample 30	300	0.1047	1.09	3.23	89.69	107.05	0.70	12.04	0.51	-0.15	94.64	0.17	0.26	5.19	0.17	0.47
Sample 31	310	0.1204	1.03	3.17	96.18	107.46	0.64	11.99	0.43	-0.13	101.56	0.16	0.22	5.89	0.19	0.51
Sample 32	320	0.1173	1.07	2.98	92.38	67.13	0.71	12.35	0.41	-0.14	114.70	0.17	0.22	5.74	0.19	0.51
Sample 33	330	0.1295	1.30	3.49	116.38	84.68	0.74	13.91	0.36	-0.11	133.37	0.21	0.21	6.24	0.19	0.60
Sample 34	340	0.1036	1.25	2.89	110.64	94.98	0.73	14.19	0.44	-0.15	137.28	0.20	0.20	6.15	0.20	0.55
Sample 35	350	0.107	1.34	3.32	116.89	124.24	0.89	14.53	0.41	-0.14	145.03	0.22	0.19	5.53	0.19	0.55
Sample 36	360	0.1027	1.67	3.59	110.54	88.82	0.68	16.34	0.43	-0.14	193.13	0.22	0.21	6.90	0.23	0.63
Sample 37	370	0.1164	1.35	3.80	121.41	76.93	0.74	17.21	0.42	-0.12	205.34	0.22	0.21	7.02	0.26	0.67
Sample 38	380	0.1614	1.30	4.51	127.65	79.28	0.69	15.43	0.41	-0.09	170.34	0.16	0.16	6.46	0.21	0.63
Sample 39	390	0.1174	1.42	3.20	114.17	89.72	0.73	14.60	0.38	-0.14	148.64	0.17	0.19	8.05	0.26	0.66
Sample 40	400	0.1134	1.61	5.11	88.32	25.81	0.49	17.32	0.23	-0.12	135.92	0.09	0.16	8.80	0.27	0.56
Sample 41	410	0.1038	1.38	3.24	61.47	21.93	0.43	16.44	0.10	-0.14	103.98	0.05	0.15	6.67	0.23	0.34
Sample 42	420	0.168	1.12	2.26	35.21	19.79	0.20	8.86	0.13	-0.09	54.03	0.03	0.07	3.36	0.10	0.16
Sample 43	430	0.1062	1.45	1.49	24.75	14.52	0.17	6.84	0.13	-0.17	39.11	0.05	0.07	2.47	0.08	0.12
Sample 44	440	0.1257	1.16	1.61	21.64	15.66	0.16	6.14	0.14	-0.14	30.65	0.04	0.07	1.88	0.06	0.10
Sample 45	450	0.1049	0.85	3.83	42.55	86.97	0.71	7.11	0.42	-0.16	50.19	0.30	0.13	3.07	0.09	0.40
Sample 46	460	0.1054	0.79	3.16	44.17	96.43	0.71	6.75	0.48	-0.16	51.55	0.37	0.16	2.64	0.09	0.37
Sample 47	470	0.1045	1.30	2.80	46.32	72.38	0.69	9.34	0.51	-0.17	92.06	0.27	0.20	3.29	0.10	0.41
Sample 48	480	0.1019	0.83	3.07	47.68	87.52	0.69	8.46	0.41	-0.17	81.64	0.32	0.19	2.70	0.09	0.38
Sample 49	490	0.1179	0.72	1.89	33.95	92.09	0.71	8.25	0.77	-0.14	78.10	0.33	0.20	2.64	0.07	0.38
Sample 50	500	0.1223	0.67	2.12	29.41	92.19	0.79	9.56	0.98	-0.14	113.14	0.35	0.26	3.40	0.09	0.43
Sample 51	510	0.1048	0.80	1.54	26.15	92.46	0.67	6.79	0.88	-0.17	48.69	0.32	0.24	2.06	0.07	0.31
Sample 52	520	0.1029	0.69	1.83	28.95	62.88	0.66	6.99	0.87	-0.17	42.05	0.27	0.25	2.25	0.07	0.31
Sample 53	530	0.1053	0.66	1.63	24.72	73.84	0.71	7.86	0.79	-0.17	67.00	0.29	0.28	2.45	0.07	0.35
Sample 54	540	0.1129	0.61	1.85	24.12	89.11	0.69	7.77	0.89	-0.16	68.71	0.33	0.27	2.20	0.07	0.35
Sample 55	550	0.1038	0.78	1.95	25.35	51.00	0.72	8.55	0.78	-0.18	74.90	0.25	0.30	2.77	0.08	0.37
Sample 56	560	0.1013	0.66	1.67	22.42	74.69	0.55	7.14	0.64	-0.17	44.44	0.25	0.27	2.36	0.07	0.32
Sample 57	570	0.1017	0.66	2.09	25.26	80.41	0.71	7.92	0.78	-0.18	58.50	0.26	0.28	2.51	0.07	0.36
Sample 58	580	0.101	0.72	6.70	51.73	84.96	0.63	8.41	0.81	-0.18	61.13	0.26	0.29	2.62	0.08	0.36
Sample 59	590	0.108	0.71	2.84	30.16	82.03	0.59	8.04	0.75	-0.16	54.62	0.25	0.28	2.73	0.07	0.36
Sample 60	600	0.1117	0.67	2.09	26.41	77.27	0.63	8.48	0.98	-0.16	69.64	0.33	0.26	2.89	0.07	0.39
Sample 61	610	0.1134	0.66	2.24	24.41	73.64	0.63	6.95	0.82	-0.16	57.41	0.28	0.25	2.48	0.07	0.36
Sample 62	620	0.1049	0.67	2.02	28.21	74.45	0.61	8.98	0.80	-0.16	84.72	0.30	0.27	2.70	0.07	0.39
Sample 63	630	0.108	0.63	1.89	24.28	62.99	0.59	8.67	0.79	-0.17	92.90	0.26	0.25	2.92	0.09	0.38
Sample 64	640	0.1043	0.68	2.59	24.12	84.20	0.72	8.66	0.85	-0.16	90.18	0.33	0.37	2.56	0.07	0.41
Sample 65	650	0.1009	0.65	2.09	25.43	106.67	0.64	8.94	0.74	-0.18	92.35	0.27	0.22	2.40	0.07	0.31
Sample 66	660	0.1033	0.66	1.90	24.56	126.20	0.58	8.63	0.63	-0.17	88.91	0.26	0.19	2.66	0.08	0.33
Sample 67	670	0.1017	0.69	2.11	22.80	89.98	0.66	8.48	0.84	-0.18	81.15	0.33	0.25	2.20	0.07	0.35
Sample 68	680	0.1071	0.62	6.61	22.15	82.40	0.65	7.06	0.77	-0.17	55.41	0.27	0.18	2.07	0.07	0.30
Sample 69	690	0.1007	0.60	1.79	25.06	69.89	0.49	7.74	0.74	-0.18	66.69	0.25	0.16	2.14	0.07	0.29
Sample 70	700	0.1068	0.74	1.83	26.79	131.27	0.54	8.12	0.72	-0.17	76.79	0.29	0.13	2.41	0.07	0.30
Sample 71	710	0.1088	0.57	1.28	26.26	86.21	0.51	7.11	0.64	-0.17	44.90	0.25	0.11	2.00	0.06	0.25
Sample 72	720	0.1024	0.70	2.84	30.31	91.24	0.86	8.88	0.80	-0.17	88.21	0.31	0.38	2.46	0.08	0.38
Sample 73	730	0.1197	0.62	1.61	29.81	99.61	0.62	8.41	0.52	-0.15	87.75	0.28	0.17	2.24	0.06	0.33
Sample 74	740	0.1141	0.64	2.04	32.90	123.62	0.56	7.28	0.56	-0.16	55.96	0.26	0.29	1.85	0.05	0.31
Sample 75	750	0.1035	0.63	2.01	30.36	123.44	0.58	7.94	0.72	-0.19	90.28	0.28	0.16	2.31	0.06	0.34
Sample 76	760	0.105	0.59	2.29	34.38	99.73	0.64	6.13	0.68	-0.17	47.82	0.28	0.38	1.98	0.06	0.36
Sample 77	770	0.1127	0.63	2.88	46.65	110.16	0.53	7.11	0.69	-0.17	56.53	0.23	0.23	1.99	0.06	0.30
Sample 78	780	0.1055	0.61	2.32	39.13	82.64	0.66	6.67	0.63	-0.18	56.44	0.22	0.26	2.19	0.06	0.34
Sample 79	790	0.115	0.65	2.23	48.29	138.19	0.67	8.90	0.78	-0.17	101.50	0.22	0.13	2.45	0.07	0.30
Sample 80	800	0.1017	0.75	2.03	50.58	92.08	0.64	8.32	0.75	-0.19	78.02	0.27	0.17	2.40	0.07	0.34
Sample 81	810	0.101	0.72	1.94	50.64	70.00	0.56	7.60	0.79	-0.18	68.03	0.24	0.17	2.37	0.06	0.32
Sample 82	820	0.1068	0.52	1.46	66.17	74.98	0.52	7.07	0.50	-0.19	37.60	0.17	0.11	1.73	0.04	0.25
Sample 83	830	0.1176	0.66	2.03	69.26	64.56	0.59	8.05	0.65	-0.16	62.16	0.21	0.18	2.23	0.06	0.33
Sample 84	840	0.1084	0.59	2.00	76.96	77.78	0.56	8.62	0.74	-0.18	73.44	0.16	0.18	2.34	0.06	0.33
Sample 85	850	0.1031	0.64	2.02	103.50	72.42	0.58	8.10	0.58	-0.19	48.45	0.14	0.15	1.83	0.05	0.30
Sample 86	860	0.1115	0.55	1.91	77.17	74.80	0.62	7.70	0.69	-0.18	69.67	0.17	0.19	2.42	0.06	0.32
Sample 87	870	0.1048	0.69	2.83	100.76	72.05	0.56	8.50	0.79	-0.19	64.43	0.21	0.26	2.13	0.06	0.36
Sample 88	880	0.1061	0.73	4.13	137.02	82.72	0.66	9.69	0.73	-0.17	73.46	0.19	0.19	2.33	0.06	0.33
Sample 89	890	0.1042	0.68	3.30	116.99	84.70	0.61	10.00	0.68	-0.19	85.17	0.18	0.23	2.64	0.07	0.38
Sample 90	900	0.1096	0.73	3.13	105.34	79.26	0.68	8.21	0.79	-0.17	59.11	0.20	0.59	2.17	0.06	0.37
Sample 91	910	0.1201	0.53	2.63	75.34	62.44	0.57	7.18	0.81	-0.13	57.77	0.19	0.40	2.04	0.06	0.34
Sample 92	920	0.103	1.38	2.30	100.93	91.96	0.54	8.75	0.72	-0.19	57.38	0.14	0.33	1.88	0.06	0.29
Sample 93	930	0.1025	0.95	2.13	82.09	93.37	0.58	8.32	0.68	-0.19	52.72	0.18	0.22	1.95	0.05	0.29
Sample 94	940	0.1219	0.55	1.93	54.17	93.90	0.62	7.30	0.68	-0.13	58.50	0.18	0.30	2.13	0.06	0.34
Sample 95	950	0.1263	0.74	2.46	52.34	76.94	0.59	7.98	0.80	-0.14	71.18	0.14	0.39	2.48	0.06	0.36
Sample 96	960	0.1293	0.57	2.22	40.98	91.99	0.57	8.79	0.64	-0.13	78.47	0.17	0.31	2.17	0.06	0.33
Sample 097	970	0.1195	0.56	2.81	39.26	77.18	0.67	10.16	0.56	-0.15	99.43	0.16	0.26	2.32	0.05	0.35
Sample 098	980	0.1082	0.65	2.41	36.44	74.44	0.65	10.27	0.60	-0.17	100.76	0.15	0.25	2.43	0.06	0.39
Sample 099	990	0.1127	0.62	2.24	30.62	73.79	0.76	12.51	0.81	-0.17	149.56	0.19	0.25	2.63	0.07	0.42
Sample 100	1000	0.1106	0.58	2.23	29.73	68.68	0.72	8.82	0.74	-0.17	86.79	0.15	0.21	2.24	0.06	0.33
Sample 101	1010	0.11	0.63	2.03	43.15	71.52	0.59	8.31	0.72	-0.18	44.60	0.14	0.17	1.73	0.04	0.27
Sample 102	1020	0.1113	0.61	2.18	43.14	58.11	0.57	8.12	0.73	-0.17	37.58	0.14	0.16	1.68	0.05	0.28
Sample 103	1030	0.108	0.61	2.93	56.74	60.23	0.50	7.93	0.68	-0.18	37.90	0.11	0.17	1.56	0.04	0.24
Sample 104	1040	0.1112	0.74	3.06	51.52	103.28	0.79	10.16	0.58	-0.18	46.84	0.14	0.31	1.90	0.05	0.31
Sample 105	1050	0.1107	0.65	2.54	37.42	58.93	0.57	9.08	0.57	-0.17	51.66	0.15	0.23	1.94	0.08	0.32
Sample 106	1060	0.1189	0.53	1.93	24.11	54.26	0.52	7.84	0.72	-0.15	51.18	0.16	0.26	2.11	0.05	0.30
Sample 107	1070	0.1179	0.59	2.33	26.42	69.30	0.59	8.88	0.76	-0.15	63.03	0.13	0.30	2.13	0.05	0.33
Sample 108	1080	0.1485	0.74	3.01	35.83	66.07	0.77	11.95	0.66	-0.07	95.28	0.14	0.53	3.02	0.08	0.42
Sample 109	1090	0.1234	0.48	1.79	17.98	54.94	0.65	6.70	0.73	-0.16	48.06	0.13	0.18	1.76	0.04	0.27
Sample 110	1100	0.1145	0.82	2.55	20.37	43.75	0.60	7.41	0.70	-0.16	55.41	0.15	0.35	2.03	0.05	0.36
Sample 111	1110	0.1058	0.50	1.71	19.46	46.85	0.54	6.71	0.65	-0.19	46.65	0.14	0.16	1.83	0.04	0.30
Sample 112	1120	0.1116	0.54	2.40	28.45	47.56	0.45	7.93	0.49	-0.17	50.33	0.12	0.25	1.77	0.04	0.27
Sample 113	1130	0.1074	0.68	2.17	36.37	48.57	0.59	9.21	0.52	-0.16	42.90	0.15	0.51	1.91	0.04	0.29
Sample 114	1140	0.1025	0.66	2.03	39.26	108.95	0.66	9.57	0.55	-0.17	42.43	0.14	0.36	1.74	0.04	0.26
Sample 115	1150	0.1091	0.65	2.63	33.43	87.30	0.75	9.14	0.98	-0.17	60.35	0.16	0.54	2.01	0.05	0.33
Sample 116	1160	0.1206	0.56	1.89	27.58	60.34	0.58	7.73	0.79	-0.15	60.06	0.17	0.31	2.08	0.05	0.32
Sample 117	1170	0.1012	0.72	2.31	39.27	55.53	0.62	8.54	0.77	-0.17	66.26	0.15	0.32	2.30	0.06	0.33
Sample 118	1180	0.1041	0.69	4.26	61.79	73.81	0.66	9.92	0.71	-0.17	49.36	0.15	0.33	1.85	0.05	0.38
Sample 119	1190	0.1068	0.74	1.55	54.38	93.54	0.61	8.71	0.57	-0.17	43.48	0.16	0.23	2.08	0.05	0.23
Sample 120	1200	0.1048	0.83	1.66	56.83	86.16	0.56	7.89	0.45	-0.17	42.32	0.13	0.21	1.92	0.04	0.23
Sample 121	1210	0.1204	6.08	2.46	64.63	52.15	0.64	6.76	0.43	-0.10	49.61	0.14	0.44	2.27	0.06	0.21
Sample 122	1220	0.1013	4.06	1.75	62.34	55.39	0.59	6.96	0.37	-0.12	51.67	0.13	0.44	2.31	0.05	0.27
Sample 123	1230	0.107	0.69	2.33	58.70	67.10	0.57	7.33	0.41	-0.13	54.84	0.14	0.54	1.92	0.06	0.30
Sample 124	1240	0.1022	0.88	2.27	58.48	87.54	0.64	7.27	0.48	-0.13	53.26	0.16	0.51	1.76	0.05	0.26
Sample 125	1250	0.1056	0.65	2.56	52.72	104.13	0.70	8.38	0.43	-0.13	77.24	0.19	0.48	2.30	0.07	0.29
Sample 126	1260	0.1005	0.78	2.48	68.06	84.02	0.71	9.60	0.42	-0.08	75.45	0.20	0.44	1.96	0.07	0.23
Sample 127	1270	0.112	1.17	2.72	58.49	60.49	0.64	8.99	0.42	-0.11	74.76	0.14	0.39	2.20	0.07	0.26
Sample 128	1280	0.1057	1.63	4.08	69.10	52.82	0.63	9.16	0.52	-0.10	67.47	0.14	0.49	1.96	0.06	0.29
Sample 129	1290	0.101	1.47	1.82	37.84	73.82	0.59	7.55	0.47	-0.15	66.44	0.12	0.48	1.89	0.06	0.27
Sample 130	1300	0.1018	0.67	2.28	47.20	94.88	0.58	7.49	0.53	-0.12	52.53	0.10	0.59	1.86	0.05	0.27
Sample 131	1310	0.1025	0.60	1.80	33.92	71.47	0.60	7.06	0.44	-0.14	59.05	0.15	0.55	1.70	0.05	0.30
Sample 132	1320	0.1109	4.35	5.19	37.52	55.24	0.61	9.31	0.47	-0.11	99.85	0.21	0.45	2.16	0.06	0.32
Sample 133	1330	0.1001	0.81	3.28	38.43	62.14	0.74	12.07	0.49	-0.13	139.84	0.15	0.49	2.82	0.08	0.40
Sample 134	1340	0.1023	0.64	3.03	32.24	52.93	0.73	7.87	0.54	-0.11	69.84	0.12	0.37	1.87	0.06	0.26
Sample 135	1350	0.1037	0.87	4.11	44.43	60.88	0.77	8.80	0.55	-0.13	63.26	0.11	0.38	2.07	0.08	0.29
Sample 136	1360	0.1017	1.03	3.18	43.15	57.90	0.62	8.01	0.52	-0.12	52.16	0.12	0.54	1.61	0.06	0.30
Sample 137	1370	0.1081	0.71	2.97	46.02	61.78	0.68	8.55	0.44	-0.10	59.54	0.14	0.94	1.91	0.06	0.34
Sample 138	1380	0.104	1.36	2.33	42.75	46.53	0.58	7.99	0.48	-0.14	59.86	0.16	0.55	1.84	0.06	0.30
Sample 139	1390	0.1022	0.65	2.54	34.55	51.84	0.56	8.10	0.49	-0.14	66.66	0.14	0.48	1.99	0.07	0.32
Sample 140	1400	0.107	1.12	2.23	35.91	44.76	0.57	7.70	0.57	-0.13	59.69	0.14	0.44	1.80	0.06	0.30
Sample 141	1410	0.104	0.60	2.32	34.88	46.32	0.58	7.68	0.61	-0.10	54.33	0.09	0.50	1.77	0.06	0.30
Sample 142	1420	0.1024	1.25	2.97	40.64	77.64	0.69	8.17	0.65	-0.11	57.17	0.13	0.59	1.84	0.06	0.35
Sample 143	1430	0.1024	1.69	2.14	41.81	57.11	0.66	7.88	0.75	-0.12	49.81	0.12	0.43	1.43	0.05	0.26
Sample 144	1440	0.1026	0.69	2.93	42.83	59.55	0.60	8.96	0.68	-0.13	75.25	0.16	0.51	2.05	0.06	0.33
Sample 145	1450	0.1032	0.65	3.04	35.25	55.25	0.62	10.08	0.59	-0.12	106.97	0.12	0.56	2.31	0.07	0.38
Sample 146	1460	0.1041	2.67	4.28	42.62	59.41	0.73	18.20	0.58	-0.12	268.11	0.12	0.63	3.40	0.09	0.46
Sample 147	1470	0.1006	0.63	3.80	34.23	60.13	0.77	9.59	0.59	-0.13	104.31	0.13	0.71	2.48	0.07	0.42
Sample 148	1480	0.1027	1.45	2.35	39.94	60.87	0.66	9.09	0.55	-0.11	64.26	0.14	0.67	1.76	0.06	0.29
Sample 149	1490	0.1087	0.65	2.78	38.45	58.21	0.65	9.32	0.66	-0.12	75.09	0.16	0.56	1.80	0.06	0.32
Sample 150	1500	0.1014	0.61	2.43	36.86	55.31	0.65	8.09	0.56	-0.12	62.22	0.12	0.55	1.67	0.06	0.29

	Depth (mm)	Sed. (ICPMS)	Li 7	B 10	Na 23	Mg 24	Al 27	Si 28	P 31	S 34	K 39	Ca 43	Cr 52	Fe 54	Mn 55	Co 59
Sample 151	1510	0.1112	2.81	21.25	441.14	386.68	3948.52	9.07	376.60	4230.09	215.26	563.22	1.24	4133.02	318.56	0.67
Sample 152	1520	0.101	2.53	24.59	372.95	341.23	3720.91	11.55	382.48	4407.17	205.33	535.71	1.31	4508.22	299.61	0.61
Sample 153	1530	0.1078	3.52	22.31	502.44	462.92	4407.03	13.35	367.57	6768.80	239.39	674.96	1.33	6466.56	391.92	0.83
Sample 154	1540	0.1048	2.25	17.61	278.66	264.46	3732.41	9.53	365.81	3699.02	176.47	422.39	2.68	4423.55	224.47	0.57
Sample 155	1550	0.109	2.09	23.17	301.97	259.76	4031.90	10.91	386.65	3481.55	199.49	445.38	1.21	3583.01	230.48	0.53
Sample 156	1560	0.1012	3.00	21.89	428.62	387.24	4128.23	10.97	381.28	4059.21	225.03	586.05	1.18	3301.65	341.80	0.66
Sample 157	1570	0.1069	2.55	14.29	330.53	334.99	4117.50	8.74	390.94	3896.07	207.55	535.44	1.27	3683.09	298.26	0.74
Sample 158	1580	0.1061	2.34	14.83	281.76	301.20	5026.43	7.33	462.50	3290.30	196.76	463.26	2.53	4020.20	232.01	0.53
Sample 159	1590	0.1106	2.58	10.26	325.09	318.72	5373.02	8.19	502.80	3766.75	222.22	505.19	1.56	3669.70	256.57	0.61
Sample 160	1600	0.1046	2.75	13.09	405.72	373.53	4015.85	8.49	361.24	3767.54	228.22	578.89	1.10	3755.08	321.68	0.62
Sample 161	1610	0.1034	2.84	15.85	426.86	377.10	3874.95	12.67	326.81	3751.76	236.21	590.85	1.01	3598.33	317.15	0.64
Sample 162	1620	0.1058	1.95	16.73	275.77	263.51	4120.19	11.27	358.77	3419.80	197.38	433.23	1.28	4313.23	223.74	0.53
Sample 163	1630	0.1042	2.07	13.60	299.25	279.63	3947.27	10.27	342.56	2710.56	206.42	478.32	1.16	3794.69	239.98	0.51
Sample 164	1640	0.1106	2.34	20.95	365.10	347.52	4322.86	11.57	336.81	3245.89	223.79	546.40	1.37	3771.39	282.26	0.55
Sample 165	1650	0.1013	2.40	20.54	363.30	346.46	3903.98	14.64	316.99	3237.37	222.76	543.48	1.07	3437.72	295.11	0.58
Sample 166	1660	0.1043	2.66	20.80	413.17	384.30	4190.34	8.86	348.67	3802.80	236.48	595.98	1.07	3308.03	314.29	0.64
Sample 167	1670	0.1079	2.65	18.54	386.06	384.70	4446.66	10.03	364.09	3693.33	244.10	579.50	2.30	4070.99	308.15	0.65
Sample 168	1680	0.106	3.11	15.82	489.32	449.83	4013.59	9.69	295.84	4540.95	242.56	647.67	1.06	3690.51	358.03	0.73
Sample 169	1690	0.1106	1.83	9.00	249.68	241.17	3501.43	5.98	275.99	2467.60	180.00	409.29	1.01	3147.10	204.28	0.47
Sample 170	1700	0.117	1.69	9.13	231.98	224.77	3816.29	6.11	286.20	2828.53	185.82	377.52	1.30	4791.94	187.99	0.46
Sample 171	1710	0.1034	2.04	11.69	288.30	265.00	4053.97	7.57	279.70	4814.47	196.73	466.87	1.21	5565.21	220.91	0.64
Sample 172	1720	0.1041	1.56	9.14	219.46	207.38	3968.78	5.90	286.17	3138.26	172.76	336.88	1.29	3674.41	171.05	0.52
Sample 173	1730	0.1107	2.11	14.38	277.79	281.00	3699.01	8.13	282.98	3614.20	186.98	418.10	1.24	3970.71	213.82	0.61
Sample 174	1740	0.1027	1.61	14.62	264.39	237.75	3452.07	10.37	258.48	4514.66	177.88	411.52	1.17	5346.38	198.08	0.58
Sample 175	1750	0.1068	1.59	10.57	252.14	235.54	3535.96	7.17	235.62	5117.88	165.17	399.07	1.36	5293.99	186.76	0.61
Sample 176	1760	0.1041	2.19	14.31	337.76	302.87	3631.10	7.87	287.99	4011.87	196.93	455.68	1.32	3785.94	251.07	0.58
Sample 177	1770	0.1016	2.67	13.14	363.51	343.82	4033.49	8.19	330.71	3590.30	215.70	527.36	1.43	3593.61	273.78	0.62
Sample 178	1780	0.1081	2.87	13.63	421.42	371.27	3737.12	6.62	275.53	4000.00	226.25	568.14	1.38	3108.51	303.04	0.63
Sample 179	1790	0.1029	2.45	12.48	366.75	313.88	4073.57	9.14	334.68	3115.33	210.91	486.28	1.55	3370.71	264.08	0.59
Sample 180	1800	0.1083	2.84	15.06	476.65	378.11	3973.50	7.54	344.59	3738.04	233.93	613.09	1.34	3314.77	318.61	0.72
Sample 181	1810	0.1013	2.26	13.15	364.34	309.77	3881.94	9.04	305.14	3267.35	213.16	465.91	1.26	3254.31	258.60	0.62
Sample 182	1820	0.1035	2.74	19.56	466.04	368.82	3719.76	7.56	329.54	3550.32	231.95	596.76	1.25	3420.84	309.53	0.69
Sample 183	1830	0.1049	2.39	20.73	419.22	317.81	3649.92	6.16	321.24	3210.53	218.21	530.85	1.21	2972.61	281.11	0.67
Sample 184	1840	0.1052	2.82	16.77	500.10	391.53	3827.38	7.91	336.91	3995.55	237.44	616.95	1.30	3194.56	327.59	0.73
Sample 185	1850	0.1043	2.20	12.09	350.43	295.41	3819.25	10.97	282.53	4227.66	214.52	484.72	1.40	3882.51	259.58	0.70
Sample 186	1860	0.1096	1.93	13.56	312.51	257.65	3513.87	8.61	271.96	4404.40	189.91	447.37	1.25	3974.48	208.27	0.60
Sample 187	1870	0.1001	2.40	14.78	408.70	316.53	3276.47	6.72	282.21	3886.88	215.37	536.52	1.11	3647.76	268.78	0.68
Sample 188	1880	0.1044	2.48	16.57	425.11	328.67	3485.42	8.63	306.59	3954.47	225.81	544.23	1.26	4012.50	277.47	0.64
Sample 189	1890	0.105	2.89	15.28	474.93	369.28	3903.66	10.42	315.81	3773.35	247.89	552.53	1.38	3145.20	394.67	1.05
Sample 190	1900	0.1058	2.07	16.15	358.62	284.05	3448.11	10.37	273.51	2940.89	200.67	459.44	1.38	3441.47	230.61	0.55
Sample 191	1910	0.1071	2.43	15.33	410.56	307.79	3466.86	9.52	250.35	3638.64	218.63	484.62	1.28	2881.51	244.35	0.57
Sample 192	1920	0.1038	2.42	15.88	441.33	339.66	3823.96	12.74	278.19	3710.67	230.06	573.13	11.85	2809.65	263.31	0.64
Sample 193	1930	0.1061	2.87	17.96	473.73	358.52	3666.95	8.11	288.45	4415.47	245.44	630.29	1.41	3847.54	340.59	0.89
Sample 194	1940	0.1016	2.33	15.19	395.43	316.14	3563.48	5.41	296.02	3767.57	217.92	500.22	1.46	3495.93	305.63	0.81
Sample 195	1950	0.1013	2.32	19.80	392.73	324.68	3707.18	6.28	282.70	4046.07	228.04	562.95	1.53	4227.49	325.21	0.91
Sample 196	1960	0.1094	2.03	17.01	356.23	280.13	3412.61	4.77	275.53	3132.51	204.57	453.46	1.43	3112.29	211.97	0.54
Sample 197	1970	0.1028	2.34	14.88	437.83	303.99	3541.44	8.05	297.99	3252.64	209.75	539.96	1.44	2588.59	247.03	0.72
Sample 198	1980	0.101	2.22	17.07	388.82	286.85	3992.02	6.56	376.27	3328.66	213.80	514.94	1.89	4217.72	456.79	1.66
Sample 199	1990	0.1031	2.41	23.44	449.81	331.90	4086.44	12.55	376.10	3917.43	231.18	517.51	2.22	5485.44	233.13	0.70
Sample 200	2000	0.1052	2.09	15.82	379.79	280.86	3731.57	6.08	317.21	3405.51	208.62	447.19	1.81	4532.47	232.06	0.80
Sample 201	2010	0.1025	2.25	29.70	460.81	313.21	2904.54	12.30	217.09	3435.11	195.92	509.02	1.01	1931.20	237.19	0.69
Sample 202	2020	0.1045	2.49	21.83	449.01	331.94	3721.81	6.86	333.63	4200.78	226.83	530.84	1.72	3886.91	231.97	0.71
Sample 203	2030	0.1052	2.49	13.93	457.20	368.81	4378.97	8.34	382.76	4154.89	234.65	549.97	2.27	3776.36	247.17	0.80
Sample 204	2040	0.1019	2.09	22.03	425.63	306.95	3656.82	8.38	326.33	4038.45	203.00	489.57	2.05	4631.80	205.25	0.63
Sample 205	2050	0.1032	2.03	17.13	364.46	282.60	3495.02	8.50	335.16	3537.86	205.79	472.18	1.70	4073.78	195.98	0.61
Sample 206	2060	0.1001	2.06	13.77	339.80	279.47	3785.58	8.82	339.46	3816.15	207.83	464.80	1.87	3924.74	184.76	0.60
Sample 207	2070	0.102	3.74	13.26	595.04	623.96	6812.38	10.54	741.16	5927.47	252.35	728.86	72.71	7674.78	425.78	2.07
Sample 208	2080	0.1064	3.45	27.91	565.46	522.64	6709.28	13.48	658.61	5421.62	249.65	687.30	59.09	6568.28	423.45	2.00
Sample 209	2090	0.1033	3.08	23.37	445.98	486.78	6347.96	10.30	729.98	3910.92	246.66	603.99	42.77	5137.48	335.20	1.57
Sample 210	2100	0.1016	2.76	15.91	410.84	484.37	5850.74	6.69	628.56	3586.83	229.41	545.43	4.67	4623.54	310.25	1.19
Sample 211	2110	0.1048	2.62	13.43	329.83	674.83	5181.25	176.54	665.02	3116.77	260.41	519.35	3.22	6264.35	255.97	1.11
Sample 212	2120	0.1022	2.59	20.13	454.94	336.97	4548.84	158.69	484.44	5507.24	243.09	547.71	2.62	5714.89	306.77	1.01
Sample 213	2130	0.1035	2.74	17.88	454.36	343.98	4832.04	188.25	442.55	5842.34	253.53	563.33	3.09	5182.53	308.54	1.03
Sample 214	2140	0.1053	1.82	13.42	301.13	239.82	3972.59	172.19	330.13	3857.64	213.60	420.56	3.63	4023.48	210.66	0.77
Sample 215	2150	0.1037	2.57	15.17	444.12	335.56	3927.40	168.48	312.63	4837.65	245.77	565.99	3.06	3911.41	298.47	0.97
Sample 216	2160	0.1029	2.01	12.74	325.19	257.53	3859.00	157.79	333.44	3971.71	222.31	458.25	2.89	4041.60	218.21	0.78
Sample 217	2170	0.1027	2.05	17.75	337.28	254.71	4183.71	170.96	395.06	3463.78	205.70	494.31	4.05	3300.36	220.00	0.86
Sample 218	2180	0.1044	1.74	8.11	329.18	291.75	4566.44	193.46	680.74	3057.91	204.68	599.95	5.00	5888.84	182.29	0.92
Sample 219	2190	0.1009	1.45	10.64	560.92	329.59	4227.41	214.16	605.45	2396.16	185.34	739.93	4.48	4932.94	159.25	0.89
Sample 220	2200	0.1037	1.86	17.49	1081.51	244.65	3582.30	158.56	290.09	3381.80	200.26	447.16	3.34	4793.03	219.46	0.71
Sample 221	2210	0.104	1.91	14.14	302.40	239.42	3465.40	145.61	257.41	3895.93	182.11	434.19	2.60	4207.83	209.28	0.71
Sample 222	2220	0.102	2.07	9.10	343.56	254.36	3435.42	139.91	239.22	4644.84	198.81	459.78	2.44	4132.40	233.27	0.75
Sample 223	2230	0.1039	2.06	14.05	324.94	240.00	3383.85	152.49	274.64	4750.22	204.59	422.99	3.12	5400.17	217.79	0.76
Sample 224	2240	0.1008	1.72	8.82	291.34	216.06	3405.92	151.28	218.71	5646.27	190.68	388.83	3.34	5475.87	184.19	0.81
Sample 225	2250	0.1062	2.01	10.57	324.94	254.95	3553.72	162.07	242.14	7742.23	207.82	458.88	3.27	7995.87	233.78	0.91
Sample 226	2260	0.1051	1.70	13.31	290.17	221.00	3418.42	152.20	235.99	4730.86	190.77	374.23	3.13	5560.12	188.07	0.72
Sample 227	2270	0.1005	2.06	16.35	355.01	260.92	3453.67	171.06	260.73	5436.98	209.16	466.96	3.39	6165.45	247.34	0.86
Sample 228	2280	0.1052	1.77	10.55	329.18	244.09	3612.59	191.58	263.52	4384.56	198.78	402.33	3.64	4954.98	216.14	0.76
Sample 229	2290	0.1039	1.28	8.09	232.51	176.26	2910.46	140.04	186.07	3194.24	158.68	307.48	1.67	3684.29	150.13	0.54
Sample 230	2300	0.1066	2.12	12.86	350.72	255.25	3462.37	167.37	212.77	3829.81	203.73	459.00	1.76	3671.96	235.02	0.69
Sample 231	2310	0.1015	2.06	15.96	340.27	286.72	3505.18	165.27	231.63	4549.59	191.81	406.74	1.89	5314.25	208.42	0.60
Sample 232	2320	0.102	1.94	13.38	287.76	267.21	3825.84	162.97	226.73	5520.03	189.46	397.37	2.77	6012.11	190.01	0.71
Sample 233	2330	0.108	2.05	17.03	293.60	257.67	3776.03	167.25	255.41	4885.40	207.28	406.78	1.98	5457.04	181.76	0.63
Sample 234	2340	0.1018	1.74	20.56	281.39	237.16	3123.77	139.73	242.28	3825.66	167.02	343.75	1.77	4467.39	171.33	0.52
Sample 235	2350	0.105	2.35	14.79	374.08	328.12	3357.55	136.01	272.51	4573.91	189.74	463.10	1.40	5646.36	249.28	0.63
Sample 236	2360	0.1062	1.61	11.29	252.96	209.91	2491.25	85.53	183.19	3005.03	134.89	301.23	1.16	2804.70	151.94	0.41
Sample 237	2370	0.104	3.08	19.36	475.36	405.79	4097.85	149.48	299.02	5409.40	230.99	524.40	2.74	4601.10	283.80	0.75
Sample 238	2380	0.1017	2.31	30.69	399.31	329.70	3580.07	151.94	299.04	4667.15	201.81	486.86	1.72	4418.05	241.98	0.68
Sample 239	2390	0.1059	2.27	22.35	356.82	332.69	4751.40	166.71	308.77	3833.72	212.95	424.57	4.51	4488.06	209.22	0.58
Sample 240	2400	0.1023	2.09	14.36	339.27	291.22	3374.26	166.91	271.61	4015.61	199.44	475.37	2.89	4718.41	217.01	0.60
241	2410	0.1033	1.33	10.96	227.88	184.89	2222.50	167.52	238.01	3532.80	157.21	310.84	1.29	2874.67	125.51	0.39
242	2420	0.1037	1.57	16.69	285.85	211.82	2280.55	157.96	219.52	4221.42	155.18	350.97	1.20	2609.41	150.15	0.46
243	2430	0.1017	1.61	23.15	297.05	222.59	2335.91	163.84	244.34	4384.14	159.42	360.03	2.48	2925.76	161.09	0.51
244	2440	0.1033	1.46	11.26	256.91	203.67	2358.99	168.71	253.93	3962.46	154.85	333.48	1.56	2885.84	145.02	0.44
245	2450	0.109	1.52	25.14	292.28	229.37	2333.34	163.11	251.39	5213.16	154.63	381.20	1.48	3828.77	164.31	0.47
246	2460	0.1016	1.51	17.89	267.14	205.38	2226.31	145.84	233.78	5007.44	162.62	332.78	1.55	3690.74	143.28	0.43
247	2470	0.1012	1.89	26.56	360.01	262.00	2316.58	139.60	250.00	5327.06	164.69	427.75	1.34	3233.77	194.43	0.55
248	2480	0.1019	1.48	22.46	301.36	216.34	2096.41	147.11	249.31	4592.25	160.54	339.41	1.68	3628.90	156.89	0.49
249	2490	0.1066	1.51	16.45	252.65	194.45	2113.62	131.84	233.89	3770.64	157.62	304.55	1.54	2874.96	121.05	0.39
250	2500	0.1015	1.61	30.12	346.08	227.13	1982.48	165.99	229.92	4935.97	154.55	380.47	1.19	2532.85	172.49	0.49
251	2510	0.1042	1.55	18.68	314.77	225.65	2354.58	145.86	286.38	4932.26	166.34	357.50	1.45	3567.10	162.38	0.51
252	2520	0.1015	1.47	22.65	292.44	213.04	2082.53	135.44	260.37	4551.12	161.56	364.30	1.30	2310.89	157.18	0.46
253	2530	0.1033	1.68	24.77	322.64	229.36	2206.03	148.82	255.04	5079.05	169.62	375.08	2.53	3155.56	165.12	0.52
254	2540	0.1006	1.34	22.06	267.45	185.00	2005.97	142.39	215.32	5143.71	154.90	298.86	3.14	3243.77	131.31	0.49
256	2550	0.1088	1.53	26.43	299.57	213.30	2055.16	139.04	243.55	4869.95	154.99	359.80	1.39	2759.72	159.30	0.49
256	2560	0.1019	1.57	18.43	307.03	224.66	2191.31	153.08	257.37	4804.56	167.03	360.36	2.28	2461.61	164.31	0.50
257	2570	0.1019	1.58	21.12	314.19	213.63	2209.15	149.22	274.41	5216.86	169.04	340.26	1.63	3670.26	157.58	0.49
258	2580	0.1031	1.25	29.01	262.94	173.08	1955.80	138.22	235.94	5648.71	154.21	280.89	1.41	4810.46	121.81	0.43
259	2590	0.1014	2.46	17.57	462.04	309.15	2461.61	145.34	252.12	7653.27	204.82	497.66	1.83	4042.39	234.93	0.67
260	2600	0.1038	1.08	15.48	202.44	148.74	2058.64	135.48	191.44	4440.50	136.81	236.32	1.55	2526.17	97.51	0.38
261	2610	0.1033	1.91	24.56	370.86	245.88	2250.33	138.26	248.51	5435.74	172.24	404.05	1.80	3088.94	179.17	0.50
262	2620	0.1013	1.32	30.99	279.85	179.65	2095.70	126.55	244.00	4914.33	152.43	292.89	1.63	3661.21	130.41	0.42
263	2630	0.1035	1.25	16.56	247.16	172.26	2207.69	140.61	248.53	4180.42	155.50	276.39	1.78	2823.75	121.67	0.40
264	2640	0.1025	1.71	21.14	325.55	215.59	2193.57	142.13	264.61	5568.14	169.15	378.47	1.94	4126.97	167.63	0.49
265	2650	0.1011	1.78	16.82	294.64	221.65	2961.64	51.19	217.31	6137.43	164.25	337.27	2.26	3949.77	138.12	0.44
266	2660	0.1001	1.78	21.34	329.76	225.34	2362.56	43.30	256.91	6559.64	164.07	384.81	1.57	4290.83	156.84	0.48
267	2670	0.1054	1.95	16.96	346.71	231.66	2470.88	42.61	266.29	5561.25	177.43	404.69	1.52	3829.75	166.89	0.50
268	2680	0.1039	1.60	13.14	299.45	204.16	2544.76	48.46	254.77	4515.86	166.76	348.76	1.69	2818.47	145.14	0.45
269	2690	0.1005	2.41	22.01	451.66	278.44	2483.71	39.52	256.89	6917.47	181.89	497.88	1.19	4058.43	222.20	0.62
270	2700	0.101	1.75	15.98	302.96	202.75	2545.10	44.13	284.69	5245.93	167.40	348.08	1.11	3312.57	146.60	0.47
271	2710	0.1054	1.61	16.85	290.92	190.17	2344.75	43.31	249.12	4578.97	152.03	314.03	1.15	2819.75	136.48	0.44
272	2720	0.1072	1.94	18.07	327.09	222.10	2559.99	42.36	250.28	6657.11	175.58	392.03	1.06	4233.95	160.61	0.49
273	2730	0.1054	1.49	17.53	280.10	184.95	2340.92	39.55	254.04	5407.29	150.12	316.18	0.95	3675.44	137.26	0.44
274	2740	0.1067	1.65	19.34	294.00	194.04	2301.60	38.46	276.35	4176.27	150.35	332.40	0.80	3096.03	141.99	0.43
275	2750	0.1045	1.66	9.04	333.20	183.09	2318.05	41.14	226.25	4298.47	156.46	300.04	0.84	2315.93	130.77	0.43
276	2760	0.1016	1.46	13.63	268.21	175.04	2309.81	43.40	231.62	3990.80	153.59	316.68	1.34	2637.60	125.30	0.41
277	2770	0.1019	1.78	16.03	618.95	196.12	2520.73	48.79	261.00	4422.74	168.97	349.68	0.92	2763.64	141.50	0.47
278	2780	0.1126	1.83	14.50	320.75	202.54	2537.82	47.73	271.95	4501.25	170.61	370.18	1.11	3229.44	152.24	0.50
279	2790	0.1006	1.83	12.14	299.64	198.72	2613.61	49.14	295.66	4653.44	170.31	348.69	0.98	3753.32	144.78	0.45
280	2800	0.1021	1.57	18.48	271.57	175.83	2351.12	45.91	257.66	5308.20	152.08	320.65	0.87	3547.24	126.88	0.40
281	2810	0.1002	2.02	11.27	330.36	208.99	2530.88	46.49	256.15	5353.15	173.41	367.42	1.01	3309.49	153.81	0.48
282	2820	0.1057	1.47	21.44	243.72	162.49	2181.64	46.58	284.98	4256.72	140.57	274.07	0.87	3983.93	109.27	0.37
283	2830	0.1122	2.16	22.52	367.18	225.28	2507.55	42.63	273.56	6134.57	170.72	415.19	0.85	3704.93	178.76	0.51
284	2840	0.1005	1.98	24.11	346.05	208.97	2351.46	38.36	274.81	4741.28	165.13	371.97	0.87	3882.06	162.61	0.49
285	2850	0.1068	1.72	20.17	304.29	185.29	2333.85	36.96	272.74	4501.07	152.25	341.37	0.67	3615.50	144.60	0.47
286	2860	0.1043	1.72	20.42	300.59	186.70	2328.88	37.47	269.25	6365.21	155.43	322.24	0.79	5021.70	138.02	0.43
287	2870	0.1013	2.42	17.53	404.34	244.27	2489.18	41.24	300.54	5831.82	187.35	455.22	0.89	4513.83	191.96	0.59
288	2880	0.1129	1.60	16.14	275.78	179.99	2193.63	42.78	300.75	4746.27	150.01	323.56	0.87	6126.20	134.05	0.47
289	2890	0.116	1.75	19.16	309.74	183.64	2415.57	43.37	263.45	5782.85	164.76	355.95	0.77	4345.73	144.79	0.46
290	2900	0.1036	1.98	18.71	357.47	204.75	2350.78	43.66	262.88	5340.13	165.21	398.33	0.69	3129.19	173.56	0.51
292	2910	0.1018	1.75	21.45	313.17	185.92	2424.55	46.19	261.98	4486.84	165.32	374.21	0.92	2615.10	149.42	0.46
292	2920	0.1039	1.59	17.22	298.68	180.37	2426.22	43.04	252.21	4837.77	159.25	333.42	1.01	3290.20	141.73	0.41
293	2930	0.1037	1.61	17.35	270.23	172.31	2504.79	42.95	232.33	7033.32	162.36	319.97	0.88	4420.26	128.25	0.42
294	2940	0.101	1.86	18.15	301.42	188.08	2811.69	48.38	317.61	3999.17	170.80	342.54	1.06	3310.58	145.61	0.46
295	2950	0.1007	2.12	23.57	356.92	209.69	2613.62	43.89	287.00	4856.83	172.26	392.32	0.92	2691.53	170.35	0.49
296	2960	0.1054	1.85	22.75	313.68	184.18	2688.29	47.58	277.19	4499.23	169.26	347.54	0.95	2904.50	145.14	0.46
297	2970	0.101	1.92	12.37	320.21	192.79	2699.80	43.38	307.94	4371.29	170.94	374.95	0.83	3358.25	147.57	0.47
298	2980	0.1032	2.07	13.88	286.00	190.13	3203.22	50.78	363.33	4158.70	175.45	346.69	1.05	3194.39	138.32	0.46
299	2990

	Depth (mm)	Sed. (ICPMS)	Ni 60	Cu 63	Zn 66	As 75	Se 82	Sr 88	Ag 109	Cd 111	Ba 137	Hg 202	Tl 205	Pb 207	Bi 209	U 238
Sample 151	1510	0.1112	0.63	2.25	39.31	45.85	0.47	8.17	0.56	-0.11	53.22	0.11	0.43	1.61	0.05	0.27
Sample 152	1520	0.101	0.56	2.28	33.19	53.99	0.53	8.06	0.50	-0.12	55.36	0.11	0.48	1.61	0.06	0.27
Sample 153	1530	0.1078	0.72	2.95	41.73	52.87	0.65	9.91	0.68	-0.13	71.13	0.12	0.82	1.82	0.07	0.32
Sample 154	1540	0.1048	1.91	2.08	25.93	48.88	0.55	7.75	0.62	-0.13	63.12	0.12	0.56	1.88	0.06	0.29
Sample 155	1550	0.109	0.54	2.16	27.06	37.98	0.60	7.80	0.79	-0.14	63.15	0.11	0.53	1.64	0.05	0.31
Sample 156	1560	0.1012	2.45	2.04	41.32	36.91	0.61	9.08	0.61	-0.14	59.80	0.10	0.50	1.68	0.05	0.30
Sample 157	1570	0.1069	7.58	2.56	35.35	35.35	0.51	9.09	0.55	-0.14	70.95	0.10	0.51	2.02	0.06	0.31
Sample 158	1580	0.1061	0.59	7.43	59.93	37.65	0.63	9.07	0.57	-0.11	83.01	0.08	0.55	1.94	0.06	0.31
Sample 159	1590	0.1106	0.71	2.91	35.06	32.34	0.71	10.61	0.52	-0.11	105.57	0.13	0.58	2.46	0.08	0.38
Sample 160	1600	0.1046	0.73	2.05	38.41	32.68	0.51	9.27	0.61	-0.09	63.96	0.09	0.44	1.56	0.05	0.26
Sample 161	1610	0.1034	1.25	2.14	45.90	33.14	0.64	9.40	0.65	-0.15	62.64	0.10	0.46	1.57	0.05	0.29
Sample 162	1620	0.1058	0.55	2.08	31.71	38.08	0.66	8.56	0.55	-0.14	76.85	0.11	0.59	1.85	0.06	0.32
Sample 163	1630	0.1042	0.53	2.63	32.54	34.73	0.61	8.49	0.57	-0.15	67.65	0.10	0.45	1.59	0.05	0.26
Sample 164	1640	0.1106	0.50	1.93	39.81	30.77	0.57	9.45	0.56	-0.14	1433.38	0.09	0.48	1.80	0.06	0.30
Sample 165	1650	0.1013	0.60	1.53	36.63	33.61	0.49	9.27	0.66	-0.15	67.96	0.09	0.43	1.62	0.07	0.27
Sample 166	1660	0.1043	0.60	1.83	42.96	31.08	0.60	10.32	0.51	-0.13	78.53	0.08	0.49	1.85	0.06	0.30
Sample 167	1670	0.1079	1.96	1.96	43.74	35.42	0.69	10.80	0.55	-0.13	87.59	0.10	0.48	1.93	0.07	0.33
Sample 168	1680	0.106	0.66	2.20	48.81	30.19	0.53	9.25	0.60	-0.08	55.23	0.08	0.45	2.23	0.04	0.32
Sample 169	1690	0.1106	0.44	1.91	29.07	29.87	0.48	7.34	0.50	-0.15	57.18	0.09	0.31	1.38	0.04	0.24
Sample 170	1700	0.117	1.33	1.98	28.77	38.53	0.62	7.43	0.47	-0.14	63.70	0.08	0.29	1.50	0.05	0.24
Sample 171	1710	0.1034	0.58	2.34	31.52	39.27	0.63	8.62	0.59	-0.14	65.27	0.10	0.91	1.78	0.04	0.36
Sample 172	1720	0.1041	0.58	2.14	25.85	34.65	0.54	7.38	0.56	-0.14	68.89	0.10	0.39	1.78	0.05	0.34
Sample 173	1730	0.1107	0.56	1.58	27.35	34.42	0.46	7.47	0.52	-0.13	58.85	0.12	0.37	1.70	0.05	0.30
Sample 174	1740	0.1027	0.56	2.05	25.91	40.32	0.55	7.40	0.48	-0.12	55.47	0.11	0.63	1.59	0.05	0.30
Sample 175	1750	0.1068	0.54	2.70	29.18	35.05	0.59	7.31	0.51	-0.13	53.08	0.11	0.83	1.74	0.04	0.33
Sample 176	1760	0.1041	0.65	2.50	61.25	34.08	0.57	7.87	0.43	-0.14	58.12	0.08	0.42	1.63	0.04	0.31
Sample 177	1770	0.1016	0.66	2.50	35.10	33.07	0.57	9.70	0.51	-0.17	76.86	0.10	0.32	2.10	0.05	0.32
Sample 178	1780	0.1081	0.66	2.92	35.18	24.49	0.46	9.96	0.47	-0.15	72.02	0.08	0.37	1.87	0.05	0.37
Sample 179	1790	0.1029	0.81	1.64	26.14	29.41	0.58	8.53	0.55	-0.15	64.53	0.10	0.39	2.01	0.05	0.27
Sample 180	1800	0.1083	1.36	2.09	30.29	32.08	0.57	9.95	0.59	-0.10	66.52	0.11	0.43	2.02	0.05	0.30
Sample 181	1810	0.1013	0.67	2.46	22.83	29.70	0.49	8.37	0.72	-0.12	63.18	0.08	0.44	1.93	0.05	0.34
Sample 182	1820	0.1035	0.77	1.98	25.95	32.32	0.58	9.48	0.69	-0.10	59.80	0.09	0.47	1.69	0.04	0.27
Sample 183	1830	0.1049	0.75	1.84	22.14	29.10	0.55	8.66	0.73	-0.11	59.89	0.08	0.47	1.66	0.05	0.25
Sample 184	1840	0.1052	0.79	2.61	27.78	37.54	0.61	9.58	0.63	-0.11	54.08	0.07	0.53	1.54	0.05	0.27
Sample 185	1850	0.1043	0.84	3.15	21.63	32.40	0.64	8.87	0.67	-0.14	67.80	0.11	0.69	2.14	0.05	0.38
Sample 186	1860	0.1096	0.69	2.42	16.93	29.90	0.55	7.79	0.68	-0.13	54.51	0.10	0.77	1.87	0.05	0.32
Sample 187	1870	0.1001	0.79	1.88	18.85	31.02	0.61	8.46	0.72	-0.13	49.75	0.08	0.63	1.62	0.04	0.27
Sample 188	1880	0.1044	0.76	2.09	19.80	32.83	0.54	8.88	0.66	-0.13	55.30	0.08	0.55	2.01	0.04	0.28
Sample 189	1890	0.105	0.94	1.88	23.10	29.21	0.57	9.33	0.69	-0.14	64.24	0.10	0.56	2.54	0.05	0.28
Sample 190	1900	0.1058	0.67	1.57	20.31	29.94	0.58	8.10	0.58	-0.14	54.52	0.09	0.46	2.54	0.05	0.24
Sample 191	1910	0.1071	0.80	2.60	21.24	24.26	0.60	8.37	0.63	-0.11	52.28	0.09	0.49	2.38	0.05	0.27
Sample 192	1920	0.1038	32.14	2.30	24.07	25.02	0.53	8.85	0.55	-0.11	53.28	0.07	0.51	2.11	0.05	0.30
Sample 193	1930	0.1061	0.67	3.04	23.52	31.10	0.82	9.50	0.73	0.66	59.77	0.10	0.67	2.11	0.05	0.34
Sample 194	1940	0.1016	0.68	2.24	21.84	30.73	0.84	8.33	0.67	0.67	55.72	0.08	0.59	1.84	0.05	0.29
Sample 195	1950	0.1013	0.63	3.57	23.92	32.63	0.79	8.41	0.60	0.64	61.04	0.10	0.59	2.30	0.06	0.35
Sample 196	1960	0.1094	0.53	2.91	20.64	31.93	0.76	7.70	0.69	0.64	54.99	0.07	0.55	1.74	0.05	0.31
Sample 197	1970	0.1028	1.19	2.39	45.41	26.36	0.62	8.45	0.66	0.66	56.88	0.07	0.64	1.85	0.06	0.28
Sample 198	1980	0.101	1.28	3.02	45.43	39.29	0.88	8.83	0.72	0.72	71.10	0.12	0.71	3.00	0.07	0.31
Sample 199	1990	0.1031	1.58	2.96	50.42	58.81	0.98	8.90	0.69	0.69	69.62	0.07	0.72	2.25	0.09	0.32
Sample 200	2000	0.1052	1.33	2.44	46.04	42.21	0.83	8.10	0.68	0.71	64.74	0.08	0.69	2.20	0.08	0.27
Sample 201	2010	0.1025	1.30	2.28	59.29	30.13	0.44	7.21	0.51	0.10	36.64	0.06	0.55	1.49	0.05	0.18
Sample 202	2020	0.1045	1.48	3.42	66.19	38.65	0.74	8.86	0.73	0.03	69.84	0.07	0.67	2.22	0.08	0.28
Sample 203	2030	0.1052	1.84	3.89	71.83	42.81	0.78	9.29	0.73	0.10	78.33	0.09	0.75	3.30	0.10	0.31
Sample 204	2040	0.1019	1.54	5.19	72.23	50.57	0.79	7.83	0.65	0.06	55.54	0.06	0.69	2.08	0.09	0.25
Sample 205	2050	0.1032	1.39	2.83	66.43	44.32	0.75	8.09	0.64	0.08	61.93	0.06	0.63	1.90	0.08	0.22
Sample 206	2060	0.1001	1.35	4.45	65.20	41.08	0.77	8.22	0.63	0.02	69.55	0.06	0.67	2.36	0.09	0.30
Sample 207	2070	0.102	38.94	12.43	77.68	91.79	0.81	9.39	0.71	0.06	104.48	0.25	0.42	8.24	0.16	0.44
Sample 208	2080	0.1064	29.14	11.36	74.91	75.17	0.92	8.88	0.78	0.07	92.12	0.28	0.41	6.74	0.18	0.44
Sample 209	2090	0.1033	20.44	7.37	55.73	64.68	0.77	8.55	0.74	0.05	106.70	0.28	0.44	6.56	0.17	0.38
Sample 210	2100	0.1016	2.62	8.53	61.96	65.50	0.76	8.78	0.73	0.01	95.93	0.25	0.45	5.08	0.17	0.33
Sample 211	2110	0.1048	2.11	2.79	36.61	79.60	0.81	8.85	0.47	0.04	83.97	0.21	0.30	3.40	0.06	0.28
Sample 212	2120	0.1022	2.26	4.91	45.41	62.88	0.76	8.03	0.44	0.11	56.40	0.13	0.35	2.25	0.04	0.38
Sample 213	2130	0.1035	2.51	4.41	50.18	55.42	0.66	8.62	0.44	0.05	66.45	0.16	0.42	2.19	0.04	0.38
Sample 214	2140	0.1053	2.40	2.80	34.23	36.88	0.67	7.19	0.44	0.04	65.77	0.11	0.42	1.68	0.04	0.27
Sample 215	2150	0.1037	2.61	4.57	45.39	35.45	0.61	7.76	0.37	0.04	58.51	0.12	0.39	1.56	0.04	0.30
Sample 216	2160	0.1029	1.86	5.32	39.28	41.82	0.72	7.35	0.32	0.02	64.02	0.07	0.38	1.58	0.08	0.27
Sample 217	2170	0.1027	2.34	7.60	39.37	35.29	0.84	8.76	0.27	0.04	80.22	0.09	0.37	1.76	0.13	0.29
Sample 218	2180	0.1044	2.25	6.87	36.02	43.60	1.28	14.95	0.29	0.04	177.67	0.08	0.35	2.07	0.27	0.19
Sample 219	2190	0.1009	2.42	3.87	38.32	36.29	1.19	17.13	0.26	0.02	195.41	0.07	0.27	2.00	0.28	0.14
Sample 220	2200	0.1037	2.06	2.48	54.30	40.10	1.07	7.51	0.28	0.01	65.10	0.15	0.28	1.49	0.04	0.21
Sample 221	2210	0.104	1.92	4.27	56.03	39.48	0.80	6.91	0.27	0.00	54.72	0.11	0.27	1.56	0.03	0.28
Sample 222	2220	0.102	2.00	4.12	64.36	39.35	0.65	7.45	0.29	0.22	58.21	0.09	0.32	1.54	0.03	0.33
Sample 223	2230	0.1039	2.02	2.47	65.61	48.36	0.69	7.17	0.36	0.05	59.98	0.10	0.44	1.60	0.12	0.28
Sample 224	2240	0.1008	2.03	2.59	62.33	42.99	0.80	6.52	0.31	0.04	56.44	0.10	0.61	1.90	0.03	0.38
Sample 225	2250	0.1062	2.39	3.78	79.78	55.86	0.70	7.51	0.31	0.06	60.06	0.11	0.74	1.93	0.04	0.38
Sample 226	2260	0.1051	2.14	3.41	69.73	46.85	0.67	6.81	0.28	0.05	59.51	0.09	0.44	1.83	0.03	0.30
Sample 227	2270	0.1005	2.71	3.46	78.83	52.69	0.69	7.58	0.35	0.07	56.08	0.13	0.40	1.73	0.03	0.29
Sample 228	2280	0.1052	2.68	3.57	72.22	48.67	0.68	7.52	0.32	0.07	61.85	0.13	0.35	1.91	0.04	0.29
Sample 229	2290	0.1039	2.06	3.30	49.15	32.54	0.55	5.60	0.26	-0.02	48.90	0.08	0.26	1.56	0.02	0.31
Sample 230	2300	0.1066	1.96	2.01	71.32	35.17	0.56	7.54	0.28	0.00	55.19	0.08	0.27	1.89	0.03	0.24
Sample 231	2310	0.1015	0.62	3.09	33.61	45.46	0.61	7.09	0.31	0.06	55.78	0.08	0.35	1.66	0.03	0.24
Sample 232	2320	0.102	0.70	5.36	46.42	46.50	0.64	6.93	0.31	0.05	55.06	0.11	0.51	1.96	0.04	0.43
Sample 233	2330	0.108	0.68	2.75	23.57	46.30	0.68	7.40	0.31	0.06	68.25	0.11	0.46	2.28	0.05	0.37
Sample 234	2340	0.1018	0.80	1.92	21.65	45.56	0.66	6.59	0.22	0.04	60.01	0.10	0.41	1.90	0.02	0.25
Sample 235	2350	0.105	0.55	1.43	30.84	43.19	0.54	7.76	0.24	0.06	53.11	0.11	0.36	1.60	0.02	0.20
Sample 236	2360	0.1062	0.55	1.25	20.31	24.30	0.40	5.55	0.22	-0.02	46.39	0.06	0.31	1.29	0.00	0.22
Sample 237	2370	0.104	1.00	6.90	62.82	41.83	0.72	8.96	0.29	0.07	69.58	0.10	0.46	2.05	0.03	0.32
Sample 238	2380	0.1017	0.91	2.08	37.30	47.90	0.58	8.24	0.27	0.04	60.40	0.11	0.43	1.76	0.03	0.30
Sample 239	2390	0.1059	1.04	14.98	87.44	46.17	0.67	8.05	0.28	0.04	71.34	0.10	0.44	2.27	0.04	0.26
Sample 240	2400	0.1023	1.32	1.70	35.28	44.95	0.62	7.88	0.34	0.05	59.89	0.10	0.42	1.95	0.03	0.26
241	2410	0.1033	0.36	1.36	22.84	33.40	0.46	5.14	0.28	-0.01	47.43	0.13	0.33	1.44	0.06	0.25
242	2420	0.1037	1.64	1.21	27.35	29.57	0.50	5.73	0.25	0.02	43.55	0.09	0.37	1.47	0.05	0.21
243	2430	0.1017	1.04	1.52	28.02	36.09	0.47	5.86	0.51	0.07	42.31	0.09	0.36	1.54	0.06	0.20
244	2440	0.1033	0.55	1.04	20.83	33.28	0.53	5.47	0.30	-0.01	44.50	0.11	0.37	1.62	0.06	0.20
245	2450	0.109	0.50	1.25	23.48	38.41	0.50	6.12	0.27	0.00	46.21	0.11	0.38	1.50	0.05	0.23
246	2460	0.1016	0.52	1.92	18.40	37.06	0.48	5.18	0.25	-0.01	40.48	0.10	0.36	1.27	0.05	0.32
247	2470	0.1012	0.50	0.96	25.32	42.60	0.48	6.01	0.18	0.01	37.50	0.10	0.31	1.22	0.05	0.20
248	2480	0.1019	0.67	0.94	20.58	44.16	0.47	5.50	0.24	0.01	41.79	0.10	0.35	1.43	0.05	0.19
249	2490	0.1066	0.49	0.82	16.48	36.78	0.42	5.31	0.24	-0.02	47.58	0.08	0.37	1.75	0.05	0.18
250	2500	0.1015	0.49	1.01	23.08	44.25	0.50	5.21	0.25	0.14	28.92	0.09	0.33	0.94	0.04	0.16
251	2510	0.1042	0.49	1.37	20.39	43.87	0.48	6.05	0.23	-0.01	50.41	0.11	0.41	1.51	0.05	0.23
252	2520	0.1015	0.52	1.02	20.74	33.16	0.42	5.38	0.20	-0.02	40.05	0.09	0.36	1.23	0.05	0.18
253	2530	0.1033	0.98	1.37	20.17	32.99	0.46	5.73	0.22	-0.01	44.67	0.12	0.45	1.47	0.05	0.23
254	2540	0.1006	2.30	1.72	16.22	35.08	0.54	4.92	0.24	0.01	40.48	0.10	0.44	1.26	0.05	0.27
256	2550	0.1088	0.52	1.31	19.68	33.70	0.41	5.43	0.21	-0.01	38.29	0.09	0.40	1.05	0.04	0.17
256	2560	0.1019	1.00	0.83	20.79	32.67	0.40	5.84	0.24	0.00	43.12	0.10	0.42	1.37	0.05	0.19
257	2570	0.1019	0.82	1.10	21.43	41.47	0.53	5.70	0.20	0.00	45.55	0.10	0.43	1.30	0.05	0.19
258	2580	0.1031	0.38	1.33	16.77	44.40	0.54	4.77	0.25	0.00	42.62	0.10	0.49	1.14	0.05	0.22
259	2590	0.1014	0.78	1.17	37.48	42.53	0.41	6.91	0.25	0.05	42.05	0.10	0.47	1.35	0.05	0.21
260	2600	0.1038	0.41	1.62	15.35	29.57	0.47	4.40	0.19	0.00	42.40	0.09	0.40	1.19	0.05	0.24
261	2610	0.1033	0.64	0.66	26.97	37.45	0.41	5.97	0.20	0.02	41.66	0.09	0.39	1.14	0.05	0.16
262	2620	0.1013	0.42	1.26	19.07	41.34	0.47	4.93	0.18	0.00	41.89	0.08	0.37	1.09	0.05	0.19
263	2630	0.1035	0.46	0.86	17.04	37.95	0.51	5.13	0.20	0.00	45.12	0.09	0.42	1.24	0.05	0.19
264	2640	0.1025	0.54	0.93	24.39	54.96	0.47	6.08	0.21	0.02	45.88	0.10	0.39	1.25	0.05	0.16
265	2650	0.1011	0.39	2.28	47.55	39.29	0.35	5.12	0.32	-0.07	43.38	0.10	0.46	1.42	0.05	0.21
266	2660	0.1001	0.51	1.40	26.87	46.86	0.35	5.35	0.30	-0.08	36.77	0.10	0.43	1.01	0.05	0.21
267	2670	0.1054	0.47	1.02	28.26	42.61	0.40	5.90	0.29	-0.07	44.14	0.08	0.42	1.18	0.05	0.17
268	2680	0.1039	0.58	1.32	28.32	39.94	0.35	5.48	0.30	-0.08	43.43	0.07	0.44	1.19	0.04	0.17
269	2690	0.1005	0.48	1.12	38.93	47.89	0.40	6.56	0.24	-0.07	35.16	0.07	0.45	1.02	0.04	0.21
270	2700	0.101	0.27	1.32	30.76	42.00	0.37	5.52	0.28	-0.08	46.92	0.07	0.46	1.35	0.05	0.21
271	2710	0.1054	0.48	1.07	28.58	41.58	0.36	5.14	0.28	-0.08	42.49	0.07	0.44	1.28	0.04	0.20
272	2720	0.1072	0.35	1.49	30.42	41.72	0.38	6.08	0.33	-0.06	47.49	0.09	0.47	1.26	0.04	0.25
273	2730	0.1054	0.23	1.14	26.68	42.30	0.46	5.13	0.23	-0.08	40.17	0.07	0.40	0.97	0.05	0.22
274	2740	0.1067	0.23	0.54	28.07	46.20	0.42	5.12	0.23	-0.07	38.15	0.08	0.39	1.07	0.04	0.15
275	2750	0.1045	0.20	1.10	27.86	27.97	0.41	5.20	0.26	-0.06	44.30	0.09	0.45	1.22	0.05	0.24
276	2760	0.1016	0.40	1.32	29.41	30.62	0.42	5.23	0.36	-0.08	45.41	0.08	0.47	1.10	0.04	0.21
277	2770	0.1019	0.28	1.02	40.72	36.36	0.38	5.72	0.35	-0.04	49.73	0.09	0.51	1.31	0.05	0.21
278	2780	0.1126	0.19	0.84	36.80	51.67	0.42	5.82	0.30	-0.05	45.23	0.09	0.48	1.15	0.05	0.17
279	2790	0.1006	0.18	0.96	36.38	52.39	0.43	5.66	0.36	-0.06	49.51	0.10	0.50	1.36	0.05	0.20
280	2800	0.1021	0.16	1.29	33.13	42.47	0.34	5.16	0.36	-0.08	46.14	0.09	0.49	1.24	0.05	0.23
281	2810	0.1002	0.23	1.53	40.41	37.52	0.40	5.59	0.33	-0.06	43.37	0.09	0.51	1.30	0.05	0.28
282	2820	0.1057	0.11	0.77	25.74	52.65	0.41	4.83	0.26	-0.08	43.91	0.10	0.41	1.14	0.04	0.19
283	2830	0.1122	0.21	0.87	48.88	54.24	0.46	6.27	0.22	-0.05	48.30	0.07	0.43	1.22	0.05	0.19
284	2840	0.1005	0.23	0.38	33.73	53.54	0.33	5.47	0.27	-0.08	43.02	0.07	0.42	1.13	0.04	0.15
285	2850	0.1068	0.12	0.48	28.79	55.83	0.34	5.32	0.22	-0.07	42.26	0.07	0.43	1.01	0.04	0.15
286	2860	0.1043	0.21	1.70	25.49	73.26	0.43	5.07	0.26	-0.08	43.90	0.09	0.48	1.27	0.05	0.26
287	2870	0.1013	0.20	0.61	34.85	69.43	0.45	6.58	0.30	-0.06	46.95	0.10	0.47	1.14	0.05	0.17
288	2880	0.1129	0.20	0.59	22.28	75.33	0.41	5.07	0.24	-0.04	42.67	0.10	0.42	1.05	0.05	0.14
289	2890	0.116	0.24	1.60	21.88	47.41	0.48	5.37	0.24	-0.04	47.26	0.09	0.47	1.11	0.04	0.22
290	2900	0.1036	0.17	1.16	22.10	51.91	0.36	5.79	0.19	-0.06	39.60	0.07	0.49	0.98	0.04	0.19
292	2910	0.1018	0.20	1.20	18.67	43.36	0.42	5.64	0.27	-0.06	47.50	0.09	0.47	1.12	0.04	0.20
292	2920	0.1039	0.16	1.70	19.71	48.56	0.33	5.59	0.30	-0.06	48.40	0.07	0.53	1.00	0.04	0.19
293	2930	0.1037	0.18	2.66	18.80	60.86	0.40	5.43	0.35	-0.06	51.27	0.08	0.61	1.32	0.05	0.27
294	2940	0.101	0.19	1.22	18.39	47.59	0.45	5.60	0.29	-0.05	52.98	0.08	0.53	1.36	0.04	0.18
295	2950	0.1007	0.19	1.07	17.99	53.71	0.46	5.94	0.23	-0.07	45.47	0.07	0.48	1.08	0.04	0.19
296	2960	0.1054	0.23	1.24	14.60	39.72	0.46	5.71	0.32	-0.05	52.34	0.08	0.52	1.30	0.04	0.21
297	2970	0.101	0.17	0.85	14.95	43.74	0.39	6.00	0.23	-0.07	51.34	0.07	0.52	1.17	0.04	0.18
298	2980	0.1032	0.20	1.22	12.77	44.65	0.45	6.69	0.29	-0.06	73.93	0.08	0.55	1.83	0.06	0.23
299	2990	0.1065	0.17	1.14	13.71	50.06	0.37	5.61	0.23	-0.04	44.51	0.09	0.48	1.10	0.04	0.20
300	3000	0.1021	0.20	1.16	13.70	46.74	0.35	5.48	0.25	-0.07	39.81	0.08	0.46	1.05	0.04	0.20

	Depth (mm)	Sed. (ICPMS)	Li 7	B 10	Na 23	Mg 24	Al 27	Si 28	P 31	S 34	K 39	Ca 43	Cr 52	Fe 54	Mn 55	Co 59
301	3010	0.1192	2.18	18.64	356.08	209.95	2462.58	39.80	245.10	5146.87	171.53	411.35	0.85	2624.80	171.86	0.47
302	3020	0.1069	1.46	19.78	243.09	152.32	2329.19	39.80	231.42	4030.57	137.49	290.74	0.79	2669.31	116.29	0.37
303	3030	0.1062	1.80	18.44	301.76	177.06	2279.40	40.27	231.46	4071.07	151.12	332.97	0.70	2472.67	140.30	0.41
304	3040	0.1027	2.36	20.38	429.52	226.62	2460.49	44.06	290.53	5930.04	178.41	438.64	0.75	4351.70	188.50	0.52
305	3050	0.1058	2.22	17.04	375.21	230.19	2749.15	49.33	289.95	6207.46	172.31	429.46	0.94	3631.48	179.19	0.52
306	3060	0.102	2.06	25.81	347.98	203.77	2534.04	48.95	278.08	7012.44	165.09	370.42	0.88	4569.71	159.71	0.46
307	3070	0.101	1.93	21.09	336.36	195.22	2349.48	44.14	222.80	6559.78	149.69	370.35	0.89	3185.94	151.97	0.44
308	3080	0.1023	2.02	22.27	353.14	208.51	2442.31	45.11	256.59	5898.50	153.89	396.86	0.91	3933.15	160.52	0.45
309	3090	0.102	1.67	18.56	279.33	164.40	2226.55	46.30	244.42	4053.21	127.82	287.87	0.79	3137.98	120.78	0.39
310	3100	0.1038	1.57	20.80	247.68	157.71	2428.02	47.69	254.07	3954.97	136.75	293.49	0.91	3669.60	111.34	0.37
311	3110	0.1016	1.97	24.43	314.17	189.77	2375.92	43.88	233.55	4717.84	157.68	326.85	0.82	4020.92	135.22	0.43
312	3120	0.1	2.23	21.77	378.00	219.87	2436.53	51.11	223.14	5384.66	139.15	390.97	1.01	2936.90	164.50	0.50
313	3130	0.1073	1.66	21.09	302.82	180.24	2313.63	46.80	253.69	4661.42	156.58	300.22	1.05	3974.00	121.10	0.43
314	3140	0.1015	1.68	18.96	308.31	201.30	2422.00	43.70	269.66	5246.79	213.83	320.48	0.87	4800.91	129.55	0.44
315	3150	0.1049	1.84	25.37	327.70	204.02	2529.18	46.10	274.32	6259.15	190.28	329.53	1.01	4777.63	125.93	0.46
316	3160	0.106	1.83	19.80	313.06	198.99	2530.34	45.37	237.10	6020.95	155.00	319.37	0.96	3287.71	122.97	0.45
317	3170	0.1095	1.62	24.61	287.83	189.15	2273.44	44.65	283.10	5015.99	213.01	294.97	1.44	3853.50	115.17	0.44
318	3180	0.1083	1.89	22.31	337.32	224.19	2460.80	43.71	284.17	5359.75	191.54	350.95	1.36	3783.85	143.01	0.52
319	3190	0.108	2.34	23.32	440.47	293.17	2473.92	42.75	297.70	5169.93	167.40	389.92	1.07	3726.09	162.99	0.58
320	3200	0.1037	2.06	22.61	327.83	249.66	2602.18	49.13	257.37	5384.22	160.96	334.97	1.67	3644.35	128.34	0.47
321	3210	0.1092	2.24	24.68	352.15	279.58	2569.49	46.47	241.01	7600.13	162.35	358.83	0.93	4334.00	144.54	0.52
322	3220	0.1007	1.89	26.01	321.91	240.75	2317.17	41.00	262.60	5618.19	151.08	311.78	1.03	4246.87	118.63	0.44
323	3230	0.1036	2.03	27.93	338.83	246.94	2398.75	42.55	264.14	5544.08	151.81	327.57	0.82	3756.14	126.68	0.48
324	3240	0.1027	2.35	30.75	381.75	282.70	2547.59	45.23	280.65	5951.33	164.75	364.50	0.90	3779.97	144.86	0.53
325	3250	0.106	2.81	28.03	441.81	328.23	2506.61	41.34	243.24	6155.02	180.67	417.72	0.77	3047.71	169.64	0.60
326	3260	0.1027	2.72	29.70	441.24	316.88	2466.55	42.74	277.57	6260.84	178.19	399.24	0.74	3595.00	162.89	0.61
327	3270	0.1056	2.19	30.76	329.57	263.35	2349.03	40.69	258.75	5914.71	154.39	341.79	0.86	3349.19	131.39	0.51
328	3280	0.1064	1.97	23.12	312.54	248.18	2111.19	41.62	216.18	6850.11	141.37	302.18	0.68	3749.65	123.70	0.47
329	3290	0.1068	2.07	26.17	341.00	262.69	2209.23	41.74	223.42	6660.16	145.44	315.79	0.73	3776.13	128.20	0.47
330	3300	0.104	2.14	24.87	338.71	271.46	2394.85	43.63	234.00	7932.05	154.97	335.83	0.79	4482.70	134.03	0.52
331	3310	0.1042	2.20	26.12	345.63	282.21	2486.53	46.80	238.54	5481.88	161.68	336.54	0.86	3018.56	132.96	0.51
332	3320	0.103	1.92	22.93	286.26	227.92	2291.05	45.43	240.33	4777.63	153.33	280.09	0.73	3123.74	106.12	0.41
333	3330	0.1076	2.09	26.72	329.42	262.69	2432.41	48.44	262.43	4969.53	160.15	322.90	0.80	3549.42	119.90	0.46
334	3340	0.1068	2.17	24.25	330.54	271.55	2490.88	48.97	237.75	4730.38	169.55	315.34	0.95	3755.44	120.39	0.46
335	3350	0.1033	1.94	28.00	292.01	249.25	2505.82	49.08	254.48	4025.46	153.26	289.43	0.93	3139.99	107.87	0.42
336	3360	0.1069	2.25	18.43	322.78	277.17	2422.21	44.73	258.91	4329.21	156.91	319.14	0.90	3777.54	120.42	0.43
337	3370	0.1049	2.14	18.31	326.78	272.30	2400.45	48.01	236.79	5150.12	161.58	325.36	0.97	3387.32	112.57	0.45
338	3380	0.1017	2.03	27.42	319.43	256.96	2344.69	46.00	242.84	5693.34	156.12	311.70	0.87	3590.89	109.10	0.44
339	3390	0.1096	2.10	25.58	342.39	283.92	2406.46	46.82	227.91	7552.10	163.89	343.04	0.95	4361.22	127.89	0.52
340	3400	0.1096	1.83	26.05	303.12	249.24	2278.81	43.06	244.79	5245.43	148.08	296.73	0.84	4360.23	106.36	0.45
341	3410	0.1023	2.38	31.57	390.86	317.42	2312.73	45.61	252.07	5520.33	164.97	381.99	0.83	3887.27	137.62	0.51
342	3420	0.1026	1.83	28.03	295.09	245.47	2336.90	45.61	236.90	5344.22	147.30	288.08	0.94	4084.22	104.55	0.43
343	3430	0.1042	2.23	21.70	360.02	302.15	2406.02	43.72	212.46	6438.70	167.94	367.47	0.98	4224.53	131.86	0.51
344	3440	0.1031	1.96	33.62	331.12	266.11	2229.66	44.75	296.06	4868.88	154.36	367.47	1.08	3773.21	117.70	0.46
345	3450	0.1013	2.09	24.91	347.72	282.01	2436.55	50.23	240.16	4549.66	169.93	330.81	1.11	3213.08	117.39	0.46
346	3460	0.1004	1.98	21.31	305.46	255.48	2269.51	47.48	243.75	4724.41	156.43	308.36	0.99	3565.40	108.04	0.45
347	3470	0.1061	2.41	25.02	387.73	331.01	2476.79	44.54	224.25	6182.16	171.08	395.26	1.00	4191.40	145.53	0.55
348	3480	0.1027	2.49	29.00	401.39	323.36	2462.44	45.01	238.09	6856.80	176.39	388.78	0.91	4668.23	140.65	0.57
349	3490	0.1022	2.47	35.87	396.00	324.73	2408.30	44.14	280.67	5114.79	164.38	374.71	0.90	3512.09	143.68	0.52
350	3500	0.1071	2.53	31.81	401.29	331.35	2418.92	43.02	241.29	6544.06	168.87	368.08	0.81	4324.83	144.29	0.56
351	3510	0.1038	2.46	34.84	379.23	313.59	2586.58	45.02	249.77	6243.19	167.93	355.52	0.92	4824.07	133.29	0.56
352	3520	0.1022	2.06	35.03	319.03	267.53	2346.68	42.92	241.85	4977.18	151.66	302.95	0.81	3554.45	112.14	0.45
353	3530	0.1014	2.44	33.65	370.26	311.78	2371.06	41.63	247.39	5602.29	167.68	354.12	0.78	4105.38	132.67	0.51
354	3540	0.1056	3.36	30.33	472.25	408.98	2806.57	45.94	255.11	6376.37	190.68	426.07	1.11	3369.26	166.40	0.60
355	3550	0.1023	2.37	29.46	341.15	308.35	2572.93	45.52	253.09	7229.16	164.64	361.62	0.95	4778.20	126.74	0.55
356	3560	0.1044	2.53	25.91	352.31	322.93	2599.84	19.31	300.15	7485.41	178.46	368.65	0.96	6087.52	133.99	0.60
357	3570	0.1026	3.39	35.57	456.18	436.90	2721.80	17.60	305.42	7739.78	203.72	477.59	0.94	5324.41	170.37	0.66
358	3580	0.1021	2.16	28.71	310.66	280.79	2448.18	20.02	295.04	6662.17	159.41	302.25	0.81	5450.57	107.53	0.47
359	3590	0.1032	2.18	29.30	322.63	301.27	2332.74	20.17	264.70	7338.98	153.28	303.18	0.76	5295.00	113.50	0.52
360	3600	0.1006	2.42	27.66	355.27	336.30	2347.92	20.27	263.31	7026.68	165.05	349.37	0.74	5250.66	126.62	0.51
361	3610	0.1029	2.73	29.94	400.06	395.32	2384.41	43.43	250.94	8103.13	171.69	394.93	0.72	6021.96	141.19	0.52
362	3620	0.1056	2.46	27.37	356.52	359.30	2527.38	44.73	294.40	5923.36	164.76	364.08	0.75	4841.99	124.71	0.46
363	3630	0.1002	2.81	26.08	395.80	408.77	2588.69	44.65	273.54	5699.43	167.15	398.32	0.72	3488.81	142.73	0.51
364	3640	0.1041	2.72	25.79	378.47	375.31	2434.44	43.31	238.35	5904.91	162.24	360.25	0.72	4103.12	134.80	0.50
365	3650	0.105	2.46	27.59	349.23	370.54	2632.69	44.46	291.30	6582.15	167.06	353.03	0.82	5241.75	123.66	0.50
366	3660	0.104	2.89	22.72	361.05	409.97	2687.90	45.27	281.17	8381.07	179.62	392.81	0.81	6008.52	140.60	0.61
367	3670	0.1034	2.39	20.88	313.31	348.28	2653.06	45.09	247.28	6661.18	162.71	340.68	0.82	4753.19	116.91	0.51
367	3680	0.1049	2.59	23.96	341.69	374.08	2576.81	46.44	250.36	5680.58	166.27	361.05	0.83	4140.31	122.98	0.47
369	3690	0.1024	2.35	20.71	303.41	351.29	2549.97	47.82	304.33	4029.06	157.06	324.68	0.79	3899.33	113.19	0.41
370	3700	0.1036	2.89	18.54	358.22	410.82	2771.79	46.21	265.81	7246.63	170.63	386.83	0.87	4701.13	139.43	0.56
371	3710	0.104	2.64	23.07	339.33	367.84	2614.30	45.21	268.26	5255.99	166.18	347.43	0.94	3985.64	125.16	0.47
372	3720	0.103	3.07	19.75	369.57	424.06	2862.64	45.23	314.33	4981.18	173.79	385.00	1.96	3969.11	137.25	0.52
373	3730	0.1011	3.33	21.90	409.49	466.04	2944.22	45.84	302.27	5367.22	184.55	428.64	1.06	3797.16	156.85	0.57
374	3740	0.1077	2.82	29.20	337.80	380.19	2889.83	46.59	289.42	7321.73	171.73	355.75	0.89	4978.23	128.65	0.50
375	3750	0.1052	3.05	24.52	353.94	398.53	3086.12	46.24	305.70	6021.31	183.11	362.42	1.11	4518.94	129.92	0.53
376	3760	0.1044	3.61	31.23	400.05	457.43	3159.77	46.37	337.90	7229.85	187.02	448.04	0.93	4998.26	152.41	0.59
377	3770	0.1053	3.40	28.43	424.12	469.03	3028.79	47.51	345.57	7142.02	184.06	437.32	0.91	5832.26	182.51	0.78
378	3780	0.1033	2.92	27.76	351.31	408.01	3020.89	46.28	330.54	6513.23	174.90	376.90	0.90	4758.06	139.16	0.53
379	3790	0.1083	3.25	33.25	390.75	443.39	2983.65	47.29	364.81	6975.60	182.57	411.58	0.85	5734.92	156.36	0.58
380	3800	0.114	4.19	35.43	504.83	614.45	3190.05	46.59	293.87	9206.29	199.98	566.03	1.20	4911.65	215.45	0.71
381	3810	0.1015	3.36	27.16	425.09	477.04	2581.54	45.10	292.09	6322.43	186.97	453.62	0.68	4439.72	173.21	0.58
382	3820	0.1064	2.88	32.50	363.40	419.23	2684.33	47.17	340.54	5912.42	173.02	399.15	0.82	5756.71	147.57	0.49
383	3830	0.1013	3.66	36.25	434.73	531.48	2974.75	49.36	380.05	5660.62	190.97	498.91	0.85	5226.96	193.03	0.58
384	3840	0.1084	2.93	24.36	336.38	400.42	2938.85	48.40	334.35	5128.49	179.33	393.97	1.08	4597.58	145.84	0.48
385	3850	0.1021	2.98	30.47	361.78	448.12	2950.53	58.14	297.22	6080.50	178.05	425.20	0.79	3707.11	157.19	0.52
386	3860	0.1048	3.17	21.92	356.82	465.55	3127.68	50.24	384.01	5461.11	179.55	427.30	0.95	4185.96	161.39	0.51
387	3870	0.1006	3.04	25.25	345.68	472.09	3275.94	49.71	486.42	4412.91	185.44	428.31	0.92	5306.74	160.98	0.54
388	3880	0.1014	3.71	30.76	425.96	553.37	3278.12	51.61	445.84	5139.79	198.37	525.46	0.86	4036.57	209.74	0.62
389	3890	0.1024	3.64	22.44	382.76	490.91	3464.72	46.47	382.75	7241.75	190.63	452.59	0.84	4871.56	185.26	0.60
390	3900	0.1008	3.92	21.69	391.75	540.89	3831.11	49.88	417.08	8562.44	199.88	538.18	0.88	5430.70	209.35	0.72
391	3910	0.1012	3.95	23.93	398.00	525.94	4386.81	53.38	492.58	7666.52	207.60	525.34	0.95	5358.98	205.87	0.72
392	3920	0.1014	3.71	32.01	346.12	482.73	4412.15	60.45	640.55	8129.30	205.08	499.68	0.81	6825.16	189.88	0.68
393	3930	0.1031	4.77	22.66	342.42	505.50	6575.91	64.96	804.16	7568.61	210.54	504.01	1.09	5160.51	191.76	0.78
394	3940	0.1062	4.98	20.99	306.90	463.42	7808.84	70.64	1282.46	5064.30	210.28	493.30	1.34	4818.17	170.34	0.75
395	3950	0.1064	4.02	24.54	322.63	472.51	6873.76	59.97	1148.18	4869.44	216.03	506.07	1.16	4115.52	173.57	0.74
396	3960	0.1012	4.29	19.83	282.82	429.04	7981.44	71.26	1411.45	4381.07	214.85	483.57	1.32	4361.81	159.60	0.73
397	3970	0.1021	3.82	16.95	290.74	434.02	6576.47	70.29	1008.65	3657.07	217.26	486.55	1.04	3257.60	165.96	0.71
398	3980	0.109	4.23	23.12	330.97	504.19	6953.63	69.60	1096.93	4235.61	233.07	533.66	1.22	3559.84	184.06	0.76
399	3990	0.1024	4.13	23.63	325.66	474.15	6468.59	71.20	1015.21	6202.21	218.19	500.62	1.17	4723.83	174.68	0.87
400	4000	0.1006	4.12	29.09	325.97	477.09	6254.88	66.78	902.22	6918.69	218.03	502.32	1.27	5570.63	172.09	0.80
401	4010	0.1027	3.92	35.12	402.25	556.70	4123.08	60.78	600.92	6193.89	212.47	540.30	1.01	6550.57	205.79	0.70
402	4020	0.1026	4.33	35.34	451.61	647.89	3690.28	58.95	392.97	6115.03	213.62	599.96	0.93	4434.50	236.87	0.69
403	4030	0.1007	3.55	27.63	378.28	547.21	3467.86	58.80	416.84	6604.03	205.03	498.55	0.90	5084.48	190.32	0.65
404	4040	0.1014	3.03	37.72	358.74	490.76	3431.22	51.37	405.92	5443.42	206.02	463.50	1.12	4434.95	155.97	0.58
405	4050	0.1026	3.01	21.42	310.42	459.24	3265.97	53.68	290.99	7793.44	187.29	411.29	0.90	5498.53	144.27	0.58
406	4060	0.1051	2.91	30.15	341.27	480.82	2826.94	51.71	282.05	7195.40	188.96	417.24	0.88	5486.66	156.29	0.55
407	4070	0.1025	3.09	21.35	354.53	529.41	2696.33	47.63	233.74	7968.89	187.22	451.52	0.92	5116.43	161.65	0.60
408	4080	0.1005	2.64	12.22	322.99	430.33	2247.29	48.30	246.43	5863.40	206.50	291.78	0.86	5149.59	111.64	0.49
409	4090	0.1022	2.50	25.64	315.70	412.63	2192.41	44.37	200.75	5973.28	155.53	267.92	0.73	3456.81	88.11	0.42
410	4100	0.1009	2.66	29.78	362.39	450.12	2293.34	52.52	205.05	6738.61	176.56	317.97	0.80	3559.82	101.55	0.46
411	4110	0.1013	2.69	25.09	385.73	453.94	2372.26	52.50	281.76	9686.96	171.17	329.03	1.07	9164.22	108.76	0.52
412	4120	0.101	2.78	18.82	367.39	435.70	2228.28	43.99	203.69	7824.50	160.33	315.50	0.91	5111.46	108.33	0.49
413	4130	0.1052	2.85	20.71	383.93	426.05	2185.05	44.77	211.62	7950.57	174.95	326.44	0.91	5507.17	109.04	0.52
414	4140	0.1027	2.58	21.04	364.23	392.32	2200.52	45.98	218.37	7945.54	196.54	309.98	0.88	5507.40	105.29	0.48
415	4150	0.1053	2.45	15.61	342.99	360.22	2117.57	45.43	219.02	7794.87	182.62	286.47	0.93	5390.09	99.35	0.46
416	4160	0.1014	2.63	21.69	381.05	388.23	2129.55	45.03	212.94	9034.24	227.70	347.37	1.39	5644.97	110.68	0.46
417	4170	0.1034	3.03	27.72	437.09	419.27	2228.38	50.81	219.78	10143.20	262.92	369.35	0.90	6256.71	124.95	0.54
418	4180	0.1013	2.71	28.55	401.69	369.10	2144.17	48.26	205.37	10209.37	261.02	345.82	0.90	6323.71	117.12	0.48
419	4190	0.1009	2.64	23.56	380.85	351.03	2035.75	47.69	175.96	9474.38	211.33	337.75	0.82	5161.69	113.14	0.46
420	4200	0.1014	3.12	20.47	458.66	386.64	2141.15	45.74	173.25	11419.55	187.42	370.87	0.82	5718.17	132.95	0.52
421	4210	0.1003	2.33	24.52	370.14	304.77	2075.48	50.01	179.93	7578.78	231.03	324.04	1.06	5390.89	106.82	0.44
422	4220	0.1079	2.84	23.02	438.89	347.38	2207.10	39.66	202.60	8447.52	245.05	368.27	0.91	7104.60	127.60	0.53
423	4230	0.1013	2.27	20.70	354.50	295.96	2184.12	49.07	187.67	8201.08	171.95	314.99	0.90	5594.26	108.90	0.49
424	4240	0.1004	1.90	14.77	299.05	235.02	1876.95	42.84	164.29	6435.34	132.12	258.15	0.78	4538.03	85.77	0.41
425	4250	0.1027	1.76	10.93	279.07	229.23	1923.03	42.69	171.19	6584.09	150.58	262.10	0.88	5078.94	85.87	0.41
426	4260	0.1029	2.12	17.61	335.39	249.27	2162.17	44.70	166.10	9668.68	157.40	286.39	0.99	5315.71	99.89	0.50
427	4270	0.1082	1.67	11.30	251.28	192.51	1882.98	40.35	165.49	6521.53	135.95	228.77	0.89	4175.01	76.09	0.39
428	4280	0.1008	2.33	16.88	345.61	250.72	2144.87	42.14	183.34	7998.81	167.29	314.46	0.99	5441.18	106.39	0.51
429	4290	0.104	1.83	13.79	285.46	212.28	2063.04	41.66	196.83	8251.46	183.08	268.19	1.14	5727.67	86.76	0.38
430	4300	0.1015	1.97	12.89	321.18	240.42	2108.67	37.61	182.43	7946.27	218.65	309.84	1.23	5556.18	97.09	0.39
431	4310	0.1031	1.49	15.89	265.20	185.94	1879.46	35.55	181.37	8115.69	182.82	238.41	1.17	6084.03	73.95	0.38
432	4320	0.1078	2.07	16.19	343.08	238.26	2052.45	41.95	196.61	8360.22	231.67	323.17	1.05	5797.96	107.61	0.44
433	4330	0.1036	2.95	16.31	460.68	296.26	2372.94	122.00	190.07	10244.67	218.21	372.23	1.03	5398.54	123.17	0.50
434	4340	0.1044	2.76	21.93	462.05	305.34	2357.28	122.08	191.38	10675.12	161.21	385.34	1.02	6153.36	130.86	0.52
435	4350	0.1001	2.19	24.52	389.20	264.81	2118.59	118.50	214.65	9897.68	164.55	358.77	0.98	7649.74	116.67	0.45
436	4360	0.1001	2.14	23.18	344.50	232.64	2110.49	124.48	161.52	8277.45	159.14	313.77	0.94	4533.53	99.91	0.39
437	4370	0.1007	2.15	20.11	376.71	240.56	2068.60	123.79	159.08	10686.93	190.08	312.16	0.82	6099.78	105.98	0.41
438	4380	0.1007	2.77	17.04	454.17	293.00	2223.30	117.70	183.14	9265.16	201.30	376.30	0.88	6181.68	133.26	0.48
439	4390	0.1007	2.16	13.99	351.93	244.98	1973.75	108.64	183.22	7802.89	219.57	308.54	0.91	5914.65	103.90	0.39
440	4400	0.1044	1.62	12.32	282.58	189.93	1896.67	118.45	163.11	6034.65	179.64	242.62	0.84	4142.99	78.46	0.32
441	4410	0.1013	1.66	14.00	256.09	190.97	1986.99	124.53	166.90	5408.68	162.24	228.68	0.99	4862.14	72.04	0.31
442	4420	0.1031	1.73	8.84	276.79	206.89	2000.96	123.95	151.67	6867.80	170.23	244.43	0.93	3921.96	79.14	0.36
443	4430	0.1037	1.81	11.42	279.75	205.80	2058.15	114.62	159.82	10199.83	142.90	253.87	0.89	6314.25	84.83	0.41
444	4440	0.1016	1.83	9.83	274.76	193.83	1981.63	109.81	152.89	8189.17	151.28	243.76	0.94	5092.39	80.63	0.35
445	4450	0.1031	1.69	17.13	287.02	198.01	1939.62	108.15	165.46	8124.31	165.85	255.37	0.88	4794.38	86.78	0.35
446	4460	0.101	2.92	12.22	461.11	309.16	2328.66	116.68	191.30	13687.29	182.80	388.20	0.94	9060.94	146.27	0.56
447	4470	0.1014	2.25	15.27	365.85	253.32	2097.02	111.66	193.76	12647.52	189.55	348.16	0.88	9050.81	122.76	0.44
448	4480	0.1009	2.20	20.72	376.16	246.60	1996.93	114.14	167.02	13821.75	173.15	332.63	0.87	7634.32	119.56	0.43
449	4490	0.101	2.31	22.34	412.38	264.69	2155.56	129.85	234.82	11135.30	250.55	370.14	1.02	8696.10	133.83	0.42

	Depth (mm)	Sed. (ICPMS)	Ni 60		Cu 63		Zn 66		As 75		Se 82		Sr 88		Ag 109		Cd 111		Ba 137		Hg 202		Tl 205		Pb 207		Bi 209		U 238	
301	3010	0.1192	0.20	0.83	13.44	41.87	0.38	5.77	0.27	-0.04	43.52	0.08	0.49	1.06	0.04	0.20														
302	3020	0.1069	0.11	1.24	9.78	41.87	0.37	5.20	0.34	-0.07	47.87	0.09	0.49	1.11	0.04	0.23														
303	3030	0.1062	0.13	0.58	11.17	39.80	0.35	5.06	0.29	-0.06	40.43	0.08	0.48	0.96	0.03	0.15														
304	3040	0.1027	0.19	4.85	17.32	64.31	0.48	6.19	0.30	-0.02	42.54	0.09	0.52	1.01	0.03	0.15														
305	3050	0.1058	0.23	1.18	17.30	61.67	0.46	6.94	0.31	-0.05	58.73	0.12	0.57	1.27	0.04	0.25														
306	3060	0.102	0.18	1.51	16.35	54.82	0.49	6.06	0.29	-0.05	47.80	0.12	0.58	1.27	0.04	0.27														
307	3070	0.101	0.17	1.71	17.23	41.16	0.43	5.52	0.24	-0.06	38.98	0.11	0.47	0.93	0.04	0.28														
308	3080	0.1023	0.16	1.23	19.71	48.77	0.43	6.18	0.29	-0.06	47.86	0.10	0.51	1.13	0.04	0.21														
309	3090	0.102	0.15	0.74	14.44	42.19	0.40	4.98	0.31	-0.05	45.48	0.07	0.51	1.14	0.04	0.17														
310	3100	0.1038	0.11	0.97	13.37	45.37	0.43	5.25	0.31	-0.04	53.05	0.11	0.53	1.45	0.04	0.18														
311	3110	0.1016	0.12	0.99	16.71	50.09	0.33	5.33	0.28	-0.07	47.15	0.10	0.52	1.44	0.04	0.18														
312	3120	0.1	0.29	0.98	20.07	49.17	0.40	5.70	0.30	-0.05	42.65	0.09	0.51	0.98	0.04	0.20														
313	3130	0.1073	0.34	1.22	16.67	59.39	0.43	4.96	0.24	-0.05	42.50	0.11	0.50	1.35	0.04	0.19														
314	3140	0.1015	0.19	1.00	18.96	76.38	0.33	5.04	0.33	-0.05	45.83	0.10	0.56	1.60	0.04	0.19														
315	3150	0.1049	0.29	1.52	19.84	58.28	0.45	5.44	0.27	-0.05	49.23	0.12	0.60	1.45	0.04	0.28														
316	3160	0.106	0.20	1.68	19.64	48.27	0.40	5.35	0.35	-0.06	49.97	0.09	0.58	1.29	0.04	0.30														
317	3170	0.1095	1.56	0.95	20.88	62.37	0.35	5.08	0.29	-0.06	46.85	0.09	0.60	1.54	0.04	0.20														
318	3180	0.1083	0.72	1.08	26.30	56.61	0.49	5.67	0.35	-0.04	49.02	0.10	0.60	1.44	0.05	0.20														
319	3190	0.108	0.69	1.05	57.21	80.73	0.34	6.07	0.39	0.04	44.71	0.10	0.52	1.36	0.05	0.16														
320	3200	0.1037	0.36	1.40	47.07	67.66	0.35	5.60	0.34	-0.01	48.57	0.10	0.55	1.45	0.04	0.22														
321	3210	0.1092	0.33	1.73	50.85	66.49	0.34	5.52	0.29	-0.05	43.51	0.11	0.61	1.30	0.04	0.24														
322	3220	0.1007	0.32	1.28	47.08	90.36	0.42	5.10	0.30	-0.03	39.05	0.09	0.48	1.05	0.04	0.17														
323	3230	0.1036	0.30	0.97	39.00	87.16	0.48	5.23	0.30	-0.06	42.39	0.10	0.52	1.20	0.04	0.21														
324	3240	0.1027	0.38	1.02	43.08	76.82	0.38	5.55	0.27	-0.06	39.81	0.17	0.50	1.18	0.04	0.20														
325	3250	0.106	1.17	0.95	52.47	64.34	0.36	6.07	0.29	-0.06	39.49	0.14	0.50	1.18	0.03	0.20														
326	3260	0.1027	0.43	0.81	49.98	79.54	0.40	5.87	0.29	-0.06	38.18	0.11	0.47	1.09	0.03	0.19														
327	3270	0.1056	0.23	1.19	42.30	68.14	0.38	5.36	0.22	-0.06	39.90	0.10	0.50	1.08	0.03	0.20														
328	3280	0.1064	0.24	1.12	42.36	70.57	0.30	4.91	0.23	-0.05	37.65	0.10	0.59	1.02	0.03	0.20														
329	3290	0.1068	0.23	1.41	42.16	60.08	0.38	4.95	0.24	-0.06	37.19	0.09	0.53	0.86	0.03	0.21														
330	3300	0.104	0.28	1.65	44.22	70.06	0.36	5.29	0.24	-0.04	39.29	0.10	0.70	1.25	0.03	0.25														
331	3310	0.1042	0.32	1.16	44.66	61.56	0.37	5.68	0.27	-0.02	47.53	0.10	0.57	1.23	0.03	0.23														
332	3320	0.103	0.15	0.98	34.50	72.49	0.35	4.95	0.28	-0.05	44.48	0.08	0.47	1.14	0.04	0.21														
333	3330	0.1076	0.24	1.05	40.46	64.06	0.42	5.44	0.24	-0.04	46.10	0.10	0.44	1.22	0.04	0.21														
334	3340	0.1068	0.36	1.41	39.25	53.97	0.40	5.44	0.26	-0.05	47.12	0.10	0.46	1.40	0.04	0.23														
335	3350	0.1033	0.18	0.96	36.36	55.55	0.38	5.25	0.27	-0.06	47.66	0.11	0.38	1.27	0.04	0.19														
336	3360	0.1069	0.63	0.80	40.66	59.89	0.35	5.19	0.20	-0.07	44.85	0.10	0.40	1.18	0.04	0.17														
337	3370	0.1049	0.23	1.43	39.48	59.36	0.46	5.08	0.22	-0.07	42.66	0.12	0.45	1.21	0.03	0.23														
338	3380	0.1017	0.23	1.34	37.91	77.00	0.42	5.20	0.20	-0.08	41.84	0.10	0.51	1.21	0.03	0.26														
339	3390	0.1095	0.37	1.66	42.45	69.74	0.41	5.38	0.20	-0.07	41.46	0.11	0.73	1.33	0.03	0.26														
340	3400	0.1096	0.30	1.26	34.00	72.10	0.41	4.91	0.20	-0.07	39.72	0.11	0.49	1.11	0.03	0.21														
341	3410	0.1023	0.22	0.95	40.80	82.39	0.41	5.55	0.22	-0.07	36.59	0.09	0.41	0.92	0.03	0.18														
342	3420	0.1026	0.21	1.27	28.46	64.69	0.52	4.84	0.20	-0.07	38.09	0.08	0.49	1.15	0.03	0.24														
343	3430	0.1042	0.23	1.40	35.55	57.63	0.43	5.52	0.23	-0.06	42.19	0.11	0.61	1.21	0.03	0.24														
344	3440	0.1031	0.29	1.04	29.20	75.33	0.41	5.06	0.22	-0.09	36.34	0.09	0.39	0.93	0.02	0.20														
345	3450	0.1013	0.48	1.01	28.51	61.98	0.40	5.26	0.37	-0.10	39.98	0.13	0.37	1.06	0.03	0.21														
346	3460	0.1004	0.20	0.97	25.92	74.65	0.45	4.93	0.26	-0.06	38.22	0.12	0.43	1.03	0.03	0.20														
347	3470	0.1061	0.32	1.29	34.75	64.57	0.47	5.89	0.29	-0.06	41.58	0.11	0.55	1.33	0.03	0.25														
348	3480	0.1027	0.24	1.63	33.62	72.36	0.45	5.70	0.29	-0.08	40.63	0.10	0.57	1.31	0.03	0.25														
349	3490	0.1022	0.24	1.14	33.35	64.30	0.41	5.78	0.23	-0.08	40.01	0.09	0.35	1.16	0.02	0.19														
350	3500	0.1071	0.22	1.06	33.54	58.98	0.37	5.68	0.21	-0.08	36.60	0.11	0.56	1.16	0.03	0.21														
351	3510	0.1038	0.26	1.53	30.94	61.15	0.41	5.75	0.24	-0.07	44.93	0.11	0.51	1.46	0.03	0.25														
352	3520	0.1022	0.24	1.17	24.80	57.20	0.39	4.98	0.20	-0.08	38.88	0.08	0.37	1.01	0.02	0.19														
353	3530	0.1014	0.19	1.33	29.60	47.37	0.35	5.41	0.19	-0.08	36.63	0.10	0.40	1.16	0.03	0.21														
354	3540	0.1056	0.63	3.08	44.41	56.28	0.42	6.56	0.20	-0.08	42.76	0.09	0.41	1.25	0.03	0.23														
355	3550	0.1023	0.26	1.58	29.03	75.89	0.52	6.02	0.27	-0.09	47.78	0.11	0.59	1.55	0.04	0.25														
356	3560	0.1044	0.28	1.42	27.88	67.82	0.44	6.00	0.51	-0.08	49.51	0.15	0.64	1.65	0.04	0.24														
357	3570	0.1026	0.32	1.38	37.77	62.87	0.42	6.85	0.54	-0.09	47.27	0.12	0.51	1.24	0.03	0.21														
358	3580	0.1021	0.14	1.43	23.97	59.55	0.42	5.39	0.65	-0.09	46.75	0.15	0.56	1.10	0.03	0.22														
359	3590	0.1032	0.18	1.43	26.13	61.17	0.42	5.27	0.69	-0.09	42.53	0.18	0.65	1.13	0.03	0.21														
360	3600	0.1006	0.18	1.35	26.65	65.41	0.42	5.38	0.68	-0.05	39.34	0.16	0.51	1.08	0.03	0.22														
361	3610	0.1029	0.25	1.75	31.21	74.25	0.37	5.80	0.55	-0.08	38.47	0.30	0.58	1.03	0.02	0.19														
362	3620	0.1056	0.17	1.29	25.09	82.27	0.38	5.55	0.56	-0.08	41.03	0.17	0.63	1.09	0.03	0.19														
363	3630	0.1002	0.19	1.24	28.40	68.42	0.42	6.01	0.48	-0.08	40.81	0.18	0.63	0.99	0.03	0.21														
364	3640	0.1041	0.19	1.26	26.57	66.72	0.39	5.37	0.47	-0.08	36.65	0.15	0.43	0.96	0.03	0.21														
365	3650	0.105	0.25	1.56	25.40	68.41	0.38	5.81	0.54	-0.09	44.74	0.18	0.46	1.34	0.03	0.24														
366	3660	0.1044	0.20	1.59	28.90	57.63	0.37	6.10	0.50	-0.06	44.99	0.18	0.76	1.34	0.03	0.25														
367	3670	0.1034	0.22	1.89	24.60	56.36	0.36	5.42	0.45	-0.09	45.68	0.15	0.54	1.33	0.03	0.28														
367	3680	0.1049	0.21	1.60	26.69	55.59	0.38	5.65	0.48	-0.07	43.99	0.18	0.54	1.23	0.03	0.22														
369	3690	0.1024	0.14	0.82	24.51	56.37	0.36	5.31	0.44	-0.06	45.40	0.15	0.32	1.01	0.03	0.16														
370	3700	0.1036	0.21	1.76	33.08	53.33	0.32	6.12	0.50	-0.08	45.10	0.17	0.58	1.32	0.03	0.25														
371	3710	0.1044	0.21	1.53	29.49	50.55	0.35	5.73	0.54	-0.09	45.86	0.22	0.48	1.17	0.03	0.22														
372	3720	0.103	0.70	1.45	32.35	56.16	0.42	6.02	0.57	-0.07	45.46	0.56	0.39	1.31	0.03	0.21														
373	3730	0.1011	0.27	1.13	34.54	57.41	0.37	6.44	0.53	-0.08	46.73	0.19	0.42	1.14	0.03	0.20														
374	3740	0.1077	0.19	1.76	27.13	56.92	0.43	5.72	0.53	-0.07	47.12	0.19	0.78	1.42	0.04	0.26														
375	3750	0.1052	0.28	1.67	28.88	63.32	0.31	6.18	0.53	-0.07	54.21	0.18	0.62	1.44	0.04	0.27														
376	3760	0.1044	0.27	1.65	32.32	71.98	0.36	6.78	0.54	-0.06	51.53	0.17	0.68	1.53	0.04	0.25														
377	3770	0.10053	0.24	1.87	35.51	73.58	0.44	6.65	0.46	-0.01	52.60	0.18	0.63	1.45	0.04	0.27														
378	3780	0.1033	0.28	1.79	30.17	57.89	0.33	6.40	0.49	0.03	58.84	0.17	0.61	1.60	0.04	0.24														
379	3790	0.1083	0.24	1.67	34.26	83.58	0.43	6.44	0.53	0.01	56.46	0.18	0.69	1.46	0.03	0.23														
380	3800	0.114	0.36	3.99	56.15	83.38	0.37	7.50	0.47	0.05	52.01	0.18	0.74	1.62	0.03	0.30														
381	3810	0.1015	0.19	2.07	36.10	77.39	0.36	6.10	0.52	0.02	43.37	0.18	0.47	1.04	0.03	0.24														
382	3820	0.1064	0.18	1.39	31.05	89.79	0.36	5.93	0.65	0.03	52.02	0.22	0.47	1.24	0.03	0.18														
383	3830	0.1013	0.40	1.00	36.48	72.13	0.42	6.96	0.70	0.05	57.10	0.21	0.45	1.34	0.04	0.17														
384	3840	0.1084	0.30	2.10	27.42	60.92	0.45	5.91	0.70	0.01	53.28	0.28	0.67	1.51	0.04	0.26														
385	3850	0.1021	0.16	2.44	28.64	57.49	0.38	5.76	0.55	-0.14	51.25	0.24	0.57	1.44	0.03	0.30														
386	3860	0.1048	1.11	2.13	29.39	65.54	0.46	6.58	0.63	-0.14	66.69	0.20	0.51	1.69	0.04	0.26														
387	3870	0.1006	0.22	1.05	27.92	73.02	0.46	6.76	0.58	-0.16	71.71	0.18	0.45	1.59	0.04	0.19														
388	3880	0.1014	0.45	1.18	35.21	63.78	0.41	6.90	0.52	-0.15	60.57	0.17	0.45	1.44	0.04	0.18														
389	3890	0.1024	0.39	3.15	32.19	54.11	0.39	6.73	0.55	-0.14	67.75	0.14	0.69	1.84	0.04	0.34														
390	3900	0.1008	0.50	2.64	35.10	49.04	0.48	7.14	0.54	-0.15	67.42	0.15	0.80	1.95	0.05	0.34														
391	3910	0.1012	0.29	2.84	37.29	50.50	0.46	7.78	0.52	-0.13	84.55	0.14	0.72	2.01	0.05	0.34														
392	3920	0.1014	0.30	4.35	33.24	55.96	0.46	7.50	0.52	-0.15	87.97	0.22	0.76	2.06	0.05	0.31														
393	3930	0.1031	0.57	4.06	35.11	40.49	0.58	10.76	0.48	-0.14	159.08	0.23	0.63	2.84	0.08	0.43														
394	3940	0.1062	0.46	4.00	33.58	41.50	0.51	13.93	0.47	-0.13	235.15	0.18	0.48	3.47	0.09	0.43														
395	3950	0.1064	0.42	3.90	30.72	39.92	0.53	13.11	0.45	-0.13	219.47	0.18	0.46	2.59	0.07	0.38														
396	3960	0.1012	0.44	4.36	31.46	37.87	0.58	15.78	0.49	-0.13	273.61	0.24	0.43	3.28	0.09	0.43														
397	3970	0.1021	0.52	4.06	29.67	33.81	0.49	11.09	0.47	-0.10	177.91	0.21	0.41	2.59	0.08	0.37														
398	3980	0.109	0.42	4.19	34.15	34.36	0.49	13.67	0.54	-0.14	217.47	0.26	0.43	2.88	0.08	0.42														
399	3990	0.1024	0.40	4.07	35.22	44.98	0.50	12.10	0.57	-0.07	186.89	0.25	0.71	2.65	0.08	0.36														
400	4000	0.1006	0.46	4.40	35.23	45.87	0.58	12.27	0.56	-0.10	189.33	0.25	0.67	2.72	0.08	0.39														
401	4010	0.1027	0.28	2.80	32.93	66.50	0.43	7.96	0.90	-0.10	86.20	0.22	0.56	1.67	0.05	0.26														
402	4020	0.1026	0.30	2.27	34.56	56.70	0.48	7.83	0.55	-0.13	67.98	0.18	0.42	1.41	0.04	0.25														
403	4030	0.1007	0.25	2.71	25.46	65.98	0.37	7.48	0.64	-0.13	74.92	0.24	0.56	1.78	0.05	0.28														
404	4040	0.1014	0.37	2.99	22.36	57.68	0.47	7.17	0.69	-0.08	74.14	0.38	0.43	1.63	0.05	0.26														
405	4050	0.1026	0.20	2.29	19.21	61.49	0.44	6.20	0.59	-0.13	60.10	0.23	0.81	1.78	0.04	0.28														
406	4060	0.1051	0.21	1.79	18.90	68.21	0.46	5.83	0.41	-0.14	51.26	0.18	0.71	1.49	0.04	0.28														
407	4070	0.1025	0.28	1.74	19.87	65.39	0.41	6.08	0.60	-0.12	48.89	0.26	0.87	1.58	0.04	0.28														
408	4080	0.1005	0.34	1.19	37.23	57.22	0.34	5.04	0.51	-0.14	42.60	0.30	0.90	2.41	0.03	0.17														
409	4090	0.1021	0.33	1.09	34.26	56.48	0.41	4.63	0.46	-0.14	39.12	0.28	0.79	1.51	0.02	0.18														
410	4100	0.1009	0.47	1.12	38.63	66.69	0.40	5.18	0.51	-0.13	38.77	0.24	0.90	1.67	0.03	0.20														
411	4110	0.1013	0.47	1.97	36.38	97.77	0.52	5.36	0.54	-0.08	39.75	0.30	1.01	1.53	0.04	0.31														
412	4120	0.101	0.45	1.55	80.72	62.05	0.43	5.12	0.47	-0.14	36.36	0.21	0.86	1.37	0.03	0.20														
413	4130	0.1052	0.75	1.12	31.46	74.07	0.34	5.06	0.46	-0.14	33.18	0.21	0.88	1.37	0.02	0.21														
414	4140	0.1027	0.34	1.06	26.92	77.81	0.36	5.05	0.62	-0.14	36.99	0.24	0.97	1.39	0.03	0.22														
415	4150	0.1053	0.30	0.95	24.06	90.30	0.49	4.86	0.59	-0.11	38.04	0.20	0.93	1.50	0.03	0.20														
416	4160	0.1014	0.30	0.96	25.02	94.71	0.40	5.08	0.60	-0.12	31.76	0.21	0.91	1.34	0.18	0.20														
417	4170	0.1034	0.53	1.07	26.31	117.81	0.56	5.70	0.58	-0.12	36.57	0.24	1.05	1.63	0.03	0.21														
418	4180	0.1013	0.35	1.10	21.61	121.99	0.54	5.49	0.68	-0.10	34.22	0.25	1.04	1.44	0.03	0.21														
419	4190	0.1009	0.34	1.16	20.20	115.16	0.45	4.95	0.64	-0.14	28.55	0.25	0.92	1.17	0.03	0.19														
420	4200	0.1014	0.34	1.54	21.89	113.98	0.51	5.51	0.59	-0.14	27.30	0.30	0.90	1.04	0.02	0.22														
421	4210	0.1003	0.36	0.79	16.88	99.55	0.42	5.07	0.71	-0.13	33.82	0.34	0.97	1.39	0.03	0.19														
422	4220	0.1079	0.30	0.64	20.93	128.55	0.44	5.54	0.62	-0.13	34.56	0.28	0.96	1.57	0.03	0.17														
423	4230	0.1013	0.27	0.92	15.80	84.73	0.46	4.98	0.59	-0.14	35.28	0.28	0.89	1.33	0.03	0.22														
424	4240	0.1004	0.18	0.75	12.54	69.18	0.45	4.32	0.53	-0.15	30.41	0.25	0.81	1.11	0.04	0.21														
425	4250	0.1027	0.17	1.01	12.94	75.04	0.39	4.36	0.60	-0.14	32.90	0.30	0.81	1.23	0.03	0.21														
426	4260	0.1029	0.25	1.68	14.17	76.34	0.40	4.56	0.62	-0.15	31.92	0.35	0.98	1.43	0.03	0.30														
427	4270	0.1082	0.15	0.98	9.98	70.80	0.37	3.92	0.55	-0.14	30.29	0.31	0.79	1.15	0.03	0.25														
428	4280	0.1008	0.22	0.96	14.01	72.51	0.41	5.06	0.61	-0.14	35.16	0.33	0.85	1.34	0.03	0.22														
429	4290	0.104	0.99	1.21	11.57	89.56	0.53	4.42	0.63	-0.12	34.61	0.41	0.86	1.45	0.03	0.26														
430	4300	0.1015	0.24	1.28	14.51	89.24	0.54	4.75	0.66	-0.14	31.11	0.34	0.82	1.39	0.04	0.22														
431	4310	0.1031	0.23	1.35	10.47	107.23	0.51	4.09	0.72	-0.06	31.67	0.40	0.82	1.67	0.06	0.25														
432	4320	0.1078	0.21	0.82	13.29	104.93	0.43	4.97	0.67	-0.14	32.08	0.51	0.90	1.58	0.04	0.21														
433	4330	0.1036	0.28	1.18	16.48	102.57	0.59	5.64	0.31	-0.11	34.65	0.32	0.79	1.48	0.03	0.24														
434	4340	0.1044	0.26	1.15	20.75	104.35	0.49	5.78	0.32	-0.13	32.77	0.31	0.74	1.10	0.03	0.21														
435	4350	0.1001	0.25	1.01	15.99	102.17	0.50	5.39	0.34	-0.15	30.03	0.30	0.71	1.06	0.02	0.19														
436	4360	0.1001	0.20	1.17	15.04	67.62	0.45	5.02	0.34	-0.15	33.51	0.26	0.69	1.32	0.02	0.22						

	Depth (mm)	Sed. (ICPMS)	Li 7	B 10	Na 23	Mg 24	Al 27	Si 28	P 31	S 34	K 39	Ca 43	Cr 52	Fe 54	Mn 55	Co 59
450	4500	0.1021	2.66	13.22	438.91	284.98	2166.01	119.68	186.92	11761.58	215.24	395.99	1.01	7243.73	149.02	0.43
451	4510	0.1007	1.92	20.40	339.60	228.30	1940.25	119.37	207.21	8275.50	262.21	307.52	0.94	6713.27	112.80	0.34
452	4520	0.1016	2.30	13.58	358.33	250.82	1982.98	123.16	162.78	11156.21	181.55	334.13	0.99	6885.62	123.60	0.48
453	4530	0.1064	2.04	19.74	364.82	241.82	1904.02	117.06	217.26	8501.61	190.25	334.49	0.98	10144.04	125.53	0.43
454	4540	0.1027	2.22	13.68	368.12	254.61	2123.47	128.67	183.81	9450.16	186.42	357.55	1.09	6846.42	133.26	0.45
455	4550	0.1031	1.84	8.93	297.64	221.69	1979.19	119.82	211.11	6610.51	167.82	279.28	1.03	5298.73	110.36	0.40
456	4560	0.101	2.33	15.04	378.87	265.58	2188.24	117.23	260.28	10159.30	195.49	361.64	1.16	6562.66	140.30	0.53
457	4570	0.1041	1.87	15.76	344.82	231.24	2057.76	174.71	802.97	6827.46	182.20	308.57	1.12	6515.53	115.00	0.41
458	4580	0.1047	1.84	10.02	335.16	237.52	2114.49	175.75	1244.34	5283.13	198.84	305.58	1.16	5029.04	112.71	0.33
459	4590	0.102	1.42	10.38	257.25	197.80	2089.13	195.50	1246.58	3326.13	197.84	244.39	1.10	4882.64	85.47	0.24
460	4600	0.1017	1.60	5.87	288.15	205.79	2253.42	190.16	685.09	3441.12	206.85	272.36	1.15	3608.77	95.47	0.25
461	4610	0.1005	1.33	15.11	266.79	188.59	2129.97	171.97	340.18	3215.38	194.22	231.09	1.93	3040.55	86.55	0.26
462	4620	0.1017	2.09	14.09	337.12	228.16	2466.61	134.77	242.82	5361.74	212.87	290.12	1.13	4539.65	114.12	0.39
463	4630	0.1006	2.29	15.42	376.05	248.07	2538.06	128.67	233.11	5961.64	218.72	336.97	1.17	4658.18	130.82	0.45
464	4640	0.101	1.98	16.15	324.13	220.17	2297.39	119.38	316.92	6494.70	192.70	308.15	1.14	5650.68	119.74	0.42
465	4650	0.1014	1.75	17.70	287.52	200.11	2154.33	120.94	528.48	8861.09	187.20	270.95	1.19	6655.31	105.21	0.48
466	4660	0.1014	2.11	9.76	344.97	227.00	2188.17	117.11	559.62	6830.19	207.61	338.88	1.19	6679.15	130.90	0.43
467	4670	0.1011	2.38	6.39	398.27	273.39	2220.92	115.55	420.99	7793.36	218.51	396.29	1.17	6855.05	157.00	0.45
468	4680	0.1013	1.76	13.95	309.25	200.36	1894.60	114.36	671.91	7017.30	185.60	290.24	1.10	6507.37	111.83	0.34
469	4690	0.1076	2.31	19.71	376.32	239.20	2025.78	117.30	1391.50	5042.33	205.79	356.05	1.19	5979.06	141.29	0.27
470	4700	0.1008	1.78	12.34	289.46	216.83	1977.84	120.27	1558.98	3312.04	209.51	293.92	1.24	5348.20	109.65	0.21
471	4710	0.1055	1.72	10.71	287.24	195.32	1839.02	119.28	1400.96	2932.60	189.67	252.49	1.22	4360.09	102.66	0.18
472	4720	0.106	2.07	9.66	344.75	226.05	1783.25	117.31	777.33	3518.98	195.94	308.10	1.10	3315.71	125.51	0.21
473	4730	0.1022	2.08	14.57	351.47	219.93	1748.78	112.53	552.63	3586.54	191.17	291.19	1.15	3334.19	120.94	0.20
474	4740	0.1026	2.76	11.29	458.14	283.87	1965.17	109.21	263.16	7891.28	227.77	412.90	1.15	5276.14	170.49	0.36
475	4750	0.1036	2.18	12.81	357.35	224.25	1966.20	107.82	248.27	6839.93	213.90	315.60	1.59	5321.08	122.21	0.34
476	4760	0.1069	2.00	15.27	322.90	224.99	1937.79	107.85	308.03	5157.10	198.78	308.32	1.42	4569.83	119.37	0.26
477	4770	0.1027	2.41	12.48	370.75	264.09	2066.70	101.21	272.00	6205.49	211.59	361.29	1.46	4903.45	144.85	0.29
478	4780	0.1053	2.28	17.36	370.74	259.63	1971.70	103.24	289.63	5830.68	208.98	337.83	1.45	4478.79	138.94	0.24
479	4790	0.1011	1.69	15.50	269.37	190.01	1728.84	102.86	674.32	3423.56	180.97	241.53	1.36	3781.82	90.25	0.14
480	4800	0.1097	1.67	12.85	268.04	197.59	1669.25	104.37	681.57	3287.61	175.37	246.65	1.35	4069.08	95.32	0.15
481	4810	0.1007	2.05	13.67	291.35	199.91	1508.44	17.05	294.38	3731.97	167.08	267.10	1.33	3947.67	117.41	0.24
482	4820	0.1022	1.93	11.37	278.08	192.91	1571.91	17.12	261.62	3404.75	167.03	228.83	1.46	3949.77	108.13	0.21
483	4830	0.1002	1.57	15.03	246.38	176.61	1460.16	16.89	270.88	2673.44	153.51	205.44	1.48	3966.70	90.40	0.20
484	4840	0.1068	2.30	9.80	320.39	238.44	1618.73	16.60	921.67	3893.90	176.11	310.61	1.86	5813.39	138.16	0.24
485	4850	0.1022	2.08	9.49	284.65	218.25	1745.06	36.39	1438.35	3391.51	180.44	252.34	2.24	6169.49	109.11	0.20
486	4860	0.1016	2.16	12.57	296.83	238.53	1817.16	27.58	1306.05	3543.66	194.39	258.80	2.48	5549.49	121.77	0.23
487	4870	0.1012	2.07	10.32	274.48	218.49	1715.28	20.10	467.17	3337.00	178.75	248.12	2.62	4254.27	103.86	0.22
488	4880	0.1036	1.87	16.34	256.27	223.56	1691.42	35.93	296.53	3673.91	188.21	245.28	2.23	4007.53	100.29	0.21
489	4890	0.1003	2.56	10.39	343.56	291.87	1679.22	24.44	779.21	3656.00	193.17	280.82	2.02	5518.51	135.90	0.22
490	4900	0.1077	2.50	11.27	321.91	300.96	1622.34	52.75	907.16	3229.62	190.93	281.78	1.81	4586.46	136.23	0.22
491	4910	0.1008	1.91	10.17	240.76	240.68	1655.66	55.42	1042.96	3183.21	183.37	226.55	2.00	5614.87	100.46	0.21
492	4920	0.1059	1.94	9.34	239.81	249.58	1706.65	81.63	1183.37	3785.05	203.46	216.62	2.22	5614.04	91.79	0.22
493	4930	0.1035	2.26	8.26	274.59	319.06	1728.85	25.51	1976.78	3663.02	237.12	248.93	2.39	7667.52	114.37	0.22
494	4940	0.1008	3.20	4.44	404.55	453.03	1691.99	13.67	2258.25	3964.44	263.37	311.92	2.45	6474.87	159.41	0.26
495	4950	0.1028	1.88	8.23	228.76	288.69	1437.00	11.14	2667.12	2657.77	230.21	188.62	2.31	7853.53	89.71	0.18
496	4960	0.1045	1.71	9.16	224.00	280.03	1160.91	12.32	1402.08	2584.16	191.31	199.64	2.46	4894.58	88.18	0.17
497	4970	0.1047	1.86	12.95	247.00	280.74	956.81	10.71	586.66	2769.70	151.89	197.65	2.23	3041.02	97.58	0.15
498	4980	0.1041	1.67	8.01	225.84	268.35	809.44	11.60	212.24	2532.88	129.34	179.03	2.19	2023.36	88.96	0.14
499	4990	0.1057	1.37	5.84	192.59	277.24	793.50	8.05	115.73	1879.51	181.43	148.24	1.41	1585.73	72.80	0.17
500	5000	0.1003	1.48	9.73	220.75	407.51	1019.31	7.13	94.52	1796.77	305.06	158.55	1.13	2337.90	83.54	0.24
501	5010	0.1061	1.09	5.03	162.88	503.05	1126.51	5.43	110.01	952.10	507.49	105.92	1.45	3119.43	53.35	0.33
502	5020	0.1074	3.67	10.71	338.26	875.33	2827.44	13.93	546.55	5244.44	311.28	398.24	8.95	6622.61	139.80	1.12
503	5030	0.1015	2.41	10.81	229.35	618.79	2980.23	17.68	380.37	3340.12	343.87	291.71	10.48	4284.18	93.29	0.81
504	5140	0.1043	2.48	13.48	284.04	248.32	2064.07	69.51	1146.97	5789.22	120.93	279.29	2.75	7300.08	102.39	0.48
505	5150	0.1055	2.22	13.30	265.65	236.04	2117.27	15.55	589.90	8592.75	219.67	305.38	2.14	8726.80	88.88	0.39
506	5160	0.1006	2.29	15.01	326.86	267.82	2149.85	9.55	321.63	8236.86	237.21	297.71	1.85	6892.05	107.80	0.50
507	5170	0.1042	2.42	20.88	314.48	259.12	2314.93	8.74	227.37	9795.90	112.25	334.20	1.97	7032.38	108.54	0.52
508	5180	0.1041	2.06	18.10	273.36	215.08	2169.18	10.11	175.38	10196.64	97.72	281.42	1.58	6821.72	95.01	0.50
509	5190	0.1063	2.08	20.66	301.54	221.67	2141.29	9.77	166.53	9557.64	246.68	293.70	1.37	7852.53	102.66	0.44
510	5200	0.1032	2.15	33.10	313.92	221.61	2251.64	8.21	182.83	7660.14	407.51	290.02	1.68	7782.15	101.18	0.41
511	5210	0.1055	2.80	12.26	363.83	258.61	2349.52	8.59	161.29	8518.66	189.02	350.14	1.78	6103.61	125.68	0.48
512	5220	0.1089	2.33	15.80	288.35	216.53	2267.53	9.43	159.08	7326.69	102.14	318.93	1.46	4649.22	106.06	0.41
513	5230	0.106	2.35	22.82	293.82	210.66	2304.93	12.09	192.41	7816.43	199.25	306.57	1.53	6083.19	105.46	0.40
514	5240	0.1044	2.01	11.40	265.65	186.84	2233.79	11.93	235.92	6416.35	156.87	262.13	1.77	6587.85	92.77	0.36
515	5250	0.1072	2.40	16.86	297.89	204.80	2332.98	12.52	209.52	7223.58	203.53	296.08	1.72	6944.22	109.56	0.42
516	5260	0.1037	1.95	11.39	244.76	172.47	2231.90	16.96	200.89	6797.20	205.97	269.88	2.16	6999.00	89.59	0.37
517	5270	0.103	2.37	10.97	289.79	198.10	2270.89	10.21	174.55	7027.14	170.77	309.15	1.67	6065.75	104.98	0.42
518	5280	0.105	2.25	14.34	295.00	201.62	2362.65	7.69	168.28	6644.95	193.67	303.65	1.68	5239.37	110.32	0.43
519	5290	0.1011	2.34	10.40	298.57	207.20	2321.36	7.42	203.60	5703.62	249.42	317.92	1.67	5698.15	112.55	0.45
520	5300	0.102	2.39	15.55	301.41	204.05	2349.21	10.02	172.82	4764.72	241.29	307.87	3.02	4364.92	111.64	0.42
521	5310	0.1061	1.90	13.48	251.17	172.99	2291.33	8.80	181.70	4129.38	160.28	281.58	1.36	4059.92	93.67	0.38
522	5320	0.1052	2.00	10.92	252.73	180.77	2386.48	10.19	177.64	5223.76	158.76	294.99	1.61	4974.44	98.98	0.43
523	5330	0.107	1.80	11.10	224.89	168.21	2454.19	8.70	187.64	4729.84	168.55	274.76	1.60	4646.90	87.76	0.44
524	5340	0.1077	2.63	12.19	318.29	224.52	2641.53	10.31	170.27	5932.98	144.32	348.27	1.36	4264.37	120.69	0.56
525	5350	0.1037	2.72	14.02	326.68	234.57	2688.63	8.82	179.92	6155.24	157.56	365.31	1.38	5026.60	129.87	0.59
526	5360	0.1022	2.20	10.04	255.23	200.04	2612.63	7.33	193.80	6094.39	154.24	329.85	1.53	6838.17	108.13	0.53
527	5370	0.1025	2.14	10.13	248.00	181.99	2642.06	7.82	164.55	5745.22	140.38	294.38	1.28	4152.48	94.61	0.46
528	5380	0.1019	2.23	11.57	268.87	193.59	2686.17	14.96	184.56	5587.74	136.05	301.96	1.28	4657.68	107.70	0.49
529	5390	0.1017	2.23	9.66	258.97	199.20	2677.95	13.10	185.15	4362.49	145.36	318.38	1.32	4747.22	109.02	0.50
530	5400	0.1031	2.70	11.50	337.07	260.42	2845.95	17.19	262.11	5252.69	155.24	410.37	1.87	6256.62	143.45	0.58
531	5410	0.1022	2.11	10.18	270.82	212.12	2820.13	15.29	215.16	4334.60	153.12	315.66	1.39	4396.25	118.24	0.53
532	5420	0.1046	2.86	9.71	341.15	273.87	2899.40	15.00	196.17	5208.91	161.29	398.66	1.37	4831.16	151.78	0.66
533	5430	0.1055	2.12	12.25	260.78	216.96	2610.36	16.03	207.17	3835.91	148.52	331.26	1.29	4173.34	123.04	0.52
534	5440	0.1014	2.23	11.34	273.38	225.61	2633.10	14.83	215.93	4507.80	161.17	342.20	1.34	4676.76	127.35	0.54
535	5450	0.1042	2.30	9.49	269.18	238.47	2627.79	13.90	230.89	3340.45	156.33	348.04	1.31	3998.05	132.41	0.54
536	5460	0.1026	2.18	10.10	281.51	245.88	2757.93	14.38	264.13	4315.85	156.78	352.57	1.40	4851.89	142.40	0.63
537	5470	0.1026	2.03	9.93	242.12	206.40	2684.42	16.36	254.39	5183.88	155.45	323.86	1.34	5838.68	125.73	0.60
538	5480	0.1034	2.15	10.46	260.22	216.07	2651.64	13.59	170.49	5210.90	156.30	327.49	1.30	4607.01	118.11	0.59
539	5490	0.1024	2.15	14.12	268.53	223.24	2555.18	14.39	188.69	4803.53	155.73	313.10	1.36	5559.95	117.83	0.56
540	5500	0.1036	2.71	12.18	343.33	276.20	2656.49	23.35	177.55	5359.19	171.04	374.88	1.31	5077.59	141.45	0.60
541	5510	0.102	2.15	13.08	268.85	220.85	2465.73	34.19	152.94	4474.58	154.32	306.59	1.45	4768.66	112.12	0.61
542	5520	0.1029	1.94	2.99	234.25	200.20	2367.52	34.97	149.48	4439.94	154.31	273.62	1.61	4298.79	95.63	0.56
543	5530	0.1021	2.06	5.30	245.64	214.03	2472.57	37.52	153.40	4803.09	150.66	294.63	1.61	4725.17	107.96	0.60
544	5540	0.1026	2.54	4.05	294.06	260.56	2457.54	42.96	154.98	5273.54	155.36	355.94	1.46	5078.53	137.77	0.68
545	5550	0.1028	2.20	3.08	256.06	237.66	2451.86	41.96	183.19	4162.33	149.83	340.10	1.64	4468.01	118.04	0.60
546	5560	0.1047	2.05	8.32	236.51	220.28	2400.46	35.64	249.91	3220.80	150.52	292.71	1.38	5343.14	105.93	0.57
547	5570	0.1053	2.51	3.08	285.77	273.68	2428.79	43.88	353.50	4479.06	156.49	356.21	1.44	4465.00	135.38	0.76
548	5580	0.1067	2.43	6.64	280.14	280.17	2456.37	40.19	362.09	3801.62	159.11	349.18	1.38	4127.00	133.55	0.65
549	5590	0.105	1.94	6.48	225.36	241.80	2219.33	38.31	268.83	2963.25	144.03	326.72	1.53	3542.85	109.59	0.57
550	5600	0.1013	1.94	5.14	205.75	209.96	2149.68	53.98	845.20	2293.79	145.13	262.44	1.78	4947.43	95.84	0.44
551	5610	0.1037	2.14	6.23	243.18	255.89	2204.28	39.08	378.62	3031.31	141.64	307.16	1.79	4001.06	116.00	0.51
552	5620	0.1051	2.25	3.29	266.55	277.91	2290.87	41.53	426.18	7220.72	152.55	362.05	1.99	6834.91	128.48	0.61
553	5630	0.1085	2.43	4.96	298.00	278.76	2235.15	29.24	381.81	8492.32	143.07	413.43	2.02	8998.77	137.28	0.68
554	5640	0.1042	2.82	9.54	364.64	387.22	2712.28	38.86	375.75	17733.93	192.54	520.69	2.13	14078.91	160.87	0.94
555	5650	0.1058	2.42	3.97	310.30	346.04	2494.66	30.39	271.61	13912.39	182.33	429.81	1.80	10844.34	147.14	1.02
556	5660	0.1037	2.14	13.35	266.27	325.60	2313.52	32.82	326.74	12078.21	183.61	390.78	1.81	11035.07	121.28	0.79
557	5670	0.1056	2.10	21.60	252.85	308.70	2121.84	31.49	368.66	8284.19	177.83	359.40	1.47	9703.22	114.83	0.70
558	5680	0.1075	1.93	8.61	239.91	312.60	1865.76	29.81	233.42	7919.52	171.55	358.01	1.56	8413.10	109.20	0.90
559	5690	0.1015	2.24	9.57	289.37	562.19	1996.85	28.61	271.27	3923.96	256.34	415.55	1.31	6438.39	124.33	0.75
560	5700	0.1061	1.86	13.35	238.16	432.17	1880.66	29.03	327.65	2406.96	234.54	377.24	1.48	6556.20	100.98	0.59
561	5710	0.107	1.91	4.36	232.36	471.66	1936.72	29.38	254.41	2372.12	203.20	390.20	1.98	4979.38	104.54	0.62
562	5720	0.1021	2.81	13.52	298.00	419.44	2627.27	44.44	249.12	2946.66	208.33	435.63	1.58	5747.67	142.37	0.84
563	5730	0.1058	2.56	11.02	274.41	386.56	2754.77	43.18	284.08	2808.59	177.33	424.45	1.78	4967.98	131.85	0.73
564	5740	0.1054	3.57	11.84	345.19	467.86	3110.01	44.96	277.84	3787.83	190.01	487.56	1.75	5652.75	176.45	0.91
565	5750	0.1016	3.44	10.53	334.11	467.76	2952.78	43.74	245.68	3930.14	187.34	490.09	1.74	5506.01	173.86	1.01
566	5760	0.1056	3.27	9.19	298.30	419.13	3032.25	44.94	263.55	3747.88	176.33	458.82	1.69	4486.69	150.18	0.93
567	5770	0.1039	3.89	9.93	373.14	530.30	2942.13	38.39	279.89	4964.22	187.97	526.17	1.79	5674.10	187.52	1.15
568	5780	0.1018	3.40	10.14	300.66	433.44	2993.77	42.20	339.80	4882.92	177.90	462.39	1.92	5182.68	157.08	0.99
569	5790	0.1058	3.96	8.66	355.90	520.63	3028.58	40.12	400.17	4384.85	180.50	526.77	1.79	5041.31	184.62	1.08
570	5800	0.1012	3.14	10.10	285.81	400.92	2762.30	39.85	384.12	3177.19	170.99	411.99	1.67	4938.39	140.12	0.75
571	5810	0.1034	2.22	3.01	278.35	244.13	2835.82	36.20	342.42	2338.09	173.67	394.75	1.80	4760.33	184.46	0.79
572	5820	0.1085	2.22	3.72	286.98	244.78	2705.79	53.05	280.93	2371.67	165.43	397.80	1.77	4805.93	199.22	0.81
573	5830	0.1067	2.02	3.64	271.05	229.80	2811.05	54.22	311.57	2367.16	168.03	387.63	1.86	5033.46	183.26	0.76
574	5840	0.1047	1.96	5.95	271.63	246.77	2585.22	51.13	284.40	2607.49	156.94	413.59	1.81	5003.63	185.56	0.87
575	5850	0.1021	2.27	3.35	295.77	235.81	2677.66	51.91	572.64	2706.07	171.12	383.28	1.74	5658.57	203.06	0.81
576	5860	0.1084	2.38	3.77	321.05	260.02	2753.79	55.02	500.18	2772.37	184.67	424.66	1.67	6014.51	238.40	0.85
577	5870	0.1215	2.71	9.04	330.98	252.48	3014.14	25.40	350.95	2970.13	181.43	433.42	1.89	4714.02	245.20	0.94
578	5880	0.1324	2.23	5.91	273.43	244.21	3099.71	21.47	456.54	3040.67	170.61	406.27	1.88	4718.33	213.38	0.93
579	5890	0.1064	1.95	7.35	241.21	216.01	3183.84	27.36	500.66	2638.26	168.60	369.68	1.82	4112.34	184.43	0.84
580	5900	0.105	2.06	3.77	268.59	327.12	3159.61	24.72	464.43	2745.58	187.84	433.12	1.91	5363.03	208.50	0.84
581	5910	0.1033	1.87	4.27	234.21	228.99	3029.50	24.79	613.34	1758.11	159.31	363.50	1.67	4863.28	180.26	0.69
582	5920	0.1079	2.11	4.75	274.63	253.37	3103.31	25.53	628.12	2067.24	174.09	439.04	2.11	5046.17	229.37	0.79
583	5930	0.1087	2.36	3.17	293.16	263.74	3182.38	22.63	575.49	2350.93	177.81	406.05	2.06	4976.40	253.97	0.87
584	5940	0.1314	2.14	1.76	262.31	257.10	3218.36	20.41	704.83	2249.50	176.14	439.10	1.62	4916.68	230.25	0.96
585	5950	0.1106	2.43	6.04	298.98	269.71	3123.95	26.31	682.92	2897.25	172.76	464.24	1.54	5605.79	274.56	1.05
586	5960	0.1007	1.87	3.90	245.78	225.73	3132.03	27.78	526.78	2420.82	178.92	374.60	1.51	5296.45	208.33	0.90
587	5970	0.1081	1.80	1.95	245.61	245.12	2918.94	24.41	743.22	2602.29	170.85	393.19	1.54	6574.85	211.26	0.86
588	5980	0.1051	2.76	2.70	387.05	337.47	3288.75	26.59	996.20	2913.08	198.55	510.29	1.76	6065.61	353.87	1.07
589	5990	0.1033	1.88	3.45	272.98	260.48	2902.54	20.59	1005.49	2043.91	170.21	428.55	1.62	5428.83	235.65	0.80
590	6000	0.1178	1.97	2.93	254.90	236.66	3018.84	19.64	795.49	1902.14	172.91	453.55	1.67	4617.81	222.55	0.80
591	6010	0.1028	2.23	3.82	297.66	245.14	2863.62	19.81	571.45	2049.86	175.01	417.94	1.40	4293.06	262.54	0.74
592	6020	0.1037	1.85	2.04	260.85	284.75	2833.09	20.73	561.89	1923.69	170.64	402.42	1.48	5237.33	212.19	0.70
593	6030	0.1179	1.90	2.25	290.39	289.65	2963.70	29.84	682.18	2334.17	174.15	441.47	1.60	5639.02	244.69	0.83
594	6040	0.1075	2.07	3.06	288.71	234.54	2920.55	25.66	852.16	3039.31	175.83	402.77	1.47	5461.14	269.39	0.94
595	6050	0.125	1.74	3.11	252.38	269.23	2885.98	18.66	548.98	2825.52	158.08	407.60	1.54	5371.88	211.71	0.85
596	6060	0.1013	2.26	3.54	330.04	309.50	2988.15	20.11	565.95	3369.60	180.77	459.91	1.74	5816.98	287.29	1.01
597	6070	0.1374	1.83	1.52	245.38	246.09	3007.12	17.52	691.14	2556.03	176.62	410.01	1.83	5179.88	209.23	0.81
598	6080	0.1077	2.38	2.46	321.74	298.78	3318.01	21.76	576.19	2935.68	191.03	466.09	1.89	5160.27	273.24	0.96
599	6090	0.105	1.96	4.06	275.21	231.88	3063.09	21.06	548.66	2851.82	171.99	383.92	1.57	5213.18	223.66	0.82

	Depth (mm)	Sed. (ICPMS)	Ni 60		Cu 63		Zn 66		As 75		Se 82		Sr 88		Ag 109		Cd 111		Ba 137		Hg 202		Tl 205		Pb 207		Bi 209		U 238	
450	4500	0.1021	0.20	1.55	24.21	103.87	0.41	5.58	0.34	-0.15	27.54	0.35	0.75	1.13	0.03	0.21														
451	4510	0.1007	0.11	1.05	18.14	95.44	0.38	4.93	0.36	-0.15	32.57	0.34	0.59	1.47	0.02	0.21														
452	4520	0.1016	0.15	1.48	19.25	92.98	0.41	5.05	0.43	-0.15	31.36	0.31	0.82	1.18	0.03	0.26														
453	4530	0.1064	0.29	1.09	18.80	136.12	0.59	5.27	0.41	-0.15	37.62	0.35	0.59	1.24	0.04	0.19														
454	4540	0.1027	0.16	1.69	20.23	163.19	0.57	5.58	0.51	-0.14	37.42	0.34	1.05	1.46	0.04	0.31														
455	4550	0.1031	0.13	1.46	17.86	144.65	0.51	4.94	0.45	-0.15	38.72	0.31	0.83	1.28	0.05	0.30														
456	4560	0.101	0.19	1.84	21.94	112.42	0.66	5.71	0.43	-0.13	37.82	0.36	1.11	1.53	0.05	0.36														
457	4570	0.1046	0.16	1.60	18.29	110.88	0.42	5.32	0.53	-0.11	37.75	0.51	0.81	1.52	0.06	0.33														
458	4580	0.1047	0.14	1.63	18.28	74.88	0.40	5.70	0.50	-0.14	45.14	0.40	0.73	1.67	0.06	0.36														
459	4590	0.102	0.21	0.89	12.01	88.66	0.48	5.27	0.51	-0.16	49.24	0.41	0.45	1.95	0.07	0.29														
460	4600	0.1017	0.10	0.92	13.83	88.60	0.49	5.10	0.47	-0.16	45.65	0.36	0.37	1.57	0.05	0.27														
461	4610	0.1005	0.47	1.35	12.73	79.88	0.46	4.69	0.40	-0.18	47.29	0.32	0.34	1.38	0.05	0.29														
462	4620	0.1017	0.15	1.57	19.88	100.78	0.49	5.37	0.25	-0.14	49.47	0.31	0.50	1.51	0.05	0.32														
463	4630	0.1006	0.19	1.48	24.33	110.25	0.52	5.52	0.27	-0.13	44.68	0.29	0.65	1.58	0.05	0.34														
464	4640	0.101	0.15	1.83	26.50	137.20	0.42	5.32	0.24	-0.13	45.24	0.32	0.71	1.44	0.05	0.31														
465	4650	0.1014	0.16	1.74	24.23	199.59	0.55	4.69	0.36	-0.12	39.58	0.34	1.14	1.58	0.05	0.36														
466	4660	0.1014	0.18	1.41	26.29	240.25	0.46	5.36	0.30	-0.13	41.81	0.34	0.82	1.48	0.05	0.31														
467	4670	0.1011	0.21	1.34	34.42	251.50	0.44	6.15	0.34	-0.15	47.24	0.38	0.60	1.38	0.08	0.31														
468	4680	0.1013	0.12	1.92	23.33	200.23	0.47	4.70	0.42	-0.14	31.98	0.39	0.49	1.30	0.06	0.36														
469	4690	0.1076	0.15	1.45	26.72	104.38	0.44	5.71	0.37	-0.16	38.64	0.53	0.25	1.58	0.06	0.33														
470	4700	0.1008	0.13	0.87	20.80	73.37	0.45	5.48	1.02	-0.17	42.31	1.09	0.22	1.65	0.06	0.31														
471	4710	0.1055	0.18	0.82	18.93	71.13	0.36	4.87	0.35	-0.16	40.62	0.44	0.23	1.59	0.05	0.28														
472	4720	0.106	0.14	1.12	23.42	99.09	0.43	5.12	0.34	-0.17	38.04	0.42	0.24	1.43	0.05	0.29														
473	4730	0.1022	0.13	1.26	22.37	92.78	0.38	4.73	0.36	-0.17	37.09	0.44	0.28	1.37	0.04	0.29														
474	4740	0.1026	0.28	1.95	33.90	211.02	0.53	5.67	0.36	-0.11	36.59	0.45	0.71	1.36	0.06	0.39														
475	4750	0.1036	0.39	1.91	23.95	202.97	0.56	5.13	0.45	-0.11	42.94	0.56	0.74	1.73	0.08	0.40														
476	4760	0.1069	0.21	1.47	20.27	183.48	0.47	4.95	0.32	-0.14	43.40	0.63	0.48	1.68	0.07	0.36														
477	4770	0.1027	0.29	1.75	24.04	183.62	0.53	5.72	0.29	-0.13	49.32	0.48	0.53	1.71	0.07	0.38														
478	4780	0.1053	0.36	2.70	23.47	144.16	0.45	5.54	0.30	-0.15	48.49	0.59	0.43	1.61	0.07	0.43														
479	4790	0.1011	0.14	1.27	14.64	110.62	0.48	4.22	0.32	-0.17	37.60	0.56	0.25	1.81	0.06	0.35														
480	4800	0.1097	0.15	0.98	16.08	148.48	0.47	4.49	0.29	-0.15	43.60	0.73	0.23	1.73	0.06	0.28														
481	4810	0.1007	0.84	1.91	19.57	236.79	0.54	4.84	0.62	-0.11	36.52	0.49	0.45	1.69	0.18	0.38														
482	4820	0.1022	0.26	1.73	18.65	190.64	0.53	4.51	0.81	-0.11	36.71	0.43	0.44	1.88	0.15	0.39														
483	4830	0.1002	0.22	1.20	16.68	266.77	0.59	4.22	0.86	-0.12	37.68	0.36	0.33	1.73	0.15	0.27														
484	4840	0.1068	0.39	1.47	26.77	201.88	0.59	5.90	0.78	-0.12	43.00	0.50	0.42	2.19	0.16	0.36														
485	4850	0.1022	0.47	1.71	20.14	162.65	0.71	5.62	0.90	-0.11	45.56	0.56	0.48	2.19	0.16	0.44														
486	4860	0.1016	0.66	1.68	24.46	172.27	0.70	5.27	0.81	-0.11	43.61	0.64	0.67	2.52	0.17	0.49														
487	4870	0.1012	0.43	2.06	23.27	219.55	0.78	5.43	0.98	-0.11	51.73	0.60	0.61	1.92	0.17	0.48														
488	4880	0.1036	0.51	2.79	24.04	184.82	0.57	4.96	0.98	-0.09	48.64	0.65	0.55	2.01	0.17	0.55														
489	4890	0.1003	0.66	1.49	30.23	177.18	0.68	5.76	0.90	-0.11	48.28	0.58	0.41	2.34	0.17	0.37														
490	4900	0.1077	0.39	1.20	30.00	229.59	0.71	5.41	0.91	-0.11	44.47	0.65	0.34	2.09	0.17	0.35														
491	4910	0.1008	0.34	2.08	21.03	337.75	0.78	5.26	1.13	-0.11	48.21	0.82	0.51	2.43	0.20	0.50														
492	4920	0.1059	0.36	2.62	20.45	313.73	0.96	5.42	1.22	-0.06	55.95	1.37	0.97	2.56	0.22	0.62														
493	4930	0.1035	0.38	2.48	22.47	270.12	0.85	5.74	1.49	-0.08	57.17	1.48	0.77	2.53	0.22	0.59														
494	4940	0.1008	0.74	2.63	31.37	195.23	0.93	5.78	1.36	-0.07	51.04	0.96	0.72	2.45	0.22	0.61														
495	4950	0.1028	0.21	2.54	16.02	342.47	0.97	4.77	1.12	-0.10	53.72	0.99	0.48	2.28	0.24	0.58														
496	4960	0.1045	0.22	2.76	17.01	389.69	1.13	4.43	1.47	-0.11	42.85	0.95	0.35	1.93	0.25	0.55														
497	4970	0.1047	0.15	2.53	16.15	400.26	1.06	4.22	1.47	-0.10	37.41	0.81	0.30	1.58	0.25	0.49														
498	4980	0.1041	0.25	2.30	16.01	412.29	1.07	3.82	1.41	-0.11	34.83	0.75	0.28	1.41	0.25	0.40														
499	4990	0.1057	0.11	1.60	13.84	249.26	0.68	2.88	1.11	-0.10	33.24	0.49	0.28	1.32	0.25	0.32														
500	5000	0.1003	0.11	1.32	17.39	194.91	0.49	2.84	0.86	-0.13	43.21	0.32	0.32	1.12	0.26	0.24														
501	5010	0.1061	0.35	1.09	9.54	94.87	0.31	2.64	0.64	-0.12	71.76	0.21	0.32	1.32	0.32	0.19														
502	5020	0.1074	4.35	2.57	42.57	66.58	0.36	5.03	0.56	-0.05	64.81	0.18	0.28	2.79	0.12	0.16														
503	5030	0.1015	4.51	12.13	81.68	42.23	0.33	4.10	0.51	-0.09	61.44	0.12	0.27	2.40	0.11	0.13														
504	5140	0.1043	0.79	2.98	21.00	280.91	1.02	6.14	1.15	-0.09	45.75	0.85	0.64	3.51	0.13	0.40														
505	5150	0.1055	0.60	3.96	16.50	197.47	0.77	6.62	1.09	-0.09	47.16	0.60	0.89	1.89	0.10	0.42														
506	5160	0.1006	0.75	2.59	20.50	179.41	0.64	5.35	1.06	-0.11	41.95	0.34	1.10	1.87	0.09	0.38														
507	5170	0.1042	0.86	3.09	21.96	135.75	0.60	5.07	1.17	-0.11	52.75	0.43	0.85	1.67	0.09	0.42														
508	5180	0.1041	0.60	2.91	18.82	128.66	0.64	4.68	1.08	-0.11	50.99	0.37	0.93	1.46	0.09	0.44														
509	5190	0.1063	0.59	2.16	18.10	139.31	0.63	5.21	0.65	-0.11	46.74	0.34	1.17	1.66	0.08	0.29														
510	5200	0.1032	0.60	1.41	18.85	157.80	0.48	5.58	0.74	-0.11	49.92	0.34	1.38	1.99	0.09	0.22														
511	5210	0.1055	0.67	1.73	21.24	147.28	0.48	5.49	0.93	-0.11	46.84	0.38	0.90	1.49	0.09	0.33														
512	5220	0.1089	0.42	1.68	16.27	135.38	0.50	4.82	0.96	-0.11	45.72	0.30	0.73	1.31	0.09	0.39														
513	5230	0.106	0.46	1.57	16.32	152.33	0.60	5.64	0.84	-0.12	51.37	0.36	0.86	1.71	0.09	0.35														
514	5240	0.1044	0.49	1.51	13.38	140.94	0.49	5.20	0.93	-0.12	47.98	0.33	0.66	1.50	0.09	0.31														
515	5250	0.1072	0.50	1.53	15.53	134.09	0.61	5.53	0.81	-0.12	53.26	0.33	0.76	1.64	0.09	0.36														
516	5260	0.1037	0.66	1.68	12.29	133.94	0.56	5.38	0.94	-0.11	52.72	0.38	0.79	1.75	0.09	0.39														
517	5270	0.103	0.49	1.90	14.35	119.21	0.51	5.22	0.78	-0.12	47.23	0.31	0.80	1.59	0.09	0.40														
518	5280	0.105	0.55	1.91	16.22	102.43	0.46	5.29	0.88	-0.11	49.52	0.30	0.75	1.66	0.10	0.40														
519	5290	0.1011	0.48	1.43	15.92	106.09	0.52	5.75	0.91	-0.12	51.84	0.32	0.69	2.06	0.11	0.35														
520	5300	0.102	1.49	1.02	16.77	80.57	0.44	5.64	0.91	-0.12	52.49	0.37	0.57	1.81	0.09	0.21														
521	5310	0.1061	0.30	1.04	12.43	67.94	0.45	5.26	0.72	-0.11	52.64	0.25	0.51	1.59	0.08	0.24														
522	5320	0.1052	0.34	1.53	13.69	65.49	0.51	5.72	0.79	-0.11	54.06	0.24	0.66	1.66	0.08	0.36														
523	5330	0.107	0.38	1.59	13.91	56.53	0.40	5.58	0.68	-0.12	58.16	0.25	0.62	1.77	0.08	0.34														
524	5340	0.1077	0.50	1.79	19.23	58.61	0.52	6.33	0.62	-0.10	52.94	0.25	0.76	1.69	0.08	0.40														
525	5350	0.1037	0.48	1.60	19.06	71.41	0.49	6.71	0.78	-0.11	59.91	0.21	0.64	1.75	0.08	0.39														
526	5360	0.1022	0.45	1.51	15.81	74.28	0.48	6.46	0.78	-0.11	58.28	0.25	0.61	1.75	0.09	0.38														
527	5370	0.1025	0.27	1.71	14.89	56.53	0.36	6.00	0.85	-0.12	57.65	0.24	0.59	1.68	0.09	0.44														
528	5380	0.1019	0.28	1.69	16.03	62.91	0.45	6.32	0.68	-0.11	58.50	0.28	0.60	1.57	0.09	0.38														
529	5390	0.1017	2.40	1.59	16.41	58.05	0.48	6.17	0.66	-0.13	58.66	0.30	0.51	1.60	0.08	0.33														
530	5400	0.1031	0.63	1.78	21.41	97.32	0.58	6.78	0.65	-0.12	61.33	0.35	0.57	1.90	0.09	0.33														
531	5410	0.1022	0.40	1.69	16.48	48.59	0.51	5.98	0.61	-0.12	61.09	0.25	0.55	1.67	0.09	0.35														
532	5420	0.1046	0.43	1.69	21.99	53.99	0.55	6.62	0.54	-0.10	58.08	0.25	0.54	1.58	0.12	0.38														
533	5430	0.1055	0.36	1.34	15.70	45.05	0.50	5.90	0.72	-0.12	58.50	0.24	0.46	1.59	0.08	0.32														
534	5440	0.1014	0.34	1.48	17.21	56.55	0.55	6.13	0.55	-0.12	55.52	0.26	0.49	1.62	0.08	0.33														
535	5450	0.1042	0.32	1.26	17.18	43.79	0.56	6.22	0.50	-0.10	61.85	0.22	0.43	1.70	0.08	0.27														
536	5460	0.1026	0.39	1.80	19.86	47.67	0.56	6.43	0.54	-0.11	64.59	0.23	0.59	1.74	0.08	0.35														
537	5470	0.1026	1.08	1.75	16.83	57.25	0.47	5.92	0.71	-0.12	61.37	0.23	0.60	1.59	0.09	0.36														
538	5480	0.1034	0.37	1.77	18.96	45.90	0.47	5.89	0.64	-0.13	57.10	0.24	0.61	1.50	0.08	0.39														
539	5490	0.1024	0.32	1.45	18.80	49.98	0.44	5.84	0.53	-0.13	61.28	0.25	0.57	1.56	0.08	0.31														
540	5500	0.1036	0.41	1.43	23.58	61.57	0.41	6.50	0.72	-0.12	57.19	0.29	0.58	1.49	0.07	0.32														
541	5510	0.102	0.42	1.52	18.48	47.77	0.48	5.81	0.65	-0.13	55.70	0.24	0.55	1.46	0.08	0.35														
542	5520	0.1029	0.48	1.60	16.40	48.22	0.46	5.18	0.62	-0.12	52.94	0.24	0.62	1.44	0.07	0.36														
543	5530	0.1021	0.44	2.14	20.29	53.65	0.56	5.66	0.52	-0.12	58.38	0.26	0.74	1.63	0.08	0.38														
544	5540	0.1026	0.55	1.64	21.72	51.60	0.56	5.82	0.55	-0.11	52.93	0.25	0.64	1.46	0.08	0.35														
545	5550	0.1028	0.63	1.63	19.14	46.14	0.44	5.93	0.48	-0.12	57.46	0.26	0.62	1.52	0.07	0.34														
546	5560	0.1047	0.37	1.49	18.45	45.65	0.45	5.56	0.48	-0.13	59.73	0.26	0.47	1.40	0.07	0.32														
547	5570	0.1053	0.48	1.45	21.63	44.86	0.49	6.01	0.52	-0.09	52.47	0.29	0.69	1.63	0.07	0.39														
548	5580	0.1067	0.45	1.69	20.75	40.67	0.55	6.06	0.62	-0.10	57.46	0.25	0.50	1.52	0.07	0.36														
549	5590	0.105	0.44	1.79	17.30	33.24	0.48	5.79	0.79	-0.14	51.01	0.27	0.43	1.61	0.08	0.42														
550	5600	0.1013	0.33	1.28	13.71	50.77	0.53	5.48	1.19	-0.14	57.77	0.39	0.34	1.93	0.09	0.31														
551	5610	0.1037	0.36	1.68	15.44	50.72	0.69	6.06	1.44	-0.14	62.77	0.54	0.30	1.74	0.09	0.37														
552	5620	0.1051	0.51	3.23	19.33	83.32	0.77	6.20	1.45	-0.13	55.40	0.70	0.43	1.78	0.09	0.59														
553	5630	0.1085	0.62	3.37	20.65	136.02	0.94	6.91	1.09	-0.12	57.70	0.61	0.68	1.78	0.07	0.55														
554	5640	0.1042	0.77	3.61	25.52	174.03	1.01	7.69	1.43	-0.10	56.14	0.57	1.21	1.92	0.08	0.49														
555	5650	0.1058	0.77	4.53	24.90	124.33	0.72	7.03	0.90	-0.08	53.23	0.42	1.04	1.72	0.07	0.49														
556	5660	0.1037	0.59	4.05	20.70	122.16	0.65	7.24	1.02	-0.13	62.49	0.35	0.58	1.44	1.73	0.35														
557	5670	0.1055	0.45	2.64	17.70	111.34	0.52	6.49	0.98	-0.13	63.80	0.30	0.35	1.23	0.07	0.28														
558	5680	0.1076	0.59	1.87	19.59	70.47	0.46	5.39	0.74	-0.09	49.67	0.20	0.73	1.52	0.07	0.32														
559	5690	0.1015	0.53	1.26	20.12	39.74	0.36	6.03	0.41	-0.14	58.73	0.14	0.37	1.47	0.10	0.19														
560	5700	0.1061	0.43	1.04	15.91	42.14	0.31	5.43	0.45	-0.13	58.91	0.14	0.36	1.47	0.10	0.15														
561	5710	0.107	0.73	1.16	17.10	31.21	0.31	5.45	0.47	-0.14	54.36	0.12	0.28	1.31	0.09	0.19														
562	5720	0.1021	0.47	1.89	21.68	30.45	0.48	7.20	0.69	-0.12	76.78	0.24	0.41	1.98	0.09	0.33														
563	5730	0.1058	0.53	2.01	19.07	37.23	0.57	6.98	0.66	-0.14	71.18	0.34	0.22	1.81	0.09	0.38														
564	5740	0.1054	0.58	2.22	23.38	35.52	0.69	8.09	0.55	-0.14	83.11	0.42	0.27	2.01	0.09	0.46														
565	5750	0.1016	0.60	2.70	26.22	36.86	0.58	8.05	0.90	-0.10	80.10	0.36	0.46	2.13	0.09	0.51														
566	5760	0.1056	0.62	2.57	25.76	36.90	0.64	7.77	0.75	-0.09	80.46	0.31	0.49	2.22	0.09	0.51														
567	5770	0.1039	0.78	2.53	31.82	43.81	0.55	8.25	0.70	-0.09	76.19	0.31	0.59	1.96	0.08	0.48														
568	5780	0.1018	0.64	2.87	26.56	47.53	0.58	7.71	0.87	-0.09	76.44	0.32	0.58	2.04	0.08	0.53														
569	5790	0.1058	0.71	3.04	29.47	40.84	0.61	8.40	0.75	-0.11	75.03	0.32	0.46	2.07	0.08	0.53														
570	5800	0.1012	0.44	2.71	20.25	45.39	0.60	7.32	0.84	-0.15	73.74	0.28	0.27	1.92	0.08	0.48														
571	5810	0.1034	0.91	2.70	13.09	32.74	0.56	7.52	0.70	-0.13	78.43	0.28	0.65	2.28	0.09	0.48														
572	5820	0.1085	0.64	2.24	14.60	30.01	0.65	7.83	0.46	-0.12	82.26	0.35	0.58	2.05	0.09	0.41														
573	5830	0.1067	0.57	2.18	14.62	33.69	0.57	7.20	0.52	-0.13	76.67	0.36	0.58	2.02	0.09	0.43														
574	5840	0.1047	0.72	3.06	17.36	38.66	0.65	7.46	0.58	0.04	78.68	0.37	0.73	2.14	0.09	0.56														
575	5850	0.1021	0.60	2.17	13.88	37.68	0.59	7.08	0.40	-0.14	70.80	0.34	0.57	2.00	0.09	0.44														
576	5860	0.1084	0.57	1.84	13.37	45.08	0.62	8.17	0.41	-0.13	86.75	0.46	0.54	2.19	0.09	0.41														
577	5870	0.1215	0.72	2.70	15.19	44.61	0.60	7.90	0.99	-0.12	84.06	0.52	0.50	1.90	0.09	0.43														
578	5880	0.1324	0.72	3.19	17.53	36.28	0.55	7.58	0.98	-0.05	74.23	0.42	0.63	2.11	0.08	0.53														
579	5890	0.1064	0.58	3.16	19.18	35.62	0.57	7.57	1.13	-0.11	86.81	0.36	0.73	2.02	0.09	0.49														
580	5900	0.105	0.65	3.18	16.74	38.89	0.51	7.57	1.03	-0.05	89.22	0.28	0.48	1.83	0.08	0.40														
581	5910	0.1033	0.43	3.09	15.90	30.14	0.52	7.11	1.12	-0.12	96.06	0.35	0.44	1.92	0.08	0.38														
582	5920	0.1079	0.46	2.94	17.08	30.69	0.48	7.61	1.07	-0.13	114.61	0.30	0.40	1.93	0.08	0.41														
583	5930	0.1087	0.59	3.45	18.42	25.61	0.51	7.81	1.10	-0.01	150.01	0.36	0.52	2.02	0.08	0.51														
584	5940	0.1314	0.72	2.98	23.03	24.63	0.60	7.73	1.01	-0.07	76.08	0.40	0.80	1.97	0.08	0.49														
585	5950	0.1106	0.60	2.76	20.99	37.81	0.60	7.97	1.05	-0.10	77.59	0.39	0.79	2.00	0.08	0.45				

	Depth (mm)	Sed. (ICPMS)	Li 7	B 10	Na 23	Mg 24	Al 27	Si 28	P 31	S 34	K 39	Ca 43	Cr 52	Fe 54	Mn 55	Co 59
600	6100	0.1217	2.23	2.44	333.96	274.12	2722.23	17.28	424.28	3375.86	175.46	456.22	1.41	4278.28	296.27	1.06
601	6110	0.1013	2.12	5.67	296.37	246.77	2777.07	27.97	576.75	2602.22	167.49	384.96	1.43	5181.01	247.87	0.72
602	6120	0.1041	1.90	6.79	298.56	300.87	2886.36	24.44	1204.43	2529.69	158.96	426.23	1.44	7827.84	232.69	0.74
603	6130	0.1095	1.62	7.10	256.51	233.41	2702.86	19.88	1084.89	3325.84	146.70	340.02	1.40	7049.90	198.32	0.82
604	6140	0.1036	1.86	1.88	312.56	303.25	2886.40	20.46	1068.59	3448.59	159.37	460.36	1.49	6365.24	244.35	1.13
605	6150	0.111	1.82	5.54	261.66	225.46	2841.68	20.83	1318.01	2897.67	161.14	356.05	1.29	6171.56	206.58	0.86
606	6160	0.1063	1.97	8.23	299.03	244.28	2883.30	21.20	1045.31	3023.19	165.85	402.86	1.24	5550.17	223.94	0.85
607	6170	0.1101	1.63	5.10	235.05	185.51	2609.36	17.53	761.67	3506.07	144.38	328.54	1.19	4983.80	178.95	0.83
608	6180	0.1128	1.84	5.21	258.72	213.86	2733.70	18.13	809.33	2549.14	166.58	321.70	1.15	4771.78	195.45	0.69
609	6190	0.103	1.96	5.22	267.05	238.54	2837.71	26.80	698.65	2409.02	163.22	335.21	1.26	4980.98	192.25	0.70
610	6200	0.1039	2.04	6.94	300.37	267.66	2902.61	22.69	852.65	2824.41	170.77	336.64	1.29	5645.85	206.65	0.72
611	6210	0.1059	2.35	3.53	355.18	286.48	2983.27	20.00	552.83	3872.95	187.08	442.37	1.31	4817.05	262.39	1.01
612	6220	0.1105	2.30	6.75	339.27	295.91	2758.26	19.34	837.28	3341.95	174.86	385.05	1.36	6160.91	251.18	0.77
613	6230	0.1096	1.87	4.91	295.76	298.45	2549.71	19.48	696.01	2962.30	154.13	373.48	1.24	6261.83	206.96	0.71
614	6240	0.1203	1.85	4.35	295.18	278.51	2625.17	18.93	412.48	2984.58	162.59	369.07	1.42	4784.69	189.75	0.69
615	6250	0.1079	2.15	4.54	318.05	269.03	2612.43	19.60	430.02	3227.91	161.92	355.88	1.33	4887.35	212.68	0.72
616	6260	0.114	2.51	5.27	358.27	287.25	2562.96	18.15	545.29	3838.64	171.20	370.71	1.26	5305.57	249.54	0.81
617	6270	0.1067	2.80	6.36	411.54	323.59	2632.03	29.75	849.65	3950.13	178.38	390.06	1.23	5405.93	272.07	0.80
618	6280	0.1017	2.15	9.56	318.53	246.87	2458.13	28.84	664.48	3585.38	181.37	330.48	1.29	6545.51	193.11	0.66
619	6290	0.1078	2.10	4.31	300.33	253.26	2567.22	19.91	477.66	3811.82	157.17	343.76	1.34	5611.43	188.68	0.68
620	6300	0.1086	2.23	9.05	314.66	253.76	2506.57	19.42	287.16	4140.92	168.25	331.08	1.19	6062.70	185.80	0.68
621	6310	0.1005	2.01	6.60	298.09	243.56	2394.28	18.53	249.89	3805.06	155.18	324.44	1.19	5792.97	181.73	0.66
622	6320	0.1205	2.14	8.58	319.55	257.35	2426.96	16.92	332.21	4166.25	172.25	371.09	1.32	8349.84	191.18	0.64
623	6330	0.1015	2.21	8.39	335.08	269.13	2351.70	17.44	220.33	5166.57	154.06	351.43	1.19	6197.55	197.11	0.79
624	6340	0.1057	2.06	6.38	302.56	244.30	2386.28	18.05	246.99	6095.19	150.60	328.30	1.18	6872.32	175.81	0.78
625	6350	0.1025	2.03	5.74	275.19	220.09	2236.23	21.39	351.24	5011.87	153.32	327.62	1.25	7068.76	168.47	0.74
626	6360	0.1044	2.12	11.84	314.37	257.09	2457.09	22.77	699.11	4557.34	164.02	388.92	1.34	7079.33	187.40	0.71
627	6370	0.1034	2.74	3.53	388.80	331.26	2722.59	19.39	582.39	5091.37	180.42	477.56	1.58	6264.24	251.64	0.90
628	6380	0.1038	2.30	5.16	328.98	292.39	2643.46	19.11	830.63	3563.28	169.72	492.13	1.56	6253.88	195.80	0.73
629	6390	0.105	2.13	5.87	319.93	283.74	2314.45	17.71	413.78	2951.48	177.86	449.59	1.30	4499.36	173.10	0.67
630	6400	0.1069	2.31	6.96	342.55	309.40	2796.93	19.36	388.59	3532.37	178.36	510.48	1.54	5632.25	202.84	0.87
631	6410	0.1046	2.27	6.21	352.02	301.23	2995.19	19.97	278.63	4047.72	189.05	538.01	1.73	5856.55	201.63	0.88
632	6420	0.1053	2.09	6.60	330.35	291.00	3189.44	20.82	358.84	3540.65	189.81	546.74	2.23	6986.77	178.89	0.76
633	6430	0.1071	2.52	4.53	377.90	311.14	3153.84	24.17	455.41	4064.31	193.05	606.47	1.67	5802.04	203.36	1.00
634	6440	0.105	2.39	4.15	375.49	313.07	3308.84	24.51	696.08	4083.16	199.47	638.24	2.01	6887.51	200.17	0.97
635	6450	0.1019	2.25	6.02	328.40	291.69	2909.36	19.87	974.83	5029.23	190.79	490.83	2.18	10274.00	189.20	0.89
636	6460	0.1028	2.89	10.54	409.16	359.78	3176.81	20.92	1307.60	7003.23	213.84	557.19	2.43	10076.48	260.81	1.02
637	6470	0.1025	2.34	5.56	346.90	296.38	2992.68	21.05	2428.61	5152.76	204.84	513.47	2.60	10947.35	202.09	0.84
638	6480	0.102	2.60	5.08	376.98	345.94	2946.14	21.34	3859.08	4913.41	217.24	530.90	2.84	13880.56	231.45	0.80
639	6490	0.1026	3.05	5.93	422.08	381.57	2943.30	22.15	3720.60	4893.50	225.59	578.40	2.86	12007.08	270.45	0.84
640	6500	0.101	2.76	1.61	391.35	386.11	2940.94	20.95	3392.09	4049.24	211.55	592.31	2.90	11211.97	242.49	0.81
641	6510	0.1088	2.79	4.93	413.28	408.74	2888.24	30.83	2320.45	4158.26	200.04	635.94	2.99	9015.85	259.46	0.78
642	6520	0.1014	2.70	6.65	416.20	400.49	3010.44	40.18	1031.32	3442.74	203.74	624.81	3.13	6331.54	220.07	0.68
643	6530	0.1035	2.59	2.99	473.16	437.05	3351.17	25.41	438.62	3596.15	202.15	877.69	3.04	5471.15	232.96	0.78
644	6540	0.1024	2.49	5.73	478.64	424.94	3571.53	21.23	359.00	3329.30	202.62	942.65	3.11	6702.98	205.80	0.82
645	6550	0.1015	2.21	3.06	430.66	361.27	3516.75	21.26	275.63	5141.14	190.54	900.93	3.00	6865.99	182.70	0.87
646	6560	0.1017	2.57	5.86	446.59	417.41	3262.51	21.89	358.65	12407.85	186.46	776.84	2.90	12365.43	251.00	0.95
647	6570	0.1025	2.12	8.02	365.88	306.98	3021.87	20.13	250.84	9814.47	163.50	644.39	2.75	9295.19	184.90	0.88
648	6580	0.1035	2.74	4.21	406.27	335.86	2581.88	18.59	275.68	8480.42	165.05	571.02	2.98	10114.06	241.79	0.70
649	6590	0.1016	2.34	4.43	347.11	309.76	2269.45	18.19	305.51	6932.61	149.45	452.34	2.22	7933.66	209.29	0.60
650	6600	0.1039	2.40	2.70	367.61	317.75	2479.62	16.81	297.65	6681.77	147.17	563.12	2.07	8255.89	226.38	0.69
651	6610	0.1033	2.41	9.09	336.16	299.41	2111.85	17.27	382.87	8640.21	143.68	400.47	1.87	9378.20	224.03	0.56
652	6620	0.1004	2.83	9.16	402.90	372.95	2342.25	18.22	1846.55	7712.38	170.00	447.78	2.16	12975.52	272.68	0.55
653	6630	0.1038	2.63	8.67	340.67	301.71	2363.21	19.76	2057.16	7694.22	162.16	412.18	2.29	11928.15	224.69	0.50
654	6640	0.1057	2.54	5.46	316.60	284.43	2517.56	20.73	4439.61	6381.20	177.27	382.48	2.48	14820.13	208.37	0.50
655	6650	0.1072	2.90	7.67	359.08	330.83	2624.30	20.89	6492.34	7414.11	191.04	381.89	2.73	17412.89	256.38	0.60
656	6660	0.1059	2.97	4.25	380.67	343.27	2669.51	21.65	6602.69	6397.97	209.83	379.78	3.29	16069.05	268.21	0.52
657	6670	0.1088	2.15	2.77	356.19	630.66	2260.05	18.43	4695.60	6499.68	131.84	450.15	3.68	15662.52	320.06	0.52
658	6680	0.1062	2.23	8.06	383.19	639.55	2120.69	20.81	2723.08	5837.09	129.03	442.89	3.51	10650.62	327.34	0.52
659	6690	0.1086	2.36	7.07	391.29	709.78	2195.82	18.29	2618.80	6622.17	146.70	500.02	3.61	10396.90	378.72	0.60
660	6700	0.1048	2.12	5.74	383.39	617.40	2074.07	18.96	811.21	6264.78	211.06	490.36	3.49	9041.13	339.48	0.53
661	6710	0.1045	1.93	10.61	361.70	548.64	1722.41	15.83	474.85	6166.80	160.07	429.25	2.97	5553.65	314.07	0.49
662	6720	0.1033	2.03	8.45	406.25	707.01	2035.61	20.23	613.90	8829.50	207.64	576.35	48.53	11058.77	362.72	0.74
663	6730	0.1066	2.12	12.01	431.75	650.15	1805.81	21.80	573.02	9556.17	290.94	528.71	3.30	9419.52	391.38	0.62
664	6740	0.1074	1.23	2.43	385.26	403.99	1222.31	18.08	245.46	5963.76	251.28	355.68	2.55	5459.32	223.53	0.39
665	6750	0.1045	1.31	4.53	360.20	462.06	1579.61	15.99	456.17	5965.74	472.59	425.59	1.89	8283.07	265.91	0.41
666	6760	0.1071	2.06	5.85	405.23	729.36	1894.10	16.84	955.07	8720.71	341.78	486.69	2.62	15149.10	482.09	0.63
667	6770	0.1026	1.69	10.13	331.01	570.55	1893.09	17.88	404.16	15785.38	185.13	478.40	2.67	12543.02	449.67	0.53
668	6780	0.1011	2.00	7.34	384.71	665.60	1957.36	19.10	402.35	8091.55	191.21	522.87	2.67	7222.06	549.41	0.62
669	6790	0.1017	1.85	12.82	387.22	740.80	1915.68	26.44	351.62	10675.72	200.73	526.79	2.70	9738.09	650.28	0.68
670	6800	0.1052	1.78	8.11	346.90	681.95	1973.71	24.44	344.11	7117.41	156.88	554.48	2.25	5975.16	623.82	0.67
671	6810	0.1062	1.59	6.91	301.41	606.28	1910.27	30.77	432.04	6775.56	117.51	514.91	2.35	6875.55	566.86	0.62
672	6820	0.1048	1.33	8.79	314.58	664.67	2100.23	25.59	640.23	8082.09	120.94	615.62	2.24	8253.73	605.57	0.77
673	6830	0.1015	1.56	8.95	318.46	721.50	2115.23	35.30	1669.86	6179.65	123.40	590.36	2.26	12002.39	773.43	0.79
674	6840	0.1015	1.87	4.54	374.69	938.18	2307.28	38.90	1026.22	6870.56	136.89	725.94	1.94	10182.55	1004.17	1.12
675	6850	0.1031	1.24	5.59	287.85	867.41	2137.06	27.57	657.32	7262.54	132.89	593.52	2.10	9706.65	649.49	1.19
676	6860	0.1055	1.51	5.82	306.21	735.30	2092.78	26.48	328.17	7803.43	135.21	572.23	1.82	9036.18	873.12	1.08
677	6870	0.1069	1.74	8.20	310.06	817.29	2071.25	27.78	375.78	5985.02	138.50	615.23	1.85	9449.98	984.85	0.99
678	6880	0.1051	1.65	7.87	319.70	804.25	2083.41	35.96	398.93	6448.86	145.11	562.60	2.06	11231.81	1029.31	1.01
679	6890	0.1033	1.58	9.42	299.85	749.15	2076.93	31.62	480.60	7744.87	144.68	537.99	1.93	11517.81	977.76	1.06
680	6900	0.103	1.54	10.70	283.40	721.25	2010.61	41.24	486.03	7428.36	144.20	510.76	1.68	10119.25	971.11	0.99
681	6910	0.1014	1.60	6.44	326.56	854.59	2093.75	29.66	349.67	6832.85	148.10	619.92	1.41	9210.90	1127.41	1.27
682	6920	0.1032	1.38	7.34	284.38	792.17	1989.09	34.66	359.96	5752.22	141.76	639.35	1.50	10423.50	1060.50	0.97
683	6930	0.1049	1.24	7.63	259.18	658.36	2058.26	30.06	210.79	8257.61	137.63	529.56	1.44	10425.57	967.96	1.06
684	6940	0.1023	1.62	9.57	293.30	818.50	1971.57	27.79	194.95	8547.68	151.27	569.84	1.45	9722.20	1251.28	1.33
685	6950	0.1057	1.53	4.22	276.08	805.38	1803.91	22.14	209.02	5994.83	143.00	613.40	1.22	8020.64	1262.01	1.26
686	6960	0.1058	1.27	6.96	262.25	701.50	1782.54	20.92	227.20	5723.27	129.97	553.51	1.05	8574.98	1202.95	1.14
687	6970	0.1082	1.41	4.19	261.57	762.25	1920.80	23.22	487.21	5556.55	131.58	544.15	1.18	9807.48	1345.21	1.58
688	6980	0.1034	1.49	6.63	272.95	785.35	1867.32	23.42	833.89	4755.85	138.54	604.80	1.02	10229.54	1350.88	0.97
689	6990	0.1038	1.17	3.87	224.20	677.86	1965.30	33.36	14810.20	2848.47	194.77	550.29	0.89	28937.58	2939.86	1.11

	Depth (mm)	Sed. (ICPMS)	Ni 60	Cu 63	Zn 66	As 75	Se 82	Sr 88	Ag 109	Cd 111	Ba 137	Hg 202	Tl 205	Pb 207	Bi 209	U 238
600	6100	0.1217	0.61	2.73	18.51	33.20	0.45	7.35	1.05	-0.06	85.08	0.66	0.91	1.85	0.07	0.48
601	6110	0.1013	0.35	2.18	10.61	42.65	0.53	7.35	1.22	-0.14	153.16	0.52	0.37	1.60	0.07	0.34
602	6120	0.1041	0.54	1.62	10.82	57.23	0.51	7.67	0.93	-0.15	122.97	0.46	0.34	1.64	0.07	0.27
603	6130	0.1095	0.63	2.92	12.83	51.94	0.65	6.98	0.97	-0.11	85.28	0.41	0.69	1.61	0.06	0.40
604	6140	0.1036	0.79	2.64	18.89	42.81	0.45	7.89	1.01	-0.10	80.91	0.36	0.89	1.53	0.06	0.37
605	6150	0.111	0.54	2.65	15.88	39.46	0.58	7.00	1.02	-0.09	84.97	0.43	0.80	1.56	0.06	0.39
606	6160	0.1063	0.52	2.16	15.16	36.77	0.46	7.15	1.04	-0.10	86.93	0.35	0.82	1.46	0.06	0.37
607	6170	0.1101	0.49	2.87	15.12	44.90	0.44	6.43	0.93	-0.08	91.71	0.32	0.93	1.56	0.06	0.40
608	6180	0.1128	0.38	2.18	11.34	34.61	0.49	6.59	1.01	-0.10	144.66	0.32	0.59	1.62	0.06	0.36
609	6190	0.103	0.43	2.35	11.63	36.22	0.48	6.92	1.07	-0.12	146.54	0.37	0.58	1.74	0.06	0.34
610	6200	0.1039	0.48	1.92	11.13	45.98	0.48	7.04	1.09	-0.13	94.20	0.39	0.56	1.67	0.07	0.35
611	6210	0.1059	0.68	3.27	16.78	45.28	0.52	7.85	1.18	-0.07	91.10	0.34	0.95	1.68	0.07	0.47
612	6220	0.1105	0.53	1.46	12.71	54.14	0.48	7.26	1.01	-0.13	99.84	0.45	0.48	1.57	0.06	0.27
613	6230	0.1096	0.49	15.51	11.51	48.87	0.45	6.68	1.72	-0.13	89.77	0.39	0.46	1.44	0.06	0.25
614	6240	0.1203	0.65	2.53	12.38	45.11	0.52	6.76	0.95	-0.11	97.45	0.41	0.59	1.33	0.06	0.34
615	6250	0.1079	0.44	2.46	14.84	46.81	0.50	6.49	0.96	-0.12	105.44	0.37	0.62	1.37	0.06	0.35
616	6260	0.114	1.24	2.28	16.64	45.11	0.55	6.90	0.79	-0.13	84.09	0.41	0.58	1.33	0.06	0.31
617	6270	0.1067	0.49	1.87	17.78	38.09	0.50	7.07	0.99	-0.14	104.99	0.36	0.51	1.53	0.06	0.28
618	6280	0.1017	0.76	2.91	17.38	55.57	0.51	6.75	1.02	-0.14	91.30	0.44	0.56	1.44	0.06	0.31
619	6290	0.1078	0.44	2.25	16.04	50.77	0.58	6.73	1.05	-0.13	90.42	0.39	0.63	1.51	0.06	0.33
620	6300	0.1086	0.40	2.18	14.63	56.91	0.50	6.12	0.96	-0.12	96.31	0.40	0.58	1.34	0.06	0.31
621	6310	0.1005	0.40	2.01	13.47	60.32	0.53	6.13	0.98	-0.14	105.52	0.40	0.50	1.24	0.06	0.26
622	6320	0.1205	0.40	1.69	13.81	86.47	0.47	6.34	0.77	-0.12	94.35	0.43	0.43	1.44	0.06	0.23
623	6330	0.1015	0.54	2.87	16.70	68.82	0.52	6.12	0.79	-0.13	75.10	0.36	0.70	1.27	0.06	0.39
624	6340	0.1057	0.41	2.72	14.78	80.69	0.47	5.98	0.85	-0.09	125.86	0.38	0.85	1.38	0.06	0.39
625	6350	0.1025	0.40	2.89	13.89	73.49	0.51	6.12	0.95	-0.12	72.54	0.53	0.84	1.43	0.06	0.36
626	6360	0.1044	0.42	2.60	13.77	65.22	0.50	6.84	1.11	-0.14	81.57	0.53	0.72	1.60	0.06	0.35
627	6370	0.1034	0.60	2.94	22.17	58.02	0.58	8.08	0.97	-0.12	88.87	0.61	0.74	1.62	0.06	0.39
628	6380	0.1038	0.49	2.53	16.57	46.85	0.40	8.15	1.04	-0.14	87.19	0.44	0.61	1.78	0.06	0.37
629	6390	0.105	0.39	2.09	13.45	39.11	0.39	7.28	0.94	-0.14	89.63	0.33	0.48	1.38	0.06	0.30
630	6400	0.1069	0.56	2.78	16.47	52.20	0.54	8.93	1.05	-0.12	117.73	0.43	0.67	1.84	0.07	0.39
631	6410	0.1046	0.54	3.91	21.38	67.79	0.52	9.20	0.97	-0.12	97.55	0.41	0.62	1.81	0.07	0.39
632	6420	0.1053	0.46	4.17	30.81	78.42	0.59	9.47	1.02	-0.14	95.22	0.47	0.45	1.64	0.07	0.33
633	6430	0.1071	0.66	3.91	22.46	59.78	0.59	11.36	0.97	-0.11	100.17	0.48	0.88	2.04	0.07	0.49
634	6440	0.105	0.56	4.73	25.60	70.33	0.58	11.40	1.13	-0.12	102.80	0.55	0.74	1.98	0.07	0.44
635	6450	0.1019	0.58	5.76	21.60	132.29	0.85	9.76	1.22	-0.14	119.27	0.88	0.79	2.09	0.09	0.50
636	6460	0.1028	0.74	6.57	28.09	139.37	1.03	10.30	1.53	-0.11	120.37	2.03	0.77	2.36	0.10	0.53
637	6470	0.1025	0.74	6.75	22.18	109.04	0.96	10.68	1.54	-0.13	125.82	2.22	0.58	2.46	0.10	0.54
638	6480	0.102	0.75	7.48	22.86	89.10	0.88	10.85	1.71	-0.12	138.65	2.70	0.46	2.55	0.10	0.60
639	6490	0.1026	0.82	7.43	23.51	76.59	0.99	11.05	1.66	-0.14	107.27	2.47	0.47	2.58	0.11	0.61
640	6500	0.101	0.78	8.36	18.19	84.30	0.95	10.52	1.56	-0.14	93.24	2.09	0.43	2.64	0.11	0.64
641	6510	0.1088	0.69	7.59	16.77	90.02	1.04	11.42	1.69	-0.13	100.73	2.24	0.30	2.57	0.10	0.55
642	6520	0.1014	0.65	6.76	13.58	123.89	0.94	12.52	1.82	-0.14	124.11	1.95	0.24	2.59	0.10	0.50
643	6530	0.1035	0.61	6.67	12.00	169.47	0.97	17.10	1.57	-0.14	121.42	1.36	0.22	2.45	0.09	0.48
644	6540	0.1024	0.57	7.18	10.38	217.04	0.94	19.82	1.67	-0.15	133.89	1.64	0.22	2.49	0.11	0.46
645	6550	0.1015	0.73	10.73	10.62	203.56	0.85	18.45	1.52	-0.15	133.88	1.24	0.33	2.21	0.10	0.57
646	6560	0.1017	0.85	8.04	17.11	312.45	1.10	13.91	1.39	-0.13	82.68	1.69	0.63	2.40	0.10	0.60
647	6570	0.1025	0.93	6.44	12.82	288.30	1.02	11.91	1.33	-0.07	90.76	1.22	0.96	2.35	0.09	0.57
648	6580	0.1035	0.95	4.27	12.60	311.81	1.03	8.73	1.22	-0.13	90.45	1.14	0.47	1.94	0.09	0.47
649	6590	0.1016	0.72	3.87	10.92	289.78	0.89	7.15	1.31	-0.15	80.60	1.35	0.46	1.89	0.07	0.46
650	6600	0.1039	0.71	3.50	12.84	268.34	0.80	7.97	1.11	-0.14	89.01	0.76	0.56	1.73	0.06	0.40
651	6610	0.1033	0.47	3.40	9.60	297.04	0.88	6.41	1.40	-0.14	94.96	1.34	0.46	1.81	0.08	0.48
652	6620	0.1004	0.53	3.09	11.51	280.83	0.98	7.18	1.60	-0.14	106.32	1.73	0.29	1.97	0.09	0.41
653	6630	0.1038	0.55	3.50	10.31	209.28	1.08	6.94	1.89	-0.15	96.41	1.85	0.43	2.46	0.10	0.57
654	6640	0.1057	0.62	3.46	11.32	157.32	1.02	7.01	1.72	-0.14	103.85	2.25	0.45	2.64	0.10	0.58
655	6650	0.1072	0.94	3.89	15.75	134.99	1.26	6.79	1.83	-0.13	94.59	3.14	0.58	2.99	0.12	0.69
656	6660	0.1059	3.01	4.97	16.94	117.19	1.36	7.31	2.23	-0.12	100.33	3.49	0.35	3.44	0.12	0.87
657	6670	0.1088	0.97	3.77	13.53	371.15	1.39	7.24	2.21	-0.13	110.41	3.48	0.47	3.55	0.14	0.57
658	6680	0.1062	0.85	4.54	15.18	608.30	1.63	7.07	2.65	-0.13	111.15	3.43	0.38	3.66	0.15	0.77
659	6690	0.1086	1.13	4.73	16.48	649.31	1.71	7.58	2.65	-0.13	118.18	3.51	0.42	4.23	0.16	0.75
660	6700	0.1048	0.67	4.16	13.59	1153.83	1.64	7.30	2.57	-0.11	133.62	3.30	0.29	3.10	0.16	0.54
661	6710	0.1045	0.68	4.52	11.74	939.87	1.58	6.11	2.47	-0.14	86.08	2.63	0.24	2.52	0.13	0.56
662	6720	0.1033	1.00	4.55	134.57	907.62	1.45	8.04	2.34	-0.14	98.42	2.68	0.32	2.75	0.14	0.49
663	6730	0.1066	1.15	5.08	13.08	807.15	1.62	7.76	2.42	-0.13	105.71	2.83	0.32	2.80	0.17	0.55
664	6740	0.1074	0.95	2.84	7.54	379.50	0.79	5.73	1.43	-0.14	91.46	0.78	0.43	1.75	0.14	0.30
665	6750	0.1045	0.48	2.48	7.89	411.06	0.86	6.91	2.02	-0.15	100.04	1.09	0.37	2.31	0.13	0.22
666	6760	0.1071	0.86	3.99	12.59	444.39	1.06	6.81	2.33	-0.14	95.21	1.90	0.24	1.97	0.10	0.39
667	6770	0.1026	0.65	6.93	10.20	391.14	1.03	6.65	2.93	-0.14	82.25	2.30	0.17	1.77	0.09	0.48
668	6780	0.1011	1.15	4.53	10.93	304.16	1.05	7.46	2.93	-0.15	97.85	1.74	0.16	2.11	0.09	0.48
669	6790	0.1017	0.94	5.31	11.65	291.09	0.88	6.90	2.81	-0.15	84.79	2.39	0.18	1.98	0.10	0.38
670	6800	0.1052	0.77	3.68	11.05	201.65	0.75	7.20	2.38	-0.14	84.48	1.42	0.20	1.78	0.08	0.41
671	6810	0.1062	1.88	3.59	10.09	214.24	0.71	7.00	2.46	-0.15	85.56	1.52	0.15	1.68	0.08	0.36
672	6820	0.1048	0.97	3.84	10.75	207.26	0.68	7.82	2.06	-0.15	90.59	1.46	0.31	1.80	0.07	0.35
673	6830	0.1015	2.48	3.14	12.46	211.22	0.68	7.71	1.85	-0.12	97.73	1.38	0.17	1.58	0.08	0.34
674	6840	0.1015	5.34	2.91	16.73	157.49	0.52	8.61	1.63	-0.11	92.36	0.79	0.26	1.42	0.07	0.30
675	6850	0.1031	1.56	3.08	16.35	176.58	0.48	8.46	1.63	-0.08	102.80	1.00	0.93	1.48	0.08	0.33
676	6860	0.1055	1.41	3.56	16.43	156.21	0.50	7.44	2.00	-0.06	99.59	0.94	0.36	1.49	0.07	0.31
677	6870	0.1069	3.14	2.48	16.73	129.38	0.50	7.13	1.71	-0.11	97.86	0.91	0.18	1.30	0.06	0.27
678	6880	0.1051	1.13	2.77	16.71	140.17	0.62	7.21	1.73	-0.12	113.98	1.05	0.28	1.43	0.07	0.29
679	6890	0.1033	1.18	2.72	16.67	143.85	0.52	7.03	1.61	-0.10	129.30	0.86	0.34	1.43	0.06	0.32
680	6900	0.103	0.95	2.92	16.81	127.71	0.54	6.65	1.73	-0.10	144.15	0.74	0.32	1.35	0.06	0.31
681	6910	0.1014	1.19	2.24	19.63	103.93	0.40	7.45	1.22	-0.07	96.33	0.66	0.68	1.33	0.06	0.27
682	6920	0.1032	0.93	1.77	15.89	116.55	0.39	7.47	1.06	-0.11	88.63	0.54	0.17	1.05	0.05	0.19
683	6930	0.1049	0.99	2.54	15.48	116.81	0.43	7.09	1.13	-0.09	103.11	0.72	0.70	1.28	0.05	0.31
684	6940	0.1023	1.04	2.21	18.77	119.20	0.36	6.67	1.08	-0.07	98.84	0.65	0.72	1.25	0.06	0.33
685	6950	0.1057	0.98	1.36	17.21	77.97	0.19	6.41	0.87	-0.08	99.75	0.32	0.63	0.94	0.03	0.21
686	6960	0.1058	0.78	1.63	15.81	71.55	0.32	6.39	0.92	-0.10	111.15	0.33	0.95	1.04	0.04	0.24
687	6970	0.1082	1.03	1.67	17.93	85.98	0.27	7.62	0.81	-0.04	149.41	0.48	2.12	1.06	0.04	0.26
688	6980	0.1034	0.70	1.75	14.62	72.37	0.26	6.81	0.96	-0.11	153.80	0.40	0.47	0.87	0.04	0.26
689	6990	0.1038	0.73	1.63	23.61	43.24	0.30	9.54	0.65	0.01	90.56	0.63	3.23	0.84	0.03	0.23

Appendix H – Carbon & nitrogen analysis

Sample	Depth (mm)	Nitrogen %	Carbon %	C:N
Sample 1	10	0.9	5.1	5.84
Sample 2	20	0.8	4.9	5.91
Sample 3	30	0.8	3.7	4.59
Sample 4	40	0.7	2.8	4.08
Sample 5	50	0.6	2.3	3.63
Sample 6	60	0.6	1.9	3.26
Sample 7	70	0.5	1.7	3.22
Sample 8	80	0.5	1.7	3.03
Sample 09	90	0.5	1.6	3.02
Sample 10	100	0.5	1.6	3.11
Sample 11	110	0.5	1.4	2.75
Sample 12	120	0.5	1.6	3.11
Sample 13	130	0.5	1.5	2.92
Sample 14	140	0.5	1.5	3.03
Sample 15	150	0.5	1.5	2.99
Sample 16	160	0.5	1.5	3.12
Sample 17	170	0.5	1.6	3.17
Sample 18	180	0.6	1.9	3.39
Sample 19	190	0.5	1.9	3.66
Sample 20	200	0.5	1.3	2.62
Sample 21	210	0.4	1.4	3.12
Sample 22	220	0.5	1.3	2.66
Sample 23	230	0.5	1.4	2.86
Sample 24	240	0.5	1.5	3.03
Sample 25	250	0.5	1.6	3.17
Sample 26	260	0.5	1.5	3.17
Sample 27	270	0.4	1.4	3.10
Sample 28	280	0.4	1.2	2.85
Sample 29	290	0.5	1.3	2.77
Sample 30	300	0.4	1.3	2.99
Sample 31	310	0.5	1.2	2.54
Sample 32	320	0.4	1.3	3.17
Sample 33	330	0.4	1.4	3.19
Sample 34	340	0.5	1.4	2.98
Sample 35	350	0.5	1.4	2.80
Sample 36	360	0.4	1.2	3.25
Sample 37	370	0.4	1.2	3.15
Sample 38	380	0.4	1.2	2.96
Sample 39	390	0.4	1.2	3.19
Sample 40	400	0.2	0.6	2.49
Sample 41	410	0.2	0.3	1.64
Sample 42	420	0.2	0.3	1.47
Sample 43	430	0.2	0.4	1.48
Sample 44	440	0.2	0.3	1.53
Sample 45	450	0.5	1.7	3.20
Sample 46	460	0.5	1.9	3.45
Sample 47	470	0.6	2.0	3.48
Sample 48	480	0.6	2.1	3.85
Sample 49	490	0.5	1.9	3.54
Sample 50	500	0.6	2.2	3.89
Sample 51	510	0.5	1.8	3.42
Sample 52	520	0.6	1.5	2.65
Sample 53	530	0.5	1.7	3.31
Sample 54	540	0.5	1.7	3.12
Sample 55	550	0.5	1.6	2.87
Sample 56	560	0.5	1.4	2.85
Sample 57	570	0.6	1.6	2.71
Sample 58	580	0.5	1.5	2.92
Sample 59	590	0.5	1.4	2.74
Sample 60	600	0.5	1.5	3.06
Sample 61	610	0.5	1.5	2.98
Sample 62	620	0.5	1.5	2.79
Sample 63	630	0.5	1.4	3.05
Sample 64	640	0.5	1.6	2.99
Sample 65	650	0.6	1.5	2.35
Sample 66	660	0.5	1.4	2.87
Sample 67	670	0.5	1.5	2.85
Sample 68	680	0.6	1.5	2.67
Sample 69	690	0.5	1.5	3.02
Sample 70	700	0.5	1.5	2.74
Sample 71	710	0.5	1.4	2.66
Sample 72	720	0.6	1.6	2.82
Sample 73	730	0.5	1.5	2.90
Sample 74	740	0.5	1.4	2.50
Sample 75	750	0.5	1.5	2.92
Sample 76	760	0.5	1.4	2.74
Sample 77	770	0.5	1.5	2.79
Sample 78	780	0.5	1.4	2.67
Sample 79	790	0.6	1.5	2.69
Sample 80	800	0.6	1.5	2.60
Sample 81	810	0.6	1.6	2.79
Sample 82	820	0.6	1.5	2.41
Sample 83	830	0.6	1.7	2.97
Sample 84	840	0.6	1.9	3.40
Sample 85	850	0.6	2.0	3.24
Sample 86	860	0.6	2.0	3.68
Sample 87	870	0.6	2.0	3.29
Sample 88	880	0.6	2.0	3.20
Sample 89	890	0.7	2.2	3.27
Sample 90	900	0.6	2.1	3.50
Sample 91	910	0.5	1.7	3.25
Sample 92	920	0.6	1.5	2.40
Sample 93	930	0.6	1.8	2.97
Sample 94	940	0.5	1.5	2.77
Sample 95	950	0.5	1.5	2.76
Sample 96	960	0.5	1.4	2.98
Sample 097	970	0.5	1.5	2.81
Sample 098	980	0.5	1.7	3.22
Sample 099	990	0.6	2.3	3.69
Sample 100	1000	0.6	2.2	3.97

Sample	Depth (mm)	Nitrogen %	Carbon %	C:N
Sample 101	1010	0.6	2.0	3.55
Sample 102	1020	0.6	1.9	3.00
Sample 103	1030	0.6	1.8	3.07
Sample 104	1040	0.6	2.7	4.34
Sample 105	1050	0.7	2.4	3.52
Sample 106	1060	0.7	1.9	2.97
Sample 107	1070	0.6	2.1	3.36
Sample 108	1080	0.6	2.0	3.49
Sample 109	1090	0.4	1.8	4.44
Sample 110	1100	0.5	1.9	3.98
Sample 111	1110	0.4	1.7	3.82
Sample 112	1120	0.5	1.7	3.48
Sample 113	1130	0.6	1.8	3.21
Sample 114	1140	0.6	2.3	3.68
Sample 115	1150	0.5	2.3	4.24
Sample 116	1160	0.5	1.8	3.90
Sample 117	1170	0.0	0.2	0.00
Sample 118	1180	1.0	4.0	4.08
Sample 119	1190	0.6	1.9	3.34
Sample 120	1200	0.6	1.9	3.31
Sample 121	1210	0.5	1.7	3.56
Sample 122	1220	0.5	1.6	3.43
Sample 123	1230	0.5	1.7	3.53
Sample 124	1240	0.5	1.6	3.03
Sample 125	1250	0.5	2.0	4.41
Sample 126	1260	0.6	2.0	3.61
Sample 127	1270	0.5	2.1	4.03
Sample 128	1280	0.4	1.6	3.70
Sample 129	1290	0.4	1.6	3.50
Sample 130	1300	0.5	1.5	3.03
Sample 131	1310	0.5	1.5	3.11
Sample 132	1320	0.4	1.5	3.47
Sample 133	1330	0.5	2.1	4.20
Sample 134	1340	0.5	1.8	3.94
Sample 135	1350	0.5	1.9	4.01
Sample 136	1360	0.5	2.0	3.90
Sample 137	1370	0.6	2.3	4.16
Sample 138	1380	0.5	2.3	4.64
Sample 139	1390	0.5	1.9	3.81
Sample 140	1400	0.5	1.7	3.54
Sample 141	1410	0.4	1.7	4.00
Sample 142	1420	0.5	1.8	3.44
Sample 143	1430	0.4	1.6	3.74
Sample 144	1440	0.5	1.7	3.27
Sample 145	1450	0.6	1.6	2.84
Sample 146	1460	0.5	1.9	3.56
Sample 147	1470	0.6	2.0	3.42
Sample 148	1480	0.6	1.8	3.14
Sample 149	1490	0.6	2.1	3.46
Sample 150	1500	0.6	1.8	3.16
Sample 151	1510	0.6	1.7	2.99
Sample 152	1520	0.5	1.6	2.95
Sample 153	1530	0.6	1.7	2.72
Sample 154	1540	0.5	1.5	3.06
Sample 155	1550	0.6	1.6	2.82
Sample 156	1560	0.6	1.6	2.47
Sample 157	1570	0.6	1.5	2.68
Sample 158	1580	0.6	1.5	2.73
Sample 159	1590	0.6	1.8	3.05
Sample 160	1600	0.6	1.6	2.84
Sample 161	1610	0.6	1.5	2.55
Sample 162	1620	0.5	1.5	2.97
Sample 163	1630	0.6	1.6	2.60
Sample 164	1640	0.6	1.6	2.74
Sample 165	1650	0.6	1.4	2.39
Sample 166	1660	0.6	1.4	2.58
Sample 167	1670	0.5	1.5	3.02
Sample 168	1680	0.6	1.4	2.60
Sample 169	1690	0.6	1.5	2.39
Sample 170	1700	0.5	1.7	3.38
Sample 171	1710	0.1	0.2	2.81
Sample 172	1720	1.0	3.9	3.88
Sample 173	1730	0.6	1.8	3.07
Sample 174	1740	0.6	1.6	2.93
Sample 175	1750	0.5	1.6	2.96
Sample 176	1760	0.6	1.6	2.54
Sample 177	1770	0.6	1.7	2.72
Sample 178	1780	0.5	1.5	2.87
Sample 179	1790	0.6	1.6	2.72
Sample 180	1800	0.6	1.6	2.70
Sample 181	1810	0.5	1.5	2.84
Sample 182	1820	0.5	1.5	2.85
Sample 183	1830	0.6	1.6	2.69
Sample 184	1840	0.6	1.5	2.47
Sample 185	1850	0.6	1.7	2.76
Sample 186	1860	0.6	1.5	2.49
Sample 187	1870	0.6	1.5	2.55
Sample 188	1880	0.6	1.5	2.50
Sample 189	1890	0.6	1.7	2.91
Sample 190	1900	0.6	1.6	2.83
Sample 191	1910	0.5	1.6	2.91
Sample 192	1920	0.5	1.6	3.13
Sample 193	1930	0.6	1.6	2.70
Sample 194	1940	0.6	1.6	2.62
Sample 195	1950	0.6	1.6	2.55
Sample 196	1960	0.6	1.6	2.63
Sample 197	1970	0.5	1.4	2.53
Sample 198	1980	0.6	1.5	2.50
Sample 199	1990	0.6	1.6	2.61
Sample 200	2000	0.6	1.5	2.54

Sample	Depth (mm)	Nitrogen %	Carbon %	C:N
Sample 201	2010	0.6	1.3	2.11
Sample 202	2020	0.5	1.5	2.90
Sample 203	2030	0.6	1.6	2.64
Sample 204	2040	0.6	1.4	2.47
Sample 205	2050	0.6	1.4	2.28
Sample 206	2060	0.6	1.5	2.55
Sample 207	2070	0.8	3.0	3.63
Sample 208	2080	0.8	2.8	3.50
Sample 209	2090	0.7	2.1	2.98
Sample 210	2100	0.6	1.9	3.00
Sample 211	2110	0.5	1.5	2.72
Sample 212	2120	0.7	2.1	3.07
Sample 213	2130	0.7	2.0	2.85
Sample 214	2140	0.5	1.6	2.94
Sample 215	2150	0.6	1.5	2.68
Sample 216	2160	0.6	1.5	2.55
Sample 217	2170	0.6	1.4	2.45
Sample 218	2180	0.5	1.2	2.24
Sample 219	2190	0.4	1.0	2.19
Sample 220	2200	0.6	1.6	2.70
Sample 221	2210	0.6	1.6	2.57
Sample 222	2220	0.5	1.5	2.79
Sample 223	2230	0.5	1.5	2.72
Sample 224	2240	0.6	1.4	2.49
Sample 225	2250	0.5	1.5	2.76
Sample 226	2260	0.5	1.5	2.81
Sample 227	2270	0.6	1.5	2.59
Sample 228	2280	0.6	1.5	2.71
Sample 229	2290	0.6	1.5	2.65
Sample 230	2300	0.6	1.5	2.55
Sample 231	2310	0.5	1.4	2.83
Sample 232	2320	0.5	1.4	3.06
Sample 233	2330	0.5	1.5	3.39
Sample 234	2340	0.5	1.4	2.77
Sample 235	2350	0.5	1.4	2.76
Sample 236	2360	0.5	1.4	2.78
Sample 237	2370	0.6	1.5	2.47
Sample 238	2380	0.5	1.6	2.94
Sample 239	2390	0.5	1.6	3.07
Sample 240	2400	0.5	1.7	3.60
241	2410	0.6	1.7	2.79
242	2420	0.5	1.6	3.21
243	2430	0.5	1.6	3.22
244	2440	0.5	1.8	3.44
245	2450	0.6	1.7	3.04
246	2460	0.5	1.7	3.38
247	2470	0.6	1.8	3.20
248	2480	0.5	1.6	3.05
249	2490	0.5	1.4	2.76
250	2500	0.6	1.5	2.73
251	2510	0.5	1.9	3.54
252	2520	0.6	1.6	2.71
253	2530	0.6	1.7	2.75
254	2540	0.6	1.6	2.51
256	2550	0.6	1.6	2.50
256	2560	0.6	1.6	2.55
257	2570	0.7	1.6	2.41
258	2580	0.6	1.6	2.69
259	2590	0.6	1.5	2.69
260	2600	0.7	1.7	2.50
261	2610	0.7	1.6	2.41
262	2620	0.6	1.7	2.66
263	2630	0.6	2.0	3.37
264	2640	0.6	1.8	2.92
265	2650	0.5	1.4	2.60
266	2660	0.7	1.8	2.59
267	2670	0.6	1.5	2.65
268	2680	0.6	1.5	2.51
269	2690	0.6	1.5	2.32
270	2700	0.6	1.7	2.84
271	2710	0.6	1.6	2.81
272	2720	0.6	1.6	2.60
273	2730	0.6	1.7	2.89
274	2740	0.6	1.5	2.49
275	2750	0.6	1.5	2.44
276	2760	0.6	1.5	2.46
277	2770	0.6	1.6	2.55
278	2780	0.7	1.9	2.79
279	2790	0.7	1.9	2.77
280	2800	0.6	1.7	2.69
281	2810	0.6	1.7	2.70
282	2820	0.6	1.7	2.76
283	2830	0.7	1.6	2.48
284	2840	0.6	1.6	2.48
285	2850	0.7	1.6	2.24
286	2860	0.6	1.6	2.63
287	2870	0.6	1.9	2.90
288	2880	0.6	1.6	2.54
289	2890	0.6	1.6	2.54
290	2900	0.7	1.5	2.09
292	2910	0.6	1.6	2.48
292	2920	0.6	1.4	2.22
293	2930	0.6	1.4	2.27
294	2940	0.7	1.5	2.26
295	2950	0.7	1.6	2.39
296	2960	0.6	1.6	2.57
297	2970	0.6	1.5	2.39
298	2980	0.5	1.7	3.31
299	2990	0.7	1.6	2.36
300	3000	0.7	1.6	2.38

Sample	Depth (mm)	Nitrogen %	Carbon %	C:N
301	3010	0.6	1.6	2.82
302	3020	0.5	1.5	2.91
303	3030	0.5	1.4	2.69
304	3040	0.6	1.5	2.59
305	3050	0.5	1.7	3.20
306	3060	0.6	1.6	2.82
307	3070	0.6	2.0	3.15
308	3080	0.6	1.7	2.88
309	3090	0.6	1.6	2.75
310	3100	0.5	1.8	3.34
311	3110	0.5	1.6	3.05
312	3120	0.5	1.7	3.33
313	3130	0.5	1.9	3.46
314	3140	0.5	1.5	3.16
415	3150	0.5	1.6	3.08
316	3160	0.5	1.6	3.32
317	3170	0.5	1.6	3.20
318	3180	0.5	1.6	3.30
319	3190	0.5	1.6	3.29
320	3200	0.6	1.6	2.65
321	3210	0.5	1.6	3.09
322	3220	0.6	1.5	2.68
323	3230	0.6	1.6	2.83
324	3240	0.6	1.8	2.80
325	3250	0.6	1.7	2.75
326	3260	0.6	1.7	2.70
327	3270	0.6	1.9	3.17
328	3280	0.5	1.6	2.97
329	3290	0.6	1.6	2.94
330	3300	0.5	1.6	3.10
331	3310	0.6	1.6	2.92
332	3320	0.5	1.6	2.90
333	3330	0.6	1.6	2.81
334	3340	0.5	1.6	2.99
335	3350	0.6	1.7	2.97
336	3360	0.5	1.6	2.94
337	3370	0.5	1.6	3.13
338	3380	0.5	1.8	3.26
339	3390	0.5	1.6	3.26
340	3400	0.5	1.4	2.83
341	3410	0.4	1.5	4.07
342	3420	0.5	1.6	3.31
343	3430	0.5	1.5	3.08
344	3440	0.5	1.5	3.27
345	3450	0.4	1.6	3.83
346	3460	0.4	1.6	3.70
347	3470	0.5	1.6	3.07
348	3480	0.4	1.6	3.60
349	3490	0.5	1.6	3.32
350	3500	0.5	1.6	3.56
351	3510	0.5	1.8	3.63
352	3520	0.5	1.7	3.34
353	3530	0.5	1.7	3.36
354	3540	0.5	1.7	3.29
355	3550	0.5	1.7	3.22
356	3560	0.5	1.7	3.20
357	3570	0.6	1.9	3.28
358	3580	0.6	2.0	3.32
359	3590	0.5	2.0	4.15
360	3600	0.5	2.1	4.09
361	3610	0.4	1.9	4.32
362	3620	0.5	1.9	3.84
363	3630	0.5	2.1	3.97
364	3640	0.5	1.7	3.51
365	3650	0.5	2.0	3.75
366	3660	0.5	1.7	3.58
367	3670	0.5	1.9	4.21
367	3680	0.5	1.7	3.64
369	3690	0.4	1.7	3.76
370	3700	0.5	1.7	3.74
371	3710	0.5	1.6	3.47
372	3720	0.5	1.6	3.26
373	3730	0.5	1.7	3.36
374	3740	0.5	1.8	3.49
375	3750	0.5	1.7	3.40
376	3760	0.5	1.6	3.12
377	3770	0.5	1.7	3.51
378	3780	0.5	1.7	3.45
379	3790	0.6	1.7	2.97
380	3800	0.5	1.7	3.13
381	3810	0.5	1.8	3.50
382	3820	0.5	1.9	3.73
383	3830	0.5	1.9	4.02
384	3840	0.5	2.1	3.90
385	3850	0.5	1.8	3.60
386	3860	0.4	1.6	3.53
387	3870	0.5	1.8	3.45
388	3880	0.5	2.1	3.91
389	3890	0.5	1.8	3.84
390	3900	0.5	1.9	3.62
391	3910	0.6	1.9	3.50
392	3920	0.5	1.8	3.37
393	3930	0.5	1.9	3.97
394	3940	0.4	1.9	4.39
395	3950	0.5	2.0	3.98
396	3960	0.5	2.1	4.62
397	3970	0.5	1.9	3.99
398	3980	0.5	2.1	4.27
399	3990	0.5	2.0	3.75
400	4000	0.6	2.1	3.70

Sample	Depth (mm)	Nitrogen %	Carbon %	C:N
401	4010	0.6	1.8	3.13
402	4020	0.4	1.7	3.77
403	4030	0.5	1.9	3.83
404	4040	0.6	2.2	3.84
405	4050	0.5	1.7	3.65
406	4060	0.5	1.8	3.63
407	4070	0.5	1.8	3.76
408	4080	0.5	1.8	3.57
409	4090	0.5	1.6	3.23
410	4100	0.5	1.6	3.51
411	4110	0.6	2.0	3.53
412	4120	0.6	1.7	2.84
413	4130	0.6	1.7	3.01
414	4140	0.5	1.8	3.41
415	4150	0.6	1.8	3.33
416	4160	0.7	1.8	2.76
417	4170	0.6	1.8	3.14
418	4180	0.6	1.7	2.78
419	4190	0.6	1.7	2.70
420	4200	0.6	1.8	2.92
421	4210	0.6	1.6	2.83
422	4220	0.6	1.6	2.62
423	4230	0.6	1.7	3.06
424	4240	0.6	1.7	2.86
425	4250	0.5	1.6	3.01
426	4260	0.6	1.8	3.34
427	4270	0.6	1.8	3.24
428	4280	0.6	1.8	3.13
429	4290	0.6	2.1	3.36
430	4300	0.7	2.2	3.38
431	4310	0.6	2.2	3.36
432	4320	0.6	2.0	3.22
433	4330	0.6	2.2	3.48
434	4340	0.7	2.0	2.95
435	4350	0.7	2.2	3.06
436	4360	0.6	1.9	3.04
437	4370	0.6	1.8	3.05
438	4380	0.6	1.9	3.16
439	4390	0.6	1.6	2.92
440	4400	0.5	1.7	3.15
441	4410	0.5	1.5	3.25
442	4420	0.5	1.6	3.18
443	4430	0.5	1.8	3.71
444	4440	0.5	1.9	3.67
445	4450	0.6	2.3	3.71
446	4460	0.6	2.1	3.66
447	4470	0.6	2.3	3.83
448	4480	0.6	2.4	4.07
449	4490	0.6	3.0	4.67
450	4500	0.6	2.3	3.58
451	4510	0.6	2.1	3.27
452	4520	0.5	1.6	3.16
453	4530	0.6	1.6	2.89
454	4540	0.5	1.5	2.94
455	4550	0.5	1.5	3.10
456	4560	0.5	1.5	3.06
457	4570	0.5	1.5	3.22
458	4580	0.4	1.5	3.26
459	4590	0.5	1.4	3.13
460	4600	0.4	1.5	3.44
461	4610	0.5	1.4	3.02
462	4620	0.5	1.4	3.08
463	4630	0.4	1.5	3.49
464	4640	0.4	1.4	3.23
465	4650	0.5	1.4	2.96
466	4660	0.5	1.4	3.03
467	4670	0.5	1.5	3.11
468	4680	0.5	1.5	2.98
469	4690	0.5	1.5	2.97
470	4700	0.4	1.5	3.34
471	4710	0.4	1.4	3.18
472	4720	0.5	1.5	2.86
473	4730	0.4	1.5	3.28
474	4740	0.5	1.5	3.21
475	4750	0.5	1.7	3.29
476	4760	0.5	1.8	3.60
477	4770	0.5	1.8	3.71
478	4780	0.5	1.7	3.57
479	4790	0.4	1.6	3.77
480	4800	0.4	1.6	3.58
481	4810	0.5	1.5	3.25
482	4820	0.5	1.6	3.65
483	4830	0.5	1.6	3.34
484	4840	0.5	1.8	3.79
485	4850	0.5	2.0	3.86
486	4860	0.5	2.1	4.47
487	4870	0.5	2.2	4.24
488	4880	0.6	2.0	3.64
489	4890	0.5	1.8	3.95
490	4900	0.5	1.9	4.02
491	4910	0.5	2.0	4.25
492	4920	0.5	2.2	4.81
493	4930	0.4	2.4	5.56
494	4940	0.5	2.5	5.39
495	4950	0.5	2.9	5.78
496	4960	0.6	3.7	6.61
497	4970	0.5	4.0	8.05
498	4980	0.5	3.5	6.96
499	4990	0.5	2.2	4.66
500	5000	0.4	1.5	3.67

Sample	Depth (mm)	Nitrogen %	Carbon %	C:N
501	5010	0.3	1.1	3.70
502	5020	0.4	1.0	2.62
503	5030	0.3	1.0	3.06
504	5140	0.5	2.6	4.94
505	5150	0.5	2.2	4.49
506	5160	0.4	1.8	4.30
507	5170	0.5	2.0	4.28
508	5180	0.4	1.9	4.21
509	5190	0.4	1.6	4.03
510	5200	0.5	1.7	3.83
511	5210	0.4	1.7	4.09
512	5220	0.5	1.7	3.81
513	5230	0.4	1.7	3.91
514	5240	0.4	1.7	3.90
515	5250	0.5	1.7	3.71
516	5260	0.4	1.7	3.97
517	5270	0.5	1.7	3.63
518	5280	0.4	1.6	3.86
519	5290	0.5	1.6	3.57
520	5300	0.4	1.3	3.47
521	5310	0.4	1.6	3.83
522	5320	0.5	1.5	3.34
523	5330	0.4	1.4	3.28
524	5340	0.4	1.5	3.39
525	5350	0.4	1.4	3.87
526	5360	0.4	1.5	3.60
527	5370	0.4	1.5	3.90
528	5380	0.5	1.5	3.30
529	5390	0.4	1.5	3.52
530	5400	0.4	1.6	3.87
531	5410	0.4	1.4	3.47
532	5420	0.4	1.4	3.31
533	5430	0.4	1.4	3.29
534	5440	0.4	1.5	3.34
535	5450	0.4	1.5	3.27
536	5460	0.4	1.4	3.33
537	5470	0.4	1.4	3.36
538	5480	0.4	1.5	3.47
539	5490	0.4	1.5	3.31
540	5500	0.4	1.5	3.33
541	5510	0.4	1.4	3.08
542	5520	0.5	1.5	3.07
543	5530	0.5	1.5	2.92
544	5540	0.5	1.4	3.04
545	5550	0.5	1.5	3.00
546	5560	0.5	1.4	2.63
547	5570	0.5	1.4	2.61
548	5580	0.6	1.4	2.57
549	5590	0.5	1.5	2.70
550	5600	0.6	1.7	2.85
551	5610	0.6	2.0	3.15
552	5620	0.6	2.1	3.33
553	5630	0.7	2.2	3.00
554	5640	0.7	1.8	2.62
555	5650	0.6	1.6	2.73
556	5660	0.6	1.4	2.43
557	5670	0.6	1.1	1.84
558	5680	0.5	0.8	1.63
559	5690	0.4	0.6	1.37
560	5700	0.5	0.7	1.53
561	5710	0.5	0.9	1.74
562	5720	0.6	1.3	2.35
563	5730	0.6	1.5	2.48
564	5740	0.6	1.7	2.77
565	5750	0.7	1.7	2.57
566	5760	0.6	1.7	2.65
567	5770	0.6	1.6	2.55
568	5780	0.6	1.6	2.48
569	5790	0.7	1.8	2.50
570	5800	0.6	1.7	2.74
571	5810	0.7	1.7	2.46
572	5820	0.6	1.7	2.75
573	5830	0.6	1.8	2.75
574	5840	0.7	1.7	2.57
575	5850	0.6	1.7	2.64
576	5860	0.7	1.7	2.55
577	5870	0.7	1.7	2.50
578	5880	0.7	1.7	2.44
579	5890	0.6	1.6	2.56
580	5900	0.6	1.5	2.42
581	5910	0.7	1.5	2.28
582	5920	0.6	1.5	2.32
583	5930	0.6	1.6	2.56
584	5940	0.6	1.6	2.53
585	5950	0.7	1.7	2.47
586	5960	0.7	1.6	2.42
587	5970	0.7	1.4	2.08
588	5980	0.7	1.6	2.27
589	5990	0.7	1.6	2.33
590	6000	0.6	1.5	2.29
591	6010	0.4	1.6	4.03
592	6020	0.4	1.4	3.66
593	6030	0.5	1.5	3.16
594	6040	0.4	1.5	3.66
595	6050	0.4	1.3	3.26
596	6060	0.4	1.5	3.49
597	6070	0.4	1.6	3.58
598	6080	0.5	1.7	3.58
599	6090	0.4	1.5	3.37
600	6100	0.4	1.4	3.18

Sample	Depth (mm)	Nitrogen %	Carbon %	C:N
601	6110	0.5	1.4	3.09
602	6120	0.4	1.3	3.04
603	6130	0.5	1.4	2.93
604	6140	0.4	1.3	3.22
605	6150	0.4	1.4	3.05
606	6160	0.5	1.3	2.88
607	6170	0.5	1.4	2.93
608	6180	0.5	1.3	2.90
609	6190	0.4	1.4	3.12
610	6200	0.4	1.4	3.21
611	6210	0.4	1.4	3.87
612	6220	0.5	1.4	3.10
613	6230	0.4	1.4	3.48
614	6240	0.4	1.4	3.26
615	6250	0.4	1.4	3.17
616	6260	0.5	1.4	3.13
617	6270	0.5	1.4	3.02
618	6280	0.4	1.5	3.36
619	6290	0.5	1.5	3.23
620	6300	0.4	1.5	3.57
621	6310	0.5	1.5	2.97
622	6320	0.5	1.5	2.83
623	6330	0.5	1.5	3.20
624	6340	0.4	1.5	3.25
625	6350	0.4	1.4	3.25
626	6360	0.4	1.4	3.07
627	6370	0.4	1.4	3.20
628	6380	0.4	1.3	3.16
629	6390	0.5	1.3	2.74
630	6400	0.4	1.3	3.12
631	6410	0.4	1.4	3.27
632	6420	0.4	1.4	3.40
633	6430	0.4	1.4	3.60
634	6440	0.4	1.6	3.96
635	6450	0.5	2.2	4.46
636	6460	0.5	2.3	4.71
637	6470	0.5	2.5	5.53
638	6480	0.5	2.8	5.35
639	6490	0.6	2.9	5.05
640	6500	0.5	2.7	5.54
641	6510	0.5	3.0	5.95
642	6520	0.5	3.2	6.02
643	6530	0.6	2.5	4.53
644	6540	0.4	2.3	5.30
645	6550	0.5	2.5	5.18
646	6560	0.5	2.3	4.32
647	6570	0.6	2.5	4.47
648	6580	0.6	2.6	4.56
649	6590	0.6	2.4	4.14
650	6600	0.5	2.1	4.41
651	6610	0.5	2.5	4.91
652	6620	0.5	2.6	5.04
653	6630	0.5	2.8	5.92
654	6640	0.6	3.1	5.65
655	6650	0.5	3.5	6.75
656	6660	0.6	4.8	7.99
657	6670	0.6	5.5	9.63
658	6680	0.6	6.1	9.75
659	6690	0.6	6.6	10.78
660	6700	0.6	5.6	9.93
661	6710	0.5	7.6	13.75
662	6720	0.5	6.5	12.27
663	6730	0.5	7.5	13.68
664	6740	0.4	4.0	10.09
665	6750	0.4	3.4	8.26
666	6760	0.5	3.8	8.31
667	6770	0.5	3.5	7.37
668	6780	0.4	3.0	7.04
669	6790	0.4	2.7	6.70
670	6800	0.4	2.1	5.34
671	6810	0.3	2.0	5.88
672	6820	0.3	1.7	5.31
673	6830	0.3	1.7	5.04
674	6840	0.3	1.5	5.74
675	6850	0.3	1.5	4.66
676	6860	0.4	1.6	4.68
677	6870	0.3	1.5	4.27
678	6880	0.3	1.3	4.28
679	6890	0.4	1.2	3.45
680	6900	0.3	1.2	3.54
681	6910	0.3	1.0	3.46
682	6920	0.3	1.0	3.24
683	6930	0.3	0.8	3.20
684	6940	0.3	0.9	3.42
685	6950	0.3	0.8	3.27
686	6960	0.3	0.8	3.05
687	6970	0.3	0.8	3.11
688	6980	0.3	0.8	3.05
689	6990	0.2	0.6	2.77
Average		0.5	1.7	3.3